I agree that, if this thesis is accepted for the award of a degree of the University of Tasmania, it may be available for photo-copying.

Jon Webb

8/11/76.

STEADY-STATE COSMIC-RAY PROPAGATION IN INTERPLANETARY SPACE

by

GARRY MICHAEL WEBB B.Sc. (Hons.)

Submitted in fulfilment of the requirements

for the degree of

Doctor of Philosophy

UNIVERSITY OF TASMANIA

HOBART

December, 1975.

CONTENTS

* * * * * * *

STATEMENT

This thesis contains no material which has been accepted for the award of any other degree or diploma in any university and, to the best of the candidate's knowledge and belief, contains no material previously published or written by another person, except when due reference is made in the text of the thesis.

.....G.M. Webb.....

G.M. WEBB

SUMMARY

This thesis is a theoretical investigation of the steady-state propagation of galactic and solar cosmic-rays in the interplanetary medium. The study is carried out by means of analytic, steady-state solutions of the equation of transport for cosmic-rays in the interplanetary medium, including the effects of convection, diffusion and energy changes.

In Chapters 2-6, analytic monenergetic-source and monoenergetic-spectrum solutions of the steady-state equation of transport are obtained and these solutions are related to previously obtained analytic solutions.

In Chapter 7, three proofs are given of a result first noted by Gleeson (1972), for the mean-time-rate-of-change of momentum for cosmic-rays in interplanetary space, reckoned for a fixed volume in a reference frame fixed in the solar system. Also discussed in Chapter 7, are the proper role of:

(i) the adiabatic deceleration momentum rate $\langle \dot{p} \rangle_{ad}$, introduced by Parker (1965), and

(ii) the mean-time-rate-of-change of momentum, $\langle \dot{p}' \rangle$, of particles with momentum p' specified relative to the solar wind frame of reference, and with position $\underline{r}$ specified in the fixed frame of reference.

The physical significance of the momentum rate $\langle \dot{p}' \rangle$ has not been understood previously, and it is derived (for the first time) in Appendix G, from the transformation of momentum between the fixed and solar wind frames of reference. It is shown that Parker (1965)

and Jokipii and Parker (1970) have misinterpreted the energy change term in the cosmic-ray continuity equation associated with $\langle \dot{p}' \rangle$, due to an insufficient distinction between the two momentum rates $\langle \dot{p} \rangle_{ad}$ and $\langle \dot{p}' \rangle$.

The cosmic-ray particle flow and momentum changes are related to each other via the continuity or transport equation. In order to elucidate this relation we introduce the concept of a flow line in position momentum space. The flow line is defined as the curve whose tangent in position momentum space is given by the ratio of the streaming velocity to the mean-time-rate-of-change-of-momentum in the fixed frame of reference.

In Chapters 8-10, the solutions developed in Chapters 2-6, are used to verify most of the principal known features of steady-state propagation in the solar cavity. Some of these are: the energy changes; the relative exclusion of low energy galactic particles; the origin within the galactic spectrum of particles of given kinetic energy at 1 A.U. say; and the flow of particles in the solar cavity. Flow lines for monoenergetic galactic and solar cosmic-rays are constructed by using the monoenergetic-source and monoenergetic-spectrum solutions of the equation of transport derived in Chapters 2-6. The flow lines show, in some detail, the radical differences in the energy changes and flow of galactic and solar cosmic-rays. In brief, Chapter 8 deals with galactic cosmic-ray propagation, Chapter 9 deals with the propagation of monoenergetic solar cosmic-rays, and Chapter 10 concerns the propagation of galactic cosmic-rays for a special model in which a monoenergetic spectrum of particles is specified at the boundary of the solar cavity which is located at a finite distance from the sun.

PUBLICATIONS

Listed below are the references of four papers that have been published on the contents of this thesis:

Gleeson, L.J. and Webb, G.M. : 1974, Cosmic-ray energy changes, *Proc.Astron.Soc.Aust.*, Vol.2, No.5, 297.

Gleeson, L.J. and Webb, G.M. : 1975, Modulation and spectral redistribution of galactic cosmic-rays, *Proc. 14th Int. Conf. on Cosmic-Rays, Munich, 3*, 893.

Webb, G.M. and Gleeson, L.J. : 1973, Monoenergetic source solutions of the steady-state cosmic-ray equation of transport, *Proc. 13th Int. Conf. on Cosmic-Rays, Denver,* (University of Denver, 1973), Conf. Papers, *5*, 3253.

Webb, G.M. and Gleeson, L.J. : 1973, Solutions of the cosmic-ray equation of transport, *Proc. Astron.Soc.Aust.*, Vol.2, No.5, 299.

In addition it is anticipated that three more papers will be forthcoming. The first will be an extensive version of the work in Chapter 7 on energy changes of cosmic-rays in the interplanetary medium, the second will deal with the particle flow and momentum changes of monoenergetic galactic and solar cosmic-rays from the work in Chapters 8 and 9, and the third will be concerned with the development of the monoenergetic-spectrum and monoenergetic-source solutions from Chapters 2-6.

ACKNOWLEDGEMENTS

I am indebted to my co-supervisors, Dr. K.B. Fenton, Dr. A.G. Fenton, of the University of Tasmania, and Dr. L.J. Gleeson of Monash University for their encouragement, criticism and advice through the period of my study.

In particular, I have benefited from frequent discussions with Dr. Leo Gleeson, and from his hospitality during extended visits to Monash University. His mathematical and physical insight into the nature of the cosmic-ray transport equations have been invaluable.

I must also express my thanks to Dr. E.D. Fackerell, now at Sydney University, for introducing me to the application of Lie groups in solving partial differential equations, contained in Chapter 2.

I would like to thank Mr. D.F. Paget, of the Mathematics Department of the University of Tasmania, for his suggestions on the numerical evaluation of the singular integrals in Chapter 10.

Mrs. Janine McClean, who typed the initial draft of Chapter 7, and Mrs. Nell Gill who typed the remaining bulk of the manuscript receive my special thanks for their careful and speedy work.

Finally, I would like to thank Di. Owens, and my sister Lynn for their astrological insight into astrophysical processes.

Financial support for the research in this thesis was

provided by a Commonwealth post-graduate award, which is gratefully acknowledged.

G.M. Webb.

December, 1975.

CHAPTER 1.

INTRODUCTION.

1.1 Introduction

This thesis is a theoretical study of the steady-state propagation of galactic and solar cosmic-ray particles in interplanetary space. In the next section we sketch the historical background of the subject. In Section 3 we consider the development of the transport equations for cosmic-rays in the interplanetary medium. In Section 4 we indicate solutions of these equations, which have been used extensively to interpret the observed cosmic-ray fluxes and anisotropies, and we discuss in some detail the steady-state solutions. In Section 4 we discuss the fundamental role of monoenergetic solutions of the steady-state equation of transport in elucidating the physical processes involved, and we give examples of the use of the analytic monoenergetic solutions obtained by the present author. Finally in Section 6 an outline of the subject matter of this thesis is given.

1.2 Historical background

Cosmic-ray research originates from the discovery of 'penetrating radiation' observed with ionisation chambers early in the 20th century. This ionisation was such that it increased with increasing altitude in the atmosphere (Hess, 1911, 1912). The results of early experiments indicated solar and sidereal diurnal variations in the cosmic-ray intensity (Hess and Steinmaurer, 1933; Compton and Getting, 1935).

In the early 1930's serious attempts were made to provide a continuous registration of cosmic-ray intensity. Hess and Graziadei (1936) subsequently reported a 27-day recurrence tendency in the intensity variations, while Forbush (1937) found that sudden decreases in cosmic-ray intensity (Forbush decreases) were accompanied by magnetic storms.

Forbush (1954) also showed that the variation in cosmic-ray intensity was in clear anti-correlation with the eleven-year cycle of solar activity as measured by the sunspot number. This phenomenon is shown in Figure 1.1, which has been reproduced from Forbush (1954). It shows the currents for four ground-based ionisation chambers and their mean current for the years 1938 to 1952. The sunspot number is also plotted with scale reversed, and there is a clear association between increase in solar activity and decrease of ionisation current or integral cosmic-ray intensity.

These time dependent phenomena (i.e., modulations) have been studied ever since, with the introduction of the neutron monitor (Simpson and Fagot, 1953; Hatton, 1971) in the 1950's being the first major attempt to record cosmic-ray intensities at a network of stations on a continuous basis.

Since the advent of balloon and satellite technology the variations in the *absolute* intensities of specific cosmic-ray nuclei and electrons could be monitored. Neutron monitor observations deep in the atmosphere consist of the registration of secondary atmospheric products of near-Earth particles of the whole cosmic-ray abundance spectrum. Satellite and balloon observations have the additional advantage that they are not subjected to atmospheric attenuation, and

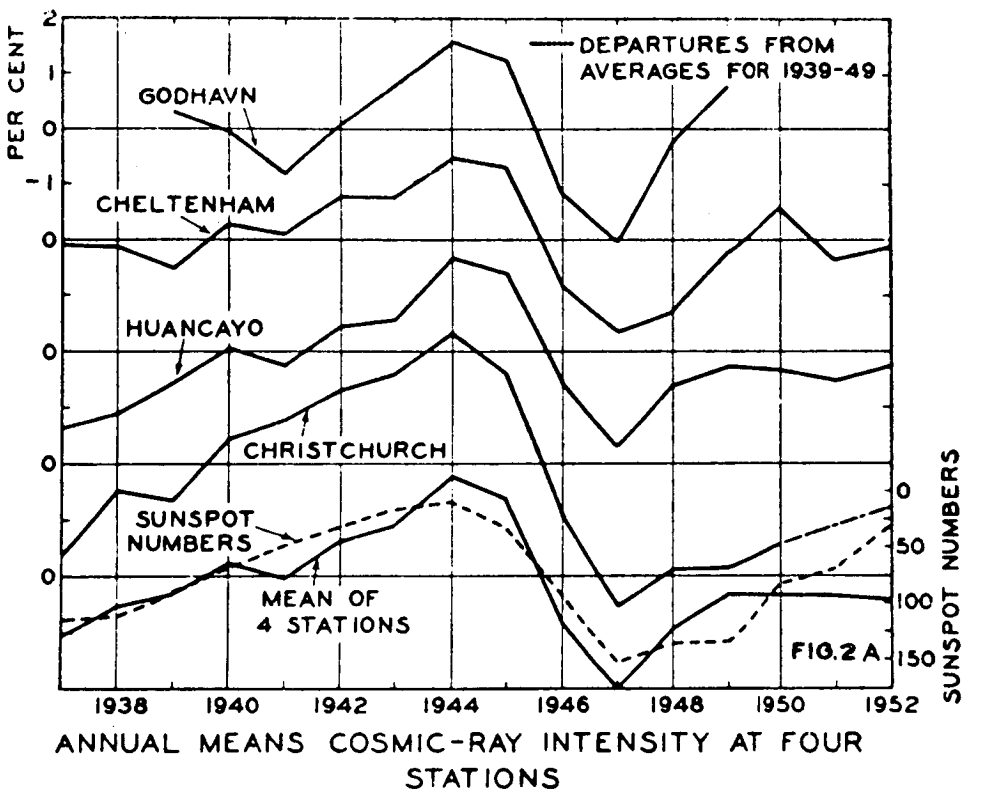

FIGURE 1.1

- shows the anti-correlation between cosmic-ray intensity at four ground-based stations and the eleven-year cycle of solar activity as measured by sunspot activity. The figure has been reproduced from Forbush (1954).

hence extend to much lower energies than observations in the atmosphere. Cosmic-ray proton and alpha particle differential intensity spectra, obtained from balloon and satellite experiments have been compiled since 1965 (e.g., Gloeckler and Jokipii 1967; Ormes and Webber 1968; Hsieh 1970; Freier *et al.*, 1971; Webber and Lezniak 1973, 1974). Intensity spectra of electrons and positrons have been measured extensively since 1965. (e.g., Webber and Chotowski, 1967; Beuerman *et.al.*1969; Fanselow *et.al.*,1969; Meyer *et.al.*,1971; Burger and Swanenburg, 1971; Fulks *et.al.*,1973; Caldwell *et.al.*,1975).

The near-Earth differential intensity spectra over solar cycle 20 of protons and alpha particles are shown in Figure 1.2 for three levels of solar modulation corresponding to: (1) sunspot minimum (1965); (2) an intermediate level; and (3) sunspot maximum (1970). The figure has been reproduced from Webber and Lezniak (1974) and the sources of the data are listed in the figure caption. The solid lines provide a smoothed best fit to the data at different epochs. The near-Earth electron spectra observed during the periods: July 1965 (Webber and Chotowski, 1967); June-July in the years 1968, 1969 and 1970 (Meyer *et.al.*,1971); and the galactic electron spectrum (Goldstein *et.al.*, 1970a; Burger *et.al.*, 1971) are shown in Figure 1.3. The figure has been reproduced from Urch and Gleeson (1972b). The range of energies observed is from 10 MeV/nuc to 1000 GeV/nuc for the proton and helium spectra of Figure 1.2 and from 10 MeV to 10 GeV for the electrons in Figure 1.3. Significant variation in the intensity (modulation) occurs only in the range 10 MeV/nuc to 10 GeV/nuc for the nuclei and 10 MeV to 10 GeV for electrons, and the work of this thesis is therefore concerned with this range.

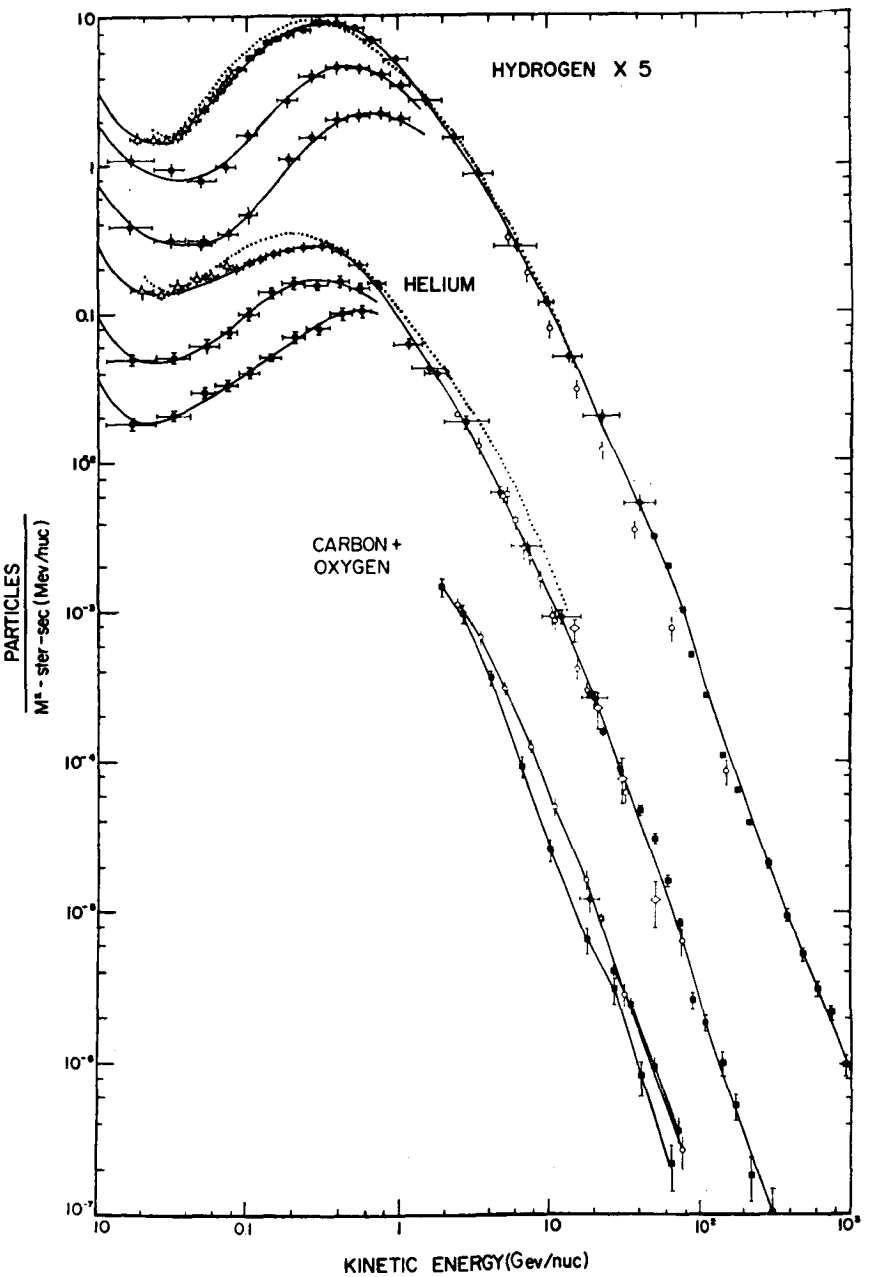

FIGURE 1.2 - Differential energy/nucleon spectra for cosmic-ray protons, helium, and carbon + oxygen nuclei for three levels of solar modulation corresponding to: (i) sunspot minimum (1965); (ii) an intermediate level; and (iii) sunspot maximum (1970). The figure has been reproduced from Webber and Lezniak (1974). Data points labelled are ♦ from Ryan *et.al.*, 1972; ♦ are from Ormes and Webber, 1965; von Rosvinge *et.al.*, 1969, and Webber *et.al.*,1973a; Δ are from Fan *et.al.*, 1966; ◊ are from Anand *et.al.*,1968; ◊ are from Smith *et.al.*,1973; ◇ are from Verma *et.al.*,1972; for C + O nuclei, ♦ are from Balasubrahmanyan and Ormes, 1973, x are from Juliusson, 1973; ◊ are from Smith *et.al.*, 1973.

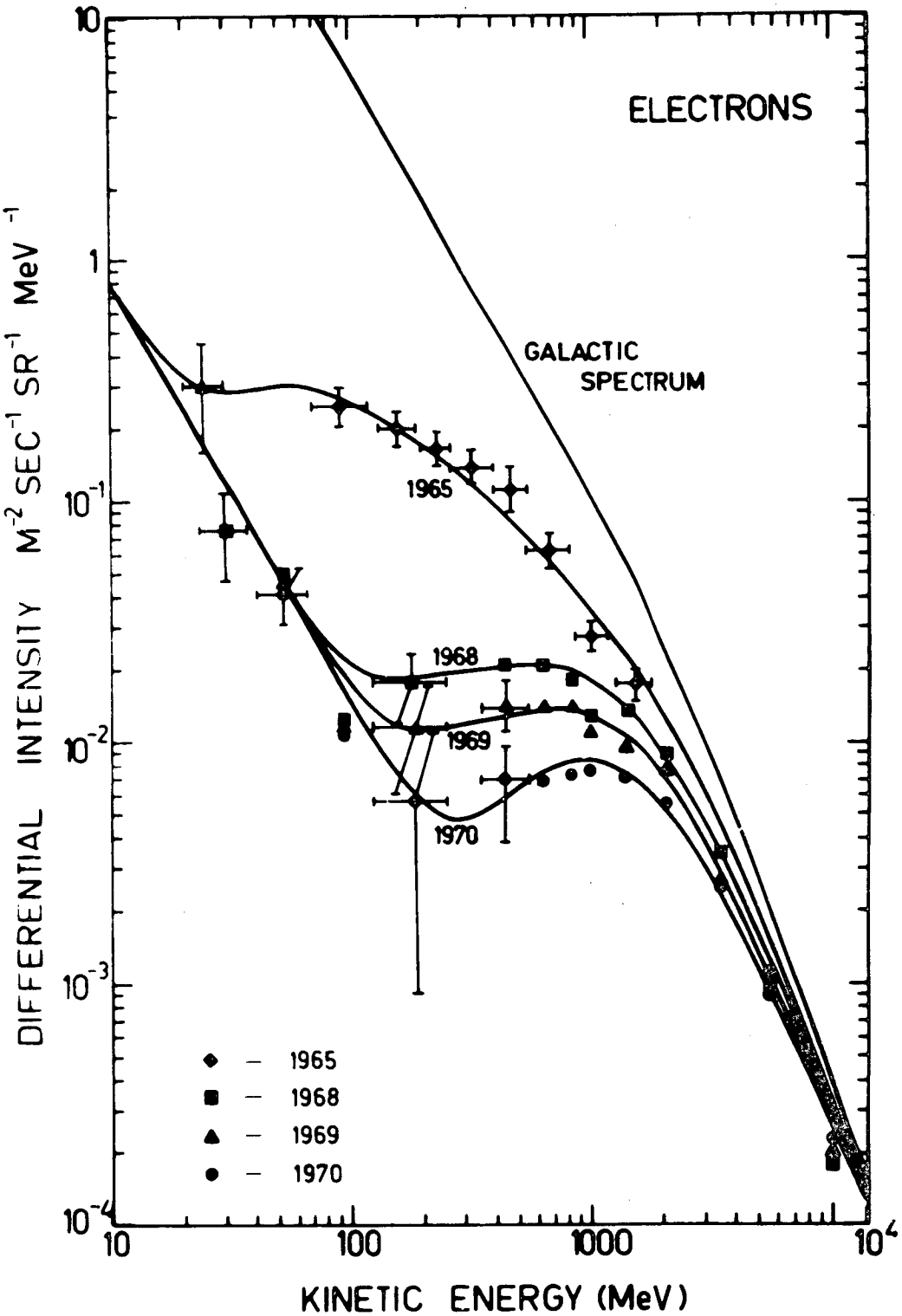

FIGURE 1.3

- The near-Earth electron spectra observed during the periods: July 1965 (Webber and Chotowski, 1967); June-July in the years 1968, 1969 and 1970 (Meyer *et.al.*, 1971); and the galactic electron spectrum (Goldstein *et.al.*,1970a; Burger *et.al.*,1971). The figure has been reproduced from Urch and Gleeson (1972b).

The basis of the theoretical understanding of these phenomena can be traced back to the original pioneering work of Fermi (1949), Cocconi (1951) and Terletskii and Logunov (1951) on the diffusion of cosmic-rays in a stochastic magnetic field. The first observational evidence that diffusion was in fact an excellent approximation to cosmic-ray motion was given by Meyer *et.al.* (1956), who showed that the intensity-time profile, during a solar flare event of particles with rigidities of 2-4GV could be accounted for quantitatively by the solution of a diffusion equation. These ad hoc applications to the propagation of cosmic-rays in interplanetary space have been put on a firm theoretical and observational basis since the observational confirmation of the existence of a continuous solar wind, first suggested by Biermann (1951) from his studies of comet tails and developed on a proper basis by Parker (1958a) with his hydrodynamical model of the extension of the solar corona into interplanetary space.

Parker predicted, and it was subsequently confirmed on Mariner II, that there would be a continuous radial flow of ionised gas (mostly protons and electrons) from the Sun into interplanetary space. The radial speed is $\approx$ 400 km s^{-1} and there are about 5 protons/c.c. and 5 electrons/c.c. at the orbit of the Earth. This expanding plasma carries with it magnetic fields from the sun's surface (Parker, 1958a). Due to the sun's rotation the steady-state interplanetary magnetic field has the form of an Archimedes spiral on the surface of a cone. In addition to the steady-state field there are irregular magnetic fields; all are convected radially with the solar wind. The irregularities or kinks in the average spiral interplanetary magnetic field convected with the solar wind (Parker, 1958a)

provide a magnetic configuration for the scattering and consequent 'random walk' of the cosmic-ray charged particles.

Since 1958 a wealth of literature has been produced on the effect of the solar wind on galactic cosmic-rays that have penetrated the inner solar system and on the propagation of solar cosmic-rays. The reader is referred to the excellent and extensive reviews by Axford (1970a, b) on the various models of propagation; to the review by Jokipii (1971), and the workshop report edited by Birmingham and Jones (1975) on the diffusion of particles in the interplanetary magnetic field; to the reviews by Gleeson (1971, 1972) on steady-state modulation of galactic cosmic-rays; to Wibberenz (1971) on solar particle propagation; to McCracken and Rao (1970) on solar particle observations; and to the Rapporteur paper by Quenby (1973) for an overall view.

1.3 Development of the cosmic-ray transport equations

We now give a development from the literature of the transport equations for cosmic-rays in the interplanetary medium which have been used extensively to interpret the modulation of galactic cosmic-rays and the propagation characteristics of solar particles.

Parker (1958b) pointed out that the continuous solar wind provides a compelling interpretation of the quasi-steady eleven-year modulation of galactic cosmic-rays. He argued that the cosmic-rays are *convected* by the magnetic fields carried by the solar wind as they *diffuse* through the solar wind due to scattering with the magnetic irregularities. He further assumed that the particles did not suffer any significant energy changes so that the equation of transport which includes the effects of convection and diffusion but neglects energy

changes is (Parker, 1963):

$$\frac{\partial U_p}{\partial t} + \underline{\nabla} \cdot (\underline{V}\, U_p - \underline{\underline{K}} \cdot \underline{\nabla}\, U_p) = 0, \qquad (1.3.1)$$

where $U_p(\underline{r},p,t)$ is the differential number density with respect to momentum p at position $\underline{r}$ and time t, $\underline{\underline{K}}$ is the diffusion tensor and $\underline{V}$ is the solar wind velocity.

He showed (Parker, 1958b) that with a spherically symmetric geometry and with isotropic diffusion the steady-state solution of Equation (1.3.1) appropriate for galactic cosmic-rays is

$$U_p(r,p) = U_p(R,p) \exp(-\int_r^R (V/K)\, dr), \qquad (1.3.2)$$

where $U_p(R,p)$ is the differential number density at the boundary of the solar cavity which is at heliocentric radius r = R, and K is the isotropic diffusion coefficient. He used this simple solution of the transport equation to qualitatively account for the quasi-steady eleven-year solar-cycle modulation of cosmic-ray intensity. This *convection-diffusion theory* has been widely used when interpreting observed cosmic-ray particle spectra and has had some success at high and intermediate energies (e.g., Fan *et.al.*, 1965; Silberberg, 1966; Gloeckler and Jokipii, 1966, 1967; Badhwar *et.al.*, 1967; O'Gallagher and Simpson, 1967; Lockwood and Webber, 1967; Ormes and Webber, 1968; Ramaty and Lingfelter, 1969; Wang, 1970).

The absolute necessity for convection in this theory can be seen directly from the steady-state solution (1.3.2) of the convection-diffusion equation. If V ≡ 0 in the solution (1.3.2) then

$$U_p(r,p) = U_p(R,p),$$

and consequently there is no modulation in the absence of convection. The presence of convection ensures that not all galactic particles

can penetrate into the inner solar system.

However Parker (1965,1966) has shown that energy changes of cosmic-ray particles in the interplanetary medium are not negligible. Parker showed that Fermi acceleration could be neglected and he argued that all cosmic-ray particles lose energy (when viewed from a frame moving with the solar wind) because of adiabatic deceleration as they move with the expanding magnetic field irregularities. The rate of change of momentum of particles due to adiabatic deceleration is (Parker, 1965; Dorman, 1965),

$$\langle \dot{p}' \rangle_{ad} = - p' (\underline{\nabla} \cdot \underline{V})/3, \qquad (1.3.3)$$

where p' is the particle momentum as seen by an observer moving with the solar wind. We note that Singer *et.al.* (1962) discussed adiabatic deceleration in connection with Forbush decreases, and the possibility of the importance of energy changes was discussed by Quenby (1965, 1967).

The transport equation, which includes the effects of convection, anisotropic diffusion and momentum changes is (Jokipii and Parker, 1970),

$$\frac{\partial U_p^*}{\partial t} + \underline{\nabla} \cdot (\underline{V} U_p^* - \underline{\underline{K}} \cdot \underline{\nabla} U_p^*) - \frac{1}{3} (\underline{\nabla} \cdot \underline{V}) \frac{\partial}{\partial p'} (p' U_p^*) = 0, \qquad (1.3.4)$$

where $U_p^* (\underline{r}, p', t)$ is the differential number density with respect to momentum p' as seen in the frame of reference moving with the solar wind, and the spatial co-ordinates $\underline{r}$ are defined in a fixed frame of reference.

Parker (1965) and Jokipii and Parker (1970) argue that the energy change term

$$- \frac{1}{3} \underline{\nabla} \cdot \underline{V} \frac{\partial}{\partial p'} (p' U_p^*),$$

occurring in the transport equation (1.3.4) is due to adiabatic deceleration. However it has been recently noted by the present author that this is not the case. In order to see this we write the transport equation (1.3.4) in the form

$$\frac{\partial U_p^*}{\partial t} + \underline{\nabla} \cdot \underline{S}_p^* + \frac{\partial}{\partial p} (\langle \dot{p}' \rangle U_p^*) = 0, \qquad (1.3.5)$$

where

$$\underline{S}_p^* = \underline{V} U_p^* - \underline{\underline{K}} \cdot \nabla U_p^* , \qquad (1.3.6)$$

is the differential current density or streaming of particles with momentum p' (specified relative to the solar wind frame) across a fixed surface at position $\underline{r}$ in the fixed frame of reference, and

$$\langle \dot{p}' \rangle = -\frac{p'}{3} \underline{\nabla} \cdot \underline{V}, \qquad (1.3.7)$$

is the corresponding mean-time-rate-of-change of momentum of particles with momentum p' at position $\underline{r}$.

The momentum rate $\langle \dot{p}' \rangle$ is due to the transformation of momentum between the fixed and solar wind frames. It arises because the solar wind frame is not an inertial reference frame on a large scale. We remark that $\langle \dot{p}' \rangle$ is not dependent on particle scattering, and a derivation of the rate $\langle \dot{p}' \rangle$ is given, (for the first time) in Appendix G.

The adiabatic deceleration rate $\langle \dot{p} \rangle_{ad}$ on the other hand is only applicable (in the discussion of cosmic-ray energy changes) in the case of convective transport or strong scattering, i.e., the components of the diffusion tensor $\underline{\underline{K}} \simeq 0$. The cosmic-rays are then effectively constrained to move with the solar wind as they scatter between the magnetic field irregularities which behave like the walls of a 'magnetic box'. Consequently the particles change momentum at

the adiabatic rate (1.3.3) within the expanding 'magnetic box' whose walls move at the solar wind velocity $\underline{V}(\underline{x})$. It thus appears that Parker (1965) and Jokipii and Parker (1970) have misinterpreted the momentum change term in the cosmic-ray continuity equation (1.3.5) associated with $\langle \dot{p}' \rangle$, as being due to adiabatic deceleration. A further discussion of this matter is given in Chapter 7.

The differential number density $U_p(r,p,t)$, defined in a fixed frame is a more useful quantity than $U_p^*(\underline{r},p,t)$ since all observations are made from the fixed frame. These densities are related by (Jokipii and Parker, 1967; Gleeson and Axford, 1968a; Forman, 1970).

$$U_p(r,p,t) = U_p^*(r,p,t)\,[1 + O(\varepsilon)] \qquad (1.3.8)$$

where $\varepsilon = (pV^2/v^2)\,|\partial\, \ell n(U_p)/\partial p\,| \ll 1$, (v is the particle speed). Hence when $\varepsilon \ll 1$ the differential number density as measured in the fixed frame $U_p(\underline{r},p,t)$ will satisfy Equation (1.3.4) and it can be used to calculate the differential number density in the fixed frame of reference, i.e., for $\varepsilon \ll 1$ we have

$$\frac{\partial U_p}{\partial t} + \underline{\nabla} \cdot (\underline{V}\, U_p - \underline{\underline{K}} \cdot \underline{\nabla}\, U_p) - \frac{1}{3}(\underline{\nabla} \cdot \underline{V}) \frac{\partial}{\partial p}(p\, U_p) = 0, \qquad (1.3.9)$$

as the equation of transport.

Alternative derivations of the transport equation (1.3.9) have also been given by Gleeson and Axford (1967), and by Dolginov and Toptygin (1967, 1968). Gleeson and Axford derived the transport equation (1.3.9) from the Boltzmann equation in a spherically symmetric model of the interplanetary medium. In this model the cosmic-rays undergo isotropic, hard-sphere scattering with scattering centres embedded in a radial solar wind. Dolginov and Toptygin derived the

equation of transport from the Boltzmann equation for a hard-sphere, small angle scattering model, but their results do not assume spherical symmetry about the sun and hence they are able to incorporate correctly the Archimedean spiral magnetic field (and hence anisotropic diffusion) and the effect of a non radial solar wind velocity. These latter authors also derived the transport equation directly from Liouville's theorem, for the case of small angle scattering, with special forms for the two point correlation tensor of the irregular component of the interplanetary magnetic field, and for a general non-spherically-symmetric model.

Gleeson and Axford, and Dolginov and Toptygin also derived an expression for the differential current density or streaming $\underline{S}_p$ per unit momentum interval. Their result can be written as

$$\underline{S}_p = C \underline{V} U_p - \underline{\underline{K}} \cdot \underline{\nabla} U_p , \qquad (1.3.10)$$

where

$$C = 1 - \frac{1}{3 U_p} \frac{\partial}{\partial p} (p U_p), \qquad (1.3.11)$$

is the Compton-Getting factor (Compton and Getting 1935, Gleeson and Axford 1968a; Forman, 1970) and $\underline{\underline{K}}$ is the diffusion tensor. In the work of Gleeson and Axford (1967), the diffusion tensor is replaced by a radial diffusion coefficient K. Gleeson (1969) has obtained the streaming (1.3.10) for a general, non spherically symmetric model by generalising the earlier results of Gleeson and Axford (1967). We note here that Gleeson and Axford (1968a) and Forman (1970), have shown that the Compton-Getting factor C and the convective flux $C \underline{V} U_p$ are consequences of transforming the streaming from the solar wind frame of reference to a stationary frame of reference taking into account the momentum spectrum of U_p.

Although the diffusion tensor arises naturally in the development of the transport equations using the Boltzmann equation, or the Liouville equation development of Dolginov and Toptygin, or by using the physical arguments of Jokipii and Parker (1970), these treatments do not give the detailed dependence of the diffusion tensor on the statistical properties of the interplanetary magnetic field. The diffusion tensor $\underline{\underline{K}}$ occurring in the transport equations (1.3.9) and (1.3.10) is in general derived from the theory of the propagation of charged particles in stochastic electromagnetic fields. This theory has been developed for both the propagation of cosmic-rays in the interstellar medium and in interplanetary space.

There is an important difference btween the cosmic-ray interaction with the magnetic field in the interstellar medium and in interplanetary space. In the former case the energy densities of the cosmic-rays and magnetic field are approximately the same, and the effect of particles on the fields (through emission and absorption of various waves) must be taken into account. This requires a self-consistent solution of the full set of Maxwell-Vlasov equations (e.g., Lerche, 1967; Kulsrud and Pearce, 1969; Melrose and Wentzel, 1970).

The magnetic field in interplanetary space is carried by the solar wind. Its energy density is roughly equal to the thermal energy density of solar wind particles and is much larger than that of cosmic-rays. In contrast to the situation in interstellar space, the effect of the cosmic-rays on the magnetic field is negligible, and the particles may be assumed to propagate in a given although complicated 'external' field (Kaiser, 1973).

Another characteristic feature of the interplanetary magnetic

field is the fact that departures from the average field are either static structures frozen into the solar wind originating in the turbulent solar plasma, or Alfven waves, whose speed relative to the wind is much smaller than that of the wind itself. Hence in a frame of reference moving with the solar wind, the magnetic field may be regarded as essentially time-independent.

The investigation of the behaviour of charged particles in the interplanetary magnetic field, and the conditions under which the particle propagation is diffusive has been studied extensively by a large number of authors (e.g., Roelof, 1966, 1968; Jokipii, 1966, 1967, 1968a, 1968b, 1971, 1972, 1974; Hall and Sturrock, 1967; Hasselman and Wibberenz, 1968, 1970; Jones *et.al.*, 1973a, 1973b; Kaiser, 1973; Kaiser *et.al.*, 1973; Jokipii and Lerche, 1973; Volk, 1973; Volk *et.al.*, 1974; Klimas and Sandri, 1971, 1972, 1973; Fisk *et.al.*, 1974; Dolginov and Toptygin 1967, 1968; Urch 1974; Lerche, 1974; Webb and Quenby, 1973b; Earl, 1973, 1974a, b; Forman *et.al.*, 1974; Owens, 1974a, 1974b; Noerdlinger, 1968; Jokipii and Parker, 1968b, 1969; Zakharchenko, 1971, 1973; Dorman and Kats, 1971). The usual procedure in these studies is to consider the propagation of the cosmic-rays in a frame of reference in which the average interplanetary magnetic field is stationary. The momentum space diffusion coefficients are then related to the statistical properties of the magnetic fluctuations.

For much of phase space of any given cosmic-ray, quasilinear theory would seem correct. In this theory the particle orbit in the first approximation is a helix about the average magnetic field which is assumed to be spatially uniform. It is a 'boot strap' procedure in which the Lorentz force on a particle due to the fluctuating

magnetic field is evaluated according to $q\,\underline{v}_o(\tau) \times \delta B(\underline{r}_o(\tau))$, where $(\underline{r}_o(\tau), \underline{v}_o(\tau))$ is the particle trajectory neglecting the effects of the fluctuations. When the interaction is weak, that is, the cosmic-ray moves out of a region of statistically correlated $\underline{\delta B}$ before the fluctuating field largely affects its orbit, the particle trajectory does not differ significantly from $\underline{r}_o(\tau)$, $\underline{v}_o(\tau)$ and the approximation is a valid one. However, there are regions of phase space for this problem, such as 90° pitch angle with respect to the average background magnetic field, where the duration of an interaction is arbitrarily long, and the theory is therefore generally thought to be invalid. It is for these regions of phase space that non linear theories have been proposed (e.g., Kaiser, 1973; Kaiser *et.al.*, 1974; Jones *et.al.*, 1973a, 1973b; Volk, 1973; Volk *et.al.*,1974).

After the momentum-space diffusion coefficients have been derived the spatial diffusion coefficients parallel and perpendicular to the average magnetic field, $K_{||}$ and $K_{\perp}$, can be obtained by 'coarse graining' the momentum space description over directions of momentum $\underline{p}$. However there is a further anti-symmetric component of the diffusion tensor, K_T, which cannot be obtained by this procedure and it is necessary to adopt another technique. Physically the term K_T provides the current density known as the perpendicular gradient drift.

A technique to obtain the complete diffusion tensor using the quasilinear theory has been developed by Forman *et. al.* (1974) and they show that in the weak scattering limit the diffusion tensor

$$\underline{\underline{K}} = \begin{bmatrix} K_{||} & 0 & 0 \\ 0 & K_{\perp} & K_T \\ 0 & -K_T & K_{\perp} \end{bmatrix} \qquad (1.3.12)$$

when written in components parallel and perpendicular to the magnetic

field. In this model the diffusion coefficients $K_{||}$, $K_{\perp}$ and K_{T} can be expressed in terms of collision times $\tau_{||}$ and $\tau_{\perp}$ parallel and perpendicular to the mean magnetic field, and if the scattering is weak, i.e., $\omega \tau_{||} >> 1$, $\omega \tau_{\perp} >> 1$,

then

$$K_{||} = \frac{v^2 \tau_{||}}{3}, \quad K_{\perp} = \frac{v^2}{3 \omega^2 \tau_{\perp}}, \quad K_{T} = \frac{v^2}{3\omega^2} = \frac{v r_g}{3} \qquad (1.3.13)$$

where $\omega = qB/m$ is the gyro-frequency, r_g is the gyro-radius and v is the particle speed.

The collision frequencies $1/\tau_{||}$ and $1/\tau_{\perp}$ in this model are related to the power spectrum tensor of the magnetic field irregularities. The collision frequency $1/\tau_{||}$ is determined by components of the power-spectrum tensor at the resonant wave number $k = 1/(r_g \cos \Theta)$ where Θ is the particle pitch angle relative to the average magnetic field. The collision frequency $1/\tau_{\perp}$ contains a resonant scattering term plus a term which represents the power in the magnetic field at zero wave number, i.e., k = 0. The power in the magnetic field at zero wave number is usually associated with random walk of the mean magnetic field (Jokipii and Parker, 1969).

In typical interplanetary conditions, the condition $\omega \tau_{\perp} >> 1$, requires the particle rigidity $\gtrsim$ 800 MV, or proton kinetic energy $\gtrsim$ 320 MeV, and at these rigidities, $K_{\perp}/K_{||} \lesssim 0.08$. At present there is no adequate theory available for $K_{\perp}$ and K_{T} below the weak perpendicular scattering limit (Forman *et.al.*, 1974; Forman and Gleeson, 1975). It should be noted that the weak scattering condition $\omega \tau_{||} >> 1$ for the validity of the derivation of $K_{||}$ is fulfilled

at all energies under typical interplanetary conditions.

We note that the form of the diffusion tensor (1.3.12) had been obtained in the less general analysis of Parker (1965), Jokipii and Parker (1969b), Dolginov and Toptygin (1967, 1968) and Gleeson (1969). In particular in the small angle scattering models of Dolginov and Toptygin (1967, 1968) and the isotropic scattering model of Gleeson (1969) with average collision time τ, the diffusion coefficients are

$$\begin{aligned} K_{||} &= v^2 \tau / 3, \\ K_{\perp} &= K_{||} / (1 + \omega^2 \tau^2), \\ K_{T} &= \omega \tau K_{\perp} = \frac{v r_g}{3} \left(\frac{\omega^2 \tau^2}{1+\omega^2 \tau^2} \right) . \end{aligned} \tag{1.3.14}$$

In the weak scattering limit, $\omega \tau >> 1$, and the diffusion coefficient K_T is identical to the result (1.3.13) obtained by Forman *et. al.* (1974).

The above completes our resume of the development of the transport equations for cosmic-rays in the interplanetary medium and the relation of the diffusion tensor to the properties of the interplanetary magnetic field.

The most extensive and complete studies of the eleven-year solar-cycle modulation of cosmic-ray intensity (see Section 2) have been carried out by means of spherically-symmetric, steady-state solutions of the equation of transport (1.3.9). In these models the solar wind is assumed to be radial, and the diffusion tensor is replaced by an effective radial diffusion coefficient.

$$K_{rr} = K_{||} \cos^2 \psi + K_{\perp} \sin^2 \psi, \tag{1.3.15}$$

where ψ is the angle between the outward spiral magnetic field and the radial direction.

In this thesis we elucidate the basic physical processes governing the steady-state propagation of cosmic-rays in interplanetary space for spherically symmetric models by using analytic solutions of the equation of transport. We remark that at present, there is no systematic study of non-spherically symmetric models for steady-state propagation incorporating the effects of the complete diffusion tensor (1.3.12).

In the next section we outline the models and solutions of the equation of transport that have been developed to describe the propagation of cosmic-rays in the interplanetary medium.

1.4 Solutions of the transport equation

Since Parker (1965) first obtained the equation of transport (1.3.9) considerable effort has been expended in obtaining solutions of the equation, with the intention of illustrating and elucidating the physical implications of the observed cosmic-ray intensity variations and anisotropies.

There are two basic types of cosmic-ray phenomena usually described by the transport equations, namely, the solar-flare events and the quasi-steady solar-cycle modulation. Solar-flare events are described by the full time dependent equation of transport after the initial flare. The typical time scale for diffusive and convective effects are of the order of seconds whereas the time scale associated with the eleven-year modulation is of the order of 10^8 seconds. Thus the eleven-year solar-cycle modulation is adequately described by quasi-steady-state solutions of the transport equation (1.3.9).

Time-dependent solutions of the equation of transport (some

analytic, some numerical) have been obtained by Fisk and Axford (1968), Englade (1971a), Forman (1971a, b), Lupton and Stone (1971, 1973), Webb and Quenby (1973a), Ng (1972), Ng and Gleeson (1971a, 1971b, 1975). Probably the most complete model at present for the propagation of solar-flare particles is that of Ng and Gleeson (1975) Excellent and extensive reviews of this earlier time-dependent work have been given by Axford (1970a, 1970b) and Wibberenz (1971).

Insight into the quasi-steady-state solar-cycle modulation of galactic and solar cosmic-rays has come from solutions of the transport equation (1.3.9), which includes the effects of convection, diffusion and particle energy changes. Observational evidence for the *necessity* to include the effects of energy changes in the equation of transport when discussing the quasi-steady modulation of the cosmic-ray intensity has been provided by Webber (1969) and Lezniak and Webber (1971), from an examination of a modulation parameter relevant to cosmic-ray fluxes at times t_1 and t_2. They found that at kinetic energies below 100 MeV/nucleon this modulation parameter plotted as a function of rigidity P splits into a separate curve for each species. This splitting is contrary to the predictions of convection-diffusion theory without energy changes; but it is present in solutions of the steady-state equation of transport including the effects of energy changes.

In the following paragraphs we discuss various steady-state solutions of the equation of transport which have been obtained and used to describe the eleven-year modulation of galactic cosmic-rays.

1.4.1 Steady-state, spherically-symmetric analytic solutions

The complete steady-state equation of transport (1.3.9) cannot in general be solved analytically. Most solutions have been obtained

for spherically-symmetric models.

Prior to the work of this thesis, Parker (1965, 1966), Dolginov and Toptygin (1967) and Fisk and Axford (1969) obtained analytic, spherically-symmetric solutions for idealised interplanetary conditions: the solar wind velocity $\underline{V}$ was assumed to be radial and constant, and the effective radial diffusion coefficient K_{rr} has restricted functional dependence on heliocentric radius r and momentum p.

Parker considered the case K_{rr} = constant, and steady release of monoenergetic particles from a free escape boundary at radius r = R (the solar cavity boundary). He obtained and evaluated a series for the differential number density U_p near r = 0. The results showed (for the first time) the effect of energy changes on the propagation of cosmic-rays in the solar cavity. Further solutions of this type for $K_{rr} = K_o(p)r^b$, where $K_o(p)$ is an arbitrary function of momentum p are presented in this thesis (Section 1.5).

The solutions of Dolginov and Toptygin (1967) and Fisk and Axford (1969) show the redistribution of galactic cosmic-rays within the solar cavity for a galactic spectrum which is a power law in momentum p or kinetic energy T. Such galactic spectra are quite realistic at kinetic energies above 1 GeV/nuc for nuclei (Figure 1.2) and for T > 1 GeV for electrons. (Figure 1.3). In the solution of Dolginov and Toptygin, the differential number density U_p is a cut-off power law spectrum at the boundary of the solar cavity, i.e.,

$$U_p(R,p) = \begin{cases} A\,p^{-\mu}, & p > p_s, \quad (A \text{ constant}) \\ 0, & 0 < p < p_s, \end{cases}$$

and the radial diffusion coefficient K_{rr} = constant, within the

modulation region $0 < r < R$. The solutions of Fisk and Axford (1969) were obtained for a more realistic diffusion coefficient of the form $K_{rr} = K_c\, p^a\, r^b$, where K_c, a and b are constants with $b > 1$ and $K_c > 0$. These latter solutions were obtained for the case where the boundary of the solar cavity was taken to be at infinity, and the differential number density U_p satisfied the boundary conditions:

(i) $U_p \rightarrow A\, p^{-\mu}$ as $r \rightarrow \infty$, and

(ii) U_p is finite as $r \rightarrow 0$.

The above analytic solutions were quite useful for illustrating the redistribution of particles in momentum with heliocentric radius, and the effects of varying the diffusion coefficient K_{rr} and the solar wind speed V in modulation models. A more detailed study of the modulation process has subsequently been carried out by means of approximate analytic solutions and numerical solutions, as discussed in the following subsections.

1.4.2 Spherically-symmetric numerical solutions.

Methods for obtaining spherically-symmetric numerical solutions were initially developed by Fisk (1969) and by Urch (1971), and solutions obtained numerically on computers have been used by, for example, Gleeson and Urch (1971), Lezniak and Webber (1971), Goldstein *et.al.* (1970b) and Urch and Gleeson (1972a, 1972b). Most of the important physical phenomena have been discovered by means of these numerical solutions.

The numerical solutions are carried out by specifying the galactic differential number density U_T (R,T) at a certain radial distance $r = R$, representing the boundary of the solar cavity. We note here that only the galactic electron spectrum is known in these

models, and this has been deduced from the galactic non-thermal radio background radiation.(Goldstein *et.al.* 1970b; Burger 1971). Boundary conditions on the number density U_T or the differential streaming S_T are specified at a boundary near the sun, and the solar-wind speed, V(r), is usually assumed to be radial and essentially constant except near the sun where it decreases rapidly to zero at one solar radius.

Diffusion coefficients are then determined which give the best match between calculated intensities and those observed at Earth at a specific time. The procedure adopted at present is as follows: From electron spectra observed near-Earth and the galactic electron spectrum inferred from the non-thermal radio noise from the galaxy, trials are made to determine a diffusion coefficient (particularly its energy dependence) at each specific time.

In order to check the modulation model, spectral forms for the galactic proton and helium nuclei are chosen which lead to a match with the near-Earth spectra during a particular epoch (note that there is no direct information about the galactic proton and helium nuclei spectra). The near-Earth proton and helium spectra are then predicted for different epochs by using these galactic spectra, and the diffusion coefficients deduced from the electron observations. Once the diffusion coefficient K_{rr} and the galactic spectra $U_T(R,T)$ are known the modulation is determined. So too are other physical quantities of interest.

1.4.3 Three dimensional solutions

At the Denver International Conference on Cosmic-Rays (1973), there was an increased acceptance for the need for three-dimensional

models of the modulation (Quenby, 1973). Early indications of the probable need for these models was recognized by Parker (1964), Krimsky (1964), who considered the effects of a non-spherical solar cavity with a boundary closer to the sun at high heliocentric latitudes. Subramanian and Sarabhai (1967), suggested that the second harmonic of the diurnal variation was due to rising off-ecliptic gradients due to a latitude dependence in solar activity. However, Lietti and Quenby (1968), were able to account for the variation with no heliolatitude dependence of the modulation parameters. Owens and Jokipii (1971) obtained an approximate analytic solution of the transport equation, depending on radial distance r, heliolatitude θ, and the kinetic energy T, for a radial magnetic field, finite $K_{\perp}$ and with a latitude dependence of $K_{||}$ and V, and used it to investigate the particle flow (i.e., the anisotropy). Belov and Dorman (1969, 1971) have also obtained analytic non spherically-symmetric solutions of the equation of transport, which describe the modulation of cosmic-rays in a region of space enclosed by a cone centred on the sun. In these models, the diffusion coefficients inside and outside the cone are different, and they simulate the effects of the asymmetry in solar activity.

Some numerical solutions of the transport equation for three dimensional models have been explored (Dorman and Milovinova, 1973; Dorman and Kobylinksi, 1973; Fisk, 1973). At the just concluded Munich International Conference (1975) only four papers on three-dimensional models were delivered (Moraal and Gleeson, 1975; Cecchini and Quenby, 1975; Fisk, 1975; Dorman and Milovinova, 1975). As yet no systematic study of the properties of such models has been carried out. When available such studies should result in a more comprehensive picture of cosmic-ray propagation in the solar cavity.

1.4.4 Approximate analytic solutions

Computer based numerical solutions are time consuming to obtain, costly and do not readily show the dependence of the solution on the parameters. Approximate analytic solutions provide in a ready form, the modulation, its dependence on the parameters of the problem and associated quantities such as the gradient with sufficient accuracy for the purposes at hand.

The simplest approximation is to use the convection-diffusion solution of Parker (1958b) (Equation (1.3.2)), i.e., to include convection and diffusion processes but exclude energy changes. This provides a simple and powerful means of rough analysis.

Gleeson and Axford (1968b, 1968c) have obtained two useful approximate steady-state solutions of the spherically-symmetric equation of transport which are valid when the modulation parameter $Vr/K(r,p)$ [$K(r,p)$ is the effective radial diffusion coefficient] is sufficiently small, i.e. $Vr/K(r,p) << 1$. In these solutions the spectrum is specified at the boundary of the solar cavity at $r = R$ by $U_T(R,T)$.

The first solution (Gleeson and Axford, 1968b), is obtained by solving the equation of transport by an iterative technique. The solution to $O(Vr/K)$ is

$$U_T(r,T) = U_T(R,T) \left[1 - \frac{2+\alpha\gamma}{3} \int_r^R \frac{V(x)}{K(x,T)} \, dx + O\left(\frac{Vr}{K}\right)^2 \right],$$

where

$$\gamma = - \partial \ell n[j_T(R,T)]/\partial T,$$

$$\alpha = (T + 2E_o)/(T + E_o),$$

and $j_T(R,T) = v\, U_T(R,T)/4\pi$ is the differential intensity spectrum on the boundary. From this last result we see that for realistic

power law spectra on the boundary ($\gamma \sim 2.6$), that the cosmic-ray intensity is reduced below its interstellar value due to solar modulation. A further feature of this approximate solution is that the differential current density

$$S_T = C V U_T - K \partial U_T / \partial r,$$

(Equation (1.3.10) is zero to O(Vr/K).

This latter observation that the differential current density is zero to O(Vr/K when $Vr/K << 1$ led to the development of another approximate analytic solution known as the force-field solution (Gleeson and Axford, 1968c). It is obtained by setting the radial differential current density

$$S_p = - 4 \pi p^2 \left(K \frac{\partial F_o}{\partial r} + \frac{Vp}{3} \frac{\partial F_o}{\partial p} \right),$$

(Equation (1.3.10) equal to zero, so that

$$v \frac{\partial F_o}{\partial r} + \frac{V p v}{3K} \frac{\partial F_o}{\partial p} = 0.$$

This latter equation is known as the force-field equation, and it has the form of a one-dimensional steady-state ($\frac{\partial F_o}{\partial t} = 0$) Liouville equation, with the quantity Vpv/(3K) having the dimensions of force. We note that Freir and Waddington (1965) observed that the modulation could be reproduced by assuming galactic particles lost energy in a force-field.

The force-field equation has the solution

$$F_o(r,p) = F_o (R, p^*),$$

where $p^*(r,p,R)$ is obtained by integrating the characteristic equation

$$\frac{dp}{dr} = \frac{pV}{3K},$$

from the point (r,p) to the point (R, p*) where the characteristic curve cuts the boundary at r = R (Urch and Gleeson, 1973).

The force-field solution only holds for a sufficiently smooth galactic spectrum, and at sufficiently small Vr/K(r,p). Urch and Gleeson (1972a) have argued that under typical interplanetary conditions, the force-field approximation is probably valid down to kinetic energies of 150 MeV/nucleon. We remark that the force-field solution has proved to be a powerful tool when used in conjunction with numerical solutions in investigations of the modulation process.

1.5 The fundamental role of monoenergetic solutions

The solutions which are investigated in detail in this thesis are the monoenergetic-source and monoenergetic-spectrum solutions of the steady-state equation of transport. By a monoenergetic-source solution we mean that monoenergetic cosmic-rays are injected at a steady rate into the interplanetary medium from some fixed heliocentric position, whereas in a monoenergetic-spectrum solution, the differential number density, U_p, is specified to be a monoenergetic spectrum on some boundary. Note that the monoenergetic-spectrum solution is quite distinct from the monoenergetic-source solution in that there are no sources within the region of position-momentum space for which the solution is valid.

These solutions do not necessarily attempt to fit any given observation, but they give very useful insight into the physics involved in the modulation process. Solutions in which the boundary spectra or sources are not monoenergetic do not display the physics so clearly since the resultant redistribution of particles in momentum

and position is the combined result of the transport processes and the boundary and source conditions.

The most basic solution is that in which monoenergetic particles are released at a steady rate from a fixed heliocentric radius and the resulting distribution in energy or momentum is determined as a function of position within the solar cavity. Except for a limited case noted below, such analytic solutions were first obtained independently by Toptygin (1973) and the present author.

The exception noted above is a solution obtained by Parker (1965, 1966). He took the case of constant radial diffusion coefficient, i.e., K = constant, a constant radial solar wind velocity, $\underline{V}$, and steady release of monoenergetic particles from a free escape boundary at radius r = R (i.e., a monoenergetic-spectrum solution). Numerical solutions have also been obtained for the distribution within the solar cavity with a boundary at r = R and the differential number density there specified to be a narrow Gaussian distribution in kinetic energy with half width ~ 10% of the mean kinetic energy (Goldstein *et. al.* 1970b; Urch, 1971; Gleeson and Urch, 1971). This Gaussian distribution represents a monoenergetic galactic spectrum. This numerical work probably shows the redistribution of particles well, but it is an approximation and restricted in that,

(i) the spectrum at r = R is near monoenergetic,

(ii) extension of the calculations to very low energies has not been carried out because of accuracy considerations, and

(iii) it is not feasible to examine a wide range of parameters.

These deficiencies are not present in the analytical solutions studied in this thesis.

We consider in detail models in which the effective radial diffusion coefficient $K = K_o(p)\ r^b$, where $K_o(p)$ is an arbitrary function of momentum p, and the solar wind velocity $\underline{V}$ is assumed to be radial and constant. We set out below the solutions which we use most intensively in Chapters 8 and 9 to study the modulation.

With the above model, the spherically-symmetric monoenergetic source solution in which:

(i) particles of momentum p_o are released at a steady rate of N per unit time from a spherical surface at radius r_o;

(ii) the momentum average distribution function $F_o(r,p) \to 0$ as $r \to \infty$;

(iii) F_o is finite as $r \to 0$;

for the case $b \neq 1$, and given in terms of F_o is:

$$F_o = \frac{3\ N}{64\ \pi^2\ V\ p_o^3\ r_o^2\ |n+1|} \left(\frac{x_o}{x}\right)^n \frac{x_o^2}{T}\ \exp\left(-\frac{x^2+x_o^2}{4T}\right) I_m\left(\frac{x\ x_o}{2T}\right). \tag{1.5.1}$$

Here $I_m(z)$ is a modified Bessel function of the first kind,

$$\begin{aligned} x &= 2(r\ p^{3/2})^{(1-b)/2} / (1-b), \\ n &= (b+1)/(1-b), \quad m = |n|, \\ T &= 3 \int_p^{p_o} K_o(z)\ z^{(1-3b)/2} dz/(2V), \end{aligned} \tag{1.5.2}$$

and $x_o = x(r_o, p_o)$. The above solution is degenerate in the case $b = 1$ and in this case

$$F_o = \frac{3\ N}{64\ \pi^{5/2} V\ p_o^3\ r_o^2} \frac{1}{\sqrt{T}}\ \exp\left[x-x_o-T-\frac{(x-x_o)^2}{4T}\right], \tag{1.5.3}$$

with $x = -\ \ell n(2r^2p^3)/2$ is the appropriate solution. The solutions (1.5.1) and (1.5.3) are derived in Chapters 3 and 4 and the solution (1.5.1) is used in Chapter 9 to study the propagation of monoenergetic

solar cosmic-rays.

The above monoenergetic-source solutions can be used to derive a monoenergetic-spectrum solution for galactic cosmic-rays (Chapter 6) in which:

(i) $U_p \rightarrow N_g\, \delta(p-p_o)$ as $r \rightarrow \infty$;

(ii) U_p is finite as $r \rightarrow 0$;

(iii) the diffusion coefficient $K = K_o(p)\, r^b$, where $K_o(p)$ is an arbitrary function of momentum p and $b > 1$.

In terms of F_o it is given by

$$F_o = \frac{3\, N_g\, K_o(p_o)\, p_o^{-3(1+b)/2}}{8\, \pi\, V\, \Gamma(m)}\, \frac{1}{T} \left(\frac{x^2}{4T}\right)^m \exp\left(\frac{-x^2}{4T}\right), \tag{1.5.4}$$

a fairly simple expression, the r dependence of the solution being in x and the p dependence in both x and T. Here $\Gamma(m)$ denotes the gamma function of argument m.

As an example of the usefulness of these solutions we display below some of the principal features of the monoenergetic-galactic-spectrum solution (1.5.4), which we have reproduced from Chapter 8. We consider the case $K = K_c\, p\, r^b$, with K_c constant and $b > 1$, in which case $(p_o^3/N_g)\, F_o$ is a function of the dimensionless variables p/p_o and $Vr/K(r,p_o)$.

Figure 1.4 shows $(p_o^3/N_g)\, F_o$ vs p/p_o for $b = 1.5$ and values 0.01, 0.1 and 1.0 of the parameter $Vr/K(r,p_o)$.

Since the solution depends on p/p_o and $Vr/K(r,p_o)$ the curves for different $Vr/K(r,p_o)$ show:

(i) the redistribution of monoenergetic galactic cosmic-rays in momentum at various heliocentric radii;

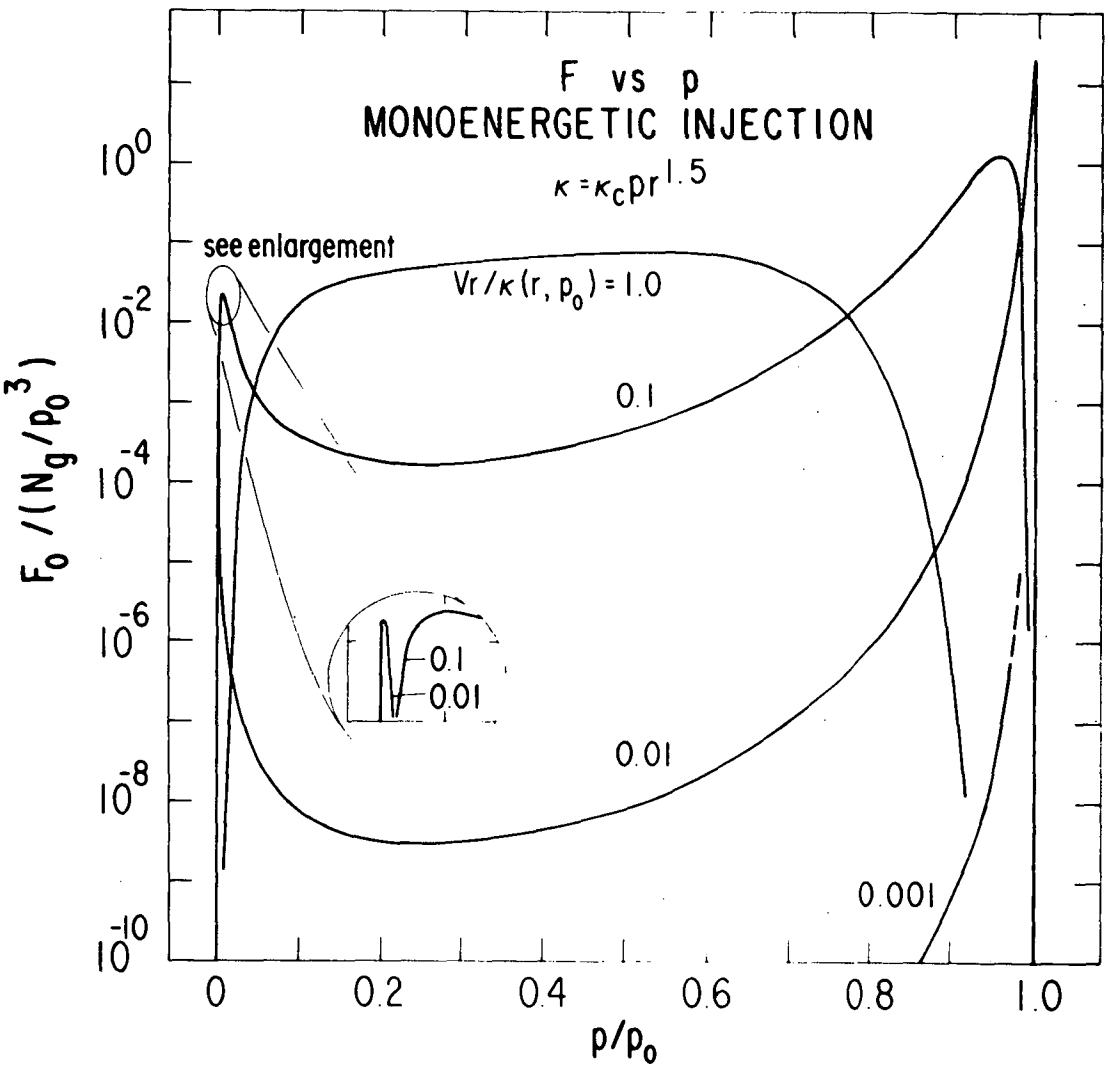

FIGURE 1.4 - The momentum spectrum of the distribution function $F_o(r,p)$ for a monoenergetic galactic spectrum at infinity, i.e., $U_p \to N_g \delta(p-p_o)$ as $r \to \infty$. The figure is drawn for a diffusion coefficient $K(r,p) = K_c\ p\ r^{1.5}$, and values 0.01, 0.1 and 1.0 of the parameter $Vr/K(r,p_o)$. It has been reproduced from Figure 8.1 in Chapter 8.

(ii) the effect of varying interplanetary conditions through the parameters V and K_c on the distribution at fixed r;

(iii) the effect of varying the source momentum p_o for fixed V, K_c and r. Thus the solution shows the basic features the propagation of monoenergetic galactic cosmic-rays in the solar cavity for a wide range of parameters; the features could of course be obtained with numerical solutions, but it would be much more difficult to display the features for such a wide range of parameters.

The monoenergetic-galactic-spectrum solution (1.5.4) can also be used to study the modulation of galactic cosmic-rays from a general galactic spectrum. For cases where the galactic spectrum is specified at infinity to be $F_o(\infty, p_o)$, the distribution at (r,p) is

$$F_o(r,p) = \int_p^\infty F_o(\infty, p_o)\, G(r,p;p_o)\, dp_o. \qquad (1.5.5)$$

Here the Green's function $G(r,p;p_o)$ is the solution of the equation of transport for $F_o(r,p)$ for a monoenergetic spectrum at infinity, i.e., $G(r,p;p_o) \to \delta(p-p_o)$ as $r \to \infty$.

From the monoenergetic-galactic-spectrum solution (1.5.4) the Green's function is given by

$$G(r,p;p_o) = \frac{3\, K_o(p_o)\, p_o^{(1-3b)/2}}{2\, V\, \Gamma(m)} \frac{1}{T}\left(\frac{x^2}{4T}\right)^m \exp\left(-\frac{x^2}{4T}\right). \qquad (1.5.6)$$

The Green's function is of fundamental importance in modulation studies since it contains the modulation properties of the interplanetary region independent of the galactic spectrum (Chapter 8).

Further examples of the usefulness of these solutions are given in Chapters 8 and 9. We remark that in regard to the steady-state propagation of monoenergetic solar cosmic-rays, that previous studies have been carried out by Urch and Gleeson (1971) by means of numerical

solutions and by Toptygin (1973) who used an analytic solution. These studies however are less extensive than the present study, and they do not display fully the physical processes.

The above completes our discussion of the role of monoenergetic solutions in modulation studies and in the next section we indicate in more detail the subject matter of this thesis.

1.6 Outline of the present thesis

As noted in the Summary, this thesis is a theoretical study of the steady-state propagation of galactic and solar cosmic-rays in the interplanetary medium. The thesis can be roughly divided into three sections:

(i) The derivation of analytic monoenergetic-source and monoenergetic-spectrum solutions of the steady-state equation of transport and the relation of these solutions to previously obtained analytic solutions (Chapters 2-6).

(ii) A clarification of the energy changes experienced by cosmic-rays in the interplanetary medium (Chapter 7).

(iii) In Chapters 8, 9 and 10 we use the solutions developed in Chapters 2-6 to verify the principal known features of steady-state cosmic-ray propagation in the solar cavity as well as elucidating various features of the transport processes which have hitherto not been displayed.

Examples of new results obtained from this study are:
(a) the particle flow and momentum changes in position-momentum space of monoenergetic galactic and solar cosmic-rays by using the

results developed in Chapter 7.

(b) the modulation properties of the interplanetary region independent of the galactic spectrum are displayed by use of the Green's function $G(r,p;p_o)$ occurring in the general galactic spectrum solution (1.5.5).

We now discuss briefly the contents of each chapter, and their relation to previous work.

In Chapter 2 we initially investigate the conditions under which the steady-state equation of transport is separable. The motivation for this study was an attempt to generalise the result obtained by Jokipii (1967) and used by Fisk and Axford (1969), that the steady-state equation was separable for a diffusion coefficient

$$K(r,p) = K_c\, p^a\, r^b,$$

where K_c, and b are constants and the solar wind velocity $\underline{V}$ is assumed to be radial and constant. We find that the equation is separable for a model with a radial magnetic field, a diffusion tensor (1.3.12) specified by

$$\begin{aligned} K_{||} &= K_o(p)\, r^b, \quad K_\perp/K_{||} = \text{constant}, \\ \frac{\partial K_T}{\partial \Theta} &= \frac{\partial K_T}{\partial \phi} = 0, \end{aligned} \tag{1.6.1}$$

where $K_o(p)$ is an arbitrary function of momentum p and the solar wind velocity $\underline{V}$ is radial and constant. Here (r,Θ,ϕ) are spherical polar co-ordinates centred on the sun, with the polar axis along the sun's rotation axis. We note again that the effects of anisotropic diffusion can be incorporated in spherically symmetric models by defining an effective radial diffusion coefficient as in Equation (1.3.15).

Having separated the steady-state equation of transport with a

constant radial solar wind velocity $\underline{V}$, and the diffusion tensor (1.6.1), we proceed to study the symmetries or group properties of the separated equation. We then use these properties to derive analytic, similarity solutions of the separated equation.

In Chapter 3 we use the similarity solutions and the group properties of the equation of transport given in Chapter 2, to obtain monoenergetic-source solutions. In these latter solutions, particles of momentum p_o, say, are released at a steady rate from a spherical surface or a point at radius r_o located within the solar cavity. We note that the spherically-symmetric monoenergetic-source solutions have been derived independently by Toptygin (1973).

In Chapter 4, the monoenergetic-source solutions of Chapter 3, and the monoenergetic-galactic-spectrum solution (1.5.4) in which we specify a monoenergetic spectrum at infinity, i.e., $U_p \to N_g\, \delta(p-p_o)$ as $r \to \infty$, and U_p is finite as $r \to 0$, are obtained by using a Laplace transform technique. We remark that the solutions of Chapter 3 are rederived in Chapter 4 by the Laplace transform technique, because it is more widely known and more easily understood than the group method.

In Chapter 5 we use the similarity solutions of Chapter 2 to derive spherically symmetric Green's functions, with the intention of obtaining solutions in which we can specify the spectrum on two boundaries at heliocentric radii $r = r_a$ and $r = r_b$. The Green's function is the solution for a monoenergetic source of momentum p_o at radius r_o and in general with the mean distribution function with respect to momentum, F_o, equal to zero at the boundaries $r = r_a$ and $r = r_b$.

In Chapter 6 we obtain analytic solutions in which we specify

the spectrum at boundary radii $r = r_a$ and $r = r_b$. We also obtain the galactic spectrum solution (1.5.5) in which a general spectrum is specified as $r \to \infty$, and we use this latter solution to obtain the solutions of Fisk and Axford (1969). These solutions are obtained by establishing an appropriate Green's theorem and using the Green's functions of Chapter 5. We remark that the Green's theorem technique used to obtain these solutions is similar to solving the one dimensional heat flow equation by Green's theorem.

In Chapter 7 we consider the momentum or energy changes of cosmic-rays in the interplanetary medium. It was noted by Gleeson (1972) and Quenby (1973) that the mean-time-rate-of-change of momentum $\langle \dot{p} \rangle$ for cosmic-rays in interplanetary space reckoned for a fixed volume in a reference frame fixed in the solar system is

$$\langle \dot{p} \rangle = \frac{p \underline{V}}{3U_p} \cdot \frac{\partial U_p}{\partial \underline{r}} = \frac{p \underline{V} \cdot \underline{G}}{3} , \qquad (1.6.2)$$

where $\underline{G} = (\partial U_p / \partial r)/U_p$, is the cosmic-ray density gradient. The result (1.6.2) for $\langle \dot{p} \rangle$ is implicit in the discussion of energy changes by Jokipii and Parker (1967). However these latter authors did not show explicitly the role of $\langle \dot{p} \rangle$ in the cosmic-ray continuity equation, and their discussion of energy changes is limited to the case of convective transport, or strong scattering.

The result (1.6.2) is proved in three ways:

(i) by a rearrangement and reinterpretation of the equation of transport or continuity equation (1.3.9);

(ii) from a consideration of particle momentum changes arising from the scattering analysis derivation of the equations of transport by Gleeson and Axford;

(iii) by a special model in which the cosmic-rays are trapped in

'magnetic boxes' moving with the solar wind. In this model the particles change momentum as they collide with the rigid walls of the box.

The third method is for a convective strong scattering model. It is particularly instructive in showing the relation between the expression (1.6.2) for $\langle \dot{p} \rangle$ and the adiabatic deceleration formula

$$\langle \dot{p} \rangle_{ad} = -\frac{p}{3} \underline{\nabla} \cdot \underline{V}, \qquad (1.6.3)$$

which is the mean rate at which particles of momentum p, change momentum in an individual 'magnetic box'. This model shows that the concept of adiabatic deceleration, as applied to cosmic-ray propagation in interplanetary space is only valid for convective transport.

In Chapter 7 we also discuss briefly the mean-time-rate-of-change of momentum $\langle \dot{p}' \rangle$ of particles with momentum p' specified relative to the solar wind frame of reference, and with position $\underline{r}$ specified in the fixed frame of reference. The physical significance of the momentum rate $\langle \dot{p}' \rangle$ has not been understood previously, and it is derived in Appendix G, from the transformation of momentum between the fixed and solar wind frames of reference. It is shown that Parker (1965) and Jokipii and Parker (1970) have misinterpreted the energy change term in the cosmic-ray continuity equation associated with $\langle \dot{p}' \rangle$, due to an insufficient distinction between the two momentum rates $\langle \dot{p} \rangle_{ad}$ and $\langle \dot{p}' \rangle$.

Having established the result (1.6.2) for $\langle \dot{p} \rangle$ we then show that the rate at which the cosmic-rays gain energy per unit volume and over the whole momentum spectrum from the solar wind is

$$\frac{dW}{dt} = V \frac{d\, P_c(r)}{dr}, \qquad (1.6.4)$$

where $P_c(r)$ is the cosmic-ray pressure at radius r. This result was initially obtained by Jokipii and Parker (1967).

The cosmic-ray particle flow and momentum changes are related to each other via the continuity or transport equation (1.3.9). In order to elucidate this relation we introduce the concept of a flow line in position-momentum space. The flow line is defined as the curve whose tangent in position-momentum space is given by the ratio of the streaming velocity

$$\langle \dot{\underline{r}} \rangle = \underline{S}_p / U_p \ , \qquad (1.6.5)$$

to the momentum rate $\langle \dot{p} \rangle$ in the fixed frame of reference (Equation (1.6.2)), i.e.,

$$\frac{d\underline{r}}{dp} = \frac{\langle \dot{\underline{r}} \rangle}{\langle \dot{p} \rangle} \ . \qquad (1.6.6)$$

We construct flow lines for monoenergetic galactic and solar cosmic-rays in Chapters 8 and 9.

In Chapter 8 we study the steady-state propagation of monoenergetic galactic cosmic-rays by using the monoenergetic galactic spectrum solution (1.5.4) in which $U_p \to N_g \, \delta(p-p_o)$ as $r \to \infty$, and U_p is finite as $r \to 0$. From the solution we show the redistribution of particles with heliocentric distance, the gradients, the particle flow and the momentum changes of monoenergetic galactic cosmic-rays. We then consider the structure of the particle flow in position-momentum space for monoenergetic galactic cosmic-rays, and to elucidate the relation between particle flow and momentum changes we construct flow lines in (r,p) space.

The redistribution of particles from a complete galactic spectrum at $r = \infty$ is obtained from the general galactic spectrum

solution (1.5.5). We use it to obtain the near-Earth spectra, gradients and anisotropies for different types of galactic spectra, and it reproduces some of the results obtained with numerical solutions, such as the relative exclusion of low energy galactic particles. We also use the solution to determine the origin within the galactic spectrum of particles observed at Earth with given momentum, and we emphasize the role of the Green's function in determining the modulation characteristics of the interplanetary region for a specific model, independent of the galactic spectrum.

In Chapter 9 we study the steady-state interplanetary propagation of solar cosmic-rays by means of the monoenergetic-source solution (1.5.1) developed in Chapters 3 and 4. We also construct flow lines in (r,p) space for the solution, and when compared with the flow lines for monoenergetic galactic cosmic-rays presented in Chapter 8, they highlight the differences between the steady-state propagation of galactic and solar particles.

In Chapter 10 we study the redistribution within the solar cavity of monoenergetic galactic cosmic-rays in a model having a free escape boundary at $r = r_b$, which corresponds to the boundary of the solar cavity. This model differs from the previous study in Chapter 8 where we considered the propagation of monoenergetic galactic cosmic-rays released from a boundary at infinity. We use this model to show the effects of a finite boundary, and we compare it with the results obtained in Chapter 8.

Three papers have been published on the contents of Chapter 8 (Webb and Gleeson, 1973; Gleeson and Webb, 1974, 1975) and one paper on the propagation of monoenergetic solar cosmic-rays from Chapter 9

(Webb and Gleeson, 1974). It is anticipated that at least three more will be forthcoming. The first will be an extensive version of the work in Chapter 7 on the energy changes of cosmic-rays in the interplanetary medium, the second will deal with the particle flow and momentum changes of monoenergetic galactic and solar cosmic-rays from the work in Chapters 8 and 9, and the third will be concerned with the development of the monoenergetic-spectrum and monoenergetic-source solutions from Chapters 2-6.

CHAPTER 2

GROUP PROPERTIES OF THE STEADY-STATE COSMIC-RAY EQUATION OF TRANSPORT

2.1 Introduction

In this chapter we study the group properties of the steady-state cosmic-ray equation of transport (1.3.9). The interplanetary magnetic field is assumed to be radial and the diffusion coefficients parallel and perpendicular to the field, denoted by $K_{||}$ and $K_{\perp}$ are given by

$$K_{||} = K_o(p)\, r^b, \quad K_{\perp}/K_{||} = e, \tag{2.1.1}$$

where e is a constant, $K_o(p)$ is an arbitrary function of momentum p and the effect of the antisymmetric component of the diffusion tensor (1.3.12), K_T, is assumed to be negligible.

With a source of monoenergetic particles of momentum p_o released at the heliocentric position (r_o, θ_o, ϕ_o) the steady-state continuity equation (1.3.9) governing the differential number density with respect to momentum $U_p(r, \theta, \phi, p)$ is

$$\underline{\nabla} \cdot \left(\underline{V}\, U_p - \underline{\underline{K}} \cdot \underline{\nabla}\, U_p \right) - \frac{1}{3}\, \underline{\nabla} \cdot \underline{V}\, \frac{\partial}{\partial p}\left(p\, U_p \right)$$

$$= \frac{N}{r_o^2}\ \delta(r-r_o)\ \delta(\mu-\mu_o)\ \delta(\phi-\phi_o)\ \delta(p-p_o). \tag{2.1.2}$$

Here $\underline{\underline{K}}$ is the diffusion tensor, $\underline{V}$ the solar wind velocity, $\mu = \cos\theta$, $\delta(z)$ is the Dirac delta function of argument z, and N is the number of particles released per second per steradian from the source point.

The density U_p is related to the mean distribution function $F_o(r, \theta, \phi, p)$ by

$$U_p = 4 \pi p^2 F_o. \qquad (2.1.3)$$

Here F_o is the isotropic part of the distribution function in position momentum space.

In Section (2), we separate the continuity equation (2.1.2) for the case where the solar wind velocity $\underline{V}$ is constant and radial, and the diffusion coefficients $K_{||}$ and $K_{\perp}$ are given by Equation (2.1.1). The separation variables in this equation are x, t, μ and ϕ where *x is a function of r and p and t is a function of p.*

The separated form of Equation (2.1.2) obtained in Section (2) may be solved analytically by the techniques:

(i) solution by separation of the variables,

(ii) solution by Laplace transform technique,

(iii) solution by group methods.

The simplest method, including boundary conditions is the Laplace transform technique. It however requires boundary conditions on the curves x = constant, and since x is a function of radius r and momentum p, we cannot obtain solutions with boundaries r = constant, except in the special cases of $r \to \infty$. Thus these solutions although very useful are more limited than we would like. *They are given in Chapter (4).*

The solution by direct application of separation of variables in x and t leads to the same solution as the Laplace transform method , since the separation function in t is exp(-st) with s the separation constant and the resultant integral over s leads to the weighting

functions being identified as an inverse Laplace transform. Because of this the separated solution is not given in this chapter.

The group method is the most useful of the above and it is developed in the present chapter. It leads to a reduction in the independent variables from four to three and to a further partial differential equation in three independent variables. This latter partial differential equation has separable solutions, and for certain special types of diffusion coefficients one of the separation variables is a function of radius r only. For these special types of diffusion coefficients it is possible to specify boundary conditions (e.g., free escape) at boundaries $r = r_a$ and $r = r_b$. The solution of boundary value problems in which spectra are specified at radii $r = r_a$ and $r = r_b$ is developed in Chapters (5) and (6).

In Section (3) a method is given for finding solutions of a system of differential equations S, from a knowledge of the groups of continuous transformations that leave S invariant.

It is noted that the homogeneous, separated, steady-state transport equation obtained in Section (2) is a linear partial differential equation of second order in one dependent variable and four independent variables. Ovsjannikov (1962) has investigated the group properties of the general second order linear partial differential equation in one dependent variable and n independent variables. Since the homogeneous, separated, steady-state transport equation of Section (2) is a special case of Ovsjannikov's work, we use his results in Section (4) to find the group of continuous infinitesimal transformations that leave the separated transport equation invariant.

In Section (5) the finite equations of the group and its

invariants are used to construct group invariant or similarity solutions of the separated transport equation by the methods of Section (3).

2.2 The separable transport equation

For diffusion coefficients $K_{||}$ and $K_{\perp}$ specified by the expressions (2.1.1), neglecting effects due to the antisymmetric component of the diffusion tensor, K_T, and assuming a constant, radial solar wind velocity $\underline{V}$, the steady-state continuity equation (2.1.2) expressed in terms of the mean distribution function with respect to momentum p $F_o(r, \theta, \phi, p)$ is

$$K_o(p)\, r^{b+1} \frac{\partial^2 F_o}{\partial r^2} + ((2+b)\, K_o(p) r^b - Vr)\frac{\partial F_o}{\partial r} + \frac{2Vp}{3} \frac{\partial F_o}{\partial p}$$
$$+ e\, K_o(p) r^{b-1} \left[(1-\mu^2)\frac{\partial^2 F_o}{\partial \mu^2} - 2\mu \frac{\partial F_o}{\partial \mu} + \frac{1}{(1-\mu^2)} \frac{\partial^2 F_o}{\partial \phi^2} \right]$$
$$= - \frac{N\, \delta(r-r_o)\, \delta(\mu-\mu_o)\, \delta(\phi-\phi_o)\, \delta(p-p_o)}{4\pi\, r_o\, p_o^2} . \qquad (2.2.1)$$

Introducing variables $\xi = \xi(r,p)$ and $t = t(p)$, and using the notation $\xi_r = \partial\xi/\partial r$, $\xi_p = \partial\xi/\partial p$, Equation (2.2.1) may be written

$$K_o(p) r^{b+1} \xi_r^2 \frac{\partial^2 F_o}{\partial \xi^2} + \left[K_o(p) r^{b+1} (\xi_{rr} + \frac{2+b}{r} \xi_r) \right.$$
$$\left. + (\frac{2p}{3} \xi_p - r\, \xi_r)\, V \right] \frac{\partial F_o}{\partial \xi} + \frac{2Vp}{3} \frac{dt}{dp} \frac{\partial F_o}{\partial t}$$
$$+ e\, K_o(p) r^{b-1} \left[(1-\mu^2) \frac{\partial^2 F_o}{\partial \mu^2} - 2\mu \frac{\partial F_o}{\partial \mu} + \frac{1}{(1-\mu^2)} \frac{\partial^2 F_o}{\partial \phi^2} \right]$$
$$= - \frac{N |\partial\xi/\partial r \, . \, dt/dp|\, \delta(\xi-\xi_o)\, \delta(t-t_o)\, \delta(\mu-\mu_o)\, \delta(\phi-\phi_o)}{4\pi\, r_o\, p_o^2} . \qquad (2.2.2)$$

In passing from Equation (2.2.1) to (2.2.2) the transformation

$$\delta(r-r_o)\ \delta(\mu-\mu_o)\ \delta(\phi-\phi_o)\delta(p-p_o) = J\ \delta(\xi-\xi_o)\ \delta(\mu-\mu_o)\ \delta(\phi-\phi_o)\ \delta(t-t_o),$$

has been used, where the Jacobian

$$J = |\ \partial\ (\xi,t,\mu,\phi)/\partial(r,p,\mu,\phi)| = |\partial\xi/\partial r \cdot dt/dp|_{r=r_o,p=p_o};$$

$$\xi_o = \xi(r_o, p_o) \text{ and } t_o = t\ (p_o).$$

Equation (2.2.2) is separable if we choose the coefficient of $\partial F_o/\partial\xi$ to be zero, such that ξ satisfies simultaneously the partial differential equations

$$\begin{aligned} \xi_{rr} + \frac{2+b}{r}\ \xi_r &= 0, \\ \frac{2p}{3}\ \xi_p - r\ \xi_r &= 0, \end{aligned} \qquad (2.2.3)$$

The solution of Equations (2.2.3) is

$$\xi = c\ (rp^{3/2})^{-(b+1)},$$

where c is an arbitrary constant. Choosing

$$\begin{aligned} \xi &= (rp^{3/2})^{-(b+1)} / (b+1), \\ t &= -3 \int^p K_o(z)\ z^{(1-3b)/2}\ dz / 2V, \end{aligned} \qquad (2.2.4)$$

Equation (2.2.2) becomes:

$$[(b+1)\xi]^{(b+3)/(b+1)}\ \frac{\partial^2 F_o}{\partial\xi^2} - \frac{\partial F_o}{\partial t}$$

$$+ e\ [(b+1)\xi]^{(1-b)/(1+b)} \left[(1-\mu^2)\frac{\partial^2 F_o}{\partial\mu^2} - 2\mu\ \frac{\partial F_o}{\partial\mu} + \frac{1}{(1-\mu^2)}\ \frac{\partial^2 F_o}{\partial\phi^2} \right]$$

$$= \frac{-\ 3\ N\ |\ \xi_r(r_o,p_o)\ |\ \delta(\xi-\xi_o)\ \delta(t-t_o)\ \delta(\mu-\mu_o)\ \delta(\phi-\phi_o)}{8\ \pi\ V\ p_o^3\ r_o}. \qquad (2.2.5)$$

We note that Equation (2.2.5) is separable.

Introducing the variables :

if $b \neq 1$,

$$x = 2(rp^{3/2})^{(1-b)/2} / (1-b) = 2\,[(b+1)\xi]^{(b-1)/(2(b+1))}/(1-b),$$

and if $b = 1$,

$$x = -\ell n(2r^2p^3)/2 = -\ell n(\xi) / 2, \qquad (2.2.6)$$

we now transform Equation (2.2.5) into two partial differential equations in x, t, μ, ϕ corresponding to the two cases in Equations (2.2.6). These partial differential equations are:

If $K_{||} = K_o(p)\, r^b$, $b \neq 1$, $K_\perp/K_{||} = e$,

$$\frac{\partial^2 F_o}{\partial x^2} + \frac{2n+1}{x}\,\frac{\partial F_o}{\partial x} - \frac{\partial F_o}{\partial t} + \frac{e(n+1)^2}{x^2}\left[(1-\mu^2)\frac{\partial^2 F_o}{\partial \mu^2} - 2\mu\frac{\partial F_o}{\partial \mu} + \frac{1}{1-\mu^2}\,\frac{\partial^2 F_o}{\partial \phi^2}\right]$$

$$= \frac{-\,3\,N\;x_o\;\delta(x-x_o)\;\delta(t-t_o)\;\delta(\mu-\mu_o)\;\delta(\phi-\phi_o)}{8\,\pi\,V\,p_o^3\,r_o^2\;\;|n+1|}\,, \qquad (2.2.7)$$

and if $K_{||} = K_o(p)r$, $b = 1$, $K_\perp/K_{||} = e$,

$$\frac{\partial^2 F_o}{\partial x^2} - 2\,\frac{\partial F_o}{\partial x} - \frac{\partial F_o}{\partial t} + e\left[(1-\mu^2)\frac{\partial^2 F_o}{\partial \mu^2} - 2\mu\,\frac{\partial F_o}{\partial \mu} + \frac{1}{(1-\mu^2)}\,\frac{\partial^2 F_o}{\partial \phi^2}\right]$$

$$= \frac{-\,3\,N\,\delta(x-x_o)\,\delta(t-t_o)\,\delta(\mu-\mu_o)\,\delta(\phi-\phi_o)}{8\,\pi\,V\,p_o^3\;\;r_o^2} \qquad (2.2.8)$$

where $x_o = x(r_o, p_o)$, $t_o = t(p_o)$ and if $b \neq 1$, $n = (b+1)/(1-b)$.

Equations (2.2.7) and (2.2.8) may be combined in the equation

$$\frac{\partial^2 F_o}{\partial x^2} + \left(\frac{a_1}{x} + a_2\right) \frac{\partial F_o}{\partial x} - \frac{\partial F_o}{\partial t} + \left(\beta + \frac{\alpha}{x^2}\right) \left[(1-\mu^2) \frac{\partial^2 F_o}{\partial \mu^2} - 2\mu \frac{\partial F_o}{\partial \mu} + \frac{1}{1-\mu^2} \frac{\partial^2 F_o}{\partial \phi^2}\right]$$

$$= Z \quad \delta(x-x_o)\ \delta(t-t_o)\ \delta(\mu-\mu_o)\ \delta(\phi-\phi_o), \qquad (2.2.9)$$

where,

(i) if $b \neq 1$, $K_{||} = K_o(p)\, r^b$, $K_\perp / K_{||} = e$, then

$$n = (b+1)/(1-b), \quad a_1 = 2n+1, \quad a_2 = 0,$$
$$\alpha = e(n+1)^2, \quad \beta = 0,$$
$$Z = -3\, N\, x_o \,/\, (8\, \pi\, V\, p_o^3\, r_o^2\, |n+1|\,), \qquad (2.2.10)$$
$$x = 2\, (r p^{3/2})^{(1-b)/2} \,/\, (1-b),$$

and

(ii) if $b = 1$, $K_{||} = K_o(p) r$, $K_\perp / K_{||} = e$ then

$$a_1 = 0, \quad a_2 = -2,$$
$$\alpha = 0, \quad \beta = e,$$
$$Z = -3N \,/\, (8\, \pi\, V\, p_o^3\, r_o^2), \qquad (2.2.11)$$
$$x = -\ell n\, (2 r^2 p^3)\, /2.$$

In the following sections we study the group properties and the group invariant solutions of the partial differential equation (2.2.9), where the parameters a_1, a_2, α, β, Z are specified in Equations (2.2.10) and (2.2.11).

The group properties and the group invariant solutions of the

transport equation (2.2.9) will be used to show the relation between the separation variables x and t given in Equations (2.2.4) and (2.2.6) and the separation variables

$$t = -3 K_c p^{\delta} / (2 V \delta), \text{ if } \delta = a + 3(1-b) / 2 \neq 0,$$

$$t = -3 K_c \ell n(p) / (2 V) \quad \text{if} \quad \delta = 0,$$

$$y = -2 V \delta r^{1-b} p^{-a} / (3 K_c (1-b)^2),$$

where the diffusion coefficient $K(r,p) = K_c p^a r^b$, which were used by Parker (1965), Jokipii (1967), Fisk and Axford (1969) in their work on analytic solutions of the steady-state cosmic-ray equation of transport.

2.3 Solutions of partial differential equations and Lie Groups

The application of group theory to the solution of partial differential equations was first considered by Lie (1881), and later by Ovsjannikov (1962), Muller and Matschat (1962) and Bluman and Cole (1969) (for a more complete account of the results of this section see Ovsjannikov (1962)).

A system of differential equations S in m dependent variables u^i and (n-m) independent variables x^j is said to admit a group of continuous transformations G if the system S is transformed into itself when the dependent and independent variables are subjected to a transformation of G. Hence any solution of S admitting a group G is transformed into another solution of S under the action of any transformation of G.

The group of continuous, infinitesimal transformations

$$\begin{aligned} x'^i &= x^i + \varepsilon \xi^i_x (x; u), \quad i = 1(1) \overline{n-m}, \\ u'^s &= u^s + \varepsilon \xi^s_u (x; u), \quad s = 1(1) m, \end{aligned} \tag{2.3.1}$$

admitted by S are found as follows. The transformations of the partial derivatives of the dependent variables u^s with respect to the independent variables x^i, i.e. $\partial u^s/\partial x^i$ etc. corresponding to the transformations (2.3.1) are calculated. We then substitute the derivative transformations and the transformations (2.3.1) into the condition of invariance of S and eliminate any relations between the partial derivatives implied by the equations of S. Equating the coefficients of the partial derivatives of $O(\varepsilon)$ in the invariance condition yields a set of partial differential equations for the functions

$$\xi^i_x , \quad \xi^s_u , \qquad i = 1(1)\ \overline{n-m}, \qquad s = 1(1)\ m.$$

known as the determining equations.

The finite equations of the group admitted by S are the integral form of the infinitesimal transformations (2.3.1), i.e., the solutions of the set of ordinary differential equations

$$\frac{d\,x'^i}{\xi^i_x\,(x';u')} = \frac{du'^s}{\xi^s_u\,(x';u')} = d\varepsilon, \tag{2.3.2}$$

known as the trajectories of the group.

Invariants of the group with infinitesimal generators (2.3.1) are functions $J(x,u)$ such that

$$J\,(x',\ u') = J\,(x,\ u). \tag{2.3.3}$$

Substituting the transformations (2.3.1) in Equation (2.3.3) and equating terms $O(\varepsilon)$ to zero we find

$$\xi^i_x \frac{\partial J}{\partial x^i} + \xi^s_u \frac{\partial J}{\partial u^s} = 0. \tag{2.3.4}$$

The characteristic equations for the first order partial differential equation (2.3.4) are given by the group trajectories (2.3.2). Thus

the invariants of the group with generators (2.3.1) are the (n-1) functionally independent solutions of the trajectories (2.3.2). The above discussion indicates that the finite equations of the group with trajectories (2.3.2) may be expressed as

$$J^{\tau}\ (x';\ u') = J^{\tau}\ (x;\ u), \qquad \tau = 1(1)\ n-1,$$
$$f\ (x',\ u',\ \varepsilon) = 0, \tag{2.3.5}$$

where J^{τ} are the invariants of the group and the function $f\ (x',\ u',\ \varepsilon)$ is determined from the trajectories (2.3.2.)

Let H be a subgroup of the main group admitted by the system S, with a complete set of functionally independent invariants $\{J^{\tau} / \tau = 1\ (1)\ t\}$. The solution $u = \psi(x)$ is known as an invariant H solution if the solution is mapped onto itself by the transformations of H. A necessary condition for the existence of an invariant H solution is that the rank of the matrix

$$|| \partial J^{\tau} / \partial u^{k} ||, \qquad \tau = 1\ (1)\ t, \qquad k = 1\ (1)\ m,$$

be equal to m (the number of dependent variables). An invariant H solution of the system S is given by

$$\phi^{k}(J) = 0, \qquad k = 1\ (1)\ m, \tag{2.3.6}$$

where the functions ϕ^{k} are functionally independent with respect to the variables J.

The transformations of the partial derivatives of the first and second order of the dependent variables u^{s} under the transformations (2.3.1) may be calculated as follows:
We introduce the total differential operators

$$\frac{D}{Dx^i} = D_i = \frac{\partial}{\partial x^i} + u_i^s \frac{\partial}{\partial u^s} , \tag{2.3.7}$$

$$\tilde{D}_i = \frac{\partial}{\partial x^i} + u_i^s \frac{\partial}{\partial u^s} + u_{ij}^s \frac{\partial}{\partial u_j^s} , \tag{2.3.8}$$

where

$$u_i^s = \frac{\partial u^s}{\partial x^i} , \tag{2.3.9}$$

$$u_{ij}^s = \frac{\partial^2 u^s}{\partial x^i \partial x^j} . \tag{2.3.10}$$

Since ξ_x^i and ξ_u^s are functions of x and u, we have

$$u'^s_i = D_\ell \left(u^s + \varepsilon \xi_u^s \right) \frac{D x^\ell}{D x'^i}$$

$$= D_\ell \left(u^s + \varepsilon \xi_u^s \right) \frac{D}{D x'^i} \left(x'^\ell - \varepsilon \xi_x^\ell \right). \tag{2.3.11}$$

Here we have used the summation convention and the notation $u_i^s = \partial u^s / \partial x^i$. Hence to $O(\varepsilon)$

$$u'^s_i = u_i^s + \varepsilon \zeta_i^s , \tag{2.3.12}$$

where

$$\zeta_i^s = D_i (\xi_u^s) - u_\ell^s D_i (\xi_x^\ell) , \tag{2.3.13}$$

gives the transformations for the first order partial derivatives.

By a similar analysis

$$u'^s_{ij} = u_{ij}^s + \varepsilon \zeta_{ij}^s \tag{2.3.14}$$

where

$$\zeta^{s}_{ij} = \tilde{D}_i (\zeta^{s}_{j}) - u^{s}_{j\ell} \tilde{D}_i (\xi^{\ell}_{x}) \qquad (2.3.15)$$

gives the transformations for the second order partial derivatives to $O(\varepsilon)$.

Associated with the transformations (2.3.1), (2.3.12) and (2.3.14) are the differential operators

$$X = \xi^{i}_{x} \frac{\partial}{\partial x^{i}} + \xi^{k}_{u} \frac{\partial}{\partial u^{k}} \qquad (2.3.16)$$

$$\tilde{X} = \xi^{i}_{x} \frac{\partial}{\partial x^{i}} + \xi^{k}_{u} \frac{\partial}{\partial u^{k}} + \zeta^{s}_{i} \frac{\partial}{\partial u^{s}_{i}} , \qquad (2.3.17)$$

$$\tilde{\tilde{X}} = \xi^{i}_{x} \frac{\partial}{\partial x^{i}} + \xi^{k}_{u} \frac{\partial}{\partial u^{k}} + \zeta^{s}_{i} \frac{\partial}{\partial u^{s}_{i}} + \zeta^{s}_{ij} \frac{\partial}{\partial u^{s}_{ij}} . \qquad (2.3.18)$$

The operators $\tilde{X}$ and $\tilde{\tilde{X}}$ are called the first and second extended operators of the operator X. If F is some arbitrary function of the x's and u's the function X F is known as the symbol of the group generated by the infinitesimal transformations (2.3.1). The functions $\tilde{X}$ F, $\tilde{\tilde{X}}$ F are the symbols of the first and second extended groups.

The general operator X of a Lie group can be expressed as a linear combination of a set of basis operators $\{X_a, \quad a = 1 (1) r\}$ with constant coefficients e^a, i.e.

$$X = e^{a} X_{a} , \qquad (2.3.19)$$

where as usual the summation convention applies. The operators X_a form a Lie Algebra with respect to the operation of commutation:

$$[X_a, X_b] = X_a X_b - X_b X_a . \qquad (2.3.20)$$

It can be shown (Eisenhart (1933)) that the operators X_a satisfy the

relations

$$[X_a, X_b] = c^e_{ab} X_e , \qquad a, b, e = 1 (1) r, \tag{2.3.21}$$

$$[X_a, X_b] = -[X_b, X_a] , \tag{2.3.22}$$

$$[[X_a, X_b], X_c] + [[X_b, X_c], X_a] + [[X_c, X_a], X_b] = 0 \tag{2.3.23}$$

The constants c^e_{ab} are known as the structure constants of the group and the relations (2.3.22) and (2.3.23) are known as the Jacobi relations. The results (2.3.21) - (2.3.23) also hold for the first extended operators $\tilde{X}_a$, $\tilde{X}_b$, $\tilde{X}_c$. Similarly the n^{th} extended operators satisfy (2.3.21)-(2.3.23).

The homogeneous, steady-state, cosmic-ray equation of transport (2.2.9) is separable and it is a second order linear homogeneous partial differential equation of the form

$$G(F) = a^{ij}(x) F_{ij} + b^i(x) F_i + cF = 0 \tag{2.3.24}$$

where a^{ij}, b^i, c are functions of the independent variables x^i and $a^{ij} = a^{ji}$. The group properties of Equation (2.3.24) have been analysed by Ovsjannikov (1962), and we outline his results below.

Consider the operators

$$X = \xi^i \frac{\partial}{\partial x^i} + \eta \frac{\partial}{\partial F} , \tag{2.3.25}$$

admitted by Equation (2.3.24). The condition of invariance of Equation (2.3.24) under the infinitesimal transformations with operators (2.3.25) is

$$\tilde{\tilde{X}} G(F) = \lambda G(F) = 0, \tag{2.3.26}$$

where

$$\overset{\approx}{X}\, G(F) = a^{ik}\,\zeta_{ik} + b^{i}\,\zeta_{i} + c\eta + X(a^{ik})\,F_{ik} + X(b^{i})\,F_{i} + X(c)F, \tag{2.3.27}$$

and $\overset{\approx}{X}$ is the second extended operator.

Equating the coefficients of the various partial derivatives of F in Equation (2.3.26) to zero yields a set of determining equations for the functions ξ^{i} and η. Ovsjannikov (1962) has shown that the determining equations for the infinitesimal transformations admitted by Equation (2.3.24), in the case where the equation is not strongly degenerate are:

$$\eta = \sigma(x)F + \Omega(x) \tag{2.3.28a}$$

$$\lambda = \lambda(x), \tag{2.3.28b}$$

$$\nu = \sigma - \lambda, \tag{2.3.28c}$$

$$a^{ik}\frac{\partial \xi^{j}}{\partial x^{k}} + a^{jk}\frac{\partial \xi^{i}}{\partial x^{k}} - \frac{\partial a^{ij}}{\partial x^{k}}\xi^{k} = \nu\, a^{ij}, \quad i, j = 1(1)n, \tag{2.3.28d}$$

$$2a^{ik}\frac{\partial \sigma}{\partial x^{k}} = a^{jk}\frac{\partial^{2}\xi^{i}}{\partial x^{k}\partial x^{j}} + b^{k}\frac{\partial \xi^{i}}{\partial x^{k}} - \xi^{k}\frac{\partial b^{i}}{\partial x^{k}} - \nu\, b^{i} \qquad i = 1(1)n, \tag{2.3.28e}$$

$$a^{ij}\frac{\partial^{2}\sigma}{\partial x^{i}\partial x^{j}} + b^{i}\frac{\partial \sigma}{\partial x^{i}} + \xi^{k}\frac{\partial c}{\partial x^{k}} + \nu\, c = 0, \tag{2.3.28f}$$

$$a^{ij}\frac{\partial^{2}\Omega}{\partial x^{i}\partial x^{j}} + b^{i}\frac{\partial \Omega}{\partial x^{i}} + c\,\Omega = 0. \tag{2.3.28g}$$

Equation (2.3.24) is strongly degenerate if in a certain system of coordinates $y = y(x)$ it is reduced to the form

$$\frac{\partial^{2}F}{\partial y^{1^{2}}} + \bar{b}\frac{\partial F}{\partial y^{1}} + \bar{c}\,F = 0, \tag{2.3.29}$$

where $\bar{b}$ and $\bar{c}$ are functions of the new coordinates $y^1, y^2, y^3, \ldots y^n$.

If the function G(F) in Equation (2.3.24) had contained an inhomogeneous term $-M\,\delta(\underline{x}-\underline{x}_o)$, where M is a constant and $\delta(\underline{x}-\underline{x}_o)$, is a Dirac delta function in the n independent variables x^i, then further conditions are imposed on the operators (2.3.25). The condition of invariance of the source point at $\underline{x}_o$ implies

$$\xi^i(\underline{x}_o) = 0, \tag{2.3.30}$$

and the n dimensional delta function transforms as

$$\delta(\underline{x}'-\underline{x}_o) = \delta(\underline{x}-\underline{x}_o)\,[1 - \varepsilon \sum_{i=1}^{n} D_i(\xi^i) + O(\varepsilon^2)]\,. \tag{2.3.31}$$

Hence we have

$$\sum_{i=1}^{n} \frac{\partial \xi^i(\underline{x}_o)}{\partial x^i} + \lambda(\underline{x}_o) = 0, \tag{2.3.32}$$

as a consequence of the invariance condition (2.3.26).

2.4 Infinitesimal transformations admitted by the steady state cosmic-ray equation of transport.

The homogeneous, separated, steady-state cosmic-ray equation of transport (2.2.9) is a linear homogeneous partial differential equation in one dependent variable F_o, and four independent variables x, t, μ and ϕ. Ovsjannikov (1962) has investigated the group properties of this type of equation and we proceed to use his results, which are outlined in Section (3) to find the group of infinitesimal transformations admitted by the separated transport equation.

Putting $(x^1, x^2, x^3, x^4) = (x, t, \mu, \phi)$, Equation (2.2.9) is then of the same form as Equation (2.3.24) with

$$a^{11} = 1, \quad a^{22} = 0,$$

$$a^{33} = (\beta + \alpha/x^2)(1-\mu^2), \quad a^{44} = (\beta + \alpha/x^2)/(1-\mu^2),$$

$$a^{ij} = 0 \text{ if } i \neq j, \quad i, j = 1\,(1)\,4, \tag{2.4.1}$$

$$b^1 = (a_1/x + a_2), \quad b^2 = -1,$$

$$b^3 = -2\mu\,(\beta + \alpha/x^2), \quad b^4 = c = 0,$$

From Equations (2.2.10) and (2.2.11) we have:

(i) if $K_{||} = K_o(p)\, r^b$, $b \neq 1$, $K_\perp/K_{||} = e$ then

$$n = (b+1)/(1-b),$$

$$a_1 = 2n+1, \quad a_2 = 0, \tag{2.4.2a}$$

$$\alpha = e(n+1)^2, \quad \beta = 0$$

and

(ii) if $K_{||} = K_o(p)\, r$ and $K_\perp/K_{||} = e$ then

$$a_1 = 0, \quad a_2 = -2, \tag{2.4.2b}$$

$$\alpha = 0, \quad \beta = e,$$

as the appropriate values of the parameters a_1, a_2, α, β to be used in Equations (2.4.1).

Using the results incorporated in Equations (2.3.28) the determining equations for the operators admitted by the separated transport equation (2.2.9) are:

$$2\frac{\partial \xi^1}{\partial x} = \nu, \tag{2.4.3a}$$

$$\frac{\partial \xi^2}{\partial x} = 0, \tag{2.4.3b}$$

$$\frac{\partial \xi^3}{\partial x} + \left(\beta + \frac{\alpha}{x^2}\right)(1-\mu^2)\frac{\partial \xi^1}{\partial \mu} = 0, \tag{2.4.3c}$$

$$\frac{\partial \xi^4}{\partial x} + \left(\beta + \frac{\alpha}{x^2}\right) \frac{1}{1-\mu^2} \frac{\partial \xi^1}{\partial \phi} = 0 , \qquad (2.4.3d)$$

$$\left(\beta + \frac{\alpha}{x^2}\right) (1-\mu^2) \frac{\partial \xi^2}{\partial \mu} = 0 , \qquad (2.4.3e)$$

$$\left(\beta + \frac{\alpha}{x^2}\right) \frac{1}{1-\mu^2} \frac{\partial \xi^2}{\partial \phi} = 0, \qquad (2.4.3f)$$

$$2\left(\beta + \frac{\alpha}{x^2}\right)(1-\mu^2) \frac{\partial \xi^3}{\partial \mu} + \frac{2\alpha}{x^3}(1-\mu^2)\,\xi^1 + 2\mu\left(\beta + \frac{\alpha}{x^2}\right)\xi^3$$

$$= \nu\left(\beta + \frac{\alpha}{x^2}\right)(1-\mu^2), \qquad (2.4.3g)$$

$$\left(\beta + \frac{\alpha}{x^2}\right)\left[(1-\mu^2) \frac{\partial \xi^4}{\partial \mu} + \frac{1}{1-\mu^2} \frac{\partial \xi^3}{\partial \phi}\right] = 0, \qquad (2.4.3h)$$

$$2\left(\beta + \frac{\alpha}{x^2}\right) \frac{1}{1-\mu^2} \frac{\partial \xi^4}{\partial \phi} + \frac{2\alpha\,\xi^1}{x^3(1-\mu^2)} - \frac{2\mu(\beta + \alpha/x^2)\xi^3}{(1-\mu^2)^2}$$

$$= \nu\left(\beta + \frac{\alpha}{x^2}\right) \frac{1}{1-\mu^2} . \qquad (2.4.3i)$$

Introducing the differential operator

$$G = \frac{\partial^2}{\partial x^2} + \left(\frac{a_1}{x} + a_2\right) \frac{\partial}{\partial x} - \frac{\partial}{\partial t} + \left(\beta + \frac{\alpha}{x^2}\right)\left[(1-\mu^2)\frac{\partial^2}{\partial \mu^2}\right.$$

$$\left. - 2\mu \frac{\partial}{\partial \mu} + \frac{1}{1-\mu^2} \frac{\partial^2}{\partial \phi^2}\right]$$

the remaining determining equations are

$$2\frac{\partial \sigma}{\partial x} = G(\xi^1) + \frac{a_1\,\xi^1}{x^2} - \nu\left(\frac{a_1}{x} + a_2\right) . \qquad (2.4.3j)$$

$$\frac{\partial \xi^2}{\partial t} = \nu , \qquad (2.4.3k)$$

$$2\left(\beta + \frac{\alpha}{x^2}\right)(1-\mu^2)\frac{\partial\sigma}{\partial\mu} = G(\xi^3) - 4\mu\frac{\alpha}{x^3} + 2\left(\beta + \frac{\alpha}{x^2}\right)(\xi^3 + \mu\nu), \tag{2.4.31}$$

$$2\frac{\left(\beta + \frac{\alpha}{x^2}\right)}{(1-\mu^2)}\frac{\partial\sigma}{\partial\phi} = G(\xi^4), \tag{2.4.3m}$$

$$G(\sigma) = 0, \tag{2.4.3n}$$

$$G(\Omega) = 0, \tag{2.4.3o}$$

The solutions of the determining equations (2.4.3) depend on the radial dependence of the diffusion coefficients $K_{||}$ and $K_{\perp}$. In the models under consideration the diffusion coefficients are of the form

$$K_{||} = K_o(p)\, r^b, \quad K_{\perp}/K_{||} = e. \tag{2.4.4}$$

In addition we require compatibility conditions of the form

$$\frac{\partial^2 \xi^i}{\partial x^j \partial x^k} = \frac{\partial^2 \xi^i}{\partial x^k \partial x^j},$$

to hold. There are three cases to consider. The solutions of the determining equations for these cases are given below.

Case 1. $K_{||} = K_o(p)\, r^b$, $b \neq 1$, $K_{\perp}/K_{||} = e$

The solutions are

$$\xi^1 = x(\beta + \gamma t) = \gamma(t-t_o)\, x, \tag{2.4.5a}$$

$$\xi^2 = \gamma t^2 + 2\beta t + \alpha = \gamma[(t-t_o)^2 + a_o], \tag{2.4.5b}$$

$$\xi^3 = A\sqrt{1-\mu^2}\,(b_2 \cos\phi - b_1 \sin\phi)$$

$$= A\sqrt{1-\mu^2}\,\sin\theta_o\,\sin(\phi_o - \phi), \tag{2.4.5c}$$

$$\xi^4 = A\left[\left(\mu / \sqrt{1-\mu^2}\right)(b_2 \sin\phi + b_1 \cos\phi) - b_3\right]$$

$$= A\left[\left(\mu / \sqrt{1-\mu^2}\right)\sin\Theta_o \cos(\phi-\phi_o) - \cos\Theta_o\right], \quad (2.4.5d)$$

$$\nu = 2\beta + 2\gamma t = 2\gamma(t-t_o), \quad (2.4.5e)$$

$$\sigma = \gamma[-x^2/4 - (n+1)\, t + \delta], \quad (2.4.5f)$$

$$\eta = \sigma F + \Omega(x), \quad (2.4.5g)$$

$$\lambda = \sigma - \nu, \quad (2.4.5h)$$

$$\text{i.e. } \lambda = -\gamma(x^2 - x_o^2)/4 - (n+3)\gamma(t-t_o) + \psi, \quad (2.4.5i)$$

where

$\Omega(x)$ is any solution of the homogeneous equation (2.2.1),

$$t_o = -\beta/\gamma, \quad a_o = (\alpha\gamma - \beta^2)/\gamma^2, \quad (2.4.5j)$$

$$\psi = \delta\gamma - \gamma(x_o^2/4 + (n+1)\, t_o), \quad (2.4.5k)$$

$$(b_1, b_2, b_3) = (\sin\Theta_o \cos\phi_o, \sin\Theta_o \sin\phi_o, \cos\Theta_o), \quad (2.4.5l)$$

and

$$\mu = \cos\Theta.$$

Case 2 $K_{||} = K_o(p)\, r, \quad K_\perp = 0.$

The solutions of the determining equations are

$$\xi^1 = K + \delta t + (\beta + \gamma t)\, x,$$

$$\text{i.e. } \xi^1 = \gamma[x(t-t_o) + d_1(t-t_o) + \omega], \quad (2.4.6a)$$

$$\xi^2 = \gamma t^2 + 2\beta t + \alpha = \gamma[(t-t_o)^2 + a_o], \quad (2.4.6b)$$

$$\nu = 2\beta + 2\gamma t = 2\gamma(t-t_o), \quad (2.4.6c)$$

$$\sigma = -\gamma x^2/4 + (\gamma t + \beta - \delta/2)x - \gamma t^2 - (2\beta + \gamma/2 - \delta)\, t + \gamma\rho_o, \tag{2.4.6d}$$

$$\eta = \sigma F + \Omega, \tag{2.4.6e}$$

$$\lambda = \sigma - \nu,$$

i.e.
$$\lambda = -\gamma(x^2-x_o^2)/4 + \gamma(t-t_o)x - \delta(x-x_o)/2 - \gamma(t-t_o)^2 - (5\gamma/2-\delta)(t-t_o) + \Sigma, \tag{2.4.6f}$$

where

$\Omega(x)$ is any solution of the homogeneous equation (2.2.1),

$$t_o = -\beta/\gamma, \quad d_1 = \delta/\gamma, \quad \omega = (K + \delta t_o)/\gamma, \tag{2.4.6g}$$

and

$$\Sigma = \gamma\rho_o - \gamma x_o^2/4 + \gamma t_o^2 - \delta x_o/2 - (\gamma/2-\delta)\, t_o. \tag{2.4.6h}$$

Case 3 $K_{||} = K_o(p)r$, $K_\perp/K_{||} = e \neq 0$

The solutions of the determining equations are

$$\xi^1 = \gamma t + \beta = \gamma(t-t_o), \tag{2.4.7a}$$

$$\xi^2 = \delta, \tag{2.4.7b}$$

$$\xi^3 = A\sqrt{1-\mu^2}\,(b_2 \cos\phi - b_1 \sin\phi), \tag{2.4.7c}$$

$$= A \sin\Theta_o \sqrt{1-\mu^2} \sin(\phi_o-\phi),$$

$$\xi^4 = A\left[\left(\mu/\sqrt{1-\mu^2}\right)(b_2 \sin\phi + b_1 \cos\phi) - b_3\right]$$

$$= A\left[\sin\Theta_o\left(\mu/\sqrt{1-\mu^2}\right)\cos(\phi-\phi_0) - \cos\Theta_o\right], \tag{2.4.7d}$$

$$\nu = 0, \tag{2.4.7e}$$

$$\sigma = \lambda = \gamma t - \gamma x/2 + k = \gamma(t-t_o) - \gamma(x-x_o)/2 + h, \tag{2.4.7g}$$

$$\eta = \sigma F + \Omega$$

where

Ω (x) is any solution of the homogeneous Equation (2.2.1),

$$t_o = -\beta/\gamma , \quad h = \gamma t_o - \gamma x_o/2 + k, \tag{2.4.7h}$$

$$(b_1, b_2, b_3) = (\sin\Theta_o, \cos\phi_o, \sin\Theta_o \sin\phi_o, \cos\Theta_o), \tag{2.4.7i}$$

and

$$\mu = \cos\Theta. \tag{2.4.7j}$$

In Equations (2.4.5), (2.4.6), and (2.4.7) Θ_o and ϕ_o are arbitrary, but constant polar and azimuthal angles and α, β, γ, δ, K, ρ, A and k are arbitrary constants.

The operators corresponding to (2.4.5)-(2.4.7) can be expressed in terms of a linear combination of basis operators [cf. Equation (2.3.19)]. For case (1) this decomposition takes the form

$$X = \xi^i \frac{\partial}{\partial x^i} + \eta \frac{\partial}{\partial F}$$

$$= A_1 X_1 + A_2 X_2 + A_3 X_3 + \alpha X_4 + \beta X_5 + \gamma X_6 + \gamma\delta X_7 + X_8, \tag{2.4.8}$$

where

$$X_1 = -\sqrt{1-\mu^2} \sin\phi \frac{\partial}{\partial\mu} + \frac{\mu}{\sqrt{1-\mu^2}} \cos\phi \frac{\partial}{\partial\phi}$$

$$= x_3 \frac{\partial}{\partial x_2} - x_2 \frac{\partial}{\partial x_3} , \tag{2.4.9a}$$

$$X_2 = \sqrt{1-\mu^2} \cos\phi \frac{\partial}{\partial\mu} + \frac{\mu}{\sqrt{1-\mu^2}} \sin\phi \frac{\partial}{\partial\phi}$$

$$= x_1 \frac{\partial}{\partial x_3} - x_3 \frac{\partial}{\partial x_1} , \tag{2.4.9b}$$

$$X_3 = -\frac{\partial}{\partial\phi} = x_2 \frac{\partial}{\partial x_1} - x_1 \frac{\partial}{\partial x_2} , \tag{2.4.9c}$$

$$X_4 = \frac{\partial}{\partial t} , \tag{2.4.9d}$$

$$X_5 = x\frac{\partial}{\partial x} + 2t\frac{\partial}{\partial t}\ , \qquad (2.4.9e)$$

$$X_6 = xt\partial/\partial x + t^2\partial/\partial t + F_o(-x^2/4 - (n+1)t)\partial/\partial F, \qquad (2.4.9f)$$

$$X_7 = F\ \partial/\partial F, \qquad (2.4.9g)$$

$$X_8 = \Omega(x)\ \partial/\partial F, \qquad (2.4.9h)$$

with $A_1 = Ab_1$, $A_2 = A\ b_2$, $A_3 = A\ b_3$, and (x_1, x_2, x_3), (A_1, A_2, A_3) position vectors in a rectangular cartesian coordinate system.

The operators X_1, X_2, X_3 correspond to infinitesimal rotations about the x_1, x_2 and x_3 axis respectively; X_4 is a translation operator, whereas X_5 and X_7 are stretching operators. A similar decomposition can be carried out for the other two cases.

The commutation relations (2.3.21) for the subgroup with operators $\{X_1, X_2, X_3, X_4, X_5, X_6, X_7\}$ defined by Equations (2.4.9) are given below:

TABLE 2.1

	X_1	X_2	X_3	X_4	X_5	X_6	X_7
X_1	0	X_3	$-X_2$	0	0	0	0
X_2	$-X_3$	0	X_1	0	0	0	0
X_3	X_2	$-X_1$	0	0	0	0	0
X_4	0	0	0	0	$2X_4$	X_5 $-(n+1)X_7$	0
X_5	0	0	0	$-2X_4$	0	$2X_6$	0
X_6	0	0	0	$(n+1)X_7-$ X_5	$-2X_6$	0	0
X_7	0	0	0	0	0	0	0

In the above table the intersection of the i^{th} row and j^{th} column gives the commutator $[X_i, X_j]$.

2.5. Invariant group solutions

In this section the finite equations of the main subgroup admitted by the separated transport equation (2.2.9) are calculated by integrating the group trajectories (2.3.2), i.e.

$$d\varepsilon = \frac{dx'^i}{\xi^i(x')} = \frac{dF'}{\sigma(x')F'+\Omega'}, \quad i = 1(1)4, \tag{2.5.1}$$

where $(x^1,x^2,x^3,x^4) = (x,t,\mu,\phi)$ and the ξ^i, σ and Ω are the infinitesimal generators of the group, which are given in Section (4). We find the solutions of Equations (2.5.1) for the main subgroup with $\Omega \equiv 0$ since this is sufficient for our purposes. Taking (x,t,μ,ϕ) as initial values of (x',t',μ',ϕ') the solutions of the trajectory equations (2.5.1) have the form

$$J_s(x',F') = J_s(x,F), \quad s = 1(1)\ 4, \tag{2.5.2}$$

where $J_s(x,F)$ are functionally independent invariants of the group.

An invariant group solution of Equation (2.2.9) has the form (cf. Equation (2.3.6)).

$$G\ (J_1,\ J_2,\ J_3,\ J_4) = 0, \tag{2.5.3}$$

where the function G in the relation (2.5.3) is compatible with the separable transport equation (2.2.9). Since only one of the invariants of Equations (2.5.1), say $J_3(x,F)$ is a function of, F, (the dependent variable), the invariant group solution (2.5.3), if it exists, may be put in the form

$$J_3\ (x,F) = f(J_1(x),\ J_2(x),\ J_4(x)\ ), \tag{2.5.4}$$

where the function f in Equation (2.5.4) is compatible with F being a solution of the separable transport equation (2.2.9).

There are three cases to consider since the generators of the

group admitted by Equation (2.2.9), given in Equations (2.4.5), (2.4.6) and (2.4.7) are dependent on the character of the diffusion coefficients.

Case 1 $\quad K_{||} = K_o(p)\ r^b, \quad b \neq 1 \quad K_\perp/K_{||} = e$

Putting $\mu = \cos\Theta$ the trajectories of the group with generators (2.4.5) are

$$d\varepsilon = \frac{dx}{\gamma(t-t_o)x} = \frac{dt}{\gamma[(t-t_o)^2+a_o]} = \frac{dF}{\gamma(-x^2/4 - (n+1)t+\delta)F}$$

$$= \frac{d\Theta}{A\ \sin\Theta_o\ \sin(\phi-\phi_o)} = \frac{d\phi}{A[\cot\Theta\ \sin\Theta_o\ \cos(\phi-\phi_o)-\cos\Theta_o]} \tag{2.5.5}$$

Equations (2.5.5) may be written

$$\frac{dx}{dt} = \frac{(t-t_o)\ x}{[(t-t_o)^2+ a_o]}\ , \tag{2.5.6a}$$

$$\frac{d\Theta}{d\phi} = \frac{\sin\Theta_o\ \sin(\phi-\phi_o)}{(\cot\Theta\ \sin\Theta_o\ \cos(\phi-\phi_o) - \cos\Theta_o)}\ , \tag{2.5.6b}$$

$$\frac{dF}{dt} = \frac{(-x^2/4 - (n+1)t + \delta)F}{(\ (t-t_o)^2 + a_o\ )}\ , \tag{2.5.6c}$$

$$\frac{d\Theta}{dt} = \frac{A\ \sin\Theta_o\ \sin(\phi-\phi_o)}{\gamma[(t-t_o)^2 + a_o]}\ . \tag{2.5.6d}$$

The solutions of Equations (2.5.6a), and (2.5.6b) are

$$\eta\ (x,t) = J_1 = \frac{x}{\sqrt{(t-t_o)^2 + a_o}}\ , \tag{2.5.7}$$

$$J_2 = \cos\Theta\ \cos\Theta_o + \sin\Theta\ \sin\Theta_o\ \cos\ (\phi-\phi_o). \tag{2.5.8}$$

The invariant J_2 is the cosine of the polar angle in a coordinate system with polar axis in the direction (Θ_o, ϕ_o).

From Equations (2.5.7) and (2.5.8)

$$x = J_1^2 (T^2 + a_o), \quad T = t-t_o, \tag{2.5.9a}$$

$$\sin(\phi-\phi_o) = \sqrt{(\sin^2\Theta \sin^2\Theta_o - (J_2 - \cos\Theta\cos\Theta_o)^2)} / \sin\Theta \sin\Theta_o. \tag{2.5.9b}$$

Using Equations (2.5.9) to eliminate x and ϕ from Equations (2.5.6c) and (2.5.6d) we find Equations (2.5.6c) and (2.5.6d) have the solutions

$$J_3 = F \exp(J_1^2 T/4+(n+1)\ell n(T^2+a_o)/2 - \chi\int^T dy/(y^2+a_o)), \tag{2.5.10}$$

$$J_4 = \Phi + (A/\gamma) \int^T dy/(y^2+a_o), \tag{2.5.11}$$

where

$$\Phi = \pm \arccos\left(\frac{\cos\Theta - J_2\cos\Theta_o}{\sqrt{(1-J_2^2)}\sin(\Theta_o)}\right), \tag{2.5.12}$$

$$\int^T dy/(y^2+a_o) = \operatorname{artan}(T/b)/b \quad \text{if } a_o = b^2 > 0, \tag{2.5.13a}$$

$$\int^T dy/(y^2+a_o) = \ell n((T-a)/(T+a))/(2a) \text{ if } a_o = -a^2 < 0, \tag{2.5.13b}$$

$$\int^T dy/y^2 = -1/T \quad \text{if } a_o = 0, \tag{2.5.13c}$$

and

$$\chi = \delta - (n+1)\, t_o . \tag{2.5.13d}$$

By simple coordinate geometry the angle Φ can be shown to be the azimuthal angle of a spherical polar coordinate system with polar axis in the direction (Θ_o, ϕ_o).

The invariants J_1, J_2, J_3, J_4 above satisfy the necessary condition for the existence of an invariant group solution given in

Section (3). The invariant group solutions of Equation (2.2.9) are of the form (2.5.4), i.e.,

$$J_3 = f(J_1, J_2, J_4). \tag{2.5.4}$$

Using the expression (2.5.10) for J_3 the invariant group solutions (2.5.4.) are

$$F = \exp[-J_1^2\, T/4 - (n+1)\ell n(T^2+a_o)/2 + \chi \int^T dy(y^2+a_o)] \cdot f(J_1,J_2,J_4), \tag{2.5.14}$$

where $f(J_1,J_2, J_4)$ is the solution of a partial differential equation in J_1, J_2, J_4 obtained by requiring that the function F in Equation (2.5.14) satisfy the separable transport equation (2.2.9).

Choosing a coordinate system such that $\Theta_o = \phi_o = 0$, and putting $\eta = J_1$ and $w = J_4$ we find that the function f satisfies the partial differential equation

$$\frac{\partial^2 f}{\partial \eta^2} + \frac{2n+1}{\eta} \frac{\partial f}{\partial \eta} + \left(\frac{a_o \eta^2}{4} - \chi\right) f - \frac{A}{\gamma} \frac{\partial f}{\partial w}$$

$$+ \frac{e(n+1)^2}{\eta^2}\left((1-\mu^2) \frac{\partial^2 f}{\partial \mu^2} - 2\mu \frac{\partial f}{\partial \mu} + \frac{1}{1-\mu^2} \frac{\partial^2 f}{\partial w^2}\right) = 0. \tag{2.5.15}$$

Note that the problem of solving a partial differential equation for F in four variables has been reduced to the solution of a partial differential equation for f in three independent variables.

If A = 0 then $w = \phi$ and Equation (2.5.15) separates, i.e.

$$f = P(\mu)\ Q(\phi)\ R(\eta), \tag{2.5.16a}$$

where

$$P''(\mu) - \frac{2\mu}{(1-\mu^2)} P'(\mu) + \left(\frac{\ell(\ell+1)}{(1-\mu^2)} - \frac{m^2}{(1-\mu^2)^2}\right) P(\mu) = 0, \tag{2.5.16b}$$

$$Q''(\phi) + m^2 Q = 0, \tag{2.5.16c}$$

$$R''(\eta) + \frac{2n+1}{\eta} R'(\eta) + \left[\frac{a_o \eta^2}{4} - \chi - \frac{e(n+1)^2}{\eta^2} \ell(\ell+1) \right] R(\eta) = 0. \qquad (2.5.16d)$$

Equation (2.5.16b) is Legendre's associated equation, Equation (2.5.16c) has solutions in terms of exponential functions, and Equation (2.5.16d) has solutions in terms of confluent hypergeometric functions or modified Bessel functions, depending on whether $a_o \neq 0$ or $a_o = 0$.

The separated solutions of Equations (2.5.16) for f are

$$f = \eta^{\zeta-n} \exp(-\sqrt{-a_o}\, \eta^2/4) \left[A.M(\chi/(2\sqrt{-a_o}) + (1+\zeta)/2,\ 1+\zeta, \sqrt{-a_o}\eta^2/2)\right.$$

$$\left. + B.U\ (\chi/(2\sqrt{-a_o}) + (1+\zeta)/2,\ 1+\zeta,\ \sqrt{-a_o}\ \eta^2/2)\right].$$

$$[C.P_\ell^m(\mu) + D.Q_\ell^m(\mu)]\ e^{\pm im\phi}\ , \qquad (2.5.17)$$

or if $a_o = 0$

$$f = \eta^{-n} [A.I_\zeta(\sqrt{\chi}\eta) + B.K_\zeta(\sqrt{\chi}\eta)].$$

$$[C.P_\ell^m(\mu) + D.Q_\ell^m(\mu)]e^{\pm im\phi}\ , \qquad (2.5.18)$$

where

$$\zeta = \sqrt{n^2 + e\ell(\ell+1)(n+1)^2}, \quad n = (b+1)/(1-b),$$

and ℓ and m are integers with $m \leq \ell$. The functions M(a,b,x) and U(a,b,x) are standard independent solutions of the equation

$$xF''(x) + (b-x)\ F'(x) - aF(x) = 0, \qquad (2.5.19)$$

which is Kummer's confluent hypergeometric equation (see Slater (1960)). The functions $I_m(x)$ and $K_m(x)$ are modified Bessel functions of the first and second kind; $P_\ell^m(\mu)$ and $Q_\ell^m(\mu)$ are associated Legendre polynomials. In the applications of the solutions (2.5.17) and (2.5.18) the coefficients of the $Q_\ell^m(\mu)$ terms are put equal to zero since these

terms have a singularity at $\mu = 1$.

Case 2 $K_{||} = K_o(p)\, r, \quad K_\perp = 0$

The generators of the group are given by Equations (2.4.6), and the trajectories of the group with $\Omega = 0$ are:

$$d\varepsilon = \frac{dx}{\gamma[x(t-t_o) + d_1(t-t_o) + \omega]} = \frac{dt}{\gamma[(t-t_o)^2 + a_o]}$$

$$= \frac{dF}{\gamma F(-x^2/4 + (t-t_o-d_1/2)x - t^2 + (2t_o-\frac{1}{2} + d_1)t + \rho_o)} . \tag{2.5.20}$$

Putting $T = t-t_o$ the trajectories (2.5.20) may be written in the alternative form

$$\frac{dx}{dT} = \frac{xT + d_1T + \omega}{(T^2 + a_o)}, \tag{2.5.20a}$$

$$\frac{dF}{dT} = \frac{F(-x^2/4 + (T-d_1/2)x - T^2 + (d_1-\frac{1}{2})T + b_1)}{(T^2 + a_o)}, \tag{2.5.20b}$$

where

$$b_1 = \rho_o + t_o^2 + (d_1 - \tfrac{1}{2})\, t_o. \tag{2.5.20c}$$

The solution of Equation (2.5.20a) is

$$\eta\,(x,T) = J_1(x,T) = \frac{x + d_1 - e_1\, T}{(T^2 + a_o)}, \tag{2.5.21}$$

where $e_1 = \omega/a_o$. From Equation (2.5.21) we have

$$x = (T^2 + a_o)\, J_1 + e_1\, T - d_1. \tag{2.5.22}$$

Substituting for x in the remaining trajectory equation (2.5.20b) we obtain a first order differential equation for F in the independent variable T, and this equation has the solution

$$J_2 = F \exp [\eta^2 T/4 + (1-e_1/2)^2 T + \ell n(T^2+a_o)/4$$
$$- \eta(1-e_1/2) \sqrt{(T^2+a_o)} - c_1 \int^T dy/(y^2+a_o)], \quad (2.5.23)$$

where

$$c_1 = t_o^2 + (d_1 - 1/2)t_o + (1-e_1/2)^2 a_o + d_1^2/4 + \rho_o.$$

The invariants J_1 and J_2 satisfy the necessary condition for the existence of an invariant group solution given in Section (3). The invariant group solution has the form:

$$J_2 = f(J_1),$$

or

$$F = f(\eta) \exp[-\eta^2 T/4 - (1-e_1/2)^2 T - \ell n(T^2+a_o)/4$$
$$+ \eta(1-e_1/2) \sqrt{(T^2+a_o)} + c_1 \int^T dy/(y^2+a_o)], \quad (2.5.24)$$

where the function $f(\eta)$ statisfies an ordinary differential equation obtained by requiring that the function F be a solution of the separable transport equation (2.2.9).

The differential equation for $f(\eta)$ is

$$\frac{d^2 f}{d\eta^2} + (a_o \eta^2/4 - c_1) f(\eta) = 0. \quad (2.5.25)$$

The Equation (2.5.25) has solutions:

if $a_o \neq 0$

$$f(\eta) = \exp(-\sqrt{-a_o}\, \eta^2/4) [A.M(c_1/(2\sqrt{-a_o}) + 1/4, 1/2, \sqrt{-a_o}\, \eta^2/2)$$
$$+ B.U(c_1/(2\sqrt{-a_o}) + 1/4, 1/2, \sqrt{-a_o}\, \eta^2/2)], \quad (2.5.26a)$$

and if $a_o = 0$,

$$f(\eta) = A.\exp(\sqrt{c_1}\, \eta) + B.\exp(-\sqrt{c_1}\, \eta). \quad (2.5.26b)$$

The functions M(a,b,x) and U(a,b,x) are standard solutions of Kummer's

confluent hypergeometric equation (2.5.19), and A and B are arbitrary constants.

Case 3 $K_{||} = K_o(p)\, r$, $K_\perp/K_{||} = e \neq 0$.

The generators of the group are given by Equations (2.4.7). The trajectories of the group with $\Omega = 0$ are

$$d\varepsilon = \frac{dx}{\gamma(t-t_o)} = \frac{dt}{\delta} = \frac{dF}{\gamma F(t-t_o-x/2+a)}$$

$$= \frac{d\theta}{A \sin\theta_o \sin(\phi-\phi_o)} = \frac{d\phi}{A(\sin\theta_o \cot\theta \cos(\phi-\phi_o)-\cos\theta_o)}, \qquad (2.5.27)$$

where $a = t_o + k/\gamma$. The integration of the group trajectories (2.5.27) falls naturally into two sub-cases according to the parameter δ, of Equations (2.4.7) is equal or not equal to zero. The case $\delta = 0$, corresponds to the monoenergetic point source solution, in which particles of momentum p_o are released at a steady rate from the heliocentric position (r_o, θ_o, ϕ_o). The condition $\delta = 0$ defines the subgroup of transformations under which the source point (r_o, θ_o, ϕ_o) remains invariant.

Without loss of generality we may choose coordinate axis such that $\theta_o = \phi_o = 0$ (cf. case (1)), and we use this to simplify the algebra in the work below, where we obtain the invariants and the group invariant solutions corresponding to the cases : (i) $\delta \neq 0$, and (ii) $\delta = 0$.

Case (i) $\delta \neq 0$

The invariants of the group with $\Omega = 0$ are given by the solutions of the trajectory equations (2.5.27), which are

$$J_1 = \eta(x,t) = x - \frac{\gamma T^2}{2\delta} \quad , \tag{2.5.28a}$$

$$J_2 = \mu \quad , \tag{2.5.28b}$$

$$J_3 = F \exp\left[\frac{\gamma}{\delta}\left(\left(\frac{J_1}{2} - a\right) T - \frac{T^2}{2} + \frac{\gamma T^3}{12\delta}\right)\right], \tag{2.5.28c}$$

$$J_4 = \phi + \frac{A.T}{\delta} = w \quad , \tag{2.5.28d}$$

where

$$T = t-t_o, \quad a = t_o + k/\gamma \tag{2.5.28e}$$

The similarity solutions are of the form

$$J_3 = f(J_1, J_2, J_4)$$

or

$$F = \exp\left[\frac{\gamma}{\delta}\left(-\frac{\gamma T^3}{12\delta} + \frac{T^2}{2} + (a - \frac{\eta}{2})T\right)\right] \quad f(\eta,\mu,w). \tag{2.5.29}$$

The function $f(\eta,\mu,w)$ is the solution of a partial differential equation obtained by requiring that the function F in Equation (2.5.29) satisfy the separable transport equation (2.2.9).

The function f satisfies the partial differential equation

$$\frac{\partial^2 f}{\partial \eta^2} - 2\frac{\partial f}{\partial \eta} + \frac{\gamma}{2\delta}(\eta-2a) f - \frac{A}{\delta}\frac{\partial f}{\partial w}$$

$$+ e\left((1-\mu^2)\frac{\partial^2 f}{\partial \mu^2} - 2\mu\frac{\partial f}{\partial \mu} + \frac{1}{1-\mu^2}\frac{\partial^2 f}{\partial w^2}\right) = 0. \tag{2.5.30}$$

If A = 0 then w = ϕ and Equation (2.5.30) has separable solutions:

$$f = P(\mu)\, Q(\phi)\, R(\eta), \tag{2.5.31a}$$

where

$$P''(\mu) - \frac{2\mu}{1-\mu^2} P'(\mu) + \left(\frac{\ell(\ell+1)}{1-\mu^2} - \frac{m^2}{(1-\mu^2)^2}\right) P(\mu) = 0, \tag{2.5.31b}$$

$$Q''(\phi) + m^2 Q(\phi) = 0, \tag{2.5.31c}$$

$$R''(\eta) - 2R'(\eta) + \left(\frac{\gamma}{2\delta}\eta - e\,\ell(\ell+1) - \frac{\gamma a}{\delta}\right) R(\eta) = 0. \tag{2.5.31d}$$

Equations (2.5.31b), (2.5.31c) have solutions in terms of associated Legendre polynomials and the exponential function. By suitable transformations Equation (2.5.31d) can be reduced to Bessel's equation. We can show that the general solution for $R(\eta)$ is

$$R(\eta) = e^{\eta}\sqrt{z}\left(A.J_{1/3}(2z^{3/2}/3) + B.J_{-1/3}(2z^{3/2}/3)\right),$$

where

$$z = (\gamma/2\delta)^{-2/3}\left[\gamma\eta/2\delta - \gamma a/\delta - 1 - e\,\ell(\ell+1)\right],$$

and $J_{1/3}(x)$ is a Bessel function of order 1/3 with argument x.

Substituting the solutions for $P(\mu)$, $Q(\phi)$ and $R(\eta)$ in Equation (2.5.31a) we obtain

$$f = e^{\eta}\sqrt{z}\left(A.J_{1/3}(2z^{3/2}/3) + B.J_{-1/3}(2z^{3/2}/3)\right)\left(C\,P_{\ell}^{m}(\mu) + D.Q_{\ell}^{m}(\mu)\right)e^{\pm im\phi}, \qquad (2.5.32)$$

where

$$z = (\gamma/2\delta)^{-2/3}\left[\gamma\eta/2\delta - \gamma a/\delta - 1 - e\,\ell(\ell+1)\right],$$

as the separated solution for f.

Case (ii) $\delta = 0$

The invariants of the group with $\Omega = 0$ are given by the solutions of the trajectory equations (2.5.27), which are:

$$J_1 = T, \qquad (2.5.33a)$$

$$J_2 = \mu, \qquad (2.5.33b)$$

$$J_3 = F\exp\left(\frac{x^2}{4T} - \frac{T+a}{T}x\right), \qquad (2.5.33c)$$

$$J_4 = \phi + \frac{Ax}{\gamma T} = w.$$

The similarity solutions are of the form

$$J_3 = f(J_1, J_2, J_4),$$

or

$$F = \exp\left(-\frac{x^2}{4T} + \frac{T+a}{T}\,x\right) \quad f(T, \mu, w). \tag{2.5.34}$$

The function $f(T,\mu, w)$ is the solution of a partial differential equation obtained by requiring that the function F in Equation (2.5.34) satisfy the separable transport equation (2.2.9).

The function f satisfies the partial differential equation

$$\frac{A^2}{\gamma^2 T^2}\,\frac{\partial^2 f}{\partial w^2} + \frac{2Aa}{\gamma T^2}\,\frac{\partial f}{\partial w} - \frac{\partial f}{\partial T} + f\left(\frac{a^2}{T^2} - 1 - \frac{1}{2T}\right)$$
$$+ e\left((1-\mu^2)\,\frac{\partial^2 f}{\partial \mu^2} - 2\mu\,\frac{\partial f}{\partial \mu} + \frac{1}{(1-\mu^2)}\,\frac{\partial^2 f}{\partial w^2}\right) = 0. \tag{2.5.35}$$

Taking A = O and $w = \phi$ Equation (2.5.35) separates into the ordinary differential equations

$$P''(\mu) - \frac{2\mu}{(1-\mu^2)}\,P'(\mu) + \left(\frac{\ell(\ell+1)}{(1-\mu^2)} - \frac{m^2}{(1-\mu^2)^2}\right)P(\mu) = 0, \tag{2.5.36a}$$

$$Q''(\phi) + m^2\,Q(\phi) = 0, \tag{2.5.36b}$$

$$R'(T) + \left(1 + \frac{1}{2T} + e\,\ell(\ell+1) - \frac{a^2}{T^2}\right)R(T) = 0, \tag{2.5.36c}$$

where

$$f = P(\mu)\;\; Q(\phi)\;\; R(T). \tag{2.5.36d}$$

Substituting the solutions for $P(\mu)$, $Q(\phi)$ and $R(T)$ in Equation (2.5.36d) we obtain

$$f(T,\mu,\phi) = \frac{1}{\sqrt{T}} \exp\left[\frac{-a^2}{T} - T\,[1+e\,\ell(\ell+1)]\right] \cdot$$
$$\left[A\,P_\ell^m(\mu) + B.Q_\ell^m(\mu)\right] \; e^{\pm im\phi} \tag{2.5.37}$$

as the separated solution for f.

The above completes the derivation of the analytic similarity solutions of the transport equation, which we use in later chapters to obtain solutions for specific boundary and source conditions.

CHAPTER 3

MONOENERGETIC SOURCE SOLUTIONS OBTAINED BY THE GROUP METHOD

3.1 Introduction

The steady state similarity solutions of the *homogeneous* equation of transport (2.2.9) of Chapter (2) are now used to obtain monoenergetic source solutions in which the distribution function F_o satisfies the boundary conditions

$$\begin{aligned} &(a) \quad F_o \to 0 \text{ as } r \to \infty, \\ &(b) \quad F_o \text{ is finite as } r \to 0. \end{aligned} \tag{3.1.1}$$

The interplanetary magnetic field is assumed to be radial and the diffusion coefficients parallel and perpendicular to the field, denoted by $K_{||}$ and $K_{\perp}$ are given by

$$K_{||} = K_o(p)\, r^b, \quad K_{\perp}/K_{||} = e, \tag{3.1.2}$$

where e is a constant and $K_o(p)$ is an arbitrary function of momentum p.

In this chapter these monoenergetic source solutions are obtained by using the group properties of the separable transport equation (Equation (2.2.9)). In Chapter (4) these solutions are obtained by using a Laplace transform method which is more widely known.

In the first solution the particles of the monoenergetic source have momentum p_o and are released from the heliocentric position (r_o, θ_o, ϕ_o) at a rate of N per second per steradian. This solution

is a function of heliocentric radius r, particle momentum p, and the angle Θ which is the polar angle referred to an axis through (Θ_o,ϕ_o).

If the source is located at the sun or infinity and the perpendicular diffusion coefficient $K_\perp \neq 0$, these solutions become spherically symmetric due to a diffusive flux perpendicular to the magnetic field at the source. For cases where $K_\perp = 0$, the particles are channelled in the direction (Θ_o,ϕ_o). We also note that if $K_\perp = K_{||}$, then diffusion is isotropic, and in this case the field need not be radial.

In the second solution particles of momentum p_o are released at a rate of N per second from a spherical surface at radius r_o. This latter solution is obtained by integrating the monoenergetic point source solution in which $N/(4\pi)$ particles per second per steradian are released from the heliocentric position (r_o, Θ_o, ϕ_o) with respect to the solid angle element $d\Omega_o = \sin\Theta_o\, d\Theta_o\, d\phi_o$, from $\Theta_o = 0$ to $\Theta_o = \pi$ and from $\phi_o = 0$ to $\phi_o = 2\pi$.

3.2 Derivation of the solutions

The monoenergetic point source solutions in which particles of momentum p_o are released at a rate of N per second per steradian from the heliocentric position (r_o, Θ_o, ϕ_o) are now obtained by using the group properties of the inhomogeneous equation of transport (2.2.9).

The infinitesimal generators of the group of transformations that leave the inhomogeneous Equation (2.2.9) invariant are a subset of the generators for the homogeneous equation (2.2.9) satisfying the conditions:

(i) The source point at (r_o, Θ_o, ϕ_o) is invariant under

transformations of G. This condition holds if the infinitesimal generators of G, namely $\xi^i(x, t, \mu, \phi)$, $i = 1(1)4$, are zero at the source point.

(ii) From Equation (2.3.32)

$$\sum_{i=1}^{n} \frac{\partial \xi^i(\underline{x}_o)}{\partial x^i} + \lambda(\underline{x}_o) = 0.$$

The conditions (i) and (ii) restrict the parameters occurring in the similarity variable η, and in the general similarity solutions of Section (2.5) to values appropriate for monoenergetic point source solutions. The boundary conditions (3.1.1) and the normalisation conditions:

If $b \neq 1$

$$F_o \to \frac{3N x_o \, \delta(x-x_o) \, \delta(\mu-\mu_o) \, \delta(\phi-\phi_o)}{8 \pi V p_o^3 r_o^2 |n+1|} \quad \text{as } T \to 0, \tag{3.2.1}$$

If $b = 1$

$$F_o \to \frac{3N \, \delta(x-x_o) \, \delta(\mu-\mu_o) \, \delta(\phi-\phi_o)}{8 \pi V p_o^3 r_o^2} \quad \text{as } T \to 0, \tag{3.2.2}$$

where

$$T = 3 \int_p^{p_o} K_o(z) \, z^{(1-3b)/2} \, dz/(2V),$$

combined with the restrictions (i) and (ii) are sufficient to determine the monoenergetic point source solutions. There are two cases to consider depending on the radial dependence of the diffusion coefficient.

Case (1) $K_{||} = K_o(p) \, r^b$, $b \neq 1$, $K_\perp/K_{||} = e$.

The generators of the group that leave the homogeneous transport equation invariant are given by Equations (2.4.5). The parameter restrictions (i) and (ii) determining the group generators of the

inhomogeneous transport equation (2.2.9) imply

$$a_o = \psi = 0, \qquad t_o = t(p_o), \quad x_o = x(r_o, p_o). \tag{3.2.3}$$

The condition $a_o = 0$, determines the similarity variable $\eta(x,t)$ of Equation (2.5.7) and we have

$$\eta = x/T,$$

where

$$x = 2(rp^{3/2})^{(1-b)/2}/(1-b).$$

$$T = 3 \int_p^{p_o} K_o(z)\, z^{(1-3b)/2}\, dz \,/\, (2V)$$

Using Equations (2.4.5) and (2.5.13d) the condition $\psi = 0$ implies

$$\delta = x_o^2/4 + (n+1)\, t_o, \qquad \chi = x_o^2/4\ , \tag{3.2.4}$$

in the similarity solution given in Equations (2.5.14) and (2.5.18).

The boundary conditions (3.1.1):

$F_o \to 0$ as $r \to \infty$;

F_o is finite as $r \to 0$;

require that coefficient of $K_\zeta(\sqrt{\chi}\,\eta)$ in the similarity solution given by Equations (2.5.14) and (2.5.18) be zero. Since $|\mu| \le 1$ the coefficient of the Legendre associated function $Q_\ell^m(\mu)$ in Equation (2.5.18) is zero from convergence considerations. Hence,

$$F_o = \frac{A\, x^{-n}}{T} \exp\left(-\frac{x^2+x_o^2}{4T}\right) \sum_{\ell=0}^{\infty} I_\zeta\left(\frac{x\, x_o}{2T}\right) \left[\sum_{m=1}^{\ell} [a_{m\ell}\cos(m\phi) + b_{m\ell}\sin(m\phi)]\, P_\ell^m(\mu) + c_\ell\, P_\ell(\mu)\right] \tag{3.2.5}$$

gives the form of the monoenergetic point source solution.

The normalisation condition (3.2.1):

$$F_o \rightarrow \frac{3N\, x_o\, \delta(x-x_o)\, \delta(\mu-\mu_o)\, \delta(\phi-\phi_o)}{8\,\pi\, V\, p_o^3\, r_o^2\, |\, n+1\,|} \quad \text{as } T \rightarrow 0, \tag{3.2.1}$$

corresponds to the release of N particles per second per steradian, of momentum p_o at the source point.

It is necessary to determine the coefficients $a_{m\ell}$, $b_{m\ell}$, c_ℓ to satisfy the condition (3.2.1). To do this we now proceed to obtain an expansion for the double Dirac delta function $\delta(\mu-\mu_o)\ \delta(\phi-\phi_o)$ in terms of $P_\ell(\mu)$, $P_\ell^m(\mu)\cos(m\phi)$, $P_\ell^m(\mu)\sin(m\phi)$. The coefficients $a_{m\ell}$, $b_{m\ell}$, c_ℓ satisfy:

$$\delta(\mu-\mu_o)\ \delta(\phi-\phi_o) = \sum_{\ell=0}^{\infty}\Big[c_\ell\, P_\ell(\mu) + \sum_{m=1}^{\ell}[a_{m\ell}\cos(m\phi) + b_{m\ell}\sin(m\phi)]\, P_\ell^m(\mu)\Big]. \tag{3.2.6}$$

The coefficients c_ℓ, $a_{m\ell}$, $b_{m\ell}$ are obtained by using the orthogonality relations

$$\int_{-1}^{1} P_\ell^m(\mu)\, P_s^m(\mu)\, d\mu = \frac{\Gamma(\ell+m+1)}{\Gamma(\ell-m+1)}\ (-1)^m\ \frac{2}{(2\ell+1)}\ \delta_{\ell s},$$

$$\int_{-1}^{1} P_\ell(\mu)\, P_s(\mu)\, d\mu = \frac{2}{(2\ell+1)}\ \delta_{\ell s}, \tag{3.2.7}$$

$$\int_0^{2\pi} \cos(m\phi)\cos(n\phi)\, d\phi = \int_o^{2\pi}\sin(m\phi)\sin(n\phi) = \pi\delta_{nm}$$

$$\int_0^{2\pi} \cos(m\phi)\sin(n\phi)\, d\phi = 0,$$

(Sneddon (1961) Sections (3.15) and (3.22))

where $\delta_{\ell s}$ is the Kronecker delta symbol and $\Gamma(z)$ is the gamma function of argument z.

Using the relations (3.2.7) we find

$$c_\ell = \frac{(2\ell+1)}{4\pi} P_\ell(\mu_o)$$

$$a_{m\ell} = \frac{(2\ell+1)}{2\pi} \frac{(-1)^m (\ell-m)!}{(\ell+m)!} P_\ell^m(\mu_o) \cos(m\phi_o). \qquad (3.2.8)$$

$$b_{m\ell} = \frac{(2\ell+1)}{2\pi} \frac{(-1)^m (\ell-m)!}{(\ell+m)!} P_\ell^m(\mu_o) \sin(m\phi_o),$$

as the expressions for c_ℓ, $a_{m\ell}$, and $b_{m\ell}$.

Substituting the coefficients c_ℓ, $a_{m\ell}$ and $b_{m\ell}$ from Equations (3.2.8) into the expansion (3.2.6) we have

$$\delta(\mu-\mu_o)\ \delta(\phi-\phi_o) = \sum_{\ell=0}^{\infty} \frac{2\ell+1}{4\pi} [P_\ell(\mu_o)\ P_\ell(\mu)$$

$$+ 2 \sum_{m=1}^{\ell} \frac{(-1)^m (\ell-m)!}{(\ell+m)!} P_\ell^m(\mu_o)\ P_\ell^m(\mu) \cos(m(\phi-\phi_o))]. \qquad (3.2.9)$$

Using the result

$$P_\ell(\cos \Theta) = P_\ell(\mu)\ P_\ell(\mu_o)$$

$$+ 2 \sum_{m=1}^{\ell} \frac{(-1)^m (\ell-m)!}{(\ell+m)!} P_\ell^m(\mu)\ P_\ell^m(\mu_o) \cos(m(\phi-\phi_o)),$$

where

$$\mu = \cos\Theta, \qquad \mu_o = \cos\Theta_o,$$

$$\cos\Theta = \cos\Theta \cos\Theta_o + \sin\Theta \sin\Theta_o \cos(\phi-\phi_o),$$

(Sneddon (1961), Section (3.23)), the expansion (3.2.9) can be expressed in the more compact form

$$\delta(\mu-\mu_o)\ \delta(\phi-\phi_o) = \sum_{\ell=0}^{\infty} \frac{2\ell+1}{4\pi} P_\ell(\cos\Theta). \qquad (3.2.10)$$

This is the expansion for $\delta(\mu-\mu_o)\ \delta(\phi-\phi_o)$ that we set out to obtain. We note that the angle Θ in Equation (3.2.10) is the polar angle referred to an axis through (Θ_o,ϕ_o).

The normalisation condition (3.2.1) is satisfied if

$$A = \frac{3N\, x_o^{n+2}}{16\,\pi\, V\, p_o^3\, r_o^2\, |(n+1)|},$$

in the expression (3.2.5) for F_o.

Substituting for the constants, A, c_ℓ, $a_{m\ell}$, $b_{m\ell}$ in the expression (3.2.5) we obtain the monoenergetic source solution corresponding to the release of N particles per steradian per second, of momentum p_o from the position (r_o,Θ_o,ϕ_o) as

$$F_o = \frac{3N\, x_o^2}{16\,\pi\, V\, p_o^3\, r_o^2\, |n+1|} \left(\frac{x_o}{x}\right)^n \frac{1}{T} \exp\left(-\frac{x^2+x_o^2}{4T}\right)$$

$$\sum_{\ell=0}^{\infty} \frac{2\ell+1}{4\pi} P_\ell(\cos\Theta) \; I_\zeta\left(\frac{x\, x_o}{2T}\right) \qquad (3.2.11)$$

where

$$\zeta = \sqrt{(n^2 + e\,\ell(\ell+1)\,(n+1)^2)},$$

$$x = 2(rp^{3/2})^{(1-b)/2} / (1-b),$$

$$T = 3\int_p^{p_o} K_o(z)\, z^{(1-3b)/2}\, dz/(2V),$$

$$n = (b+1) / (1-b),$$

$$e = K_\perp / K_{||}.$$

We note again that the diffusion coefficients in (3.2.11) are $K_{||} = K_o(p)r^b$ and $K_\perp = e\, K_{||}$, where e is a constant.

We now consider the structure of the monoenergetic source solution (3.2.11) as the source radius $r_o \to 0$. For particles to escape from $r_o = 0$ it is necessary to choose the parameter b, determining

the radial dependence of the diffusion coefficients to be less than one i.e. $b < 1$. If the perpendicular diffusion coefficient $K_\perp = e = 0$, $b < 1$, and we let $r_o \to 0$ in the solution (3.2.11) we find that

$$F_o = \frac{3N(n+1)^{2n+2}}{2^{2n+4}\,\pi\, V\, \Gamma(n+2)} \frac{1}{T^{n+1}} \exp\left(\frac{-x^2}{4T}\right) \sum_{\ell=0}^{\infty} \frac{2\ell+1}{4\pi} P_\ell(\cos\Theta), \tag{3.2.12}$$

which is a steady state solution of the equation of transport for solar cosmic-rays. The series in Equation (3.2.12) is an expansion for $\delta(\mu-\mu_o)\ \delta(\phi-\phi_o)$ (cf. Equation (3.2.10)), so that with $K_\perp = 0$, particles from the sun are channelled in the direction (Θ_o,ϕ_o).

However if $K_\perp \neq 0$, $b < 1$, and $r_o \to 0$ in the monenergetic point source solution (3.2.11) the only term in the right hand side of Equation (3.2.11) which remains non zero corresponds to $\ell = 0$ and the solution (3.2.11) becomes spherically symmetric due to a diffusive flux perpendicular to the magnetic field at the source. Hence the solar source solution in which N particles per second of momentum p_o are released from $r_o = 0$ is

$$F_o = \frac{3N\,(n+1)^{2n+2}}{2^{2n+6}\, V\, \pi^2\, \Gamma(n+2)} \frac{1}{T^{n+1}} \exp\left(\frac{-x^2}{4T}\right), \tag{3.2.13}$$

where $K_{||} = K_o(p)r^b$, $b < 1$, $K_\perp/K_{||} = e \neq 0$.

We now consider the character of the monoenergetic source solution (3.2.11) as the source radius $r_o \to \infty$, which corresponds to the case of galactic cosmic rays. In order to obtain a finite solution as $r_o \to \infty$ it is necessary to choose the parameter b, determining the radial dependence of the diffusion coefficients, to be greater

than one, i.e. $b > 1$, and to choose the injection rate N to be proportional to r_o^{b+1}.

If we choose

$$N = (b+1)N_g K_o(p_o) r_o^{b+1},$$

$$K_{||} = K_o(p) r^b, \; b > 1, \quad K_\perp = 0,$$

and let $r_o \to \infty$ in the monoenergetic point source solution (3.2.11) we obtain the solution for a monoenergetic galactic spectrum at infinity, i.e.

$$U_p = 4\pi p^2 F_o \to N_g \delta(p-p_o) \delta(\mu-\mu_o) \delta(\phi-\phi_o) \quad \text{as} \quad r \to \infty . \tag{3.2.14}$$

The solution is

$$F_o = \frac{3N_g K_o(p_o) p_o^{-3(1+b)/2}}{8 \pi V \Gamma(m)} \frac{1}{T} \left(\frac{x^2}{4T}\right)^m \exp\left(\frac{-x^2}{4T}\right)$$

$$\sum_{\ell=0}^{\infty} \frac{(2\ell+1)}{4\pi} P_\ell(\cos \Theta) , \tag{3.2.15}$$

where $K_\perp = 0$, $K_{||} = K_o(p) r^b$, $b > 1$, $m = (b+1)/(b-1)$. The solution (3.2.15) shows that with $K_\perp = 0$, monoenergetic galactic particles released from $r_o = \infty$ are channelled in the direction (Θ_o, ϕ_o). We note that the corresponding solar source solution (3.2.12) with $K_\perp = 0$ also has this property.

However if the perpendicular diffusion coefficient $K_\perp \neq 0$,

$$K_{||} = K_o(p) r^b, \quad b > 1, \quad K_\perp/K_{||} = e,$$

and

$$N = 4\pi(b+1) N_g K_o(p_o) r_o^{b+1} ,$$

and we let $r_o \to \infty$ in the monoenergetic point source solution (3.2.11), the only term on the right hand side of (3.2.11) which remains non

zero corresponds to $\ell = 0$. In this way we obtain the monoenergetic, spherically symmetric galactic spectrum solution in which

$$U_p \rightarrow N_g \, \delta(p-p_o) \quad \text{as} \quad r \rightarrow \infty \, . \tag{3.2.16}$$

This solution is

$$F_o = \frac{3 N_g K_o(p_o) p_o^{-3(1+b)/2}}{8 \pi V \Gamma(m)} \frac{1}{T} \left(\frac{x^2}{4T}\right)^m \exp\left(\frac{-x^2}{4T}\right) , \tag{3.2.17}$$

where $K_\perp \neq 0$, $K_{||} = K_o(p) \, r^b$, $b > 1$, $m = (b+1)/(b-1)$.

The solution (3.2.17) may also be obtained by a Laplace transform technique (see Section (4.3)), or by use of Green's theorem (see Section (6.3)).

To obtain the spherically symmetric monoenergetic source solution in which particles of momentum p_o are released at a rate of N particles per second from a spherical surface at radius r_o, we simply replace N by $N/(4\pi)$ in the monoenergetic point source solution (3.2.11) and integrate over the solid angle element $d\Omega_o = \sin\Theta_o \, d\Theta_o \, d\phi_o$ from $\Theta_o = 0$ to $\Theta_o = \pi$ and from $\phi_o = 0$ to $\phi_o = 2\pi$. Using the orthogonality relations (3.2.7) for the Legendre and associated Legendre polynomials, and carrying out the solid angle integrations we obtain

$$F_o = \frac{3N}{64 \pi^2 V p_o^3 r_o^2 \, |n+1|} \left(\frac{x_o}{x}\right)^n \frac{x_o^2}{T} \exp\left(-\frac{x^2+x_o^2}{4T}\right) I_m\left(\frac{x \, x_o}{2T}\right) . \tag{3.2.18}$$

For ready reference we note again

$$x = 2(rp^{3/2})^{(1-b)/2} / (1-b),$$

$$T = 3\int_p^{p_o} K_o(z) \, z^{(1-3b)/2} \, dz/(2V),$$

$$n = (b+1)/(1-b), \qquad m = |\, n \,|,$$

$$K_{||} = K_o(p) \, r^b, \quad b \neq 1, \quad K_\perp/K_{||} = e.$$

Case (2) $K_{||} = K_o(p)r, \quad K_\perp/K_{||} = e \neq 0$

For monoenergetic source solutions, the group generators (2.4.7) must satisfy the additional parameter restrictions (2.3.30) and (2.3.32), i.e.,

$$\xi^i(\underline{x}_o) = \sum_{i=1}^{4} \frac{\partial \xi^i(\underline{x}_o)}{\partial x^i} + \lambda(\underline{x}_o) = 0,$$

so that

$$\begin{aligned} \delta &= h = 0, \\ k &= \gamma(x_o/2 - t_o), \\ x_o &= x(r_o, p_o), \quad t_o = t(p_o). \end{aligned} \tag{3.2.19}$$

Using Equation (2.5.28e) the condition $k = \gamma(x_o/2 - t_o)$ is equivalent to

$$a = x_o/2. \tag{3.2.20}$$

Substituting the parameters (3.2.19), (3.2.20) into the similarity solution given by Equations (2.5.34) and (2.5.37) we find that the monoenergetic point source solution has the form

$$F_o = \frac{A}{\sqrt{T}} \exp\left[\frac{-(x-x_o)^2}{4T} + x - T\right],$$

$$\sum_{\ell=0}^{\infty} \left[c_\ell P_\ell(\mu) + \sum_{m=1}^{\ell} [a_{m\ell} \cos(m\phi) + b_{m\ell} \sin(m\phi)] P_\ell^m(\mu) \right]$$

$$\exp(-e\,\ell(\ell+1)\,T). \tag{3.2.21}$$

The normalisation condition (3.2.2) :

$$F_o \to \frac{3N\,\delta(x-x_o)\,\delta(\mu-\mu_o)\,\delta(\phi-\phi_o)}{8\,\pi\,V\,p_o^3\,r_o^2} \quad \text{as } T \to 0, \tag{3.2.2}$$

corresponds to the release of N particles per steradian per second of momentum p_o from the source point (r_o, Θ_o, ϕ_o). The constants c_ℓ, $a_{m\ell}$, $b_{m\ell}$ are determined from the expansion of the Double Dirac delta function $\delta(\mu-\mu_o)\,\delta(\phi-\phi_o)$ in terms of $P_\ell(\mu)$, $P_\ell^m(\mu)\cos(m\phi)$ and

$P_\ell^m(\mu)\ \sin(m\phi)$. These constants are the same as in case (1) and they are given by Equations (3.2.8). The normalisation condition (3.2.2) also implies

$$A = \frac{3\ N\ e^{-x_o}}{16\ \pi^{3/2}\ V\ p_o^3\ r_o^2}\ , \qquad (3.2.22)$$

in the expression (3.2.21) for F_o.

Substituting c_ℓ, $a_{m\ell}$, $b_{m\ell}$ from the Equations (3.2.8), and A from (3.2.22) in the solution (3.2.21), we obtain the monoenergetic point source solution in which particles of momentum p_o are released at a rate of N per second per steradian from the heliocentric position (r_o,Θ_o,ϕ_o). This solution is

$$F_o = \frac{3\ N}{6\ 4\ \pi^{5/2}\ V\ p_o^3\ r_o^2}\ \frac{1}{\sqrt{T}}\ \exp\left(x - x_o - \frac{(x-x_o)^2}{4T} - T\right)$$

$$\sum_{\ell=0}^{\infty}\ (2\ell+1)\ P_\ell(\cos\ \Theta\ )\ \exp\ (-e\ \ell(\ell+1)\ T), \qquad (3.2.23)$$

where

$$x = -\ell n(2\ r^2\ p^3)\ /2,$$

$$T = 3 \int_p^{p_o} K_o(z)\ z^{(1-3b)/2}\ dz\ /\ (2V),$$

$$\cos\ \Theta = \cos\ \Theta\ \cos\ \Theta_o + \sin\ \Theta\ \sin\ \Theta_o\ \cos(\phi-\phi_o),$$

i.e. Θ is the polar angle relative to an axis in the direction (Θ_o,ϕ_o).

Replacing N by $N/(4\pi)$ in the monenergetic point source solution (3.2.23), and integrating Equation (3.2.23) with respect to the solid angle element $d\Omega_o = \sin\ \Theta_o\ d\Theta_o\ d\phi_o$ from $\Theta_o = 0$ to $\Theta_o = \pi$ and from $\phi_o = 0$ to $\phi_o = 2\pi$ we obtain the spherically symmetric monoenergetic source solution in which particles of momentum p_o are released at a rate of N per second from a spherical surface at radius r_o. This

solution is:

$$F_o = \frac{3\,N}{6\,4\,\pi^{5/2}\,V\,p_o^3\,r_o^2}\;\frac{1}{\sqrt{T}}\;\exp\left(x-x_o-T-\frac{(x-x_o)^2}{4T}\right). \tag{3.2.24}$$

We note that the solutions (3.2.23) and (3.2.24) both tend to zero as $r_o \to 0$.

3.3 Remarks

The monoenergetic point source solutions in which particles of momentum p_o are released at a rate of N per second per steradian from the heliocentric position (r_o,Θ_o,ϕ_o) are given by Equations (3.2.11), (3.2.23). In these solutions the diffusion coefficients parallel and perpendicular to the "radial interplanetary magnetic field" have the form $K_{||} = K_o(p)\,r^b$, $K_\perp/K_{||} = e$. However if we have isotropic diffusion, i.e. $K_\perp = K_{||}$ the interplanetary magnetic field need not be assumed to be radial.

The spherical symmetric monoenergetic source solutions in which particles of momentum p_o are released at a rate of N per second from a spherical surface at radius r_o are given by Equations (3.2.18) and (3.2.24).

The monoenergetic galactic and solar source solutions are given in Equations (3.2.13) and (3.2.17) for the cases where $K_\perp \neq 0$. These solutions are spherical symmetric due to a diffusive flux perpendicular to the magnetic field at the source. For the case where $K_\perp = 0$, the monoenergetic galactic and solar point source solutions are given by Equations (3.2.15) and (3.2.12). In these solutions the particles are channelled in the direction (Θ_o, ϕ_o).

CHAPTER 4

THE LAPLACE TRANSFORM DERIVATION OF THE MONOENERGETIC SOURCE SOLUTIONS

4.1 Introduction

In this chapter the monoenergetic point source solutions of Chapter (3) are derived using a Laplace transform technique. In these solutions the distribution function F_o satisfies the boundary conditions

$$\begin{aligned} &\text{(a)} \quad F_o \to 0 \quad \text{as} \quad r \to \infty, \\ &\text{(b)} \quad F_o \text{ is finite as } r \to 0, \end{aligned} \tag{4.1.1}$$

and these solutions are derived in Section (2).

The interplanetary magnetic field is assumed to be radial and the diffusion coefficients parallel and perpendicular to the field denoted by $K_{||}$ and $K_{\perp}$ are given by

$$K_{||} = K_o(p)\, r^b, \quad K_{\perp}/K_{||} = e, \tag{4.1.2}$$

where e is a constant and $K_o(p)$ is an arbitrary function of momentum p. The solar wind velocity $\underline{V}$ is assumed to be radial and constant.

In Section (3) we derive the solution of the boundary value problem

$$\begin{aligned} &\text{(i)} \quad U_p = 4\pi p^2 F_o \to N_g\, \delta(p-p_o) \quad \text{as} \quad r \to \infty, \\ &\text{(ii)} \quad U_p \text{ is finite as } r \to 0, \\ &\text{(iii)} \quad \text{The diffusion coefficient } K = K_o(p)\, r^b, \quad b > 1, \end{aligned} \tag{4.1.3}$$

by the Laplace transform technique. The solution of the boundary

value problem (4.1.3) was given, without derivation, in Chapter (3).

4.2 Monoenergetic point source solutions

With a source of monoenergetic particles of momentum p_o released at heliocentric position (r_o, Θ_o, ϕ_o) at a rate of N particles per second, per steradian, the steady-state cosmic-ray equation of transport has the separable forms (2.2.7) and (2.2.8), i.e.,

if $K_{||} = K_o(p)\, r^b$, $b \neq 1$, $K_\perp/K_{||} = e$,

$$\frac{\partial^2 F_o}{\partial x^2} + \frac{2n+1}{x}\frac{\partial F_o}{\partial x} - \frac{\partial F_o}{\partial t} + e\frac{(n+1)^2}{x^2}\left[(1-\mu^2)\frac{\partial^2 F_o}{\partial \mu^2} - 2\mu\frac{\partial F_o}{\partial \mu} + \frac{1}{(1-\mu^2)}\frac{\partial^2 F_o}{\partial \phi^2}\right]$$

$$= \frac{-3\,N\,x_o\,\delta(x-x_o)\,\delta(t-t_o)\,\delta(\mu-\mu_o)\,\delta(\phi-\phi_o)}{8\,\pi\,V\,p_o^3\,r_o^2\,|n+1|} \qquad (4.2.1)$$

where

$$x = 2(rp^{3/2})^{(1-b)/2}/(1-b),$$

$$t = -3\int^p K_o(z)\, z^{(1-3b)/2}\, dz/(2V), \qquad (4.2.2)$$

$$n = (b+1)/(1-b);$$

if $K_{||} = K_o(p)\, r$, $K_\perp/K_{||} = e$, $b = 1$,

$$\frac{\partial^2 F_o}{\partial x^2} - 2\frac{\partial F_o}{\partial x} - \frac{\partial F_o}{\partial t} + e\left[(1-\mu^2)\frac{\partial^2 F_o}{\partial \mu^2} - 2\mu\frac{\partial F_o}{\partial \mu} + \frac{1}{(1-\mu^2)}\frac{\partial^2 F_o}{\partial \phi^2}\right]$$

$$= -\frac{3N\,\delta(x-x_o)\,\delta(t-t_o)\,\delta(\mu-\mu_o)\,\delta(\phi-\phi_o)}{8\,\pi\,V\,p_o^3\,r_o^2}, \qquad (4.2.3)$$

where

$$x = -\ell n\,(2r^2p^3)\,/\,2,$$

$$t = -3\int^{p} K_o(z)\, z^{(1-3b)/2}\, dz\,/\,(2V), \qquad (4.2.4)$$

and

$$t_o = t(p_o), \qquad x_o = x(r_o,p_o).$$

Using the Laplace transform technique there are two mono-energetic point source problems to consider according as the parameter b (determining the radial dependence of the diffusion coefficients) is equal or not equal to one.

To derive these solutions we first obtain separated solutions of the angular part of the partial differential equations (4.2.1) and (4.2.3) determining F_o, and hence we obtain

$$F_o = \sum_{\ell=0}^{\infty} \Big[\sum_{m=1}^{\ell} \left[a_{m\ell}\cos(m\phi) + b_{m\ell}\sin(m\phi)\right] P_\ell^m(\mu) + c_\ell\, P_\ell(\mu)\Big]$$

$$R\,(x,\, t,\, \ell), \qquad (4.2.5)$$

where $P_\ell^m(\mu)$ is a Legendre associated function and $P_\ell(\mu)$ is a Legendre polynomial of order ℓ. The second solution of Legendre's associated equation $Q_\ell^m(\mu)$ has not been included in the solution (4.2.5) since it has a singularity at $\mu = 1$ and hence is inappropriate for the present problem.

The coefficients $a_{m\ell}$, $b_{m\ell}$, and c_ℓ in the solution (4.2.5) are then determined from the normalisation conditions (3.2.1) and (3.2.2): If $b \neq 1$

$$F_o \to \frac{3N\, x_o\, \delta(x-x_o)\, \delta(\mu-\mu_o)\, \delta(\phi-\phi_o)}{8\,\pi\, V\, p_o^3\, r_o^2\, |n+1|} \quad \text{as } t \to t_o, \qquad (4.2.6)$$

if $b = 1$

$$F_o \rightarrow \frac{3N\ \delta(x-x_o)\ \delta(\mu-\mu_o)\ \delta(\phi-\phi_o)}{8\ \pi\ V\ p_o^3\ r_o^2} \quad \text{as} \quad t \rightarrow t_o. \tag{4.2.7}$$

The conditions (4.2.6) and (4.2.7) imply

$$\delta(\mu-\mu_o)\ \delta(\phi-\phi_o) = \sum_{\ell=0}^{\infty}\Big[\sum_{m=1}^{\ell}\ [a_{m\ell}\cos(m\phi) + b_{m\ell}\ \sin(m\phi)]\ P_\ell^m(\mu) + c_\ell\ P_\ell(\mu)\Big]. \tag{4.2.8}$$

The determination of the coefficients $a_{m\ell}$, $b_{m\ell}$, c_ℓ from the conditions (4.2.8) has been carried out in Chapter (3) in Equations (3.2.6)-(3.2.10). In Equation (3.2.10) it is shown that

$$\delta(\mu-\mu_o)\ \delta(\phi-\phi_o) = \sum_{\ell=0}^{\infty}\ \frac{2\ell+1}{4\pi}\ P_\ell(\cos\Theta), \tag{4.2.9}$$

where

$$\cos\Theta = \cos\Theta\cos\Theta_o + \sin\Theta\sin\Theta_o\cos(\phi-\phi_o), \tag{4.2.10}$$

and Θ is the polar angle referred to an axis through (Θ_o, ϕ_o).

Hence the solution of the Equations (4.2.1) and (4.2.3) for monoenergetic point source solutions reduces to the solution of a boundary value problem for the function $R(x, t, \ell)$ referred to in the expansion (4.2.5).

Putting $T = t-t_o$ and since $x = x(r,p)$, the function $R(x,t,\ell)$ must satisfy the conditions

(i) $R(x,T,\ell) \rightarrow 0$ as $r \rightarrow \infty$, (4.2.11a)

(ii) $R(x,T,\ell) \rightarrow$ a finite value as $r \rightarrow 0$, (4.2.11b)

(iii) If $b \neq 1$

$$R(x,T,\ell) \rightarrow \frac{3N\, x_o\, \delta(x-x_o)}{8\,\pi\, V\, p_o^3\, r_o^2 |n+1|} \quad \text{as } T \rightarrow 0, \tag{4.2.11c}$$

and if $b = 1$

$$R(x,T,\ell) \rightarrow \frac{3N\, \delta(x-x_o)}{8\,\pi\, V\, p_o^3\, r_o^2} \quad \text{as } T \rightarrow 0. \tag{4.2.11d}$$

The boundary value problem (4.2.11) for the function $R(x,t,\ell)$ is now solved by the Laplace transform method for the two types of diffusion coefficient mentioned previously in this section.

Case (1) $K_{||} = K_o(p)\, r^b$, $b \neq 1$, $K_\perp / K_{||} = e$

The function $R(x,t,\ell)$ satisfies the partial differential equation

$$\frac{\partial^2 R}{\partial x^2} + \frac{2n+1}{x}\,\frac{\partial R}{\partial x} - \frac{e\,\ell(\ell+1)(n+1)^2}{x^2}\,R = \frac{\partial R}{\partial T}\,. \tag{4.2.12}$$

Consider the Laplace transform of $R(x,t,\ell)$ with respect to T

$$u(x,s) = \int_0^\infty e^{-sT}\, R(x,T,\ell)\, dT. \tag{4.2.13}$$

Taking the Laplace transform of Equation (4.2.12) and the boundary conditions (4.2.11a) and (4.2.11b), the boundary value problem (4.2.11) for $R(x,T,\ell)$ reduces the boundary value problem for $u(x,s)$ given below.

$$\frac{d^2u}{dx^2} + \frac{2n+1}{x}\,\frac{du}{dx} - \left[\frac{e\,\ell(\ell+1)(n+1)^2}{x^2} + s\right] u = -R(x,0), \tag{4.2.14a}$$

$$R(x,0) = \frac{3N\, x_o\, \delta(x-x_o)}{8\,\pi\, V\, p_o^3\, r_o^2\, |n+1|}\,, \tag{4.2.14b}$$

$$u(x,s) \rightarrow 0 \quad \text{as} \quad r \rightarrow \infty, \tag{4.2.14c}$$

$$u(x,s) \quad \text{is finite as} \quad r \rightarrow 0. \tag{4.2.14d}$$

Since

$$x = 2(rp^{3/2})^{(1-b)/2} / |(1-b)|,$$

the boundary conditions (4.2.14c) and (4.2.14d) expressed in terms of x are:

<u>if b < 1</u>,

$$u(x,s) \rightarrow 0 \quad \text{as} \quad x \rightarrow \infty, \tag{4.2.14e}$$

$$u(x,s) \quad \text{is finite as} \quad x \rightarrow 0$$

and <u>if b > 1</u>,

$$u(x,s) \quad \text{is finite as} \quad x \rightarrow \infty, \tag{4.2.14f}$$

$$u(x,s) \rightarrow 0 \quad \text{as} \quad x \rightarrow 0.$$

The general solution of the inhomogeneous Equation (4.2.14a) is

$$u(x,s) = u_1(x,s)\left(c + \int^x \frac{R(z,0)\, u_2(z,s)}{W(u_1(z,s),u_2(z,s))}\, dz\right) + u_2(x,s)\left(d - \int^x \frac{R(z,0)\, u_1(z,s)}{W(u_1(z,s),\, u_2(z,s))}\, dz\right), \tag{4.2.15}$$

where $u_1(x,s)$ and $u_2(x,s)$ are independent solutions of the homogeneous Equation (4.2.14a), with wronskian $W(u_1(x,s), u_2(x,s))$ (Morse and Feshback, Methods of theoretical physics, Vol.1, Section (5.2.), p.529-530). The constants c and d are determined by the boundary conditions that are placed on u(x,s).

Two independent solutions of the homogeneous form of Equation

(4.2.14a) are:

$$u_1(x,s) = x^{-n} I_\zeta(\sqrt{s}\, x). \tag{4.2.16}$$

$$u_2(x,s) = x^{-n} K_\zeta(\sqrt{s}\, x), \tag{4.2.17}$$

where

$$\zeta = \sqrt{n^2 + e\,\ell(\ell+1)(n+1)^2}$$

The wronskian of $u_1(x,s)$ and $u_2(x,s)$ is

$$W(u_1, u_2) = -x^{-2n-1}. \tag{4.2.18}$$

The functions $u_1(x,s)$ and $u_2(x,s)$ have the properties:

$$u_1(x,s) \to \infty \text{ as } x \to \infty, \tag{4.2.19a}$$

$$u_1(x,s) \to 0 \text{ as } x \to 0, \tag{4.2.19b}$$

$$u_2(x,s) \to 0 \text{ as } x \to \infty, \tag{4.2.19c}$$

$$u_2(x,s) \to \infty \text{ as } x \to 0. \tag{4.2.19d}$$

Substituting the expressions (4.2.16) and (4.2.17) for $u_1(x,s)$ and $u_2(x,s)$ in the general solution (4.2.15) and using the properties of $u_1(x,s)$ and $u_2(x,s)$ for small and large x, to fit the boundary conditions (4.2.14) we obtain

$$u(x,s) = \frac{3N x_o}{8\pi V p_o^3 r_o^2 |n+1|} \left[x^{-n} K_\zeta(\sqrt{s}\, x) \int_0^x \delta(z-x_o)\, z^{n+1} I_\zeta(\sqrt{s}z)\,dz \right.$$

$$\left. + x^{-n} I_\zeta(\sqrt{s}\, x) \int_x^\infty \delta(z-x_o)\, z^{n+1} K_\zeta(\sqrt{s}\, z)\, dz \right]. \tag{4.2.20}$$

Carrying out the integrations in Equations (4.2.20) we have

$$u(x,s) = \frac{3 N x_o^{n+2}}{8 \pi V p_o^3 r_o^2 |n+1|} x^{-n} I_\zeta(\sqrt{s}\, x_o) K_\zeta(\sqrt{s}\, x) \text{ if } x > x_o,$$

and,

$$u(x,s) = \frac{3N\, x_o^{n+2}}{8\,\pi\, V\, p_o^3\, r_o^2\, |n+1|}\, x^{-n}\, I_\zeta(\sqrt{s}\, x)\, K_\zeta(\sqrt{s}\, x_o) \quad \text{if } x \le x_o. \tag{4.2.21}$$

The inverse Laplace transform of $u(x,s)$ gives the required solution of the boundary value problem (4.2.11) for $R(x,T,\ell)$. This solution is given by the Bromwich integral formula

$$R(x,T,\ell) = \frac{1}{2\pi i} \int_{c-i\infty}^{c+i\infty} u(x,s)\, e^{sT}\, ds. \tag{4.2.22}$$

From Erdelyi's Tables of integral transforms (vol.1, Section (5.16), p.284, formula (56))

$$\frac{1}{2\pi i} \int_{c-i\infty}^{c+i\infty} K_\zeta((\sqrt{\alpha}+\sqrt{\beta})\sqrt{s})\; I_\zeta(\sqrt{\alpha}-\sqrt{\beta})\sqrt{s})\; e^{sT}\, ds$$

$$= \frac{1}{2T}\; \exp\left(-\frac{\alpha+\beta}{2T}\right)\; I_\zeta\left(\frac{\alpha-\beta}{2T}\right) \tag{4.2.23}$$

where $\mathrm{Re}(\alpha) > 0$ and $\mathrm{Re}(\beta) > 0$. Substituting the expressions (4.2.21) for $u(x,s)$ in the Bromwich integral formula (4.2.22), and using the transform (4.2.23) with

$$\alpha = (x + x_o)^2/4, \quad \beta = (x - x_o)^2/4,$$

we obtain

$$R(x,T,\ell) = \frac{3N\, x_o^{n+2}}{16\,\pi\, V\, p_o^3\, r_o^2\, |n+1|}\; \frac{x^{-n}}{T}\; \exp\left(-\frac{x^2+x_o^2}{4T}\right)\; I_\zeta\left(\frac{x\, x_o}{2T}\right) \tag{4.2.24}$$

as the solution for $R(x,T,\ell)$.

Combining the expansion (4.2.9) for $\delta(\mu-\mu_o)\,\delta(\phi-\phi_o)$ and the expression (4.2.24) for $R(x,t,\ell)$ we obtain the monoenergetic point

source solution in which particles of momentum p_o are released at a rate of N per second per steradian from the heliocentric position (r_o, Θ_o, ϕ_o). The solution is

$$F_o = \frac{3 N x_o^2}{16 \pi V p_o^3 r_o^2 |n+1|} \left(\frac{x_o}{x}\right)^n \frac{1}{T} \exp\left(-\frac{x^2+x_o^2}{4T}\right)$$

$$\sum_{\ell=0}^{\infty} \frac{(2\ell+1)}{4\pi} P_\ell(\cos \Phi) I_\zeta\left(\frac{x x_o}{2T}\right) . \qquad (4.2.25)$$

where

$$K_{||} = K_o(p) r^b, \quad b \neq 1, \quad K_\perp/K_{||} = e,$$

$$n = (b+1)/(1-b),$$

$$\zeta = \sqrt{n^2 + e \ell(\ell+1)(n+1)^2},$$

$$x = 2(rp^{3/2})^{(1-b)/2} / (1-b),$$

$$T = 3 \int_p^{P_o} K_o(z) z^{(1-3b)/2} dz / (2V).$$

$$\cos \Phi = \cos \Theta \cos \Theta_o + \sin \Theta \sin \Theta_o \cos (\phi-\phi_o).$$

The result (4.2.25) has been given in Equation (3.2.11) of Chapter (3).

Case (2) $K_{||} = K_o(p)r, \quad K_\perp/K_{||} = e$

The function $R(x,T,\ell)$ satisfies the partial differential equation

$$\frac{\partial^2 R}{\partial x^2} - 2 \frac{\partial R}{\partial x} - e \ell(\ell+1) R = \frac{\partial R}{\partial T} . \qquad (4.2.26)$$

Consider the Laplace transform of $R(x,T,\ell)$ with respect to T:

$$u(x.s) = \int_o^\infty e^{-sT} R(x,T,\ell) dT.$$

Taking the Laplace transform of Equation (4.2.26) and the boundary

conditions (4.2.11a) and (4.2.11b), the boundary value problem (4.2.11) for $R(x,T,\ell)$ is reduced to the following boundary value problem for $u(x,s)$

$$\frac{d^2u}{dx^2} - 2\frac{du}{dx} - (e\,\ell(\ell+1) + s)\,u = -R(x,0), \tag{4.2.27a}$$

$$R(x,0) = \frac{3N\,\delta(x-x_o)}{8\,\pi\,V\,p_o^3\,r_o^2}, \tag{4.2.27b}$$

$$\begin{aligned} &u(x,s) \to 0 \text{ as } r \to \infty, \\ &u(x,s) \text{ is finite as } r \to 0. \end{aligned} \tag{4.2.27c}$$

Since $x = -\ell n(2r^2p^3)/2$, the boundary conditions expressed in terms of x are

$$\begin{aligned} &u(x,s) \to 0 \text{ as } x \to -\infty, \\ &u(x,s) \text{ is finite as } x \to \infty. \end{aligned} \tag{4.2.27d}$$

The general solution of the inhomogeneous form of Equation (4.2.27a) is:

$$u(x,s) = u_1(x,s)\left(c + \int^x \frac{R(z,0)\,u_2(z,s)}{W(u_1(z,s),u_2(z,s))}\,dz\right) + u_2(x,s)\left(d - \int^x \frac{R(z,0)\,u_1(z,s)}{W(u_1(z,s),u_2(z,s))}\,dz\right), \tag{4.2.28}$$

where $u_1(x,s)$ and $u_2(x,s)$ are independent solutions of the homogeneous form of Equation (4.2.27a), $W(u_1(x,s), u_2(x,s))$ is the wronskian of u_1 and u_2 and c and d are constants determined by the boundary conditions (cf. case (1)).

Two independent solutions of the homogeneous form of Equation (4.2.27a) are

$$u_1(x,s) = \exp\left[\left(1 + \sqrt{1+s+e\,\ell(\ell+1)}\right)x\right], \tag{4.2.29}$$

and

$$u_2(x,s) = \exp\left[\left(1 - \sqrt{1 + s + e\,\ell(\ell+1)}\right) x\right]. \tag{4.2.30}$$

The wronskian of u_1 and u_2 is

$$W(u_1(x,s),\, u_2(x,s)) = -\,2\sqrt{1 + s + e\,\ell(\ell+1)}\ \exp(2x). \tag{4.2.31}$$

For large positive x and large negative x we have:

$$u_1(x,s) \to 0 \quad \text{as} \quad x \to -\infty, \quad u_1(x,s) \to \infty \quad \text{as} \quad x \to \infty, \tag{4.2.32a}$$

$$u_2(x,s) \to \infty \quad \text{as} \quad x \to -\infty, \quad u_2(x,s) \to 0 \quad \text{as} \quad x \to \infty\ . \tag{4.2.32b}$$

Substituting the expressions (4.2.29) and (4.2.30) for $u_1(x,s)$ and $u_2(x,s)$ in the general solution (4.2.28), and using the properties (4.2.32) of $u_1(x,s)$ and $u_2(x,s)$ for large $|x|$ to fit the boundary conditions (4.2.27d), we obtain

$$u(x,s) = \frac{3N}{16\,\pi\,V\,p_o^3\,r_o^2\sqrt{1+s+e\,\ell(\ell+1)}}\Big[\exp\left[\left(1-\sqrt{1+s+e\,\ell(\ell+1)}\right)x\right]\cdot$$
$$\int_{-\infty}^{x}\delta(z-x_o)\exp\left[\left(\sqrt{1+s+e\,\ell(\ell+1)}-1\right)z\right]dz$$
$$+\exp\left[\left(1+\sqrt{1+s+e\,\ell(\ell+1)}\right)x\right]\int_{x}^{\infty}\delta(z-x_o)\exp\left[-\left(1+\sqrt{1+s+e\,\ell(\ell+1)}\right)z\right]dz\Big]. \tag{4.2.33}$$

Carrying out the integrations in (4.2.33) we have

$$u(x,s) = \frac{3N}{16\,\pi\,V\,p_o^3\,r_o^2\sqrt{1+s+e\,\ell(\ell+1)}}\exp\left[\left(1-\sqrt{1+s+e\ell(\ell+1)}\right)(x-x_o)\right]$$
$$\text{if } x > x_o, \tag{4.2.34a}$$

and

$$u(x,s) = \frac{3N}{16\,\pi\,V\,p_o^3\,r_o^2\sqrt{1+s+e\,\ell(\ell+1)}}\exp\left[\left(1+\sqrt{1+s+e\ell(\ell+1)}\right)(x-x_o)\right]$$
$$\text{if } x < x_o, \tag{4.2.34b}$$

as the required solution for u(x,s).

The inverse Laplace transform of u(x,s) :

$$R(x,T,\ell) = \frac{1}{2\pi i} \int_{c-i\infty}^{c+i\infty} u(x,s)\, e^{sT}\, ds, \tag{4.2.35}$$

is the solution of the boundary value problem (4.2.11). Putting $p = 1 + s + e\,\ell(\ell+1)$ and using the expressions (4.2.34) for $u(x,s)$ in the transform (4.2.35) we have

$$R(x,T,\ell) = \frac{3N}{16\,\pi\,V\,p_o^3\,r_o^2} \exp\left[x-x_o-(1+e\,\ell(\ell+1))\,T\right] \frac{1}{2\pi i} \int_{c-i\infty}^{c+i\infty} \exp(pT)\, \frac{\exp(-\sqrt{p}\,|x-x_o|)}{\sqrt{p}}\, dp. \tag{4.2.36}$$

From Erdelyi, Tables of integral transforms (vol.1, Section (5.6), p. 246, formula (6)):

$$\frac{1}{2\pi i} \int_{\sigma-i\infty}^{\sigma+i\infty} \frac{1}{\sqrt{p}}\, e^{-\sqrt{\alpha}\sqrt{p}}\, e^{pt}\, dp = \frac{1}{\sqrt{\pi t}} \exp\left(-\frac{\alpha}{4t}\right). \tag{4.2.37}$$

Using the transform (4.2.37) with

$$\alpha = (x-x_o)^2 \quad \text{and} \quad t = T,$$

in the result (4.2.36) we obtain

$$R(x,T,\ell) = \frac{3N}{16\,\pi^{3/2}\,V\,p_o^3\,r_o^2} \frac{1}{\sqrt{T}} \exp\left[x - x_o - [1+e\,\ell(\ell+1)]\,T - \frac{(x-x_o)^2}{4T}\right] \tag{4.2.38}$$

as the solution for $R(x,T,\ell)$.

Combining the expansion (4.2.9) for $\delta(\mu-\mu_o)\,\delta(\phi-\phi_o)$ and the solution (4.2.38) for $R(x,T,\ell)$ we obtain the monoenergetic point source solution in which particles of momentum p_o are released at a radius r_o at a rate of N per second per steradian from the heliocentric position (r_o, Θ_o, ϕ_o).

The solution is :

$$F_o = \frac{3\,N}{16\,\pi^{3/2}\,V\,p_o^3\,r_o^2}\,\frac{1}{\sqrt{T}}\,\exp\left[x - x_o - T - \frac{(x-x_o)^2}{4T}\right].$$

$$\sum_{\ell=0}^{\infty} \frac{(2\ell+1)}{4\pi}\,P_\ell(\cos\Theta)\,\exp\left[-e\,\ell(\ell+1)\,T\right], \tag{4.2.39}$$

where

$$K_{||} = K_o(p)\,r, \qquad K_\perp/K_{||} = e,$$

$$x = -\ell n(2r^2p^3)/2,$$

$$T = 3\int_p^{p_o} K_o(z)\,z^{(1-3b)/2}\,dz\,/(2V),$$

$$\cos\Theta = \cos\theta\cos\theta_o + \sin\theta\sin\theta_o\cos(\phi-\phi_o).$$

The solution (4.2.39) has been given previously in Equation (3.2.23) of Chapter (3).

4.3. The monoenergetic galactic spectrum solution

We now proceed to solve the boundary value problem (4.1.3) in which the number density U_p is a monoenergetic spectrum at infinity and U_p is finite as $r \to 0$, i.e. in terms of F_o:

$$\text{(i)} \quad F_o \to \frac{N_g\,\delta(p-p_o)}{4\,\pi\,p_o^2} \quad \text{as} \quad r \to \infty,$$

$$\text{(ii)} \quad F_o \text{ is finite as } r \to 0, \tag{4.3.1}$$

$$\text{(iii)} \quad \text{the diffusion coefficient } K = K_o(p)\,r^b,\ b > 1.$$

For the problem (4.3.1) the distribution function F_o satisfies the spherically symmetric equation of transport with zero source term. Hence from Equation (2.2.7) we have:

$$\frac{\partial^2 F_o}{\partial x^2} + \frac{2n+1}{x} \frac{\partial F_o}{\partial x} = \frac{\partial F_o}{\partial T} \tag{4.3.2}$$

where

$$x = 2(rp^{3/2})^{(1-b)/2} / |(1-b)|,$$

$$n = (b+1)/(1-b),$$

$$T = 3 \int_p^{p_o} K_o(z)\, z^{(1-3b)/2}\, dz / (2V),$$

Since

$$\delta(p-p_o) = \delta(T) \left|\frac{dT}{dp}\right| = \frac{3\, K_o(p_o)\, p_o^{(1-3b)/2}}{2\, V}\, \delta(T), \tag{4.3.3}$$

the boundary value problem (4.3.1) expressed in terms of x and T is

$$\text{(i)}\quad F_o \to \frac{3\, K_o(p_o)\, p_o^{-3(1+b)/2}\, N_g\, \delta(T)}{8\, \pi\, V} \quad \text{as} \quad x \to 0, \tag{4.3.4}$$

$$\text{(ii)}\quad F_o \text{ is finite as } x \to \infty.$$

Consider the Laplace transform of F_o with respect to T:

$$u(x,s) = \int_0^{\infty} e^{-sT}\, F_o(x,T)\, dT. \tag{4.3.5}$$

Taking the Laplace transform of Equation (4.3.2) and the boundary conditions (4.3.4) the boundary value problem (4.3.1) becomes the following boundary value problem for u(x,s)

$$\frac{d^2 u}{dx^2} + \frac{2n+1}{x} \frac{du}{dx} - s\, u = 0, \tag{4.3.6a}$$

$$u(x,s) \to 0 \quad \text{as} \quad x \to \infty, \tag{4.3.6b}$$

$$u(x,s) \to \frac{3\, K_o(p_o)\, p_o^{-3(1+b)/2}}{8\, \pi\, V}\, N_g \quad \text{as} \quad x \to 0. \tag{4.3.6c}$$

The general solution of the ordinary differential equation (4.3.6a) is

$$u(x,s) = [A \cdot I_m(\sqrt{s}\, x) + B \cdot K_m(\sqrt{s}\, x)]\, x^m, \qquad (4.3.7)$$

where $m = |n|$ and $I_m(z)$ and $K_m(z)$ are modified Bessel functions of the first and second kind of argument z.

The boundary condition at $x = \infty$, (4.3.6b) is satisfied if we choose $A = 0$ in the general solution (4.3.7). Using the result

$$K_m(z) \sim \Gamma(m)\, (z/2)^{-m}/2 \quad \text{as} \quad z \to 0, \qquad (4.3.8)$$

we find that the boundary condition at $x = 0$, (4.3.6c) is satisfied for

$$B = \frac{3N_g\, K_o(p_o)\, p_o^{-3(1+b)/2}\, s^{m/2}}{2^{m+2}\, \pi\, V\, \Gamma(m)}, \qquad (4.3.9)$$

and

$$u(x,s) = \frac{3\, N_g\, K_o(p_o) p_o^{-3(1+b)/2}}{2^{m+2}\, \pi\, V\, \Gamma(m)}\; s^{m/2}\, x^m\, K_m(\sqrt{s}\, x). \qquad (4.3.10)$$

Inverting the Laplace transform (4.3.10) for u(x,s) we obtain

$$F_o = \frac{3N_g\, K_o(p_o)\, p_o^{-3(1+b)/2}}{2^{m+2}\, \pi\, V\, \Gamma(m)}\; \frac{1}{2\pi i} \int_{c-i\infty}^{c+i\infty} s^{m/2}\, K_m(\sqrt{s}\, x)\, e^{sT}\, x^m\, ds. \qquad (4.3.11)$$

Using the result

$$\frac{1}{2\pi i} \int_{c-i\infty}^{c+i\infty} \alpha^{-\nu/2}\, p^{\nu/2}\, K_\nu(2\sqrt{\alpha}\sqrt{p})\, e^{pt}\, dp = t^{-\nu-1}\, e^{-\alpha/t}/2, \qquad (4.3.12)$$

(Erdelyi et.al. (1954), Vol.1, Section (5.16), p. 283), the expression (4.3.11) for F_o becomes:

$$F_o = \frac{3\, N_g\, K_o(p_o)\, p_o^{-3(1+b)/2}}{8\,\pi\, V\, \Gamma(m)} \left(\frac{x^2}{4T}\right)^m \frac{1}{T} \exp\left(\frac{-x^2}{4T}\right). \qquad (4.3.13)$$

The solution (4.3.13) is the monoenergetic galactic spectrum solution (3.2.17), which was given, without derivation in Chapter (3).

CHAPTER 5

GREEN'S FUNCTIONS

5.1 Introduction

In this chapter we use the results of Chapter (2) to determine general solutions for cases in which we can specify the distribution function F_o on two boundaries at radii $r = r_a$ and $r = r_b$, with the intention of obtaining spherically symmetric Green's functions. The Green's function is the solution for a monoenergetic source of momentum p_o, at radius r_o and in general with $F_o = 0$ at boundaries $r = r_a$ and $r = r_b$, where $r_a < r_o < r_b$.

The expressions (2.5.7) and (2.5.21) for the similarity variable $\eta(x,t)$ are in general functions of radius r and momentum p. The curves

$$\eta(x,t) = \text{constant},$$

where,

$$\begin{aligned} t &= -(3/(2V))\int^{p} K_o(z)\, z^{(1-3b)/2}\, dz, \\ x &= [2/(1-b)](rp^{3/2})^{(1-b)/2} \quad \text{if} \quad b \neq 1, \\ \text{and} \qquad & \qquad (5.1.1) \\ x &= -\ell n(2r^2p^3)/2 \quad \text{if} \quad b = 1, \end{aligned}$$

may be used as boundary curves for the general similarity solutions of Section (2.5).

In Section (2) we show that the variable $z = \alpha\eta$ (where α is a constant which may be made infinitely large) is a function

of radius only for diffusion coefficients of the form $K_{||} = K_o\, r^b$ or $K_{||} = K_o\, r^b\, p^{3/4(b-1)}$ and appropriate choice of the parameters a_o, t_o, e_1, d_1 which define η in Equations (2.5.7) and (2.5.21). The case b = 1 is degenerate so three separate similarity solutions arise for which z = z(r); they are for

$$\begin{aligned} &(1)\quad K_{||} = K_o\, r^b\, p^{3/4(b-1)}, \quad b \neq 1, \\ &(2)\quad K_{||} = K_o\, r^b, \quad b \neq 1, \\ &(3)\quad K_{||} = K_o\, r, \end{aligned} \tag{5.1.2.}$$

and these solutions are given below.

In Section (3) we use the general similarity solutions of Section (2) to obtain the spherical symmetric Green's functions for cases where z = z(r) and boundaries at r_a and r_b. In the case where $r_b = \infty$ and there is no inner boundary we obtain a spherical symmetric Green's function for general diffusion coefficients $K_{||} = K_o(p)\, r^b$, $K_\perp/K_{||} = e$. These latter solutions are the spherical symmetric monoenergetic-source solutions (3.2.18) and (3.2.24) with appropriate values of the normalisation constant N.

5.2. Similarity solutions for cases where z = z(r)

Case (1) $K_{||} = K_o\, r^b\, p^{3(b-1)/4}$, $b \neq 1$

The similarity variable $\eta(x,t)$ is given by Equation (2.5.7):

$$\eta = \frac{x}{\sqrt{(t-t_o)^2 + a_o}}, \tag{5.2.1}$$

with x and t given by Equations (5.1.1)

Choosing $a_o = t_o = 0$ we have

$$t = 2K_o\, p^{3(1-b)/4}/(V(b-1)), \tag{5.2.2}$$

$$z = \eta = x/t = Vr^{(1-b)/2}/K_o, \tag{5.2.3}$$

and the similarity solution given by Equations (2.5.14) and (2.5.18) becomes

$$F_o(r,p) = \exp(-z^2t/4-\chi/t)z^{-n}\, t^{-n-1}\ [A.I_\zeta(\sqrt{\chi}\, z) + B.K_\zeta(\sqrt{\chi}\, z)]$$
$$.\ [C.P_\ell^s(\mu) + D.Q_\ell^s(\mu)]\ e^{\pm is\phi}, \tag{5.2.4}$$

where

$$n = (b+1)/(1-b),$$
$$\zeta = \sqrt{n^2 + e(n+1)^2\ \ell(\ell+1)},$$

and s and ℓ are positive integers with $s \le \ell$.

The spherical symmetric part of the solution (5.2.4) is

$$F_o(r,p) = \exp(-z^2t/4-\chi/t)z^{-n}\, t^{-n-1}\ .\ [A.I_m(\sqrt{\chi}\, z) + B.K_m(\sqrt{\chi}\, z)], \tag{5.2.5}$$

where $m = |\, n\, |$.

Case (2) $K_{||} = K_o\, r^b$, $b \neq 1$

The similarity variable $\eta(x,t)$ for this case is given by the expression (2.5.7):

$$\eta(x,t) = x/\sqrt{((t-t_o)^2 + a_o)}\ , \tag{5.2.6}$$

where x and t are defined in (5.1.1).

We now let $a_o = -t_o^2 \to \infty$ and we introduce a new similarity variable

$$z = \lim_{t_o \to \infty} \frac{-t_o \eta^2}{2} = x^2/(4t). \tag{5.2.7}$$

For a diffusion coefficient $K_{||} = K_o\, p^a\, r^b$, the expression (5.1.1) for t is

$$t = -\frac{3K_o}{2V}\,\frac{p\delta}{\dot{\delta}}\,, \tag{5.2.8}$$

where

$$\delta = a + 3(1-b)/2,$$

and the expression (5.2.7) for z is

$$z = -2V\,\delta\, r^{1-b}\, p^{-a}/(3(1-b)^2 K_o). \tag{5.2.9}$$

Hence if $K_{||} = K_o\, r^b$, $b \neq 1$, from the results (5.2.9) and (5.2.8) we have

$$t = K_o\, p^{3(1-b)/2}/(V(b-1)), \tag{5.2.10}$$

$$z = V\, r^{1-b}/\,(K_o(b-1))\,, \tag{5.2.11}$$

as the appropriate expressions for t and z.

The similarity solution for a diffusion coefficient $K_{||} = K_o\, r^b$, is given by the expressions (2.5.14) and (2.5.17). Letting $a_o = -t_o^2 \to \infty$ in (2.5.14) and (2.5.17), defining

$$\nu = \lim_{a_o \to \infty} \frac{x}{2t_o}\,, \tag{5.2.12}$$

and scaling the expression (2.5.17) so that we obtain a finite result we find

$$F_o = t^{\nu-(n+1)/2}\, z^{(\zeta-n)/2}\, e^{-z}\, [A_o \,.\, M((1+\zeta)/2 + \nu,\ 1+\zeta,\ z) + B_o \,.\, U(1+\zeta)/2 + \nu,\ 1+\zeta,\ z)] \,.\, [C.P_\ell^s(\mu) + D.Q_\ell^s(\mu)]\, e^{\pm is\phi}, \tag{5.2.13}$$

where

$$n = (b+1)/(1-b),$$

$$\zeta = \sqrt{n^2 + e\ \ell(\ell+1)(n+1)^2}\ ,$$

s and ℓ are positive integers with $s \leq \ell$, and A_o and B_o are arbitrary constants.

The spherical symmetric part of the solution (5.2.13) is

$$F_o = t^{\nu-(n+1)/2}\, e^{-z}\, [A_o \,.\, M((1+n)/2 + \nu,\ 1+n,\ z) + B_o \,.\, U(1+n)/2 + \nu,\ 1+n,\ z)], \tag{5.2.14}$$

and this is the form of the solution that we will use later in our analysis.

Case (3) $K_{||} = K_o\, r$

For a diffusion coefficient $K_{||} = K_o\, r$ the similarity variable $\eta(x,t)$ is given by the expression (2.5.21):

$$\eta(x,t) = \frac{x + d_1 + e_1\ (t-t_o)}{(t-t_o)^2 + a_o}\ , \tag{5.2.15}$$

where

$$x = -\ln(2)/2 - \ln r - (3/2)\ln(p),$$

$$t = -(3K_o/(2V))\ln(p), \quad t_o = t(p_o),$$

$$T = t - t_o,$$

and e_1, d_1, and a_o are arbitrary constants.

We now let $a_o = a^2 \to \infty$ and we introduce a new similarity variable z:

$$z = \lim_{a \to \infty} a^{2\eta}$$

$$= d_1 - \ln(2)/2 - (3K_o/(2V))e_1 \ln(p_o) - (3/2)\ln(p)$$

$$+(3K_o e_1/(2V))\ln(p) - \ln(r). \qquad (5.2.16)$$

We choose e_1 and d_1 so that z is a function of radius r only and hence putting

$$e_1 = V/K_o, \quad d_1 = \ln(2)/2 + (3/2)\ln(p_o), \qquad (5.2.17)$$

we obtain

$$z = -\ln(r), \qquad (5.2.18)$$

as the appropriate expression for our similarity variable.

The similarity solution for this case is given by the results (2.5.24) and (2.5.26a) :

$$F_o = \exp\Big[-\eta^2 T/4 - (1-e_1/2)^2 T - \ell n(T^2+a_o)/4 + \eta(1-e_1/2)\sqrt{T^2+a_o} + c_1 \int^T dy/(y^2+a_o)\Big] \cdot \exp(-\sqrt{-a_o}\,\eta^2/4)\Big[A_o \cdot M(c_1/(2\sqrt{-a_o}) + 1/4,\ 1/2,\ \sqrt{-a_o}\,\eta^2/2) + B_o \cdot \sqrt{(\sqrt{-a_o}\,\eta^2/2)}\ M(c_1/(2\sqrt{-a_o}) + 3/4,\ 3/2,\ \sqrt{-a_o}\,\eta^2/2)\Big]$$

(5.2.19)

Letting $a_o = a^2 \to \infty$, defining

$$\nu^2 = \lim_{a \to \infty} c_1/a^2, \quad c = 1 - V/(2K_o), \tag{5.2.20}$$

and using the results

$$\lim_{a \to \infty} M(-i\nu^2 a/2+1/4,1/2,iz^2/(2a)) = (e^{\nu z} + e^{-\nu z})/2,$$

$$\lim_{a \to \infty} \sqrt{iz^2/2}\ M(3/4 - ia\nu^2/2,\ 3/2,\ iz^2/(2a)) = \frac{(e^{\nu z} - e^{-\nu z})\sqrt{i}}{2\sqrt{2}\,\nu}$$

(5.2.21)

(Abramowitz and Stegun (1964), Section 13.5).

the similarity solution (5.2.19) becomes

$$F_o = (A\, e^{\nu z} + B\, e^{-\nu z}) \exp((\nu^2 - c^2)\, T + c\, z). \tag{5.2.22}$$

An alternative form of the solution (5.2.22) in terms of radius r and momentum p is

$$F_o = r^{-c}\,(A\, r^{-\nu} + B\, r^{\nu})\ p^{-3d(\nu^2-c^2)/2}, \tag{5.2.23}$$

where

$$c = 1 - V/(2K_o), \quad d = K_o/V.$$

5.3 The Green's Functions

We now extend the general solutions for F_o in cases with η a function of r only, given in Section (2), and obtain the Green's functions for those particular cases. The Green's function is the solution for monoenergetic release with momentum p_o, at radius r_o, and in general with $F_o = 0$ at boundaries r_a, r_b with $r_a < r_o < r_b$. We denote it by G_F $(r, p; r_o, p_o, r_a, r_b)$ and here restrict ourselves to the spherically symmetric problem.

Solutions which have $F_o = 0$ at r_a and r_b are in general sums of eigensolutions of the general solution. For example in the case $K_{||} = K_o r^b p^{3(b-1)/4}$ where the general solution is given by Equation (5.2.5), the constants χ must have values χ_s set by the eigenvalue equation

$$I_m[\sqrt{\chi_s}\, z(r_a)]\; K_m[\sqrt{\chi_s}\, z(r_b)] - I_m[\sqrt{\chi_s}\, z(r_b)]\, K_m[\sqrt{\chi_s}\, z(r_a)] = 0. \qquad (5.3.1)$$

The Green's function solution is then obtained by a summation of the terms corresponding to the right hand side of Equation (5.2.5), with suitable coefficients c_s.

The determination of the constants c_s is awkward if done directly from (5.2.5). However the problem is basically of Sturm Liouville type and the determination of the constants is expedited by using Sturm Liouville theory. To achieve this we use a change of variables.

$$t \to \tau, \qquad (5.3.2)$$

and manipulate the solutions of Section (2) into the form

$$F_o = a(z, t)\ g(z, \tau), \tag{5.3.3}$$

in which we choose $a(z, t)$. Then in place of the partial differential equation for F_o in terms of z and t (see e.g., Equation (5.3.8)) we obtain a partial differential equation for $g(z, \tau)$.

$$\frac{1}{q(z)}\ \frac{\partial}{\partial z}\left(p(z)\ \frac{\partial g}{\partial z}\right) = \frac{\partial g}{\partial \tau}\ . \tag{5.3.4}$$

This is immediately separable with solutions of the form

$$g(z, \tau) = y(z, \lambda)\ e^{-\lambda\tau}\ , \tag{5.3.5}$$

and y satisfying

$$\frac{1}{q(z)}\ \frac{d}{dz}\left(p(z)\ \frac{dy}{dz}\right) + \lambda\ y(z) = 0, \tag{5.3.6}$$

which is an equation of standard Sturm Liouville form.

The transformations (5.3.2) and the function $a(z, \tau)$ are different in each case as are the functions $q(z)$, $p(z)$ and the resultant algebraic equation for the eigenvalues λ_s, which is obtained in solving Equation (5.3.6). This procedure gives the Green's function in z and τ for g as an expansion of the form

$$G_g\ (z, \tau; z_o, z_a, z_b) = \sum_{s=1}^{\infty}\ c_s\ y_s\ (z, \lambda_s)\ e^{-\lambda_s\tau}\ , \tag{5.3.7}$$

and the Green's function for F_o follows immediately from (5.3.3).

The transformations (5.3.2) are listed for each case of K(r,p) of interest here : $K_o\, r^b\, p^{3/4(b-1)}$, $b \neq 1$; $K_o\, r^b$, $b > 1$; $K_o\, r^b$, $b < 1$; $K_o\, r$. To facilitate presentation we work through the method in general here in the text following standard Sturm Liouville procedure, and simply list the eigenfunctions, the eigenvalue equations and any special information with the transformations in Table (5.1.).

For completeness we note that the partial differential equation for F_o in the spherical symmetric case in terms of z and t referred to above is obtained in the most general case from Equations (2.2.7) and (2.2.8) by transforming the independent variables from $(x, t) \rightarrow (z, t)$. For the case $K_{||} = K_o\, r^b\, p^{3(b-1)/4}$ it has the form:

$$\frac{\partial^2 F_o}{\partial z^2} + \left(\frac{2n+1}{z} + z\,t\right)\frac{\partial F_o}{\partial z} = t^2 \frac{\partial F_o}{\partial t} . \quad (5.3.8)$$

In contrast to Equation (5.3.4) the form of the partial differential equation for F_o is not standard being different for each of the diffusion coefficients of interest in this section (see Appendix (A)). That the substitutions (5.3.3) listed in Table (5.1) lead to the standard form (5.3.4) may be verified by direct substitution with some considerable labour.

We now proceed to give a more precise definition of the Green's functions $G_F(z, \tau;\ z_o, \tau_o, z_a, z_b)$ and $G_g(z, \tau; z_o, \tau_o, z_a, z_b)$ where $z_o = z(r_o)$, $z_a = z(r_a)$, $z_b = z(r_b)$, $\tau_o = \tau(p_o)$ referred to

above, and using Sturm Liouville theory we obtain an eigenfunction expansion of the form (5.3.7) for the Green's function G_g.

Definition

The Green's function $G_F(z, \tau; z_o, \tau_o, z_a, z_b)$ for the steady-state spherically symmetric cosmic-ray equation of transport in the similarity variable z and the energy parameter τ is defined by:

(i) G_F satisfies the spherical symmetric transport equation

$$\frac{1}{r^2}\frac{\partial}{\partial r}\left(r^2 V F_o - r^2 K \frac{\partial F_o}{\partial r}\right) - \frac{2V}{3rp^2}\frac{\partial}{\partial p}\left(p^3 F_o\right) = M\,\delta(p-p_o)\delta(r-r_o). \tag{5.3.9a}$$

The constant M is determined by the condition :

$$\text{(ii)} \quad \lim_{\tau \to \tau_o} G_F(z, \tau; z_o, \tau_o, z_a, z_b) = \delta(z - z_o), \tag{5.3.9b}$$

where $\tau > \tau_o$ and $\delta(z)$ is the Dirac delta function of argument z.

$$\text{(iii)} \quad G_F(z_a, \tau; z_o, z_a, z_b) = G_F(z_b, \tau; z_o, z_a, z_b) = 0. \tag{5.3.9c}$$

Definition

The Green's function for $g(z, \tau)$ namely $G_g(z, \tau; z_o, z_a, z_b)$ is the solution of the partial differential equation

$$\frac{1}{q(z)}\frac{\partial}{\partial z}\left(p(z)\frac{\partial g}{\partial z}\right) = \frac{\partial g}{\partial \tau} - M\,\delta(z - z_o)\,\delta(\tau), \tag{5.3.10a}$$

where the constant M is determined by the condition

$$\text{(i)} \qquad \lim_{\tau \to \tau_o} G_g(z, \tau;\ z_o, \tau_o, z_a, z_b) = \delta(z - z_o), \qquad (5.3.10b)$$

and

$$\text{(ii)} \qquad G_g(z_a, \tau;\ z_o, \tau_o, z_a, z_b) = G_g(z_b, \tau;\ z_o, \tau_o, z_a, z_b) = 0. \qquad (5.3.10c)$$

We also have

$$G_F(z, \tau; z_o, \tau_o, z_a, z_b) = \frac{a(z,t)}{a(z_o,t_o)}\ G_g(z, \tau; z_o, \tau_o, z_a, z_b), \qquad (5.3.11)$$

relating the Green's functions G_F and G_g.

The Green's functions with boundary surface at $r = \infty$ and no inner boundary are :

If $K_{||} = K_o(p) r^b, \quad b \neq 1,$

$$G_F(x, t; x_o, t_o) = \frac{x_o^{n+1} x^{-n}}{2T} \exp\left(-\frac{x^2+x_o^2}{4T}\right) I_m\left(\frac{x\, x_o}{2T}\right), \qquad (5.3.12)$$

and if $b = 1$

$$G_F(x, t; x_o, t_o) = \frac{1}{2\sqrt{\pi}\sqrt{T}} \exp\left(x - x_o - T - \frac{(x-x_o)^2}{4T}\right), \qquad (5.3.13)$$

where

$$T = t - t_o = (3/(2V)) \int_p^{p_o} K_o(z)\ z^{(1-3b)/2}\, dz,$$

if $b \neq 1$,

$$x = (2/(1-b))(r p^{3/2})^{(1-b)/2}, \qquad (5.3.14)$$

and if $b = 1$,

$$x = -\tfrac{1}{2} \ln(2r^2 p^3).$$

The Green's functions (5.3.12) and (5.3.13) are the mono-energetic source solutions (3.2.18) and (3.2.24) with appropriate values of the normalisation constant N. The solutions (5.3.12) and (5.3.13) have the properties:

$$\text{(i)} \quad G_F(x, t; x_o, t_o) \to \delta(x - x_o) \quad \text{as} \quad t \to t_o , \tag{5.3.15}$$

$$\text{(ii)} \quad G_F(x, t; x_o, t_o) \to 0 \quad \text{as} \quad r \to \infty.$$

The Green's function $G_g(z, \tau; z_o, \tau_o, z_a, z_b)$ is obtained as follows. Since G_g must satisfy the partial differential equation for $g(z, \tau)$ (Equation (5.3.4)) we have

$$G_g = \sum_{s=1}^{\infty} c_s \, y_s(z, \lambda_s) \, e^{-\lambda_s \tau}, \tag{5.3.16}$$

where the eigenfunctions $y_s(z, \lambda_s)$ satisfy Equation (5.3.6) with $\lambda = \lambda_s$. In certain cases where z_a or z_b is a singular point of Equation (5.3.6) the eigenfunction expansion (5.3.16) is an integral over a continuous eigenspectrum λ_s. At the moment we restrict ourselves to cases where the eigenspectrum for λ is discrete. In general the eigenfunctions $y_s(z, \lambda_s)$ are a linear combination of two independent solutions $Y_1(z, \lambda_s)$ and $Y_2(z, \lambda_s)$ of Equation (5.3.6). Hence

$$y_s(z, \lambda_s) = A \, . \, Y_1(z, \lambda_s) + B \, . \, Y_2(z, \lambda_s). \tag{5.3.17}$$

Since G_g is zero at $z = z_a$ and $z = z_b$ the eigenfunctions $y_s(z, \lambda_s)$ must also be zero at z_a and z_b, and from Equation (5.3.17) we have

$$A \cdot Y_1(z_a, \lambda_s) + B \cdot Y_2(z_a, \lambda_s) = 0, \tag{5.3.18a}$$

$$A \cdot Y_1(z_b, \lambda_s) + B \cdot Y_2(z_b, \lambda_s) = 0. \tag{5.3.18b}$$

Solving Equations (5.3.18) for A / B we find

$$\frac{A}{B} = \frac{-Y_2(z_a,\lambda_s)}{Y_1(z_a,\lambda_s)} = \frac{-Y_2(z_b, \lambda_s)}{Y_1(z_b,\lambda_s)}. \tag{5.3.19}$$

It follows from Equation (5.3.19) that the eigenvalues λ_s must satisfy the eigenvalue equation

$$Y_1(z_1,\lambda_s)\, Y_2(z_2,\lambda_s) - Y_1(z_2,\lambda_s)\, Y_2(z_1,\lambda_s) = 0, \tag{5.3.20}$$

where the convention

$$\begin{aligned} z_1 &= \text{minimum of } (z_a, z_b), \\ z_2 &= \text{maximum of } (z_a, z_b), \end{aligned} \tag{5.3.21}$$

has been adopted.

Choosing A and B to satisfy Equation (5.3.19) we may define the eigenfunctions (5.3.17) to be

$$y_s(z, \lambda_s) = Y_2(z_1,\lambda_s)\, Y_1(z,\lambda_s) - Y_1(z_1,\lambda_s)\, Y_2(z,\lambda_s). \tag{5.3.22}$$

The eigenfunctions $y_s(z, \lambda_s)$ satisfy the relations

$$(\lambda_m-\lambda_n)\int_{z_1}^{z_2} q(x)y_m(x)y_n(x)dx = \left[p(z)(y_m(z)\frac{dy_n(z)}{dz} - y_n(z)\frac{dy_m(z)}{dz})\right]_{z=z_1}^{z=z_2},$$

(5.3.23)

(see Morse and Feshback, Methods of theoretical physics, Vol.1, p. 720) from which it follows that they satisfy the orthogonality relations

$$\int_{z_1}^{z_2} q(x)y_m(x)y_n(x)\,dx = N_m^{(1)}\,\delta_{mn}\,, \tag{5.3.24}$$

with

$$N_n^{(1)} = \underset{\lambda_m\to\lambda_n}{\text{limit}} \frac{1}{(\lambda_m-\lambda_n)} \left[p(z)(y_m(z)\frac{dy_n(z)}{dz} - y_n(z)\frac{dy_m(z)}{dz})\right]_{z=z_1}^{z=z_2}.$$

Using Hospital's rule and the result

$$\partial y_n(z, \lambda_n) / \partial\lambda_n \,|_{z=z_1} = 0,$$

we have

$$N_n^{(1)} = p(z)(\partial y_n(z,\lambda_n) / \partial\lambda_n).\,(\partial y_n(z,\lambda_n) / \partial z)\,|_{z=z_2} \tag{5.3.25}$$

as the expression for $N_n^{(1)}$.

Since the Green's function expansion for G_g is given by Equation (5.3.16) and G_g satisfies the source condition (5.3.10b) we have

$$G_g(z,\tau_o;\, z_o,\, \tau_o, z_a, z_b) = \delta(z-z_o) = \sum_{s=1}^{\infty} c_s\, y_s(z,\, \lambda_s)\, e^{-\lambda_s\tau_o} \tag{5.3.26}$$

Using the orthogonality relations (5.3.24) and Equation (5.3.26) we find the constants c_s are given by

$$c_s = q(z_o)\, y(z_o)\, e^{\lambda_s \tau_o} / N_s^{(1)}. \qquad (5.3.27)$$

Substituting for the constants c_s in the expansion (5.3.16) we have

$$G_g(z, \tau; z_o, \tau_o, z_a, z_b) = q(z_o) \sum_{n=1}^{\infty} \frac{y_n(z)\, y_n(z_o)\, e^{-\lambda_n(\tau-\tau_o)}}{N_n^{(1)}} \qquad (5.3.28)$$

This is the Green's function for $g(z, \tau)$ and the important result we seek. Note that y_n and λ_n must be determined in each case.

From the expression (5.3.28) for the Green's function G_g we have

$$q(z)\, G_g(z, \tau; z_o, \tau_o, z_a, z_b) = q(z_o)\, G_g(z_o, \tau; z, \tau_o, z_a, z_b), \tag{5.3.29}$$

which is a reciprocity relation for G_g.

The above has been developed with z_1 the explicit boundary variable in the eigensolution y_n and z_2 implicit via the eigenvalue equation. Alternative solutions with z_2 explicit and z_1 implicit can be written. Thus using the eigensolutions

$$v_n(z, \lambda_n) = Y_2(z_2, \lambda_n)\, Y_1(z, \lambda_n) - Y_1(z_2, \lambda_n)\, Y_2(z, \lambda_n), \tag{5.3.30}$$

the Green's function is

$$G_g(z, \tau; z_o, \tau_o, z_a, z_b) = q(z_o) \sum_{n=1}^{\infty} \frac{v_n(z_o) v_n(z)}{N_n^{(2)}}\, e^{-\lambda_n(\tau - \tau_o)}, \tag{5.3.31}$$

where

$$N_n^{(2)} = - p(z) \frac{\partial v_n(z, \lambda_n)}{\partial \lambda_n} \frac{\partial v_n(z, \lambda_n)}{\partial z} \Big|_{z=z_1}. \tag{5.3.32}$$

The functions $v_n(z)$ $y_n(z)$ and the normalisation constants $N_n^{(1)}$ and $N_n^{(2)}$ are related by :

$$Y_2(z_1, \lambda_n)\, v_n(z) = Y_2(z_2, \lambda_n)\, y_n(z), \tag{5.3.33}$$

$$N_n^{(1)} \left[Y_2(z_2, \lambda_n)\right]^2 = N_n^{(2)} \left[Y_2(z_1, \lambda_n)\right]^2. \qquad (5.3.34)$$

In the cases where z_a or z_b is a singular point of Equation (5.3.6) and the eigenspectrum for λ is continuous the Green's function G_g is derived using a Laplace transform technique (for an example see Appendix (B)). For a discussion of eigenfunction expansions when the spectrum is discrete or continuous see Titchmarsh (1962).

The Green's functions for the cases where $z = z(r)$ may be constructed from the table below by using the expansions (5.3.28) and (5.3.31). In this table it is also shown how the eigenfunction expansions for G_g and G_F behave as the outer boundary at $r_b \to \infty$ and the inner boundary at r_a (if any) tends to zero.

TABLE 5.1

GREEN'S FUNCTIONS

A. Diffusion coefficient

$$K = K_o r^b p^{3(b-1)/4}, \quad b > 1.$$

Variables

$$z = V r^{(1-b)/2} / K_o,$$

$$t = 2 K_o p^{3(1-b)/4} / (V(b-1)),$$

$$\tau = -1 / t,$$

$$x = zt = 2(rp^{3/2})^{(1-b)/2} / (b-1), \quad T = t - t_o,$$

$$z_1 = z(r_b), \quad z_2 = z(r_a), \quad t_o = t(p_o),$$

$$m = |(b+1) / (b-1)|, \quad n = (b+1) / (1-b).$$

a(z, t), p(z), q(z)

$$a(z, t) = t^{m-1} \exp(-z^2 t/4),$$

$$p(z) = q(z) = z^{1-2m}.$$

The eigenvalue equation

Putting $s_n = \sqrt{\lambda_n}$ the eigenvalue equation is in general

$$J_m(s_n z_1) Y_m(s_n z_2) - J_m(s_n z_2) Y_m(s_n z_1) = 0.$$

If $z_1 = 0$, i.e. $r_b = \infty$ the eigenvalue equation is

$$J_m(s_n z_2) = 0.$$

If $z_2 = \infty$, i.e. $r_a = 0$ the eigenspectrum is continuous and $0 \leq \lambda < \infty$.

Eigenfunctions

$$y_n(z) = z_1^m z^m [Y_m(s_n z_1) J_m(s_n z) - J_m(s_n z_1) Y_m(s_n z)]$$

If $z_1 = 0$, i.e. $r_b = \infty$ then

$$y_n(z) = z^m J_m(s_n z).$$

$$v_n(z) = z_2^m z^m [Y_m(s_n z_2) J_m(s_n z) - J_m(s_n z_2) Y_m(s_n z)].$$

Normalisation constants

$$N_n^{(1)} = (z_2/2)[J_{m+1}(s_n z_2) Y_m(s_n z_1) - J_m(s_n z_1) Y_{m+1}(s_n z_2)]$$

$$[z_2 (J_{m+1}(s_n z_2) Y_m(s_n z_1) - J_m(s_n z_1) Y_{m+1}(s_n z_2))$$

$$+ z_1 (J_m(s_n z_2) Y_{m+1}(s_n z_1) - Y_m(s_n z_2) J_{m+1}(s_n z_1))] z_1^{2m}$$

If $z_1 = 0$ i.e. $r_b = \infty$,

$$N_n^{(1)} = z_2^2 J_{m+1}^2 (s_n z_2) / 2.$$

$$N_n^{(2)} = (z_1/2)[J_{m+1}(s_n z_1) Y_m(s_n z_2) - J_m(s_n z_2) Y_{m+1}(s_n z_1)]$$

$$[z_2 (J_{m+1}(s_n z_2) Y_m(s_n z_1) - J_m(s_n z_1) Y_{m+1}(s_n z_2))$$

$$+ z_1 (J_m(s_n z_2) Y_{m+1}(s_n z_1) - Y_m(s_n z_2) J_{m+1}(s_n z_1))] z_2^{2m}$$

Asymptotic form for large n

For n sufficiently large

$$\lambda_n \sim n^2 \pi^2 / (z_2 - z_1)^2 ,$$

and the terms of the eigenfunction expansion have the form

$$u_n = \frac{2}{(z_2-z_1)} \sin\left(\frac{n\pi(z_1-z)}{(z_2-z_1)}\right) \sin\left(\frac{n\pi(z_1-z_o)}{(z_2-z_1)}\right)\left(\frac{z}{z_o}\right)^{\frac{1}{2}-m}$$
$$\exp\left[\frac{-n^2\pi^2(\tau-\tau_o)}{(z_2-z_1)^2}\right] ,$$

and the series for G_g is uniformly convergent for $\tau > \tau_o$.

Effect of varying the boundaries

If $z_1 = 0$, i.e. $r_b = \infty$ then

$$G_g = (2/z_2^2) z_o^{1-m} z^m \sum_{n=1}^{\infty} \frac{J_m(s_n z) J_m(s_n z_o)}{J_{m+1}^2(s_n z_2)} e^{-s_n^2(\tau-\tau_o)} ,$$

(5.3.35)

and the Green's function for F is given by the result (5.3.11), i.e.,

$$G_F = (t/t_o)^{m-1} \exp(z_o^2 t_o/4 - z^2 t/4) G_g.$$

We note that for $\tau = \tau_o$ then expression (5.3.35) is the Fourier Bessel expansion of $\delta(z-z_o)$ [see Titchmarsh (1962)].

If $z_2 = \infty$, i.e. $r_a = 0$, the Green's function for $g(z, \tau)$ is :

$$G_g = z^m z_o^{1-m} \int_0^{\infty} s.e^{-s^2(\tau-\tau_o)} . [J_m(sz) Y_m(sz_1) - J_m(sz_1) Y_m(sz)]$$
$$[J_m(sz_o) Y_m(sz_1) - Y_m(sz_o) J_m(sz_1)]/[J_m^2(sz_1) + Y_m^2(sz_1)] \, ds,$$

(5.3.36)

and

$$G_F = (t/t_o)^{m-1} \exp(z_o^2 t_o/4 - z^2 t/4) G_g.$$

For a derivation of the result (5.3.36) see Appendix (B). If $\tau = \tau_o$ the expression (5.3.36) gives the Weber formula expansion of $\delta(z-z_o)$ [see Titchmarsh (1962)].

As $z_2 \to \infty$, i.e. $r_a \to 0$ in the solution (5.3.35) or as $z_1 \to 0$, i.e. $r_b \to \infty$ in the solution (5.3.36) we find

$$G_F \to z^m z_o^{1-m} (t/t_o)^{m-1} \exp(z_o^2 t_o/4 - z^2 t/4)$$
$$\int_0^\infty e^{-y^2(\tau-\tau_o)} J_m(yz_o) J_m(yz) y \, dy.$$

This latter result is essentially the Green's function for F_o with a free escape boundary at $r = \infty$. To show this explicitly we use the result

$$\int_0^\infty e^{-x^2\alpha} J_m(2\delta x) J_m(2\sigma x) x \, dx$$
$$= \frac{1}{2\alpha} \exp\left(-\frac{\sigma^2+\delta^2}{\alpha}\right) I_m\left(\frac{2\delta\sigma}{\alpha}\right), \qquad \text{Re } (m) > -1$$

(see Gradshteyn and Ryzhik (1965) p. 710), and hence obtain

$$G_F = (t/t_o)^{m-1} \exp((z_o^2 t_o - z^2 t)/4) \frac{z^m z_o^{1-m}}{2(\tau-\tau_o)} \exp\left[-\frac{z^2+z_o^2}{4(\tau-\tau_o)}\right]$$
$$I_m\left(\frac{z\, z_o}{2(\tau-\tau_o)}\right).$$

Using the relations

$$x = 2(rp^{3/2})^{(1-b)/2} / (b-1) = zt,$$
$$\tau = -1/t, \qquad T = t - t_o,$$

(see Variables), we may write this last expression for G_F as

$$G_F = t_o \frac{x^m x_o^{1-m}}{2T} \exp\left(-\frac{x^2+x_o^2}{4T}\right) I_m\left(\frac{x\, x_o}{2T}\right),$$

which is t_o times the Green's function (5.3.12) for F_o with an outer free escape boundary at $r = \infty$.

B. Diffusion coefficient.

$$K(r,p) = K_o r^b, \quad b < 1$$

Variables

$$z = V r^{1-b} / (K_o(1-b)),$$

$$t = -K_o p^{3(1-b)/2} / (V(1-b)),$$

$$\tau = -3(1-b) \ln(p)/2,$$

$$t = t_o \exp[-(\tau-\tau_o)], \quad T = t - t_o,$$

$$z = -x^2/(4t),$$

$$x = 2(rp^{3/2})^{(1-b)/2} / (b-1),$$

$$z_1 = z(r_a), \quad z_2 = z(r_b), \quad t_o = t(p_o),$$

$$m = (b+1) / (1-b).$$

a(z,t), p(z), q(z)

$$a(z,t) = 1,$$

$$p(z) = z^{1+m} e^{-z}, \quad q(z) = z^m e^{-z}.$$

The eigenvalue equation

The eigenvalue equation is in general

$$M(-\lambda_n,1+m,z_1)\, U(-\lambda_n,1+m,z_2) - U(-\lambda_n,1+m,z_1)\, M(-\lambda_n,1+m,z_2) = 0,$$

where M(a,b,z) and U(a,b,z) are standard solutions of Kummers' confluent

hypergeometric equation. If there is no inner boundary and the Green's function G_g is finite as $r \to 0$ then the eigenvalue equation is

$$M(-\lambda_n, 1+m, z_2) = 0.$$

Eigenfunctions

$$y_n(z) = U(-\lambda_n,1+m,z_1)\, M(-\lambda_n,1+m, z) - M(-\lambda_n,1+m,z_1)\, U(-\lambda_n,1+m,z),$$

$$v_n(z) = U(-\lambda_n,1+m,z_2)\, M(-\lambda_n,1+m,z) - M(-\lambda_n,1+m,z_2)\, U(-\lambda_n,1+m,z).$$

If there is no inner boundary

$$y_n(z) = M(-\lambda_n,1+m,z).$$

Normalisation constants

The normalisation constants are given by Equations (5.3.25) and (5.3.32).

Asymptotic form for large n

For n sufficiently large the eigenvalues are

$$\lambda_n \sim \frac{n^2\pi^2}{4(\sqrt{z_1}-\sqrt{z_2})^2} - \frac{1+m}{2},$$

and the terms of the eigenfunction expansion for G_g are

$$u_n \sim e^{(z-z_o)/2} z_o^{m/2-\frac{1}{4}} z^{-m/2-\frac{1}{4}} \frac{1}{(\sqrt{z}_2 - \sqrt{z}_1)}$$

$$\sin\left[\frac{n\pi(\sqrt{z}_1 - \sqrt{z}_o)}{(\sqrt{z}_1 - \sqrt{z}_2)}\right] \sin\left[\frac{n\pi(\sqrt{z}_1 - \sqrt{z})}{(\sqrt{z}_1 - \sqrt{z}_2)}\right] e^{-\lambda_n(\tau-\tau_o)} ,$$

and the series for G_g is uniformly convergent for $\tau > \tau_o$.

Effect of varying the boundaries

If we have no inner boundary and let the outer boundary at $r = r_b$ tend to infinity the eigenfunction expansion becomes

$$G_g = z_o^m e^{-z_o} \sum_{n=0}^{\infty} \frac{\Gamma(n+1)}{\Gamma(m+n+1)} L_n^m(z_o) L_n^m(z) e^{-n(\tau-\tau_o)}.$$

Since $a(z,t) = 1$, $G_g = G_F$ and using the result

$$\sum_{n=0}^{\infty} \frac{\Gamma(n+1)}{\Gamma(m+n+1)} L_n^m(x) L_n^m(y) z^n$$

$$= \frac{(xyz)^{-m/2}}{1-z} \exp\left(\frac{-z(x+y)}{(1-z)}\right) I_m\left(\frac{2\sqrt{xyz}}{(1-z)}\right), \qquad |z| < 1$$

where $L_n^m(z)$ is a generalised Laguerre function and $I_m(z)$ a modified Bessel function of the first kind (see Gradshteyn and Ryzhik (1965), p. 1038) we have

$$G_g = G_F = z_o^m e^{-z_o} \left[\frac{[z\, z_o \exp(-(\tau-\tau_o))]^{-m/2}}{[1 - \exp(-(\tau-\tau_o))]}\right]$$

$$\exp\left[\frac{-\exp(-(\tau-\tau_o))(z+z_o)}{[1 - \exp(-(\tau-\tau_o))]}\right] \cdot I_m\left(\frac{2\sqrt{z\, z_o \exp(-(\tau-\tau_o))}}{[1 - \exp(-(\tau-\tau_o))]}\right).$$

Since

$$z = -x^2/(4t),$$

$$t = t_o \exp(-(\tau-\tau_o)), \quad T = (t-t_o),$$

(see Variables), this last result for G_g and G_F may be written

$$G_g = G_F = \frac{x_o}{2z_o} \cdot \frac{x_o^{m+1} x^{-m}}{2T} \exp\left(-\frac{x^2+x_o^2}{4T}\right) I_m\left(\frac{x\, x_o}{2T}\right)$$

which is $x_o/(2z_o)$ times the Green's function (5.3.12) for F_o with an outer free escape boundary at $r = \infty$.

C. Diffusion coefficient

$$K(r,p) = K_o\, r^b, \qquad b > 1,$$

Variables

$$z = V\, r^{1-b}/(K_o(b-1)),$$

$$t = K_o\, p^{3(1-b)/2} / (V(b-1)),$$

$$\tau = -3(b-1)\, \ell n(p)/2,$$

$$t = t_o \exp(\tau-\tau_o), \qquad T = t - t_o,$$

$$z = x^2/(4t),$$

$$x = 2(rp^{3/2})^{(1-b)/2} / (b-1),$$

$$z_1 = z(r_b), \quad z_2 = z(r_a), \quad t_o = t(p_o),$$

$$m = (b+1) / (b-1).$$

a(z,t), p(z), q(z)

$$a(z,t) = 1,$$

$$p(z) = z^{1-m} e^z, \quad q(z) = z^{-m} e^z$$

The eigenvalue equation

The eigenvalue equation is in general

$$M(1-\lambda_n, 1+m, z_1)\, U(1-\lambda_n, 1+m, z_2) - U(1-\lambda_n, 1+m, z_1)\, M(1-\lambda_n, 1+m, z_2) = 0,$$

where M(a,b,z) and U(a,b,z) are standard solutions of Kummer's confluent hypergeometric equation. If $z_1 = 0$, i.e. $r_b = \infty$ then the eigenvalue equation is

$$M(1-\lambda_n,\ 1+m,\ z_2) = 0.$$

If $z_2 = \infty$, i.e. $r_a = 0$ then the eigenvalue equation is

$$U(1-\lambda_n,\ 1+m,\ z_1) = 0.$$

Eigenfunctions

$$y_n(z) = e^{-z_1-z}(z\ z_1)^m [M(1-\lambda_n,1+m,z_1)\ U(1-\lambda_n,1+m,z) - U(1-\lambda_n,1+m,z_1)\ M(1-\lambda_n,1+m,z)],$$

If $z_1 = 0$, or $r_b = \infty$ then

$$y_n(z) = e^{-z}z^m\ M(1-\lambda_n,\ 1+m,\ z),$$

and if $z_2 = \infty$, i.e. $r_a = 0$ then

$$y_n(z) = e^{-z}z^m\ U(1-\lambda_n,\ 1+m,\ z)$$

Normalisation constants

The normalisation constants $N_n^{(1)}$ and $N_n^{(2)}$ are given by Equations (5.3.32).

Asymptotic form for large n

For n sufficiently large the eigenvalues are

$$\lambda_n \sim \frac{n^2\pi^2}{4(\sqrt{z_2}-\sqrt{z_1})^2} + \frac{1-m}{2},$$

and the terms of the eigenfunction expansion for G_g have the form

$$u_n \sim z_o^{-m/2-\frac{1}{4}}\, z^{m/2-\frac{1}{4}}\, e^{(z-z_o)/2} \,/\, (\sqrt{z_2}-\sqrt{z_1})$$

$$\sin\left[\frac{n\pi(\sqrt{z_o}-\sqrt{z_2})}{(\sqrt{z_1}-\sqrt{z_2})}\right] \quad \sin\left[\frac{n\pi(\sqrt{z}-\sqrt{z_2}}{(\sqrt{z_1}-\sqrt{z_2})}\right] \quad \exp(-\lambda_n(\tau-\tau_o)),$$

and the series for G_g is uniformly convergent for $\tau > \tau_o$.

Effect of varying the boundaries

If we let the outer boundary at $r = r_b$ tend to infinity and the inner boundary at $r = r_a$ tend to zero the eigenfunction expansion becomes

$$G_g = z^m\, e^{-z-(\tau-\tau_o)} \sum_{n=0}^{\infty} L_n^m(z_o)\, L_n^m(z)\,(\Gamma(n+1) \,/\, \Gamma(1+n+m))\, e^{-n(\tau-\tau_o)}.$$

where $L_n^m(z)$ is a generalised Laguerre function of argument z.

Since $a(z,t) = 1$, $G_g = G_F$ and using the result

$$\sum_{n=0}^{\infty} \frac{\Gamma(n+1)}{\Gamma(m+n+1)}\, L_n^m(x)\, L_n^m(y)\, z^n$$

$$= \frac{(xyz)^{-m/2}}{1-z} \exp\left(\frac{-z(x+y)}{(1-z)}\right) I_m\left(\frac{2\sqrt{xyz}}{(1-z)}\right), \qquad |z| < 1,$$

(see Gradshteyn and Ryzhik (1965), p.1038), we have

$$G_g = G_F = z^m\, e^{-z-(\tau-\tau_o)} \left[\frac{[z\, z_o\, e^{\tau_o-\tau}]^{-m/2}}{(1-\exp(\tau_o-\tau))}\right]$$

$$\exp\left(\frac{-(z+z_o)\exp(\tau_o-\tau)}{(1-\exp(\tau_o-\tau))}\right) \cdot I_m\left(\frac{2\sqrt{z\, z_o \exp(\tau_o-\tau)}}{1-\exp(\tau_o-\tau)}\right).$$

Using the relations

$$z = x^2 / (4t),$$

$$t = t_o \exp(\tau-\tau_o), \quad T = t - t_o,$$

(see Variables), this last result for G_g and G_F may be written

$$G_g = G_F = \frac{x_o}{2z_o} \frac{x_o^{1-m} x^m}{2T} \exp\left(-\frac{x^2+x_o^2}{4T}\right) I_m\left(\frac{x\, x_o}{2T}\right),$$

which is $x_o/(2z_o)$ times the Green's function (5.3.12) for F_o, with an outer free escape boundary at $r = \infty$.

D. Diffusion coefficient

$$K(r,p) = K_o\, r$$

Variables

$$z = \ell n\,(r),$$

$$t = \tau = -(3K_o/(2V))\ell n(p), \quad T = t - t_o,$$

$$x = -\tfrac{1}{2}\ell n(2r^2p^3) = 2(1-c)\tau - \ell n(2)/2 - z$$

$$z_1 = z(r_a), \quad z_2 = z(r_b), \quad t_o = t(p_o)$$

$$c = 1 - V/(2K_o).$$

a(z,t), p(z), q(z)

$$a(z,t) = 1,$$

$$p(z) = q(z) = e^{2cz}.$$

The eigenvalue equation

The eigenvalues are given by

$$\lambda_n = c^2 + \frac{n^2\pi^2}{(z_2-z_1)^2} = c^2 + \frac{n^2\pi^2}{[\ln(r_b/r_a)]^2}$$

Eigenfunctions

$$y_n(z) = e^{-c(z+z_1)} \sin(n\pi(z-z_1) / (z_1-z_2)).$$

Normalisation const

$$N_n^{(1)} = \frac{z_2 - z_1}{2} \exp(-2c\, z_1)$$

Green's function

In this case it is relatively simple to give the Green's functions G_g and G_F

$$G_g = G_F = \frac{2}{(z_2-z_1)} e^{c(z_o-z)} \sum_{n=1}^{\infty} \sin\left(\frac{n\pi(z-z_1)}{(z_1-z_2)}\right) \sin\left(\frac{n\pi(z_o-z_1)}{(z_1-z_2)}\right) \exp\left[-\left(c^2 + \frac{n^2\pi^2}{(z_2-z_1)^2}\right)\cdot(\tau-\tau_o)\right]. \quad (5.3.38)$$

Effect of varying the boundaries

If $z_1 \to -\infty$ i.e. $r_a \to 0$ we find

$$G_F = G_g = \frac{1}{2\sqrt{\pi(\tau-\tau_o)}} \exp[\, c(z_o-z) - c^2(\tau-\tau_o)] \left[\exp\left(-\frac{(z-z_o)^2}{4(\tau-\tau_o)}\right) - \exp\left(-\frac{(z+z_o-2z_2)^2}{4(\tau-\tau_o)}\right)\right]. \quad (5.3.39)$$

If we let $z_2 \to \infty$, i.e. $r_b \to \infty$, and keep the inner boundary at $r = r_a$ fixed, $r_a \neq 0$ the eigenspectrum becomes continuous and we have

$$G_F = G_g = \frac{1}{2\sqrt{(\tau-\tau_o)\pi}} \exp(c(z_o-z) - c^2(\tau-\tau_o)) \cdot$$

$$\left[\exp\left(-\frac{(z-z_o)^2}{4(\tau-\tau_o)}\right) - \exp\left(-\frac{(z+z_o-2z_1)^2}{4(\tau-\tau_o)}\right)\right]. \qquad (5.3.40)$$

Hence if we let $r_b \to \infty$ and $r_a \to 0$ the solutions (5.3.39) and (5.3.40) give

$$G_F = G_g = \frac{1}{2\sqrt{\pi(\tau-\tau_o)}} \exp\left[c(z_o-z) - c^2(\tau-\tau_o) - \frac{(z-z_o)^2}{4(\tau-\tau_o)}\right]. \qquad (5.3.41)$$

Since

$$x = 2(1-c)\tau - \tfrac{1}{2}\ln(2) - z,$$

$$T = \tau - \tau_o,$$

(see Variables) the solution (5.3.41) may be expressed in the alternative form

$$G_F = G_g = \frac{1}{2\sqrt{\pi T}} \exp\left[x - x_o - T - \frac{(x-x_o)^2}{4T}\right],$$

which is the Green's function (5.3.13) with boundary surface at $r = \infty$.

The negative terms in the Green's functions (5.3.39) and (5.3.40) are due to boundary effects, whereas the positive term is due to the source at (z_o, τ_o).

CHAPTER 6

GREEN'S THEOREM AND BOUNDARY VALUE PROBLEMS

6.1 Introduction

In this chapter solutions in which the distribution function F_o is specified on boundaries at $r=r_a$ and $r=r_b$ are obtained from the cases where the similarity variable z of Chapter (5) is a function of radius only, namely when the diffusion coefficient $K_{\parallel}$ has one of the forms:

$$K_{\parallel} = K_o r^b p^{3(b-1)/4},$$

$$K_{\parallel} = K_o r^b, \quad b \neq 1,$$

$$K_{\parallel} = K_o r,$$

where K_o is a constant. We also obtain galactic spectrum solutions in which F_o is specified as $r \to \infty$ and as $r \to 0$, with a diffusion coefficient $K = K_o(p)\, r^b$, $b>1$.

In cases where the similarity variable $z=z(r)$, the distribution function F_o has the form

$$F_o = a(z,\tau)\, g(z,\tau), \tag{6.1.1}$$

where the function $a(z,\tau)$ is chosen such that $g(z,\tau)$ satisfies the partial differential equation

$$\frac{1}{q(z)} \frac{\partial}{\partial z} \left(p(z) \frac{\partial g}{\partial z} \right) = \frac{\partial g}{\partial \tau}, \tag{6.1.2}$$

(see Equations (5.3.3) and (5.3.4)). Hence a boundary value problem for the distribution function F_o in which spectra are specified at radii r_a and r_b may be reduced to an equivalent boundary value problem for $g(z,\tau)$ by using the relation (6.1.1) with the functions $a(z,\tau)$, $p(z)$ and $q(z)$ given in Table (5.1).

We note that Equation (6.1.2) is similar to the one dimensional heat flow equation. It is well known that boundary value problems for the heat equation may be solved by using Green's theorem for the heat equation in conjunction with appropriate Green's functions (see Snedden Elements of Partial Differential Equations (1957)). The basic procedure we adopt to solve boundary value problems for F_o with boundaries at r_a and r_b is to solve the equivalent boundary value problem for $g(z,\tau)$ by using Green's theorem for Equation (6.1.2) in conjunction with Green's functions $G_g(z,\tau;z_o,\tau_o,z_a,z_b)$ for $g(z,\tau)$ given in Table (5.1).

In Section (2) we establish Green's theorem for Equation (6.1.2), and for the sake of completeness we incorporate a source term $-Q(z,\tau)$ on the right-hand side of this equation.

In Section (3) we use the Green's theorem technique to solve the general boundary value problem for F_o in which the galactic spectrum is specified and the diffusion coefficient is of the form $K = K_o(p)r^b$ with $b > 1$. The monoenergetic galactic spectrum solution given by Equation (3.2.17) and the solutions of Fisk and Axford (1969) in which:

(i) $F_o(r,p) \to Ap^{-\mu-2}$ as $r \to \infty$,

(ii) $F_o(r,p)$ is finite as $r \to 0$,

(iii) the diffusion coefficient $K(r,p) = K_o p^a r^b$ with $b > 1$,

are derived as special cases of the general galactic spectrum solution.

In Section (4) the Green's theorem technique is used to solve boundary value problems for F_o with boundaries at radii $r = r_a$ and $r = r_b$, and these solutions are given in Table (6.2).

In Section (5) we conclude the Chapter with a discussion of the various solutions obtained by the Green's theorem technique.

6.2 Green's Theorem for $g(z,\tau)$

Green's theorem for Equation (6.1.2) with a source term $Q(z,\tau)$ gives the solution of the partial differential equation

$$\frac{1}{q(z)} \frac{\partial}{\partial z}\left(p(z) \frac{\partial g}{\partial z} \right) = \frac{\partial g}{\partial \tau} - Q(z,\tau), \tag{6.2.1}$$

in which the function $g(z,\tau)$ is specified on boundaries at $z = z_1$, $z = z_2$ and $\tau = \tau_i$ where τ_i is some initial value of the variable τ. This solution is valid in the region $z_1 < z < z_2$ and $\tau > \tau_i$. For brevity of exposition we denote the Green's function solution of Equation (6.1.2) with boundaries at z_1 and z_2 by $G(z, z_o, \tau - \tau_o)$. This solution of (6.1.2) has the properties

$$\text{(i)} \quad G(z, z_o, \tau - \tau_o) \to \delta(z - z_o) \text{ as } \tau \to \tau_o, \tag{6.2.2a}$$

$$\text{(ii)} \quad G(z_1, z_o, \tau - \tau_o) = G(z_2, z_o, \tau - \tau_o) = 0. \tag{6.2.2b}$$

Green's theorem for the partial differential equation (6.2.1) is obtained as follows: Since $g(z,\tau)$ satisfies Equation (6.2.1) we have

$$\frac{1}{q(z_o)} \frac{\partial}{\partial z_o}\left(p(z_o) \frac{\partial g(z_o,\tau_o)}{\partial z_o} \right) = \frac{\partial g(z_o,\tau_o)}{\partial \tau_o} - Q(z_o, \tau_o). \tag{6.2.3}$$

The Green's function G satisfies the equation

$$\frac{1}{q(z_o)} \frac{\partial}{\partial z_o}\left(p(z_o) \frac{\partial}{\partial z_o} G(z_o, z, \tau - \tau_o) \right) = - \frac{\partial G (z_o, z, \tau - \tau_o)}{\partial \tau_o} . \quad (6.2.4)$$

From Equations (6.2.3) and (6.2.4)

$$q(z_o) \frac{\partial}{\partial \tau_o}\left(g(z_o, \tau_o) G(z_o, z, \tau - \tau_o) \right)$$

$$= \left[q(z_o) Q(z_o, \tau_o) + \frac{\partial}{\partial z_o}\left(p(z_o) \frac{\partial g(z_o, \tau_o)}{\partial z_o} \right) \right] G(z_o, z, \tau - \tau_o)$$

$$- \frac{\partial}{\partial z_o}\left(p(z_o) \frac{\partial}{\partial z_o} G(z_o, z, \tau - \tau_o) \right) \cdot g(z_o, \tau_o). \quad (6.2.5)$$

Rearranging Equation (6.2.5) we have

$$q(z_o) \frac{\partial}{\partial \tau_o}\left(g(z_o, \tau_o) G(z_o, z, \tau - \tau_o) \right)$$

$$= q(z_o) Q(z_o, \tau_o) G(z_o, z, \tau - \tau_o)$$

$$+ \frac{\partial}{\partial z_o}\left[p(z_o) \left(G(z_o, z, \tau-\tau_o) \frac{\partial g(z_o, \tau_o)}{\partial z_o} - g(z_o, \tau_o) \frac{\partial G(z_o, z, \tau-\tau_o)}{\partial z_o} \right) \right]. \quad (6.2.6)$$

Integrating Equation (6.2.6) with respect to z_o and τ_o from $z_o = z_1$ to $z_o = z_2$ and from $\tau_o = \tau_i$ to $\tau_o = \tau$:

$$\int_{z_1}^{z_2} dz_o \cdot q(z_o) \int_{\tau_i}^{\tau} d\tau_o \frac{\partial}{\partial \tau_o}\left(g(z_o, \tau_o) G(z_o, z, \tau-\tau_o) \right)$$

$$= \int_{z_1}^{z_2} dz_o \int_{\tau_i}^{\tau} d\tau_o \, q(z_o) G(z_o, z, \tau-\tau_o) Q(z_o, \tau_o)$$

$$+\int_{\tau_i}^{\tau} d\tau_o \int_{z_1}^{z_2} dz_o \frac{\partial}{\partial z_o}\left[p(z_o)\left(G(z_o, z, \tau-\tau_o) \frac{\partial g(z_o, \tau_o)}{\partial z_o}\right.\right.$$

$$\left.\left. -g(z_o, \tau_o) \frac{\partial G}{\partial z_o} (z_o, z, \tau-\tau_o)\right)\right]. \qquad (6.2.7)$$

Carrying out the inner integrations in (6.2.7) we obtain

$$\int_{z_1}^{z_2} dz_o\, q(z_o) \left[g(z_o, \tau_o)\, G(z_o, z, \tau-\tau_o)\right]_{\tau_o=\tau_i}^{\tau_o=\tau}$$

$$= \int_{z_1}^{z_2} dz_o \int_{\tau_i}^{\tau} d\tau_o\, q(z_o)\, Q(z_o, \tau_o)\, G(z_o, z, \tau-\tau_o)$$

$$+ \int_{\tau_i}^{\tau} d\tau_o \left[p(z_o)\left(G(z_o,z,\tau-\tau_o) \frac{\partial g(z_o,\tau_o)}{\partial z_o} - g(z_o,\tau_o)\frac{\partial G(z_o,z,\tau-\tau_o)}{\partial z_o}\right)\right]_{z_o=z_1}^{z_o=z_2}. \qquad (6.2.8)$$

Using the singularity property (6.2.2a) of the Green's function

$$G(z_o, z, \tau-\tau_o) \to \delta(z_o-z) \text{ as } \tau \to \tau_o,$$

the left hand side of Equation (6.2.8) reduces to

$$q(z)\, g(z, \tau) - \int_{z_1}^{z_2} dz_o\, q(z_o)\, g(z_o, \tau_i)\, G(z_o, z, \tau-\tau_i).$$

This last result shows that we can rearrange the result (6.2.8) to obtain the required solution for $g(z, \tau)$.

Since the Green's function for $g(z, \tau)$ is zero on the boundaries at $z=z_1$ and $z=z_2$ (see Equation (6.2.2b))

$$G(z_1, z, \tau-\tau_o) = G(z_2, z, \tau-\tau_o) = 0,$$

the second integral in the right hand side of Equation (6.2.8) becomes

$$\int_{\tau_i}^{\tau} d\tau_o \left[p(z_1)\, g(z_1, \tau_o) \frac{\partial G(z_o, z, \tau-\tau_o)}{\partial z_o} \Big| z_o=z_1 \right.$$

$$\left. -p(z_2)\, g(z_2,\tau_o) \frac{\partial G(z_o,z,\tau-\tau_o)}{\partial z_o} \Big| z_o = z_2 \right].$$

Hence solving Equation (6.2.8) for $g(z,\tau)$

$$g(z,\tau) = \frac{1}{q(z)} \left[\int_{z_1}^{z_2} dz_o \int_{\tau_i}^{\tau} d\tau_o\, q(z_o)\, Q(z_o, \tau_o)\, G(z_o, z, \tau-\tau_o) \right.$$

$$+ \int_{z_1}^{z_2} q(z_o)\, g(z_o, \tau_i)\, G(z_o, z, \tau-\tau_i)\, dz_o$$

$$+ \int_{\tau_i}^{\tau} d\tau_o \left(p(z_1)\, g(z_1, \tau_o) \frac{\partial G(z_o, z, \tau-\tau_o)}{\partial z_o} \Big| z_o = z_1 \right.$$

$$\left. \left. - p(z_2)\, g(z_2, \tau_o) \frac{\partial G(z_o, z, \tau-\tau_o)}{\partial z_o} \Big| z_o=z_2 \right) \right]. \qquad (6.2.9)$$

This result is Green's theorem for the partial differential equation (6.2.1) and we shall use this result in Section (3), to obtain solutions of boundary value problems for $g(z,\tau)$ and the distribution function $F_o(r,p)$.

The double integral over z_o and τ_o in the result (6.2.9) involving $Q(z_o,\tau_o)$ gives the effects of sources within the region $z_1 < z_o < z_2$ and $\tau_i < \tau_o < \tau$. The second integral gives the "initial conditions"

and the third and fourth integrals give the effects of boundary conditions at z_1 and z_2.

Note that if

$$Q(z_o,\tau_o) = \delta(z_o-z_s)\ \delta(\tau_o-\tau_s),$$

and,

$$g(zo,\tau_i) = g(z_1,\tau) = g(z_2,\tau) = 0,$$

the solution of (6.2.9) is

$$g(z,\tau) = \frac{q(z_s)}{q(z)}\ G(z_s, z, \tau-\tau_s). \tag{6.2.10}$$

Using the reciprocity relation for the Green's function given in Equation (5.3.29) the solution (6.2.10) becomes

$$g(z,\tau) = G(z, z_s, \tau-\tau_s). \tag{6.2.11}$$

The solution (6.2.11) is the Green's function of the partial differential equation (6.2.1), which satisfies homogeneous Dirichlet boundary conditions at $z=z_1$ and $z=z_2$, and the source is located at (z_s, τ_s).

Since the variables z and τ given in Table (5.1) have the properties:

(i) the variable $z=z(r)$ and $\tau=\tau(p)$ with r heliocentric radius and p the particle momentum,

(ii) $\tau(p)$ is a monotonic decreasing function of p, and hence

(iii) if $p < p_o < p_i$, $\tau_o=\tau(p_o)$, $\tau_i=\tau(p_i)$ then $\tau > \tau_o > \tau_i$,

(iv) $\tau(p) \to -\infty$ as $p \to \infty$, (6.2.12)

(v) the variable z(r) is restricted to the range

$$z_1 < z < z_2,$$

where

z_1 = minimum of $(z(r_a), z(r_b))$,

z_2 = maximum of $(z(r_a), z(r_b))$,

and

$$r_a < r < r_b \text{ (see Equation(5.3.21))},$$

we may interpret the Green's theorem (6.2.9) for cosmic ray problems in the following way.

The double integral over z_o and τ_o in Equation (6.2.9) gives the effects of sources located within the region $r_a < r_o < r_b$ and $p < p_o < p_i$. The second integral gives the effects of specifying the radial variation of the distribution function at momentum p_i and the third and fourth integrals give the effects of specifying the spectrum at radii r_a, r_b.

In certain problems of physical interest we have

(i) $Q(z_o, \tau_o) = 0$ corresponding to no sources within the solar cavity.

(ii) $\tau_i = -\infty$ or $p_i = \infty$ since we are interested in all particles with momentum $o < p < \infty$,

(iii) $F_o(r,p)$ and $g(z,\tau) \to 0$ as $p \to \infty$ or $\tau_i \to -\infty$ since we cannot have particles with infinite momentum.

Hence in these cases Green's theorem (6.2.9) takes the form

$$g(z,\tau) = \frac{1}{q(z)}\left[\int_{\tau(\infty)}^{\tau} d\tau_o\, p(z_1)\, g(z_1,\tau_o)\, \frac{\partial G}{\partial z_o}(z_o,z,\tau-\tau_o) \,\Big|\, z_o = z_1 \right.$$

$$\left. - \int_{\tau(\infty)}^{\tau} d\tau_o\, p(z_2)\, g(z_2,\tau_o)\, \frac{\partial G(z_o,z,\tau-\tau_o)}{\partial z_o} \Big|\, z_o = z_2 \right], \qquad (6.2.13)$$

where $\tau(p) \to \tau(\infty)$ as $p \to \infty$.

Since the Green's function expansions (5.3.28) and (5.3.31) are uniformly convergent we may obtain expressions for $\partial G(z_o,z,\tau-\tau_o)/\partial z_o$ by differentiating the series for $G(z_o,z,\tau-\tau_o)$ term by term.

From the Green's function expansion (5.3.28)

$$\frac{\partial G(z_o,z,\tau-\tau_o)}{\partial z_o}\Big|_{z_o=z_2} = q(z)\sum_{n=1}^{\infty}\frac{y_n(z)\,\partial y_n(z_o)/\partial z_o\, e^{-\lambda_n(\tau-\tau_o)}}{N_n^{(1)}}\Big|_{z_o=z_2}$$

Using the expression (5.3.25) for $N_n^{(1)}$ we obtain

$$\frac{\partial G(z_o,z,\tau-\tau_o)}{\partial z_o}\Big|_{z_o=z_2} = \frac{q(z)}{p(z_2)}\sum_{n=1}^{\infty}\frac{y_n(z)\, e^{-\lambda_n(\tau-\tau_o)}}{\partial y_n(z_o,\lambda_n)/\partial\lambda_n\,|_{z_o=z_2}}, \qquad (6.2.14)$$

as the expansion for $[\partial G(z_o,z,\tau-\tau_o)/\partial z_o]_{z_o=z_2}$.

Also from the result (5.3.31)

$$\frac{\partial G(z_o,z,\tau-\tau_o)}{\partial z_o}\Big|_{z_o=z_1} = q(z)\sum_{n=1}^{\infty}\frac{v_n(z)\,\partial v_n(z_o)/\partial z_o\, e^{-\lambda_n(\tau-\tau_o)}}{N_n^{(2)}}\Big|_{z_o=z_1}.$$

Using the expression (5.3.32) for $N_n^{(2)}$ we have

$$\frac{\partial G(z_o,z,\tau-\tau_o)}{\partial z_o}\Big|_{z_o=z_1} = -\frac{q(z)}{p(z_1)}\sum_{n=1}^{\infty}\frac{v_n(z)\, e^{-\lambda_n(\tau-\tau_o)}}{\partial v_n(z_o,\lambda_n)/\partial\lambda_n\,|_{z_o=z_1}} \qquad (6.2.15)$$

as the expansion for $\partial G(z_o,z,\tau-\tau_o)/\partial z_o\,|_{z_o=z_1}$.

Substituting the expressions (6.2.14) and (6.2.15) for $\partial G(z_o,z,\tau-\tau_o)/\partial z_o$ in the result (6.2.13) we obtain the Green's theorem solution

$$g(z,\tau) = -\int_{\tau(\infty)}^{\tau} d\tau_s\, g(z_1,\tau_s)\sum_{n=1}^{\infty}\frac{v_n(z)\, e^{-\lambda_n(\tau-\tau_s)}}{\partial v_n(z_o,\lambda_n)/\partial\lambda_n\,|_{z_o=z_1}}$$

$$-\int_{\tau(\infty)}^{\tau} d\tau_s\, g(z_2,\tau_s)\sum_{n=1}^{\infty}\frac{y_n(z)\, e^{-\lambda_n(\tau-\tau_s)}}{\partial y_n(z_o,\lambda_n)/\partial\lambda_n\,|_{z_o=z_2}}, \qquad (6.2.16)$$

for the partial differential equation (6.2.1) when the eigenspectrum is discrete.

In Sections (3) and (4) we use the Green's theorems (6.2.13) and (6.2.16) to solve boundary value problems for the distribution function $F_o(r,p)$, with boundaries at radii $r=r_a$ and $r=r_b$. If the eigenspectrum is continuous we use the Green's theorem (6.2.13) whereas if the eigenspectrum is discrete we use the Green's theorem (6.2.16).

6.3 Galactic spectrum solutions

From the separable form of the cosmic ray equation of transport (2.2.7) we have

$$\frac{\partial^2 F_o}{\partial x^2} + \frac{2n+1}{x} \frac{\partial F_o}{\partial x} = \frac{\partial F_o}{\partial t} , \tag{6.3.1}$$

where the diffusion coefficient

$$K(r,p) = K_o(p)\, r^b , \quad b > 1, \tag{6.3.2}$$

and

$$\begin{aligned} x &= (2/(1-b))(rp^{3/2})^{(1-b)/2} , \\ t &= -(3/(2V))\int^p K_o(z)\, z^{(1-3b)/2} dz, \end{aligned} \tag{6.3.3}$$

are the independent variables. For particles, initially at infinity to penetrate to a finite radius it is necessary to choose $b > 1$ in (6.3.2).

Since the partial differential equation (6.3.1) has the same form as Equation (6.1.2) i.e.

$$\frac{1}{q(x)} \frac{\partial}{\partial x} \left(p(x) \frac{\partial F_o}{\partial x} \right) = \frac{\partial F_o}{\partial t} , \tag{6.3.4}$$

with

$$p(x) = q(x) = x^{2n+1}, \tag{6.3.5}$$

we may use Green's theorem for Equation (6.1.2), derived in Section (2) to obtain solutions for F_o in which F_o is specified on boundaries at $x = x_1$ and $x = x_2$.

In general the curves x = constant, describe a curve in the r-p plane. However for boundary radii at $r = 0$ and $r = \infty$, and with $b > 1$ we have

$$x \to 0 \quad \text{as} \quad r \to \infty, \tag{6.3.6a}$$

$$x \to \infty \quad \text{as} \quad r \to 0, \tag{6.3.6b}$$

so that we can use Green's theorem (6.2.13) and the Green's function (5.3.12) to obtain galactic spectrum solutions.

We now proceed to obtain the general galactic spectrum solution in which the distribution function $F_o(r,p)$ satisfies:

(i) $F_o(r,p)$ is finite as $r \to 0$, (6.3.7a)

(ii) $F_o(r,p) \to A(p) = Z(t)$ as $r \to \infty$, (6.3.7b)

where A(p) is the galactic spectrum and Z(t) is the corresponding form of A(p) expressed in terms of the variable t,

(iii) the diffusion coefficient $K(r,p) = K_o(p)\, r^b$ with $K_o(p)$ an arbitrary function of p and $b > 1$, (6.3.7c)

(iv) the solar wind speed V is assumed constant. (6.3.7d)

Using Green's theorem (6.2.13) and the results (6.3.4), (6.3.5) and 6.3.6), the solution of the galactic boundary value problem (6.3.7) is

$$F_o = (1/x^{2n+1}) \left[\int_{t(\infty)}^{t} dt_o \lim_{x_o \to 0} x_o^{2n+1} F_o(r_o,p_o) \partial G(x_o,x,t-t_o)/\partial x_o \right.$$

$$- \int_{t(\infty)}^{t} dt_o \lim_{x_o \to \infty} x_o^{2n+1} F_o(r_o,p_o) \partial G(x_o,x,t-t_o)/\partial x_o \Big], \tag{6.3.8}$$

where the appropriate Green's function (5.3.12) is

$$G(x,x_o,t-t_o) = \frac{x_o^{n+1} x^{-n}}{2T} \exp\left(- \frac{x^2+x_o^2}{4T}\right) I_m \left(\frac{x\, x_o}{2T}\right) \tag{6.3.9}$$

and

$$\begin{aligned} T &= t-t_o, \\ t_o &= t(p_o), \\ x_o &= x(r_o,p_o), \\ n &= (b+1)/(1-b),\ m = |n|,\ b > 1. \end{aligned} \tag{6.3.10}$$

Since the modified Bessel function $I_m(z)$ has the properties

$$I_m'(z) = \frac{m}{z} I_m(z) + I_{m+1}(z), \tag{6.3.11}$$

$$I_m(z) \to \frac{e^z}{\sqrt{2\pi z}} \quad \text{as} \quad z \to \infty, \tag{6.3.12}$$

$$I_m(z) \to \frac{z^m}{2^m \Gamma(m+1)} \quad \text{as} \quad z \to 0, \tag{6.3.13}$$

(Abramowitz and Stegun (1964), Sections (9.6) and (9.7)),

we have

$$\frac{\partial G(x_o,x,t-t_o)}{\partial x_o} = \frac{x^{n+1} x_o^{-n} e^{-\frac{x^2+x_o^2}{4(t-t_o)}}}{2(t-t_o)} \left[\left(\frac{2m}{x_o} - \frac{x_o}{2(t-t_o)}\right) I_m \left(\frac{x\, x_o}{2(t-t_o)}\right) + \frac{x}{2(t-t_o)} I_{m+1} \left(\frac{x\, x_o}{2(t-t_o)} \right) \right], \tag{6.3.14}$$

$$\lim_{x_o \to \infty} x_o^{2n+1} \frac{\partial G(x_o, x, t-t_o)}{\partial x_o} = 0, \tag{6.3.15}$$

$$\lim_{x_o \to 0} x_o^{2n+1} \frac{\partial G(x_o,x,t-t_o)}{\partial x_o} = \frac{x \quad e^{-x^2/(4(t-t_o))}}{2^{2m}\,\Gamma(m)\,(t-t_o)^{m+1}} \quad , \tag{6.3.16}$$

as expressions for $\partial G(x_o,x,t-t_o)/\partial x_o$.

Substituting the expressions (6.3.15), and (6.3.16) for $\partial G(x_o,x,t-t_o)/\partial x_o$ and the boundary conditions (6.3.7) into the Green's theorem solution (6.3.8) we obtain the general galactic spectrum solution

$$F_o(r,p) = \frac{x^{2m}}{2^{2m}\Gamma(m)} \int_{t(\infty)}^{t} \frac{Z(t_s)}{(t-t_s)^{m+1}} \exp\left(\frac{-x^2}{4(t-t_s)}\right) dt_s, \tag{6.3.17}$$

where

$$\begin{aligned} x &= 2(rp^{3/2})^{(1-b)/2}/\ (1-b), \quad b > 1\ , \\ t &= -3 \int^{p} K_o(z)\ z^{(1-3b)/2}\ dz/2V,\ t_s = t(p_s), \\ m &= (b+1)/(b-1), \end{aligned} \tag{6.3.18}$$

and $Z(t_s) = F_o(\infty,p_s)$ specifies the galactic spectrum.

Expressing the integral over t_s in the solution (6.3.17) in terms of the momentum variable p_s of (6.3.18) we obtain

$$F_o(r,p) = \int_{p}^{\infty} G(r,p,p_s)\ F_o(\infty,p_s)\ dp_s, \tag{6.3.19}$$

where

$$G(r,p,p_s) = \frac{3\ K_o(p_s)\ p_s^{(1-3b)/2}}{2VT\ \Gamma(m)}\ u^m\ e^{-u}\ ,$$

$$\begin{aligned} T &= 3 \int_{p}^{p_s} K_o(z)\ z^{(1-3b)/2}\ dz\ /\ 2V, \\ u &= x^2/(4T)\ , \\ x &= 2(rp^{3/2})^{(1-b)/2}/(1-b), \end{aligned} \tag{6.3.20}$$

as an alternative form of the general galactic spectrum solution.

The monoenergetic galactic spectrum solution in which

$$F_o(\infty, p_s) = N_g \delta(p_s - p_o) / (4\pi p_o^2), \tag{6.3.21}$$

is obtained by substituting the galactic spectrum (6.3.21) in the general solution (6.3.19). Thus we obtain the monoenergetic galactic spectrum solution

$$F_o(r,p) = \frac{3N_g K_o(p_o)}{8\pi V p_o^{3(1+b)/2} \Gamma(m)} \left(\frac{x^2}{4T}\right)^m \frac{1}{T} \exp\left(\frac{-x^2}{4T}\right), \tag{6.3.22}$$

where

$$T = t - t_o.$$

We note that this solution has also been given in Equations (3.2.17) and (4.3.13).

The solutions of Fisk and Axford (1969), which satisfy the boundary conditions

(i) $F_o \to N_g p^{-\mu-2}$ as $r \to \infty$, (6.3.23a)

(ii) F_o is finite as $r \to 0$, (6.3.23b)

(iii) the diffusion coefficient $K(r,p) = K_o p^a r^b$, with $b > 1$, $a > 0$, are obtained by choosing the galactic momentum spectrum $F_o(\infty,p)$ and the corresponding function $Z(t)$ of (6.3.7) to be

$$Z(t) = F_o(\infty,p) = N_g p^{-\mu-2}, \tag{6.3.24}$$

and substituting for $Z(t)$ in the general galactic spectrum solution (6.3.17).

There are three solutions of the boundary value problem (6.3.23) corresponding to the cases

(i) $1 < b < 1 + 2a/3$,

(ii) $b = 1 + 2a/3$,

(iii) $b > 1 + 2a/3$.

Introducing the parameters

$$\nu = 2/(1-b+2a/3),$$

$$m = (b+1)/(b-1),$$

the solutions corresponding to cases (i), (ii) and (iii) are

case (i) $1 < b < 1 + 2a/3$

The solution of (6.3.23) in terms of $F_o(r,p)$ is

$$F_o = N_g\, p^{-\mu-2}\, \frac{\Gamma(\nu(\mu+2)/3+m)}{\Gamma(m)} \cdot U(\nu(\mu+2)/3, 2/(1-b), 2Vr^{1-b}p^{-a}/(\nu K_o(1-b)^2)). \tag{6.3.25a}$$

case (ii) $b = 1 + 2a/3$

The solution of (6.3.23) is

$$F_o = 2N_g\, p^{-\mu-2}\, (2(\mu+2)\, Vr^{1-b}p^{-a}/(3(1-b)^2K_o))^{m/2}/\Gamma(m).$$

$$K_m(\, 2(2(\mu+2)\, Vr^{1-b}\, p^{-a}/\, (3(1-b)^2\, K_o))^{\frac{1}{2}}\,). \tag{6.3.25b}$$

case (iii) $b > 1 + 2a/3$

The solution of (6.3.23) is

$$F_o = N_g\, p^{-\mu-2} \frac{\Gamma(1-\nu(\mu+2)/3)}{\Gamma(m)} \exp(2Vr^{1-b}p^{-a}/(\nu(1-b)^2K_o))$$

$$U(1-m-\nu(\mu+2)/3,\ 1-m,\ -2Vr^{1-b}\, p^{-a}/(\,\nu(1-b)^2K_o)), \tag{6.3.25c}$$

In Equations (6.3.25) $K_m(z)$ is a modified Bessel function of the second kind of order m, and U(a,b,z) is one of the standard solutions of Kummer's confluent hypergeometric equation (Abramowitz and Stegun (1964) Section (13.1)).

We now derive the solution (6.3.25a) from the general galactic spectrum solution (6.3.17). The solutions (6.3.25b) and (6.3.25c) can also be obtained from the general galactic spectrum solution and the derivation of these results are given in Appendix (C).

In the case of interest the general galactic spectrum solution (6.3.17) becomes

$$F_o = \frac{x^{2m}}{2^{2m}\Gamma(m)} \int_{t(\infty)}^{t} \frac{Z(t_o)}{(t-t_o)^{m+1}} \exp\left(\frac{-x^2}{4(t-t_o)}\right) dt_o , \qquad (6.3.26)$$

where

$$t = -\varepsilon p^{\delta}/\delta ,$$

$$\delta = a + 3(1-b)/2 > 0,$$

$$\varepsilon = 3K_o/2V,$$

and the diffusion coefficient $K(r,p) = K_o\, p^a r^b$.

Introducing the variables

$$u = t-t_o = \varepsilon(p_o^{\delta} - p^{\delta})/\delta , \qquad (6.3.27)$$

$$y = (\mu+2)/\delta,$$

and

$$s = x^2/(4(t-t_o)),$$

we have

$$p_o = p(1 + \delta x^2/(4\varepsilon p^{\delta} s))^{1/\delta},$$

$$Z(t_o) = N_g\, p_o^{-\mu-2} = N_g\, p^{-\mu-2}\, s^{y}(s + \delta x^2/(4\varepsilon p^{\delta}))^{-y}, \qquad (6.3.28)$$

$$dt_o = x^2/(4s^2)\, ds,$$

$$\text{as } t_o \to t,\ s \to \infty;\ \text{as } t_o \to t(\infty)\ s \to 0. \qquad (6.3.29)$$

Using the transformations (6.3.27), (6.3.28) and (6.3.29) the solution (6.3.26) for $F_o(r,p)$ becomes

$$F_o = \frac{N_g\, p^{-\mu-2}}{\Gamma(m)} \int_0^{\infty} \left(s + \frac{\delta x^2}{4\varepsilon p^{\delta}}\right)^{-y} s^{y+m-1} e^{-s}\, ds. \qquad (6.3.30)$$

Since the solution U(a,b,x) of Kummer's confluent hypergeometric equation is defined by

$$U(a,b,x) = x^{1-b} \int_0^{\infty} e^{-s}\, s^{a-1}\, (s+x)^{b-a-1}\, ds/\Gamma(a), \qquad (6.3.31)$$

and from Kummer's transformation

$$U(a,b,x) = x^{1-b}\, U(1 + a-b,\ 2-b,\ x), \qquad (6.3.32)$$

(see Slater 1960), the solution (6.3.30) becomes

$$F_o = N_g\, p^{-\mu-2}\, \frac{\Gamma\left(\frac{\nu(\mu+2)}{3} + m\right)}{\Gamma(m)} \cdot U\left(\frac{\nu}{3}(\mu+2),\ \frac{2}{1-b},\ \frac{2V\, r^{1-b} p^{-a}}{(1-b)^2 K_o \nu}\right), \qquad (6.3.33)$$

where $\nu = 2/(1-b + 2a/3) > 0$, i.e. $1 < b < 2a/3$.

This is the result we set out to obtain and it is identical to the solution (6.3.25a).

6.4 Solutions with finite boundaries

Solutions in which the distribution function $F_o(r,p)$ is specified on boundaries at $r = r_a$ and $r = r_b$ can be obtained for cases where the diffusion coefficient $K(r,p)$ has the forms

(i) $K = K_o r^b p^{3(b-1)/4}$, $b > 1$,

(ii) $K = K_o r^b$, $b < 1$,

(iii) $K = K_o r^b$, $b > 1$,

(iv) $K = K_o r$.

The general Green's theorem with source term in $r_a < r < r_b$ set equal to zero as given in Equations (6.2.13) or (6.2.16) and the Green's functions of Chapter (5) (see Table (5.1)) are used to obtain these solutions. Green's theorem in the form (6.2.16) may be used when the eigenspectrum is discrete, whereas Green's theorem in the form (6.2.13) must be used if the eigenspectrum is continuous.

The solutions are obtained for the following cases.

TABLE 6.1

K(r,p)	$F(r_a,p)$	$F(r_b,p)$
$K_o r^b p^{3(b-1)/4}$, $b > 1$	0	$N_o \delta(p-p_o)$
	$N_o \delta(p-p_o)$	0
$K_o r^b$, $b < 1$	0	$N_o \delta(p-p_o)$
	$N_o \delta(p-p_o)$	0
$K_o r^b$, $b > 1$	0	$N_o \delta(p-p_o)$
	$N_o \delta(p-p_o)$	0
$K_o r$	0	$N_o \delta(p-p_o)$
	$N_o \delta(p-p_o)$	0

The determination of these solutions from those of Chapter (5) (Table (5.1)) is straight forward, but in particular cases is quite lengthy. These details have been omitted and the solutions together with the appropriate variables have been given in Table (6.1). For completeness the eigenvalue equations for λ_n are repeated from Table (5.1).

TABLE 6.2

SOLUTIONS WITH FINITE BOUNDARIES

A. Diffusion coefficient

$$K(r,p) = K_o r^b p^{3(b-1)/4}, \quad b > 1$$

Boundary conditions

$$F_o(r_a,p) = 0,$$

$$F_o(r_b, p) = N_o \delta(p-p_o),$$

$$r_a < r < r_b , \quad 0 < p < p_o$$

Variables

$$z = V r^{(1-b)/2} / K_o ,$$

$$t = 2K_o p^{3(1-b)/4} / (V(b-1)),$$

$$u = (t-t_o)/ (t\, t_o),$$

$$x = zt = 2(r\, p^{3/2})^{(1-b)/2} / (b-1), \quad T = (t-t_o),$$

$$z_1 = z(r_b) , \; z_2 = z(r_a), \; t_o = t(p_o),$$

$$m = (b+1.0) / (b-1.0) .$$

Solution

$$F_o(r,p) = \frac{3N_o (b-1)^2 V p_o^{(3b-7)/4}}{4K_o} (z/z_1)^m (t/t_o)^{m-1} \exp((z_1^2 t_o - z^2 t)/4)$$

$$\sum_{n=1}^{\infty} s_n [Y_m(s_n z_2) J_m(s_n z) - J_m(s_n z_2) Y_m(s_n z)] e^{-s_n^2 u} /$$

$$[z_1 (Y_m(s_n z_2) J_{m+1}(s_n z_1) - J_m(s_n z_2) Y_{m+1}(s_n z_1)) +$$

$$z_2 (J_m(s_n z_1) Y_{m+1}(s_n z_2) - Y_m(s_n z_1) J_{m+1}(s_n z_2))], \qquad (6.4.1)$$

where,

$$J_m(s_n z_1) Y_m(s_n z_2) - J_m(s_n z_2) Y_m(s_n z_1) = 0,$$

and $J_m(z)$, $Y_m(z)$ are Bessel functions, of order m, and of the first and second kind respectively.

Effect of varying the boundaries

If we let the outer boundary at $r=r_b$ tend to infinity then $z_1 = z(r_b) \to 0$ and the eigenvalue equation becomes

$$J_m(s_n z_2) = 0.$$

Using Green's theorem (6.2.16) and the Green's function (5.3.35) for $z_1 = 0$ and z_2 finite we have

$$F_o(r,p) = \frac{3N_o V(b-1)^2 p_o^{(3b-7)/4}}{2^{m+1}\Gamma(m)} z^m (t/t_o)^{m-1} \exp(-z^2 t/4).$$

$$\sum_{n=1}^{\infty} s_n^m J_m(s_n z) e^{-s_n^2 u} / (z_2^2 J_{m+1}^2(s_n z_2)), \qquad (6.4.2)$$

as the solution with inner boundary at $r=r_a \neq 0$ and the outer boundary at $r = \infty$.

If we let the inner boundary at $r=r_a$ tend to zero in the solution (6.4.2), then $z_2 = z(r_a) \to \infty$, the eigenspectrum becomes continuous and we find

$$F_o(r,p) = \frac{3\,N_o\,V(b-1)^2\,p_o^{(3b-7)/4}}{2^{m+2}\,\Gamma(m)\,K_o}\; z^m\,(t/t_o)^{m-1}\,\exp(-z^2\,t/4).$$

$$\int_0^\infty s^{m+1}\,J_m(sz)\,e^{-s^2 u}\,ds, \qquad (6.4.3)$$

as the solution for $r_a = 0$ and $r_b \to \infty$.

The solution (6.4.3) is equivalent to the monoenergetic galactic spectrum solution (6.3.22). To show this explicitly we put

$$N_g = 4\pi\,p_o^2\,N_o,$$

and we use the result

$$\int_0^\infty x^{m+1}\,e^{-ax^2}\,J_m(bx)\,dx = \frac{b^m}{(2a)^{m+1}}\,\exp(-b^2/(4a)),$$

where Re (a) > 0, b > 0, Re(m) > -1 (Gradshteyn and Ryszhik p.717) in the solution (6.4.3). Hence we obtain

$$F_o(r,p) = \frac{3\,N_g(b-1)^2\,V\,p_o^{(3b-7)/4}}{2^{m+4}\,\pi\,p_o^2\,K_o\,\Gamma(m)}\; z^m(t/t_o)^{m-1}\exp(-z^2t/4).$$

$$[\; z^m \exp(-z^2/(4u)) \,/\, (2u)^{m+1}\;].$$

Since

$$x = zt, \quad T = (t-t_o) \qquad u = T/(t\,t_o),$$

(see Variables), this latter result reduces to

$$F_o(r,p) = \frac{3\,N_g\,K_o\,p_o^{3(b-1)/4}}{8\,\pi\,V\,p_o^{3(1+b)/2}\,\Gamma(m)}\;\left(\frac{x^2}{4T}\right)^m \frac{1}{T}\;\exp\left(\frac{-x^2}{4T}\right),$$

which is the monoenergetic galactic spectrum solution (6.3.22).

In the case where the inner boundary is at $r_a=0$ ($z_2 \to \infty$), and the outer boundary at some finite radius r_b (z_1 finite), the eigenspectrum is continuous and the appropriate Green's function is given by Equation (5.3.36). Using Green's theorem (6.2.13) and the Green's function (5.3.36) we obtain

$$F_o(r,p) = \frac{3\ N_o(b-1)}{2\pi\ p_o} (z/z_1)^m\ t^{m-1}\ t_o^{-m} \exp\ ((z_1^2\ t_o - z^2 t)/4).$$

$$\int_0^\infty \frac{[J_m\ (sz_1)\ Y_m(sz) - Y_m(sz_1)\ J_m(sz)]}{[J_m^{\ 2}\ (sz_1) + Y_m^{\ 2}\ (sz_1)]}\ s \cdot \exp\ (-s^2\ u)\ ds, \qquad (6.4.4)$$

as the solution for $r_a = 0$ and r_b finite.

If we let the outer boundary at r_b tend to infinity (i.e. $z_1 \to 0$) in the solution (6.4.4) we obtain

$$F_o\ (r,p) = \frac{3\ N_o\ (b-1)}{2^{m+1}\ \Gamma(m)\ p_o}\ t^{m-1}\ t_o^{-m}\ z^m \exp\ (-z^2\ t/4).$$

$$\int_0^\infty s^{m+1}\ e^{-s^2 u}\ J_m\ (sz)\ ds, \qquad (6.4.5)$$

which is equivalent to the monoenergetic galactic spectrum solution (6.3.22), or the solution (6.4.3).

B. Diffusion Coefficient

$$K\ (r,p) = K_o\ r^b\ p^{3(b-1)/4},\ b > 1.$$

Boundary Conditions

$$F_o(r_a,p) = N_o\ \delta(p-p_o),$$

$$F_o(r_b,p) = 0,$$

$$r_a < r < r_b, \qquad 0 < p < p_o.$$

Variables

$$z = V r^{(1-b)/2} / K_o ,$$

$$t = 2 K_o p^{3(1-b)/4} / (V(b-1)),$$

$$u = (t-t_o) / (t\, t_o),$$

$$x = zt = 2 (r p^{3/2})^{(1-b)/2} / (b-1),\ T = t-t_o,$$

$z_1 = z(r_b)$, $z_2 = z(r_a)$, $t_o = t(p_o)$,

$$m = (b+1.0) / (b-1.0) .$$

Solution

$$F_o(r,p) = \frac{3(b-1)^2 N_o V p_o^{(3b-7)/4}}{4K_o} (z/z_2)^m (t/t_o)^{m-1} \exp[(z_2^2 t_o - z^2 t)/4].$$

$$\sum_{n=1}^{\infty} s_n [Y_m(s_n z_1) J_m(s_n z) - J_m (s_n z_1) Y_m(s_n z)] e^{-s_n^2 u} /$$

$$[z_1 (J_m (s_n z_2) Y_{m+1} (s_n z_1) - Y_m (s_n z_2) J_{m+1} (s_n z_1))$$

$$+ z_2 (Y_m (s_n z_1) J_{m+1} (s_n z_2) - J_m (s_n z_1) Y_{m+1} (s_n z_2))] \qquad (6.4.6)$$

where,

$$J_m(s_n z_1)\ Y_m(s_n z_2) - J_m (s_n z_2) Y_m (s_n z_1) = 0$$

is the eigenvalue equation.We note that the solution (6.4.6) can be obtained from the solution (6.4.1) by interchanging z_1 and z_2.

Effect of Varying the Boundaries

If we let the outer boundary at $r = r_b$ tend to infinity then z_1 tends to zero and the eigenvalue equation becomes

$$J_m(s_n z_2) = 0.$$

Using Green's theorem (6.2.16) and the Green's function (5.3.35) for $z_1 = 0$ and z_2 finite we have

$$F_o(r,p) = \frac{3N_o V(b-1)^2 p_o^{(3b-7)/4}}{4K_o} (t/t_o)^{m-1} z^m z_2^{-m-1} \exp((z_2^2 t_o - z^2 t)/4).$$

$$\sum_{n=1}^{\infty} s_n J_m(s_n z) e^{-s_n^2 u} / J_{m+1}(s_n z_2), \qquad (6.4.7)$$

as the solution with an inner boundary at $r=r_a \neq 0$, and the outer boundary at $r = \infty$.

C. Diffusion Coefficient

$$K(r,p) = K_o r^b , \quad b < 1$$

Boundary conditions

$$F_o(r_a,p) = 0,$$

$$F_o(r_b,p) = N_o \delta(p-p_o),$$

$$r_a < r < r_b , \quad 0 < p < p_o.$$

Variables

$$z = V r^{1-b} / (K_o(1-b)),$$

$$u = 3(1-b) \ln(p_o/p) /2,$$

$$z_1 = z(r_a), \quad z_2 = z(r_b),$$

$$m = (b+1) / (1-b)$$

Solution

$$F_o(r,p) = \frac{3(b-1)}{2p_o} N_o \sum_{n=1}^{\infty} [U(-\lambda_n,1+m,z_1)M(-\lambda_n,1+m,z)-M(-\lambda_n,1+m,z_1).$$

$$U(-\lambda_n, 1+m, z)] e^{-\lambda_n u} /$$

$$\frac{\partial}{\partial\lambda_n} [U(-\lambda_n,1+m,z_1)M(-\lambda_n,1+m,z_o)-M(-\lambda_n,1+m,z_1)U(-\lambda_n,1+m,z_o)]_{zo=z2},$$

(6.4.8)

where the eigenvalues λ_n satisfy

$$U(-\lambda_n,1+m,z_1)M(-\lambda_n,1+m,z_2)-M(-\lambda_n,1+m,z_1)U(-\lambda_n,1+m,z_2) = 0$$

Effect of Varying the Boundary

If there is no inner boundary, but we require that $F_o(r,p)$ be finite as $r \to 0$, then the solution is

$$F_o(r,p) = \frac{3(b-1)}{2p_o} N_o \sum_{n=1}^{\infty} M(-\lambda_n, 1+m, z) e^{-\lambda_n u} /$$

$$\frac{\partial}{\partial\lambda_n} [M(-\lambda_n, 1+m, z_o)]_{z_o=z_2}, \qquad (6.4.9)$$

and the eigenvalue equation is

$$M(-\lambda_n, 1+m, z_2) = 0$$

D. Diffusion Coefficient

$$K(r,p) = K_o r^b, \quad b < 1 ,$$

Boundary conditions

$$F_o(r_a, p) = N_o \delta(p - p_o),$$

$$F_o(r_b, p) = 0,$$

$$r_a < r < r_b, \qquad 0 < p < p_o.$$

Variables

$$z = Vr^{1-b}/(K_o(1-b)),$$

$$u = 3(1-b) \ln (p_o/p)/2,$$

$$z_1 = z(r_a), \quad z_2 = z(r_b),$$

$$m = (b+1)/(1-b).$$

Solution

$$F_o(r,p) = \frac{3(b-1)}{2 p_o} N_o \sum_{n=1}^{\infty} \Big[U(-\lambda_n, 1+m, z_2) M(-\lambda_n, 1+m, z) - M(-\lambda_n, 1+m, z_2) U(-\lambda_n, 1+m, z) \Big] e^{-\lambda_n u} \Big/ \frac{\partial}{\partial \lambda_n} \Big(U(-\lambda_n, 1+m, z_2) M(-\lambda_n, 1+m, z_o) - M(-\lambda_n, 1+m, z_2) U(-\lambda_n, 1+m, z_o) \Big) \Big| z_o = z_1, \tag{6.4.10}$$

where

$$U(-\lambda_n, 1+m, z_2) M(-\lambda_n, 1+m, z_1) - U(-\lambda_n, 1+m, z_1)$$

$$M(-\lambda_n, 1+m, z_2) = 0,$$

is the eigenvalue equation. We note that the solution (6.4.10) can be obtained from the solution (6.4.8) by interchange of z_1 and z_2.

E. Diffusion coefficient

$$K(r,p) = K_o r^b, \quad b > 1$$

Boundary conditions

$$F_o(r_a, p) = 0$$

$$F_o(r_b, p) = N_o \delta(p - p_o),$$

$$r_a < r < r_b, \qquad 0 < p < p_o.$$

Variables

$$z = V r^{1-b}/(K_o (b-1)),$$

$$t = K_o p^{3(1-b)/2}/ (V (b-1)),$$

$$u = 3(b-1) \ln (p_o/p) /2,$$

$$x = (4zt)^{\frac{1}{2}} = 2(rp^{3/2})^{(1-b)/2}/ (b-1),$$

$$T = t - t_o = t [1 - \exp(-u)],$$

$$z_1 = z(r_b), \quad z_2 = z(r_a), \quad t_o = t(p_o),$$

$$m = (b+1)/(b-1).$$

Solution

$$F_o(r,p) = \frac{-3N_o(b-1)}{2p_o} (z/z_1)^m e^{z_1-z}$$

$$\sum_{n=1}^{\infty} \left[U(1-\lambda_n, 1+m, z_2) M(1-\lambda_n, 1+m, z) - M(1-\lambda_n, 1+m, z_2) U(1-\lambda_n, 1+m, z)\right] e^{-\lambda_n u} /$$

$$\frac{\partial}{\partial \lambda_n} \left(U(1-\lambda_n, 1+m, z_2) M(1-\lambda_n, 1+m, z_o) - M(1-\lambda_n, 1+m, z_2) U(1-\lambda_n, 1+m, z_o) \right) \Big| z_o = z_1,$$

(6.4.11)

where

$$U(1-\lambda_n, 1+m, z_2) M(1-\lambda_n, 1+m, z_1) - M(1-\lambda_n, 1+m, z_2) U(1-\lambda_n, 1+m, z_1) = 0,$$

is the eigenvalue equation.

Effect of varying the boundaries

If we let the inner boundary at $r = r_a$ tend to zero, then $z_2 \to \infty$ and the eigenvalue equation becomes

$$U(1-\lambda_n, 1+m, z_1) = 0,$$

and we obtain

$$F_o(r,p) = \frac{-3(b-1)}{2p_o} N_o (z/z_1)^m e^{z_1-z} \sum_{n=1}^{\infty} \frac{U(1-\lambda_n, 1+m, z) e^{-\lambda_n u}}{\frac{\partial}{\partial \lambda_n} U(1-\lambda_n, 1+m, z_o) \mid z_o = z_1} \qquad (6.4.12)$$

as the solution with outer boundary at $r = r_b$ and inner boundary at $r = 0$.

If we let the outer boundary at $r = r_b$ tend to infinity (i.e. $z_1 \to 0$) in the solution (6.4.12), the eigenvalue equation becomes

$$\frac{1}{\Gamma(1-\lambda_n)} = 0,$$

so that the eigenvalues are

$$\lambda_n = 1, 2, 3, 4, \ldots\ldots$$

Since

$$U(-n, 1+m, z) = (-1)^n n! L_n^m(z),$$

$$\lim_{z \to 0} \partial U(-n, 1+m, z)/\partial n \sim z^{-m} \Gamma(m) \Gamma(n+1)(-1)^{n+1},$$

where $L_n^m(z)$ is a generalised Laguerre function and $\Gamma(z)$ is the

gamma function, we obtain

$$F_o(r,p) = \frac{3(b-1)N_o}{2p_o} \frac{z^m e^{-z}}{\Gamma(m)} \sum_{n=0}^{\infty} L_n^m(z)\, e^{-nu-u}, \tag{6.4.13}$$

as the solution with inner boundary at $r_a = 0$ and the outer boundary r_b at infinity.

The solution (6.4.13) is equivalent to the monoenergetic galactic spectrum solution (6.3.22). To show this explicity we put

$$N_g = 4\pi p_o^2 N_o,$$

and we use the result

$$\sum_{n=0}^{\infty} L_n^m(x) y^n = (1-y)^{-m-1} \exp(xy/(y-1)),$$

where $| y | < 1$ (see Gradshteyn and Ryzhik p. 1038) in Equation (6.4.13) and thus obtain

$$F_o(r,p) = \frac{3(b-1)N_g}{8\pi p_o^3} \frac{z^m e^{-z}}{\Gamma(m)} \left[e^{-u}(1-e^{-u})^{-m-1} \exp\left(\frac{z e^{-u}}{e^{-u}-1}\right) \right]$$

Since

$$x^2 = 4zt, \quad T = t(1-e^{-u}), \quad t = K_o p^{3(1-b)/2} / (V(b-1)),$$

(see Variables), this latter result reduces to

$$F_o(r,p) = \frac{3N_g K_o}{8\pi V p_o^{3(1+b)/2} \Gamma(m)} \left(\frac{x^2}{4T}\right)^m \frac{1}{T} \exp\left(\frac{-x^2}{4T}\right),$$

which is the monoenergetic galactic spectrum solution (6.3.22).

F. Diffusion coefficient

$$K(r,p) = K_o r^b, \quad b > 1$$

Boundary conditions

$$F_o(r_a,p) = N_o\ \delta(p-p_o),$$

$$F_o(r_b,p) = 0,$$

$$r_a < r < r_b, \quad 0 < p < p_o$$

Variables

$$z = V\, r^{1-b}/\, K_o(1-b),$$

$$u = 3(b-1)\ \ln\ (p_o/p)/2,$$

$$z_1 = z(r_b), \quad z_2 = z(r_a)$$

$$m = (b+1)/(b-1)$$

Solution

$$F_o(r,p) = \frac{-3(b-1)}{2p_o}\ (z/z_2)^m\ \exp(z_2-z).$$

$$\sum_{n=1}^{\infty} \left[U(1-\lambda_n,\ 1+m,\ z_1)\ M(1-\lambda_n,\ 1+m,\ z) - M(1-\lambda_n,\ 1+m,\ z_1)\right.$$
$$\left. U(1-\lambda_n,\ 1+m,\ z)\right]\ e^{-\lambda_n u} \Big/ \frac{\partial}{\partial\lambda_n}\Big(U(1-\lambda_n,\ 1+m,\ z_1)\ M(1-\lambda_n,\ 1+m,\ z_o)$$
$$- M(1-\lambda_n,\ 1+m,\ z_1)\ U(1-\lambda_n,\ 1+m,\ z_o)\Big)\Big|\ z_o = z_2, \qquad (6.4.14)$$

and the eigenvalue equation is

$$U(1-\lambda_n,\ 1+m,\ z_1)\ M(1-\lambda_n,\ 1+m,\ z_2) - M(1-\lambda_n,\ 1+m,\ z_1)$$
$$U(1-\lambda_n,\ 1+m,\ z_2) = 0.$$

Effect of varying the boundaries

If we let the outer boundary at $r = r_b$ tend to infinity (i.e., $z_1 \to 0$) the eigenvalue equation becomes

$$M(1-\lambda_n,\ 1+m,\ z_2) = 0,$$

and

$$F_o(r,p) = \frac{-3N_o(b-1)}{2p_o} (z/z_2)^m e^{z_2-z} \sum_{n=1}^{\infty} \frac{M(1-\lambda_n, 1+m, z) e^{-\lambda_n u}}{\partial M(1-\lambda_n, 1+m, z_o)/\partial\lambda_n \mid z_o = z_2}, \quad (6.4.15)$$

is the solution for an inner boundary at $r = r_a \neq 0$ and an outer boundary at infinity.

G. Diffusion coefficient

$$K(r,p) = K_o r$$

Boundary conditions

$$F(r_a,p) = 0,$$

$$F(r_b,p) = N_o \delta(p-p_o),$$

$$r_a < r < r_b, \quad 0 < p < p_o.$$

Variables

$$z = \ln(r)$$

$$u = 3K_o \ln(p_o/p)/2V,$$

$$c = 1 - V/2K_o$$

$$z_1 = z(r_a), \quad z_2 = z(r_b)$$

Solution

$$F_o(r,p) = \frac{3N_oK_o}{Vp_o(z_2-z_1)^2} \exp(c(z_2-z) - c^2u).$$

$$\sum_{n=1}^{\infty} (-1)^n \; n\pi \; \sin\left[n\pi(z-z_1)/(z_2-z_1)\right] \exp\left[-n^2\pi^2 u/(z_2-z_1)^2\right] \tag{6.4.16}$$

Effect of varying the boundaries

If we let the inner boundary at r_a tend to zero then $z_1 \to -\infty$ and the solution (6.4.16) becomes

$$F_o(r,p) = \frac{3N_oK_o}{4Vp_o\sqrt{\pi}} \; (z_2-z) \exp\left[c(z_2-z)-c^2u - (z-z_2)^2/(4u)\right] / u^{3/2}. \tag{6.4.17}$$

H. Diffusion coefficient

$$K(r,p) = K_o r$$

Boundary conditions

$$F(r_a,p) = N_o \, \delta(p-p_o),$$

$$F(r_b,p) = 0,$$

$$r_a < r < r_b, \qquad 0 < p < p_o,$$

Variables

$$z = \ln(r),$$

$$u = 3K_o \, \ell n(p_o/p) / \, 2V,$$

$$c = 1 - V/2K_o,$$

$$z_1 = z(r_a), \quad z_2 = z(r_b).$$

Solution

$$F_o(r,p) = \frac{3N_oK_o}{V \, p_o(z_2-z_1)^2} \exp\left[c(z_1-z) - c^2u\right].$$

$$\sum_{n=1}^{\infty} n\pi \sin\left[n\pi(z-z_1)/(z_2-z_1)\right] \exp\left[-n^2\pi^2 u/(z_2-z_1)^2\right] \tag{6.4.18}$$

Effect of varying the boundaries

If we let the outer boundary at $r = r_b$ tend to infinity then $z_2 \to \infty$ and we obtain

$$F_o(r,p) = \frac{3\ N_o K_o}{4\ V p_o \sqrt{\pi}}\ (z-z_1)\ \exp[c(z_1-z) - c^2 u - (z-z_1)^2/(4u)]/u^{3/2}, \quad (6.4.19)$$

as the solution for an inner boundary at $r_a \neq 0$, and an outer boundary at infinity.

6.5 Concluding Remarks

In each case considered, solutions in this chapter have been given for a monoenergetic boundary spectrum of the form $F_o = N_o\ \delta(p-p_o)$. Only in the case of Fisk and Axford (1969) with $K = K_o\ p^a\ r^b$, $b > 1$ has to solution included the effects of a full boundary spectrum, viz. $F \to N_o\ p^{-u-2}$ as $r \to \infty$. Full spectrum cases can of course be determined by integration but numerical methods may be necessary. Examples of this will be given later in Chapter (8).

Note again that the interior sources have been set equal to zero, this corresponding to the cosmic ray case in the solar cavity. These sources can also be included if necessary by evaluation of the Green's theorem integral (see Equation (6.2.9)).

CHAPTER 7

COSMIC-RAY ENERGY CHANGES

7.1 Introduction

In this chapter we show that the average time rate of change of momentum of cosmic-ray particles propagating in interplanetary space, reckoned for a fixed volume in a frame of reference fixed in the solar system is given by

$$\langle \dot{p} \rangle = \frac{p\,\underline{V}}{3U_p} \cdot \frac{\partial U_p}{\partial \underline{r}} = \frac{p\,\underline{V} \cdot \underline{G}}{3}, \qquad (7.1.1)$$

where $U_p(\underline{r},p,t)$ is the differential number density (w.r.t. momentum), $\underline{V}$ is the solar wind velocity, and $\underline{G} = (1/U_p)(\partial U_p/\partial \underline{r})$ is the density gradient. The expression (7.1.1) for $\langle \dot{p} \rangle$ was first noted by Gleeson (1972), Quenby (1973), Gleeson and Webb (1974), and it is implicit in the discussion of cosmic-ray energy changes by Jokipii and Parker (1967). It shows that particles on average gain energy when there is a positive density gradient, and that they lose energy in a negative density gradient.

There are two further momentum rates that are useful in discussing cosmic-ray energy changes, which have been discussed briefly in Section 1.3. We reiterate the basic argument of that section in order to show the proper use of these two rates.

The equation of transport for the propagation of cosmic-rays in the interplanetary medium is (Jokipii and Parker, 1970),

$$\frac{\partial U_p^*}{\partial t} + \underline{\nabla}.\left(\underline{V}\,U_p^* - \underline{\underline{K}}.\underline{\nabla}\,U_p^*\right) - \frac{1}{3}\,\underline{\nabla}.\underline{V}\,\frac{\partial}{\partial p}\left(p' U_p^*\right) = 0, \qquad (7.1.2)$$

where U^*_p ($\underline{r}$,p',t) is the differential number density with respect to momentum p' as seen in a frame of reference moving with the solar wind, and the spatial coordinates, $\underline{r}$, are defined in a fixed frame of reference. The equation of transport (7.1.2) can be written in an alternative form, which displays the physics more clearly:

$$\frac{\partial U^*_p}{\partial t} + \underline{\nabla} \cdot \underline{S}^*_p + \frac{\partial}{\partial p'}\left(\langle \dot{p}' \rangle U^*_p\right) = 0, \qquad (7.1.3)$$

where

$$\underline{S}^*_p = \underline{V} U^*_p - \underline{\underline{K}} \cdot \underline{\nabla} U^*_p, \qquad (7.1.4)$$

is the streaming of particles with momentum p' (specified relative to the solar wind frame) across a fixed surface at position $\underline{r}$ in the fixed frame, and

$$\langle \dot{p}' \rangle = -\frac{p'}{3} \underline{\nabla} \cdot \underline{V}, \qquad (7.1.5)$$

is the corresponding mean rate of change of momentum of particles with momentum p' at position $\underline{r}$.

The momentum rate $\langle \dot{p}' \rangle$ is due to the transformation of momentum between the fixed and solar wind frames. It arises because the solar wind frame is not an inertial frame of reference on a large scale. We remark that $\langle \dot{p}' \rangle$ is not dependent on particle scattering, and a derivation of the rate $\langle \dot{p}' \rangle$ is given (for the first time) in Appendix G.

In addition to the rates $\langle \dot{p} \rangle$ and $\langle \dot{p}' \rangle$ referred to in Equations (7.1.1) and (7.1.5) there is the adiabatic deceleration rate of Parker (1965). The term adiabatic arises from thermodynamics. An adiabatic enclosure is one which is isolated or thermally insulated from its surroundings. If a gas is allowed to expand under adiabatic conditions it will do work at the expense of its internal energy (the total kinetic

energy of the individual particles composing the gas). The adiabatic deceleration formula

$$\langle \dot{p} \rangle_{ad} = -\frac{p}{3} \underline{\nabla} \cdot \underline{V} , \qquad (7.1.6)$$

gives the rate of change of momentum that the particles of momentum p undergo when the external boundaries of the gas expand at the velocity $\underline{V}(\underline{x})$.

In the case of cosmic-ray propagation in the interplanetary medium, the concept of adiabatic deceleration is only applicable in the limit of strong scattering, i.e., the components of the diffusion tensor $\underline{\underline{K}} \simeq 0$. The cosmic-rays are then effectively constrained to move with the solar wind as they scatter between the magnetic field irregularities which behave like the walls of a 'magnetic box'. Consequently they change momentum at the adiabatic rate (7.1.6) within the 'magnetic box' whose walls expand at the solar wind velocity $\underline{V}(\underline{x})$. A derivation of the adiabatic rate (7.1.6) is given in Section 4.

It is obvious from the above discussion that the appropriate rate to use when deriving the transport equation in terms of $U_p^*(\underline{r},p',t)$ is $\langle \dot{p}' \rangle$. We remark that Parker (1965) and Jokipii and Parker (1970) obtained the equation of transport (7.1.2) by using the adiabatic rate $\langle \dot{p} \rangle_{ad}$, which is of course incorrect. However they obtained the correct equation of transport because the momentum rate $\langle \dot{p}' \rangle$ and the adiabatic deceleration rate $\langle \dot{p}' \rangle_{ad}$ are given by the same formula.

As indicated in Section 1.3, the equation of transport in the fixed frame of reference is

$$\frac{\partial U_p}{\partial t} + \underline{\nabla} \cdot (\underline{V} U_p - \underline{\underline{K}} \cdot \underline{\nabla} U_p) - \frac{1}{3} \underline{\nabla} \cdot \underline{V} \frac{\partial}{\partial p} (p U_p) = 0, \qquad (7.1.7)$$

where U_p ($\underline{r}$, p,t) is the differential number density with respect to momentum p at position $\underline{r}$ in the fixed frame, and it is readily obtained from Equation (7.1.2),

The principal contents of this chapter concern the derivation of the meant-time-rate-of-change of momentum $\langle\dot{p}\rangle$ in the fixed frame of reference, referred to in Equation (7.1.1). We derive $\langle\dot{p}\rangle$ in three ways:

(i) by a rearrangement and reinterpretation of the equation of transport (7.1.7),

(ii) from a consideration of particle momentum changes arising from the scattering analysis of Gleeson and Axford (1967),

(iii) by considering the collisions of the cosmic-rays with the walls of a collection of 'magnetic boxes' moving with the solar wind.

We develop it by the first method in Section 2, the second method in Section 3 and by the third method in Section 4. The first derivation has been published (Gleeson 1972; Quenby 1973; Gleeson and Webb 1974). The third method is particularly instructive in the derivation of the relativistic adiabatic deceleration formula and for showing the relation between this and the result (7.1.1).

For completeness a result of Jokipii and Parker (1967) is also derived. These authors have shown that the total rate of energy transfer from the solar wind to the cosmic-rays, per unit volume is :-

$$\frac{dW}{dt} = V \frac{d P_c (r)}{dr} , \qquad (7.1.8)$$

where $P_c(r)$ is the cosmic-ray pressure at radius r. In Section 5 we show that the result (7.1.8) follows from the momentum rate $\langle\dot{p}\rangle$ given in Equation (7.1.1).

In Section (6) we give a summary and discussion of the results of this chapter and we define a momentum-position flow line in terms of the flow velocity $\langle \dot{\underline{r}} \rangle$ and the average time rate of change of momentum $\langle \dot{\underline{p}} \rangle$.

In the work that follows we use two frames of reference; one of the frames, denoted by S is fixed in the solar system and the other frame S_m moves with the solar wind. Physical quantities in the moving frame S_m are denoted by the subscript m. The Lorentz transformations for momentum $\underline{p}$ and total energy E between the moving frame S_m and the fixed frame S are:

$$\begin{aligned} \underline{p}_m &= \underline{p} + \left(\frac{(\gamma-1)\underline{p} \cdot \underline{V}}{V^2} - \gamma m \right) \underline{V}, \\ E_m &= \gamma(E - \underline{V}\cdot\underline{p}), \\ \gamma &= (1-V^2/c^2)^{-\frac{1}{2}}, \end{aligned} \tag{7.1.9}$$

and $m=m_o(1-v^2/c^2)^{-\frac{1}{2}}$ is the relativistic mass of a particle with rest mass m_o. To $O(V/c)^2$ we have $\gamma=1$ and the transformations (7.1.9) are

$$\underline{p}_m = \underline{p} - m\underline{V} \tag{7.1.10}$$

$$E_m = E - \underline{V} \cdot \underline{p} \tag{7.1.11}$$

It can also be shown (see e.g. Forman (1970)) that the momentum position distribution function $F(\underline{r},\underline{p})$ and the volume element $d^3\underline{r}\, d^3\underline{p}$ centred on the point $(\underline{r},\underline{p})$ of position momentum space are Lorentz invariant, i.e.,

$$F_m(\underline{r}_m, \underline{p}_m, t_m) = F(\underline{r},\underline{p},t), \tag{7.1.12}$$

$$d^3\underline{r}_m\, d^3\underline{p}_m = d^3\underline{r} d^3\underline{p}, \tag{7.1.13}$$

and we will use these relationships in our analysis.

7.2 The transport equation approach

The basic equations describing the cosmic ray gas in the interplanetary region are:-

$$\frac{\partial U_p}{\partial t} + \underline{\nabla} \cdot \left(\underline{V} U_p - \underline{\underline{K}} \cdot \frac{\partial U_p}{\partial \underline{r}} \right) - \frac{1}{3} (\underline{\nabla} \cdot \underline{V}) \frac{\partial}{\partial p} \left(p U_p \right) = 0, \tag{7.2.1}$$

$$\underline{S}_p = \underline{V} U_p - \frac{\underline{\underline{V}}}{3} \frac{\partial}{\partial p} (p U_p) - \underline{\underline{K}} \cdot \frac{\partial U_p}{\partial \underline{r}}, \tag{7.2.2}$$

where $\underline{S}_p$ is the differential current density or streaming. The result (7.2.2) was first obtained by Gleeson and Axford (1967) in a spherically symmetric model of the interplanetary region.

The basis for the present work is to note that particles are conserved; thus we may write down a continuity equation and identify the terms in it by comparison with (7.2.1). Taking into account the momentum of the cosmic ray particles the general continuity equation for $U_p(\underline{r},p,t)$ is

$$\frac{\partial U_p}{\partial t} + \underline{\nabla} \cdot \underline{S}_p + \frac{\partial}{\partial p} (\langle \dot{p} \rangle U_p) = 0. \tag{7.2.3}$$

In order to identify terms in our case we rearrange (7.2.1) so that the terms in the first parenthesis are equal to $\underline{S}_p$. It becomes

$$\frac{\partial U_p}{\partial t} + \underline{\nabla} \cdot \left(\underline{V} \left[U_p - \frac{1}{3} \frac{\partial}{\partial p} (p U_p) \right] - \underline{\underline{K}} \cdot \frac{\partial U_p}{\partial \underline{r}} \right) + \frac{\partial}{\partial p} \left(\frac{p \underline{\nabla}}{3} \cdot \frac{\partial U_p}{\partial \underline{r}} \right) = 0. \tag{7.2.4}$$

Identification with (7.2.3) now gives the relationship

$$\langle \dot{p} \rangle U_p = \frac{\underline{\nabla} p}{3} \cdot \frac{\partial U_p}{\partial \underline{r}}. \tag{7.2.5}$$

Alternatively we write this result as

$$\langle \dot{p} \rangle = \frac{p \underline{\underline{V}} \cdot \underline{G}}{3} \tag{7.2.6}$$

in which $\underline{G} = (1/U_p) \partial U_p / \partial \underline{r}$ is the density gradient.

7.3 The scattering model approach

We now obtain the momentum rate $\langle \dot{p} \rangle$ derived in Section (7.2) and given in Equations (7.1.1) and (7.2.6) by using the scattering analysis of Gleeson and Axford (1967). We first give details of their analysis and then use the same model to calculate:

(i) the total momentum change of particles with momentum in (p,p+dp) and position in $d^3\underline{r}$ about $\underline{r}$ at time t, due to scattering in the time interval (t,t+dt);

(ii) the total momentum change of particles with momentum in (p,p+dp) and position in $d^3\underline{r}$ about $\underline{r}$ at time t+dt, due to previous scattering in the time interval (t,t+dt).

The momentum changes obtained in (i) and (ii) are found to be different, and to calculate $\langle \dot{p} \rangle$ we take the average of these momentum changes, and divide this average by the time interval dt and the number of particles with momentum in (p,p+dp) and position in $d^3\underline{r}$ about $\underline{r}$ at time t.

In the scattering analysis the interplanetary medium is modelled by magnetic irregularities moving radially with the solar wind and deflecting or scattering cosmic-ray particles. We assume:

(i) the steady interplanetary magnetic field is radial;

(ii) the scattering is isotropic in the solar wind frame S_m, and since there are no electric fields in S_m particles are scattered without change of speed.

The number of scatterers per unit volume and the scattering cross section in S_m are denoted by $N_m(r)$ and $\sigma(p_m)$ respectively. The Boltzmann equation

$$\frac{\partial F}{\partial t} + \frac{\partial}{\partial \underline{r}} \cdot (\underline{v}\, F) + \frac{\partial}{\partial \underline{p}} \cdot (\dot{\underline{p}}\, F) = \left(\frac{\delta F}{\delta t}\right)_c , \qquad (7.3.1)$$

for this situation becomes

$$\frac{\partial F}{\partial t} + v \cos\theta \frac{\partial F}{\partial r} - \frac{v \sin\theta}{r} \frac{\partial F}{\partial \theta} = \left(\frac{\delta F}{\delta t}\right)_c , \qquad (7.3.2)$$

where θ is the angle between $\underline{v}$ and $\underline{r}$ and $\left(\frac{\delta F}{\delta t}\right)_c$ represents the effect of scattering (cf. Gleeson and Axford, 1967). The scattering rate $\left(\frac{\delta F}{\delta t}\right)_c$ is initially evaluated in the moving frame S_m, and a relativistic transformation gives the result in the fixed frame. Thus for isotropic scattering

$$\left(\frac{\delta F}{\delta t}\right)_c = -4\pi N \left(1 - \frac{Vv \cos\theta}{c^2}\right) v_m \sigma(p_m) F(r,p,\theta,t)$$

$$+2\pi N \left(1 - \frac{Vv \cos\theta}{c^2}\right) v_m \sigma(p_m) \int_0^{\pi} F(r,p',\theta',t) \sin\theta'_m \, d\theta'_m , \qquad (7.3.3)$$

where primed superscripts refer to the particle momentum before scattering. The first and second terms in Equation (7.3.3) represent scattering out of and into a given element of phase space respectively.

It is assumed that the distribution function can be written as a Legendre expansion as follows:

$$F(r,p,\theta,t) = \sum_{i=0}^{\infty} F_i (r,p,t) P_i(\cos\theta). \qquad (7.3.4)$$

Substituting this expression for $F(r,p,\theta,t)$ into Equations (7.3.2) and (7.3.3), making a Taylor expansion of $\left(\frac{\delta F}{\delta t}\right)_c$ in powers of $\frac{V}{v}$, assuming near isotropy so that $F_i << F_o$, F_1 $(i \geq 2)$, a set of coupled partial differential equations for the functions $F_i(r,p,t)$ are obtained by equating the coefficients of the P_i $(\cos\theta)$. The first two of these equations are

$$\frac{\partial F_o}{\partial t} + \frac{1}{3r^2} \frac{\partial}{\partial r} (r^2 v F_1) = \frac{4\pi NV}{3p^2} \frac{\partial}{\partial p} \left[p^3 \sigma \left(F_1 + mV \frac{\partial F_o}{\partial p}\right)\right] ,$$

$$+ O\left[\left(\frac{V}{v}\right)^3 4\pi N \sigma v F_o\right] , \qquad (7.3.5)$$

$$\frac{\partial F_1}{\partial t} + v\frac{\partial F_o}{\partial r} = -4\pi N\sigma v(F_1 + mV\frac{\partial F_o}{\partial p}) + O(\frac{V^2}{v^2} 4\pi N\sigma v F_o). \quad (7.3.6)$$

In the derivation of (7.3.5) and (7.3.6) it is assumed that the distribution function is sufficiently smooth for F, $p\frac{\partial F}{\partial p}$ and $p^2\frac{\partial^2 F}{\partial p^2}$ to be considered of the same order of magnitude and $F_1 = O(\frac{V}{v} F_o)$.

The term $\frac{\partial F_1}{\partial t}$, (which represents the effects of inertia of the cosmic-ray gas) can usually be neglected in Equation (7.3.6), and this equation becomes

$$v\frac{\partial F_o}{\partial r} = -4\pi N\sigma v(F_1 + mV\frac{\partial F_o}{\partial p}). \quad (7.3.7)$$

On eliminating F_1 between (7.3.5) and (7.3.7) and replacing $N\sigma$ by the diffusion coefficient

$$K = v/12\pi N\sigma,$$

we obtain the equations of transport:

$$\frac{\partial F_o}{\partial t} + \frac{1}{r^2}\frac{\partial}{\partial r}(r^2\frac{Vp}{3}\frac{\partial F_o}{\partial p} - r^2 K\frac{\partial F_o}{\partial r}) + \frac{V}{3p^2}\frac{\partial}{\partial p}(p^3\frac{\partial F_o}{\partial r}) = 0, \quad (7.3.8)$$

$$v F_1 = -pV\frac{\partial F_o}{\partial p} - 3K\frac{\partial F_o}{\partial r}. \quad (7.3.9)$$

In terms of the differential current density

$$S_p = 4\pi p^2 v F_1/3,$$

and the momentum number density

$$U_p = 4\pi p^2 F_o,$$

these equations are

$$\frac{\partial U_p}{\partial t} + \frac{1}{r^2}\frac{\partial}{\partial r}(r^2 S_p) + \frac{\partial}{\partial p}(\frac{Vp}{3}\frac{\partial U_p}{\partial r}) = 0, \quad (7.3.10)$$

$$S_p = VU_p - \frac{V}{3}\frac{\partial}{\partial p}(pU_p) - K\frac{\partial U_p}{\partial r}, \quad (7.3.11)$$

which are the usual form of the transport equations.

The above completes the resume of the scattering analysis used to obtain the equations of transport. We now proceed to use these same ideas to calculate directly the average - time - rate of change of momentum $\langle \dot{p} \rangle$ for cosmic-rays. In the analysis we use the following relativistic relations between the moving and the fixed frames

$$F_m(r_m, p_m, \theta_m, t_m) = F(r, p, \theta, t), \tag{7.3.12a}$$

$$d^3\underline{r}_m \, d^3\underline{p}_m = d^3\underline{r} d^3\underline{p}, \tag{7.3.12b}$$

$$dt_m = \gamma\left(1 - \frac{V v \cos\theta}{c^2}\right) dt, \tag{7.3.12c}$$

$$N_m = N/\gamma, \tag{7.3.12d}$$

$$\underline{p}_m = \underline{p} - m\underline{V} + O(V^2/c^2 p), \tag{7.3.12e}$$

$$E_m = E - \underline{V}\cdot\underline{p} + O(V^2/c^2 E), \tag{7.3.12f}$$

where $\gamma = (1-V^2/c^2)^{-\frac{1}{2}}$, m is the relativistic mass of a particle with rest mass m_o, and speed v, $d^3\underline{r}_m \, d^3\underline{p}_m$ and $d^3\underline{r} d^3\underline{p}$ are volume elements about the points $(\underline{r}_m, \underline{p}_m)$ and $(\underline{r},\underline{p})$ of position - momentum space, and N(r) is the number of scatterers per unit volume.

Consider the momentum changes of particles initially in the volume $d^3\underline{r} \, d^3\underline{p}$ about $(\underline{r},\underline{p})$ at time t, which are scattered out of the momentum volume $d^3\underline{p}$ about $\underline{p}$ in the time interval (t,t+dt).

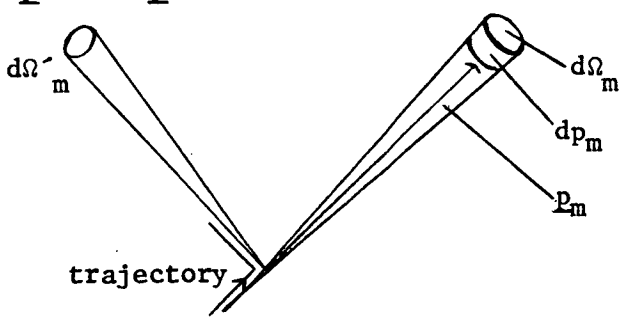

Figure 7.3a.

Showing particles scattered out of the momentum volume $d^3\underline{p}_m$ about $\underline{p}_m$ into the volume $d^3\underline{p}'_m$ about $\underline{p}'_m$

In the moving frame S_m, the number of particles initially with momentum in $d^3\underline{p}_m$ around $\underline{p}_m$ and position in $d^3\underline{r}_m$ which are scattered into the element of phase space $d^3r_m\ d^3p'_m$ around $(\underline{r}_m,\underline{p}'_m)$ in time dt_m is

$$[v_m\ F_m(r_m,p_m,\theta_m,t_m)\ d^3\underline{p}_m]\ [\sigma(p'_m)\ d\Omega'_m]\ [N_m d^3\underline{r}_m]\ dt_m. \qquad (7.3.13)$$

The first bracket in (7.3.13) is the flux of particles with momentum in $d^3\underline{p}_m$ around $\underline{p}_m$ incident on a surface with unit normal $\underline{p}_m/p_m$, the second bracket is the fraction of particles, incident on a single scatterer, which are scattered into the solid angle $d\Omega'_m$, and the third bracket is the number of scatterers located in $d^3\underline{r}_m$ at $\underline{r}_m$.

The number in (7.3.13) is Lorentz invariant, so it is the number of particles initially in the volume $d^3\underline{r}\ d^3\underline{p}$ around $(\underline{r},\underline{p})$ at time t, which are scattered into the volume $d^3\underline{r}\ d^3\underline{p}'$ around $(\underline{r},\underline{p}')$ in the time interval (t,t+dt). Using the relativistic transformations (7.3.12), i.e.

$$F_m(r_m,p_m,\theta_m,t_m) = F(r,p,\theta,t),$$

$$d^3\underline{r}_m\ d^3\underline{p}_m = d^3\underline{r}\ d^3\underline{p},$$

$$N_m = N/\gamma,$$

$$dt_m = \gamma\ dt\left(1-\frac{V\ v\ \cos\theta}{c^2}\right),$$

noting that $d^3\underline{p} = p^2 dp d\Omega$, $d\Omega = 2\pi \sin\theta\ d\theta$ and that particles are scattered without change of speed in the moving frame (i.e. $p'_m = p_m$)

$$4\pi^2 v_m\ \sigma(p_m)\ F(r,p,\theta,t)\ N\left(1-\frac{V\ v\ \cos\theta}{c^2}\right)\ p^2 \sin\theta \sin\theta'_m\ d\theta'_m d\theta$$

$$dp\ d^3\underline{r}\ dt$$

is the number of particles initially in the volume $d^3\underline{r}\ d^3\underline{p}$ around $(\underline{r},\underline{p})$ at time t, which are scattered into the volume $d^3\underline{r}\ d^3\underline{p}'$ around $(\underline{r},\underline{p}')$ in the time interval (t,t+dt).

Each of these particles changes momentum by $(p'-p)$ in the fixed frame, so that

$$(p'-p)\ [4\Pi^2\ v_m\ \sigma(p_m)\ F(r,p,\theta,t)\ N(1-\frac{V\ v\ \cos\ \theta}{c^2})\ p^2 \sin\theta\ \sin\theta'_m d\theta'_m d\theta$$

$$dp\ d^3\underline{r}dt],$$

is the momentum change of these particles.

Integrating this last result from $\theta=0$ to $\theta=\Pi$ and from $\theta'_m=0$ to $\theta'_m=\Pi$ we find

$$4\Pi^2\ N\ p^2 \int_0^{\Pi}\ \int_0^{\Pi} v_m\ \sigma(p_m)\ F(r,p,\theta,t)(1-\frac{V\ v\ \cos\ \theta}{c^2})(p'-p)\ \sin\theta\ \sin\theta'_m\ d\theta'_m\ d\theta$$

$$d^3\underline{r}\ dp\ dt, \qquad (7.3.14)$$

is the total momentum change of particles with momentum in $(p,p+dp)$ and position in $d^3\underline{r}$ about $\underline{r}$ at time t, due to scattering in the time interval $(t, t+dt)$.

To evaluate the integrals in (7.3.14) to the order we require we need to obtain expressions for p', $\cos\theta'$ and p_m in terms of θ, θ'_m and p. These expressions follow from the Lorentz transformations for momentum (7.3.12e) and the result that the particle speed in the moving frame is conserved during a collision, i.e.

$$\underline{p}_m = \underline{p} - m\underline{V} + O(V^2/c^2)p, \qquad (7.3.15)$$

$$p'_m = p_m. \qquad (7.3.16)$$

Putting $\mu = \cos\theta$ and $\mu'_m = \cos\theta'_m$ from (7.3.15) we deduce

$$p_m = p\ (1-\frac{2mV}{p}\ \mu + \frac{m^2V^2}{p^2})^{\frac{1}{2}} + O(V^2/c^2\ p).$$

Expanding this result by the Binomial Theorem

$$p_m = p\ -mV\mu + O(V^2/v^2\ p),$$

i.e.,

$$p_m - p = -mV\mu + O(V^2/v^2\ p). \qquad (7.3.17)$$

Also from the transformation (7.3.15) and using $p'_m = p_m$, we find

$$p' = p_m \left(1 + \frac{2mV}{p_m}\mu'_m + \frac{m^2V^2}{p_m^2}\right)^{\frac{1}{2}} + O\left(\frac{V^2}{c^2}p'\right).$$

Using the Binomial Theorem and the result (7.3.17) this expression for p' becomes

$$p' = p - mV\mu + mV\mu'_m + O\left(\frac{V^2}{v^2}p\right),$$

i.e.,

$$p' - p = mV(\mu'_m - \mu) + O\left(\frac{V^2}{v^2}p\right). \tag{7.3.18}$$

From (7.3.15) we have

$$\underline{p}'_m = \underline{p}' - m\underline{V} + O(V^2/c^2\, p'),$$

so that

$$p'\cos\theta' = p_m \cos\theta'_m + mV + O(V^2/v^2\, p'),$$

i.e.,

$$\cos\theta' = \frac{mV + p_m \cos\theta'_m}{p'}.$$

Using the expansions (7.3.17) and (7.3.18) for p_m and p' we obtain

$$\mu' = \mu'_m + \frac{V}{v}(1 - \mu'^2_m) + O(V^2/v^2),$$

i.e.,

$$\mu' - \mu'_m = \frac{V}{v}(1 - \mu'^2_m) + O(V^2/v^2), \tag{7.3.19}$$

as an expansion for $\cos\theta'$.

We note, for later reference that the distribution function $F(r,p',\theta',t)$ can be expressed in terms of the variables r,p,θ,θ'_m,t. This expansion is obtained as follows. We first note that we can expand $F(r,p',\theta',t)$ using the Legendre expansion (7.3.4)

$$F(r,p',\theta',t) = \sum_{i=0}^{\infty} F_i(r,p',t)\, P_i(\cos\theta'),$$

and we then expand the functions $F_i(r,p',t)$ and $P_i(\mu')$ in Taylor series

about the points p and μ'_m respectively. We have

$$F(r,p',\theta',t) = \sum_{i=0}^{\infty} [F_i(r,p,t) + (p'-p) \frac{\partial F_i(r,p,t)}{\partial p} + O(\frac{V^2}{v^2} p^2 \frac{\partial^2 F_i}{\partial p^2})]$$

$$[P_i(\mu'_m) + (\mu' - \mu'_m) \frac{dP_i(\mu'_m)}{d\mu'_m} + O(\frac{V^2}{v^2}) P_i].$$

From this and using the expressions for $p'-p$ and $\mu'-\mu'_m$ given in Equations (7.3.18) and (7.3.19), and using the assumptions of the scattering model, namely $F_i << F_o$, $F_1 (i \geq 2)$, $F_1 = O(V/v\ F_o)$ and $p\ \partial F_i/\partial p = O(F_i)$ etc., we obtain

$$F(r,p',\theta',t) = F_o + \frac{V}{v} (\mu'_m - \mu) p \frac{\partial F_o}{\partial p} + \mu'_m F_1 + O(\frac{V^2}{v^2} F_o) \qquad (7.3.20)$$

as the expansion for $F(r,p',\theta',t)$ to $O(V^2/v^2\ F_o)$.

Similarly expanding $v_m \sigma(p_m)$ about p in a Taylor series, and using the expression for $p_m - p$ given in (7.3.17) we have

$$v_m\ \sigma(p_m) = v\ \sigma(p) - mV\mu \frac{\partial}{\partial p} (v\ \sigma(p)) + O(\frac{V^2}{v^2} v\ \sigma\ (p)), \qquad (7.3.21)$$

as the expansion for $v_m\ \sigma(p_m)$.

Substituting the expressions for $v_m\ \sigma(p_m)$, $F(r,p,\theta,t)$ and $p'-p$

from Equations (7.3.21), (7.3.4) and (7.3.18) in the result (7.3.14), we have that

$$4\Pi^2 Np^2 \int_{-1}^{1} [v\sigma - p\frac{V}{v}\mu \frac{\partial}{\partial p}(v\sigma) + O(\frac{V^2}{v^2} v\sigma)] (1 - \frac{Vv\mu}{c^2})$$

$$[F_o + \mu F_1 + O(V^2/v^2 F_o)] \int_{-1}^{1} [mV(\mu'_m - \mu) + O(\frac{V^2}{v^2} p)] d\mu'_m d\mu \cdot d^3\underline{r}\, dp\, dt$$

$$= -8\Pi^2 p^3 \frac{V}{v} N \int_{-1}^{1} [v\sigma - p\frac{V}{v}\mu \frac{\partial}{\partial p}(v\sigma) + O(\frac{V^2}{v^2} v\sigma)] (1 - \frac{Vv\mu}{v^2})$$

$$\cdot [\mu F_o + \mu^2 F_1 + O(V^2/v^2 F_o)] d\mu \cdot d^3\underline{r}\, dp\, dt$$

$$= -\frac{16\Pi^2 p^3 V N\sigma}{3} [F_1 - [\frac{Vv}{c^2} + p\frac{V}{v}\frac{\partial}{\partial p}(v\sigma)] F_o$$

$$+ O(\frac{V^2}{v^2} F_o)] d^3\underline{r}\, dp\, dt, \qquad (7.3.22)$$

is the total momentum change of particles with momentum in (p,p+dp) and position in $d^3\underline{r}$ about $\underline{r}$ at time t due to scattering in the time interval (t,t+dt).

We now consider the momentum changes of particles in the volume $d^3\underline{r}\ d^3\underline{p}$ about $(\underline{r},\underline{p})$ at time t+dt, due to particles scattering into the momentum volume $d^3\underline{p}$ about $\underline{p}$ in the time interval (t,t+dt).

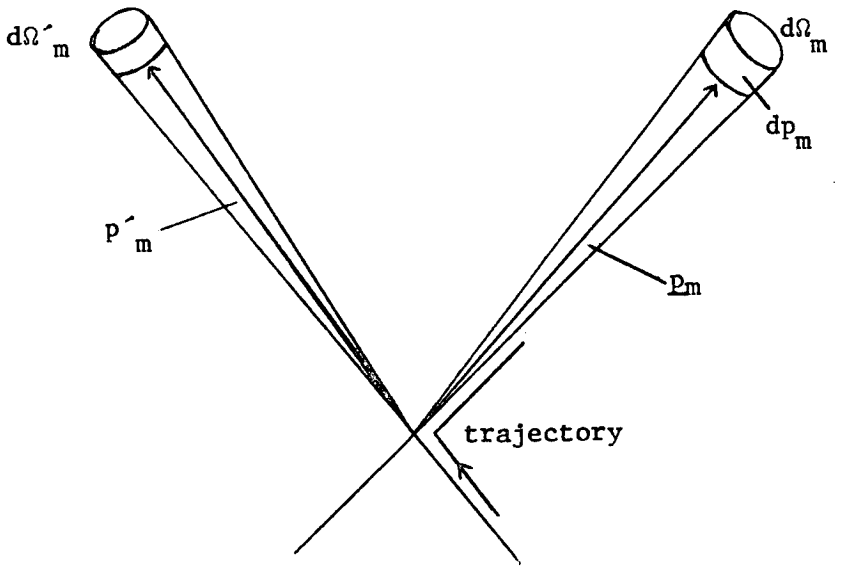

Figure 7.3b

Showing particles scattered into the volume $d^3\underline{r}_m\ d^3\underline{p}_m$ about $(\underline{r}_m, \underline{p}_m)$.

In the moving frame S_m, the number of particles initially in the volume $d^3\underline{r}_m\ d^3\underline{p}'_m$ about $(\underline{r}_m, \underline{p}'_m)$, at time t_m which are scattered into the volume element of phase space $d^3\underline{r}_m\ d^3\underline{p}_m$ in time dt_m is

$$[v'_m\ F_m(r_m,p'_m,\ \theta'_m,t_m)\ d^3\underline{p}'_m]\ [\sigma(p_m)\ d\Omega_m]\ [N_m\ d^3\underline{r}_m]\ dt_m. \qquad (7.3.23)$$

The physical significance of the three bracketed quantities in (7.3.23) are analagous to the interpretation of (7.3.13).

The number in (7.3.23) is Lorentz invariant, so it is the number of particles initially in the volume $d^3\underline{r}\ d^3\underline{p}'$ about $(\underline{r},\underline{p}')$ at time t, which are scattered into the volume $d^3\underline{r}\ d^3\underline{p}$ about $(\underline{r},\underline{p})$ in the time interval (t,t+dt). Since $p'_m = p_m$, $d^3\underline{p} = p^2 dp\ d\Omega$, we make the substitution

$$d^3\underline{p}'_m\ d^3\underline{r}_m\ d\Omega_m = d^3\underline{p}_m\ d^3\underline{r}_m\ d\Omega'_m,$$

in (7.3.23). However from Equation (7.3.12b) we have

$$d^3\underline{p}_m \, d^3\underline{r}_m = d^3\underline{p} \, d^3\underline{r},$$

so that this last result may be written in an alternative form

$$d^3p'_m \, d^3r_m \, d\Omega_m = d^3\underline{r} \, p^2 \, dp \, d\Omega \, d\Omega'_m. \tag{7.3.24}$$

Thus using the relativistic transformations (7.3.12) i.e.

$$F_m(r_m, p'_m, \theta'_m, t_m) = F(r,p',\theta',t),$$

$$N_m = N/\gamma,$$

$$dt_m = \gamma dt\left(1 - \frac{Vv \cos\theta}{c^2}\right),$$

noting $d\Omega = 2\Pi \sin\theta \, d\theta$, and using the result (7.3.24) in Equation (7.3.23) we have

$$4\Pi^2 Np^2 \, v_m \sigma(p_m) \, F(r,p',\theta',t) \left(1 - \frac{Vv \cos\theta}{c^2}\right) \sin\theta \sin\theta'_m \, d\theta \, d\theta'_m \, dp d^3\underline{r} \, dt$$

is the number of particles initially in the volume $d^3\underline{r} \, d^3\underline{p}'$ about $(\underline{r},\underline{p}')$ at time t which are scattered into the volume $d^3\underline{r} \, d^3\underline{p}$ about $(\underline{r},\underline{p})$ in the time interval (t,t+dt).

Each of these particles changes momentum by $p-p'$ in the fixed frame in the time interval (t,t+dt) so that

$$(p-p')[4\Pi^2 Np^2 \, v_m \, \sigma(p_m) \, F(r,p',\theta',t) \left(1 - \frac{Vv \cos\theta}{c^2}\right) \sin\theta \sin\theta'_m \, d\theta \, d\theta'_m$$

$$dp \, d^3\underline{r} \, dt],$$

is the momentum change of these particles.

Integrating this last result from $\theta = 0$ to $\theta = \Pi$ and from $\theta'_m = 0$ to $\theta'_m = \Pi$, and using the expansions for $v_m \, \sigma(p_m)$, $F(r,p',\theta',t)$ and $p-p'$ given in Equations (7.3.21), (7.3.20) and (7.3.18), we find

$$4\Pi^2 Np^2 \int_0^{\Pi}\int_0^{\Pi} v_m\, \sigma(p_m)(p-p')\, F(r,p',\theta',t)\left(1-\frac{Vv\cos\theta}{c^2}\right)\sin\theta\sin\theta'_m$$

$$d\theta\, d\theta'_m\, dp\, d^3\underline{r}\, dt$$

$$= 4\Pi^2 Np^2 \int_{-1}^{1} [v\sigma - p\frac{V}{v}\mu\frac{\partial}{\partial p}(v\sigma(p)) + O(\frac{V^2}{v^2} v\sigma(p))]\left(1-\frac{Vv\mu}{c^2}\right)$$

$$\int_{-1}^{1} [p\frac{V}{v}(\mu-\mu'_m) + O(\frac{V^2}{v^2} p)]\,[F_o + \frac{V}{v}(\mu'_m - \mu)\, p\frac{\partial F_o}{\partial p} + \mu'_m F_1 + O(\frac{V^2}{v^2} F_o)]$$

$$d\mu'_m\, d\mu\, dp d^3\underline{r}\, dt$$

$$= 4\Pi^2 Np^2 \int_{-1}^{1} [v\sigma - p\frac{V}{v}\mu\frac{\partial}{\partial p}(v\sigma) + O(\frac{V^2}{v^2} v\sigma)]\,[1 - \frac{Vv\mu}{c^2}]$$

$$p\frac{V}{v}\,[2\mu F_o - \frac{V}{v} p\frac{\partial F_o}{\partial p}(2\mu^2 + 2/3) - 2/3 F_1 + O(\frac{V^2}{v^2} F_o)]\, d\mu\, dp d^3\underline{r}\, dt$$

$$= -\frac{16\Pi^2 p^3 V N\sigma}{3}\,[F_1 + 2p\frac{V}{v}\frac{\partial F_o}{\partial p} + (\frac{Vv}{c^2} + \frac{p\frac{V}{v}}{v\sigma}\frac{\partial}{\partial p}(v\sigma))\, F_o + O(\frac{V^2}{v^2}) F_o]$$

$$d^3\underline{r}\, dp\, dt, \qquad (7.3.25)$$

is the total momentum change of particles with momentum in (p,p+dp) and position in $d^3\underline{r}$ about $\underline{r}$ at time t+dt, due to previous scattering in the time interval (t,t+dt).

In summary, the basic results (7.3.22) and (7.3.25) concerning the momentum changes of particles with momentum in (p,p+dp) are:

(i) we have

$$-\frac{16\Pi^2 p^3 V N\sigma}{3}\,[F_1 - [\frac{Vv}{c^2} + \frac{p\frac{V}{v}}{v\sigma}\frac{\partial}{\partial p}(v\sigma)]\, F_o + O(\frac{V^2}{v^2} F_o)]$$

$$d^3\underline{r}\, dp\, dt,$$

is the total momentum change of particles with momentum in (p,p+dp)

and position in $d^3\underline{r}$ about $\underline{r}$ at time t due to scattering in the time interval $(t,t+dt)$ and,

$$\text{(ii)} \qquad \frac{-16\Pi^2 p^3 V N\sigma}{3} \left[F_1 + 2p \frac{V}{v} \frac{\partial F_o}{\partial p} + \left[\frac{Vv}{c^2} + \frac{pV/v}{v\sigma} \frac{\partial}{\partial p} (v\sigma)\right] F_o \right.$$

$$\left. + O\left(\frac{V^2}{v^2} F_o\right)\right] d^3\underline{r}\, dp\, dt,$$

is the total momentum change of particles with momentum in $(p,p+dp)$ and position in $d^3\underline{r}$ about $\underline{r}$ at time $t+dt$, due to previous scattering in the time interval $(t,t+dt)$.

As noted at the beginning of this section the momentum changes in (i) and (ii) are different, and to calculate $\langle\dot{p}\rangle$ we take the average of these momentum changes, and divide this average by the time interval dt and the number of particles with momentum in $(p,p+dp)$ and position in $d^3\underline{r}$ about $\underline{r}$, viz. $4\Pi p^2 F_o(r,p,t)\, dp\, d^3\underline{r}$. Hence we obtain.

$$\langle\dot{p}\rangle = -\frac{pV}{3} \frac{4\Pi N\sigma}{F_o} \left[F_1 + p \frac{V}{v} \frac{\partial F_o}{\partial p} + O\left(\frac{V^2}{v^2} F_o\right)\right], \qquad (7.3.26)$$

as the expression for average time rate of change of momentum of the cosmic rays.

If we express the distribution function in the moving frame by

$$F_m(\underline{r}_m, p_m) = F_{m_o}(\underline{r}_m, p_m) + F_{m_1}(\underline{r}_m, p_m) \cos\theta_m + O\left(\frac{V^2}{v^2} F_{m_o}\right)$$

we can show that

$$F_{m_1} = F_1 + p \frac{V}{v} \frac{\partial F_o}{\partial p}. \qquad (7.3.27)$$

Since the streaming in the moving frame is given by

$$\underline{S}_{pm} = \frac{4\Pi p_m^2 v_m}{3} F_{m_1}(\underline{r}_m, p_m), \qquad (7.3.28)$$

the result (7.3.27) when substituted in the expression (7.3.26) for $\langle \dot{p} \rangle$ indicates that $\langle \dot{p} \rangle$ is proportional to the net inward streaming in the moving frame. Since the streaming in the moving frame is a diffusive flux

$$\underline{S}_{pm} = -4\Pi p^2 K(r,p) \frac{\partial F_o}{\partial r} , \qquad (7.3.29)$$

arising from the scattering, we find that $\langle \dot{p} \rangle$ is proportional to the radial gradient $1/F_o \; \partial F_o/\partial r$. The result $\langle \dot{p} \rangle \propto \underline{S}_{pm}$ also makes physical sense, since the streaming in the moving frame is due to the combined effect of overtaking and head on collisions between the cosmic rays and the scatterers.

To show the relationship (7.3.27) explicitly and to obtain the dependence of $\langle \dot{p} \rangle$ on the radial gradient $(1/F_o)$ $(\partial F_o/\partial r)$ we note that from the equation of transport (7.3.9)

$$F_1 + p \frac{V}{v} \frac{\partial F_o}{\partial p} = \frac{-1}{4\Pi N\sigma} \frac{\partial F_o}{\partial r} . \qquad (7.3.30)$$

Since the diffusion coefficient $K = v/(12\Pi N\sigma)$ we may write this last result as

$$F_1 + p \frac{V}{v} \frac{\partial F_o}{\partial p} = - \frac{3K}{v} \frac{\partial F_o}{\partial r} ,$$

or using Equations (7.3.28) and (7.3.29) we have

$$F_1 + p \frac{V}{v} \frac{\partial F_o}{\partial p} = \frac{3 \underline{S}_{pm}}{4\Pi \; p^2 \; v} = F_{m_1} ,$$

which is the result (7.3.27). Finally using the result (7.3.30) in the expression (7.3.26) for $\langle \dot{p} \rangle$ we find

$$\langle \dot{p} \rangle = \frac{Vp}{3F_o} \frac{\partial F_o}{\partial r} . \qquad (7.3.31)$$

Alternatively in terms of the radial gradient $G_r(r,p) = (1/U_p)\ (\partial U_p/\partial r)$ we write this result as

$$\langle \dot{p} \rangle = \frac{Vp}{3} G_r . \qquad (7.3.22)$$

This is the result we seek and it was obtained in Section (7.2) by proper interpretation of the equations of transport.

7.4 The moving cell approach

In this section we consider a special model (see Figure (7.4a)) in which the particles are considered to be confined within "boxes", the walls of which are moving with velocity $\underline{V}(r)$ ($\underline{V}(\underline{r})$ is in general a function of position).

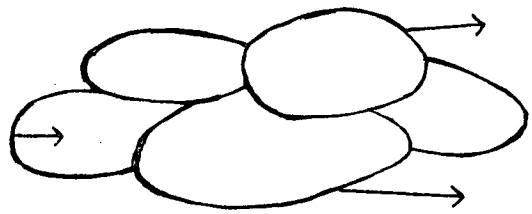

Figure 7.4a.
Illustrating the boxes of Section (7.4). The surfaces at each point move with the local velocity $\underline{V}(\underline{r})$.

In the cosmic ray case $\underline{V}$ is the velocity of the solar wind. We first consider momentum changes within a single box or cell and then the momentum changes associated with a set of cells within a volume fixed in space and not moving.

A single cell is shown in Figure (7.4b) and the following conditions apply

(i) The particle speed $v >> V$.

(ii) As seen by an observer moving anywhere within the cell the distribution function $F_m(\underline{p}_m)$ is uniform and isotropic and we write

$$F_m(\underline{p}_m) = F_{m_o}(p_m)$$

with $F_{m_o}(p_m)$ changing from cell to cell.

(iii) The particles are considered to have elastic collisions with the rigid walls of the enclosure i.e. the incident and rebound speed as seen moving relative to the contact point of the wall are the same.

The Lorentz transformations for the momentum $\underline{p}$ and the total energy

E between the moving frame S_m and the fixed frame S to $O(V/c)^2$ are given in Equations (7.1.10) and (7.1.11):

$$\underline{p}_m = \underline{p} - m\underline{V} , \tag{7.4.1}$$

$$E_m = E - \underline{V} \cdot \underline{p} . \tag{7.4.2}$$

From the Lorentz invariance of the position-momentum distribution function

$$F(\underline{r},\underline{p}) = F_m (\underline{r}_m, \underline{p}_m). \tag{7.4.3}$$

Expanding $F_m(\underline{r}_m, \underline{p}_m)$ about $\underline{p}$ in a Taylor series we have

$$F(\underline{r},\underline{p}) = F_m(\underline{r}_m,\underline{p}) + (\underline{p}_m - \underline{p}) \cdot \frac{\partial}{\partial \underline{p}} F(\underline{r}_m,\underline{p}) + ... \tag{7.4.4}$$

Since $F_m(\underline{r}_m,\underline{p}_m)$ is essentially isotropic (see (ii)) and using the Lorentz transformations (7.4.1) we have

$$F(\underline{r},\underline{p}) = F_{m_o}(\underline{r}_m,p) + O(\frac{V}{v} p \frac{\partial F_o}{\partial p}),$$

as an approximate relation between the moving and fixed frame distribution functions.

We now proceed to calculate the rate at which the particles change momentum due to collisions with the walls of the enclosure.

Consider the collision of a particle of momentum p with an element dA of the wall centred around the boundary point at $\underline{b}$ where the inward normal is $\underline{n}$. Let $\underline{p}_i$ and $\underline{p}_f$ denote the particle momenta before and after the collision.

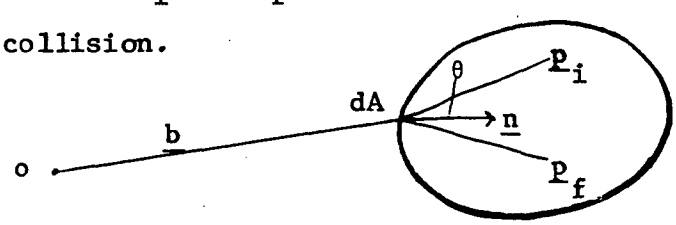

Figure 7.4b.

Schematic of particle collision with wall at $\underline{b}$.

The inward normal to the surface at $\underline{b}$ is $\underline{n}$.

Since collisions are elastic relative to the wall (see (iii)) we can easily show

$$\underline{p}_{mf} = (\underline{p}_{mi} - p_{mi} \cdot \underline{n}\,\underline{n}) - \underline{p}_{mi} \cdot \underline{n}\,\underline{n} = \underline{p}_{mi} - 2\underline{p}_{mi} \cdot \underline{n}\,\underline{n} \tag{7.4.6}$$

Using the Lorentz transformations (7.4.1) we have

$$\underline{p}_f = \underline{p}_i - \underline{p}_i \cdot \underline{n}\,\underline{n} - (\underline{p}_i - 2m\,\underline{V}) \cdot \underline{n}\,\underline{n} + O(V^2/c^2\, p_i). \tag{7.4.7}$$

Hence

$$\underline{p}_f^{\,2} = p_i^{\,2} - 4(m\underline{V} \cdot \underline{n})\,(\underline{p}_i \cdot \underline{n}) + O(V^2/c^2\, p_i^{\,2}). \tag{7.4.8}$$

Using the Binomial theorem in Equation (7.4.8),

$$\Delta p = p_f - p_i = -2(m\,\underline{V} \cdot \underline{n})\,(\underline{p}_i \cdot \underline{n})/p_i + O(V^2/c^2)\, p_i. \tag{7.4.9}$$

With θ the angle between $\underline{p}_i$ and $-\underline{n}$ ($\underline{p}_i \cdot \underline{n} = -p_i \cos\theta$) and dropping the subscript i, Equation (7.4.9) gives

$$\Delta p = 2(m\,\underline{V} \cdot \underline{n}) \cos\theta + O(V^2/c^2\, p), \tag{7.4.10}$$

as the momentum change in the fixed frame.

The number of particles with momentum in $d^3\underline{p}$ about $\underline{p}$ which intercept dA in time dt is

$$F(\underline{r},\underline{p})\,(v\cos\theta - \underline{V} \cdot \underline{n})\, dA\, dt\, d^3\underline{p}.$$

Using the relation between distribution functions given in (7.4.5) we have

$$[F_{mo}(\underline{r}_m,p) + O(\frac{V}{v}\, p\, \frac{\partial F_{mo}}{\partial p})]\,(v\cos\theta - \underline{V} \cdot \underline{n})\, dA\, dt\, d^3\underline{p},$$

as the number of particles with momentum in $d^3\underline{p}$ about $\underline{p}$ which intercept the area dA in time dt.

Each of these particles changes momentum by Δp given by Equation (7.4.10) and

$$2(m\,\underline{V}\cdot\underline{n})\cos\theta\,F_{mo}(\underline{r}_m,\,p)\,(v\cos\theta-\underline{V}\cdot\underline{n})\,dA\,d^3\underline{p}\,dt$$

$$+\,O(p^2\underline{V}\,V/v\,(\partial F_{mo}/\partial p))\cdot dA\,d^3\,\underline{p}\,dt.$$

is their total momentum change in time dt.

Using $d^3\underline{p} = p^2\delta p d\Omega$, $d\Omega = 2\Pi \sin\theta\ d\theta$ and integrating this last result over the solid angle $d\Omega$ corresponding to incident particles we obtain

$$4\Pi(\underline{V}\cdot\underline{n})\,p^3/v\,F_{mo}(\underline{r}_m,\,p)\,\delta p dA\,dt\int_o^{\Pi/2}(v\cos\theta-\underline{V}\cdot\underline{n})$$

$$\cos\theta\sin\theta\,d\theta+O(p^2V^2/v\,(\partial F_{mo}/\partial p))\cdot p^2\,\delta p\,dA\,dt$$

$$=\frac{4\Pi\,p^3}{3}\,F_{mo}(\underline{r}_m,\,p)\,\underline{V}\cdot\underline{n}\,\delta p\,dA\,dt\,(1+O(\tfrac{V}{v})),\qquad(7.4.11)$$

as the total momentum change in time dt from particles with momentum in $(p,p+\delta p)$ irrespective of direction.

Dividing by dt, noting that $F_{mo}(\underline{r}_m,p)$ is constant within a cell and integrating over the entire interior surface we have

$$4\Pi\,F_{mo}\,(\underline{r}_m,\,p)\,p^3/3\int_S\underline{V}\cdot\underline{n}\,dA\,\delta p\,(1+O(\tfrac{V}{v})),$$

as the total momentum change per unit time of particles with momentum in $(p,p+\delta p)$ due to collisions with the cell wall.

The exterior normal to the surface S is $-\underline{n}$, and using Gauss's theorem this result can be written alternatively as

$$-4\Pi/3\,p^3\,F_{mo}(\underline{r}_m,p)\,\delta p\int_{V_o}\underline{\nabla}\cdot\underline{V}\,d^3\underline{r}.$$

Noting that the number of particles in $(p,p+\delta p)$ is $4\Pi p^2\,F_{mo}(\underline{r}_m,p)\delta p.V_o$, this result shows that although due to surface collisions, the momentum changes can be reckoned as due to the momentum changing at each point of space at a rate

$$\langle\dot{p}\rangle_{ad} = -(p/3)\underline{\nabla}\cdot\underline{V}\ .\qquad(7.4.12)$$

Since it is independent of the shape of the surfaces this is a useful general interpretation. The result (7.4.12) is the adiabatic deceleration rate referred to in (7.1.6), and it is independent of the frame of reference.

We now consider a collection of adjoining cells moving through a volume V_o enclosed by a surface S_o which is fixed relative to the rest frame (Figure 7.4c).

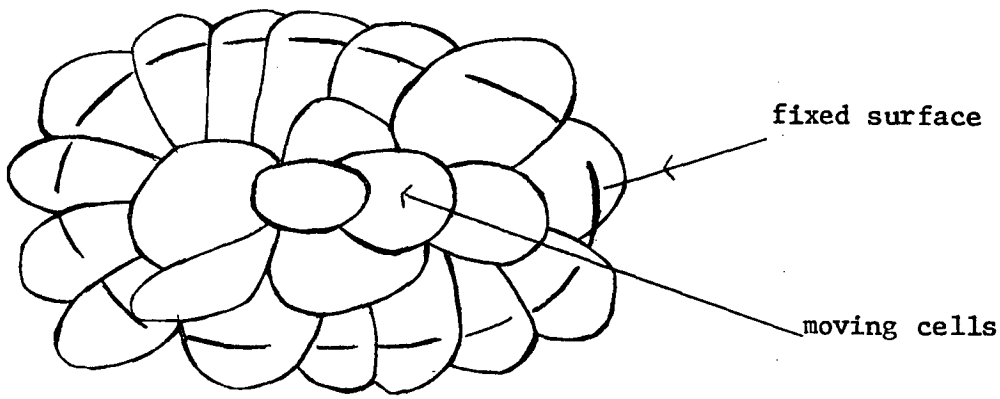

Figure 7.4c.
The volume V_o enclosed by the surface S_o which is fixed in the rest frame.

The total change of momentum per unit time for particles in $(p,p+\delta p)$ due to collisions with the walls of all the cells follows from (7.4.11) and it is given by

$$\frac{4\Pi p^3}{3} \int_S F_{mo}(\underline{r}_m,p)\, \underline{V} \cdot \underline{n}\, dA\, \delta p\, [1 + o(\tfrac{V}{v})],$$

where the surfaces S are the complete set of the walls of the cells which are totally or partially enclosed by S_o. Note that although $F_{mo}(\underline{r}_m,p)$ is a function of position, it is constant within each cell.

Labelling the cells totally enclosed by S_o by the index i, we find that the total momentum change per unit time in these cells is

$$\frac{4\Pi p^3}{3}\, \delta p \sum_i F_{mo}(\underline{r}_{mi},p) \int_{Si} \underline{V} \cdot \underline{n}\, dA.$$

Since $-\underline{n}$ is the outward normal and using Gauss's theorem,

$$-4\Pi p^3 \delta p \sum_i F_{mo}(\underline{r}_{mi}, p) \int_{V_i} \underline{V} \cdot \underline{V} \, d^3\underline{r}. \tag{7.4.13}$$

is the momentum change per unit time in these cells.

We now consider the contribution to the momentum change in a cell partially enclosed by S_o. The volume of the cell within S_o is denoted by V_k; the portion of the surface S_o which cuts the cell is labelled S_k and the surfaces of the cell interior to S_o are labelled S* (Figure 7.4d).

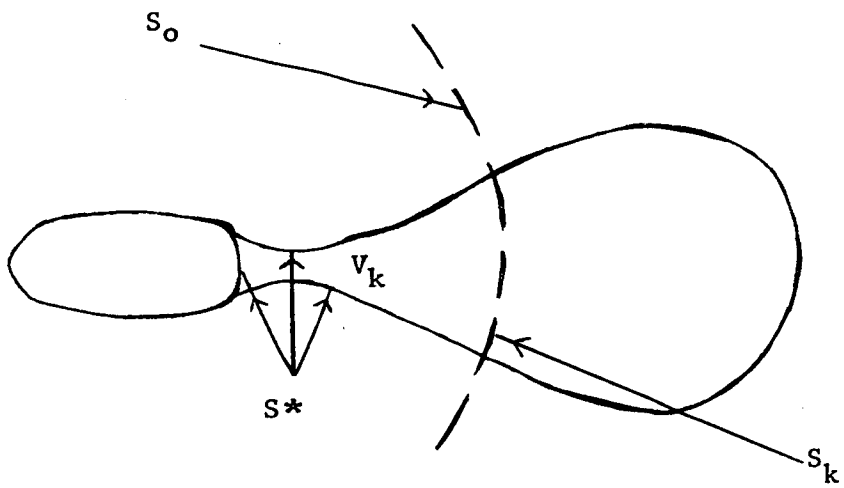

Figure 7.4d
A cell partially enclosed by S_o.

Using the result (7.4.11) the total change of momentum per unit time of particles with momenta $(p, p+\delta p)$ within this cell is

$$\frac{4\Pi p^3}{3} \int_{S^*} F_{mo}(\underline{r}_m, p) \, \underline{V} \cdot \underline{n} \, dA \, \delta p.$$

This result may also be written

$$\frac{4\Pi p^3}{3} \left[\int_{S_k} + S^* \; \underline{V} \cdot \underline{n} \, F_{mo}(\underline{r}_m, p) \, dA - \int_{S_k} \underline{V} \cdot \underline{n} \, F_{mo}(\underline{r}_m, p) \, dA \right] \delta p,$$

with $S_k + S^*$ the surface enclosing V_k and S_k the stationary part of that surface. Using Gauss's theorem in the usual way

$$\frac{-4\Pi p^3}{3} \left[F_{mo}(\underline{r}_{mk}, p) \int_{V_k} \underline{\nabla} \cdot \underline{V} \, d^3\underline{r} + \int_{S_k} F_{mo}(\underline{r}_m, p) \, \underline{V} \cdot \underline{n} \, dA \right] \delta p,$$

is the momentum change per unit time within this cell.

Combining this with the result (7.4.13) for cells completely enclosed by the fixed surface S_o, we find the total change of momentum per unit time to be

$$\frac{-4\Pi p^3}{3} \delta p \left[\sum_k F_{mo}(\underline{r}_{mk}, p) \int_{V_k} \underline{\nabla} \cdot \underline{V} \, d^3\underline{r} + \sum_i F_{mo}(\underline{r}_{mi}, p) \int_{V_i} \underline{\nabla} \cdot \underline{V} \, d^3\underline{r} \right]$$

$$- \frac{4\Pi p^3 \delta p}{3} \sum_k \int_{S_k} F_{mo}(\underline{r}_m, p) \, \underline{V} \cdot \underline{n} \, dA;$$

where the subscript i labels the cells totally interior to S_o, and the subscript k labels the cells partially enclosed by S_o.

Noting that $\Sigma V_k + \Sigma V_i = V_o$, the enclosed volume, ΣS_k is the fixed surface S_o and that $F_{mo}(\underline{r}_m, p)$ is constant within a cell,

$$\frac{-4\Pi p^3 \delta p}{3} \int_{V_o} F_{mo}(\underline{r}_m, p) \, \underline{\nabla} \cdot \underline{V} \, d^3\underline{r} - \frac{4\Pi p^3 \delta p}{3} \int_{S_o} F_{mo}(\underline{r}_m, p) \, \underline{V} \cdot \underline{n} \, dA,$$

is the total momentum change per unit time for cells within S_o. Finally using $F_{mo}(\underline{r}_m, p) = F_o(\underline{r}, p)$ to the order required the total change of momentum per unit time is

$$\frac{-4\Pi p^3 \delta p}{3} \int_{V_o} F_o(\underline{r}, p) \, \underline{\nabla} \cdot \underline{V} \, d^3\underline{r} - \frac{4\Pi p^3 \delta p}{3} \int_{S_o} F_o(\underline{r}, p) \, \underline{V} \cdot \underline{n} \, dA.$$

The first term is the adiabatic deceleration term discussed earlier. The second term is from the exterior surfaces. It too can be converted to an equivalent volume effect by using Gauss's theorem and noting again that $\underline{n}$ is the inward normal to S_o.

It follows that the change of momentum per unit time of particles in $(p,p+\delta p)$ is

$$-\frac{4\Pi p^3\,\delta p}{3}\int_{V_o}\left[F_o(\underline{r},p)\,\underline{\nabla}\cdot\underline{V}-\underline{\nabla}\cdot(F_o(\underline{r},p)\,\underline{V})\right]d^3\underline{r}$$

$$=\frac{4\Pi p^3\,\delta p}{3}\int_{V_o}\underline{V}\cdot\underline{\nabla}\,F_o(\underline{r},p)\,d^3\underline{r}\,.$$

Since the number of particles with momenta in $(p,p+\delta p)$ inside S_o is $4\Pi p^2\delta p\int_{V_o}F_o(\underline{r},p)\,d^3\underline{r}$ this result shows that although due to surface collisions with the cell walls, the momentum changes can be reckoned as due to the momentum changing at each point of space at a rate

$$\langle\dot{p}\rangle=\frac{p}{3\,F_o(\underline{r},p)}\,\underline{V}\cdot\underline{\nabla}\,F_o(\underline{r},p). \qquad (7.4.14)$$

This result expressed in terms of the number density $U_p=4\Pi p^2F_o(\underline{r},p)$ is

$$\langle\dot{p}\rangle=\frac{p}{3\,U_p}\,\underline{V}\cdot\frac{\partial U_p}{\partial\underline{r}}\,, \qquad (7.4.15)$$

which is the expression for $\langle\dot{p}\rangle$ given in (7.1.1).

This result can be written in terms of the spatial gradient of particles

$$\underline{G} = \frac{1}{F_o} \underline{\nabla} F_o = \frac{1}{U_p} \underline{\nabla} U_p ,$$

as

$$\langle \dot{p} \rangle = (p/3) \underline{V} \cdot \underline{G} .$$

It shows that whenever there is a positive heliocentric density gradient cosmic-ray particles are, on average, gaining energy.

7.5 Cosmic-ray energy changes over the whole momentum spectrum

Jokipii and Parker (1967) showed that the total rate of change of energy transfer per unit volume from the solar wind to the cosmic rays is

$$\frac{dW}{dt} = V \frac{dP_c(r)}{dr} , \qquad (7.5.1)$$

where $P_c(r)$ is the isotropic cosmic-ray pressure at heliocentric radius r. In this section we derive this result from the expression for $\langle \dot{p} \rangle$ given in (7.1.1).

The relation between the average time rate of change of kinetic energy $\langle \frac{dT}{dt} \rangle$ and $\langle \dot{p} \rangle$ is

$$\langle \frac{dT}{dt} \rangle = \frac{dT}{dp} \langle \dot{p} \rangle . \qquad (7.5.2)$$

Using the relativistic relations

$$E^2 = p^2c^2 + E_o^2 ,$$

$$T = E - E_o ,$$

where E is the total particle energy, E_o, the rest energy and T the

kinetic energy it is easy to show that

$$\frac{dT}{dp} = v, \tag{7.5.3}$$

where v is the particle speed. From the expression for $\langle \dot{p} \rangle$ given in (7.1.1) and the relations (7.5.2) and (7.5.3) we have

$$\left\langle \frac{dT}{dt} \right\rangle = \frac{v\ Vp}{3\ U_p} \frac{\partial U_p}{\partial r}, \tag{7.5.4}$$

as the average time rate of change of kinetic energy.

Hence

$$\left\langle \frac{dT}{dt} \right\rangle U_p\ dp\ d^3\underline{r},$$

is the total average rate of change of kinetic energy of particles with momentum in (p,p+dp) and position in $d^3\underline{r}$ about $\underline{r}$.

Using the expression for $\left\langle \frac{dT}{dt} \right\rangle$ given in (7.5.4), integrating over the whole momentum spectrum, and dividing by $d^3\underline{r}$ we obtain

$$\frac{dW}{dt} = \int_0^\infty \left\langle \frac{dT}{dt} \right\rangle U_p\ dp$$

$$= V \int_0^\infty \frac{vp}{3} \frac{\partial U_p}{\partial r}\ dp, \tag{7.5.5}$$

as the total rate of energy transfer per unit volume from the solar wind to the cosmic rays.

To relate the expressions (7.5.1) and (7.5.5) for $\frac{dW}{dt}$ we need an expression for the cosmic ray pressure $P_c(r)$ in terms of the momentum number density U_p. The pressure $P_c(r)$ is the force per unit area exerted on a plane rigid surface at radius r. To calculate $P_c(r)$ consider collisions of particles with an element of area dA of the surface, with normal $\underline{n}$ (Figure (7.5a).

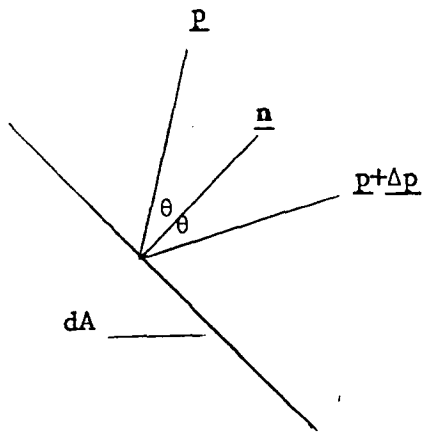

Figure 7.5a

Illustrating the collisions of particles of momentum $\underline{p}$ with the area dA.

The number of particles with momentum in $d^3\underline{p}$ about $\underline{p}$ striking the area dA in time dt is

$$v \cos\theta \, F(\underline{r},\underline{p}) \, dA \, dt \, d^3\underline{p},$$

where θ is the angle between the initial particle momentum $\underline{p}$ and $-\underline{n}$.

Each of these particles changes momentum by $\Delta p = 2p \cos\theta$ and

$$2p \cos\theta \, v \cos\theta \, F(\underline{r},\underline{p}) \, dA \, dt \, d^3\underline{p},$$

is the total momentum change from these particles.

Assuming that the momentum distribution function is essentially isotropic i.e. $F(\underline{r},\underline{p}) = F_o(\underline{r},p)$ and using the relations

$$d^3\underline{p} = p^2 dp d\Omega, \quad d\Omega = 2\pi \sin\theta \, d\theta, \quad U_p = 4\pi p^2 F_o, \quad \text{then}$$

$$\int_0^{\pi/2} \int_0^{\infty} 4\pi p^3 \, v \, F_o(\underline{r},p) \, dp \cos^2\theta \sin\theta \, d\theta \, dA \, dt$$

$$= \int_0^{\infty} \frac{vp}{3} \, U_p \, dp \, dA \, dt,$$

is the total momentum change corresponding to all particles from $p=0$ to $p=\infty$ and incident on one side of dA.

Since the cosmic ray pressure is the momentum change per unit area per unit time we have

$$P_c(r) = \int_0^\infty \frac{vp}{3} U_p \, dp. \qquad (7.5.6)$$

The gradient of the cosmic ray pressure is

$$\frac{dP_{c(r)}}{dr} = \int_0^\infty \frac{vp}{3} \frac{\partial U_p}{\partial r} \, dp. \qquad (7.5.7)$$

Noting that the integrals on the left hand sides of Equations (7.5.7) and (7.5.5) are identical we obtain

$$\frac{dW}{dt} = V \frac{dP_{c(r)}}{dr} , \qquad (7.5.8)$$

and this is the result (7.5.1) obtained by Jokipii and Parker in (1967).

7.6 Summary and discussion

In this chapter we have obtained a new expression for $\langle \dot{p} \rangle$, the time average rate of change of momentum for cosmic rays in the interplanetary medium, given by

$$\langle \dot{p} \rangle = p \, \underline{V} \cdot \underline{G} \, /3, \qquad (7.6.1)$$

with $\underline{G}\ (\underline{r},p) = (1/U_p)\ \partial U_p/\partial \underline{r}$, the density gradient.

This result was obtained in three different ways:

(i) by a rearrangement and reinterpretation of the general continuity equation for the cosmic rays.

(ii) by using the scattering analysis of Gleeson and Axford (1967), to calculate directly the momentum changes of the particles due to collisions with the radially moving scattering centres.

(iii) by using a special model in which the particles are trapped in 'boxes' moving with the solar wind. In this model the particles change momentum as they collide with the rigid walls of the box.

The first method is the simplest, but in fact it is built on the results obtained from the scattering analysis.

The second method is quite complex because it involves calculating directly the momentum changes of the particles due to scattering, and had to be treated with great care to obtain the final result.

The third method employs a special model with particles trapped in boxes moving with the solar wind. However, this model is very instructive since the adiabatic deceleration result is derived in the process. The model demonstrates that particles within a moving cell lose energy at the adiabatic rate, but when a volume fixed in the rest frame is considered, a further 'surface effect' must be included, and this together with adiabatic deceleration gives the new result (7.6.1).

The most significant difference between the adiabatic deceleration rate and the new result (7.6.1) is that particles can, on average gain kinetic energy when there is a positive radial density gradient.

In any use of the equations we consider that it is particularly instructive that they be written as the set: the continuity equation, the streaming equation and the momentum rate i.e.

$$\frac{\partial U_p}{\partial t} + \underline{\nabla} \cdot \underline{S}_p + \frac{\partial}{\partial p} \left(\langle \dot{p} \rangle U_p\right) = 0, \tag{7.6.2}$$

$$\underline{S}_p = -\underline{V} U_p - \underline{V}/3 \frac{\partial}{\partial p} (pU_p) - \underline{\underline{K}} \cdot \frac{\partial U_p}{\partial \underline{r}}, \tag{7.6.3}$$

$$\langle \dot{p} \rangle = \frac{\underline{V}p}{3U_p} \cdot \frac{\partial U_p}{\partial \underline{r}}. \tag{7.6.4}$$

These display clearly the entire set of physical phenomenon and on substitution of the results (7.6.4) and (7.6.3) in the continuity equation (7.6.2) we obtain the equation of transport given by Parker (1965). The fact that $\langle\dot{p}\rangle$ may be positive will require us to reinterpret energy exchange processes of cosmic rays in interplanetary space. For example galactic cosmic rays have a positive density gradient in the vicinity of the earth and hence are gaining energy.

A useful way to visualise the transport of particles in position and momentum is by means of flow lines in (r,p) space. The flow lines are the solutions of the simultaneous ordinary differential equations

$$\frac{d\underline{r}}{dt} = \langle\dot{\underline{r}}\rangle = \underline{S}_p/U_p, \tag{7.6.5}$$

$$\frac{dp}{dt} = \langle\dot{p}\rangle = (Vp/3U_p)\ (\partial U_p/\partial r), \tag{7.6.6}$$

where $\underline{S}_p$ is the differential current density. Since the time t in (7.6.5) and (7.6.6) is a parameter we have

$$\frac{d\underline{r}}{dp} = 3\underline{S}_p \Big/ \left(Vp \frac{\partial U_p}{\partial r}\right), \tag{7.6.7}$$

as an alternative form of the flow line equations.

We note that the tangent to the flow line passing through the point $(\underline{r},p)$, gives the ratio of the streaming velocity $\langle\dot{\underline{r}}\rangle$ to the momentum rate $\langle\dot{p}\rangle$ at that point. Hence if we cannot identify individual particles with momentum in (p,p+dp) and position in $d^3\underline{r}$ about $\underline{r}$, these particles would appear to follow the flow line passing through the point $(\underline{r},p)$ of position-momentum space.

In the scattering model, a consideration of the collisions between an individual particle with a collection of radially moving scatterers

shows that the particle cannot gain momentum greater than

$$\Delta p = 2mV\ (1 + O(\frac{V}{v})),$$

but the particle may continuously lose energy. This aspect of the collision process needs to be kept in mind in the interpretation of the momentum rate $\langle \dot{p} \rangle$.

In spherical symmetric models of the interplanetary medium the differential current density

$$\underline{S}_p = -4\Pi p^2 \left(\frac{Vp}{3} \frac{\partial F_o}{\partial p} + K(r,p) \frac{\partial F_o}{\partial r}\right) \underline{e}_r,$$

where $K(r,p)$ is the diffusion coefficient and $\underline{e}_r$ is the radial unit vector. The flow line equations for this case are

$$\frac{dr}{dt} = -[Vp/3(\partial F_o/\partial p) + K(r,p)\ \partial F_o/\partial r]/F_o, \qquad (7.6.8)$$

$$\frac{dp}{dt} = \frac{Vp}{3F_o} \frac{\partial F_o}{\partial r}, \qquad (7.6.9)$$

or

$$\frac{dr}{dp} = -3\left(\frac{Vp}{3} \frac{\partial F_o}{\partial p} + K(r,p) \frac{\partial F_o}{\partial r}\right) / \left(Vp \frac{\partial F_o}{\partial r}\right). \qquad (7.6.10)$$

We shall construct flow lines for monoenergetic source and monoenergetic spectrum solutions of the transport equations in later chapters.

CHAPTER 8

GALACTIC SPECTRUM SOLUTIONS

8.1 Introduction

In this chapter we present calculations showing features of the monenergetic galactic spectrum solution (6.3.22):

$$F_o(r,p) = \frac{3\, N_g\, K_o(p_o)\, p_o^{-3(1+b)/2}}{8\,\pi\, V\, \Gamma(m)}\ \frac{1}{T}\left(\frac{x^2}{4T}\right)^m \exp\left(\frac{-x^2}{4T}\right) \tag{8.1.1}$$

and the general galactic spectrum solution (6.3.19):

$$F_o(r,p) = \int_p^\infty G(r,p;p_o)\, F_o(\infty,p_o)\, d\, p_o, \tag{8.1.2}$$

where

$$G(r,p;p_o) = \frac{3\, K_o(p_o) p_o^{(1-3b)/2}}{2\, V\, \Gamma(m)}\ \frac{1}{T}\left(\frac{x^2}{4T}\right)^m \exp\left(\frac{-x^2}{4T}\right), \tag{8.1.3}$$

$$x = 2(r\, p^{3/2})^{(1-b)/2} / (1-b),$$

$$T = 3 \int_p^{p_o} K_o(z)\, z^{(1-3b)/2}\, dz/(2V),$$

the diffusion coefficient $K(r,p) = K_o(p) r^b$, with $b > 1$, and $F_o(\infty,p_o)$ specifies the distribution function at $r = \infty$.

Some of the results of this chapter concerning the propagation of galactic cosmic-rays have been obtained previously by means of numerical solutions of the equation of transport. Here the features are obtained more easily, with more precision, and over a wider range of parameters. In particular, the results concerning the momentum changes and the flow of monenergetic galactic cosmic-rays within the solar cavity are new.

In Section (2) we show the characteristics of the monoenergetic

galactic spectrum solution (8.1.1) for a diffusion coefficient $K(r,p) = K_c\ p\ r^{1.5}$ and we present the results published in Webb and Gleeson (1973).

Previous studies of the redistribution of monoenergetic or near monoenergetic galactic cosmic-rays within the solar cavity have been carried out by Parker (1965, 1966), Gleeson and Urch (1971), and Goldstein *et al.* (1970b). Parker considered the case where the diffusion coefficient K(r,p) = constant, and monoenergetic particles were released from a free escape boundary at r = R. He obtained and evaluated a series for the distribution near r = 0. Gleeson and Urch, and Goldstein *et al.* studied the redistribution of near monoenergetic galactic cosmic rays using extensive numerical solutions of the equation of transport. In the latter solutions, the differential number density was specified to be a narrow Gaussian distribution in kinetic energy with a half width $\sim$ 10% of the mean kinetic energy. The numerical solutions probably show the redistribution of particles well, but they are restricted in that,

(i) the spectrum at r = R is near monoenergetic,

(ii) extension of the calculations to very low energies has not been carried out because of accuracy considerations, and

(iii) it is not feasible to examine a wide range of parameters.

These deficiencies are not present in the analytical solution (8.1.1).

In Section (3) we show the structure of the streaming $\underline{S}_p$ in the (r,p) plane arising from monoenergetic galactic cosmic-rays for the case where the diffusion coefficient $K(r,p) = K_c\ p\ r^{1.5}$, and $V\ r_e/K(r_e,p_o) = 0.1$ in the solution (8.1.1). To understand the

physics of the flow it is necessary to recognise that the particles change momentum at the average rate (7.1.1), i.e.

$$\langle \dot{p} \rangle = p \underline{V} \cdot \underline{\nabla} U_p / (3 U_p), \qquad (8.1.4)$$

and not at the adiabatic rate

$$\langle \dot{p} \rangle_{ad} = - p \underline{\nabla} \cdot \underline{V} / 3, \qquad (8.1.5)$$

as given in Equation (7.1.6).

The variation of the streaming velocity $\langle \dot{\underline{r}} \rangle = \underline{S}_p / U_p$, and the momentum rate $\langle \dot{p} \rangle$ in the (r,p) plane are best seen by constructing solutions of the flow line equation (7.6.7), i.e.,

$$\frac{d\underline{r}}{dp} = \langle \dot{\underline{r}} \rangle / \langle \dot{p} \rangle = 3 \underline{S}_p / (V p \partial U_p / \partial r), \qquad (8.1.6)$$

and in Section (3) we obtain numerical and analytic solutions of this equation for the case $K(r,p) = K_c p r^{1.5}$ and $V r_e / K(r_e, p_o) = 0.1$, where r_e is some fixed radius.

In Section (4) we give examples of the general galactic spectrum solution (8.1.2) and we obtain features similar to those in Urch and Gleeson's (1972a) numerical solutions of the equation of transport.

In the general galactic spectrum solution (8.1.2) the distribution function $F_o(r,p)$ is the convolution of the Green's function $G(r,p;p_o)$ of Equation (8.1.3) and the galactic distribution function $F_o(\infty,p_o)$. The Green's function determines the modulation properties of a model, independent of the galactic spectrum and thus warrants particular consideration. In Section (5) we investigate the dependence of $G(r,p;p_o)$ on the momentum p_o, for a range of interplanetary conditions. We use it to study the fraction of particles with kinetic energy in the interval (T, T + dT) at radius r which originated in the kinetic energy

interval $(T_o, T_o + dT_o)$ in a general galactic spectrum. In specific examples we show the origin of protons, electrons and helium nuclei in the galactic spectrum. Some of these results for particular interplanetary conditions are similar to those of Urch and Gleeson (1972b, 1973), but for other conditions the results are different. The calculations involved in the approach presented here are much simpler than the calculations of Urch and Gleeson (1972b, 1973) who investigated the origin of particles in the galactic spectrum by using numerical solutions of the equation of transport.

8.2 The monoenergetic - galactic - spectrum solution

For a diffusion coefficient $K(r,p) = K_c\, p\, r^b$, the monoenergetic galactic spectrum solution (8.1.1) may be written

$$\frac{p_o^3 F_o}{N_g} = \frac{(5-3b)}{8\pi\Gamma(m)} \frac{1}{[1-(p/p_o)^{(5-3b)/2}]} \left(\frac{x^2}{4T}\right)^m \exp\left(-\frac{x^2}{4T}\right), \tag{8.2.1}$$

where

$$\frac{x^2}{4T} = \frac{(5-3b)}{3(1-b)^2} \frac{Vr}{K(r,p_o)} \frac{(p/p_o)^{3(1-b)/2}}{[1-(p/p_o)^{(5-3b)/2}]} . \tag{8.2.2}$$

The parameter $V\, r/K(r,p_o)$ is dimensionless, and it contains the complete dependence of the solution on heliocentric distance r, the diffusion coefficient constant K_c, and the solar wind speed V. A useful and more explicit formulation of the radial dependence is obtained by noting that

$$Vr/K(r,p_o) = V\, r_e/K(r_e,p_o)\, (r_e/r)^{b-1}, \tag{8.2.3}$$

and we have some knowledge of $V\, r/K(r,p_o)$ at 1 A.U. which we may take as r_e.

The differential number density with respect to momentum U_p,

and the mean differential intensity with respect to kinetic energy, $j_T(r,T)$, are related to the mean distribution function with respect to momentum $F_o(r,p)$, by

$$U_p = 4\pi p^2 F_o = 4\pi j_T, \qquad (8.2.4)$$

and we will use each of these in the following.

Some of the principal features of the monoenergetic galactic spectrum solution (8.2.1) are displayed in Figure 8.1. It shows $p_o^3 F_o/N_g$ versus p/p_o on a log-linear scaling for a diffusion coefficient $K(r,p) = K_c\, p\, r^{1.5}$, and values 0.01, 0.1 and 1.0 of the parameter $V\, r/K(r,p_o)$.

The particles injected with momentum p_o are seen to be redistributed over the whole momentum interval, $0 < p \leq p_o$, due to the momentum changes. For sufficiently small $V\, r/K(r,p_o)$ there is a substantial peak in the distribution in the vicinity of p_o. As $V\, r/K(r,p_o)$ decreases, either because r or p_o or K_c increases, or V decreases, the peak moves towards p_o, increases in value, and narrows in width. Since the differential number density U_p tends to a delta function as $r \to \infty$, we have

$$U_p \to N_g\, \delta(p-p_o) \qquad \text{as } V\, r/K(r,p_o) \to 0.$$

The distribution function $F_o(r,p) \to 0$ as $p \to 0$, we have $x^2/T \to \infty$ and the term $\exp(-x^2/(4T))$ dominates in the expression (8.2.1) for $F_o(r,p)$. For the two smaller values of $V\, r/K(r,p_o)$ of Figure 8.1, there is a second peak at the low end of the momentum range. There is apparently a buildup of particles which have most momentum due to interaction with the irregular mangnetic fields moving with the solar wind. At $V\, r/K(r,p_o) = 1.0$ this second peak is not present, and the distribution has a single peak, which diminishes sharply in amplitude as

V $r/K(r,p_o)$ increases, e.g., for V $r/K(r,p_o)$ = 10.0, the maximum of $p_o^3 F_o/N_g$ is 1.19×10^{-21} at $p/p_o = 0.32$.

The curves of Figure 8.1 can be interpreted as indicating the changes in the distribution function $F_o(r,p)$ at fixed r for various diffusion coefficients, or the changes at fixed r for various p_o in interstellar space (recall $K(r,p_o) = K_c\ p_o\ r^b$). In this latter case the figure shows that particles of lower p_o are more spread from the delta function distribution of injection, and are more attenuated. To establish the relationship of these curves to practical modulation problems, we note that using values of K used by Urch and Gleeson (1972b) to reproduce the modulation of 1965, i.e., solar minimum ($K(r,p) = 3 \times 10^{17}$ m^2 s^{-1} at a radius of 1 A U and 1 G V rigidity, and $V = 4 \times 10^5$ m s^{-1}), the curves V $r/K(r,p_o)$ = 0.01, 0.1 and 1.0 represent, respectively the distributions to be obtained at r = 1 A U from injection of protons at kinetic energies, T_o, of 19 GeV, 1260 MeV and 20.9 MeV.

Alternative to the previous paragraph, the three curves of Figure 8.1, can be interpreted as indicating the changes in distribution with heliocentric distance r. In this example V $r/K(r,p_o) \propto r^{-1/2}$ and the heliocentric distances, represented by the curves V $r/K(r,p_o)$ = 1.0, 0.1 and 0.01 are in the ratio 0.01 : 1 : 100. Thus if the curve for V $r/K(r,p_o)$ = 0.1 represents the distribution at r = 1 A U, the curves V $r/K(r,p_o)$ = 1.0 and 0.01 represent, respectively, the corresponding distributions at r = 0.01 A U and r = 100 A U.

Observational results for cosmic-ray spectra are usually shown as j_T vs T and, in view of this, we have redrawn the curves of Figure 8.1 in this form in Figure 8.2. The same general features noted above

are to be seen, except that, due to the factor p^2 in the relation between F_o and j_T, viz., $j_T = p^2 F_o$, the peaks at the low energy end of the spectrum are not as pronounced. Although generally representing the form of the spectra, Figure 8.2 has been drawn for the particular case of the kinetic energy of injection T_o equal to the rest energy E_o.

As a confirmation of previous results, Figures 8.1 and 8.2 demonstrate again the reduction in momentum and energy cosmic ray particles, on average, undergo.

Figures 8.1 and 8.2 also provide an extension of previous results for they show a hitherto unknown peak in the distribution at low energies. However, this might not be important in relation to the population of very low energy particles since

(i) the peak occurs at very low energies $T \sim 0.001$ MeV for $T_o = E_o = 938.211$ MeV protons,

(ii) at these energies the diffusion coefficient $K(r,p) = K_c\ p\ r^{1.5}$ may not be appropriate,

(iii) other sources, e.g. the sun, may be more important contributors in practical situations.

An example of a previous notion to be refuted is the hypothesis advanced by Urch and Gleeson (1972b), based on a wide range of numerical solutions, that monoenergetic galactic sources produced, within the solar cavity, distributions with $j_T \propto T$ at the low (non-relativistic) energy end of the spectrum. The condition $j_T \propto T$ corresponds to $\partial F_o/\partial p = 0$, i.e., F_o = constant over the range in which $j_T \propto T$, and the results displayed in Figures 8.1 and 8.2 shows that this is not generally the case.

The results of a more comprehensive investigation of the mono-

energetic galactic spectrum solution (8.2.1) for the case $K(r,p) = K_c\ p\ r^{1.5}$ are presented in Figures 8.3 and 8.4. The figures show the physical quantities:

(i) the distribution function F_o,

(ii) the differential number density $U_p = 4\ \pi\ p^2\ F_o$,

(iii) the radial gradient $G_r(r,p) = (1/U_p)\ \partial U_p/\partial r$, (8.2.5)

(iv) the radial differential current density S_p, and the convective and diffusive components of S_p, which we denote by S_c and S_d, i.e.,

$$S_c = - 4\ \pi\ p^3 (V/3)\ \partial F_o/\partial p,$$

$$S_d = - 4\ \pi\ p^2\ K(r,p)\ \partial F_o/\partial r\ ,$$

$$S_p = S_c + S_d\ ,$$

(v) the bulk flow speed $\langle \dot{r} \rangle = S_p/U_p$, the related component quantities $S_p/(V\ U_p)$, $S_d/(V\ U_p)$, and the Compton Getting factor $C = S_c/(V\ U_p)$,

(vi) the time average rate of change of momentum

$$\langle \dot{p} \rangle = V\ p\ G_r\ /\ 3,$$

and $\langle \dot{p} \rangle\ /\ \langle \dot{p} \rangle_{ad}$, where

$$\langle \dot{p} \rangle_{ad} = - 2\ V\ p/(3r),$$

is the adiabatic deceleration rate.

In Figures 8.3a, and 8.3b, these physical quantities are plotted against p/p_o for values 0.01, 0.1 and 1.0 of the parameter $V\ r/K(r,p_o)$. In Figures 8.4a and 8.4b they are shown on contour plots in the (r,p)plane, on a log-log scale for the case $V\ r_e/K(r_e,p_o) = 0.1$.

To conclude this section we discuss some of the physical characteristics of the cosmic-ray propagation shown by this set of

graphs. We look at the distribution of particles, gradient, streaming and mean momentum changes in (r,p) space for K_c given. Thus we regard the curves V r/K(r,p_o) = 0.01, 0.1 and 1.0 of Figures 8.3 as being for different heliocentric distance, and in this case, since K = K_c p $r^{1.5}$, the parameter V r/K(r,p_o) α $r^{-1/2}$. The contour plots of Figures 8.4 are particularly useful here.

The curves for F_o or U_p in Figures 8.3 and 8.4 show that for each p, ($p < p_o$) as r increases from zero the number density increases to a peak and then decreases. This represents particles simultaneously being fed into (p, p + dp) by the energy changes but being excluded from the inner regions by the outwardly moving scattering centres.

Corresponding to this peak (which shows as a 'ridge' in the (r,p) plane) we have a positive gradient near r = 0, changing to negative at heliocentric distances past the peak. At large radii the negative gradient is independent of p over a large portion of the spectrum.

The structure of the streaming is very complex, particularly near $p = p_o$. The contours of S_p in Figure 8.4 give the clearer picture of the streaming structure. They show that near the sun S_p changes from -ve to +ve as p increases from 0 to p_o and at larger radii S_p changes through the sequence -ve, +ve, -ve, +ve as p increases from 0 to p_o. At low momenta ($p << p_o$) the magnitude of the Compton-Getting factor is much greater than $|S_d / V U_p|$ and the flow is convective.

The regions in (r,p) space in which particles are gaining or losing momentum are readily seen from the contour plots of $(dp/dt)/(dp/dt)_{ad}$ of Figure 8.4b. We note that at large radii, $\langle\dot{p}\rangle$ is approximately equal to the adiabatic deceleration rate over a large portion of the momentum spectrum.

At sufficiently small p we note that the distribution function contours are of the form

$$r\, p^{3/2} = \text{constant.}$$

This form is characteristic of the convective solution of the transport equation (Appendix D, Gleeson, 1970), and it can also be seen from the analytic expression (8.2.1) for $F_o(r,p)$: for $K(r,p) = K_c\, p\, r^{1.5}$, we have as $p \to 0$

$$x^2/(4T) \to 2\, V\, r_e/K(r_e,p_o) \cdot \left[(r/r_e)\,(p/p_o)^{3/2}\right]^{-1/2} / 3,$$

and F_o is a function of $r\, p^{3/2}$. However for diffusion coefficients of the form $K = K_c\, p^a\, r^b$, with $b > 1 + 2a/3$, an investigation of the analytic expression (8.1.1) for $F_o(r,p)$ shows that it is not a function of the single variable $r\, p^{3/2}$ for small p, and hence in these cases the solution might not be convective as $p \to 0$.

The particle flow and momentum changes are related since the momentum changes form effective sources of particles. We investigate this more fully for monoenergetic galactic cosmic-rays in the next section.

8.3 The flow pattern of monoenergetic galactic cosmic-rays

In this section we investigate the particle flow and momentum changes in position-momentum space. These aspects are examined together because they are related by the fact that particles are conserved and the continuity equation

$$\frac{1}{r^2}\frac{\partial}{\partial r}\,(r^2\, S_p) + \frac{\partial}{\partial p}\,(\langle \dot{p} \rangle\, U_p) = 0, \qquad (8.3.1)$$

applies. The momentum changes provide an effective source of particles;

without them we would have

$$r^2 S_p = \text{constant.}$$

in general, and $S_p \equiv 0$ in the galactic case.

We first calculate the streaming $S_p(r,p)$ for the case $K = K_c\, p\, r^b$ and show the regions of (r,p) space in which particles have a net inflow or net outflow for the particular conditions $K(r,p) = K_c\, p\, r^{1.5}$ and $V\, r_e/K(r_e,p_o) = 0.1$ where r_e is some fixed heliocentric distance.

Then in order to elucidate the physics of the flow we obtain analytic and numerical solutions of the flow line equations (7.6.8) and (7.6.9). We note again that the tangent to a flow line at any point of (r,p) space gives the ratio of the streaming speed $\langle \dot{r} \rangle$ to the momentum change rate $\langle \dot{p} \rangle$ (cf. Section (7.6)).

From the expression (7.6.3) for the streaming we have

$$S_p = -4\pi p^2 \left(\frac{V p}{3} \frac{\partial F_o}{\partial p} + K(r,p) \frac{\partial F_o}{\partial r} \right). \qquad (8.3.2)$$

For a diffusion coefficient $K(r,p) = K_c\, p\, r^b$, $b > 1$ substitution of the expression (8.2.1) for F_o in the result (8.3.2) gives

$$S_p = -4\pi p^2 V F_o \left[\frac{(5-3b)z}{6(1-z)} + \left(\frac{2z+3-3b}{6(1-z)} + (1-b) \frac{K(r,p)}{Vr} \right) \left(m - \frac{(5-3b)}{3(b-1)^2} \frac{V r}{K(r,p)} \frac{z}{(1-z)} \right) \right], \qquad (8.3.3)$$

where

$$z = (p/p_o)^{(5-3b)/2},$$

$$m = (b+1)/(b-1),$$

as the formula for the streaming arising from monoenergetic galactic cosmic-rays.

The general structure of $S_p(r,p)$ is given in Figure 8.5, it shows an (r,p) plane and the arrows indicate schematically the direction of S_p (either inward or outward). Note that the total flux of particles inward equals that outward at every r. At r_1, say we note four momenta p_o, p_1, p_2 and p_3 (see Figure 8.5). The significant net inward flow occurs between p_1 and p_2 and the bulk of this moves outward at lower momenta between p_2 and p_3. There is always a region $p_1 < p < p_o$ with a net outflow and these particles have momentum greater than that of the inflow region. This flow pattern is readily understood in terms of particles entering within r_1 and gaining momentum at the rate (8.1.4) i.e.,

$$\langle \dot{p} \rangle = V\, p\, (\partial U_p/\partial r) \,/\, (3\, U_p) \;; \qquad (8.3.4)$$

the outflow in $p_1 < p < p_o$ could not arise if cosmic-ray particles lost momentum continuously at the adiabatic rate (8.1.6).

The relationship between the mean rate of change of momentum $\langle \dot{p} \rangle$ and the streaming is conveniently illustrated by plotting the flow lines in (r,p) space of the *average* particle. These are defined parametrically by Equations (7.6.8) and (7.6.9):

$$\frac{dr}{dt} = \langle \dot{r} \rangle = \frac{S_p}{U_p} = \frac{-1}{F_o}\left(\frac{V\, p}{3} \frac{\partial F_o}{\partial p} + K(r,p) \frac{\partial F_o}{\partial r} \right), \qquad (8.3.5)$$

$$\frac{dp}{dt} = \langle \dot{p} \rangle = \frac{p\, V}{3F_o} \frac{\partial F_o}{\partial r} \;. \qquad (8.3.6)$$

Alternatively by eliminating time we obtain

$$\frac{dr}{dp} = \frac{\langle \dot{r} \rangle}{\langle \dot{p} \rangle} = -3\left(\frac{V\, p}{3} \frac{\partial F_o}{\partial p} + K(r,p) \frac{\partial F_o}{\partial r} \right) \Big/ \left(V\, p \frac{\partial F_o}{\partial r} \right), \qquad (8.3.7)$$

the direct equation of the flow line.

We now obtain the analytic solution of these flow line equations

for the monoenergetic galactic spectrum solution (8.1.1). Substituting the expression (8.1.1) for F_o in the flow line equations (8.3.5) and (8.3.6) we have

$$\frac{dr}{dt} = \left(1 - \frac{m}{u}\right)\left(\frac{V\,u}{(1-m)} + (1+u-m)\,\frac{K_o(p)\,p^{(3-3b)/2}}{2\,T}\right)$$

$$- K_o(p)\,p^{(3-3b)/2}\,/\,(2T), \qquad (8.3.8)$$

$$\frac{dp}{dt} = \frac{2\,V\,p\,(m-u)}{3\,r\,(1-m)}, \qquad (8.3.9)$$

where

$$u = x^2/(4T).$$

and as previously

$$T = 3\int_p^{p_o} K_o(z)\,z^{(1-3b)/2}\,dz\,/\,(2V), \qquad (8.3.10)$$

$$x = 2\,(r\,p^{3/2})^{(1-b)/2}\,/\,(1-b).$$

Regarding u and T as independent variables and using the derivative transformations

$$\frac{dr}{dt} = \left(\frac{\partial r}{\partial u}\right)_T \frac{du}{dt} + \left(\frac{\partial r}{\partial T}\right)_u \frac{dT}{dt},$$

$$\frac{dp}{dt} = \left(\frac{\partial p}{\partial u}\right)_T \frac{du}{dt} + \left(\frac{\partial p}{\partial T}\right)_u \frac{dT}{dt},$$

$$\left(\frac{\partial r}{\partial u}\right)_T = \frac{1-m}{2}\,\frac{r}{u}, \qquad (8.3.11)$$

$$\left(\frac{\partial r}{\partial T}\right)_u = \frac{(1+m)\,r}{2T} + \frac{V\,r}{K_o(p)\,p^{(3-3b)/2}},$$

$$\left(\frac{\partial p}{\partial u}\right)_T = 0,$$

$$\left(\frac{\partial p}{\partial T}\right)_u = \frac{-\,2\,V}{3\,K_o(p)\,p^{(1-3b)/2}},$$

the flow line Equations (8.3.8) and (8.3.9) may be expressed as

$$\frac{du}{dt} = \frac{m}{(1-m)} \frac{K_o(p)\ p^{(3-3b)/2}}{T\ r} (m-1-u), \qquad (8.3.12)$$

$$\frac{dT}{dt} = \frac{K_o(p)\ p^{(3-3b)/2}(m-u)}{(m-1)r} . \qquad (8.3.13)$$

Dividing Equation (8.3.12) by Equation (8.3.13) we obtain

$$\frac{du}{dT} = \frac{m(u + 1 - m)}{T\ (m-u)} , \qquad (8.3.14)$$

as the flow line equation for monoenergetic galactic cosmic-rays. Note that it contains only u and T as variables.

The general solution of the flow line Equation (8.3.14) is

$$A\ T^m = (u+1-m)\ \ e^{-u}, \qquad (8.3.15)$$

with A an arbitrary constant.

The flow lines in (u,T) coordinates are shown in Figure 8.6a, for the case $K(r,p) = K_o(p)\ r^{1.5}$, for $0 < u < 10$, and for $A = \pm 0.1$, ± 1, ± 10, on a log-linear scaling. There are two distinct sections corresponding to $A \gtrless 0$, and separated by the critical solution

$$u = m - 1 = 4, \qquad (8.3.16)$$

obtained with $A = 0$. The curves in each section, have the same slope with a logarithmic T scale. The peaks occur at $u = m = 5$, and

$$T = 1/(e\ A^{1/m}) = 1/(e\ A^{1/5}),$$

where e is the base of Napierian logarithms, at this peak. In order to show the structure of the flow lines for large u we have redrawn the flow lines in Figure 8.6b for $A = \pm 0.01$, ± 1, ± 100 and for $0.1 < u < 100$ on a log-log scaling.

We note particularly that these flow lines apply to the general case $K(r,p) = K_o(p)\ r^b$, $(b = 1.5)$, and not just the case $K(r,p) = K_c\ p\ r^b$. They may, of course, be expressed in terms of r and p when required and we do this next to illustrate the general features.

For a diffusion coefficient $K(r,p) = K_c\ p\ r^b$, $b > 1$,

we have

$$u = \frac{x^2}{4T} = \frac{(5-3b)}{3(b-1)^2} \frac{V r_e}{K(r_e,p_o)} \left(\frac{r}{r_e}\right)^{1-b} \frac{p_o}{p} \frac{z}{(1-z)} ,$$

$$T = 3 K_c p_o^{(5-3b)/2} (1-z) / ((5-3b)V),$$

where

$$z = (p/p_o)^{(5-3b)/2} ,$$

$$m = (b+1)/(b-1).$$

Note that we have again introduced r_e and the non-dimensional parameter $V r_e/K(r_e,p_o)$.

The flow lines for the case $b = 1.5$ and $V r_e/K(r_e,p_o) = 0.1$ are given in Figure 8.7. Although it is possible to use the solution (8.3.15) to construct the flow lines in (r,p) space, the flow lines of Figure 8.7 were obtained by numerically solving the flow equations (8.3.8) and (8.3.9) as an initial value problem.

The general features to note are that the lines are of two main forms:

(i) those that go inward, drop monotonically in p and emerge again with lower p, and

(ii) those that enter inwards, and return with p increased, indicating momentum increases.

There is a critical curve separating the two forms and it corresponds to $u = m - 1$ of Figures 8.6 obtained with $A = 0$.

Further loci which assist in assessing the structure of the flow lines are the locus of the minimum values of p/p_o (when it exists) and the locus of the minimum values of r. The first is the locus $\langle \dot{p} \rangle = 0$ and is given by

$$u = m$$

and corresponds to the peaks in the distribution function in Figure 8.4a. The second are the loci $\langle\dot{r}\rangle = 0$ or $S_p = 0$; they cannot be expressed in terms of u and T without a knowledge of $K_o(p)$ and are found by solving the equation $\langle\dot{r}\rangle = 0$, with $\langle\dot{r}\rangle$ given by Equation (8.3.8).

For sufficiently small p/p_o Figure 8.8 shows that the critical curve, the locus $\langle\dot{p}\rangle = 0$ and the right hand locus $\langle\dot{r}\rangle = 0$ are of the form $r\, p^{3/2}$ = constant. We note from Section (8.2) that the distribution function contours for the case $K = K_c\, p\, r^{1.5}$ and $V\, r_e/K(r_e,p_o) = 0.1$, are of the form $r\, p^{3/2}$ = constant, at small p/p_o, and that this form is characteristic of the convective solution of the transport equation. However for diffusion coefficients $K = K_c\, p^a\, r^b$, with $b > 1 + 2a/3$ the solution (8.1.1), the flow lines (8.3.15) and the locus $\langle\dot{p}\rangle = 0$, at small p/p_o cannot be expressed in terms of the single variable $r\, p^{3/2}$ and the convective solution of the transport equation does not seem to apply.

Finally, in this section we remark that these flow patterns show clearly the regions in (r,p) space of the inflow and outflow and momentum gains and losses of the *average* particles. The momentum gains occurring make the flow pattern variations explicable. We stress however that the flow lines represent the mean or *average* effects on the particles and *not* the path in (r,p) space of any individual particle. The individual particle paths in (r,p) space are random with some order (the average effects discussed here) superimposed.

8.4 Composite galactic spectrum solutions

In this section we give examples of the general galactic spectrum solution (8.1.2), i.e.,

$$F_o(r,p) = \int_p^\infty G(r,p;p_o)\, F_o(\infty, p_o)\, d\, p_o, \qquad (8.4.1)$$

where

$$G(r,p;p_o) = \frac{3\, K_o(p_o)\, p_o^{(1-3b)/2}}{2\, V\, \Gamma(m)}\, \frac{1}{T} \left(\frac{x^2}{4T}\right)^m \exp\left(-\frac{x^2}{4T}\right), \qquad (8.4.2)$$

$$x = 2(r\, p^{3/2})^{(1-b)/2}/\,(1-b)\,, \qquad (8.4.3)$$

$$T = 3 \int_p^{P_o} K_o(z)\, z^{(1-3b)/2}\, dz/(2V), \qquad (8.4.4)$$

the diffusion coefficient $K(r,p) = K_o(p)\, r^b$, $b > 1$ and $F_o(\infty,p_o)$ specifies the distribution function at $r = \infty$.

In terms of the differential number density with respect to kinetic energy U_T, the three forms of the galactic spectrum used are:

$$\text{(a)} \quad U_T(\infty,T) = A_1(T + E_o)^{-2.5} \times \begin{cases} 1 & (T > 186 \text{ MeV}) \\ \exp(-25\, \ell n(2)((T-186)/155)^2) & (T < 186 \text{ Mev}) \end{cases}$$

$$\text{(b)} \quad U_T(\infty,T) = A_2(T + E_o)^{-2.5}\,, \qquad (8.4.5)$$

$$\text{(c)} \quad U_T(\infty,T) = A_3[(1 + T/E_o)^{-2.5} + (1/2)(T/0.15\, E_o)^{-2}]$$

hereafter referred to as (a), (b) and (c) respectively.

In these examples we use a diffusion coefficient

$$K(r,p) = 6 \times 10^{21}\, r^{1.237}\, P\, \beta \text{ cm}^2/\text{s}, \qquad (8.4.6)$$

$\beta \equiv$ particle speed/speed of light, P is in GV and r is in A U. For this diffusion coefficient, with the boundary of the solar cavity at $r = \infty$, and the solar wind speed $V = 4 \times 10^5$ m s^{-1}, the value of the force field parameter, ϕ, (Gleeson and Axford, 1968c) is 0.14 G V at 1 A U.

The galactic spectra (8.4.5), the value of the diffusion coefficient at a radius of 1 A U and a rigidity of 1 G V, and the value of the force field parameter at a radius of 1 A U are the same as Urch and Gleeson (1972a) have used in numerical solutions of the equation of transport. Hence we may directly compare the results obtained from the general galactic spectrum solution (8.4.1) and the work of Urch and Gleeson (1972a).

We investigate the kinetic energy spectra of the differential intensity with respect to kinetic energy

$$j_T(r,T) = p^2 F_o(r,p), \qquad (8.4.7)$$

the radial gradient

$$G_r(r,T) = (1/U_p)\ \partial U_p/\partial r\ , \qquad (8.4.8)$$

and the radial anisotropy

$$\xi_r(r,T) = 3\ S_p\ /\ (v\ U_p), \qquad (8.4.9)$$

where v is the particle speed, to be obtained at r = 1 A U for the three forms of the galactic proton spectra (8.4.5).

In Figures 8.9a, 8.9b, 8.9c we show the differential intensity, the radial gradient and the radial anisotropies to be obtained at r = 1 A U for the three types of galactic proton spectra (8.4.5).

These spectra were obtained as follows. We first expressed j_T, G_r and ξ_r given in Equations (8.4.7)-(8.4.9) in terms of F_o, $\partial F_o/\partial r$ and $\partial F_o/\partial p$, i.e.,

$$\begin{aligned} j_T &= p^2 F_o \\ G_r &= (1/F_o)\ (\partial F_o/\partial r\ ), \qquad (8.4.10) \\ \xi_r &= -\ 3\ (K\ \partial F_o/\partial r + (V\ p/3)\ \partial F_o/\partial p)\ /\ (v\ F_o). \end{aligned}$$

Using the galactic spectrum solution (8.4.1) we then evaluated the integrals

$$F_o = \int_p^\infty G(r,p;p_o)\ F_o(\infty,p_o)\ d\,p_o.$$

$$\partial F_o/\partial r = \int_p^\infty [\partial G(r,p;p_o)/\partial r]\ F_o(\infty,p_o)\ d\,p_o, \qquad (8.4.11)$$

$$\partial F_o/\partial p = \int_p^\infty [\partial G(r,p;p_o)/\partial p]\ F_o(\infty,p_o)\ d\,p_o,$$

for F_o, $\partial F_o/\partial r$ and $\partial F_o/\partial p$ directly by using Simpson's rule and neglecting contributions to the integral above p_o = 100 GeV/c. Thus using the expressions (8.4.10) we obtained numerical values for j_T, G_r and ξ_r.

Although the three galactic spectra are very different for $T \leq 200$ MeV they all lead to similar differential intensity spectra at r = 1 A U. The results of Figure 8.9a show that low energy particles are being excluded from near earth, and that a large proportion of the low energy particles observed near earth must have originated from above 200 MeV in the galactic spectrum (cf. Goldstein *et al.* 1970b, Urch and Gleeson 1972a).

In contrast to the differential intensity spectra, the gradients and anisotropies in the energy range $T < 60$ MeV are very sensitive to the form of the galactic spectrum. The case (a) is quite distinct, for it yields negative gradients and positive radial anisotropies at low energies. The positive radial anisotropy is due to an accumulation of low energy particles at r < 1 A U, which originated from much higher energies in the galactic spectrum.

Since the time-average-rate-of-change of momentum is given by

$$\langle \dot{p} \rangle = V\ p\ G_r/3,$$

the radial gradient curves of Figure 8.9b show that in cases (b) and (c) that particles with kinetic energy $T \geq 10$ MeV are on average gaining energy, whereas in case (a) particles with T > 60 MeV are gaining energy and particles with T < 60 MeV are losing energy.

The differential intensities, the radial gradients, and the radial anisotropies obtained by Urch and Gleeson (1972a) from numerical solutions of the equation of transport are displayed in Figures 8.10a, 8.10b and 8.10c respectively. The differential intensity spectra obtained at r = 1 A U by Urch and Gleeson are virtually identical to the results obtained from the galactic spectrum solution (8.4.1). The radial gradients and the radial anisotropies obtained at r = 1 A U by the two methods show similar positive and negative regions. However due to the different radial dependence of the diffusion coefficient and the position of the outer boundary used in the two methods, they differ considerably in fine details.

8.5 The origin of particles in a galactic spectrum

In the general galactic spectrum solution (8.1.2) the distribution function $F_o(r,p)$ is the convolution of the kernel $G(r,p;p_o)$ of Equation (8.1.3) and the galactic distribution function $F_o(\infty,p_o)$. In this section we investigate the properties of the kernel $G(r,p;p_o)$ and then use it to determine the relative contribution of the galactic spectrum to intensities measured at (r,p).

The kernel regarded as a function of p_o provides a direct measure of the sensitivity of the intensity at position r and momentum p to particles of momentum p_o in the galactic spectrum. It thus provides the essential features of the modulating region without reference to galactic spectra and enables us to establish the most sensitive regions of the galactic spectrum. This concept studying the modulation characteristics via G is new and has not been possible before because of the difficulty of obtaining G by numerical solution of the equation of transport.

As an example of the form of G we note that for a diffusion coefficient $K(r,p) = K_c\ p\ r^b$, $b > 1$, the function $G(r,p;p_o)$ is given by

$$G(r,p;p_o) = \frac{(5-3b)}{\Gamma(m)p}\ \frac{z}{(z-1)}\ \left(\frac{p}{p_o}\right)\ u^m\ e^{-u}\ , \qquad (8.5.1)$$

where

$$\begin{aligned} m &= (b+1)/(b-1), \\ z &= (p_o/p)^{(5-3b)/2}, \qquad (8.5.2) \\ u &= \frac{x^2}{4T} = \frac{(5-3b)}{3(1-b)^2}\ \frac{1}{(z-1)}\ \frac{V\ r}{K(r,p)} \end{aligned}$$

and $\Gamma(m)$ is the gamma function of argument m. The diffusion coefficient constant K_c, r and V dependence is completely contained in the non-dimensional parameter V r/K(r,p).

This function G is plotted in Figure 8.11 as a function of p_o/p for a diffusion coefficient $K(r,p) = K_c\ p\ r^{1.5}$ and values 0.01, 1.0 and 10.0 of the parameter V r/K(r,p).

The curves show:

(i) that particles with momentum p at radius r, arise from particles in the whole momentum range $p_o > p$ in the galactic spectrum and

(ii) as V r/K(r,p) increases the peak which represents the most sensitive region moves to higher p_o and becomes broader.

For a diffusion coefficient $K = K_c\ p\ r^b$, $b > 1$, the peak is located at

$$p_o/p = [(B + \sqrt{B^2 - 4AC}\ )/(2A)]^{2/(5-3b)}, \qquad (8.5.3)$$

where

$$B = \frac{5-3b}{b-1} + 2 + \frac{(5-3b)^2}{6(b-1)^2}\ \frac{V\ r}{K(r,p)}\ , \qquad (8.5.4)$$

$$A = 1 + (5-3b)(b+1)/(2(b-1)),$$

$$C = 3(b-1)/2.$$

As $V\ r/K(r,p) \to 0$, either because the radius r, or momentum p or diffusion coefficient constant K_c increases (recall $K = K_c\ p\ r^{1.5}$), or because V decreases, the peak narrows in width, increases in peak value and moves towards $p_o = p$, and $G(r,p;p_o) \to \delta(p_o-p)$.

The parameter $V\ r/K(r,p)$ determines the modulation of galactic cosmic-rays when a $p^{-\mu}$, $\mu > 0$, galactic spectrum for $F_o(\infty,p_o)$ is used [see Section (6.3)]; the modulation increases as $V\ r/K(r,p)$ increases. We note that only when the modulation is small and the function $G(r,p;p_o)$ is sharply peaked at p_o near p can the galactic spectrum near $p_o = p$ contribute significantly to the intensity at (r,p). At the higher modulation the contribution from $p_o \simeq p$ decreases markedly as the curves in Figure 8.11 shift to the right and the contribution is predominantly from the higher momentum range. This low contribution from $p_o \simeq p$ when the modulation is large is the exclusion of low energy galactic cosmic rays shown from numerical solutions of the equation of transport by Urch and Gleeson (1972a), Goldstein *et al.* (1970b), and from the galactic spectrum solution (8.1.2) results discussed in the previous section. These present curves give a more direct demonstration of the exclusion and it is quite clear that this exclusion becomes more marked as the modulation increases.

The curves of Figure 8.11 can be interpreted as indicating the changes in $G(r,p;p_o)$ at fixed r for various diffusion coefficients (recall $K = K_c\ p\ r^{1.5}$), or the changes at fixed r, for particles of various momenta p. In this latter case, if $V = 4 \times 10^5$ m s^{-1}, r = 1 A U and $K(r,p) = 3 \times 10^{17}$ m^2 s^{-1} at a radius of 1 A.U. and a momentum of

1 GeV/c, the curves V r/K(r,p) = 10, 1, 0.1 and 0.01, represent, respectively, the number of particles with momentum p_o in a galactic spectrum with $F_o(\infty,p_o)$ = constant, which are observed at r = 1 A U with momenta of 20, 200 MeV/c, 2 and 20 GeV/c.

Alternatively the curves of Figure 8.11 can be interpreted as indicating the changes in $G(r,p;p_o)$ with heliocentric radius r. In this example V r/K(r,p) α $r^{-1/2}$ and the heliocentric distances represented by the curves V r/K(r,p) = 10, 1, 0.1 and 0.01 are in the ratio 0.01 : 1 : 10^2 : 10^4. Thus if the curve V r/K = 1 corresponds to r = 1 A U, the curves V r/K(r,p) = 10, 1, 01, and 0.01 represent, respectively, the distribution of particles with momentum p_o in a galactic spectrum with $F_o(\infty,p_o)$ = constant, which are observed with momentum p at radii of 0.01, 1, 100 and 10^4 A U.

The Green's function $G(r,p;p_o)$ can be used to determine where within the galactic spectrum particles observed at position r and momentum p have originated. If the galactic spectrum at p_o is $F_o(\infty,p_o)$, then there are

$$4\pi p^2 F_o(\infty,p_o) \; G(r,p;p_o) \; dp \; dp_o$$

particles per unit volume at r in (p, p+dp) arising from the momentum interval (p_o, p_o + dp_o). The fraction of particles at (r,p) originating within dp_o about p_o is thus

$$\psi_p(r,p;p_o)dp_o = \frac{F_o(\infty,p_o)\; G(r,p;p_o)\; dp_o}{\int_p^\infty F_o(\infty,p_o)\; G(r,p,p_o)\; dp_o} \quad . \quad (8.5.5)$$

If we work in terms of kinetic energy T, the fraction of particles at (r,T) originating in dT_o about T_o is

$$\psi_T(r,T;T_o)\; dT_o = \psi_p(r,p;p_o)\; \frac{dp_o}{dT_o}\; dT_o = \frac{1}{v_o}\; \psi_p(r,p;p_o) d\, T_o. \quad (8.5.6)$$

The mean kinetic energy of the particles observed at r with kinetic energy T is

$$\langle T_o(T) \rangle = \int_o^\infty T_o \ \psi_T \ (r,T;T_o) \ dT_o \qquad (8.5.7)$$

and a similar result applies to momentum.

Using these formulae we now calculate the contribution from different portions of the galactic spectrum to the near earth differential intensity at kinetic energy T, for electron, proton, and helium galactic spectra and interplanetary conditions appropriate for 1965 and 1969. The only previous study of this nature was carried out by Urch and Gleeson (1972b, 1973) using numerical solutions of the equation of transport; that study made no reference to Green's function $G(r,p;p_o)$.

The galactic spectra and the momentum dependence of the diffusion coefficient assumed have been taken from Urch and Gleeson (1973), denoted U G for further reference. The galactic proton and helium nuclei spectra are

$$U_T(\infty,T) = A(T + a\ E_o)^{-2.5}, \qquad (8.5.8)$$

with a = 1.0, E_o = 938.211 MeV for protons and a = 0.5, E_o = 3726.78 MeV for helium. The known galactic electron spectrum (see Figure 1, Burger, 1971; Goldstein *et al.* 1970a), is used in the electron calculations. We approximate this galactic spectrum by

$$j_T(\infty,T) = p^2 F_o(\infty,p) = \begin{cases} B_1 T^{A_1}, & T < T_2, \\ B_2 T^{A_2}, & T_2 < T < T_3, \\ B_3 T^{A_3}, & T > T_2, \end{cases} \qquad (8.5.9)$$

where T is the kinetic energy in MeV,

$$T_2 = 1279.8,$$

$$T_3 = 425.1,$$

$$B_1 = 1.77826 \times 10^4, \quad A_1 = -1.75, \qquad (8.5.10)$$

$$B_2 = 6.95517 \times 10^5, \quad A_2 = -2.262,$$

$$B_3 = 7.60505 \times 10^7, \quad A_3 = -2.824,$$

and $j_T(\infty,T)$ is the differential intensity with respect to kinetic energy in units of $m^{-2}\ s^{-1}\ sr^{-1}\ MeV^{-1}$.

The diffusion coefficient is assumed to be of the form

$$K(r,p) = K_c\ K_2(P)\ \beta\ r^b, \qquad (8.5.11)$$

where

$$K_2(P) = \begin{cases} P, & P > P_2, \\ \sqrt{P_2\ P}, & P_1 < P \leq P_2, \\ \sqrt{P_1\ P_2}, & 0 < P \leq P_1, \end{cases} \qquad (8.5.12)$$

P is the rigidity in G V, β = particle speed/speed of light. With K_c in $m^2\ s^{-1}$ and r in A U, and for $K(r,p) \propto r^{1.5}$, the parameters (K_c, P_1, P_2) appropriate for 1965 and 1969 are $(1.139 \times 10^{17}, 0.038, 1.0)$ and $(5.316 \times 10^{16}, 0.248, 0.7)$ respectively. These values of K_c and $b = 1.5$ together give the force-field parameter, $\phi(r)$, values of 0.35 GV and 0.75 GV at 1 A U. These are the same as used by U G to reproduce the observed modulation for 1965 and 1969. Note that the general form (8.1.3) for the Green's function $G(r,p;p_o)$ must be used because of the sectioned form of $K_2(P)$, in Equation (8.5.12).

In Figures 8.12a, 8.12b, 8.12c we show the origin, within the galactic spectrum of protons, helium and electrons observed near Earth during 1965 and 1969. The kinetic energies of the proton and helium nuclei are 50, 100, 200 and 500 MeV/nucleon, and for the electrons they are 100, 200, 500 and 1000 MeV. The arrows indicate the mean energies

of the distribution $\langle T_o \rangle$ and these are also listed on the figures.

It has been shown previously (Goldstein *et al.*, 1970b, Gleeson and Urch, 1971; Urch and Gleeson 1973) that low energy nuclei ($T \leq 80$ MeV/nucleon at sunspot minimum) are virtually excluded from near Earth. For example in 1969, Figure 8.12a shows that only a few percent of the proton differential intensity near Earth at T = 50 MeV comes from galactic protons with kinetic energies T < 400 MeV. The mean energy of the distribution for 50 MeV protons in 1969 was $\langle T_o \rangle$ = 777 MeV, whereas based upon the mean energy loss of monoenergetic galactic protons with T = 50 MeV near Earth should have come from T ~ 150 MeV in the galactic spectrum (Gleeson and Urch, 1971; Urch and Gleeson, 1972b, 1973).

In contrast the electron distributions of Figure 8.12c show that there is no virtual exclusion of the electrons. This contrasting behaviour of the electrons and nuclei is due to their different galactic spectra at low energies. Both low energy galactic electrons and protons have only a small probability of penetrating to the orbit of the Earth (see Figure 8.11, in which the curve $Vr/K(r,p) = 1.0$ corresponds to 30 MeV protons or 200 MeV electrons at r = 1 A U if $K_c = 3 \times 10^{17}$ m^2 s^{-1}), and for nuclei, for which the spectrum is flat at low energies, this leads to virtual exclusion, but for electrons the galactic intensity increases rapidly as the energy decreases and this enables enough galactic electrons of all energies to reach Earth so that there is no virtual exclusion of this cosmic-ray species (cf. Urch and Gleeson, 1973).

The distributions shown in Figures 8.12 are quite close to those obtained numerically by Urch and Gleeson (1973). We note however that with the $r^{1.5}$ dependence of K(r,p) the radial gradients given approximately

by $$G_r = C V / K(r,p),$$

where C is the Compton Getting factor (the force-field approximation) are higher than those of Urch and Gleeson which are in turn higher than those reported observationally from Pioneer 10 and 11 Jupiter missions (Lentz *et al.*, 1973; Van Allen, 1973).

We have therefore repeated the distribution calculations using a diffusion coefficient which leads to gradients of about 1/5 that calculated by Urch and Gleeson, but maintaining their values of ϕ. This has been achieved by using a diffusion coefficient with $K \alpha r^{1.038}$ replacing $K \alpha r^{1.5}$, and values 1.5×10^{18} m^2 s^{-1} and 7×10^{17} m^2 s^{-1} for the diffusion coefficient constant K_c during 1965 and 1969. The results of these calculations are presented in Figures 8.13a, 8.13b and 8.13c, which show, respectively, the proton, helium nuclei and electron distributions for the same near Earth kinetic energies, T, as those listed in Figures 8.12.

The distributions in Figures 8.13 are in general narrower than those obtained by U G and those presented in Figures 8.12. The narrowing of these distributions are illustrated more clearly in Figures 8.14a, 8.14b, and 8.14c, which display, respectively, the distributions $\psi_T(r,T;T_o)$ for protons and helium nuclei with T = 200 MeV/nucleon and for electrons with T = 200 MeV at Earth for 1965. Conditions assumed here and later are

$$\begin{aligned} &\text{(a)} \quad K_c \sim 5 \text{ times that of U G ,} \\ &\text{(b)} \quad K_c \sim 0.3 \text{ times that of U G,} \end{aligned} \qquad (8.5.13)$$

with ϕ(1 A U) = 0.35 G V for 1965 and ϕ(1 A U) = 0.75 G V for 1969, which correspond to the interplanetary parameters used in Figures 8.13

and 8.12 respectively. For comparison the histogram ψ_T obtained by U G with conditions

$$\text{(c)}\quad K_c = 3 \times 10^{17}\ m^2\ s^{-1}, \quad \phi(1\ A\ U) = 0.35\ G\ V, \qquad (8.5.14)$$

have also been reproduced in Figures 8.14.

The mean energy $\langle T_o \rangle$ of each of the distributions in Figures 8.14 are indicated by arrows. In the case of electrons (Figure 8.14c) there is a substantial difference in $\langle T_o \rangle$ for conditions (a) and (b), but $\langle T_o \rangle$ for (b) and(c) are closely equal. This difference is shown more generally in Figure 8.15.

In Figure 8.15 we have reproduced from U G, the mean energy loss $\langle T_o \rangle - T$, for electrons, obtained by them for 1965 and 1969 conditions (full curves) and the force-field energy loss Φ (dotted curves). On this we have superimposed the values of $\langle T_o \rangle - T$ for 1965 and 1969 obtained here with conditions (a) and (b). Results for conditions (a) are indicated by crosses, those for conditions (b) by circles.

The substantial differences in $\langle T_o \rangle - T$ obtained with conditions (a) and (b), noted above, are apparent in both 1965 and 1969. These results show that in the case of electrons the distribution ψ_T and the mean energy loss is a function of the magnitude of the diffusion coefficient, despite the fact that $\phi(1\ A\ U)$, and hence the modulation is maintained.

A further result, apparent in Figure 8.15, is that with conditions (a) the mean energy losses obtained (the crosses) are almost equal to the force-field energy changes Φ (the dotted curve). Under these conditions the force-field energy loss would be a good approximation to $\langle T_o \rangle - T$. This is in contrast to the results (cf. Figure 8.15)

for conditions (c), given and stressed by U G, that Φ is not a good approximation to $\langle T_o \rangle - T$ in the case of electrons. Since the Pioneer 10 and Pioneer 11 gradient observations indicate that conditions (a) may be more appropriate it is likely that the force field energy losses Φ can be used to obtain good approximations to the mean energy loss $\langle T_o \rangle - T$ for electrons.

A similar pattern of mean energy loss applies for proton and helium nuclei save that the differences are much less significant. In Figure 8.16 we have reproduced from U G the energy loss $\langle T_o \rangle - T$ for protons and helium obtained by them for 1965 (full curves) and the force-field energy loss Φ (dotted curves). Figure 8.17 shows the corresponding results for 1969 conditions. As in Figure 8.15 we have superimposed the values of $\langle T_o \rangle - T$ for 1965 and 1969 conditions obtained here with conditions (a) (the crosses) and conditions (b) (the circles). Conditions (a) lead to energy losses close to the values obtained by U G. These differences are not significant however because the energy losses for protons and helium obtained by U G were themselves close to Φ.

In conclusion we remark that in determining these distributions that even with the somewhat complex dependence of K on p, only two simple numerical integrations were required. The first was in the determination of the function T (Equation (8.1.3)) and the second in convolving the spectrum with $G(r,p;p_o)$.

FIGURES 8.1 - 8.17

Figure 8.1 - The momentum spectrum of the distribution function $F_o(r,p)$ for a monoenergetic galactic spectrum at infinity, i.e., $U_p \to N_g \, \delta(p-p_o)$ as $r \to \infty$. The figure is drawn for a diffusion coefficient $K(r,p) = K_c \, p \, r^{1.5}$, and values 0.001, 0.01, 0.1 and 1.0 of the parameter $Vr/K(r,p_o)$.

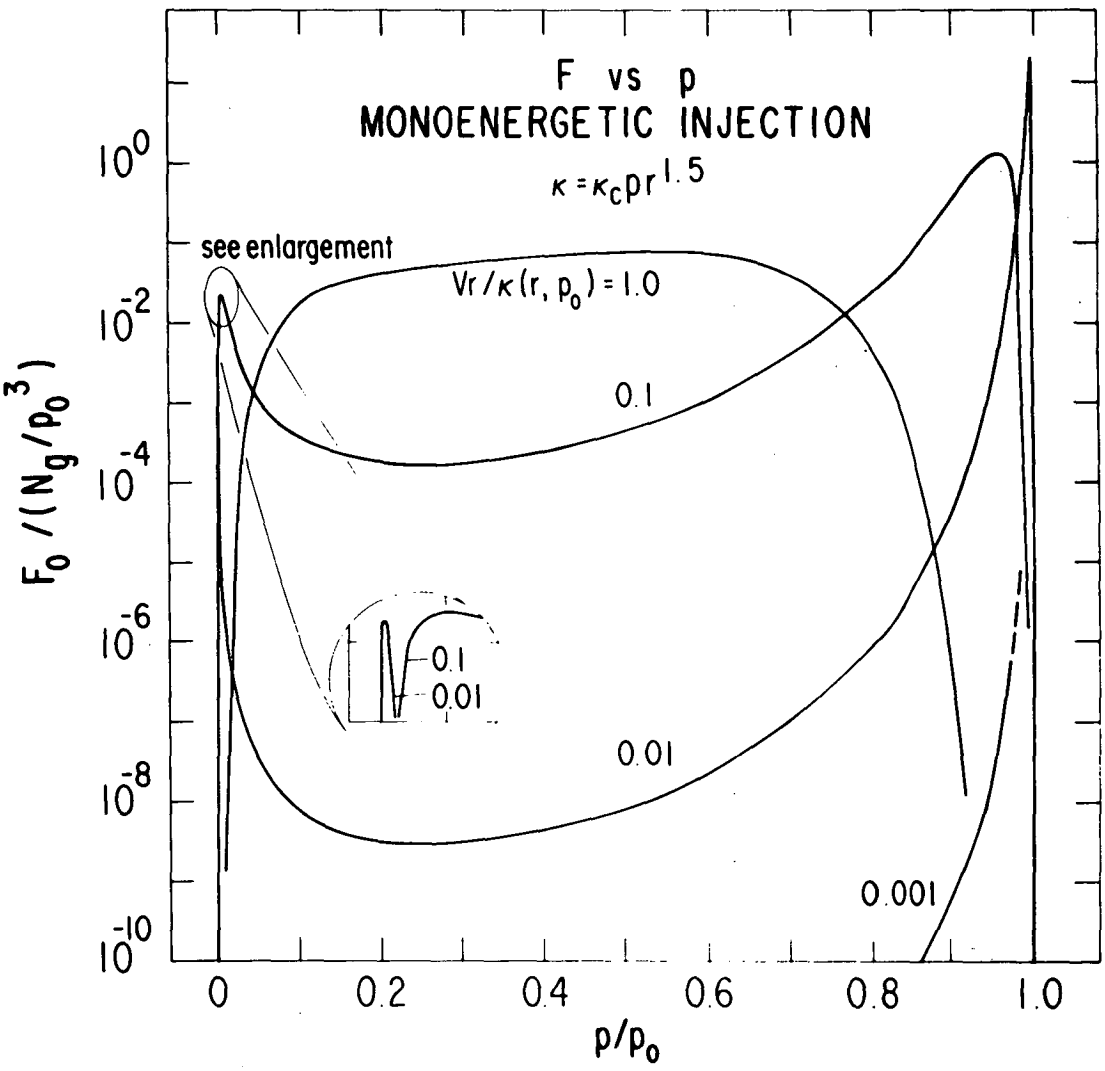
F vs p
MONOENERGETIC INJECTION
$\kappa = \kappa_c pr^{1.5}$
see enlargement
$Vr/\kappa(r, p_0) = 1.0$
0.1
0.01
0.001
$F_0/(N_g/p_0^3)$
10^0
10^{-2}
10^{-4}
10^{-6}
10^{-8}
10^{-10}
0
0.2
0.4
0.6
0.8
1.0
p/p_0

Figure 8.1

Figure 8.2 - The kinetic energy spectrum of the differential intensity $j_T(r,T)$ for a mono-energetic galactic spectrum at infinity, i.e., $U_p \to N_g \delta(p-p_o)$ as $r \to \infty$. The figure is drawn for a diffusion coefficient $K(r,p) = K_c\, p\, r^{1.5}$ and the parameter $Vr/K(r,p_o) = 0.01$, 0.1 and 1.0. The kinetic energy of injection T_o is equal to the rest energy E_o.

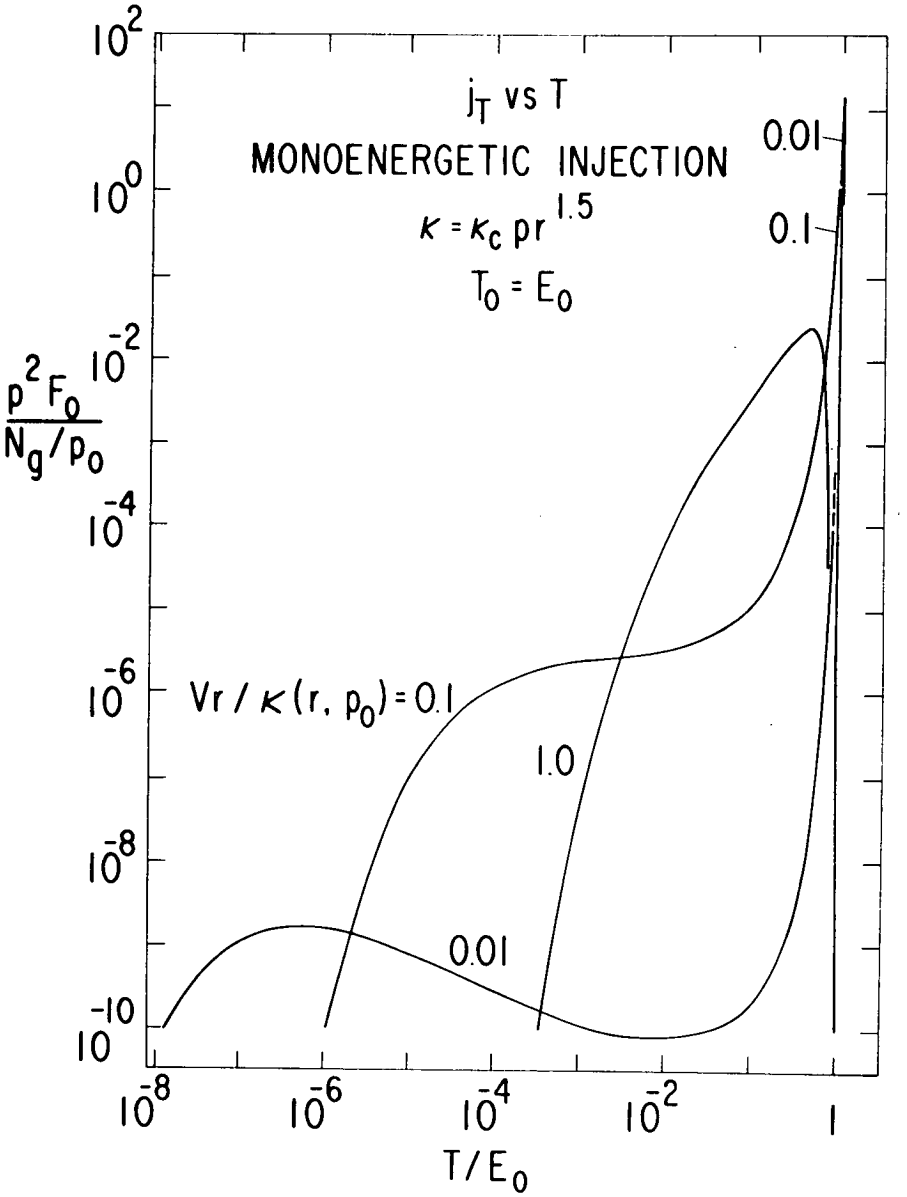
j_T vs T
MONOENERGETIC INJECTION
$\kappa = \kappa_c\, pr^{1.5}$
$T_0 = E_0$
0.01
0.1
1.0
0.01
$Vr / \kappa(r, p_0) = 0.1$
$\frac{p^2 F_0}{N_g / p_0}$
10^2
10^0
10^{-2}
10^{-4}
10^{-6}
10^{-8}
10^{-10}
10^{-8}
10^{-6}
10^{-4}
10^{-2}
1
T/E_0

Figure 8.2

Figure 8.3a - The momentum dependence of various physical quantities, arising from a monoenergetic galactic spectrum of particles at infinity, i.e., $U_p \to N_g\ \delta(p-p_o)$ as $r \to \infty$. The figure is drawn for a diffusion coefficient $K(r,p) = K_c\ p\ r^{1.5}$, and for values 0.01, 0.1 and 1.0 of the dimensionless parameter $Vr/K(r,p_o)$. Shown (in dimensionless form) are :

(a) the momentum average distribution function $F_o(r,p)$,
(b) the differential number density $U_p = 4\ \pi\ p^2\ F_o$,
(c) the radial gradient $G_r = (1/U_p).(\partial U_p/\partial r)$,
(d) the radial differential current density S_p and its convective and diffusive components S_c and S_d, i.e.,

$$S_c = -\ 4\ \pi p^3 (V/3)\ \partial F_o/\partial p,$$

$$S_d = -\ 4\ \pi\ p^2\ K(r,p)\ \partial F_o/\partial r,$$

$$S_p = S_c + S_d.$$

Here

$$\overline{F}_o = (p_o^3 / N_g)\ F_o,$$

$$\overline{U}_p = (p_o/N_g)\ U_p,$$

$$\mathrm{Grad}(\log(U_p)) = r_e\ G_r,$$

$$\overline{S}_c = (p_o / V\ N_g)\ S_c,$$

$$\overline{S}_d = (p_o / V\ N_g)\ S_d;$$

$$\overline{S}_p = \overline{S}_c + \overline{S}_d = (p_o / V\ N_g)\ \underline{S}_p,$$

are dimensionless forms of F_o, U_p, G_r, S_c, S_d and S_p, and

$$r/r_e = \left([Vr/K(r,p_o)] / [Vr_e/K(r_e,p_o)] \right)^{1/(1-b)},$$

$$Vr_e/K(r_e,p_o) = 0.1, \quad b = 1.5.$$

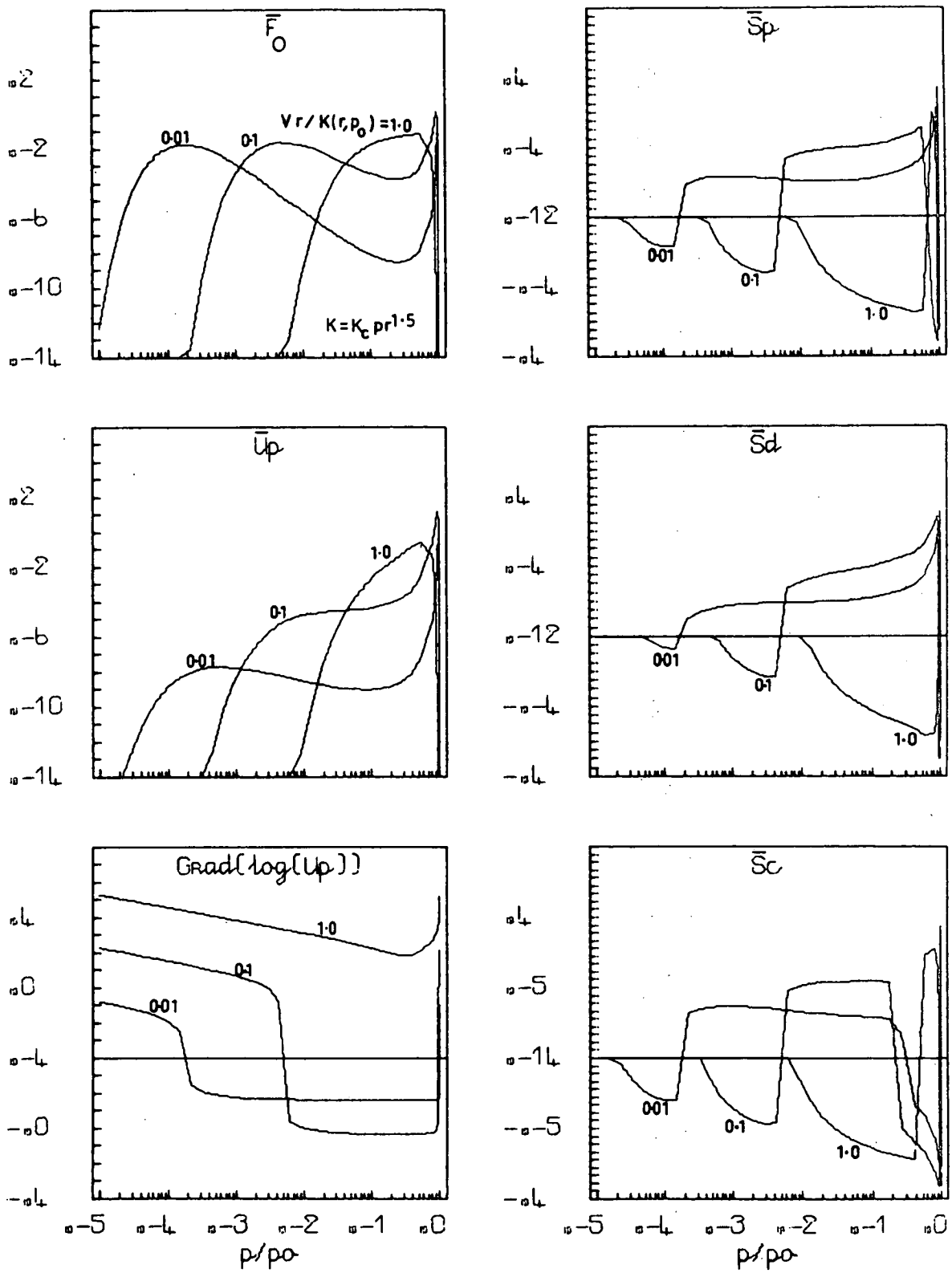
$\bar{F}_O$
Vr / K(r,p_o) =1·0
0·01
0·1
K=K_c pr^1·5
$\bar{S}p$
0·01
0·1
1·0
$\bar{U}p$
1·0
0·1
0·01
$\bar{S}d$
001
0·1
1·0
Grad[log[Up]]
1·0
0·1
0·01
$\bar{S}c$
001
0·1
1·0
p/po
p/po

Figure 8.3a

Figure 8.3b - The momentum dependence of various physical quantities arising from a monoenergetic spectrum of particles at infinity, i.e., $U_p \rightarrow N_g \ \delta(p-p_o)$ as $r \rightarrow \infty$. The figure is drawn for a diffusion coefficient $K(r,p) = K_c \ p \ r^{1.5}$, and for values 0.01, 0.1 and 1.0 of the dimensionless parameter $Vr/K(r,p_o)$. Shown are:

(e) the ratio of the bulk streaming velocity $\langle \dot{r} \rangle$ to the solar wind speed V, i.e., $dR/dt = S_p/(V \ U_p)$, and the related component quantities $S_d/(V \ U_p)$ and the Compton-Getting factor $C = S_c/(V \ U_p)$,

(f) the time average rate of change of momentum $\langle \dot{p} \rangle$, expressed in dimensionless form, i.e.,

$$dp/dt = (r_e/(V \ p_o)) \ \langle \dot{p} \rangle$$

(g) the ratio of $\langle \dot{p} \rangle$ and the adiabatic deceleration rate

$$\langle \dot{p} \rangle_{ad} = - 2 \ V \ p \ / \ 3 \ r,$$

i.e.,

$$(dp/dt) \ / \ (dp/dt) \ ad = \langle \dot{p} \rangle \ / \ \langle \dot{p} \rangle_{ad}.$$

As in Figure 8.3a, r_e is some fixed radius and

$$r/r_e = \left([Vr/K(r,p_o)] \ / \ [Vr_e/K(r_e,p_o)] \right)^{1/(1-b)},$$

$$Vr_e/K(r_e,p_o) = 0.1, \quad b = 1.5.$$

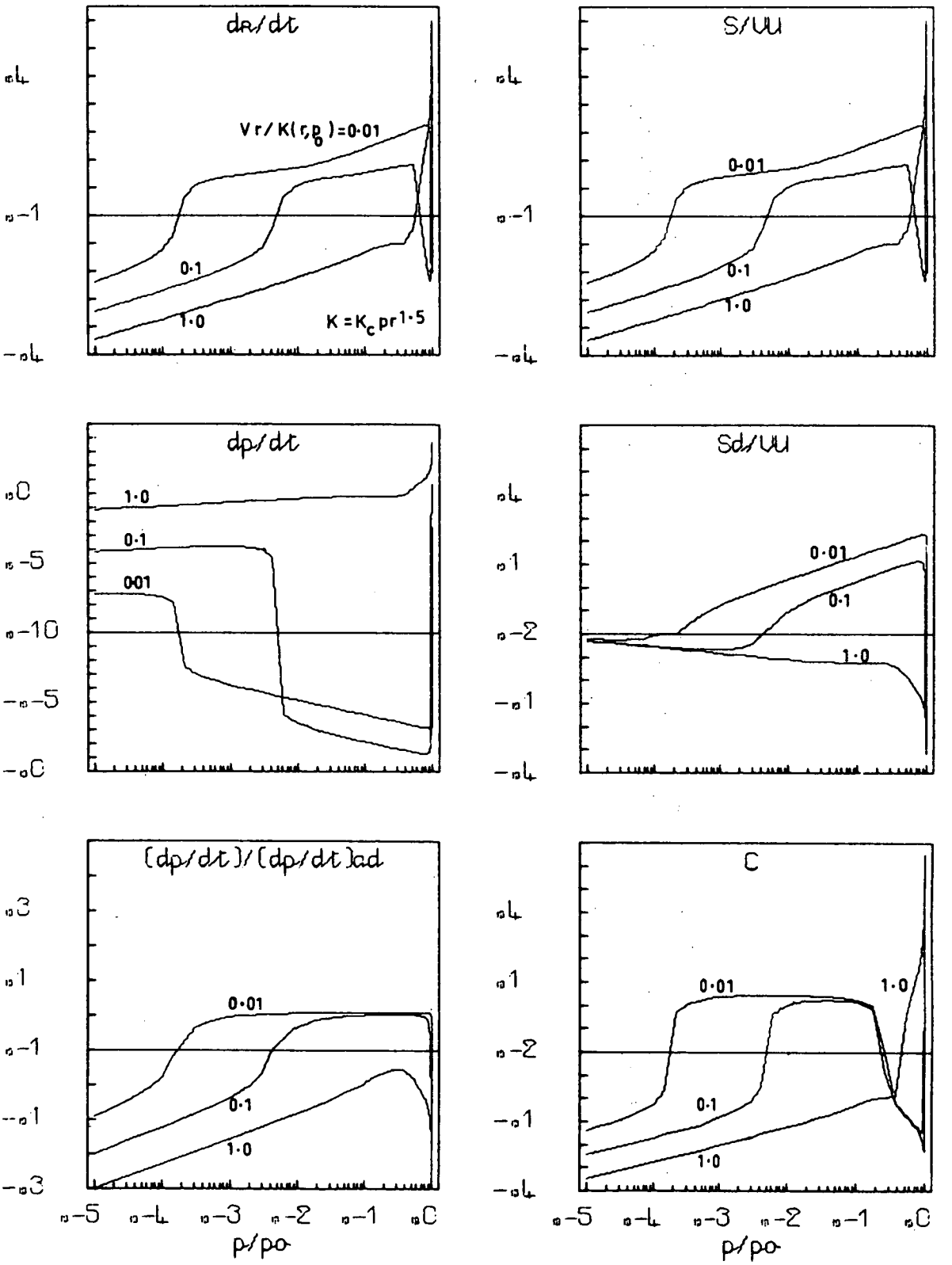
dR/dt
Vr/K(r,ρ0)=0·01
0·1
1·0
K=Kc pr1·5
S/UU
0·01
0·1
1·0
dp/dt
1·0
0·1
001
Sd/UU
0·01
0·1
1·0
(dp/dt)/(dp/dt)ad
0·01
0·1
1·0
C
0·01
1·0
0·1
1·0
p/po
p/po

Figure 8.3b

Figure 8.4a - Contours in the (r,p) plane of various physical quantities associated with a monoenergetic galactic spectrum of particles at infinity, i.e. $U_p \to N_g\, \delta(p-p_o)$ as $r \to \infty$. The figure is drawn for a diffusion coefficient $K(r,p) = K_c\, p\, r^{1.5}$, and the parameter $Vr_e/K(r_e,p_o) = 0.1$ where r_e is some fixed radius. Shown (in dimensionless form) are:

(a) the momentum average distribution function $F_o(r,p)$,

(b) the differential number density $U_p = 4\,\pi\, p^2\, F_o$,

(c) the radial gradient $G_r = (1/U_p)(\partial U_p/\partial r)$,

(d) the radial differential current density S_p and its convective and diffusive components, S_c and S_d, i.e.,

$$S_c = -4\,\pi\, p^3 (V/3)\, \partial F_o/\partial p\ ,$$

$$S_d = -4\,\pi\, p^2\, K(r,p)\, \partial F_o/\partial r\ ,$$

$$S_p = S_c + S_d .$$

Here

$$\overline{F}_o = (p_o^3 / N_g)\ F_o ,$$

$$\overline{U}_p = (p_o / N_g)\ U_p ,$$

$$\text{Grad}\,(\log(U_p)) = r_e\, G_r ,$$

$$\overline{S}_c = (p_o / (V\, N_g))\ S_c ,$$

$$\overline{S}_d = (p_o / (V\, N_g))\ S_d ,$$

$$\overline{S}_p = \overline{S}_c + \overline{S}_d = (p_o / (V\, N_g))\ S_p ,$$

are dimensionless forms of F_o, U_p, G_r, S_c, S_d and S_p.

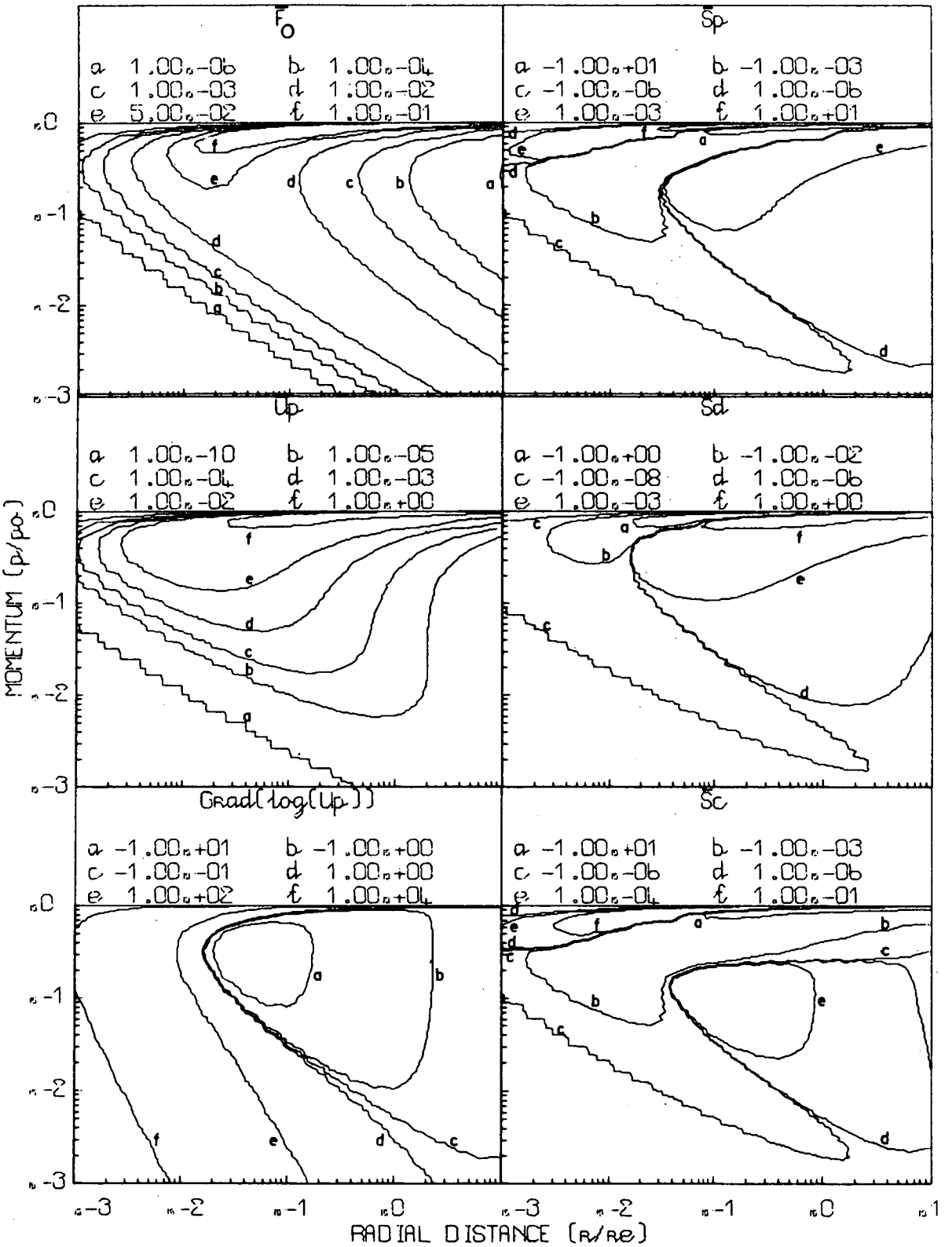
F0
a 1.00E-06 b 1.00E-04
c 1.00E-03 d 1.00E-02
e 5.00E-02 f 1.00E-01
Sp
a -1.00E+01 b -1.00E-03
c -1.00E-06 d 1.00E-06
e 1.00E-03 f 1.00E+01
Up
a 1.00E-10 b 1.00E-05
c 1.00E-04 d 1.00E-03
e 1.00E-02 f 1.00E+00
Sd
a -1.00E+00 b -1.00E-02
c -1.00E-08 d 1.00E-06
e 1.00E-03 f 1.00E+00
Grad(log(Up))
a -1.00E+01 b -1.00E+00
c -1.00E-01 d 1.00E+00
e 1.00E+02 f 1.00E+04
Sc
a -1.00E+01 b -1.00E-03
c -1.00E-06 d 1.00E-06
e 1.00E-04 f 1.00E-01
MOMENTUM (p/po)
RADIAL DISTANCE (R/Re)

Figure 8.4a

Figure 8.4b - Contours in the (r,p) plane of various physical quantities associated with a monoenergetic galactic spectrum of particles at infinity, i.e., $U_p \to N_g\ \delta(p-p_o)$ as $r \to \infty$. The figures is drawn for a diffusion coefficient $K(r,p) = K_c\ p\ r^{1.5}$, and the parameter $Vr_e/K(r_e,p_o) = 0.1$ where r_e is some fixed radius. Shown are:

(e) the ratio of the bulk streaming velocity $\langle \dot{r} \rangle$ to the solar wind speed V, i.e, $dR/dt = S_p/(V\ U_p)$, and the related component quantities $S_d/(V\ U_p)$, and the Compton-Getting factor $C = S_c/(V\ U_p)$,

(f) the time average rate of change of momentum $\langle \dot{p} \rangle$ expressed in dimensionless form, i.e.,

$$dp/dt = \left[r_e/(V\ p_o)\right] \langle \dot{p} \rangle$$

(g) the ratio of $\langle \dot{p} \rangle$ and the adiabatic deceleration rate

$$\langle \dot{p} \rangle_{ad} = -2\ V\ p\ /\ (3r),$$

i.e.,

$$(dp/dt)/(dp/dt)\ ad = \langle \dot{p} \rangle\ /\ \langle \dot{p} \rangle_{ad}\ .$$

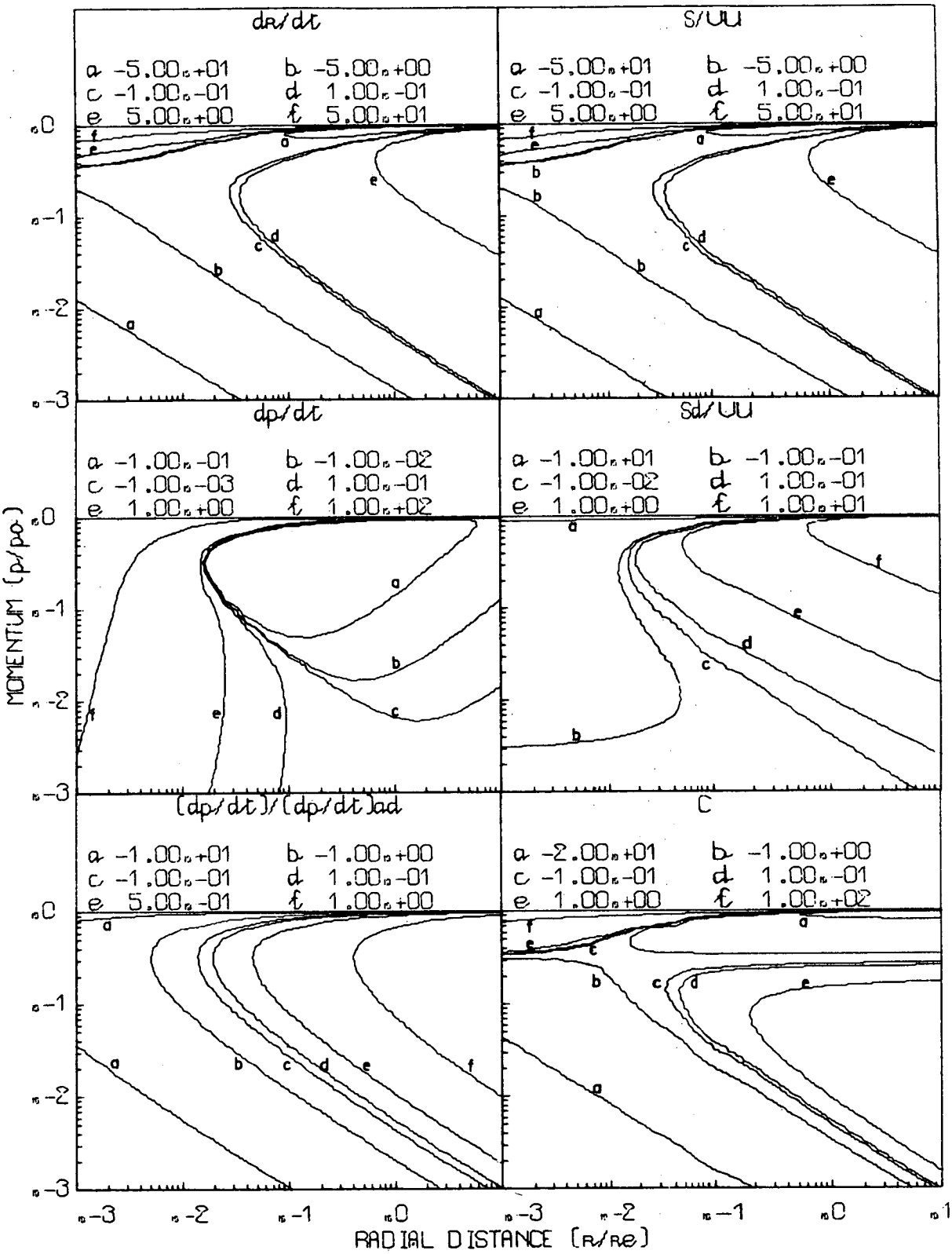
dR/dt
a -5.00E+01 b -5.00E+00
c -1.00E-01 d 1.00E-01
e 5.00E+00 f 5.00E+01
S/UU
a -5.00E+01 b -5.00E+00
c -1.00E-01 d 1.00E-01
e 5.00E+00 f 5.00E+01
dp/dt
a -1.00E-01 b -1.00E-02
c -1.00E-03 d 1.00E-01
e 1.00E+00 f 1.00E+02
Sd/UU
a -1.00E+01 b -1.00E-01
c -1.00E-02 d 1.00E-01
e 1.00E+00 f 1.00E+01
(dp/dt)/(dp/dt)ad
a -1.00E+01 b -1.00E+00
c -1.00E-01 d 1.00E-01
e 5.00E-01 f 1.00E+00
C
a -2.00E+01 b -1.00E+00
c -1.00E-01 d 1.00E-01
e 1.00E+00 f 1.00E+02
MOMENTUM (p/po)
RADIAL DISTANCE (R/Re)
E0
E-1
E-2
E-3
E1

Figure 8.4b

Figure 8.5 - Schematic of the differential current density S_p in the (r, p) plane for a monoenergetic galactic spectrum at infinity, i.e., $U_p \to N_g \, \delta(p-p_o)$ as $r \to \infty$. The figure is drawn for $K(r,p) = K_c \, p \, r^{1.5}$ and $Vr_e/K(r_e,p_o) = 0.1$. The arrows represent the direction of S_p.

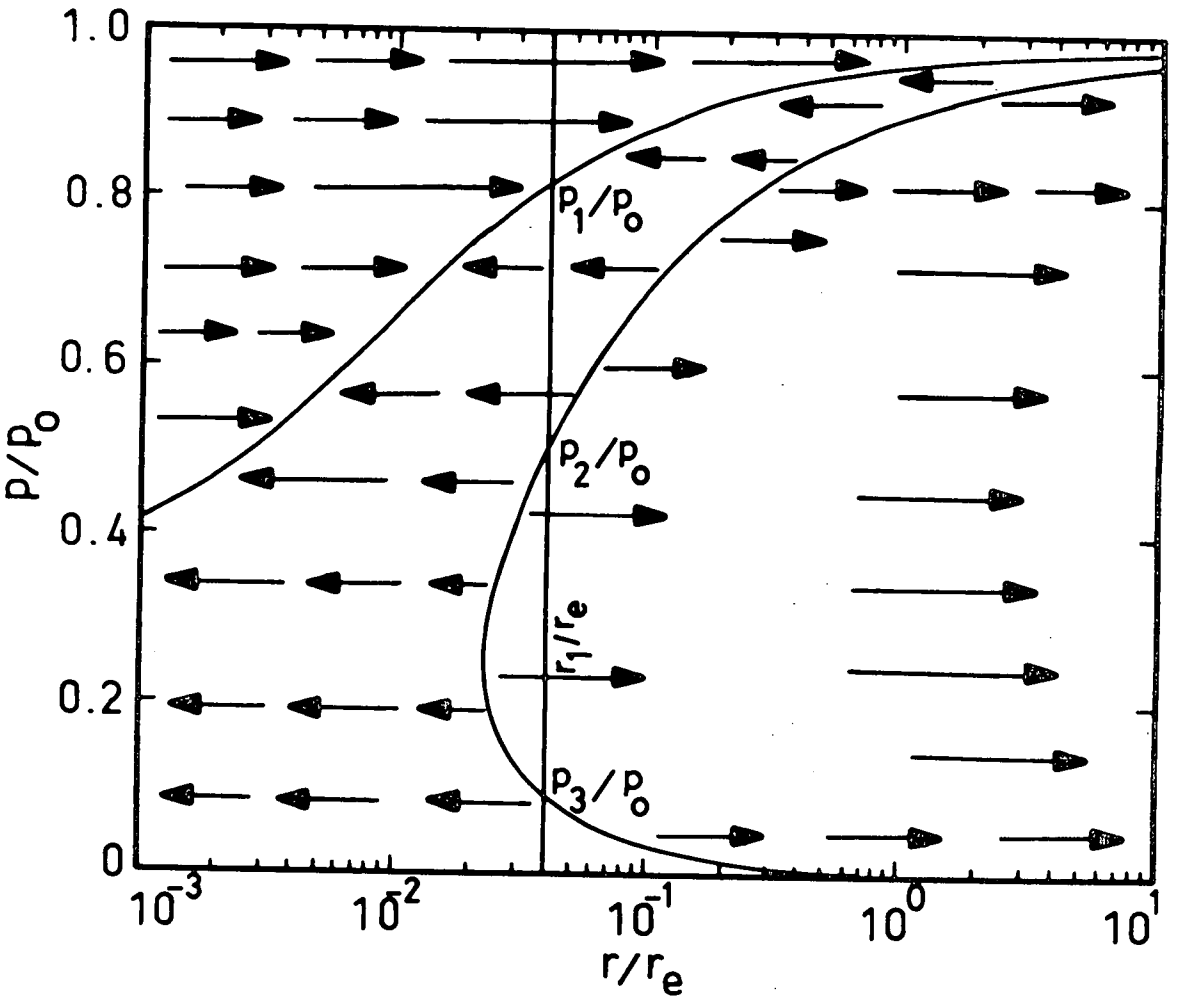

Figure 8.5

Figure 8.6a – The flow lines (8.3.15) in (u,T) co-ordinates for a monoenergetic galactic spectrum of particles at infinity. The figure is drawn for a diffusion coefficient $K(r,p) = K_o(p)\ r^{1.5}$, where $K_o(p)$ is an arbitrary function of momentum p and for $A = \pm 0.1, \pm 1, \pm 10$. Also shown are the critical curve and the locus $\langle \dot{p} \rangle = 0$.

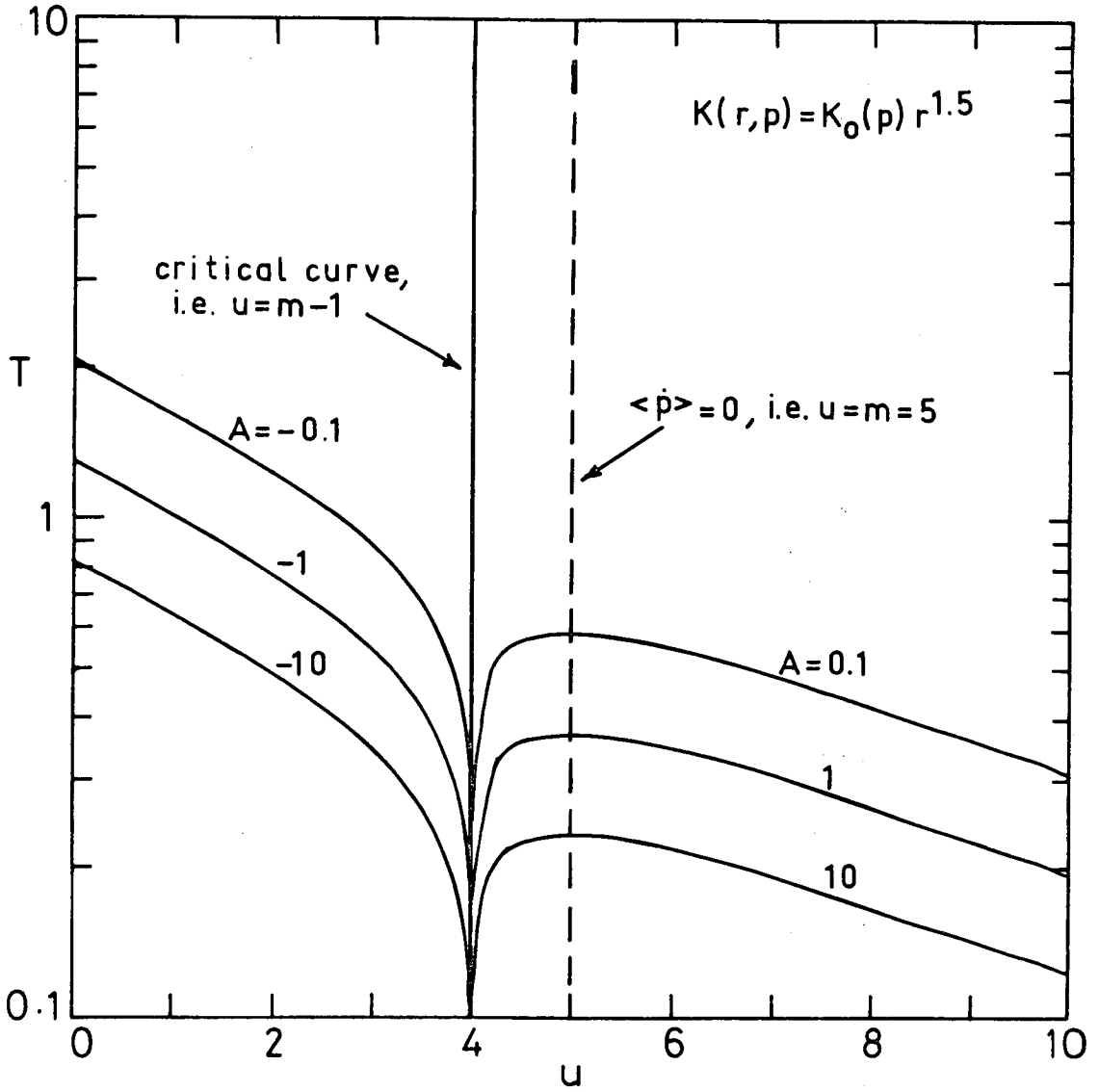
10
1
0.1
T
0
2
4
6
8
10
u
K(r,p) = K0(p) r^1.5
critical curve,
i.e. u=m-1
<ṗ> = 0, i.e. u=m=5
A=-0.1
-1
-10
A=0.1
1
10

Figure 8.6a

Figure 8.6b - The flow lines (8.3.15) in (u,T) coordinates for a monoenergetic galactic spectrum of particles at infinity. The figure is drawn for a diffusion coefficient $K(r,p) = K_o(p)\, r^{1.5}$, where $K_o(p)$ is an arbitrary function of momentum p and for $A = \pm 0.01, \pm 1, \pm 100$. Also shown are the critical curve and the locus $\langle \dot{p} \rangle = 0$.

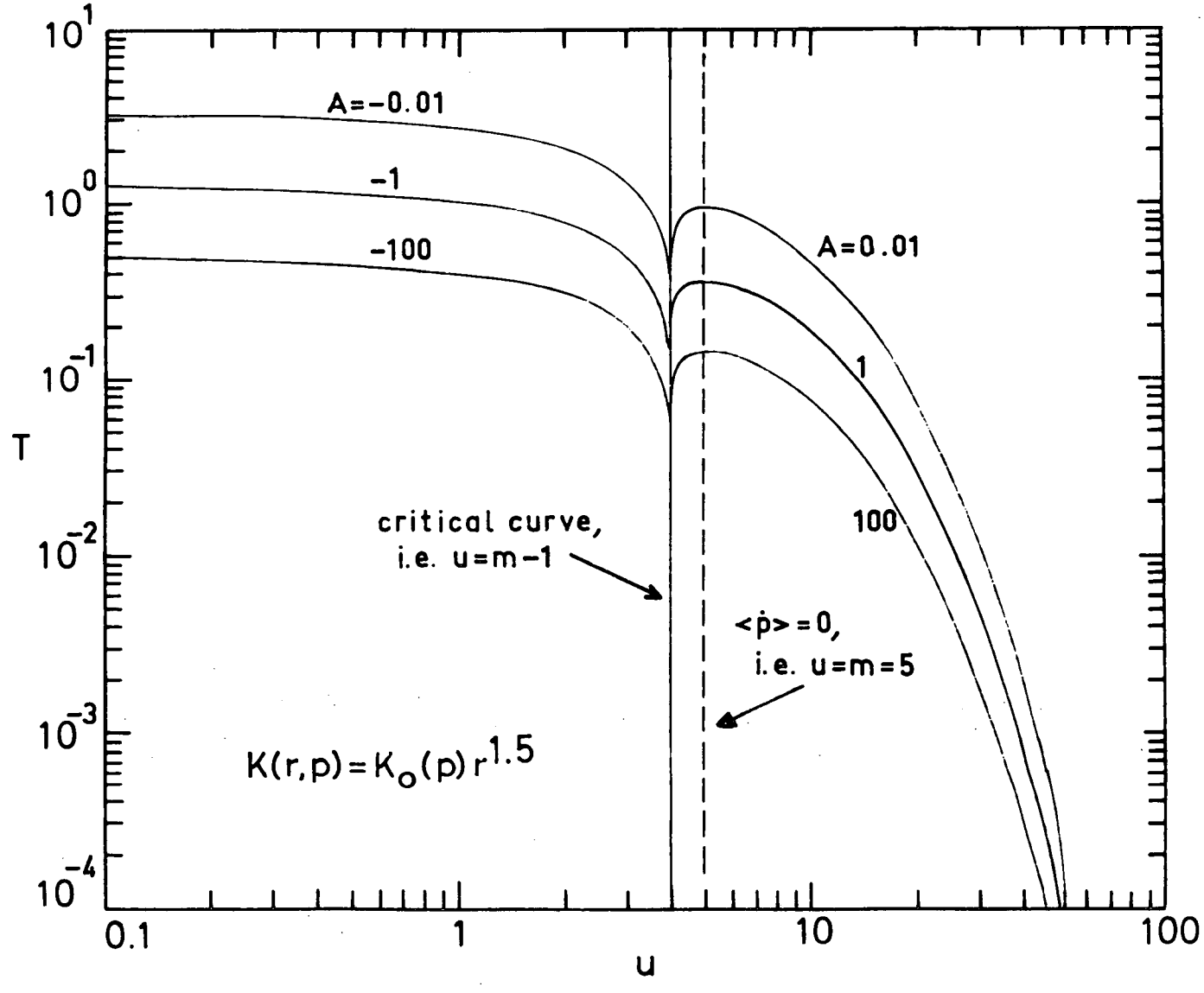
10^1
10^0
10^{-1}
10^{-2}
10^{-3}
10^{-4}
T
A=-0.01
-1
-100
A=0.01
1
100
critical curve,
i.e. u=m-1
<ṗ>=0,
i.e. u=m=5
$K(r,p)=K_o(p)\,r^{1.5}$
0.1
1
10
100
u

Figure 8.6b

Figure 8.7 - Flow lines in the (r,p) plane for a mono-energetic galactic spectrum of particles at infinity, i.e., $U_p \to N_g\, \delta(p-p_o)$ as $r \to \infty$. The figure is drawn for a diffusion coefficient $K(r,p) = K_c\, p\, r^{1.5}$, and $Vr_e/K(r_e,p_o) = 0.1$. The flow lines are shown by the full lines whereas the loci $\langle \dot{r} \rangle = 0$, $\langle \dot{p} \rangle = 0$ and the critical curve are shown by broken lines.

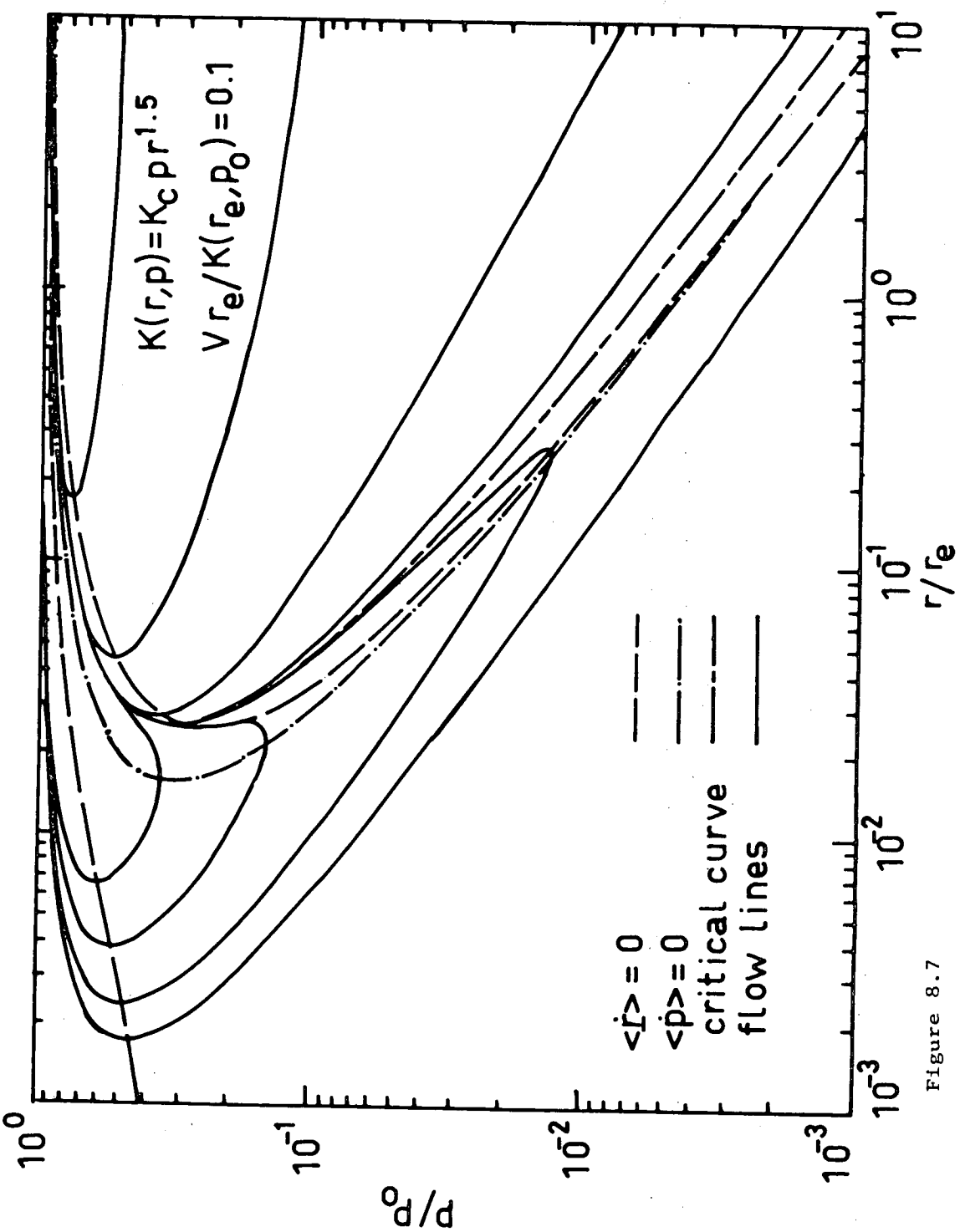
K(r,p)=K_c p r^1.5
V r_e/K(r_e,P_0)=0.1
<ṙ> = 0
<ṗ> = 0
critical curve
flow lines
P/P_0
r/r_e
10^0
10^-1
10^-2
10^-3
10^1

Figure 8.7

Figure 8.8 - Loci in the (r,p) plane which assist in assessing the flow lines for a monoenergetic spectrum of particles at $r = \infty$. The figure is drawn for a diffusion coefficient $K(r,p) = K_c\ p\ r^{1.5}$ and $Vr_e/K(r_e,p_o) = 0.1$. Shown are the curves $\langle \dot{r} \rangle = 0$, $\langle \dot{p} \rangle = 0$, and the critical curve which separates the two different types of flow lines displayed in Figure 8.7.

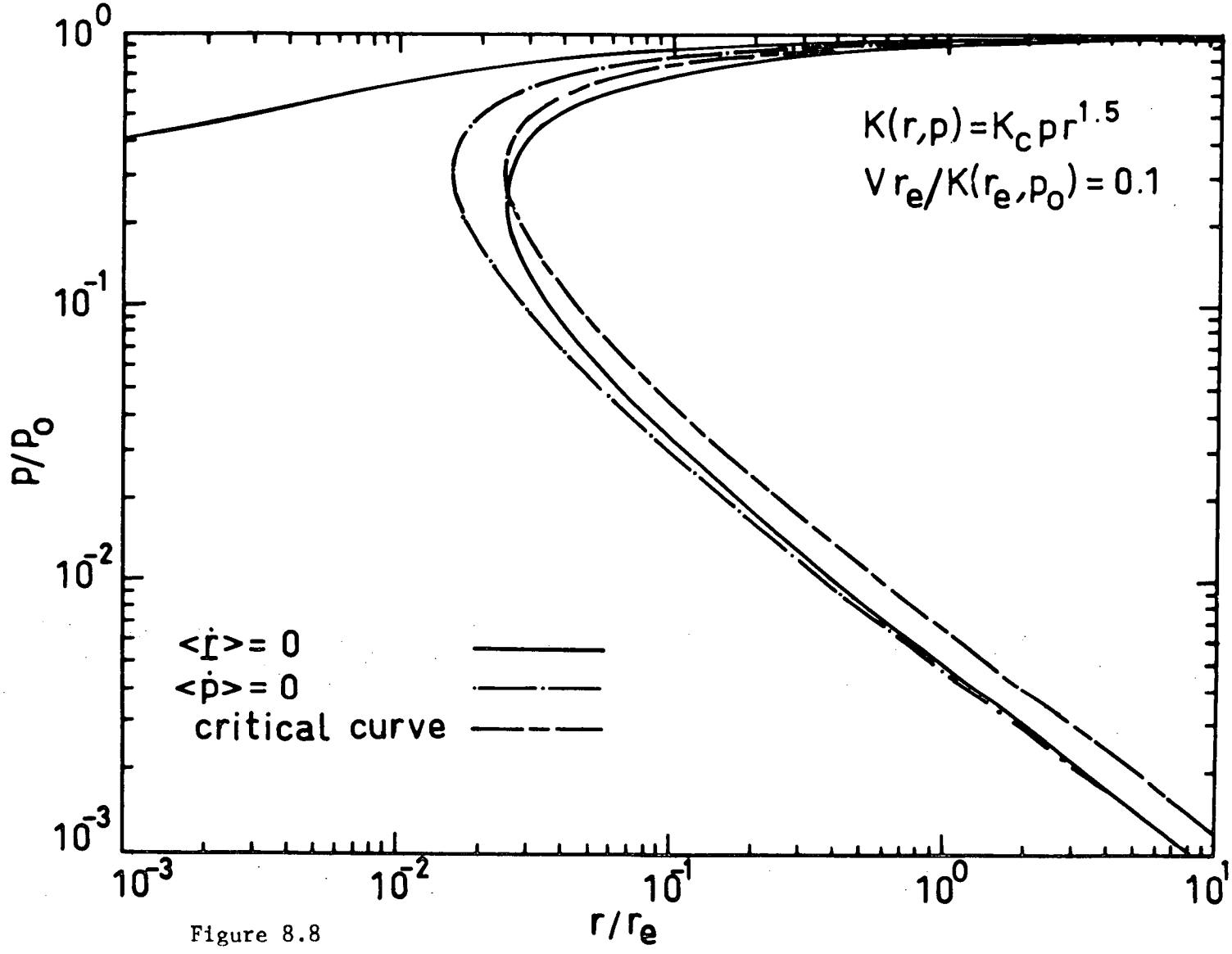
10^0
10^{-1}
10^{-2}
10^{-3}
p/p_o
10^{-3}
10^{-2}
10^{-1}
10^0
10^1
r/r_e
$K(r,p)=K_c p r^{1.5}$
$V r_e/K(r_e,p_o)=0.1$
$<\dot{r}>=0$
$<\dot{p}>=0$
critical curve

Figure 8.8

Figure 8.9a - Showing the insensitivity of the near-Earth proton spectrum to the form of the low energy galactic spectrum. These results were obtained from the general galactic spectrum solution (8.4.1), with the galactic spectra (a), (b) and (c) specified in Equations (8.4.5), the diffusion coefficient $K = 6 \times 10^{21}\ r^{1.237}\ P\ \beta\ cm^2\ s^{-1}$ (P in G V and r in A U) and the solar wind speed $V = 4 \times 10^5\ m\ s^{-1}$.

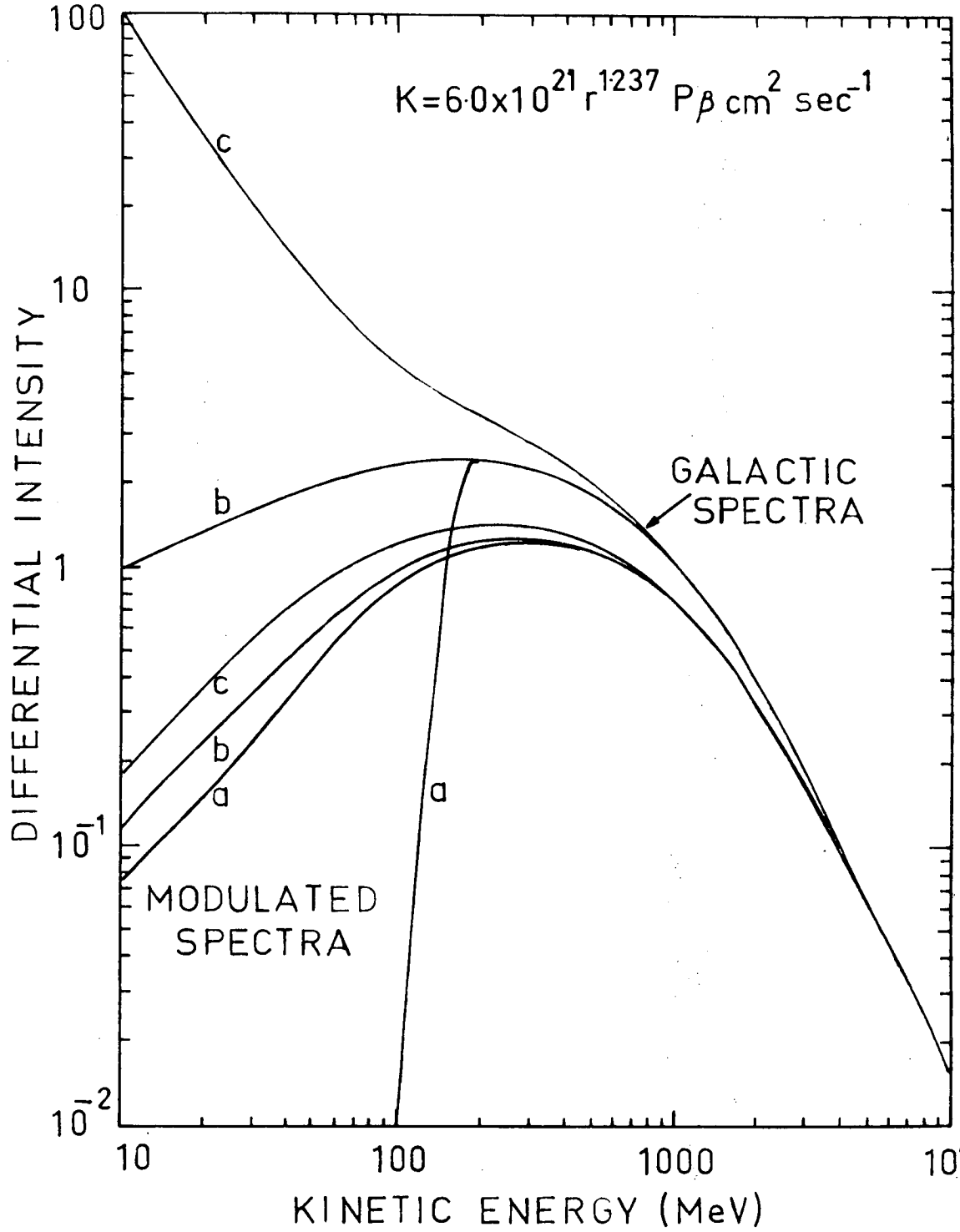
100
10
1
10^{-1}
10^{-2}
DIFFERENTIAL INTENSITY
$K=6{\cdot}0\times10^{21}\,r^{1{\cdot}237}\,P\beta\,cm^2\,sec^{-1}$
c
b
a
GALACTIC
SPECTRA
c
b
a
a
MODULATED
SPECTRA
10
100
1000
10^4
KINETIC ENERGY (MeV)

Figure 8.9a

Figure 8.9b - The radial gradients of protons at r = 1 A U for three different galactic spectra (a), (b) and (c). These results were obtained from the general galactic spectrum solution (8.4.1), with the galactic spectra (a), (b) and (c) specified in Equations (8.4.5), the diffusion coefficient $K(r,p) = 6 \times 10^{21} r^{1.237} P \beta$ cm^2 s^{-1} (P in G V and r in A U) and the solar wind speed $V = 4 \times 10^5$ m s^{-1}.

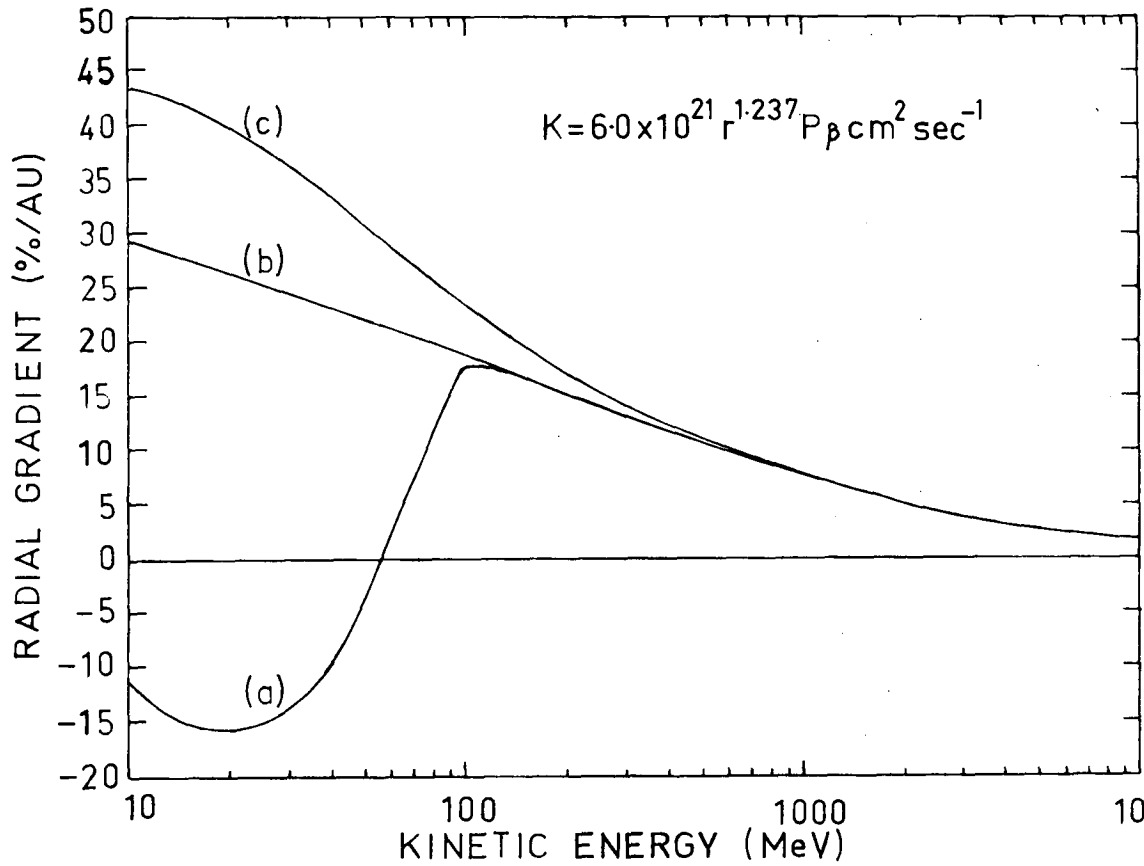
50
45
40
35
30
25
20
15
10
5
0
-5
-10
-15
-20
RADIAL GRADIENT (%/AU)
(c)
(b)
(a)
K=6·0x10^21 r^1·237 Pβ cm^2 sec^-1
10
100
1000
10^4
KINETIC ENERGY (MeV)

Figure 8.9b

Figure 8.9c - The radial anisotropies of protons at r = 1 A U for three different galactic spectra (a), (b) and (c). These results were obtained from the general galactic spectrum solution (8.4.1), with the galactic spectra (a), (b) and (c) specified in Equations (8.4.5), the diffusion coefficient $K(r,p) = 6 \times 10^{21} r^{1.237} P \beta$ cm^2 s^{-1} (P in G V and r in A U), and the solar wind speed $V = 4 \times 10^5$ m s^{-1}.

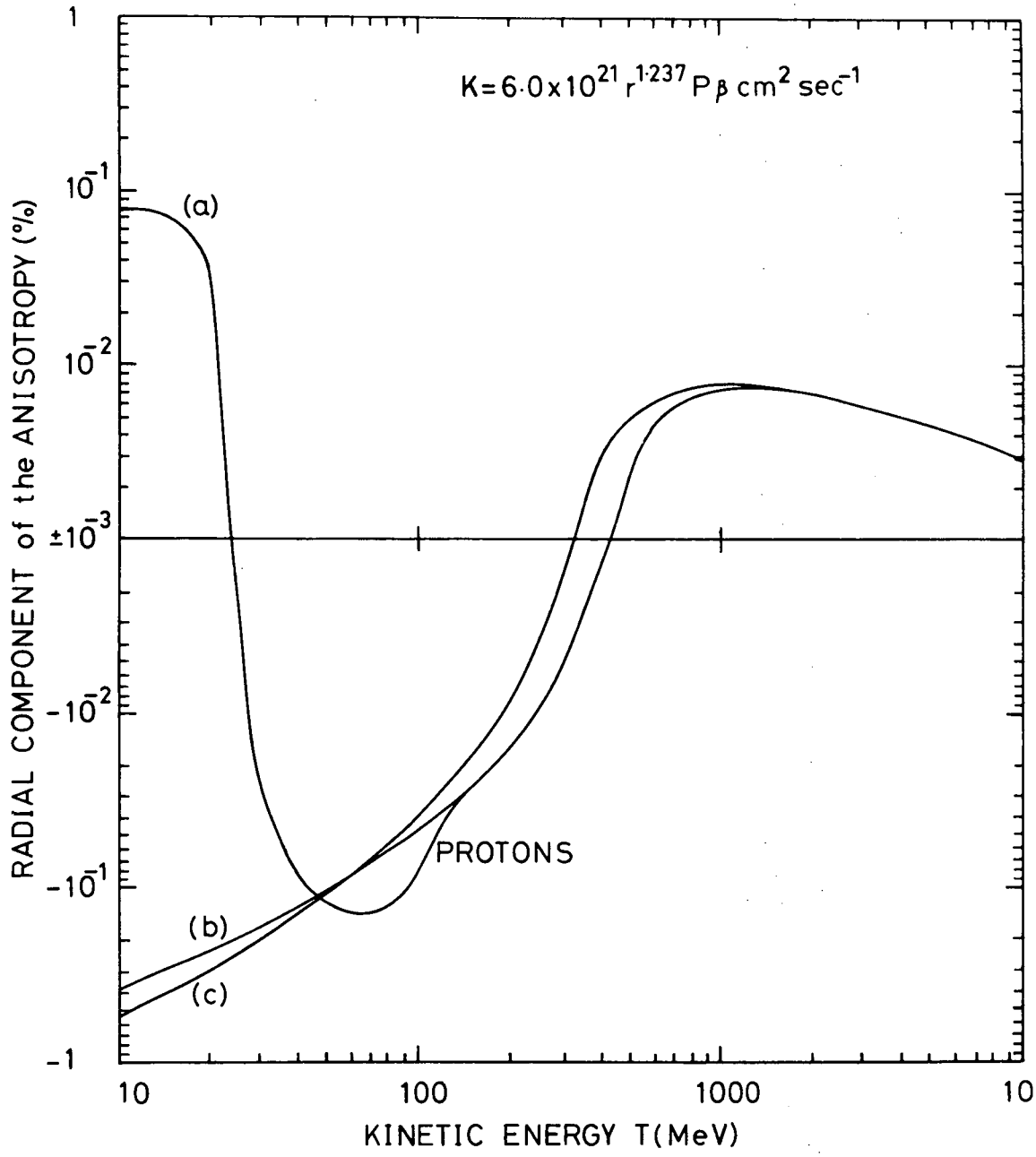
K=6·0x10^21 r^1·237 Pβ cm^2 sec^-1
RADIAL COMPONENT of the ANISOTROPY (%)
1
10^-1
10^-2
±10^-3
-10^-2
-10^-1
-1
(a)
(b)
(c)
PROTONS
10
100
1000
10^4
KINETIC ENERGY T(MeV)

Figure 8.9c

Figure 8.10a - Showing the insensitivity of the near-Earth proton spectrum to the form of the low energy galactic spectrum. These results were obtained by Urch and Gleeson (1972a) from numerical solutions of the equation of transport. Three forms of galactic spectra (a), (b) and (c) given in Equations (8.4.5) were used. In the model the diffusion coefficient $K = 6 \times 10^{21} \sqrt{r}\ P\ \beta\ cm^2\ s^{-1}$ (P in G V and r in A U), the force field parameter at r = 1 A U, ϕ(1 A U) = 0.14 G V, and the boundary of the solar cavity was taken to be at r = 10 A U.

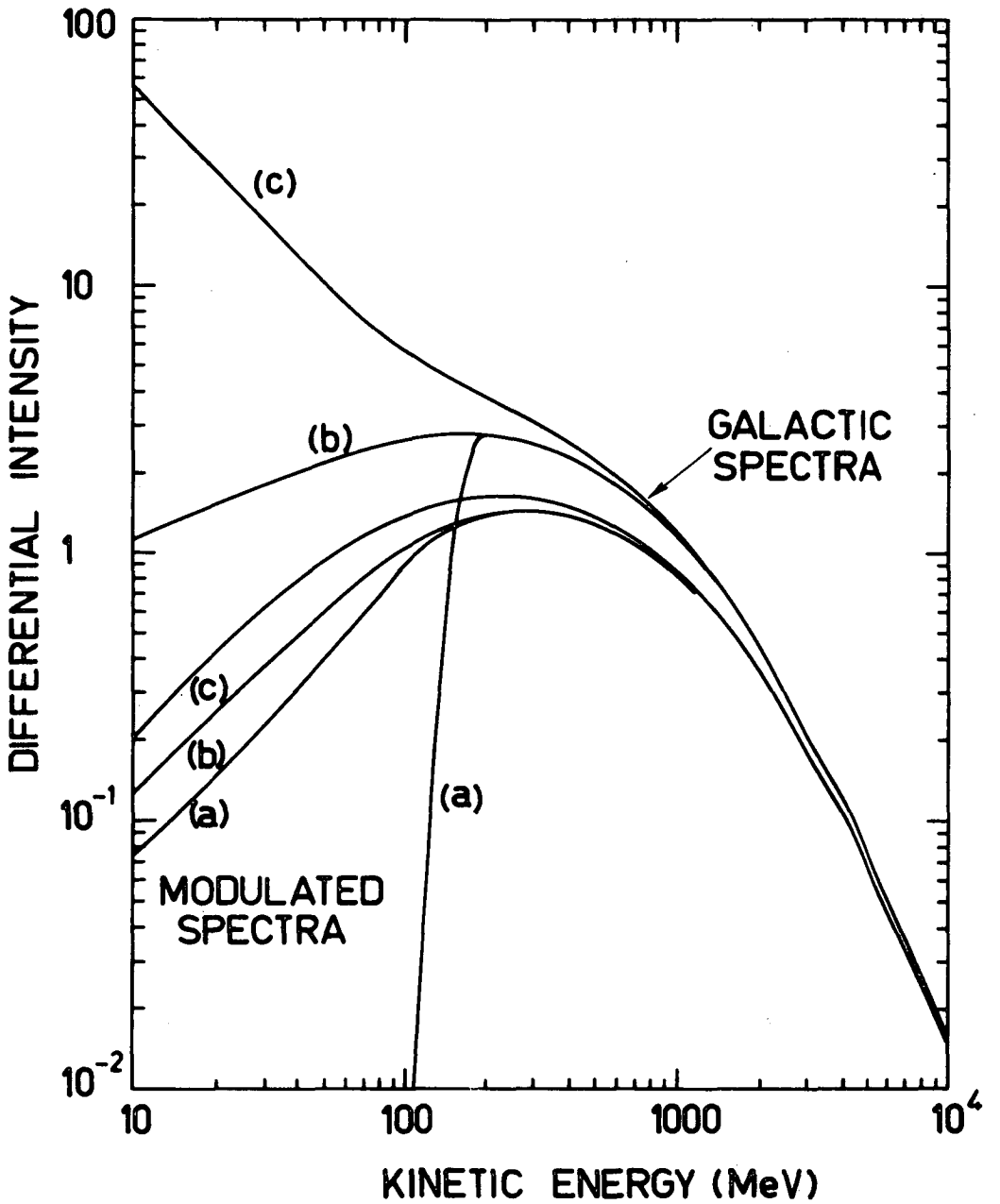
100
10
1
10^{-1}
10^{-2}
DIFFERENTIAL INTENSITY
(c)
(b)
GALACTIC
SPECTRA
(c)
(b)
(a)
(a)
MODULATED
SPECTRA
10
100
1000
10^4
KINETIC ENERGY (MeV)

Figure 8.10a

Figure 8.10b - Showing the radial gradient of protons at $r = 1$ A U for the diffusion coefficient $K = 6 \times 10^{21} \sqrt{r}\ P\ \beta\ cm^2\ s^{-1}$ (P in G V and r in A U) and the three forms (a), (b) and (c) for the galactic proton spectra given in Equations (8.4.5). These results were obtained by Urch and Gleeson (1972a) from numerical solutions of the equation of transport. The gradients for cases (a) and (b) computed from the force-field approximate solution are shown by broken lines.

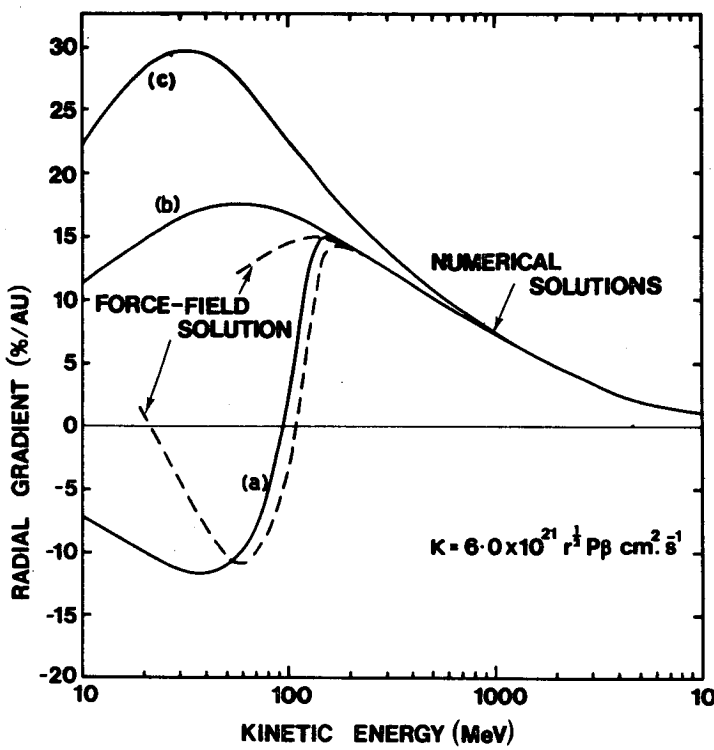
30
25
20
15
10
5
0
-5
-10
-15
-20
10
100
1000
10⁴
(c)
(b)
(a)
NUMERICAL
SOLUTIONS
FORCE-FIELD
SOLUTION
K = 6·0x10²¹ r^½ Pβ cm.² s⁻¹
RADIAL GRADIENT (%/AU)
KINETIC ENERGY (MeV)

Figure 8.10b

Figure 8.10c - showing the radial component of the anisotropy of protons at r = 1 A U for the diffusion coefficient $K = 6 \times 10^{21} \sqrt{r}\ P\ \beta\ cm^2\ s^{-1}$ (P in G V and r in A U) and the three forms (a), (b) and (c) of the galactic proton spectra given in Equations (8.4.5). These results are reproduced from Urch and Gleeson (1972a) who obtained them from numerical solutions of the equation of transport.

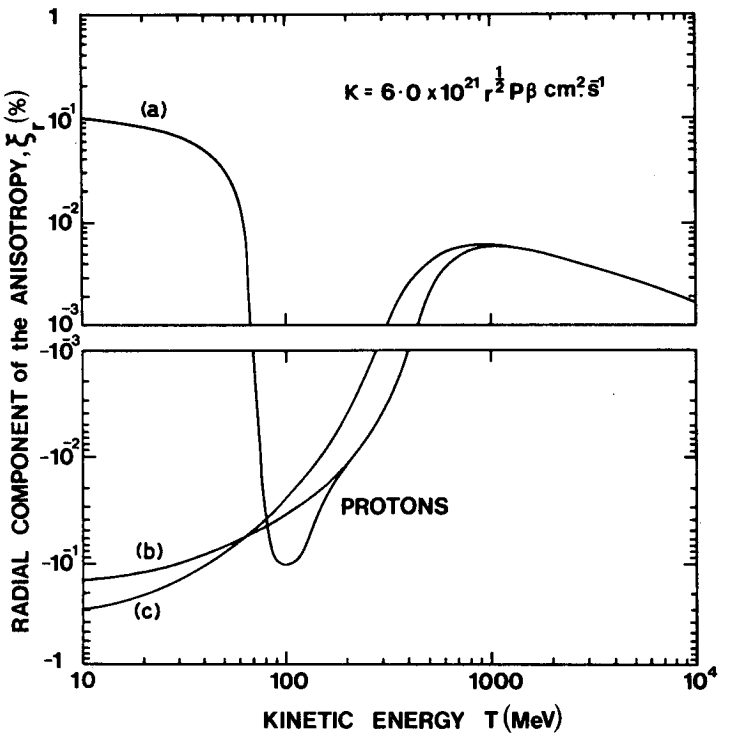
K = 6·0 x 10^21 r^½ Pβ cm²s⁻¹
(a)
(b)
(c)
PROTONS
RADIAL COMPONENT of the ANISOTROPY, ξr (%)
KINETIC ENERGY T (MeV)
1
10⁻¹
10⁻²
10⁻³
-10⁻³
-10⁻²
-10⁻¹
-1
10
100
1000
10⁴

Figure 8.10c

Figure 8.11 - Showing the dependence of the Green's function $G(r,p;p_o)$ given in Equation (8.5.1) on the momentum variable p_o/p. It provides a direct measure of the sensitivity of the intensity, at position r and momentum p, to particles of momentum p_o in the galactic spectrum. The figure is drawn for a diffusion coefficient $K = K_c\ p\ r^{1.5}$ and for values 0.01, 0.1, 1.0 and 10 of the parameter $Vr/K(r,p)$.

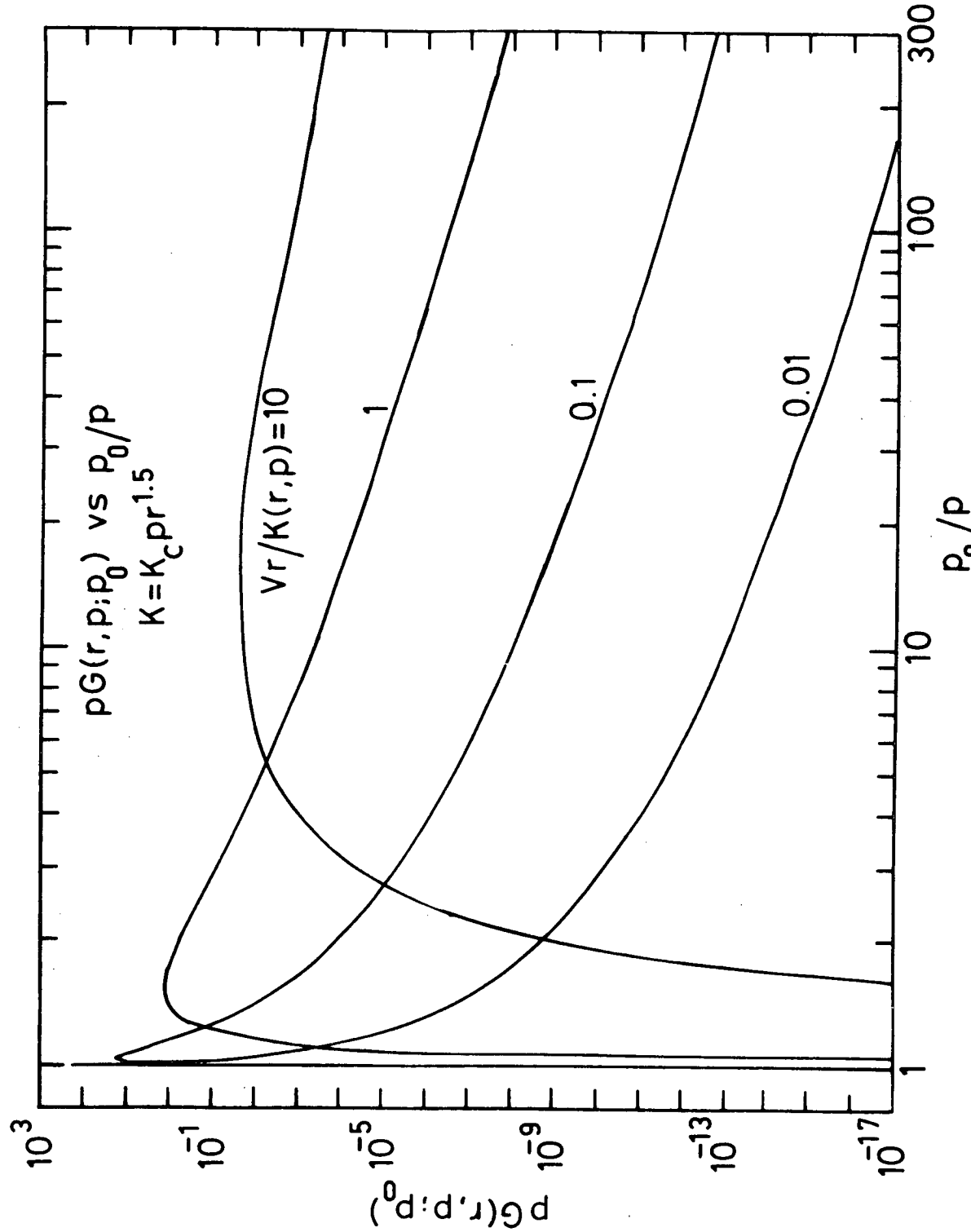
pG(r,p;p0) vs p0/p
K=Kc pr1.5
Vr/K(r,p)=10
1
0.1
0.01
pG(r,p;p0)
p0/p
10^3
10^-1
10^-5
10^-9
10^-13
10^-17
1
10
100
300

Figure 8.11

Figure 8.12a - Showing the distribution $\psi_T(r,T;T_o)$ of protons observed at r = 1 A U during 1965 and 1969 with kinetic energies T = 50, 100, 200 and 500 MeV, which originated with kinetic energy T_o in the galactic spectrum. The galactic spectrum is given in Equation (8.5.8) and the diffusion coefficients used are of the form given in Equations (8.5.11) and (8.5.12) with the parameters (K_c, P_1, P_2, b) appropriate for 1965 and 1969 being (1.139×10^{17}, 0.038, 1.0, 1.5) and (5.316×10^{16}, 0.248, 0.7, 1.5) respectively. The arrows indicate the mean energies $\langle T_o \rangle$ of the distributions and these are also listed in the figure.

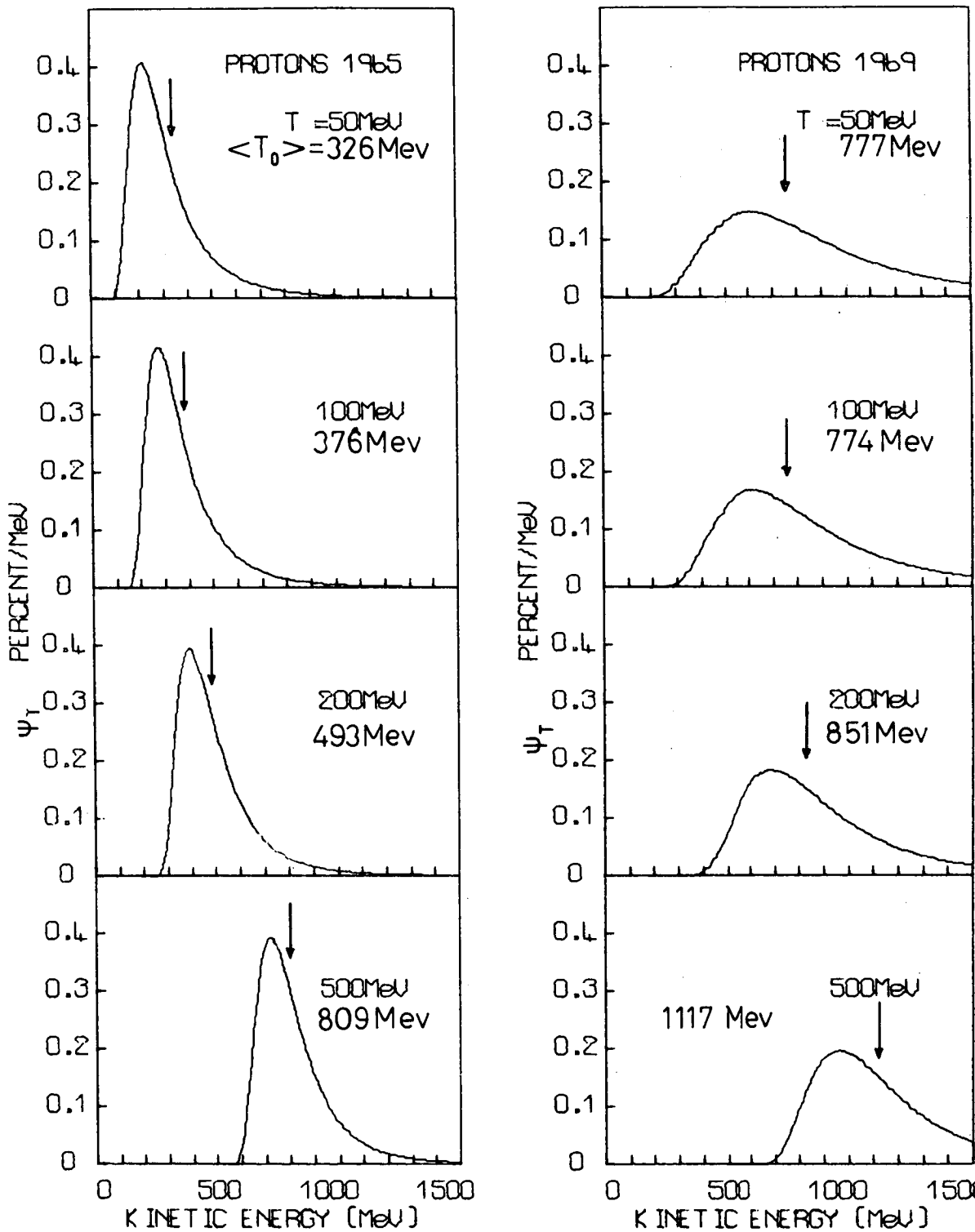
PROTONS 1965
T =50MeV
<T0>=326Mev
100MeV
376Mev
200MeV
493Mev
500MeV
809Mev
PROTONS 1969
T =50MeV
777Mev
100MeV
774 Mev
200MeV
851Mev
500MeV
1117 Mev
PERCENT/MeV
ψT
0.4
0.3
0.2
0.1
0
0
500
1000
1500
KINETIC ENERGY (MeV)

Figure 8.12a

Figure 8.12b - Showing the distribution $\psi_T(r,T;T_o)$ of helium nuclei observed at r = 1 A U with kinetic energies T = 50, 100, 200 and 500 MeV/ nucleon, which originated with kinetic energy T_o in the galactic spectrum. The galactic spectrum is given in Equation (8.5.8) and the diffusion coefficients used are of the form given in Equations (8.5.11) and (8.5.12), with parameters (K_c, P_1, P_2, b) appropriate for 1965 and 1969 being (1.139×10^{17}, 0.038, 1.0, 1.5) and (5.316×10^{16}, 0.248, 0.7, 1.5) respectively. The arrows indicate the mean energies $\langle T_o \rangle$ of the distribution and these are also listed on the figure.

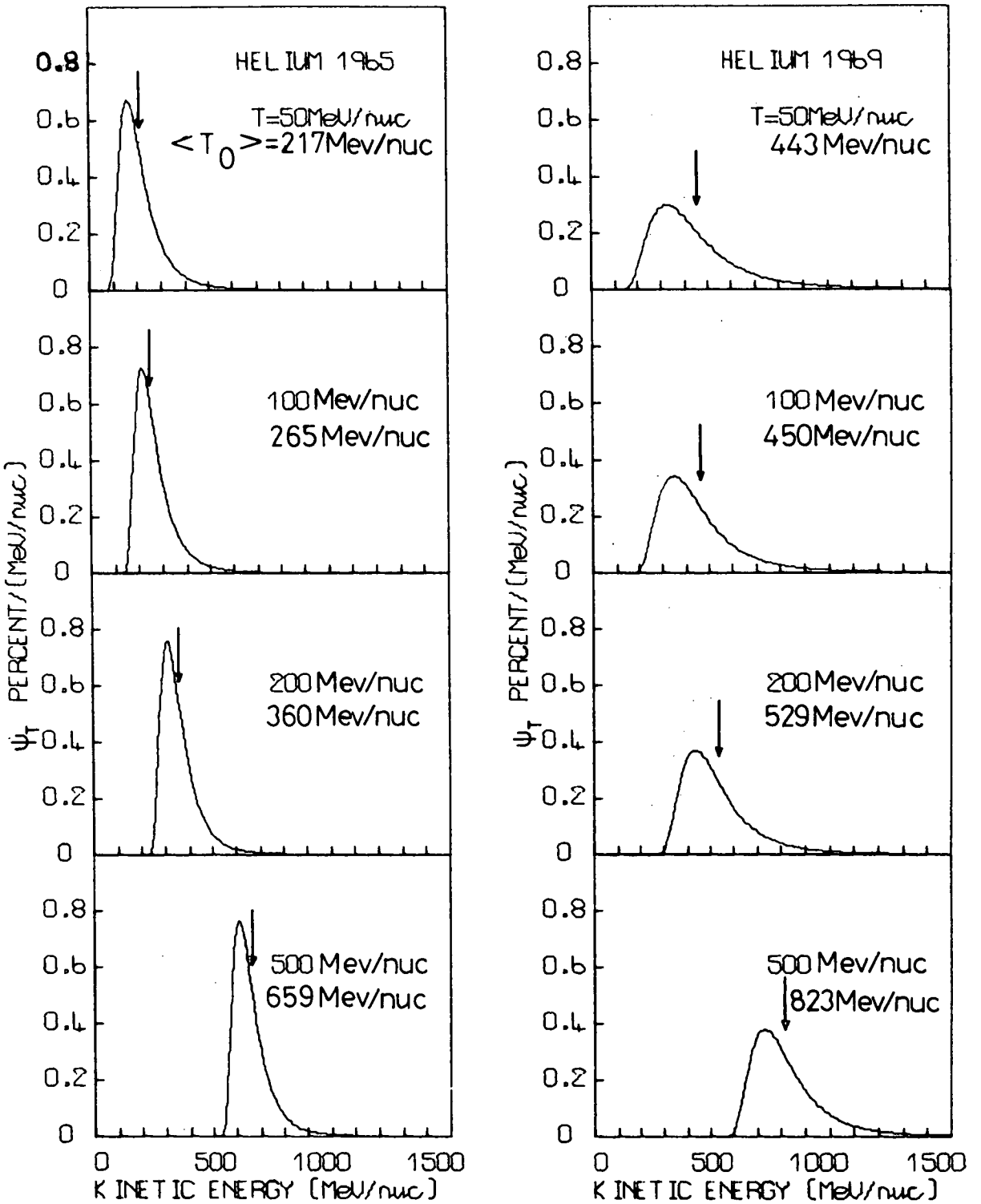
HELIUM 1965
T=50MeV/nuc
<T0>=217Mev/nuc
100 Mev/nuc
265 Mev/nuc
200 Mev/nuc
360 Mev/nuc
500 Mev/nuc
659 Mev/nuc
HELIUM 1969
T=50MeV/nuc
443 Mev/nuc
100 Mev/nuc
450 Mev/nuc
200 Mev/nuc
529 Mev/nuc
500 Mev/nuc
823 Mev/nuc
ψT PERCENT/(MeV/nuc)
KINETIC ENERGY (MeV/nuc)
0
0.2
0.4
0.6
0.8
500
1000
1500

Figure 8.12b

Figure 8.12c - Showing the distribution $\psi_T(r,T;T_o)$ of electrons observed at r = 1A U with kinetic energies T = 100, 200, 500 and 1000 MeV, which originated with kinetic energy T_o in the galactic spectrum. The galactic spectrum is given in Equations (8.5.9) and (8.5.10) and the diffusion coefficients employed are of the form given in Equations (8.5.11) and (8.5.12), with the parameters (K_c, P_1, P_2, b) appropriate for 1965 and 1969 being (1.139×10^{17}, 0.038, 1.0, 1.5) and (5.316×10^{16}, 0.248, 0.7, 1.5) respectively. The arrows indicate the mean energies $\langle T_o \rangle$ of the distributions, and these are also listed on the figure.

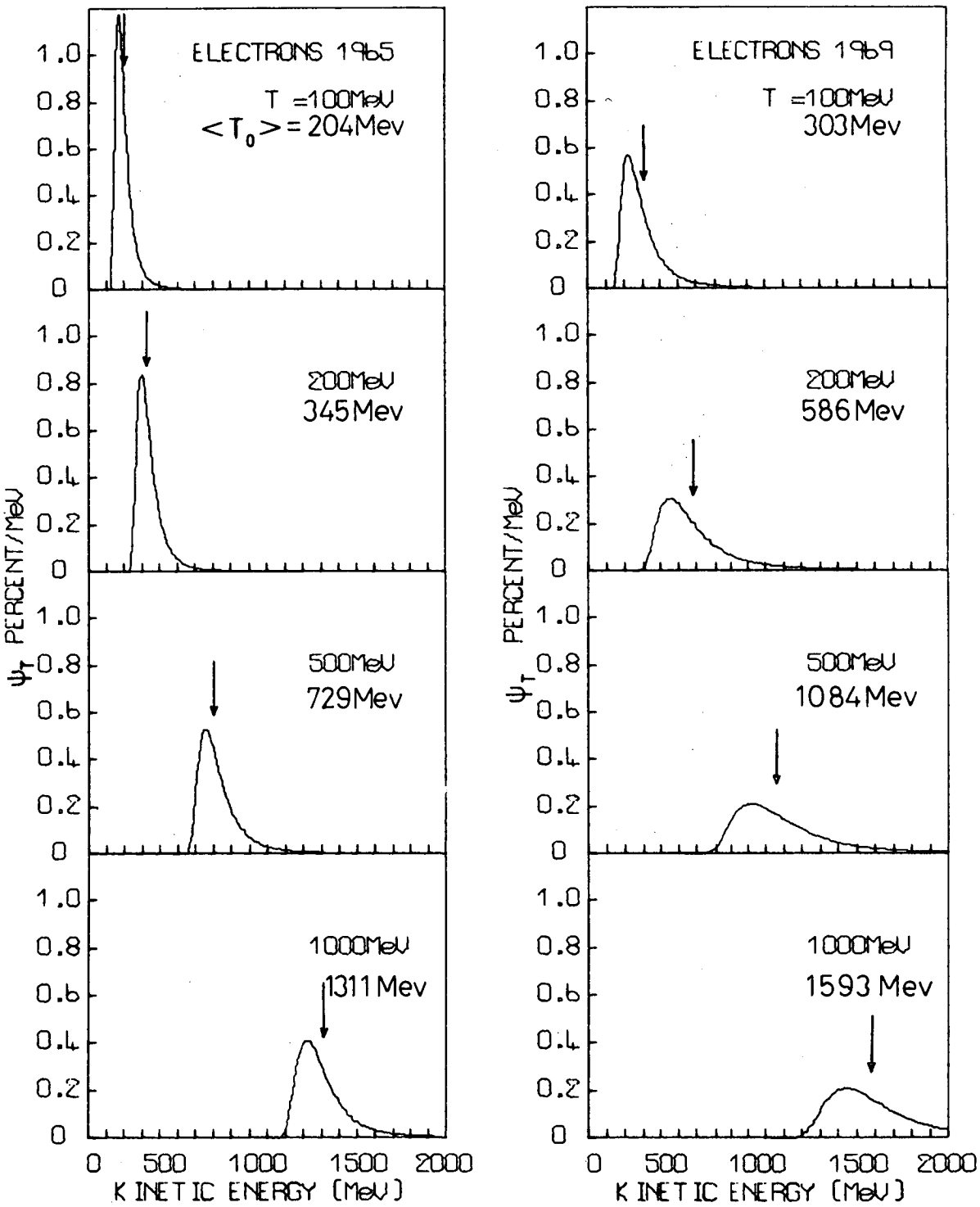
ELECTRONS 1965
T =100MeV
<T0> = 204Mev
200MeV
345Mev
500MeV
729Mev
1000MeV
1311 Mev
ELECTRONS 1969
T =100MeV
303Mev
200MeV
586Mev
500MeV
1084Mev
1000MeV
1593 Mev
ψT PERCENT/MeV
KINETIC ENERGY (MeV)
0
500
1000
1500
2000
0.2
0.4
0.6
0.8
1.0

Figure 8.12c

Figure 8.13a - Showing the distribution $\psi_T(r,T;T_o)$ of protons observed at r = 1 A U with kinetic energies T = 50, 100, 200 and 500 MeV, which originated with kinetic energy T_o in the galactic spectrum. The galactic spectrum is given in Equation (8.5.8) and the diffusion coefficients employed are of the form given in Equations (8.5.11) and (8.5.12), with the parameters (K_c, P_1, P_2, b) appropriate for 1965 and 1969 being (1.5×10^{18}, 0.038, 1.0, 1.038) and (7.0×10^{17}, 0.248, 0.7, 1.038) respectively. With these diffusion coefficients, the radial gradients are in accord with the observations from Pioneer 10 and 11 Jupiter missions. The arrows indicate the mean energies $\langle T_o \rangle$ of the distributions, and these are also listed on the figure.

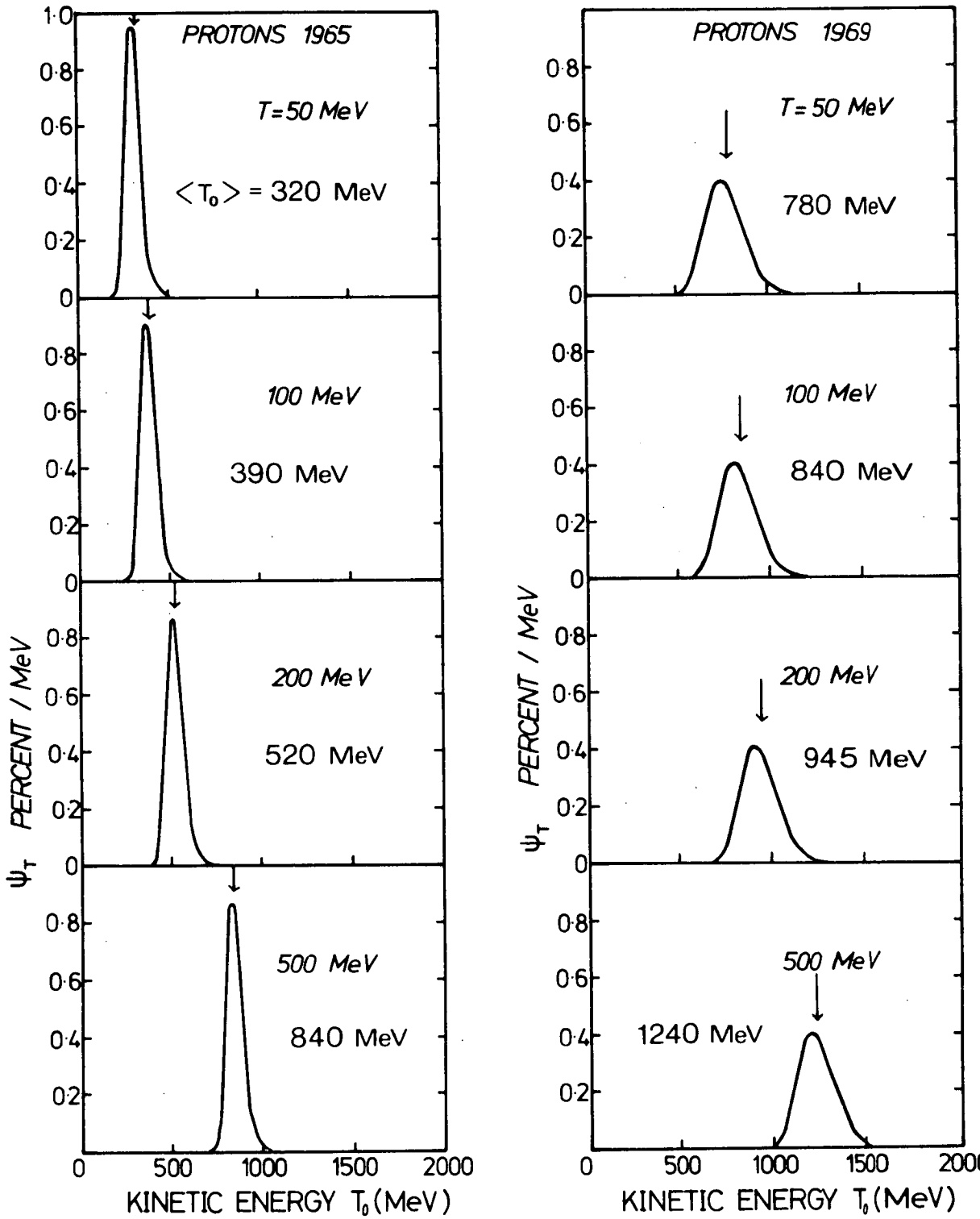
PROTONS 1965
T=50 MeV
<T₀> = 320 MeV
100 MeV
390 MeV
200 MeV
520 MeV
500 MeV
840 MeV
PROTONS 1969
T=50 MeV
780 MeV
100 MeV
840 MeV
200 MeV
945 MeV
500 MeV
1240 MeV
ψT PERCENT / MeV
KINETIC ENERGY T₀(MeV)
0
500
1000
1500
2000

Figure 8.13a

Figure 8.13b - Showing the distribution $\psi_T(r,T;T_o)$ of helium observed at r = 1 A U, with kinetic energies T = 50, 100, 200 and 500 MeV/nucleon, which originated with kinetic energy T_o in the galactic spectrum. The galactic spectrum is given in Equation (8.5.8), and the diffusion coefficients employed are of the form given in Equations (8.5.11) and (8.5.12), with the parameters (K_c, P_1, P_2, b) appropriate for 1965 and 1969 being (1.5×10^{18}, 0.038, 1.0, 1.038) and (7.0×10^{17}, 0.248, 0.7, 1.038) respectively. With these diffusion coefficients, the radial gradients in the model are in accord with the observations from the Pioneer 10 and 11 Jupiter missions. The arrows indicate the mean energies $\langle T_o \rangle$ of the distributions, and these are also listed on the figure.

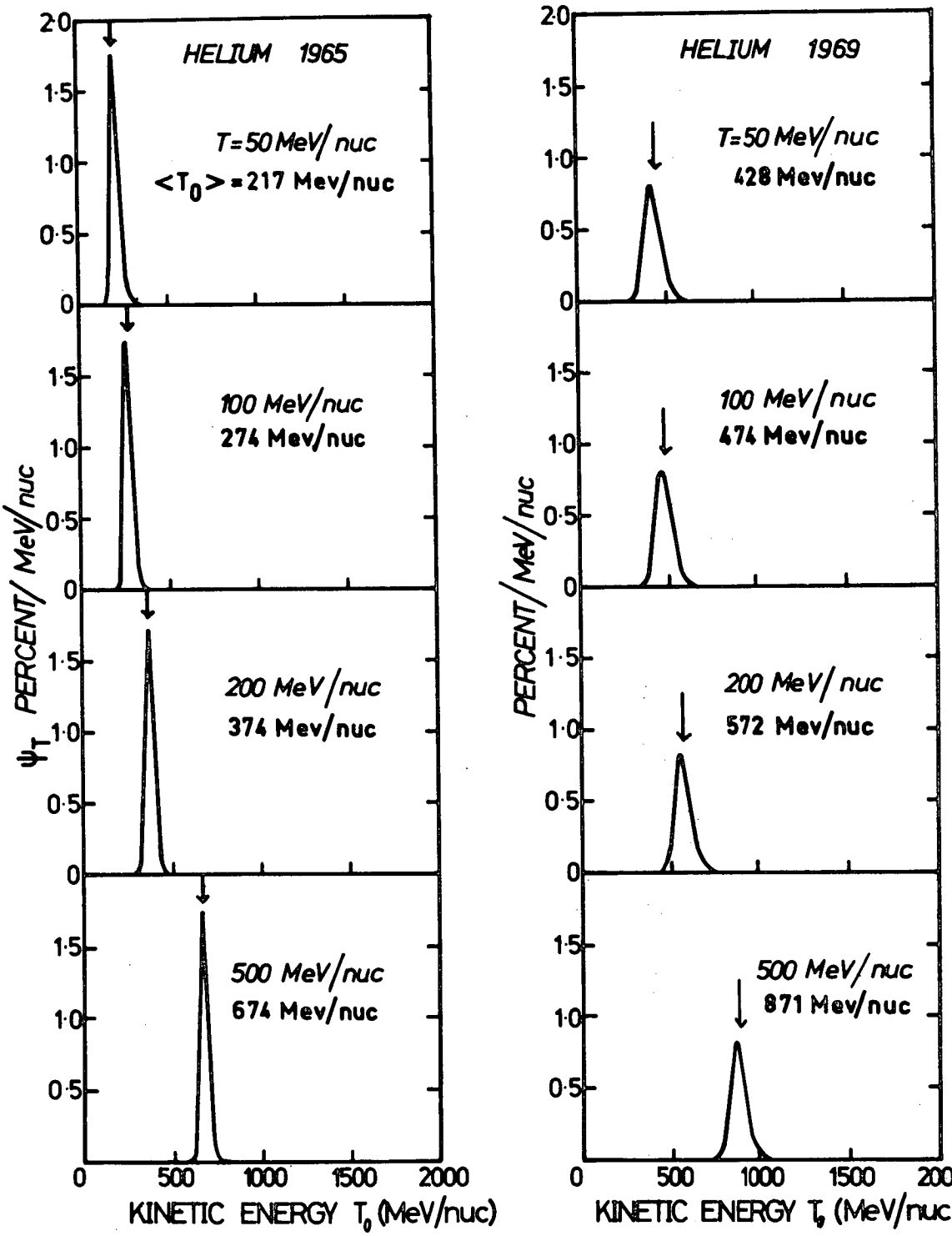
HELIUM 1965
T=50 MeV/nuc
<T0> = 217 Mev/nuc
100 MeV/nuc
274 Mev/nuc
200 MeV/nuc
374 Mev/nuc
500 MeV/nuc
674 Mev/nuc
HELIUM 1969
T=50 MeV/nuc
428 Mev/nuc
100 MeV/nuc
474 Mev/nuc
200 MeV/nuc
572 Mev/nuc
500 MeV/nuc
871 Mev/nuc
ψT PERCENT/MeV/nuc
KINETIC ENERGY T0 (MeV/nuc)
KINETIC ENERGY T0 (MeV/nuc)

Figure 8.13b

Figure 8.13c - Showing the distribution $\psi_T(r,T;T_o)$ of electrons at r = 1 A U, with kinetic energies T = 100, 200, 500 and 1000 MeV, which originated with kinetic energy T_o in the galactic spectrum. The galactic spectrum is given in Equations (8.5.9) and (8.5.10), and the diffusion coefficients used are of the form given in Equations (8.5.11) and (8.5.12), with the parameters (K_c, P_1, P_2, b) appropriate for 1965 and 1969 being (1.5×10^{18}, 0.038, 1.0, 1.038) and (7.0×10^{17}, 0.248, 0.7, 1.038) respectively. With these diffusion coefficients, the radial gradients are in accord with the observations from the Pioneer 10 and 11 Jupiter missions. The arrows indicate the mean energy $\langle T_o \rangle$ of the distributions, and these are also listed on the figure.

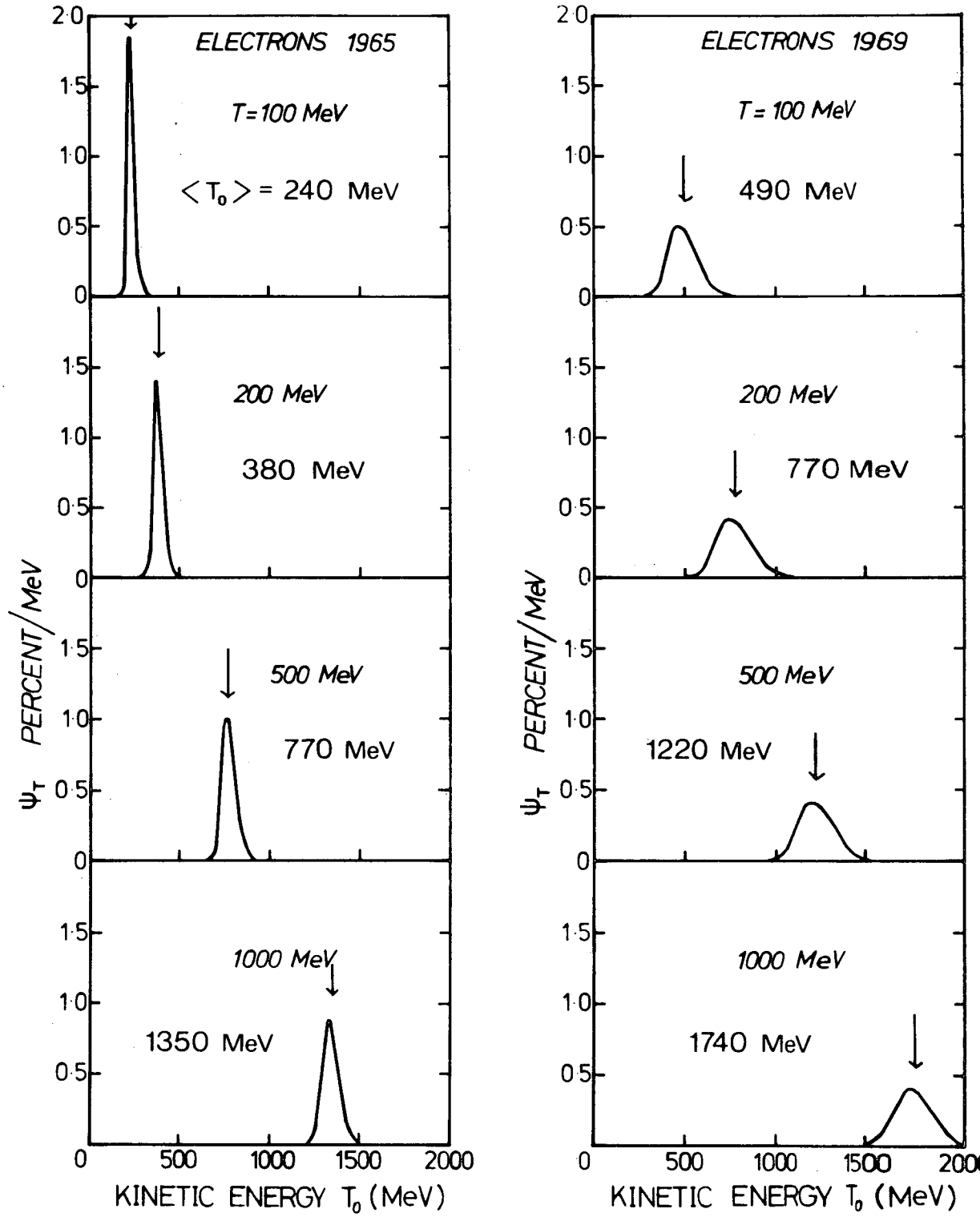
ELECTRONS 1965
T=100 MeV
<T₀> = 240 MeV
200 MeV
380 MeV
500 MeV
770 MeV
1000 MeV
1350 MeV
ELECTRONS 1969
T= 100 MeV
490 MeV
200 MeV
770 MeV
500 MeV
1220 MeV
1000 MeV
1740 MeV
ψT PERCENT/MeV
KINETIC ENERGY T₀ (MeV)
0
500
1000
1500
2000
0.5
1.0
1.5
2.0

Figure 8.13c

Figure 8.14a - Showing $\psi_T(r,T;T_o)$, the percentage of protons per MeV at r = 1 A U at kinetic energy T which originated in the kinetic energy interval $(T_o, T_o + dT_o)$ of the galactic spectrum. The figure is drawn for T = 200 MeV. It shows the effect of varying the magnitude of the diffusion coefficient K_c ($K(r,p) = K_c K_2(P) \beta r^b$, $b > 1$, P in G V, r in A U, Equation (8.5.11)). Curves (a), (b) and (c) are drawn for

(a) $K_c = 1.5 \times 10^{18}$ m^2 s^{-1},

(b) $K_c = 1.139 \times 10^{17}$ m^2 s^{-1},

(c) $K_c = 3 \times 10^{17}$ m^2 s^{-1}.

(see Equations (8.5.13) and (8.5.14) and these conditions are appropriate for 1965. The histogram (conditions (c)) has been reproduced from Urch and Gleeson (1973). The arrows indicate the mean energies $\langle T_o \rangle$ of the distributions.

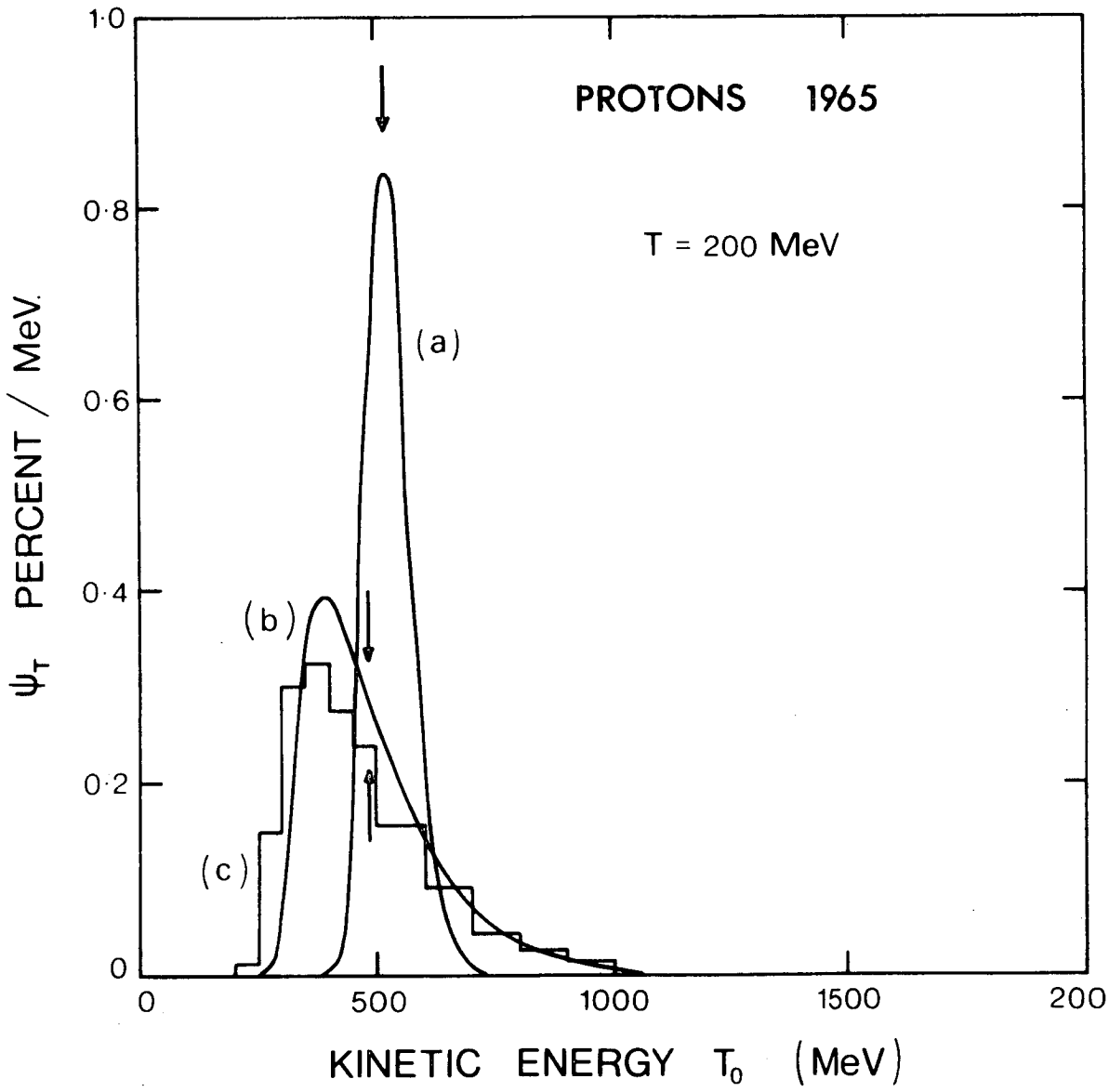
PROTONS 1965
T = 200 MeV
(a)
(b)
(c)
1·0
0·8
0·6
0·4
0·2
0
ψ_T PERCENT / MeV
0
500
1000
1500
2000
KINETIC ENERGY T_0 (MeV)

Figure 8.14a

Figure 8.14b - Showing $\psi_T(r,T;T_o)$, the percentage per MeV/nucleon of helium nuclei at r = 1 A U at kinetic energy T which originated in the kinetic energy interval $(T_o, T_o + dT_o)$ of the galactic spectrum. The figure is drawn for T = 200 MeV/nucleon. It shows the effect of varying the magnitude of the diffusion coefficient K_c ($K(r,p) = K_c K_2(P) r^b$, P in G V, r in A U, Equations (8.5.11)). Curves (a), (b) and (c) are drawn for

(a) $K_c = 1.5 \times 10^{18}$ m^2 s^{-1},

(b) $K_c = 1.139 \times 10^{17}$ m^2 s^{-1},

(c) $K_c = 3 \times 10^{17}$ m^2 s^{-1},

(see Equations (8.5.13) and (8.5.14)) and these conditions are appropriate for 1965. The histogram (conditions (c)) has been reproduced from Urch and Gleeson (1973). The arrows indicate the mean energies $\langle T_o \rangle$ of the distributions.

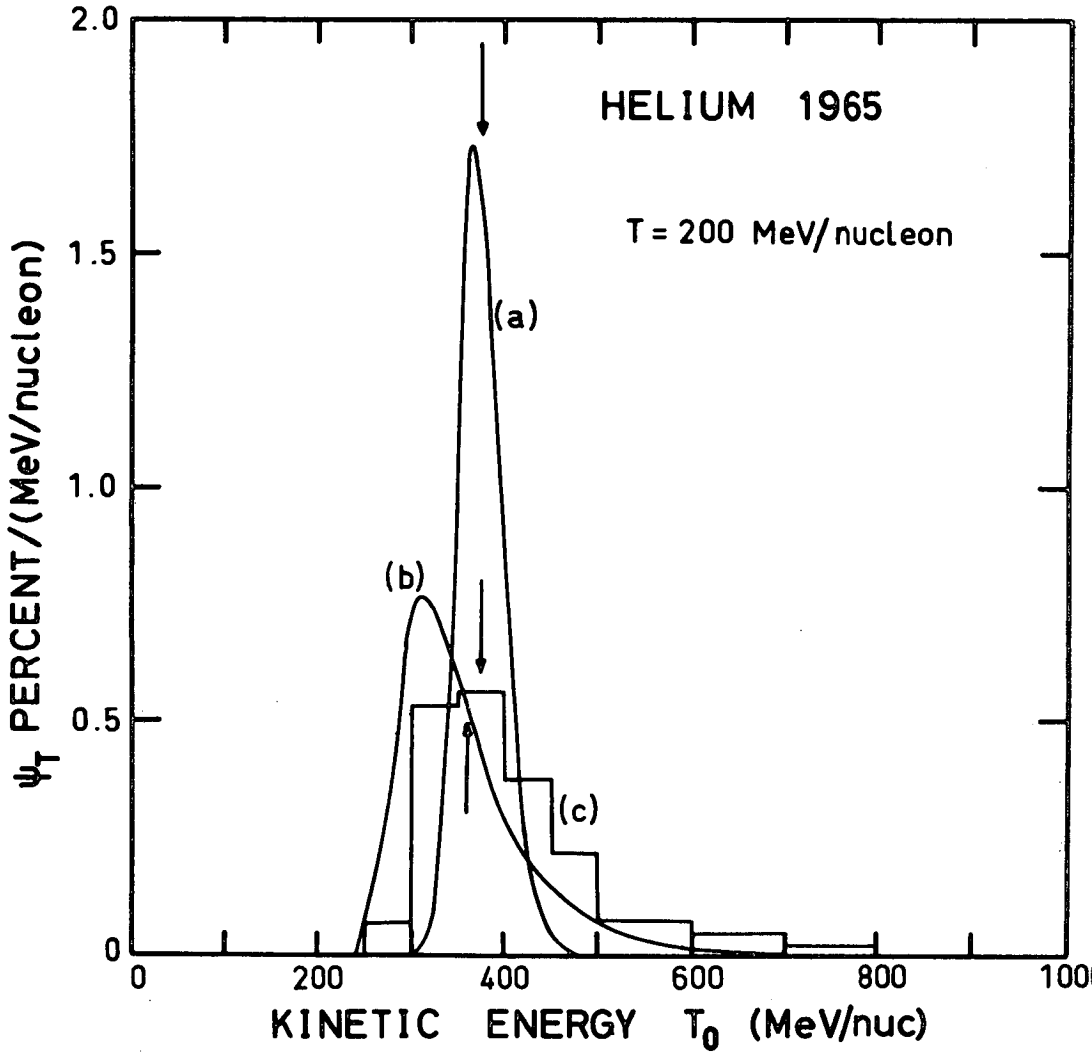
HELIUM 1965
T = 200 MeV/nucleon
(a)
(b)
(c)
2.0
1.5
1.0
0.5
0
0
200
400
600
800
1000
ψ_T PERCENT/(MeV/nucleon)
KINETIC ENERGY T_0 (MeV/nuc)

Figure 8.14b

Figure 8.14c - Showing $\psi_T(r,T;T_o)$, the percentage of electrons per MeV at r = 1 A U at kinetic energy T, which originate in the kinetic energy interval $(T_o, T_o + dT_o)$ of the galactic spectrum. The figure is drawn for T = 200 MeV. It shows the effect of varying the magnitude of the diffusion coefficient K_c, ($K(r,p) = K_c\, K_2(P)\, \beta\, r^b$, r in A U, P in G V, Equation (8.5.11)). Curves (a), (b) and (c) are drawn for

(a) $K_c = 1.5 \times 10^{18}\ m^2\ s^{-1}$,

(b) $K_c = 1.139 \times 10^{17}\ m^2\ s^{-1}$,

(c) $K_c = 3 \times 10^{17}\ m^2\ s^{-1}$,

(see Equations (8.5.13) and (8.5.14)), and these conditions are appropriate for 1965. The histogram (conditions (c)) has been reproduced from Urch and Gleeson (1973). The arrows indicate the mean energies $\langle T_o \rangle$ of the distributions.

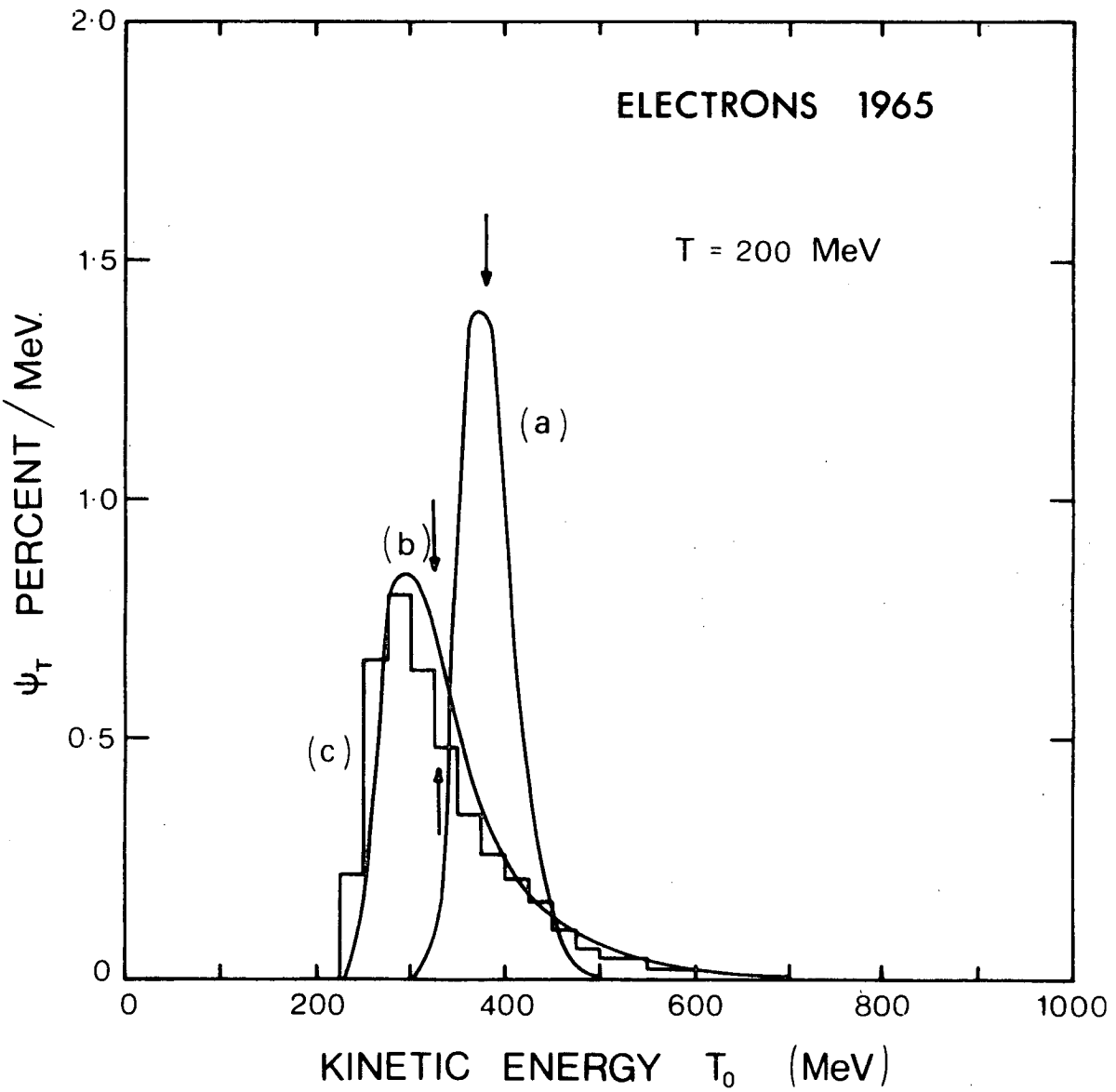
ELECTRONS 1965
T = 200 MeV
(a)
(b)
(c)
2·0
1·5
1·0
0·5
0
ψ_T PERCENT / MeV
0
200
400
600
800
1000
KINETIC ENERGY T_0 (MeV)

Figure 8.14c

Figure 8.15 - The energy losses $\langle T_o \rangle - T$ for galactic electrons for 1965 and 1969. The energy losses obtained by Urch and Gleeson (1973) from numerical solutions of the equation of transport (full curves), and the force field energy losses, Φ, (broken curves) have been reproduced from their study. The energy losses obtained here with conditions (a) (the crosses) and conditions (b)(the circles) have been obtained from the distributions $\psi_T(r,T;T_o)$ displayed in Figures 8.13c and 8.12c respectively. Conditions (a) and (b) are specified in Equations (8.5.13).

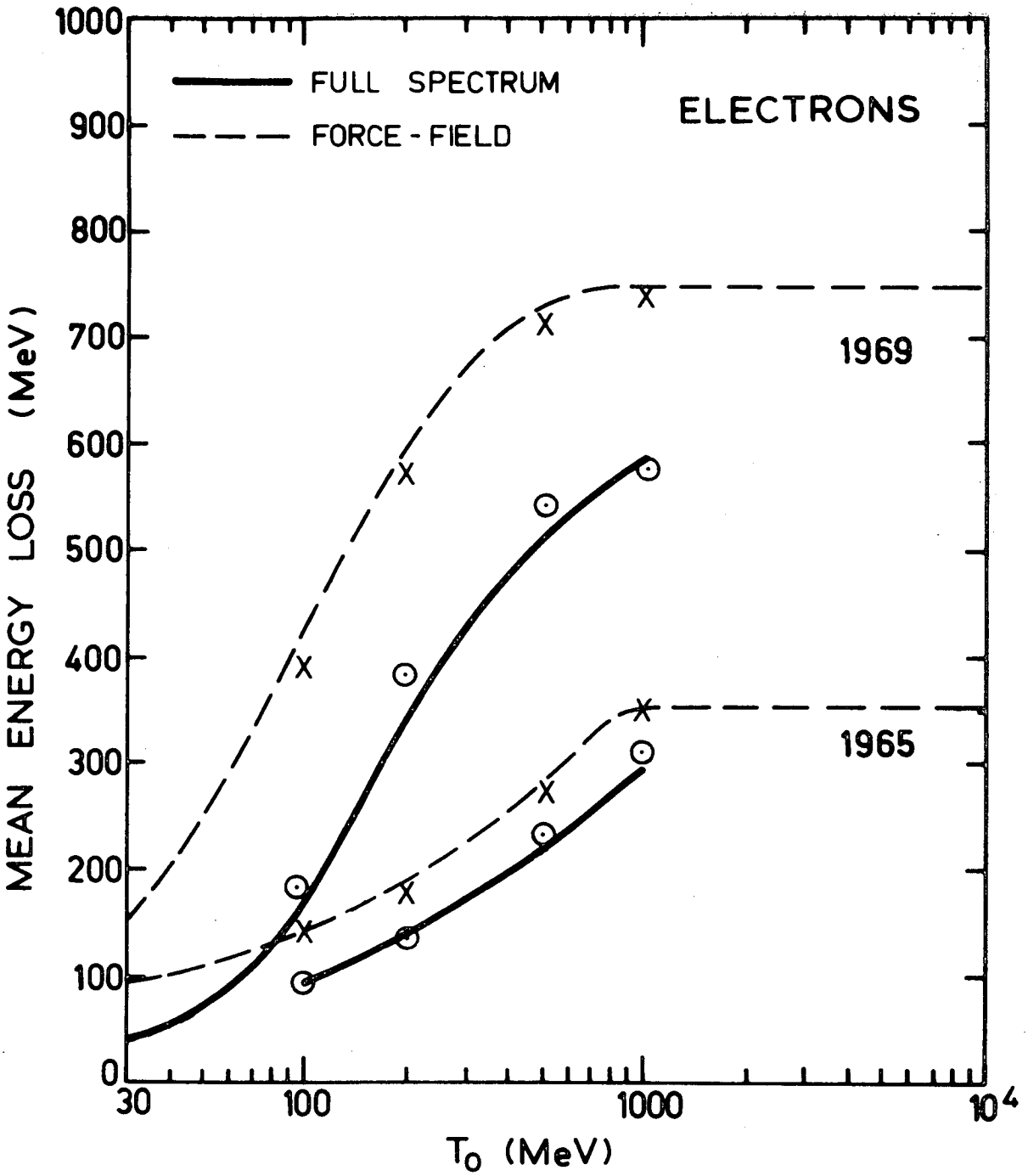
FULL SPECTRUM
FORCE - FIELD
ELECTRONS
1969
1965
MEAN ENERGY LOSS (MeV)
T_0 (MeV)
0
100
200
300
400
500
600
700
800
900
1000
30
100
1000
10^4

Figure 8.15

Figure 8.16 - The energy losses $\langle T_o \rangle - T$ for galactic protons and helium nuclei for 1965. The energy losses obtained by Urch and Gleeson (1973) from numerical solutions of the equation of transport (full curves), and the force field energy losses, Φ, (broken curves) have been reproduced from their study. The energy losses obtained here with conditions (a) (the crosses) and conditions (b) (the circles) have been obtained from the distributions $\psi_T(r,T;T_o)$ displayed in Figures 8.13a, 8.13b and Figures 8.12a, 8.12b respectively. Conditions (a) and (b) are specified in Equations (8.5.13).

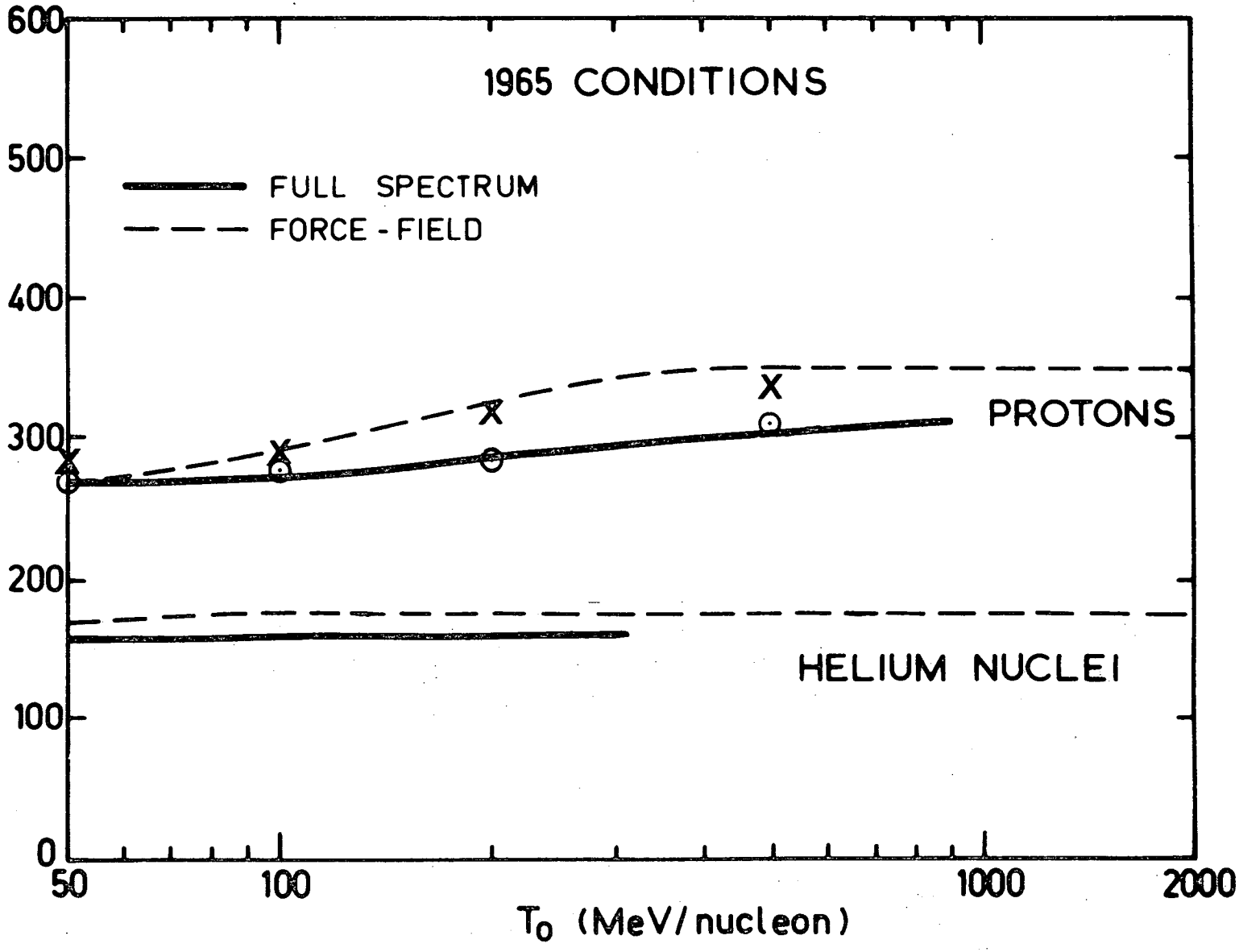
1965 CONDITIONS
FULL SPECTRUM
FORCE - FIELD
PROTONS
HELIUM NUCLEI
600
500
400
300
200
100
0
50
100
1000
2000
T0 (MeV/nucleon)

Figure 8.16

Figure 8.17 - The energy losses $\langle T_o \rangle - T$ for galactic protons and helium nuclei for 1969. The energy losses obtained by Urch and Gleeson (1973) from numerical solutions of the equation of transport (full curves), and the force field energy losses, Φ, (broken curves) have been reproduced from their study. The energy losses obtained here with conditions (a) (the crosses) and conditions (b) (the circles) have been obtained from the distributions $\psi_T(r,T;T_o)$ displayed in Figures 8.13a, 8.13b and Figures 8.12a, 8.12b respectively. Conditions (a) and (b) are specified in Equations (8.5.13).

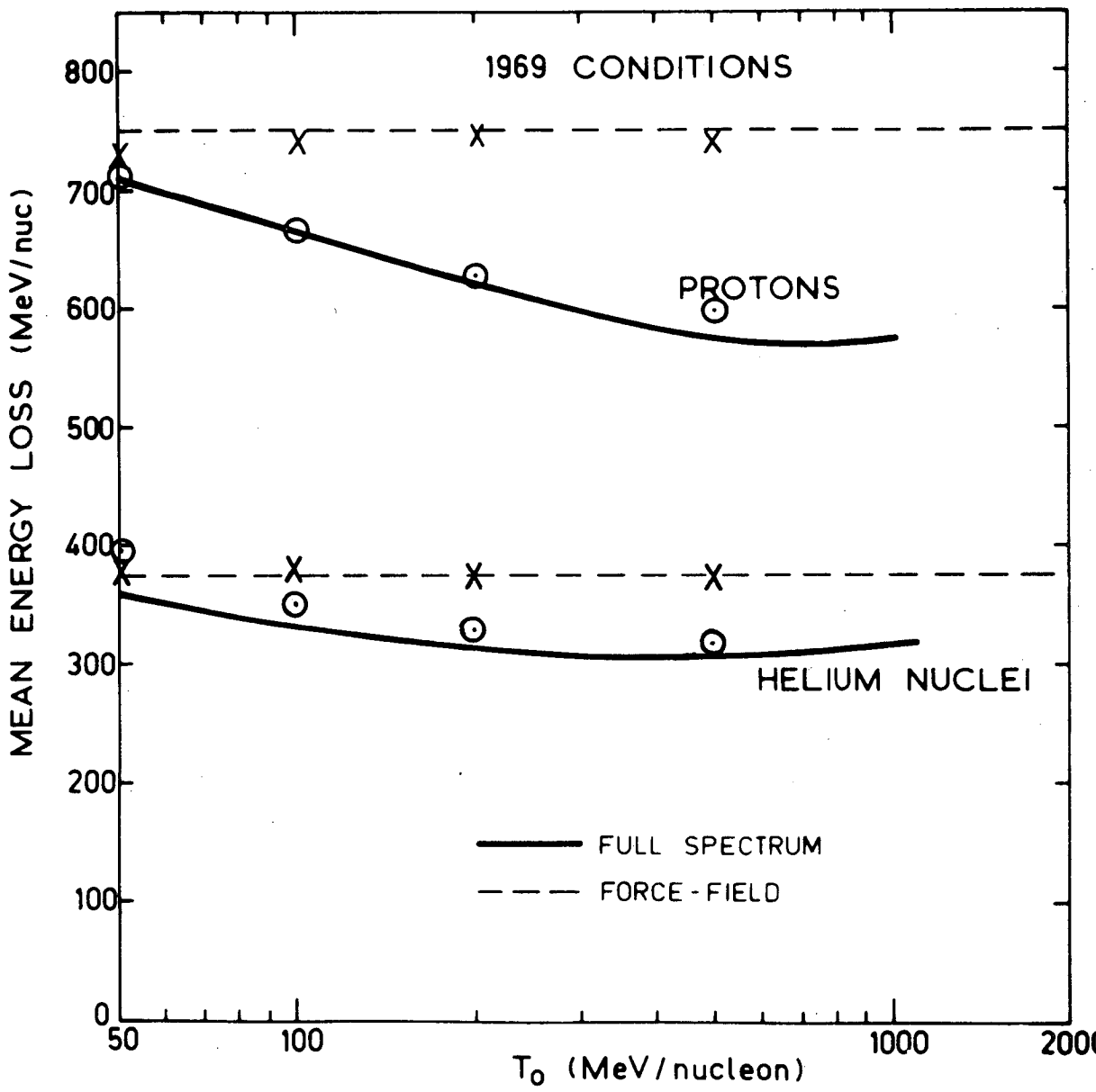
1969 CONDITIONS
PROTONS
HELIUM NUCLEI
FULL SPECTRUM
FORCE-FIELD
MEAN ENERGY LOSS (MeV/nuc)
T_0 (MeV/nucleon)
0
100
200
300
400
500
600
700
800
50
100
1000
2000

Figure 8.17

CHAPTER 9

SOLAR SOURCE SOLUTIONS

9.1 Introduction

In this chapter we study the steady-state interplanetary propagation of solar cosmic-rays by means of monoenergetic source solutions (3.2.13) and (3.2.18) of the transport equation.

In these solutions particles are released monoenergetically from a spherical surface at radius r_o with momentum p_o. The solution (3.2.18), expressed in terms of the distribution function F_o is

$$F_o = \frac{3\,N}{64\pi^2\,V\,p_o^3\,r_o^2|n+1|}\left(\frac{x_o}{x}\right)^n \frac{x_o^2}{T}\exp\left(-\frac{x^2+x_o^2}{4\,T}\right) I_m\left(\frac{x\,x_o}{2\,T}\right) \tag{9.1.1}$$

where

$$\begin{aligned} T &= 3\int_p^{p_o} K_o(z)\, z^{(1-3b)/2} dz/(2V), \\ n &= (b+1)\,/\,(1-b), \quad m = |n|\,, \\ x &= 2\,(rp^{3/2})^{(1-b)/2}/\,(1-b), \quad x_o = x(r_o,p_o), \end{aligned} \tag{9.1.2}$$

the diffusion coefficient $K(r,p) = K_o(p)\,r^b$, with $b \neq 1$, $I_m(z)$ is a modified Bessel function of the first kind of order m and argument z, and N is the rate at which particles are released from the source. The solution (3.2.13), for release at the origin, is obtained by letting $r_o \to 0$ and choosing $b < 1$ in the solution (9.1.1). Note that it is necessary to choose $b < 1$ for particles to escape from $r_o = 0$. This solution is

$$F_o = \frac{3\,N\,(n+1)^{2n+1}}{2^{2n+6}\,V\,\pi^2\,\Gamma(n+1)}\,T^{-n-1}\exp\left(\frac{-x^2}{4T}\right), \tag{9.1.3}$$

In Section (2) we study the solar source solution (9.1.3) with release at $r_o = 0$ for a diffusion coefficient $K(r,p) = K_c\ p\ \sqrt{r}$, and the general solution (9.1.1) with $r_o \neq 0$ for the case $K(r,p) = K_c\ p\ r^{1.5}$, and with parameters in the solution appropriate for solar cosmic rays. Some of the results of this section are published in Webb and Gleeson (1974).

In Section (3) we study the structure of the particle flow and momentum changes in (r,p) space by constructing solutions of the flow line equation (7.6.7) for the monoenergetic source solution (9.1.3) with release at $r_o = 0$ for the case

(i) $K(r,p) = K_c\ p\ \sqrt{r}$

and for the solution (9.1.1) with release at r_o for the cases

(ii) $K = K_c\ p\ r^{1.5}$ and $V\ r_o/K(r_o,p_o) = 1.46$,

(iii) $K = K_c\ p\ \sqrt{r}$ and $V\ r_o/K(r_o,p_o) = 0.4$.

The flow lines for these three cases are quite distinct, and when compared with the flow lines for monoenergetic galactic cosmic-rays presented in Chapter (8), (Figure 8.7), they highlight the difference between the steady state propagation of galactic and solar cosmic-rays.

9.2 Monoenergetic solar source solutions.

For a diffusion coefficient $K(r,p) = K_c\ p^a\ r^b$, $b < 1$ the monoenergetic solar source solution (9.1.3) with $r_o = 0$, is

$$\frac{r_s^2\ p_o^3\ V\ F_o}{N} = \frac{3(n+1)^{2n+1}}{2^{2n+6}.\pi^2\ \Gamma(n+1)}\ [\ 1 - (p/p_o)^{\delta}]^{-n-1}\ \exp\left(\frac{-x^2}{4T}\right)\ , \tag{9.2.1}$$

where

$$\delta = a + 3(1-b)/2,$$

$$r_s = (3\, K_c\, p_o^a /(2V\delta))^{1/(1-b)},$$

$$n = (b+1)\,/\,(1-b),$$

$$\frac{x^2}{4T} = \frac{2\delta}{3(1-b)^2}\,\frac{V\,r}{K(r,p_o)}\,\frac{(p/p_o)^{3(1-b)/2}}{(1-(p/p_o)^{\delta})} \quad . \qquad (9.2.2)$$

Here the parameter $V\,r/K(r,p_o)$ is dimensionless, and it contains the complete dependence of the solution on heliocentric radius r, the diffusion coefficient constant K_c, and the solar wind speed V. A more explicit formulation of the radial dependence is obtained by observing that

$$V\,r/K(r,p_o) = [V\,r_e/K(r_e,p_o)]\,(r/r_e)^{1-b}, \qquad (9.2.3)$$

where r_e is some fixed heliocentric radius.

Similarly, for a diffusion coefficient $K(r,p) = K_c\, p^a\, r^b$, the general monenergetic source solution (9.1.1) may be written as

$$\frac{r_o^2\, p_o^3\, V}{N}\, F_o(r,p) = \frac{3}{64\pi^2|n+1|}\left(\frac{x_o}{x}\right)^n \frac{x_o^2}{T}\exp\left(-\frac{x^2+x_o^2}{4T}\right) I_m\left(\frac{x\,x_o}{2T}\right), \qquad (9.2.4)$$

where

$$x = 2\,(r\,p^{3/2})^{(1-b)/2}/\,(1-b),$$

$$x/x_o = (r/r_o)^{(1-b)/2}\,(p/p_o)^{3(1-b)/4},$$

$$n = (b+1)/(1-b), \quad m = |n|\,,$$

$$\frac{x^2}{4T} = \frac{2\delta}{3(1-b)^2}\,\frac{V\,r_o}{K(r_o,p_o)}\,\frac{(r/r_o)^{1-b}\,(p/p_o)^{3(1-b)/2}}{(1-(p/p_o)^{\delta})}\,,$$

$$\frac{x_o^2}{4T} = \frac{2\delta}{3(1-b)^2}\,\frac{V\,r_o}{K(r_o,p_o)}\,\frac{1}{(1-(p/p_o)^{\delta})}\,, \qquad (9.2.5)$$

$$\frac{x\, x_o}{2T} = \frac{4\delta}{3(1-b)^2}\,\frac{V\, r_o}{K(r_o,p_o)}\,\frac{(r/r_o)^{(1-b)/2}\,(p/p_o)^{3(1-b)/4}}{(1-(p/p_o)^{\delta})},$$

$$\delta = a + 3(1-b)/2.$$

Here the solution depends on the three dimensionless quantities $V\, r_o/K(r_o,p_o)$, r/r_o and p/p_o. This is in direct contrast with the case $r_o \to 0$ in which $Vr/K(r,p_o)$ and p/p_o were the dimensionless quantities specifying $F_o(r,p)$ and also in contrast to the galactic case for which $r_o \to \infty$. This additional parameter makes the range of solution forms more difficult to display.

Some of the principal features of these solutions are shown in Figures 9.1, 9.2 and 9.3 which display F_o, U_p and S_p as functions of p/p_o. Figure 9.1 is for the case $r_o = 0$ and the radial dependence and the dependence on V, K_c and p_o are contained in the single parameter $V\, r/K(r,p_o)$. Figures 9.2 and 9.3 are for the cases $r_o \neq 0$; here, because of the increase in the number of parameters in the solution two sets of curves are necessary. Figure 9.2 represents the effects seen at a fixed position obtained by changing V, K_c or p_o while Figures 9.3a and 9.3b show the dependence on position r/r_o with fixed $V\, r_o/K(r_o,p_o)$.

Figure 9.1 shows the momentum dependence of F_o, U_p and S_p for the solution with $r_o = 0$ (Equation (9.2.1)) for $K = K_c\, p\, \sqrt{r}$, and values 0.001, 0.01, 0.1, 1.0 and 10.0 of the parameter $V\, r/K(r,p_o)$. Particles injected with momentum p_o are seen to be redistributed over the whole momentum range $0 < p \leq p_o$. For the three smaller values of $V\, r/K(r,p_o)$ there is a substantial peak in the spectrum in the vicinity of p_o. As $V\, r/K(r,p_o)$ decreases, either because V or r decreases or because K_c or p_o increases the peaks move toward p_o

narrow in width and increase in peak value. Since particles are released monoenergetically with momentum p_o from $r_o = 0$ we have

$$F_o(r,p_o) = \lim_{r_o \to 0} \frac{3\ N\ \delta(r-r_o)}{32\pi^2\ V\ p_o^3\ r_o}\ , \qquad (9.2.6)$$

where $\delta(x)$ is the Dirac delta function of argument x, and hence $F_o(r,p_o) \to \infty$ as $V\ r/K(r,p_o) \to 0$.

For large values of $V\ r/K(r,p_o)$ in Figure 9.1 the distributions are strongly attenuated at the upper end of the momentum range. These results indicate that as the solar wind speed V, or the heliocentric distance r increase, or as p_o or the diffusion coefficient constant K_c decrease, particles lose a larger fraction of their initial momentum. We can also see these characteristics of the particle propagation from the mean momenta

$$\overline{p} = \int_0^{p_o} p\ U_p\ dp \ / \int_0^{p_o} U_p\ dp, \qquad (9.2.7)$$

which are indicated on the U_p plots by arrows.

At the low end of the momentum range the distribution function curves show that there is an accumulation of particles which have lost momentum due to interaction with the irregular component of the magnetic field moving with the solar wind. As $p \to 0$ we have

$$\frac{r_s^2\ p_o^3\ V}{N}\ F_o \to 0.203,$$

for all values of $V\ r/K(r,p_o)$, with $b = 0.5$, $r_o = 0$, and r_s defined by Equations (9.2.2), and hence the distribution function is independent of heliocentric distance as $p \to 0$. The result $F_o \to$ constant as $p \to 0$ is characteristic of the monoenergetic source solutions (9.2.1) and (9.2.4) for cases where r_o is general and $K(r,p) = K_c\ p^a\ r^b$, $a > 0$, $b < 1$. For the solution (9.2.4) with $r_o \neq 0$ we find that as $p \to 0$,

with $a > 0$, $b < 1$,

$$F_o \rightarrow \frac{3N}{16\pi^2 V p_o^3 r_o^2 |n+1|} \left[\frac{2\delta}{3(1-b)^2} \frac{V r_o}{K(r_o,p_o)} \right]^{n+1} \frac{1}{\Gamma(n+1)}$$

$$\exp\left(\frac{-2\delta}{3(1-b)^2} \frac{V r_o}{K(r_o,p_o)} \right), \quad (9.2.8)$$

where

$$\delta = a + 3(1-b)/2 \neq 0, \quad n = (b+1)/(1-b) .$$

For a source at $r_o = 0$ with $a > 0$ and $b < 1$, as $p \rightarrow 0$ we have

$$\frac{r_s^2 p_o^3 V}{N} \quad F_o \rightarrow \frac{3(n+1)^{2n+1}}{2^{2n+6} \pi^2 \Gamma(n+1)}, \quad (9.2.9)$$

where

$$r_s = [3K_c p_o^a /(2V\delta)]^{1/(1-b)} .$$

The above result may be obtained directly from the solution (9.2.1) with $r_o = 0$, or by letting $r_o \rightarrow 0$ in the result (9.2.8).

The S_p curves show that for $r_o = 0$, $K = K_c p \sqrt{r}$, the streaming is positive (outward) for all p and $V r/K(r,p_o)$. We can also show (Equation (9.3.11)) that S_p is positive at all r and p when the source is located at $r_o = 0$ and $K = K_o(p) r^b$, $b < 1$.

The curves of Figure 9.1 can be interpreted as indicating the changes in the spectra at fixed r for various diffusion coefficients or the changes at fixed r for particles of various source momenta p_o. In this latter case, since $V r/K(r,p_o)$ increases as p_o decreases, the U_p curves show that particles of lower p_o lose a larger fraction of their initial momentum. We note that with values of K used by Urch and Gleeson (1972b) to reproduce the modulation of 1965, i.e., solar

minimum ($K(r,p) = 3 \times 10^{17}$ m^2 s^{-1} at a radius of 1 A.U. and a rigidity of 1 G V, $V = 4 \times 10^5$ m s^{-1}), the curves $Vr/K(r,p_o) = 0.001$, 0.01, 0.1, 1.0 and 10.0 represent, respectively, the spectra to be obtained at r = 1 A U from injection of protons at $r_o = 0$ with kinetic energies, T_o, of 198, 19, 1.26 GeV, 20 and 0.2 MeV.

The curves of Figure 9.1 can alternatively be interpreted as indicating the changes in the spectra with heliocentric distance r. Since $V\ r/K(r,p_o) \propto \sqrt{r}$ in this example, the heliocentric distances represented by the curves of Figure 9.1 are in the ratio of $10^{-4} : 10^{-2} : 1 : 10^2 : 10^4$. Hence if $V\ r/K(r,p_o) = 0.1$ represents the spectra at r = 1 A U obtained from particles released monoenergetically at $r_o = 0$, the curves $V\ r/K(r,p_o) = 0.001$, 0.01, 1.0 and 10.0 represent the spectra at 10^{-4}, 10^{-2} 10^2 and 10^4 A U respectively.

We now turn to the examination of the cases with $r_o \neq 0$, for which examples of F_o, U_p and S_p are displayed in Figures 9.2 and 9.3. Two figures are provided in order to show the dependence of the solution on each of the parameters $V\ r_o/K(r_o,p_o)$ and r/r_o.

Figure 9.2 indicates the dependence of F_o, U_p and S_p on $V\ r_o/K(r_o,p_o)$ for fixed r/r_o; it is constructed for the case $K = K_c\ p\ r^{1.5}$ and $r/r_o = 214.95$. The principal features are again the spread in momentum over the range $0 < p \leq p_o$ and the peaked nature of the spectrum in the vicinity of p_o for small $V\ r_o/K(r_o,p_o)$. As in the case of $r_o = 0$ [Figure 9.1] the mean momentum decreases as $V\ r_o/K(r_o,p_o)$ increases.

At small p/p_o the spectrum of Figure 9.2 has a second peak for small $V\ r_o/K(r_o,p_o)$, apparently indicating some accumulation of particles after energy changes.

As $p \to 0$, $F_o \to 0$ for $b > 1$, but for $K = K_c\, p^a\, r^b$, $b < 1$, $a > 0$, from the result (9.2.8)

$$F_o \to \text{constant} = \frac{3N}{16\pi^2 V p_o^3 r_o^2 |n+1|} \left[\frac{2\delta}{3(1-b)^2} \frac{V r_o}{K(r_o,p_o)} \right]^{n+1} \frac{1}{\Gamma(n+1)}$$

$$\exp\left[- \frac{2\delta}{3(1-b)^2} \frac{V r_o}{K(r_o,p_o)} \right].$$

we recall that for $r_o = 0$, $K = K_c\, p^a\, r^b$, $a > 0$, $b > 1$, the distribution function tended to the constant (9.2.9) as $p/p_o \to 0$, and this behaviour of F_o for small p/p_o is also shown in Figure 9.1.

The structure of the streaming S_p is more complex than for the case $r_o = 0$. Here S_p is positive for p near p_o but becomes negative, indicating inward flow at low p, whereas in the case $r_o = 0$ we had $S_p > 0$ for all p. This pattern is discussed in more detail in Section (9.3). For $K(r,p) = 3 \times 10^{17}$ m^2/s at 1 A U and 1 G V rigidity, $V = 4 \times 10^5$ m/s, the curves $V\, r_o/K(r_o, p_o) = 0.03$, 0.3 and 3.0 of Figure 9.2, represent, respectively, the momentum dependence of F_o, U_p and S_p to be obtained at r = 1 A U from injection of protons at $r_o = 1$ solar radius and kinetic energies, T_o, of 96.5, 8.85 GeV and 414 MeV.

The curves of Figures 9.3a and 9.3b show the dependence of the spectra on heliocentric distance. They show F_o, U_p and S_p as functions of p/p_o for $r/r_o = 1$, 2, 100 and 1000 and are for the cases $K = K_c\, p\, r^{1.5}$ and $V\, r_o/K(r_o,p_o) = 1.46$ (Figure 9.3a) and $V\, r_o/K(r_o,p_o) = 0.1$ (Figure 9.3b).

Figure 9.3a shows that F_o and U_p are peaked near $r/r_o \simeq 1$ and that the spectrum spreads and becomes concentrated at lower mean values of p/p_o as r/r_o increases. Figure 9.3b which is for smaller

$V\, r_o/K(r_o,p_o)$ shows that as we decrease $V\, r_o/K(r_o,p_o)$ the peak near $p/p_o = 1$, persists even at large radii, and that the shape of the spectrum is critically dependent on this parameter. Since the particles are released monoenergetically with momentum p_o at radius r_o we have

$$F(r,p_o) = \frac{3\, N\, \delta(r-r_o)}{32\, \pi^2\, V\, p_o^3\, r_o} ,$$

where $\delta(r-r_o)$ is the Dirac delta function, so that $F(r,p_o) \to \infty$ as $r \to r_o$.

The spectra of Figures 9.3a and 9.3b have $F_o \to 0$ as $p \to 0$ because $b > 1$ (recall $K = K_c\, p^a\, r^b$, $b = 1.5$, $a = 1.0$). If $b < 1$ and $a > 0$, then F_o tends to the constant (9.2.8) as $p \to 0$.

The dependence of S_p upon p of Figures 9.3a and 9.3b is again complex, but very interesting. As in the case of Figure 9.2 we have a region of $S_p > 0$ near $p = p_o$ and a region of $S_p < 0$ for low p; the crossover point in p/p_o decreases as r/r_o increases. As $r/r_o \to 1^+$, the range of p/p_o of net outflow ($S_p > 0$) decreases and tends to a double delta form with large positive flow close to p_o and a large negative inward flow for p just below this. It represents the particles first flowing outward and being turned around with energy loss (overtaking 'collisions') and passing into $r < r_o$. The (r,p) flow patterns are given in Section 9.3.

If we choose $r_o = 1$ solar radius in Figures 9.3, the curves $r/r_o = 2$, 100, 1000 represent, respectively, the spectra obtained at heliocentric distances of 9.3×10^{-3}, 0.465 and 4.65 A U.
For $K(r,p) = 3 \times 10^{17}\ m^2\ s^{-1}$ at a rigidity of 1 G V and r = 1 A U, $V = 4 \times 10^5\ m\ s^{-1}$, the curves of Figure 9.3a show the redistribution and streaming of monoenergetic protons released from $r_o = 1$ solar radius,

with a momentum p_o = 2 GeV/c whereas in Figure 9.3b, p_o = 29.3 GeV/c.

The results presented so far in this section show the main features associated with steady state monoenergetic release with $r_o = 0$ and $r_o \neq 0$. We now present the results of a more detailed investigation of the dependence on p and r of these solutions in particular, but representative cases.

As in a similar study for the monoenergetic galactic spectrum case of Chapter (8) we calculate the quantities specified in the list (8.2.5) and we use contour plots in the (r,p) plane to represent them. We look at the distribution of particles, gradient, streaming and momentum changes, and use the set of graphs produced to discuss some of the physical characteristics of the steady state propagation of solar cosmic rays.

The particular cases studied are

(i) $r_o = 0$ and $K = K_c\ p\ \sqrt{r}$ with $V\ r_e/K(r_e,p_o) = 0.1$, and

(ii) $r_o \neq 0$ and $K = K_c\ p\ r^{1.5}$ with $V\ r_o/K(r_o,p_o) = 1.46$.

The results for (i) follow from the solution (9.2.1) and are presented in Figures 9.4 while those for (ii) follow from the solution (9.2.4) and are presented in Figures 9.5.

The contours for F_o or U_p show that the number density is sharply peaked about the source at r = 0 and $p = p_o$ in Figure 9.4a and about the source at $r = r_o \neq 0$, and $p = p_o$ in Figure 9.5a.

The redistribution of particles initially injected into the interplanetary medium with momentum p_o in these two examples are very different and this is essentially a consequence of the differing radial dependence of the two diffusion coefficients employed, and the helio-

centric position of the source.

For the case $K = K_c\ p\ \sqrt{r}$ and $r_o = 0$ the contours of Figure 9.4a show that for a fixed momentum F_o decreases montonically with increasing r. As a consequence the radial gradient is negative and the diffusive flux is outward at all radii. Since the diffusive flux is outward the cosmic-rays undergo more overtaking than head on collisions with the magnetic field irregularities moving with the solar-wind and hence on average particles are losing momentum at all r and p and $\langle\dot{p}\rangle$ is negative. From the $(dp/dt)/(dp/dt)_{ad}$ contours of Figure 9.4b we see that the cosmic-rays are losing momentum over a large portion of the (r,p) plane at a rate less than the adiabatic rate.

As noted previously the streaming S_p and the bulk flow velocity are outward over the whole (r,p) plane, and hence the particles on average lose momentum as they flow outward.

For the case $K = K_c\ p\ r^{1.5}$ and $r_o \neq 0$, the F_o or U_p contours of Figure 9.5a show that for each p, as r increases from zero the number density increases to a peak and then decreases. This represents particles simultaneously being fed into (p,p+dp) by the energy changes, but being excluded from the inner regions by the outwardly moving scattering centres. Corresponding to this peak (which shows as a ridge in the r-p plane) we have a positive gradient near r = 0, changing to negative at heliocentric distances past the peak.

The contours of S_p in Figure 9.5a show that the streaming changes from inward to outward as p increases from 0 to p_o, and the outflow region decreases in width and S_p increases as $r \to r_o^+$ or as $r \to r_o^-$. The outflow region of the momentum spectrum is in general much wider at heliocentric radii $r > r_o$ than for $r < r_o$. At low

momenta, the magnitude of the Compton Getting factor, C, is much greater than $|S_d/V\ U_p|$ and the flow is convective.

The regions of (r,p) space in which particles are gaining and losing momentum are readily seen from the contour plots of dp/dt of Figure 9.5b. At a fixed p, as r increases the momentum rate $<\dot{p}>$ changes from positive to negative.

At sufficiently small p the distribution function contours are of the form

$$r\ p^{3/2} = \text{constant}.$$

This form is characteristic of the convective solution of the transport equation (Appendix D, Gleeson 1970) and for the case $K = K_c\ p\ r^{1.5}$ it can also be seen from the analytic expression (9.2.4) for $F_o(r,p)$. However for a diffusion coefficient $K = K_c\ p^a\ r^b$ with $b > 1 + 2a/3$, the expression (9.2.4) for F_o cannot be expressed solely in terms of the variable $r\ p^{3/2}$ at small p/p_o, and the solution does not seem to be convective.

The redistribution of particles, the streaming, the gradient and the momentum changes in the region $r << r_o$ of Figures 9.5 are similar to the corresponding features of the monoenergetic galactic spectrum solution (8.1.1) for $K = K_c\ p\ r^{1.5}$ near $r = 0$. (See Figures 8.4).

The particle flow and momentum changes are related since the momentum changes form effective sources of particles. We investigate this more fully for monoenergetic solar cosmic-rays in the next section.

9.3 The flow pattern of monoenergetic solar cosmic-rays.

In this section we investigate the particle flow and momentum changes in position-momentum space arising from a source of monoenergetic cosmic-rays of momentum p_o released at a rate of N particles per second from the heliocentric radius $r = r_o$. These aspects are examined together because they are related by the fact that particles are conserved and the continuity equation

$$\frac{1}{r^2}\frac{\partial}{\partial r}\left(r^2 S_p\right) + \frac{\partial}{\partial p}\left(\langle \dot{p} \rangle U_p\right) = \frac{N\,\delta(r-r_o)\,\delta(p-p_o)}{4\pi r_o^2}\,, \qquad (9.3.1)$$

applies. Equation (9.3.1) shows that the momentum changes provide an effective source of particles.

Using the continuity equation (9.3.1) we first consider the conservation of particles over the whole momentum range $0 \leq p < \infty$, and we obtain a relation between the total flux across a spherical surface at radius r and the injection rate N.

We then calculate the streaming $S_p(r,p)$, and show the regions of the (r,p) plane in which particles have a net inflow or outflow for the particular cases

(i) $K = K_c\, p\sqrt{r}$, $\qquad r_o = 0$,

(ii) $K = K_c\, p\, r^{1.5}$, $\qquad V\, r_o/K(r_o,p_o) = 1.46$, $\quad r_o \neq 0$,

(iii) $K = K_c\, p\sqrt{r}$, $\qquad V\, r_o/K(r_o,p_o) = 0.4$, $\quad r_o \neq 0$.

Then in order to elucidate the physics of the flow we obtain analytic and numerical solutions of the flow line equations (7.6.8) and (7.6.9). We note again that the tangent to a flow line at any point of (r,p) space gives the ratio of the streaming speed $\langle \dot{r} \rangle$ to the

momentum change rate $\langle \dot{p} \rangle$ (cf. Sections 7.6 and 8.3).

We now consider the conservation of particles over the whole momentum range $0 \leq p < \infty$. Under steady state conditions particles which enter the region $r < r_o$ must flow out again, so that the net flow of particles over the whole momentum range $0 < p < \infty$ across any spherical surface at heliocentric radius r, with $r < r_o$ must be zero. In the region $r > r_o$, the net outflow of particles of all momenta across the spherical surface at radius r must equal the injection rate, i.e., N particles per second. We may express these results by the equation

$$4 \pi r^2 \int_0^\infty S_p (r,p)\, dp = N \cdot H(r-r_o), \qquad (9.3.3)$$

where $H(r-r_o)$ is the Heaviside step function with argument $r-r_o$, i.e.,

$$H(r-r_o) = \begin{cases} 1 & \text{if } r > r_o, \\ 0 & \text{if } r < r_o, \end{cases} \qquad (9.3.4)$$

and $S_p(r,p)$ is the radial differential current density.

To show the conservation relation (9.3.3) directly from the continuity equation (9.3.1) we proceed as follows. Using the expression (7.1.1) for $\langle \dot{p} \rangle$, i.e.,

$$\langle \dot{p} \rangle = \frac{V\, p}{3U_p} \frac{\partial U_p}{\partial r} , \qquad (9.3.5)$$

putting r = x in the continuity equation and integrating over the whole momentum range from p = 0 to p = ∞ we have

$$\frac{1}{x^2} \frac{\partial}{\partial x} \left(x^2 \int_0^\infty S_p(x,p)dp \right) + \left[\frac{Vp}{3} \frac{\partial U_p(x,p)}{\partial x} \right]_{p=0}^{p=\infty} = \frac{N.\delta(x-r_o)}{4 \pi r_o^2} \qquad (9.3.6)$$

Since $U_p (x,\infty) = 0$ we have $\partial U_p(x,\infty)/\partial x = 0$, the term in square braces

in the above equation is zero and it becomes

$$\frac{\partial}{\partial x}\left(4\pi x^2 \int_0^\infty S_p(x,p)dp\right) = N \cdot \delta(x-r_o), \qquad (9.3.7)$$

showing that the divergence of the total particle flux over all p has a singularity at $x = r_o$, but it is zero for $x \neq r_o$.

Integrating Equation (9.3.7) from x = 0 to x = r we find

$$\left[4\pi x^2 \int_0^\infty S_p(x,p)dp\right]_{x=0}^{x=r} = N \cdot H(r-r_o),$$

i.e.,

$$4\pi r^2 \int_0^\infty S_p(r,p)dp = N \cdot H(r-r_o), \qquad (9.3.8)$$

which is the conservation relation (9.3.3).

From the monoenergetic source solutions (9.1.1) and (9.1.3) we can show that for $x \neq r_o$ we have $U_p(x,p) = 0$ for $p \geq p_o$, and hence the conservation relation (9.3.8) for these solutions can be written as

$$4\pi r^2 \int_0^{p_o} S_p(r,p)dp = N \cdot H(r-r_o). \qquad (9.3.9)$$

The result (9.3.8) shows that the net flux of particles across a spherical surface at radius r, with $r < r_o$, is zero and hence either $S_p \equiv 0$ or the momentum spectrum of S_p must have positive and negative regions at these radii. At $r > r_o$, the streaming flux across the spherical surface at radius r equals the injection rate N, and S_p can be positive over the whole momentum range $0 \leq p < \infty$.

The positive and negative regions of the streaming in the (r,p) plane can be calculated from the expression (7.6.3) for S_p, i.e.,

$$S_p = -4\pi p^2 \left(\frac{Vp}{3}\frac{\partial F_o}{\partial p} + K(r,p)\frac{\partial F_o}{\partial r}\right). \qquad (9.3.10)$$

For a general diffusion coefficient $K = K_o(p)r^b$, $b < 1$, substituting the expression (9.1.3) for F_o in the result (9.3.10) gives the streaming arising from a monoenergetic source at $r_o = 0$ to be

$$S_p = 4\pi p^2 V F_o\left(\frac{x^2}{4T}\right)\left(\frac{1}{(n+1)} + \frac{K_o(p)\, p^{(3-3b)/2}}{2VT}\right), \quad (9.3.11)$$

where as usual

$$\begin{aligned} x &= 2(r\, p^{3/2})^{(1-b)/2}/(1-b), \\ T &= 3\int_p^{p_o} K_o(z)\, z^{(1-3b)/2}\, dz\, /\, (2V). \end{aligned} \quad (9.3.12)$$

Since T and $x^2/(4T)$ are positive Equation (9.3.11) shows that for the solution (9.1.3) for a source at $r_o = 0$, with $b < 1$, the streaming is positive (outward) over the whole momentum range $0 \le p \le p_o$.

Substituting the general monoenergetic source solution (9.1.1) for F_o in the expression (9.3.9) for the streaming and using the result

$$I'_m(z) = I_{m+1}(z) + \frac{m}{z} I_m(z),$$

for the modified Bessel function of the first kind $I_m(z)$ (Abramowitz and Stegun, 1965, Section 9.6), we have

$$\begin{aligned} S_p = 4\pi p^2 F_o \Bigg[& \frac{K_o(p)\, p^{(3-3b)/2}}{2TV}\left(m-n+(m-n)(n+1)\frac{2T}{x^2}\right. \\ & - \frac{x^2+x_o^2}{4T} + \left[(n+1)\frac{x_o}{x} + \frac{x\, x_o}{2T}\right] I_{m+1}\left(\frac{x\, x_o}{2T}\right) \Big/ I_m\left(\frac{x\, x_o}{2T}\right) \Big) \\ & + \frac{1}{2(n+1)}\left(m-n-\frac{x^2}{2T} + \frac{x\, x_o}{2T}\, I_{m+1}\left(\frac{x\, x_o}{2T}\right) \Big/ I_m\left(\frac{x\, x_o}{2T}\right)\right) \Bigg] \end{aligned} \quad (9.3.13)$$

as the streaming for a monoenergetic source located at radius $r_o \neq 0$, and $b \neq 1$.

The general structure of $S_p(r,p)$ in the (r,p) plane resulting from a monoenergetic source located at radius $r_o \neq 0$ for the particular cases

(i) $K = K_c\ p\ r^{1.5}$ and $V\ r_o/K(r_o,p_o) = 1.46$,

(ii) $K = K_c\ p\ \sqrt{r}$ and $V\ r_o/K(r_o,p_o) = 0.4$,

are shown in Figures 9.6b and 9.6c. Figure 9.6a shows for comparison the structure of $S_p(r,p)$ in the (r,p) plane for a monoenergetic source located at $r_o = 0$, and a diffusion coefficient $K = K_c\ p\ \sqrt{r}$. The figures show an (r,p) plane and the arrows indicate schematically the direction of S_p (either inward or outward).

In both examples with $r_o \neq 0$, there are two outflow regions and one inflow region. The inflow regions include the source point at (r_o,p_o). For $K = K_c\ p\ r^{1.5}$, Figure 9.6b shows that the inflow region extends to radial distances $r >> r_o$ at low momenta, and there is a net inflow of particles with momenta between the curves $p = 0$ and $S_p = 0$. However for $K = K_c\ p\ \sqrt{r}$, the inflow region does not extend far beyond $r = r_o$ and in contrast to the case $K = K_c\ p\ r^{1.5}$, there is an outflow of particles at low momenta at radii $0 < r < r_o$. In both cases there is an outflow of particles at the upper end of the momentum range at radii $r < r_o$.

These flow patterns can readily be understood in terms of the momentum change term in the continuity equation (9.3.1) providing an effective source of particles and of particles changing momentum at the average rate (9.3.5)

$$\langle p^{\cdot} \rangle = V\ p\ \partial U_p/\partial r\ /\ (3\ U_p), \qquad (9.3.14)$$

over the whole (r,p) plane. The outflow of particles at the upper end

of the momentum range at radii $r < r_o$ could not occur if cosmic-ray particles lost momentum continuously at the adiabatic rate (7.1.6).

The relationship between the mean rate of change of momentum $\langle \dot{p} \rangle$ and the streaming is conveniently illustrated by plotting the flow lines in (r,p) space of the *average* particle. These are defined parametrically by Equations (7.6.8) and (7.6.9):

$$\frac{dr}{dt} = \langle \dot{r} \rangle = \frac{S_p}{U_p} = -\left(\frac{V\, p}{3} \frac{\partial F_o}{\partial p} + K(r,p) \frac{\partial F_o}{\partial r} \right) / F_o , \tag{9.3.15}$$

$$\frac{dp}{dt} = \langle \dot{p} \rangle = \frac{p\, V}{3F_o} \frac{\partial F_o}{\partial r} . \tag{9.3.16}$$

Alternatively eliminating time we obtain

$$\frac{dr}{dp} = \frac{\langle \dot{r} \rangle}{\langle \dot{p} \rangle} = -3\left(\frac{V\, p}{3} \frac{\partial F_o}{\partial p} + K(r,p) \frac{\partial F_o}{\partial r} \right) / \left(V\, p \frac{\partial F_o}{\partial r} \right) , \tag{9.3.17}$$

the direct equation of the flow line.

We now obtain the analytic solution of the flow line equation (9.3.17) for the monoenergetic solar source solution (9.1.3) with $r_o = 0$. Substituting the expression (9.1.3) for F_o in the flow line equations (9.3.15) and (9.3.16) we have

$$\frac{dr}{dt} = \frac{V\, u}{(n+1)} + \frac{K_o(p)\, p^{(3-3b)/2}\, u}{2\, T} , \tag{9.3.18}$$

$$\frac{dp}{dt} = \frac{-2\, V\, p}{3r} \frac{u}{(n+1)} , \tag{9.3.19}$$

where

$$u = x^2/(4T).$$

$$x = 2(r\, p^{3/2})^{(1-b)/2} / (1-b), \tag{9.3.20}$$

$$T = 3 \int_p^{p_o} K_o(z)\, z^{(1-3b)/2}\, dz / (2V).$$

Regarding u and T as independent variables and using the derivative transformations

$$\frac{dr}{dt} = \left(\frac{\partial r}{\partial u}\right)_T \frac{du}{dt} + \left(\frac{\partial r}{\partial T}\right)_u \frac{dT}{dt} ,$$

$$\frac{dp}{dt} = \left(\frac{\partial p}{\partial u}\right)_T \frac{du}{dt} + \left(\frac{\partial p}{\partial T}\right)_u \frac{dT}{dt} ,$$

$$\left(\frac{\partial r}{\partial u}\right)_T = \frac{(n+1)r}{2u} ,$$

$$\left(\frac{\partial r}{\partial T}\right)_u = \frac{(n+1)r}{2T} + \frac{V\, r}{K_o(p)\, p^{(3-3b)/2}} , \qquad (9.3.21)$$

$$\left(\frac{\partial p}{\partial u}\right)_T = 0,$$

$$\left(\frac{\partial p}{\partial T}\right)_u = \frac{-2V}{3\, K_o(p)\, p^{(1-3b)/2}} ,$$

(cf. Equations (8.3.11)) the flow line equations (9.3.18) and (9.3.19) become

$$\frac{dT}{dt} = K_o(p)\, p^{(3-3b)/2} \frac{u}{(n+1)r} , \qquad (9.3.22)$$

$$\frac{du}{dt} = 0, \qquad (9.3.23)$$

Dividing Equation (9.3.23) by (9.3.22) we obtain

$$\frac{du}{dT} = 0, \qquad (9.3.24)$$

as the flow line for monoenergetic solar cosmic-rays released from $r_o = 0$, and we note that it contains only u and T as variables.

The general solution of the flow line equation (9.3.24) is

$$u = \text{constant}, \tag{9.3.25}$$

a particularly simple result. The flow lines in (u,T) space are straight lines parallel to the T axis. In physically realistic cases, the integration constant of Equation (9.3.25) is positive.

We note particularly that these flow lines apply to the general case $K = K_o(p)\ r^b$, $b < 1$, and not just the case $K = K_c\ p\ r^b$. They may of course be expressed in terms of r and p and we do this next in particular cases to illustrate the general features.

For a diffusion coefficient $K = K_c\ p^a\ r^b$, $(a > 0,\ b < 1)$ we have

$$u = \frac{x^2}{4T} = \frac{2\delta}{3(1-b)^2}\ \frac{V\ r_e}{K(r_e,p_o)}\ \frac{[\ (r/r_e)\ (p/p_o)^{3/2}\ ]^{1-b}}{(1-\ (p/p_o)^{\delta})} \tag{9.3.26}$$

where

$$\delta = a + 3(1-b)/2,$$

and r_e is some fixed heliocentric radius. Using the results (9.3.26) in the flow line equation (9.3.25) we have

$$r/r_i = [(1-(p/p_o)^{\delta})/(1-(p_i/p_o)^{\delta})\ ]^{1/(1-b)}\ (p/p_i)^{-3/2}\ , \tag{9.3.27}$$

as the flow line passing through the point $(r_i,\ p_i)$ of position momentum space. An important and striking feature of the flow line (9.3.27) is that it is independent of the solar wind speed V and the diffusion coefficient constant K_c.

The flow lines (9.3.27) for a monoenergetic source located at $r_o = 0$ for the case $K = K_c\ p\ \sqrt{r}$ are shown in Figure 9.7 on a linear-linear scaling in the (r,p) plane. We have redrawn these flow lines

on a log-log scale in Figure 9.8 in order to emphasize the nature of the flow lines at low momenta.

The flow lines for a monoenergetic source located at radius $r_o \neq 0$, for the particular cases

(i) $K = K_c\ p\ r^{1.5}$ and $V\ r_o/K(r_o,p_o) = 1.46$,

(ii) $K = K_c\ p\ \sqrt{r}$ and $V\ r_o/K(r_o,p_o) = 0.4$,

are shown in Figures 9.9 and 9.10 respectively. These flow lines were obtained by substituting the expression (9.1.1) for F_o in the flow line differential equations (9.3.15) and (9.3.16) and numerically integrating the resultant differential equations as an initial value problem.

For $r_o \neq 0$ the flow lines of Figures 9.9 and 9.10 are of two main forms:

(i) those that circulate around the source, and

(ii) those that go outward from the source with p decreasing with increasing r.

As in the flow lines obtain for monoenergetic galactic cosmic rays , there is a critical curve separating the two forms (cf. Figure 8.7).

The general features in common of the flow lines of Figures 9.7 - 9.10 are:

(i) every flow line passes through the source point (r_o,p_o).

(ii) At low p/p_o, the flow lines are of the form

$$r\ p^{3/2} = \text{constant}.$$

As noted previously, this result is characteristic of the convective solution of the equation of transport. We note that for the case $K = K_c\ p\ \sqrt{r}$ and $r_o = 0$ the above features can be seen directly from

the analytic solution (9.3.27).

For the cases with $r_o \neq 0$, further loci which assist in assessing the structure of the flow lines are the locus of the minimum values of p/p_o along a flow line (when it exists) and the locus of the minimum values of r. The first is the locus $\langle \dot{p} \rangle = 0$, i.e. $\partial F_o/\partial r = 0$, and it corresponds to a maximum in the distribution function considered as a function of r, with p fixed. The second are the loci $\langle \dot{r} \rangle = 0$ or $S_p = 0$. The loci $\langle \dot{r} \rangle = 0$ and $\langle \dot{p} \rangle = 0$ are shown by broken lines on the flow line plots of Figures 9.9 and 9.10. These curves were obtained by substituting the expression (9.1.3) for F_o in the flow line equations (9.3.15) and (9.3.16) and solving the equations $\langle \dot{r} \rangle = 0$ and $\langle \dot{p} \rangle = 0$ numerically.

At large radii the flow lines of Figures 9.7 - 9.10 show that nearly all particles, on average are losing momentum as they stream outwards. For the cases where $K = K_c\, p \sqrt{r}$, all particles, are on average behaving in this manner (Figures 9.7, 9.8 and 9.10) but for the case $K = K_c\, p\, r^{1.5}$, displayed in Figure 9.9 there is a small proportion of low momentum particles which are, on average, gaining momentum and flowing inwards.

In contrast to the above results, the flow pattern for monoenergetic galactic cosmic-rays for the case $K = K_c\, p\, r^{1.5}$, $V\, r_e/K(r_e,p_o) = 0.1$, displayed in Figure 8.7, shows that at all radii, there are particles with momentum near $p = p_o$ which, on average, are gaining momentum as they stream outwards. In other respects the flow lines of Figure 8.7 are quite similar (particularly near $r = 0$) to the flow lines for a monenergetic source located at radius r_o ($r_o \neq 0$, $r_o \neq \infty$), for $K = K_c\, p\, r^{1.5}$ and $V\, r_o/K(r_o,p_o) = 1.46$ displayed in Figure 9.9.

To conclude this section we reiterate the comments about flow patterns made at the end of Section (8.3). The flow patterns show clearly the regions in (r,p) space of the inflow and outflow and momentum gains and losses of the *average* particles. The momentum gains occurring make the flow pattern variations explicable. We stress however that the flow lines represent the mean or *average* effects on the particles and *not* the path in (r,p) space of any individual particle. The individual particle paths in (r,p) space are random with some order (the average effects discussed here) superimposed.

FIGURES 9.1 - 9.10

Figure 9.1 - the momentum dependence of F_o, U_p and S_p for a monoenergetic source of particles of momentum p_o released from radius $r_o = 0$. The diffusion coefficient $K(r,p) = K_c\, p\, \sqrt{r}$ and the parameter $Vr/K(r,p_o)$ has values 0.001, 0.01, 0.1, 1.0 and 10.0. The functions

$$\overline{F}_o = \frac{r_s^2\, p_o^3\, V}{N}\, F_o,$$

$$\overline{U}_p = \frac{r_s^2\, p_o\, V}{N}\, U_p,$$

$$\overline{S}_p = \frac{r_s^2\, p_o}{N}\, S_p,$$

are dimensionless forms of F_o, U_p and S_p, and

$$r_s = \left[3K_c\, p_o^a \;/\; (2V\delta)\right]^{1/(1-b)},$$

is a characteristic length (see Equations (9.2.2)),

$a = 1$, $b = 0.5$, $\delta = 1.75$.

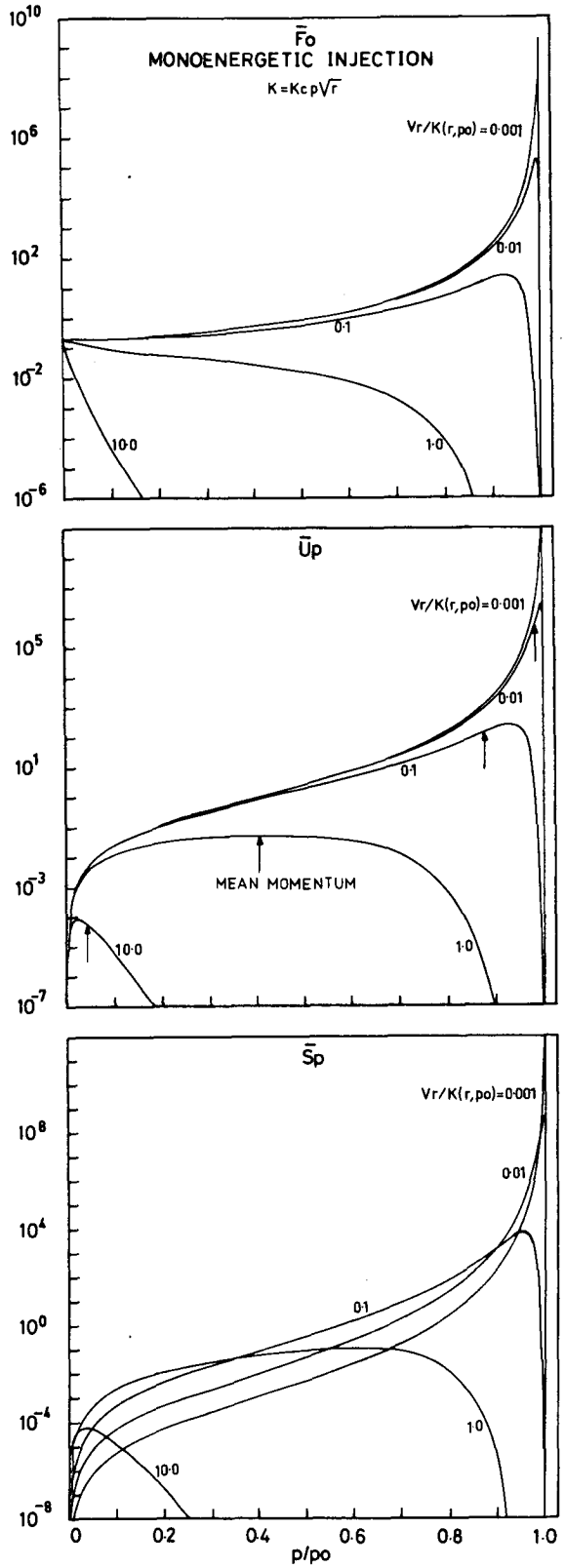
$\bar{F}o$
MONOENERGETIC INJECTION
$K = Kc\,p\sqrt{r}$
Vr/K(r,po) = 0·001
0·01
0·1
1·0
10·0
$\bar{U}p$
Vr/K(r,po)=0·001
0·01
0·1
MEAN MOMENTUM
1·0
10·0
$\bar{S}p$
Vr/K(r,po)=0·001
0·01
0·1
1·0
10·0
10^{10}
10^{6}
10^{2}
10^{-2}
10^{-6}
10^{5}
10^{1}
10^{-3}
10^{-7}
10^{8}
10^{4}
10^{0}
10^{-4}
10^{-8}
0
0·2
0·4
0·6
0·8
1·0
p/po

Figure 9.1

Figure 9.2 - The momentum dependence of F_o, U_p and S_p for a monenergetic source of particles of momentum p_o, released from radius $r_o (r_o \neq 0)$. The diffusion coefficient $K(r,p) = K_c\, p\, r^{1.5}$, the heliocentric radius variable $r/r_o = 214.95$, and the parameter $V\, r_o/K(r_o,p_o)$ has values 0.03, 0.3 and 3.0. The functions

$$\overline{F}_o = \frac{r_o^2\, p_o^3\, V}{N}\, F_o,$$

$$\overline{U}_p = \frac{r_o^2\, p_o\, V}{N}\, U_p,$$

$$\overline{S}_p = \frac{r_o^2\, p_o}{N}\, S_p,$$

are dimensionless forms of F_o, U_p and S_p.

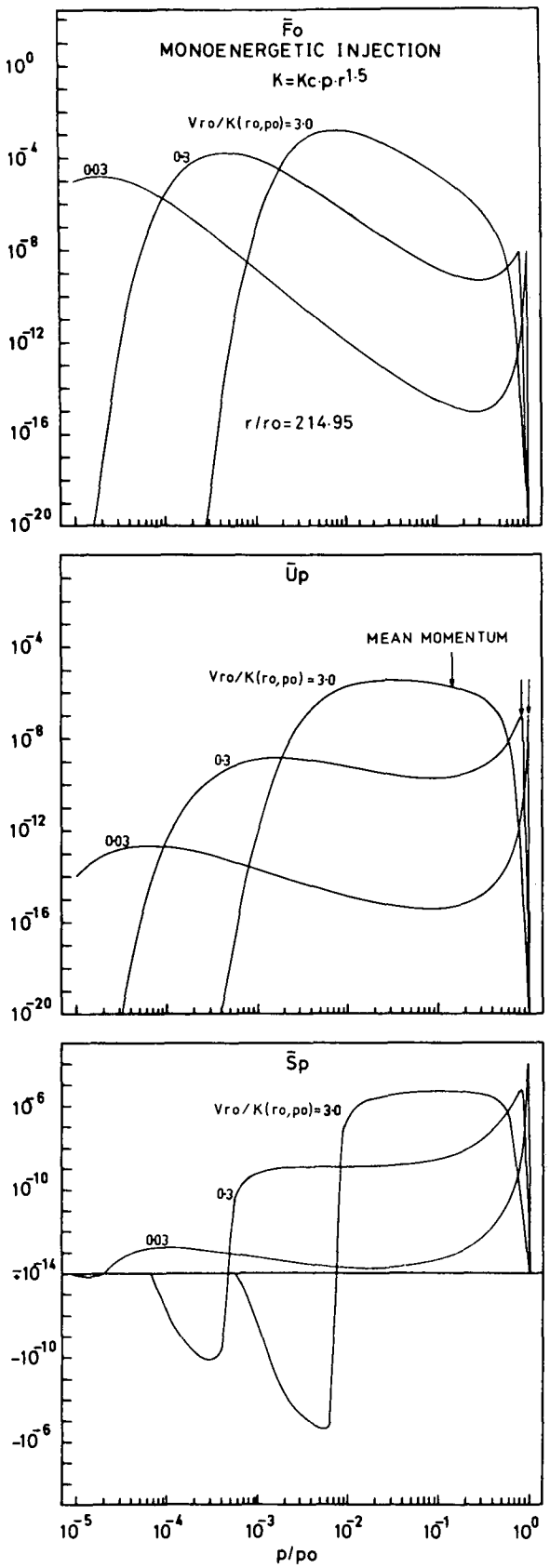
F̄o
MONOENERGETIC INJECTION
K=Kc·p·r^1.5
Vro/K(ro,po)=3·0
0·3
0·03
r/ro=214·95
Ūp
MEAN MOMENTUM
Vro/K(ro,po)=3·0
0·3
0·03
S̄p
Vro/K(ro,po)=3·0
0·3
0·03
p/po

Figure 9.2

Figure 9.3a - The momentum dependence of F_o, U_p and S_p for a monoenergetic source of particles of momentum p_o, released from radius $r_o (r_o \neq 0)$. The diffusion coefficient $K(r,p) = K_c\ p\ r^{1.5}$, $V\ r_o/K(r_o,p_o) = 1.46$, and the heliocentric radius variable r/r_o has values 1, 2, 100 and 1000. The functions

$$\overline{F}_o = \frac{r_o^2\ p_o^3\ V}{N}\ F_o,$$

$$\overline{U}_p = \frac{r_o^2\ p_o\ V}{N}\ U_p,$$

$$\overline{S}_p = \frac{r_o^2\ p_o}{N}\ S_p,$$

are dimensionless forms of F_o, U_p and S_p.

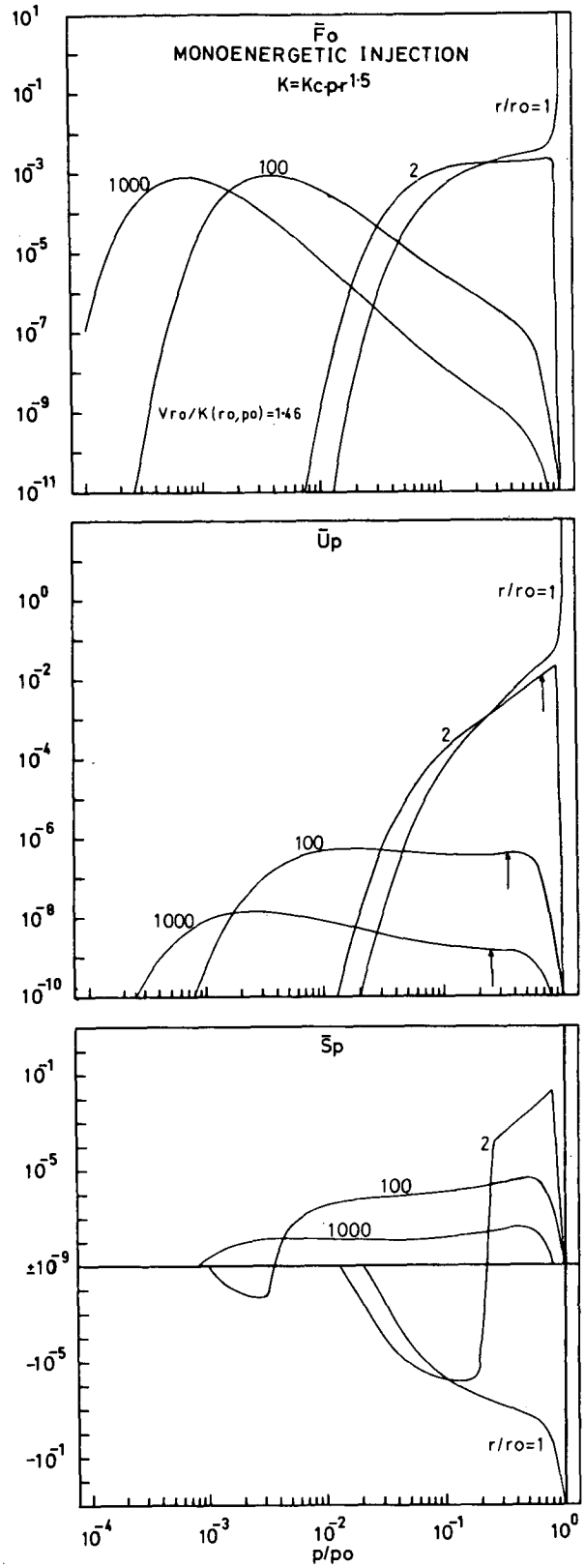
F̄o
MONOENERGETIC INJECTION
K=Kc·pr^1.5
r/ro=1
1000
100
2
Vro/K(ro,po)=1·46
Ūp
r/ro=1
2
100
1000
S̄p
2
100
1000
r/ro=1
p/po

Figure 9.3a

Figure 9.3b - The momentum dependence of F_o, U_p and S_p for a monoenergetic source of particles of momentum p_o, released from radius $r_o (r_o \neq 0)$. The diffusion coefficient $K(r,p) = K_c\, p\, r^{1.5}$, $Vr_o/K(r_o,p_o) = 0.1$, and the heliocentric distance variable r/r_o has values, 1, 2, 100 and 1000. The functions

$$\overline{F}_o = \frac{r_o^2\, p_o^3\, V}{N} F_o,$$

$$\overline{U}_p = \frac{r_o^2\, p_o\, V}{N} U_p,$$

$$\overline{S}_p = \frac{r_o^2\, p_o}{N} S_p,$$

are dimensionless forms of F_o, U_p and S_p.

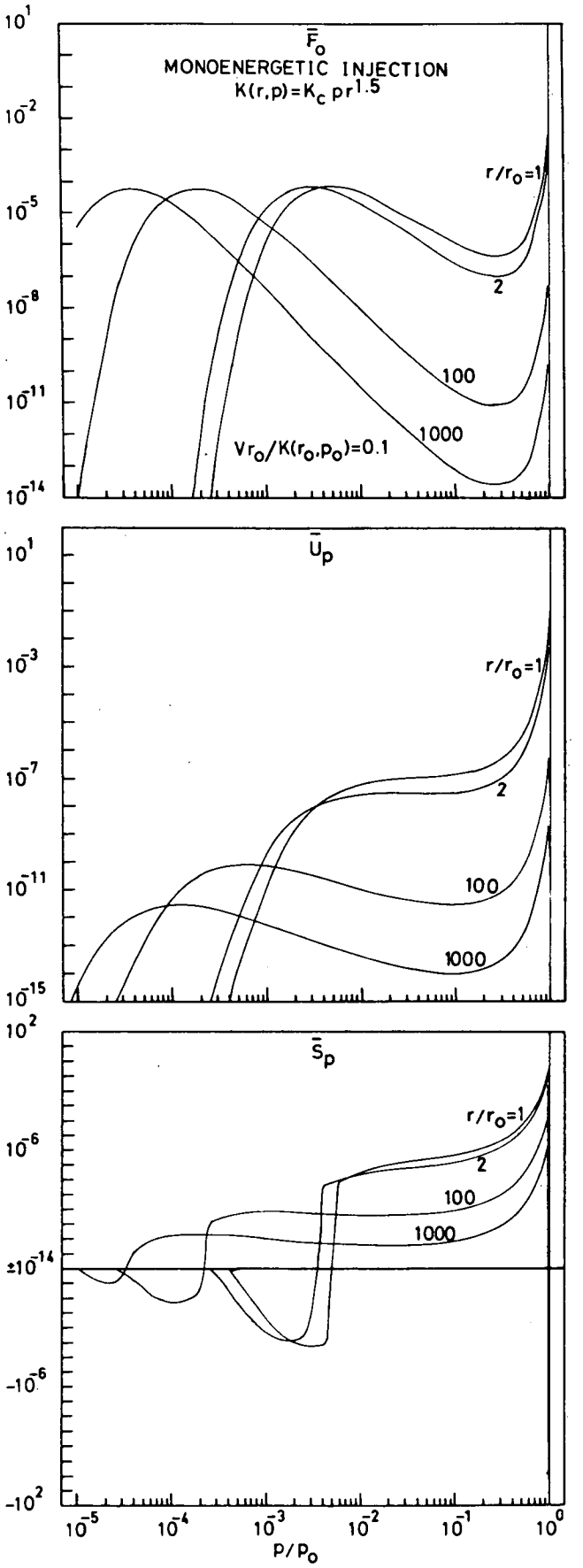
$\bar{F}_o$
MONOENERGETIC INJECTION
$K(r,p)=K_c\, p r^{1.5}$
$r/r_o=1$
2
100
1000
$Vr_o/K(r_o,p_o)=0.1$
$\bar{U}_p$
$r/r_o=1$
2
100
1000
$\bar{S}_p$
$r/r_o=1$
2
100
1000
10^{1}
10^{-2}
10^{-5}
10^{-8}
10^{-11}
10^{-14}
10^{-3}
10^{-7}
10^{-11}
10^{-15}
10^{2}
10^{-6}
$\pm 10^{-14}$
-10^{-6}
-10^{2}
10^{-5}
10^{-4}
10^{-3}
10^{-2}
10^{-1}
10^{0}
p/p_o

Figure 9.3b

Figure 9.4a - Contours in the (r,p) plane of the characteristics of a monoenergetic source of particles of momentum p_o released from heliocentric radius $r_o = 0$. The figure is drawn for a diffusion coefficient $K(r,p) = K_c\ p\ \sqrt{r}$, and the parameter $V\ r_e/K(r_e,p_o) = 0.1$, where r_e is some fixed heliocentric radius. Shown (in dimensionless form) are

(a) the mean distribution function F_o,
(b) the differential number density $U_p = 4\ \pi\ p^2\ F_o$,
(c) the radial gradient $G_r = (1/U_p)(\partial U_p/\partial r)$,
(d) the radial differential current density S_p, and its convective and diffusive components S_c and S_d, i.e.,

$$S_c = -\ 4\ \pi\ p^3\ (V/3)\ \partial F_o/\partial p,$$

$$S_d = -\ 4\ \pi\ p^2\ K(r,p)\ \partial F_o/\partial r,$$

$$S_p = S_c + S_d.$$

Here

$$\overline{F}_o = (r_s^2\ p_o^3\ V/N)\ F_o,$$

$$\overline{U}_p = (r_s^2\ p_o\ V/N)\ U_p,$$

$$\text{Grad}\ (\log(U_p)) = \alpha\ r_s\ G_r,$$

$$\overline{S}_c = (r_s^2\ p_o/N)\ S_c,$$

$$\overline{S}_d = (r_s^2\ p_o/N)\ S_d,$$

$$\overline{S}_p = \overline{S}_c + \overline{S}_d = (r_s^2\ p_o/N)\ S_p;$$

$$r_s = [3\ K_c\ p_o^a\ /(2V\delta)]^{\ 1/(1-b)},$$

is a characteristic length (Equation (9.2.2)), and

$$a = 1,\quad b = 0.5,\quad \delta = 1.75,\quad \alpha = 36/49.$$

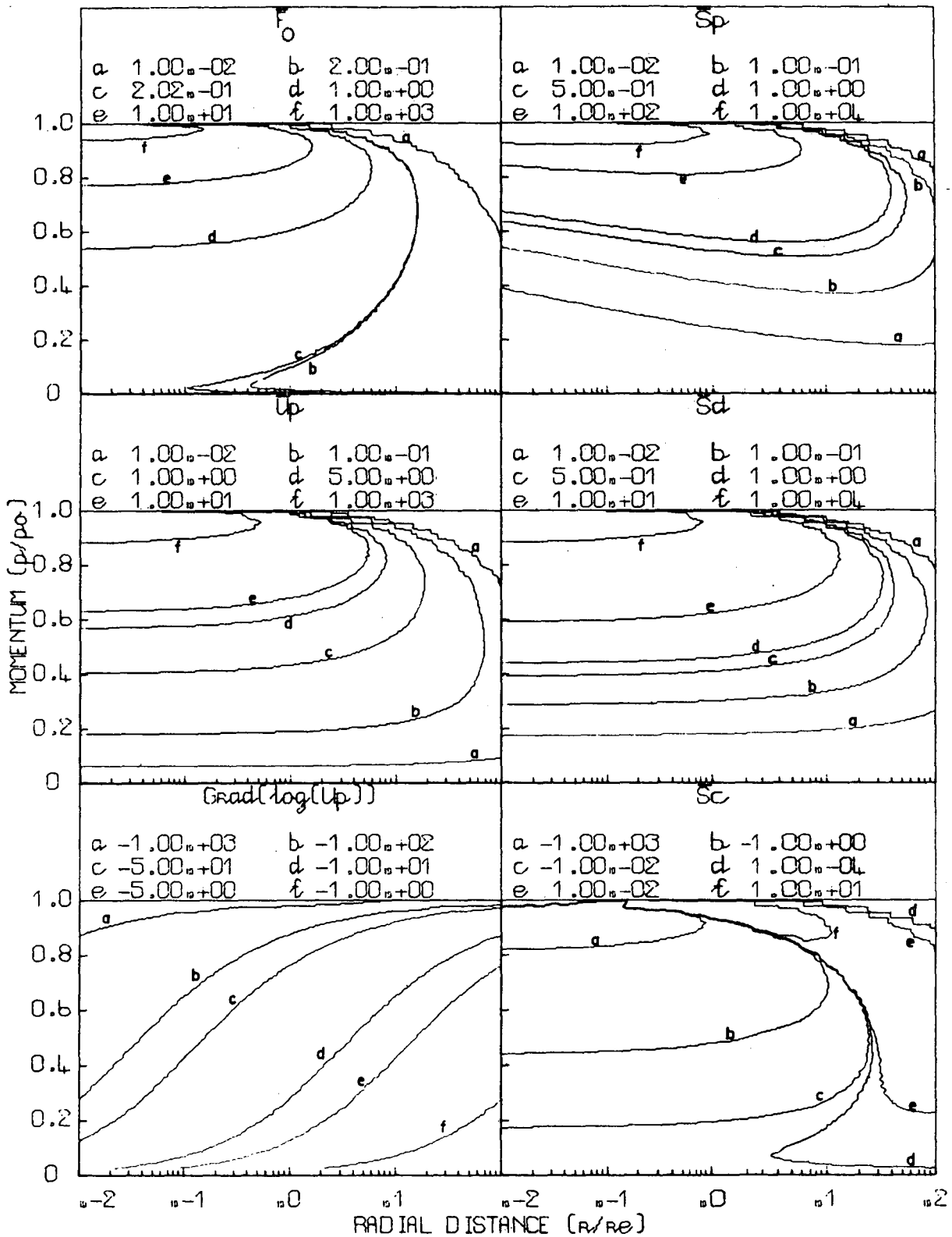
Fo
a 1.00E-02 b 2.00E-01
c 2.02E-01 d 1.00E+00
e 1.00E+01 f 1.00E+03
Sp
a 1.00E-02 b 1.00E-01
c 5.00E-01 d 1.00E+00
e 1.00E+02 f 1.00E+04
Up
a 1.00E-02 b 1.00E-01
c 1.00E+00 d 5.00E+00
e 1.00E+01 f 1.00E+03
Sd
a 1.00E-02 b 1.00E-01
c 5.00E-01 d 1.00E+00
e 1.00E+01 f 1.00E+04
Grad[log(Up)]
a -1.00E+03 b -1.00E+02
c -5.00E+01 d -1.00E+01
e -5.00E+00 f -1.00E+00
Sc
a -1.00E+03 b -1.00E+00
c -1.00E-02 d 1.00E-04
e 1.00E-02 f 1.00E+01
MOMENTUM (p/po)
RADIAL DISTANCE (R/Re)
0
0.2
0.4
0.6
0.8
1.0
E-2
E-1
E0
E1
E2

Figure 9.4a

Figure 9.4b - Contours in the (r,p) plane of the characteristics of a monoenergetic source of particles of momentum p_o released from heliocentric radius $r_o = 0$. The figure is drawn for a diffusion coefficient $K(r,p) = K_c\ p\ \sqrt{r}$, and the parameter $V\ r_e/K(r_e,p_o) = 0.1$, where r_e is some fixed heliocentric radius. Shown are:

(e) the ratio of the bulk flow speed $\langle \dot{r} \rangle$ to the solar wind speed V, i.e., $dR/dt = S_p/(V\ U_p)$, and the related component quantities $S_d/(V\ U_p)$, and the Compton-Getting factor $C = S_c/(V\ U_p)$,

(f) the time average rate of change of momentum $\langle \dot{p} \rangle$, expressed in dimensionless form, i.e.,

$$dp/dt = (\alpha\ r_s/(V\ p_o)\ \langle \dot{p} \rangle = [\alpha\ r_s\ p/(3\ p_o)]\ G_r$$

where G_r is the radial gradient,

(g) the ratio of $\langle \dot{p} \rangle$ and the adiabatic deceleration rate

$$\langle \dot{p} \rangle_{ad} = -2\ V\ p/\ (3\ r),$$

i.e.,

$$(dp/dt)/(dp/dt)\ ad = \langle \dot{p} \rangle\ /\langle \dot{p} \rangle_{ad}\ .$$

As in Figure (9.4a)

$$r_s = [3\ K_c\ p_o^a\ /\ (2V\delta)]^{1/(1-b)},$$

is a characteristic length and

$$a = 1,\quad b = 0.5,\quad \delta = 1.75,\quad \alpha = 36/49.$$

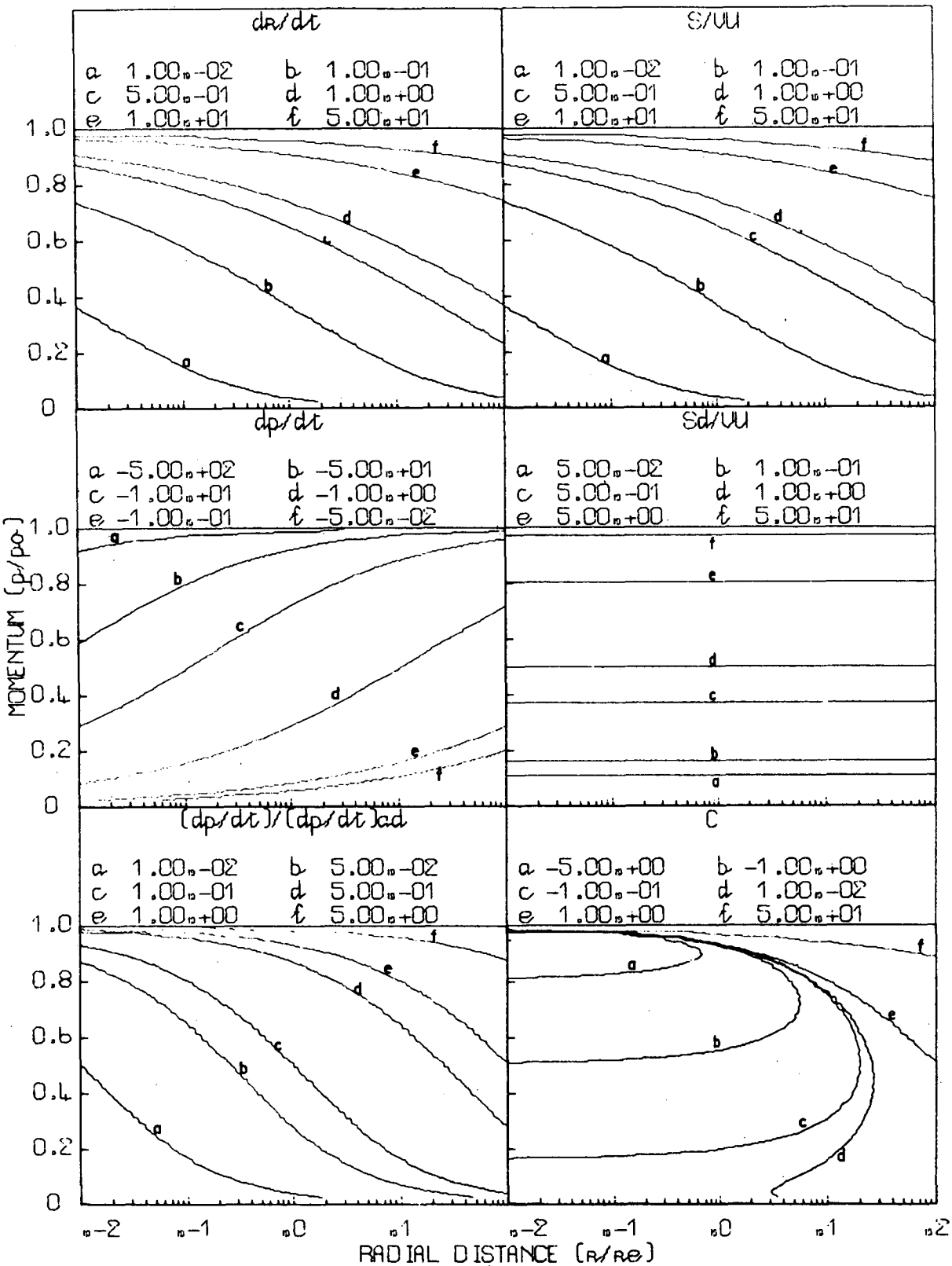
dR/dt
a 1.00E-02 b 1.00E-01
c 5.00E-01 d 1.00E+00
e 1.00E+01 f 5.00E+01
S/UU
a 1.00E-02 b 1.00E-01
c 5.00E-01 d 1.00E+00
e 1.00E+01 f 5.00E+01
dp/dt
a -5.00E+02 b -5.00E+01
c -1.00E+01 d -1.00E+00
e -1.00E-01 f -5.00E-02
Sd/UU
a 5.00E-02 b 1.00E-01
c 5.00E-01 d 1.00E+00
e 5.00E+00 f 5.00E+01
(dp/dt)/(dp/dt)ad
a 1.00E-02 b 5.00E-02
c 1.00E-01 d 5.00E-01
e 1.00E+00 f 5.00E+00
C
a -5.00E+00 b -1.00E+00
c -1.00E-01 d 1.00E-02
e 1.00E+00 f 5.00E+01
MOMENTUM (p/po)
1.0
0.8
0.6
0.4
0.2
0
E-2
E-1
E0
E1
E2
RADIAL DISTANCE (R/Re)

Figure 9.4b

Figure 9.5a - Contours in the (r,p) plane of the characteristics of a monoenergetic source of particles of momentum p_o released from heliocentric radius r_o ($r_o \neq 0$). The figure is drawn for a diffusion coefficient $K(r,p) = K_c\ p\ r^{1.5}$ and the parameter $V\ r_o/K(r_o,p_o) = 1.46$. Shown (in dimensionless form) are :

(a) the distribution function F_o,
(b) the differential number density $U_p = 4\ \pi\ p^2\ F_o$,
(c) the radial gradient $G_r = (1/U_p)(\partial U_p/\partial r)$,
(d) the differential current density S_p, and its convective and diffusive components, i.e.,

$$S_c = -\ 4\ \pi\ p^3\ (V/3)\ \partial F_o/\partial p\ ,$$

$$S_d = -\ 4\ \pi\ p^2\ K(r,p)\ \partial F_o/\partial r,$$

$$S_p = S_c + S_d.$$

Here

$$\overline{F}_o = (r_o^2\ p_o^3\ V/N)\ F_o,$$

$$\overline{U}_p = (r_o^2\ p_o\ V/N)\ U_p,$$

$$\text{Grad}\ (\log\ (U_p)) = r_o\ G_r,$$

$$\overline{S}_c = (r_o^2\ p_o/N)\ S_c,$$

$$\overline{S}_d = (r_o^2\ p_o/N)\ S_d,$$

$$\overline{S}_p = \overline{S}_c + \overline{S}_d = (r_o^2\ p_o/N)\ S_p.$$

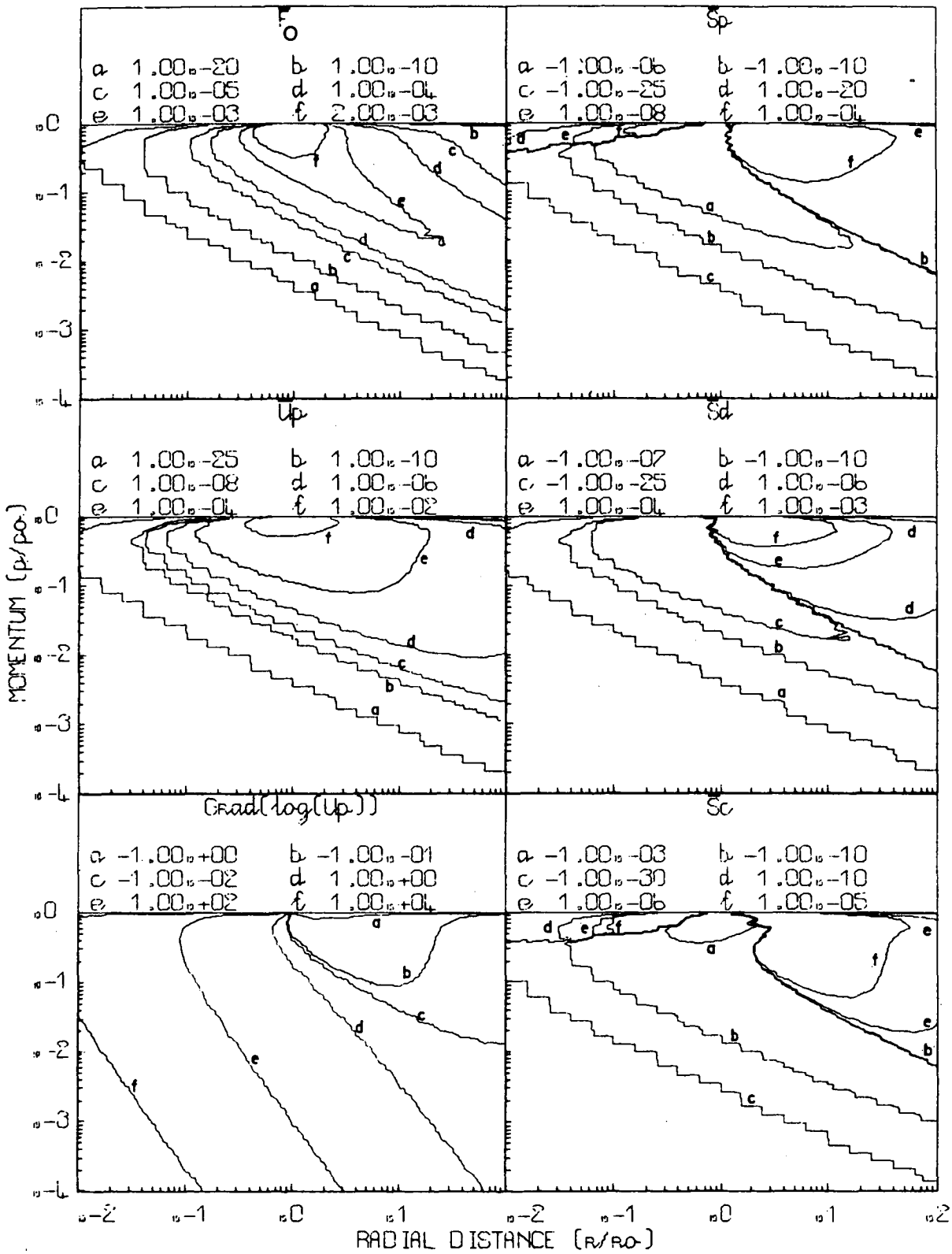
Fo
a 1.00E-20 b 1.00E-10
c 1.00E-05 d 1.00E-04
e 1.00E-03 f 2.00E-03
Sp
a -1.00E-06 b -1.00E-10
c -1.00E-25 d 1.00E-20
e 1.00E-08 f 1.00E-04
Up
a 1.00E-25 b 1.00E-10
c 1.00E-08 d 1.00E-06
e 1.00E-04 f 1.00E-02
Sd
a -1.00E-07 b -1.00E-10
c -1.00E-25 d 1.00E-06
e 1.00E-04 f 1.00E-03
Grad(log(Up))
a -1.00E+00 b -1.00E-01
c -1.00E-02 d 1.00E+00
e 1.00E+02 f 1.00E+04
Sc
a -1.00E-03 b -1.00E-10
c -1.00E-30 d 1.00E-10
e 1.00E-06 f 1.00E-05
MOMENTUM (p/po)
RADIAL DISTANCE (R/Ro)

Figure 9.5a

Figure 9.5b - Contours in the (r,p) plane of the characteristics of a monoenergetic source of particles of momentum p_o released from heliocentric radius r_o ($r_o \neq 0$). The figure is drawn for a diffusion coefficient $K(r,p) = K_c\ p\ r^{1.5}$, and the parameter $V\ r_o/K(r_o,p_o) = 1.46$. Shown are :

(e) the ratio of the bulk flow speed $\langle \dot{r} \rangle$ to the solar wind speed V, i.e., $dR/dt = S_p/(V\ U_p)$, and the related component quantities $S_d/(V\ U_p)$, and the Compton-Getting factor $C = S_c/\ V\ U_p$,

(g) the time average rate of change of momentum $\langle \dot{p} \rangle$, expressed in dimensionless form, i.e.

$$dp/dt = [r_o/(V\ p_o)]\ \langle \dot{p} \rangle = [r_o\ p/(3p_o)]\ G_r,$$

where G_r is the radial gradient,

(g) the ratio

$$(dp/dt)\ /\ (dp/dt)_{ad} = \langle \dot{p} \rangle\ /\ \langle \dot{p} \rangle_{ad}\ ,$$

where

$$\langle \dot{p} \rangle_{ad} = -\ 2\ V\ p/(3r),$$

is the adiabatic deceleration rate.

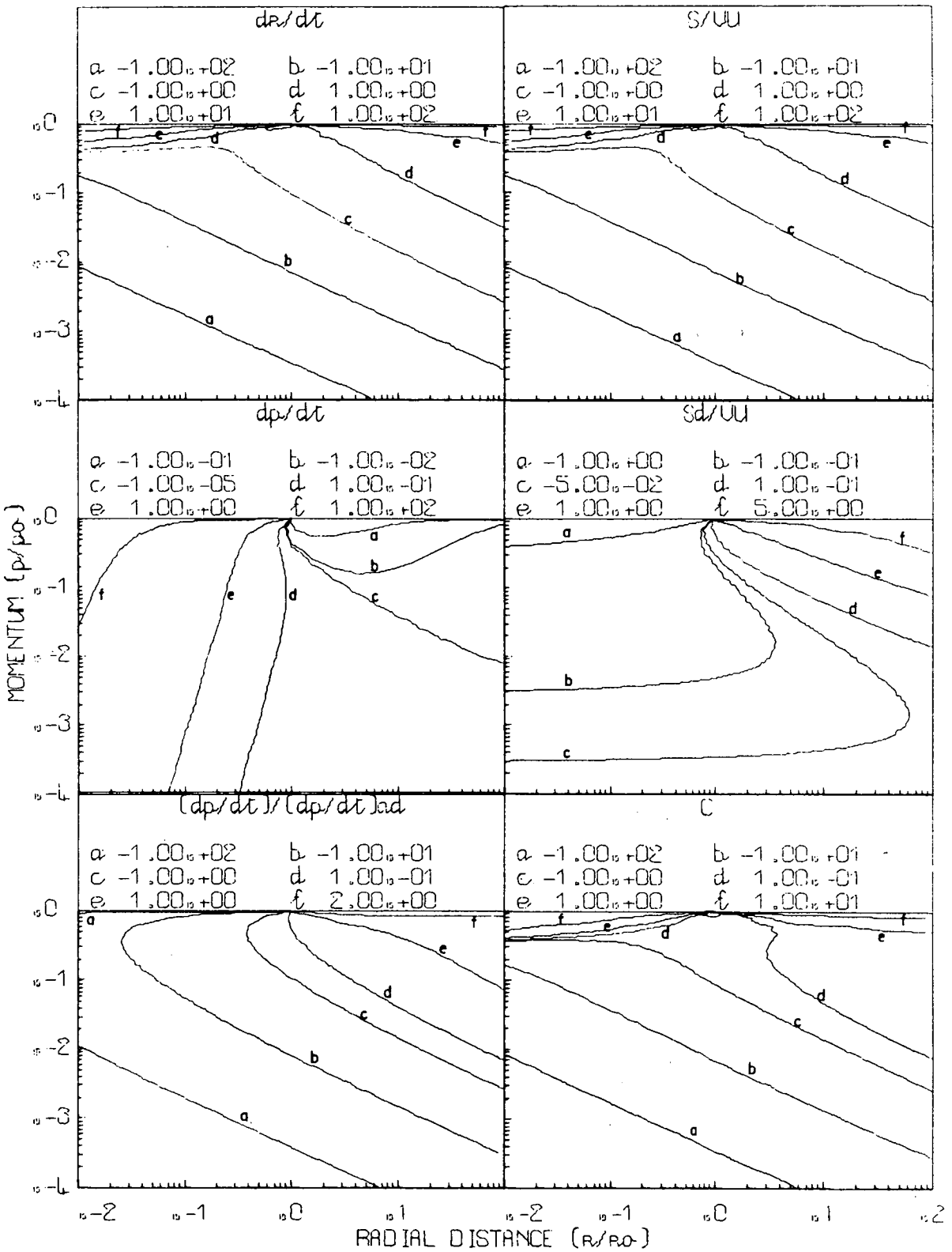
dR/dt
S/UU
dp/dt
Sd/UU
(dp/dt)/(dp/dt)ad
C
MOMENTUM (p/ρo)
RADIAL DISTANCE (R/Ro)

Figure 9.5b

Figures 9.6 - show schematically the differential current density S_p in the (r,p) plane for three different models, in which particles of momentum p_o are released monoenergetically from heliocentric radius r_o. The models are specified by the position of the source ($r_o = 0$ or $r_o \neq 0$), the diffusion coefficient K(r,p), and in cases (b) and (c) by the dimensionless parameter $V\ r_o/K(r_o,p_o)$. The figures are drawn for the cases:

(a) $r_o = 0$, $K(r,p) = K_o(p)\ r^b$, $b < 1$, where $K_o(p)$ is an arbitrary function of momentum p;

(b) $r_o \neq 0$, $K(r,p) = K_c\ p\ r^{1.5}$, $V\ r_o/K(r_o,p_o) = 1.46$;

(c) $r_o \neq 0$, $K(r,p) = K_c\ p\ \sqrt{r}$, $V\ r_o/K(r_o,p_o) = 0.4$.

The arrows represent the direction of S_p.

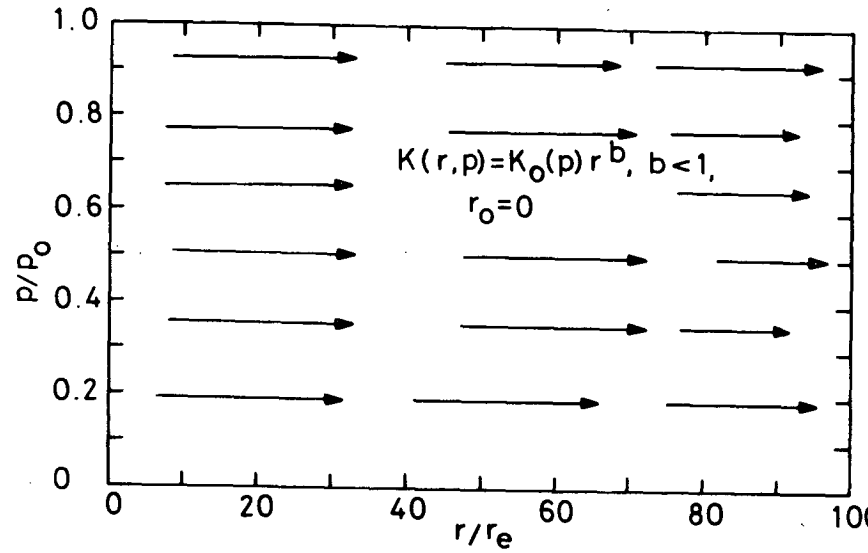

Figure 9.6a

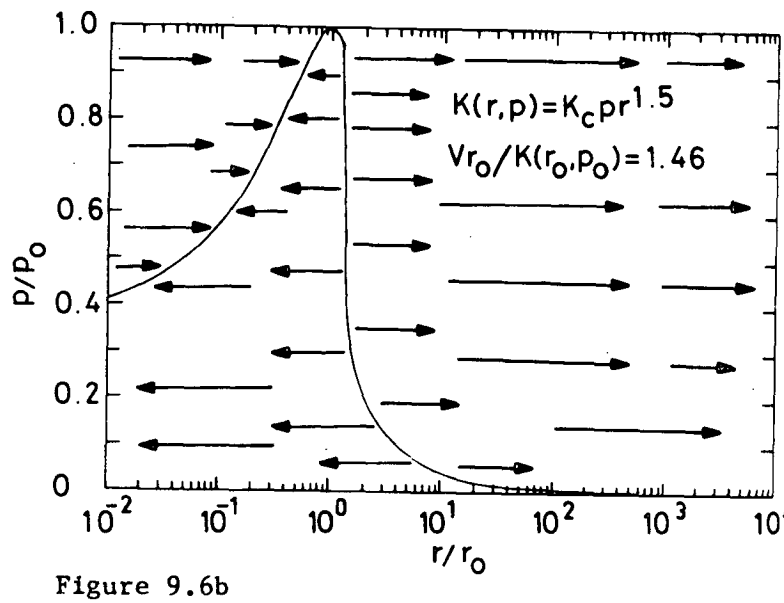

Figure 9.6b

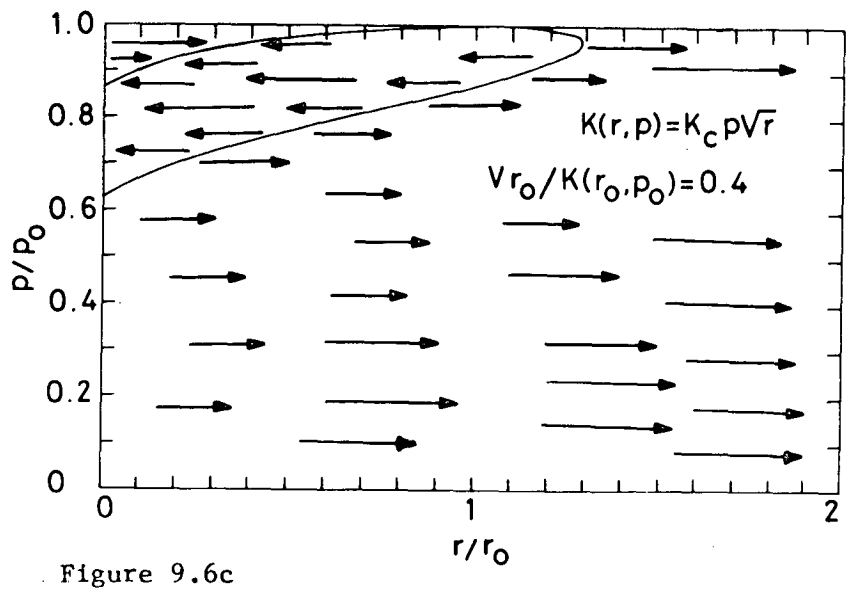

Figure 9.6c

Figure 9.7 - Flow lines in the (r,p) plane for a monoenergetic source of particles of momentum p_o, released at a steady rate from the source point $r_o = 0$. The diagram is drawn on a log-linear scaling, for the particular case where the diffusion coefficient $K(r,p) = K_c\ p\ \sqrt{r}$, and r_e is some fixed heliocentric radius.

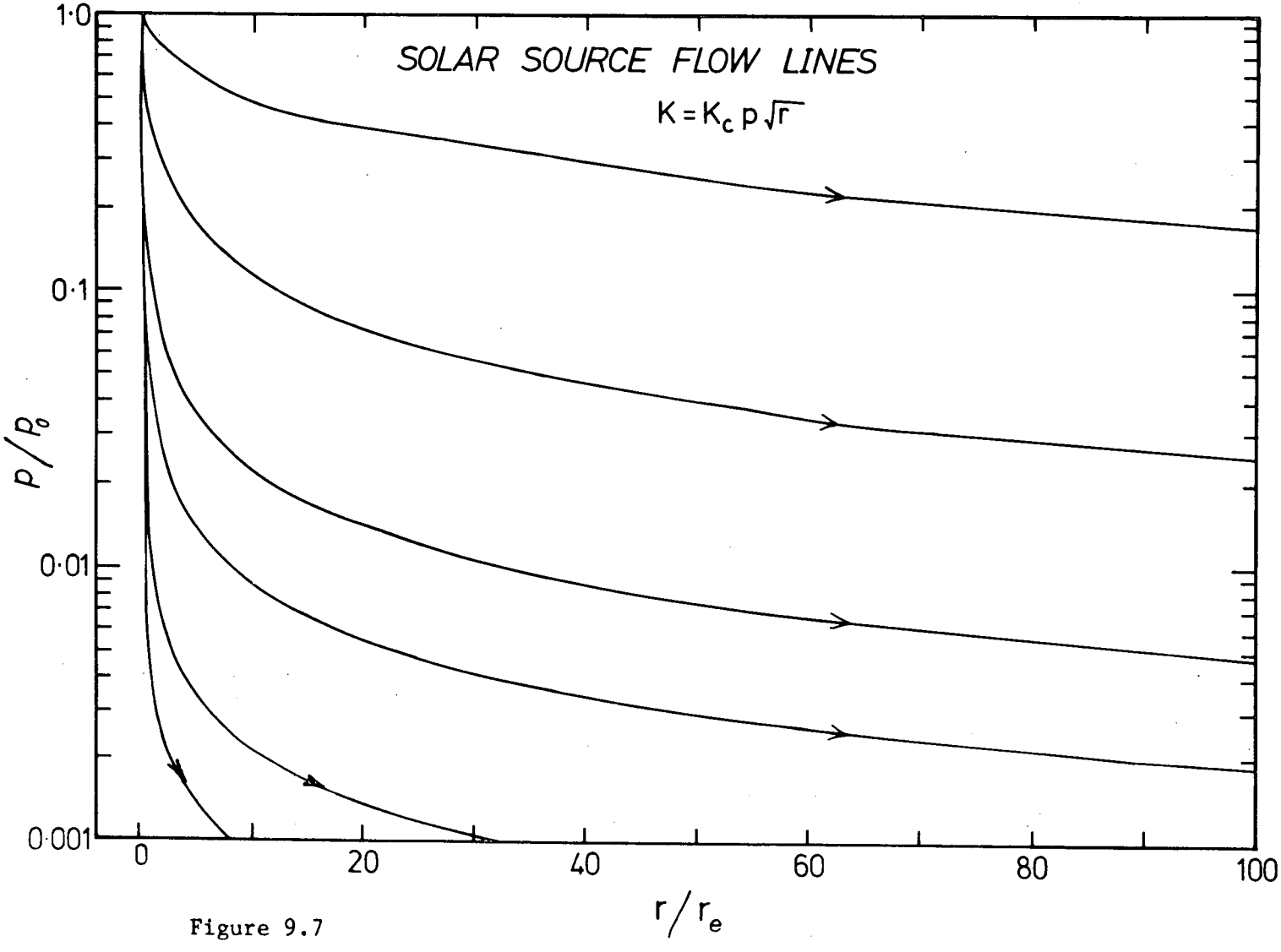
SOLAR SOURCE FLOW LINES
K = K_c p √r
1·0
0·1
0·01
0·001
p/p_o
0
20
40
60
80
100
r/r_e

Figure 9.7

Figure 9.8 - Flow lines in the (r,p) plane for a monoenergetic source of particles of momentum p_o released at a steady rate from the source point $r_o = 0$. The diagram is drawn on a log-log scaling for the particular case where the diffusion coefficient $K(r,p) = K_c\ p\sqrt{r}$, and r_e is some fixed heliocentric radius.

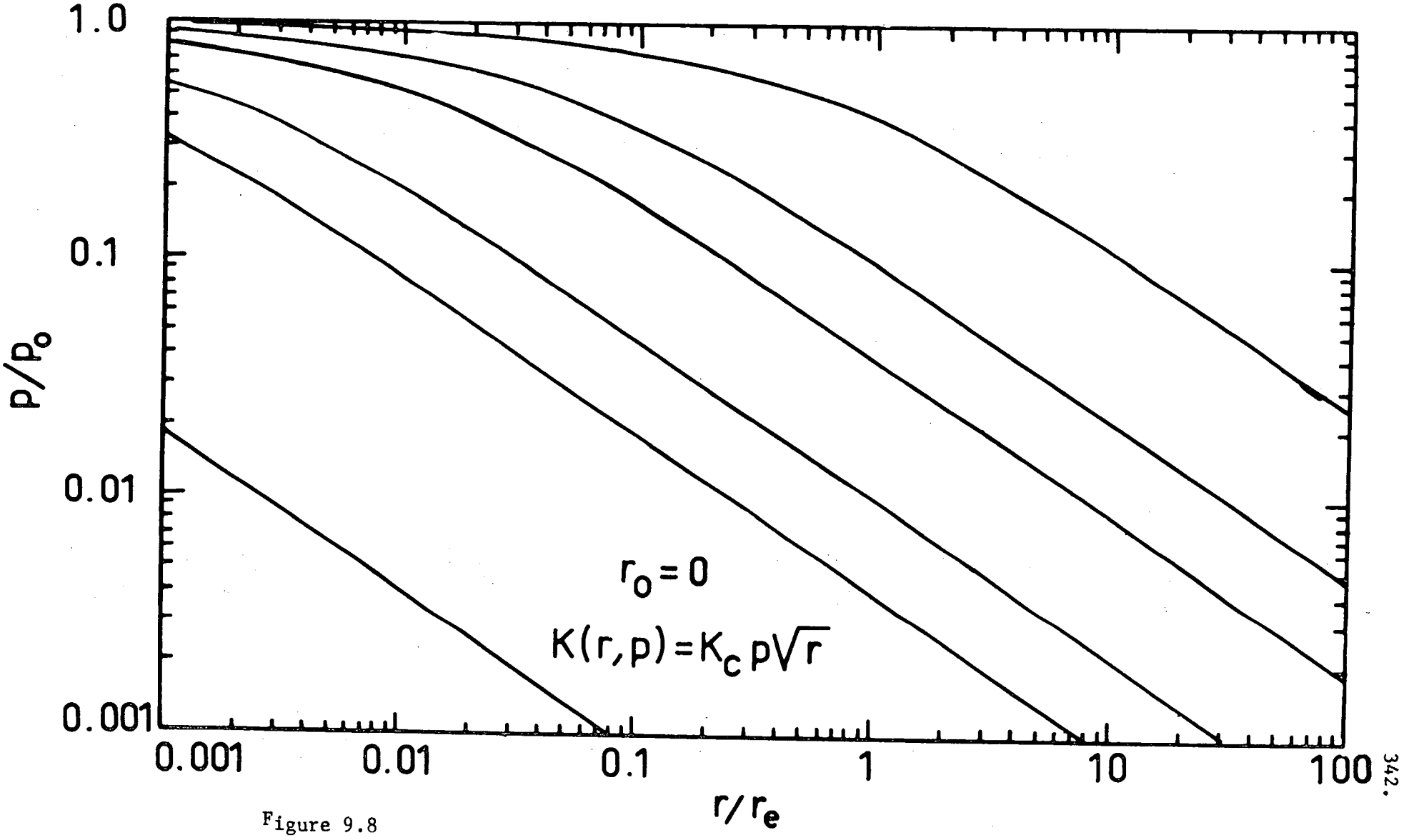

Figure 9.8

Figure 9.9 - Flow lines in the (r,p) plane for a monenergetic source of particles of momentum p_o, released at a steady rate from a spherical surface at heliocentric radius r_o ($r_o \neq 0$). The diagram is drawn for a diffusion coefficient $K(r,p) = K_c\ p\ r^{1.5}$ and $V\ r_o/K(r_o,p_o) = 1.46$. The flow lines are indicated by the full curves, whereas the loci $\langle \dot{r} \rangle = 0$ and $\langle \dot{p} \rangle = 0$ are indicated by broken curves.

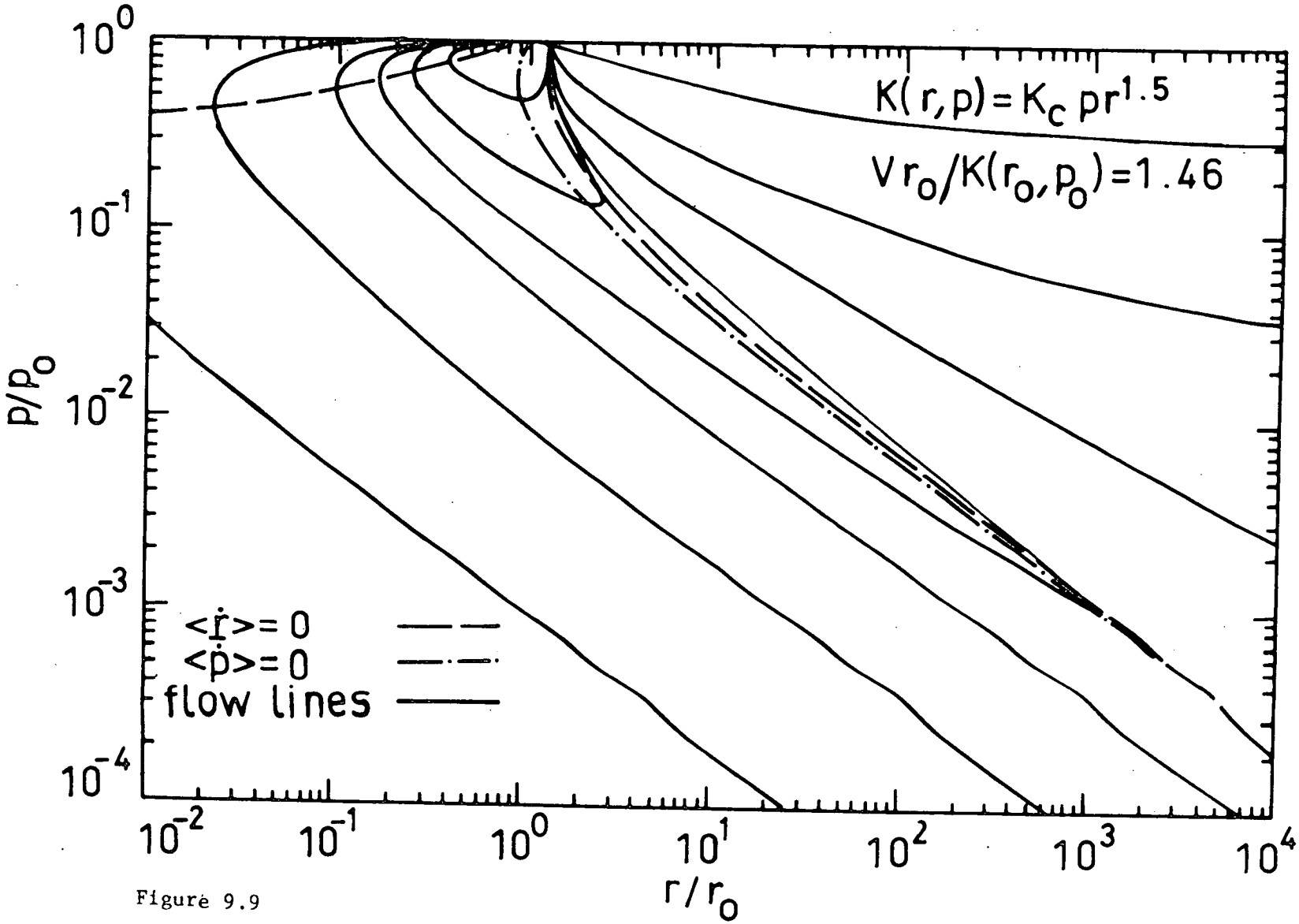
10^0
10^{-1}
10^{-2}
10^{-3}
10^{-4}
p/p_o
$K(r,p)=K_c\, p r^{1.5}$
$V r_o/K(r_o,p_o)=1.46$
$\langle \dot{r} \rangle = 0$
$\langle \dot{p} \rangle = 0$
flow lines
10^{-2}
10^{-1}
10^{0}
10^{1}
10^{2}
10^{3}
10^{4}
r/r_o

Figure 9.9

Figure 9.10 - Flow lines in the (r,p) plane for a monoenergetic source of particles of momentum p_o, released at a steady rate from a spherical surface at heliocentric radius r_o ($r_o \neq 0$). The figure is drawn for a diffusion coefficient $K(r,p) = K_c\, p\, \sqrt{r}$ and $V\, r_o/K(r_o,p_o) = 0.4$. The flow lines are indicated by the full curves, whereas the loci $\langle \dot{r} \rangle = 0$ and $\langle \dot{p} \rangle = 0$ are indicated by broken curves.

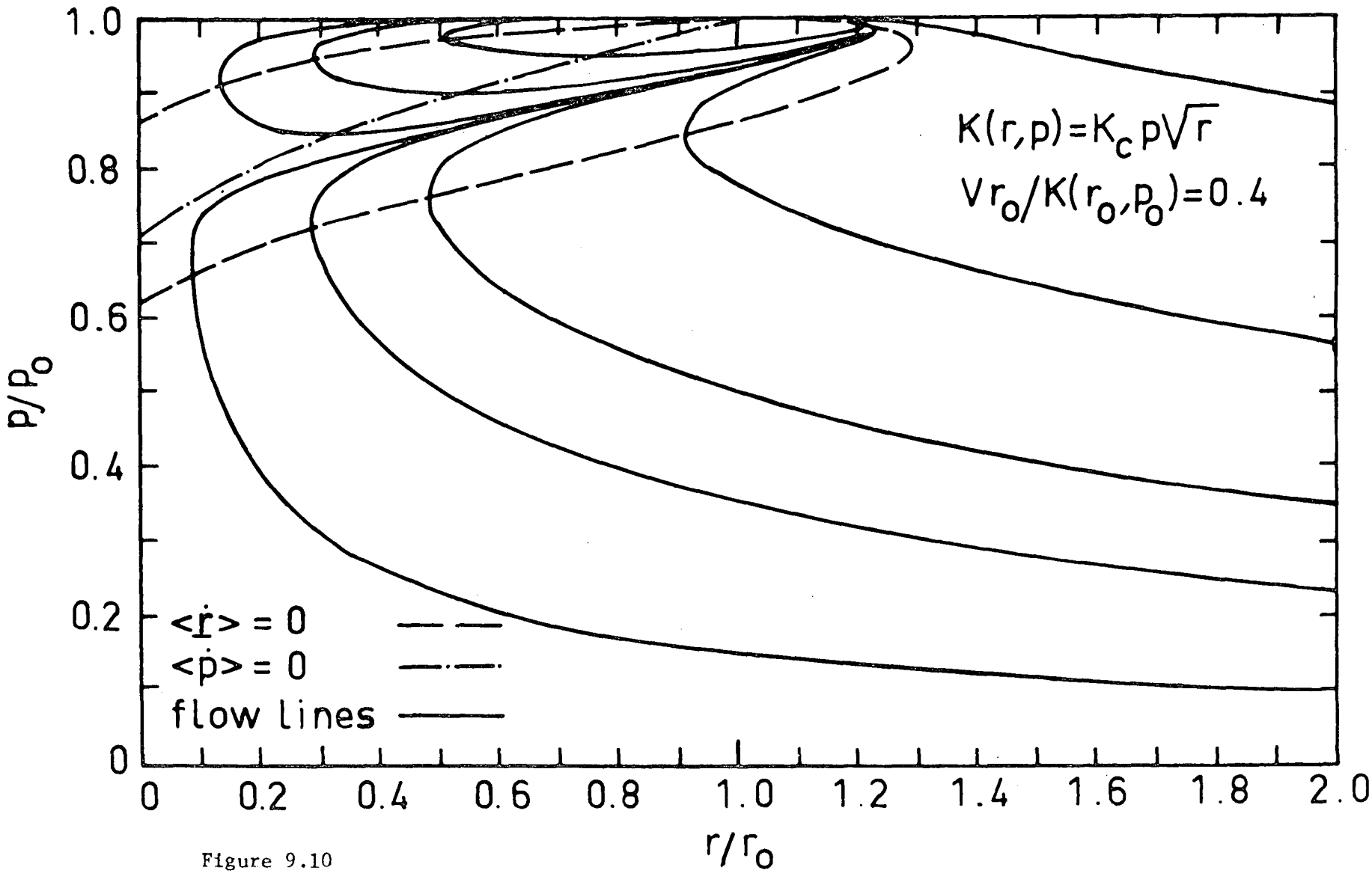
1.0
0.8
0.6
0.4
0.2
0
p/p_o
0
0.2
0.4
0.6
0.8
1.0
1.2
1.4
1.6
1.8
2.0
r/r_o
K(r,p)=K_c p√r
Vr_o/K(r_o,p_o)=0.4
<ṙ> = 0
<ṗ> = 0
flow lines

Figure 9.10

CHAPTER 10

A FREE ESCAPE BOUNDARY SOLUTION

10.1 Introduction

In this chapter we study the steady state propagation, within the solar cavity of monoenergetic galactic cosmic rays, in a model having a free escape boundary at $r = r_b$. In this problem the differential number density U_p satisfies the boundary conditions

$$\text{(i)} \quad U_p \to N_g \, \delta(p-p_o) \quad \text{as} \quad r \to r_b, \qquad (10.1.1)$$

$$\text{(ii)} \quad U_p \text{ is finite as } r \to 0,$$

and in the region $r > r_b$ the diffusion coefficient $K \to \infty$, corresponding to free escape conditions.

The solution differs from the previous cases of Chapter (8), where we considered the propagation of galactic cosmic-rays with a boundary at infinity. In general it is given by an eigenfunction expansion as outlined in Chapter (6). We recall from Chapter (6), that we could only obtain solutions with finite boundaries for cases where the diffusion coefficient $K(r,p)$ has one of the forms

$$\text{(i)} \quad K = K_c \, r^b,$$

$$\text{(ii)} \quad K = K_c \, r^b \, p^{3(b-1)/4},$$

and the solar wind speed V is assumed to be constant.

The evaluation of the finite boundary solution is in general much more complex than the case where the boundary is at infinity. If the eigenspectrum in the solution is discrete it is necessary to evaluate the eigenvalues and eigenfunctions and then sum an appropriately weighted series of eigenfunctions. However if the eigenspectrum is

continuous the solution is given by an integral over the continuous range of eigenvalues. In the former case the terms of the eigenfunction series decrease with increasing eigenvalue λ_n and the series is in general slowly convergent for p near p_o. For a continuous eigenspectrum, the evaluation of the integral can be quite difficult, particularly when the integral is highly oscillatory and there is an infinite range of eigenvalues.

We consider the case where the diffusion coefficient $K = K_c\, r^b\, p^{3(b-1)/4}$, with b = 7/3 i.e., $K = K_c\, p\, r^{7/3}$. The solution of the boundary value problem (10.1.1) for this type of diffusion coefficient is given by a semi-finite integral, corresponding to a continuous eigenspectrum. It has been derived, in detail in Chapter (6) and using the result (6.4.4), the solution, expressed in terms of $F_o(r,p)$ and valid for $0 < r < r_b$, $0 < p < p_o$ is

$$F_o(r,p) = \frac{N_g}{2\pi^2\, p_o^3}\, \frac{\zeta^{5/2}\, \mu^{-3/2}}{\eta}\, \exp\,[\eta(1-\zeta^2/\mu)/4\,]$$

$$\int_0^\infty s\, \exp\,[-s^2(1-\mu)/\eta]\, [J_{5/2}(s)Y_{5/2}(s\zeta) - J_{5/2}(s\zeta)Y_{5/2}(s)]/$$

$$[J^2_{5/2}(s) + Y^2_{5/2}(s)]\, ds, \qquad (10.1.2)$$

where

$$\mu = p/p_o,$$

$$\eta = 3\,(V\, r_b/K(r_b,p_o))/2,$$

$$\zeta = (r/r_b)^{-2/3},$$

and $J_{5/2}(s)$ and $Y_{5/2}(s)$ are Bessel functions of the first and second kind of order 5/2. Note that three quantities specify the solution: p/p_o, r/r_b and $V\, r_b/K(r_b,p_o)$.

Parker (1965) has considered a similar solution of the steady-state

equation of transport satisfying the boundary conditions (10.1.1), for a constant diffusion coefficient in the region $0 < r < r_b$ and a constant solar wind speed V. He obtained and evaluated a series for the distribution near r = 0. The present study is more extensive than Parker's and we show the characteristics of the solution (10.1.2) over the whole range of heliocentric radii $0 < r < r_b$, and for a range of values of the parameter $V\ r_b/K(r_b,p_o)$.

In Section (2) we outline the numerical methods used to evaluate the solution (10.1.2). The reader who is not particularly interested in these details, can omit this section without losing the physical implications of the solution.

In Section (3) we show the characteristics of the solution as a function of p/p_o for a range of values of the radial variable r/r_b and for a range of the parameter $V\ r_b/K(r_b,p_o)$. We also show the effect of varying the free escape boundary at r_b, for $V\ r/K(r,p_o)$ fixed, and we compare the momentum spectra thus obtained with the mono-energetic galactic spectrum solution (8.1.1) results obtained when $r_b \to \infty$.

10.2 Evaluation of the solution

In this section we discuss methods of evaluating the solution (10.1.2). We first obtain expressions for F_o, $\partial F_o/\partial r$ and $\partial F_o/\partial p$. We note that having computed F_o, $\partial F_o/\partial r$ and $\partial F_o/\partial p$ it is relatively simple to calculate the basic physical quantities, such as the differential number density, the radial gradient, the streaming S_p, and its convective and diffusive components. The computation of F_o, $\partial F_o/\partial r$ and $\partial F_o/\partial p$ reduces to the evaluation of six infinite integrals of the

form

$$i = \int_{-\infty}^{\infty} e^{-x^2} \sin(\alpha x)\, h(x, \nu, \zeta)\, dx, \qquad (10.2.1a)$$

$$j = \int_{-\infty}^{\infty} e^{-x^2} \cos(\alpha x)\, g(x, \nu, \zeta)\, dx, \qquad (10.2.1b)$$

where

$$\begin{aligned} \nu &= \eta / (1 - \mu), \\ \alpha &= (\zeta - 1)\sqrt{\nu}\ , \\ \mu &= p / p_o, \\ \eta &= 3\,(V\, r_b / K(r_b, p_o)) / 2, \\ \zeta &= (r/r_b)^{-2/3}\ , \end{aligned} \qquad (10.2.2)$$

and $h(x,\nu,\zeta)$ and $g(x,\nu,\zeta)$ are odd and even rational functions of x respectively.

We then give two methods of evaluating the integrals (10.2.1) In the first method we approximate the functions $h(x,\nu,\zeta)$ and $g(x,\nu,\zeta)$ by Hermite polynomial expansions, and using the properties of Hermite polynomials we devise an algorithm to numerically evaluate the integrals, and estimate the errors involved. For sufficiently large values of the parameter α, given in Equations(10.2.2), the errors increase and we then use the second method of computing the integrals (10.2.1). In this latter method the integrals (10.2.1) are evaluated by solving a system of first order linear ordinary differential equations as an initial value problem.

From the solution (10.1.2) we have

$$F_o = \frac{N_g}{2\pi p_o^3} \frac{\zeta^{5/2}\, \mu^{-3/2}}{\eta} \exp\left[/\eta\, (1-\zeta^2/\mu)/4\right]\ I_1$$

$$\frac{\partial F_o}{\partial r} = \frac{F_o}{r_b}\, 2\zeta\, (\eta\, \zeta/\, 2\mu - I_3/I_1)\ /\ (3\ (r/r_b)), \qquad (10.2.3)$$

$$\frac{\partial F_o}{\partial p} = \frac{F_o}{p_o}\ (\eta\, \zeta^2/(4\ \mu^2) - \ 3/(2\mu) + I_2/I_1),$$

where

$$I_1 = \int_0^\infty s \exp[-s^2(1-\mu)/\eta] \; [J_m(s)Y_m(s\zeta) - Y_m(s)J_m(s\zeta)] / [J_m^2(s) + Y_m^2(s)] \; ds, \qquad (10.2.4a)$$

$$I_2 = \partial I_1/\partial\mu = (1/\eta) \int_0^\infty s^3 \exp[-s^2(1-\mu)/\eta] \; [J_m(s)Y_m(s\zeta) - Y_m(s)J_m(s\zeta)] / [J_m^2(s) + Y_m^2(s)] \; ds, \qquad (10.2.4b)$$

$$I_3 = (m/\zeta)I_1 + \partial I_1/\partial\zeta = \int_0^\infty s^2 \exp[-s^2(1-\mu)/\eta] \; [Jm(s)Y_{m-1}(\zeta s) - J_{m-1}(s\zeta)Y_m(s)] / [J_m^2(s) + Y_m^2(s)] \; ds, \qquad (10.2.4c)$$

and m = 5/2.

Since m is a half integer in Equations (10.2.4) we may express the ordinary Bessel functions in these equations in terms of spherical Bessel functions. Using the relations between the spherical Bessel functions $j_n(x)$, $y_n(x)$ (n is an integer) and the ordinary Bessel functions $J_{n+\frac{1}{2}}(x)$, $Y_{n+\frac{1}{2}}(x)$, i.e.,

$$j_n(x) = \sqrt{\pi/(2x)} \; J_{n+\frac{1}{2}}(x), \qquad y_n(x) = \sqrt{\pi/(2x)} \; Y_{n+\frac{1}{2}}(x), \qquad (10.2.5)$$

and the results

$$j_1(x) = \sin(x)/x^2 - \cos(x)/x,$$
$$j_2(x) = (3/x^3 - 1/x)\sin(x) - (3/x^2)\cos(x), \qquad (10.2.6)$$
$$y_1(x) = -\cos(x)/x^2 - \sin(x)/x,$$
$$y_2(x) = (-3/x^3+1/x)\cos(x) - (3/x^2)\sin(x),$$

(Abramowitz and Stegun 1964, Section 10.1), we may write Equations (10.2.4) as

$$I_1 = \zeta^{-5/2}\,[\nu\, i_1 + \sqrt{\nu}\, j_1]\,/2,$$
$$I_2 = \zeta^{-5/2}\,[\nu^2 i_2 + \nu^{3/2}\, j_2]\,/\,(2\eta), \qquad (10.2.7)$$
$$I_3 = \zeta^{-3/2}\,[\nu^2 i_3 + \nu^{3/2}\, j_3]\,/2,$$

where

$$i_1 = \int_{-\infty}^{\infty} e^{-u^2} \sin(\alpha u)\,[9+\nu(9\zeta-3-3\zeta^2)u^2 + \zeta^2\nu^2u^4]\; u/s_o(u,\nu)\; du,$$
$$i_2 = \int_{-\infty}^{\infty} e^{-u^2} \sin(\alpha u)\,[9+\nu(9\zeta-3-3\zeta^2)u^2 + \zeta^2\nu^2u^4]\; u^3/s_o(u,\nu)\; du,$$
$$i_3 = \int_{-\infty}^{\infty} e^{-u^2} \sin(\alpha u)\,[3+(3\zeta-1)\nu\, u^2]\; u^3/s_o(u,\nu)\; du,$$
$$j_1 = \int_{-\infty}^{\infty} e^{-u^2} \cos(\alpha u)\,[9(1-\zeta)\nu + 3(\zeta-\zeta^2)\nu^2u^2]\; u^2/s_o(u,\nu)\; du,$$
$$j_2 = \int_{-\infty}^{\infty} e^{-u^2} \cos(\alpha u)\,[9(1-\zeta)\nu + 3(\zeta-\zeta^2)\nu^2u^2]\; u^4/s_o(u,\nu)\; du,$$
$$j_3 = \int_{-\infty}^{\infty} e^{-u^2} \cos(\alpha u)\,[-3\nu(\zeta-1) + \nu^2\zeta\, u^2]\; u^4/s_o(u,\nu)\; du,$$
$$s_o(u,\nu) = 9 + 3\nu u^2 + \nu^2u^4, \qquad (10.2.8)$$

$$\nu = \eta\,/\,(1-\mu),$$
$$\alpha = (\zeta-1)\,\sqrt{\nu}\;.$$

The results (10.2.8), show, as mentioned previously in Equations (10.2.1) that the computation of F_o, $\partial F_o/\partial r$ and $\partial F_o/\partial p$ reduces to the evaluation of infinite integrals of the form

$$i = \int_{-\infty}^{\infty} e^{-x^2} \sin(\alpha x)\; h(x)\; dx, \qquad (10.2.9a)$$
$$j = \int_{-\infty}^{\infty} e^{-x^2} \cos(\alpha x)\; g(x)\; dx, \qquad (10.2.9b)$$

where

$$h(x) = m(x,\nu,\zeta)\;/\;s_o(x,\nu), \qquad (10.2.10a)$$
$$g(x) = t(x,\nu,\zeta)\;/\;s_o(x,\nu), \qquad (10.2.10b)$$
$$s_o(x,\nu) = \nu^2(x-z_1)(x-\bar{z}_1)(x+z_1)(x+\bar{z}_1), \qquad (10.2.10c)$$
$$z_1 = \sqrt{3/\nu}\; e^{i\pi/3}, \qquad (10.2.10d)$$

$m(x,\nu,\zeta)$ and $t(x,\nu,\zeta)$ are odd and even polynomials of x respectively.

To compute integrals of the form (10.2.9) we approximate the

rational functions h(x) and g(x) by Hermite polynomial expansions $h_n(x)$ and $g_n(x)$ of degree n. These expansions are

$$h_n(x) = \sum_{k=0}^{n} a_k\, p_k(x) = \sum_{i=0}^{n} \frac{h(t_i)\; p_{n+1}(x)}{(x-t_i)p'_{n+1}(t_i)} \quad , \qquad (10.2.11a)$$

$$g_n(x) = \sum_{k=0}^{n} c_k\, p_k(x) = \sum_{i=0}^{n} \frac{g(t_i)\; p_{n+1}(x)}{(x-t_i)p'_{n+1}(t_i)} \quad , \qquad (10.2.11b)$$

where

$$p_k(x) = \frac{(-1)^k\, e^{x^2}}{\sqrt{2^k\, k!\, \sqrt{\pi}}} \quad \frac{d^k}{dx^k}\,(e^{-x^2}) = \frac{1}{\sqrt{2^k\, k!\, \sqrt{\pi}}}\; H_k(x). \qquad (10.2.12)$$

Here $H_k(x)$ is a Hermite polynomial of degree k, $p_k(x)$ is the normalised form of $H_k(x)$ and the constants t_i are the roots of $p_{n+1}(x)$, i.e.,

$$p_{n+1}(t_i) = 0, \quad i = 0(1)n, \qquad (10.2.13)$$

and

$$\int_{-\infty}^{\infty} e^{-x^2}\, p_k(x)\, p_\ell(x)\, dx = \delta_{k\ell} \qquad (10.2.14)$$

Note that since

$$h_n(t_i) = h(t_i), \qquad i = 0(1)n, \qquad (10.2.15a)$$

$$g_n(ti) = g(t_i), \qquad i = 0(1)n, \qquad (10.2.15b)$$

the polynomial expansions $h_n(x)$ and $g_n(x)$ are the Lagrange interpolation polynomials for h(x) and g(x) with interpolation points located at $x = t_i$, i = 0(1)n.

The coefficients a_k and c_k occurring in the expansions (10.2.11a) and (10.2.11b) are given by

$$a_k = \frac{1}{(n+1)} \sum_{i=0}^{n} h(t_i)\; p_k(t_i)/p_n^2(t_i), \quad k = 0(1)n, \qquad (10.2.16a)$$

$$c_k = \frac{1}{(n+1)} \sum_{i=0}^{n} g(t_i)\; p_k(t_i)/p_n^2(t_i), \quad k = 0(1)n, \qquad (10.2.16b)$$

(See Appendix (E)).

The roots of t_i of $p_{n+1}(x)$ and the constants $p_k(t_i)$, $k = 0(1)n$, $i = 0(1)n$, occurring in the expansions (10.2.16) for a_k and c_k can be computed as follows. The normalised Hermite polynomials satisfy the recurrence relation

$$p_{k+1}(x) = \sqrt{2/(k+1)}\ x\ p_k(x) - \sqrt{k/(k+1)}\ p_{k-1}(x), \quad k = 0(1)n, \tag{10.2.17}$$

(Abramowitz and Stegun 1964, Section 22.7). We can write the result (10.2.17) in the form

$$x\ p_k(x) = M_{k\ell}\ p_\ell(x) + \sqrt{(n+1)/2}\ p_{n+1}(x)\delta_{k,n}, \quad k, \ell = 0(1)n, \tag{10.2.18}$$

where the summation convention has been assumed and

$$M_{k\ell} = \sqrt{(k+1)/2}\ \delta_{\ell,k+1} + \sqrt{k/2}\ \delta_{\ell+1,k}. \tag{10.2.19}$$

We can regard the $M_{k\ell}$ as the elements of a symmetric tridiagonal matrix $\underline{\underline{M}}$. Noting that at $x = t_i$ we have $p_{n+1}(t_i) = 0$ so that the second term in (10.2.18) is zero and

$$t_i\ p_k(t_i) = M_{k\ell}(t_i)\ p_\ell(t_i), \quad k, \ell = 0(1)n. \tag{10.2.20}$$

Introducing the column vector $\underline{P}(i) = (p_o(t_i), p_1(t_i), \ldots, p_n(t_i))^T$ where the superscript T denotes the transpose, the set of linear equations (10.2.20) can be expressed in the matrix form

$$t_i\ \underline{P}(i) = \underline{\underline{M}} \cdot \underline{P}(i), \qquad i = 0(1)n. \tag{10.2.21}$$

This latter result shows that the roots t_i and the column vectors $[p_o(t_i), p_1(t_i), \ldots, p_n(t_i)]^T$, $i = 0(1)n$, are the eigenvalues and eigenvectors of the symmetric tridiagonal matrix $\underline{\underline{M}}$. This eigenvalue problem for the roots t_i and the eigenvectors $\underline{P}(i)$ is readily solved by using the theory of Sturm sequences (Hammarling, 1970).

Substituting the Hermite polynomial approximations (10.2.11) for $h(x)$ and $g(x)$ in the integrals (10.2.9) we obtain approximations

$i^{(n)}$ and $j^{(n)}$ to the integrals i and j:

$$i^{(n)} = \int_{-\infty}^{\infty} e^{-x^2} \sin(\alpha x)\, h_n(x)\, dx = \sum_{k=0}^{n} a_k J_k(\alpha), \qquad (10.2.22a)$$

$$j^{(n)} = \int_{-\infty}^{\infty} e^{-x^2} \cos(\alpha x)\, g_n(x)\, dx = \sum_{k=0}^{n} c_k K_k(\alpha), \qquad (10.2.22b)$$

where

$$J_k(\alpha) = \int_{-\infty}^{\infty} e^{-x^2} \sin(\alpha x)\, p_k(x)\, dx$$

$$= \pi^{\frac{1}{4}} \sin(k\pi/2)\, \alpha^k\, e^{-\alpha^2/4} / \sqrt{2^k\, k!}\,, \qquad (10.2.23a)$$

$$K_k(\alpha) = \int_{-\infty}^{\infty} e^{-x^2} \cos(\alpha x)\, p_k(x)\, dx$$

$$= \pi^{\frac{1}{4}} \cos(k\pi/2)\, \alpha^k\, e^{-\alpha^2/4} / \sqrt{2^k\, k!}\,, \qquad (10.2.23b)$$

This is the algorithm we use in the next section to evaluate the integrals (10.2.8) and hence F_o, $\partial F_o/\partial r$ and $\partial F_o/\partial p$.

We have changed the problem of evaluating the infinite integrals (10.2.8) to one of finding the eigenvalues and eigenvectors of a symmetric tridiagonal matrix. The accuracy can be increased by increasing n, the degree of the polynomial approximation and the procedure is satisfactory when the parameter α is sufficiently small for $i^{(n)}$ and $j^{(n)}$ to be good approximations to i and j.

The results (10.2.23a) and (10.2.23b) are standard integrals for Hermite polynomials (Erdelyi *et.al.*, 1954, Vol.1, Sections 1.11, 2.10). Since the functions $J_k(\alpha)$ and $K_k(\alpha)$ satisfy the recurrence relations

$$\begin{aligned} J_{2k+1} &= -(\alpha^2/\sqrt{8k(2k+1)})\, J_{2k-1}\,, \quad k \geq 1, \\ K_{2k} &= -(\alpha^2/\sqrt{8k(2k-1)})\, K_{2k-1}, \quad k \geq 1, \end{aligned} \qquad (10.2.24)$$

and

$$\begin{aligned} J_{2k} &= K_{2k+1} = 0, \\ J_1 &= \pi^{\frac{1}{4}} e^{-\alpha^2/4}, \\ K_0 &= \alpha\, \pi^{\frac{1}{4}} e^{-\alpha^2/4}, \end{aligned} \qquad (10.2.25)$$

we may sum the series (10.2.22a) and (10.2.22b) most efficiently by using Clenshaws algorithm, (Clenshaw, 1955). In the present application we construct sequences $\{b_k\}$, k = M(-1)0, $\{e_j\}$, j = N(-1)0,

$$\begin{aligned} b_k &= a_{2k+1} - (\alpha^2 / \sqrt{8(k+1)(2k+3)}\ )\ b_{k+1}, \\ e_j &= c_{2j} - (\alpha^2 / \sqrt{8(j+1)(2j+1)}\ )\ e_{j+1}, \end{aligned} \tag{10.2.26}$$

where

$$\begin{aligned} M &= \begin{cases} (n-2)/2 & \text{if } n \text{ even}, \\ (n-1)/2 & \text{if } n \text{ odd}, \end{cases} \\ N &= \begin{cases} n/2 & \text{if } n \text{ even}, \\ (n-1)/2 & \text{if } n \text{ odd}. \end{cases} \end{aligned} \tag{10.2.27}$$

$$b_{M+1} = e_{N+1} = 0,$$

then the series (10.2.22a) and (10.2.22b) are given by

$$\begin{aligned} i^{(n)} &= \sum_{k=0}^{M} a_{2k+1}\ J_{2k+1} = b_0\ J_1 \\ j^{(n)} &= \sum_{k=0}^{N} c_{2k}\ K_{2k} = e_0\ K_0. \end{aligned} \tag{10.2.28}$$

Summarizing we determine the integrals (10.2.9) by evaluating the a_k and c_k and then summing appropriately to find b_0 and e_0. The a_k and c_k in turn have been found from the expressions (10.2.16) which require $p_k(t_i)$ and t_i which are obtained as the eigenvalues and eigenvectors of the symmetric tridiagonal matrix (10.2.19).

Another important aspect of calculating the integrals (10.2.9a) and (10.2.9b) by using Hermite polynomial expansions for h(x) and g(x) is that we may obtain asymptotic estimates of the errors $R_i^{(n)} = i - i^{(n)}$ and $R_j^{(n)} = j - j^{(n)}$ for large n by using methods of complex integration (Donaldson and Elliot, 1972; Paget and Elliot 1972). Using these methods we can show that the errors $R_i^{(n)}$ and $R_j^{(n)}$ for functions

h(x) and g(x) of the form (10.2.10), are given by

$$R_i^{(n)} = \int_{-\infty}^{\infty} e^{-x^2} \sin(\alpha x)\,[h(x) - h_n(x)]\,dx.$$

$$= -2\,\mathrm{Im}\,(m(z_1)\,q(z_1,\alpha) / (3\sqrt{3}\,\nu\,z_1\,p_{n+1}(z_1))), \qquad (10.2.29a)$$

$$R_j^{(n)} = \int_{-\infty}^{\infty} e^{-x^2} \cos(\alpha x)\,(g(x) - g_n(x))\,dx$$

$$= -2\,\mathrm{Im}(t(z_1)\,Q(z_1,\alpha) / (3\sqrt{3}\,\nu\,z_1\,p_{n+1}(z_1))), \qquad (10.2.29b)$$

where

$$q(z_1,\alpha) = \int_{-\infty}^{\infty} e^{-x^2} \sin(\alpha x)\,p_{n+1}(x) / (z_1 - x)\,dx, \qquad (10.2.30a)$$

$$Q(z_1,\alpha) = \int_{-\infty}^{\infty} e^{-x^2} \cos(\alpha x)\,p_{n+1}(x) / (z_1 - x)\,dx, \qquad (10.2.30b)$$

$$h(x) = m(x)/s_o(x,\nu), \qquad (10.2.30c)$$

$$g(x) = t(x)/s_o(x,\nu), \qquad (10.2.30d)$$

$$s_o(x,\nu) = \nu^2\,(x-z_1)(x-\bar{z}_1)(x+z_1)(x+\bar{z}_1), \qquad (10.2.30e)$$

$$z_1 = \sqrt{3/\nu}\;e^{i\pi/3}, \qquad (10.2.30f)$$

m(x) is an odd polynomial and t(x) is an even polynomial (Appendix(F)). The result (10.2.29a) is exact for n > the degree of m(x) and the result (10.2.29b) is exact for n > the degree of the polynomial t(x), but it is only practicable to evaluate these errors for large n.

Asymptotic estimates of the errors are obtained by using asymptotic expansions of the functions $q(z_1,\alpha)$, $Q(z_1,\alpha)$ and $p_{n+1}(z_1)$. To obtain these expansions we express the functions $q(z_1,\alpha)$, $Q(z_1,\alpha)$ in the alternative form:

$$q(z_1,\alpha) = (C_{n+1}(z_1)\,\sin(\alpha z_1) - \sqrt{\pi}\,\cos((n+1)\pi/2)\,d_1$$

$$+ \sqrt{\pi}\,\sin((n+1)\,\pi/2)\,d_2)/k_{n+1}, \qquad (10.2.31a)$$

$$Q(z_1,\alpha) = (C_{n+1}(z_1)\,\cos(\alpha z_1) + \sqrt{\pi}\,\sin((n+1)\,\pi/2)\,d_1$$

$$+ \sqrt{\pi}\,\cos((n+1)\,\pi/2)\,d_2)/k_{n+1}, \qquad (10.2.31b)$$

where

$$d_1 = \int_0^\alpha x^{n+1} e^{-x^2/4} \cos\left((\alpha-x) z_1\right) dx$$

$$= \alpha^{n+2} \int_0^\infty \exp\left(-(n+2)x - \alpha^2 e^{-2x}/4\right) \cos\left(\alpha(1-e^{-x}) z_1\right) dx, \quad (10.2.31c)$$

$$d_2 = \int_0^\alpha x^{n+1} e^{-x^2/4} \sin\left((\alpha-x) z_1\right) dx$$

$$= \alpha^{n+2} \int_0^\infty \exp\left(-(n+2)x - \alpha^2 e^{-2x}/4\right) \sin\left(\alpha (1-e^{-x}) z_1\right) dx, \quad (10.2.31d)$$

$$C_{n+1}(z_1) = \int_{-\infty}^{\infty} e^{-x^2} H_{n+1}(x) / (z_1-x) dx / k_{n+1}$$

$$= e^{-i(n+2)\pi/2} \sqrt{\pi}\, (n+1)!\, U\left((n+2)/2, 1/2, e^{-i\pi} z_1^2\right), \quad (10.2.31e)$$

$$k_{n+1} = \sqrt{2^{n+1}\, (n+1)!\, \sqrt{\pi}}\,, \quad (10.2.31f)$$

$H_n(x)$ is the usual Hermite polynomial and $U(a,b,x)$ is a standard solution of Kummer's confluent hypergeometric equation (Abramowitz and Stegun, 1964, Chapter 13).

We then substitute asymptotic expansion for $C_{n+1}(z_1)$, d_1 and d_2 of Equations (10.2.31c) - (10.2.31e) into the expressions (10.2.31a), (10.2.31b) for $q(z_1\alpha)$ and $Q(z_1,\alpha)$ to obtain the asymptotic behaviour of $q(z_1,\alpha)$ and $Q(z_1,\alpha)$. Finally we substitute the asymptotic expansions for $q(z_1\alpha)$, $Q(z_1,\alpha)$ and $p_{n+1}(z_1)$ in the results (10.2.29a) and (10.2.29b) and obtain asymptotic estimates of $R_i^{(n)}$ and $R_j^{(n)}$.

The asymptotic behaviour of $C_{n+1}(z_1)$ and $p_{n+1}(z_1)$ for large n is given in Elliot (Technical report 21), and

$$d_1 \sim \frac{\alpha^{n+2} e^{-\alpha^2/4}}{(n+2)} \left[1 + \alpha^2/(2(n+2)) + (\alpha^4/4 - \alpha^2 - \alpha^2 z_1^2)\ /(n+2)^2 + O\left(\alpha^6/(n+1)^3\right)\right], \quad (10.2.32a)$$

$$d_2 \sim \frac{\alpha^{n+3} z_1 e^{-\alpha^2/4}}{(n+2)^2} \left[1 + (\alpha^2-1) / (n+2) + (\alpha^2 (3\alpha^2 - z_1^2 - 9/2) + 1) /(n+2)^2 + O(\alpha^6/(n+2)^3)\right], \quad (10.2.32b)$$

are the asymptotic expansions of the integrals d_1 and d_2. The asymptotic expansions (10.2.32a) and (10.2.32b) were obtained by expanding the integrals (10.2.31c) and (10.2.31d) by integration by parts (cf. Erdelyi, 1956).

In the computations of F_o, $\partial F_o/\partial r$ and $\partial F_o/\partial p$ presented in the next section, the errors $R_i^{(n)}$ and $R_j^{(n)}$ in evaluating the integrals (10.2.8) in general decrease with increasing n. However as $\mu = p_o/p \to 1$, the parameters $\nu = \eta/(1-\mu)$ and $\alpha = (\zeta-1)/\nu$ increase very rapidly and the errors eventually become so large that we cannot use the approximations $i^{(n)}$ and $j^{(n)}$ of Equations (10.2.22a) and (10.2.22b) to evaluate the integrals (10.2.8). Hence an alternative method of evaluating the integrals (10.2.8) for $\mu = p/p_o \gtrsim 1$, $(p/p_o < 1)$, was devised and we outline the method below.

In this method we first express the integrals (10.2.8) in a slightly different form and we introduce integrals $y_i(\varepsilon,\zeta)$, i = 1(1)8 where

$$\varepsilon = (1-\mu) / \eta,$$

which are closely related to the integrals (10.2.8). Noting that $1-\mu = (1-p/p_o)$, we see that ε is small when $p \to p_o$. We then show that $\{y_i(\varepsilon,\zeta)\}$ and $\{\frac{d\, y_i(\varepsilon,\zeta)}{d\varepsilon}\}$, i = 1(1)8 are linearly related and the y_i's satisfy a system of linear, first order, ordinary differential equations with the independent variable being ε. Since we can obtain analytic expressions for $y_i(0,\zeta)$, (i.e., the value of $y_i(\varepsilon,\zeta)$ for $p/p_o = 1$) we can solve this system of differential equations for $y_i(\varepsilon,\zeta)$, numerically as an initial value problem, and hence we evaluate the integrals (10.2.8).

The integrals i_1, i_2, i_3, j_1, j_2, and j_3 given in Equations (10.2.8) are related to the integrals $y_i(\varepsilon,\zeta)$, i = 1(1)8 as follows:

$$i_1 = 2\,\varepsilon\, y_1(\varepsilon,\zeta)\,. \tag{10.2.33a}$$

$$i_2 = -2\,\varepsilon^2\, y_2(\varepsilon,\zeta), \tag{10.2.33b}$$

$$i_3 = 2\,\varepsilon^2\, y_5(\varepsilon,\zeta), \tag{10.2.33c}$$

$$j_1 = 2\sqrt{\varepsilon}\, y_3(\varepsilon,\zeta), \tag{10.2.33d}$$

$$j_2 \quad -2\,\varepsilon^{3/2}\, y_4(\varepsilon,\zeta). \tag{10.2.33e}$$

$$j_3 = 2\,\varepsilon^{3/2}\, y_7(\varepsilon,\zeta), \tag{10.2.33f}$$

where

$$\varepsilon = 1/\nu = (1-\mu)/\eta, \tag{10.2.34a}$$

$$y_1(\varepsilon,\zeta) = \int_0^\infty e^{-s^2\varepsilon}\, \frac{s(9+(9\zeta-3-3\zeta^2)s^2+\zeta^2 s^4)}{(9+3s^2+s^4)}\, \sin((\zeta-1)s)\, ds, \tag{10.2.34b}$$

$$y_2(\varepsilon,\zeta) = \frac{dy_1}{d\varepsilon} = -\int_0^\infty e^{-s^2\varepsilon}\, s^3\, \frac{(9+(9\zeta-3-3\zeta^2)s^2+\zeta^2 s^4)}{(9+3s^2+s^4)}\, \sin((\zeta-1)s)\, ds, \tag{10.2.34c}$$

$$y_3(\varepsilon,\zeta) = \int_0^\infty e^{-s^2\varepsilon}\, s^2\, \frac{(9(1-\zeta) + 3(\zeta-\zeta^2)s^2)}{(9+3s^2+s^4)}\, \cos((\zeta-1)s)\, ds, \tag{10.2.34d}$$

$$y_4(\varepsilon,\zeta) = \frac{dy_3}{d\varepsilon} = -\int_0^\infty e^{-s^2\varepsilon}\, \frac{s^4(9(1-\zeta) + 3(\zeta-\zeta^2)s^2)}{(9+3s^2+s^4)}\, \cos((\zeta-1)s)\, ds, \tag{10.2.34e}$$

$$y_5(\varepsilon,\zeta) = \int_0^\infty e^{-s^2\varepsilon}\, \frac{s^3(3+(3\zeta-1)\, s^2)}{(9+3s^2+s^4)}\, \sin\,((\zeta-1)s)\, ds, \tag{10.2.34f}$$

$$y_6(\varepsilon,\zeta) = \frac{dy_5(\varepsilon,\zeta)}{d\varepsilon} = -\int_0^\infty e^{-s^2\varepsilon}\, \frac{s^5(3+(3\zeta-1)s^2)}{(9+3s^2+s^4)}\, \sin((\zeta-1)s)\, ds, \tag{10.2.34g}$$

$$y_7(\varepsilon,\zeta) = \int_0^\infty e^{-s^2\varepsilon}\, \frac{s^4(3-3\zeta+\zeta s^2)}{(9+3s^2+s^4)}\, \cos((\zeta-1)s)\, ds, \tag{10.2.34h}$$

$$y_8(\varepsilon,\zeta) = \frac{dy_7(\varepsilon,\zeta)}{d\varepsilon} = -\int_0^\infty e^{-s^2\varepsilon}\, \frac{s^6(3-3\zeta+\zeta s^2)}{(9+3s^2+s^4)}\, \cos\,((\zeta-1)s)\, ds, \tag{10.2.34i}$$

Note that the variable of integration s is related to that used in Equations (10.2.8) by $s^2 = \nu\, u^2$.

The integrals (10.2.34) satisfy the system of ordinary differential equations

$$\frac{dy_1}{d\varepsilon} = y_2, \qquad \frac{dy_2}{d\varepsilon} = q_1 + 3\,y_2 - 9\,y_1,$$

$$\frac{dy_3}{d\varepsilon} = y_4, \qquad \frac{dy_4}{d\varepsilon} = q_3 + 3\,y_4 - 9\,y_3, \tag{10.2.35}$$

$$\frac{dy_5}{d\varepsilon} = y_6, \qquad \frac{dy_6}{d\varepsilon} = q_5 + 3\,y_6 - 9\,y_5.$$

$$\frac{dy_7}{d\varepsilon} = y_8, \qquad \frac{dy_8}{d\varepsilon} = q_7 + 3\,y_8 - 9\,y_7,$$

where

$$\begin{aligned} q_1 &= \int_0^\infty e^{-s^2\varepsilon}\, s(9+(9\zeta-3-3\zeta^2)s^2 + \zeta^2 s^4)\, \sin((\zeta-1)s)\, ds, \\ q_3 &= \int_0^\infty e^{-s^2\varepsilon}\, s^2(9(1-\zeta) + 3(\zeta-\zeta^2)s^2)\, \cos((\zeta-1)s)\, ds, \\ q_5 &= \int_0^\infty e^{-s^2\varepsilon}\, s^2(3+(3\zeta-1)s^2)\, \sin((\zeta-1)s), \\ q_7 &= \int_0^\infty e^{-s^2\varepsilon}\, s^4(3(1-\zeta) + \zeta s^2)\, \cos((\zeta-1)s)\, ds. \end{aligned} \tag{10.2.36}$$

In the system of ordinary differential equations (10.2.35) the quantities q_1, q_3, q_5 and q_7 are independent of the y_i's and are functions of ε and ζ only.

We now obtain analytic expressions for q_1, q_3, q_5 and q_7. Expressing the polynomial parts of the integrands of the integrals (10.2.36) in terms of Hermite polynomials and then using the results

$$\int_0^\infty e^{-s^2} H_k(s)\, \sin(\alpha s)\, ds = \sqrt{\pi}\,\alpha^k\, e^{-\alpha^2/4} \sin(k\pi/2)/2, \tag{10.2.37a}$$

$$\int_0^\infty e^{-s^2} H_k(s)\, \cos(\alpha s)\, ds = \sqrt{\pi}\,\alpha^k\, e^{-\alpha^2/4} \cos(k\pi/2) \tag{10.2.37b}$$

where $H_k(s)$ is an Hermite polynomial of degree k (Erdelyi *et.al.*, 1954,

Vol.1, Sections 1.11, 2.10), we obtain

$$\begin{aligned} q_1 &= 9\,\ell_1 + (9\zeta - 3 - 3\zeta^2)\,\ell_3 + \zeta^2\,\ell_5, \\ q_3 &= 9(1-\zeta)\,m_2 + s(\zeta-\zeta^2)\,m_4, \\ q_5 &= 3\,\ell_3 + (3\zeta-1)\,\ell_5, \\ q_7 &= 3(1-\zeta)\,m_4 + \zeta m_6, \end{aligned} \tag{10.2.38}$$

where

$$\begin{aligned} \ell_1 &= \sqrt{\pi}\,\alpha\, e^{-\alpha^2/4} / (4\epsilon), \\ \ell_3 &= \sqrt{\pi}\,(6\alpha-\alpha^3)\, e^{-\alpha^2/4} / (16\epsilon^2), \\ \ell_5 &= \sqrt{\pi}\,(\alpha^5 - 20\alpha^3 + 60\alpha)\, e^{-\alpha^2/4} /(64\epsilon^3), \\ m_2 &= \sqrt{\pi}\,(2-\alpha^2)\, e^{-\alpha^2/4} / (8\epsilon^{3/2}), \\ m_4 &= \sqrt{\pi}\,(\alpha^4-12\alpha^2+12)\, e^{-\alpha^2/4} / (32\epsilon^{5/2}), \\ m_6 &= \sqrt{\pi}\,(-\alpha^6+30\alpha^4 - 180\alpha^2+120)\, e^{-\alpha^2/4} / (128\epsilon^{7/2}), \\ \alpha &= (\zeta-1)/\nu\,, \qquad \epsilon = 1/\nu = (1-\mu)/\eta. \end{aligned} \tag{10.2.39}$$

The expressions (10.2.38) for q_1, q_3, q_5 and q_7 and the associated quantities (10.2.39) are easily evaluated and we use these results when we numerically integrate the differential equations (10.2.35) to obtain the y_i's.

Finally we evaluate the integrals (10.2.34), i.e., $y_i(\epsilon,\zeta)$, $i = 1(1)8$ at $\epsilon = 0$ by using the methods of complex integration. For $\epsilon = 0$ these integrals have one of the forms

$$I = \int_0^\infty u(s) \sin[(\zeta-1)s] / (s^4 + 3s^2 + 9)\, ds,$$

or

$$J = \int_0^\infty \omega(s) \cos[(\zeta-1)s] / (s^4 + 3s^2 + 9)\, ds, \tag{10.2.40}$$

where $u(s)$ is an odd polynomial and $\omega(s)$ is an even polynomial.

Using Cauchy's theorem in the complex s plane we can show that the integrals (10.2.40) have values

$$I = \pi \, \mathrm{Im} \, (u(s_1) \, e^{i(\zeta-1)s_1/s_1}) \, / \, 3\sqrt{3}$$

and (10.2.41)

$$J = \pi \, \mathrm{Re} \, (\omega(s_1) \, e^{i(\zeta-1)s_1/s_1}) \, / \, 3\sqrt{3}$$

where

$$s_1 = \sqrt{3} \; e^{i\pi/3}. \tag{10.2.42}$$

and we use these results to evaluate the integrals $y_i(0,\zeta)$, $i = 1(1)8$.

In this way we obtain

$$\begin{aligned} y_1(0,\zeta) &= -y_3(0,\zeta) = b_1 P + a_1 Q, \\ y_2(0,\zeta) &= -y_4(0,\zeta) = b_2 P + a_2 Q, \\ y_5(0,\zeta) &= -y_7(0,\zeta) = b_5 P + a_5 Q, \\ y_8(0,\zeta) &= -y_6(0,\zeta) = b_6 P + a_6 Q, \end{aligned} \tag{10.2.43}$$

where

$$\begin{aligned} a_1 &= 27(1-\zeta)/2, & b_1 &= 9\sqrt{3}\,(3\zeta-1-\zeta^2)/2, \\ a_5 &= -27\zeta/2, & b_5 &= 9\sqrt{3}\,(2-3\zeta)/2, \\ a_2 &= 3(a_1+\sqrt{3}\,b_1)/2, & b_2 &= 3(b_1-\sqrt{3}\,a_1)/2, \\ a_6 &= 3(a_5+\sqrt{3}\,b_5)/2, & b_6 &= 3(b_5-\sqrt{3}\,a_5)/2, \\ P &= \pi \exp[-3(\zeta-1)/2] \cos[\sqrt{3}(\zeta-1)/2\,], \\ Q &= \pi \exp[-3(\zeta-1)/2] \sin[\sqrt{3}(\zeta-1)/2\,], \end{aligned} \tag{10.2.44}$$

as values for $y_i(0,\zeta)$, $i = 1(1)8$.

Upon substitution of the expressions (10.2.38), (10.2.39) for q_1, q_3, q_5 and q_7 in the differential equations (10.2.35) and numerically integrating the latter set of equations with initial values $y_i(0,\zeta)$, $i = 1(1)8$, given by Equations (10.2.43), (10.2.44) we obtain

numerical values for $y_i(\varepsilon,\zeta)$. Hence using the results (10.2.33), (10.2.7) and (10.2.3) we evaluate $F_o, \partial F_o/\partial r$, and $\partial F_o/\partial p$.

We note that the expressions (10.2.7) for I_1, I_2 and I_3, given in terms of $y_i(\varepsilon,\zeta)$ are :

$$\begin{aligned} I_1 &= \zeta^{-5/2}\,[y_1(\varepsilon,\zeta) + y_3(\varepsilon,\zeta)], \\ I_2 &= -\zeta^{-5/2}\,[y_2(\varepsilon,\zeta) + y_4(\varepsilon,\zeta)]\,/\eta\,, \\ I_3 &= \zeta^{-3/2}\,[y_5(\varepsilon,\zeta) + y_7(\varepsilon,\zeta)]\,. \end{aligned} \tag{10.2.45}$$

Using the values of $y_i(0,\zeta)$, i = 1(1)8, given in Equations (10.2.43), (10.2.44) in Equations (10.2.45) we find that at

$$\begin{aligned} &\varepsilon = 0, \quad r \neq r_b \ (\text{i.e., } p = p_o,\ r \neq r_b), \\ &I_1 = I_2 = I_3 = 0. \end{aligned} \tag{10.2.46}$$

Substituting the above values of I_1, I_2 and I_3 into the expressions (10.2.3) for F_o, $\partial F_o/\partial r$ and $\partial F_o/\partial p$ we find that for $r \neq r_b$

$$F_o(r,p_o) = \partial F_o(r,p_o)/\partial r = \partial F_o(r,p)/\partial p\big|_{p=p_o} = 0, \tag{10.2.47}$$

which shows that the differential number density, the streaming and the gradient $\partial F_o/\partial r$ are all zero at $p = p_o$ and for $r \neq r_b$, $0 < r < r_b$.

The numerical methods presented in this section are quite complex; we use them in the next section to investigate the physical characteristics of the solution (10.1.2).

10.3 Characteristics of the solution

In this section we show some of the basic physical characteristics of the solution (10.1.2) which has $U_p \to N_g\,\delta(p-p_o)$ as $r \to r_b$. We note against that the solution depends on the dimensionless quantities $V\,r_b/K(r_b,p_o)$, r/r_b and p/p_o and the diffusion coefficient has the form $K = K_c\,p\,r^{7/3}$. Since

$$V\, r_b/K(r_b,p_o) \;=\; (V\, r/K(r,p_o))\,.\,(r/r_b)^{4/3},$$

the solution may alternatively be expressed in terms of $V\, r/K(r,p_o)$, r/r_b and p/p_o. The latter formulation in terms of $V\, r/K(r,p_o)$, r/r_b and p/p_o is particularly useful in showing the relation of the solution (10.1.2) to the monoenergetic galactic spectrum solution (8.1.1) for $K = K_c\, p\, r^{7/3}$ obtained by letting $r_b \to \infty$.

Using the methods of Section (2) we calculate F_o, $\partial F_o/\partial r$ and $\partial F_o/\partial p$ and we investigate the momentum dependence of

(i) the distribution function F_o,

(ii) the differential number density $U_p = 4\pi p^2 F_o$,

(iii) the radial gradient $G_r = (1/U_p)\,\partial U_p/\partial r$, and

(iv) the radial differential current density S_p, and the convective and diffusive components of S_p which we denote by S_c and S_d, i.e.,

$$S_c = -4\pi p^3 (V/3)\,\partial F_o/\partial p,$$

$$S_d = -4\pi p^2 K\,\partial F_o/\partial r,$$

$$S_p = S_c + S_d.$$

In Figure 10.1 these quantities are plotted against p/p_o for $V\, r_b/K(r_b,p_o) = 0.005$ and $r/r_b = 0.01$, 0.1 and 0.9. In Figure 10.2 they are plotted against p/p_o for $r/r_b = 0.1$ and values 0.0005, 0.005 and 0.1 of the parameter $V\, r_b/K(r_b,p_o)$ and Figure (10.3) shows similar plots for $V\, r/K(r,p_o) = 0.11753$ and $r_b/r = 1.01$, 1.1, 2.0 and ∞.

The F_o or U_p curves of Figure 10.1 show the radial redistribution of particles, initially injected with momentum p_o from the free escape boundary at $r = r_b$. There is a substantial peak in the distribution in the vicinity of p_o. As we approach the boundary, i.e. $r/r_b \to 1$, the peak moves towards p_o, narrows in width and increases

in peak value and $U_p \rightarrow N_g \quad (p-p_o)$.

The F_o curves also show that $F_o \rightarrow 0$ as $p \rightarrow 0$. For $r/r_b = 0.9$ and 0.1, there is a second peak in the distribution function at the low end of the momentum range due to an accumulation of particles which have lost momentum to the solar wind. As r increases towards the boundary radius r_b, the peak moves towards $p = 0$ and diminishes in peak value.

The radial gradient curves of Figure 10.1 show that for each p, $(p < p_o)$ that as r increases from zero the number density increases to a peak and then decreases, and that the radial position of the peak moves outward as p decreases. This represents particles being fed into (p, p + d p) by the energy changes but being excluded from the inner regions by the outwardly moving scattering centres.

The streaming curves of Figure 10.1 are quite complex, but have the same basic structure as the monoenergetic galactic spectrum solution (8.1.1) results presented in Figure 8.3a . Although it is not obvious from the curves of Figure 10.1 the calculations show that near the sun S_p changes from - ve to + ve as p increases from 0 to p_o, and at larger radii S_p changes through the sequence -ve, + ve, - ve, + ve as p increases from 0 to p_o.

The curves of Figure 10.1 show the dependence of the solution on heliocentric radius for a range of interplanetary conditions. For example if $K(r,p) = 3 \times 10^{17}$ m^2 s^{-1} at a radius of 1 A U, and 1 G V rigidity, $V = 4 \times 10^5$ m s^{-1} and r_b = 10 A U, the F_o curves for r/r_b = 0.9, 0.1 and 0.01 of Figure 10.1 represent, respectively, the distributions to be obtained at r = 9, 1 and 0.1 A U from protons injected with a kinetic energy of 1.14 GeV from the boundary at

r_b = 10 A U.

The curves of Figure 10.2 show the dependence of the solution on the parameter V $r_b/K(r_b,p_o)$, and they can be interpreted as indicating the changes in the solution due to changes in the solar wind speed V, the diffusion coefficient constant K_c (recall $K = K_c\ p\ r^{7/3}$), or the injection momentum p_o. The curves are very similar to those of Figure 10.1, and as a consequence we shall not discuss them in great detail.

For the two smaller values of V $r_b/K(r_b,p_o)$ in Figure 10.2 the distribution function has a substantial peak in the vicinity of p_o. As V $r_b/K(r_b,p_o) \to 0$, the peak moves towards p_o, decreases in width and increases in peak value and $U_p \to N_g\ \delta(p-p_o)$.

For V $r_b/K(r_b,p_o)$ = 0.005 and 0.0005, there is a second peak in the distribution function at the low end of the momentum range. As V $r_b/K(r_b,p_o)$ decreases, the peak decreases in amplitude and moves towards p = 0.

If we interpret the curves as indicating the changes in the number density, the gradient and the streaming at fixed r for various p_o, they show that particles of lower p_o are more spread from the delta function of injection and are more attenuated. The radial gradient curves show that a greater proportion of particles with lower p_o are excluded from the region enclosed by a spherical surface at radius r, due to the decreased diffusion coefficient for these particles. Assuming a diffusion coefficient $K(r,p) = 3 \times 10^{17}\ m^2\ s^{-1}$ at r = 1 A U and P = 1 G V, $V = 4 \times 10^5$ m/s and r_b = 10 A U, the F_o curves of Figure 10.2 represent, respectively, the distributions to be obtained at r = 1 A U from monoenergetic protons, intially at r_b = 10 A U with

kinetic energies, T_o, of 17.6, 1.14 GeV and 4.53 MeV.

The curves of Figure 10.3 show the changes in the momentum dependence of the solution at fixed r and p_o when we vary the position of the free escape boundary at radius r_b. As r_b/r decreases, F_o and U_p decrease fairly uniformly over most of the spectrum. For smaller values of r/r_b (i.e., larger values of r_b/r) we might expect F_o and U_p to decrease due to the exclusion of particles from the inner regions. However the F_o and U_p curves of Figure 10.3 show that this is not the case, and that there is a reduction in the number density as r_b/r decreases which must be due to the free escape of particles across the boundary. The curves for $r_b = \infty$ in Figure 10.3 were calculated from the monoenergetic galactic spectrum solution (8.1.1) for $K = K_c\ p\ r^{7/3}$ and $V\ r/K(r,p_o) = 0.11753$. We note that at radii $r/r_b < 1/2$ there is little difference between the monoenergetic galactic spectrum solution (8.1.1) curves and the corresponding results for the free escape boundary solution (10.1.2). Using the numerical values of the diffusion coefficient at 1 A U and 1 G V,and the solar wind speed V, assumed in the previous paragraph, the F_o curves r_b/r = 1.01, 1.1, 2.0 and ∞ of Figure 10.3 represent, respectively, the distributions to be obtained at r = 1 A U from protons released from r_b = 1.01, 1.1, 2.0 A U and infinity with kinetic energy T_o = 1 GeV.

The features of the free escape boundary solution (10.1.2) investigated in this chapter are quite similar to the monoenergetic galactic spectrum solution (8.1.1) results displayed in Figure 8.3a . Finally we remark that the basic effect of the free escape boundary is to reduce the values of F_o and U_p below the values obtained for the corresponding monoenergetic galactic spectrum solution obtained when $r_b \to \infty$, and at $r/r_b << 1$ there is virtually no difference between the solutions.

FIGURES 10.1 - 10.3

Figure 10.1 - The momentum dependence of various physical quantities associated with a monoenergetic galactic spectrum of particles at heliocentric radius r_b, for the solution (10.1.2), in which $U_p \to N_g\, \delta(p-p_o)$ as $r \to r_b$, and the diffusion coefficient $K(r,p) = K_c\, p\, r^{7/3}$. The figure is drawn for $V\, r_b/K(r_b,p_o) = 0.005$, and for values 0.9, 0.1 and 0.01 of the heliocentric radius variable r/r_b. Shown (in dimensionless form) are

(a) the momentum average distribution function $F_o(r,p)$,

(b) the differential number density $U_p = 4\,\pi\, p^2\, F_o$,

(c) the radial gradient $G_r = (1/U_p)(\partial U_p/\partial r)$,

(d) the radial differential current density S_p and its convective and diffusive components S_c and S_d, i.e.,

$$S_c = -\,4\,\pi\, p^3 (V/3)\, \partial F_o/\partial p\ ,$$

$$S_d = -\,4\,\pi\, p^2\, K(r,p)\, \partial F_o/\partial r\ ,$$

$$S_p = S_c + S_d .$$

Here

$$\overline{F}_o = p_o^3\, F_o/N_g ,$$

$$\overline{U}_p = p_o\, U_p/N_g ,$$

$$\mathrm{Grad}(\log(U_p)) = r_b\, G_r ,$$

$$\overline{S}_c = p_o\, S_c\, /\, (V\, N_g) ,$$

$$\overline{S}_d = p_o\, S_d\, /\, (V\, N_g) ,$$

$$\overline{S}_p = \overline{S}_c + \overline{S}_d = p_o\, S_p\, /\, (V\, N_g) ,$$

are dimensionless forms of F_o, U_p, G_r, S_c, S_d and S_p.

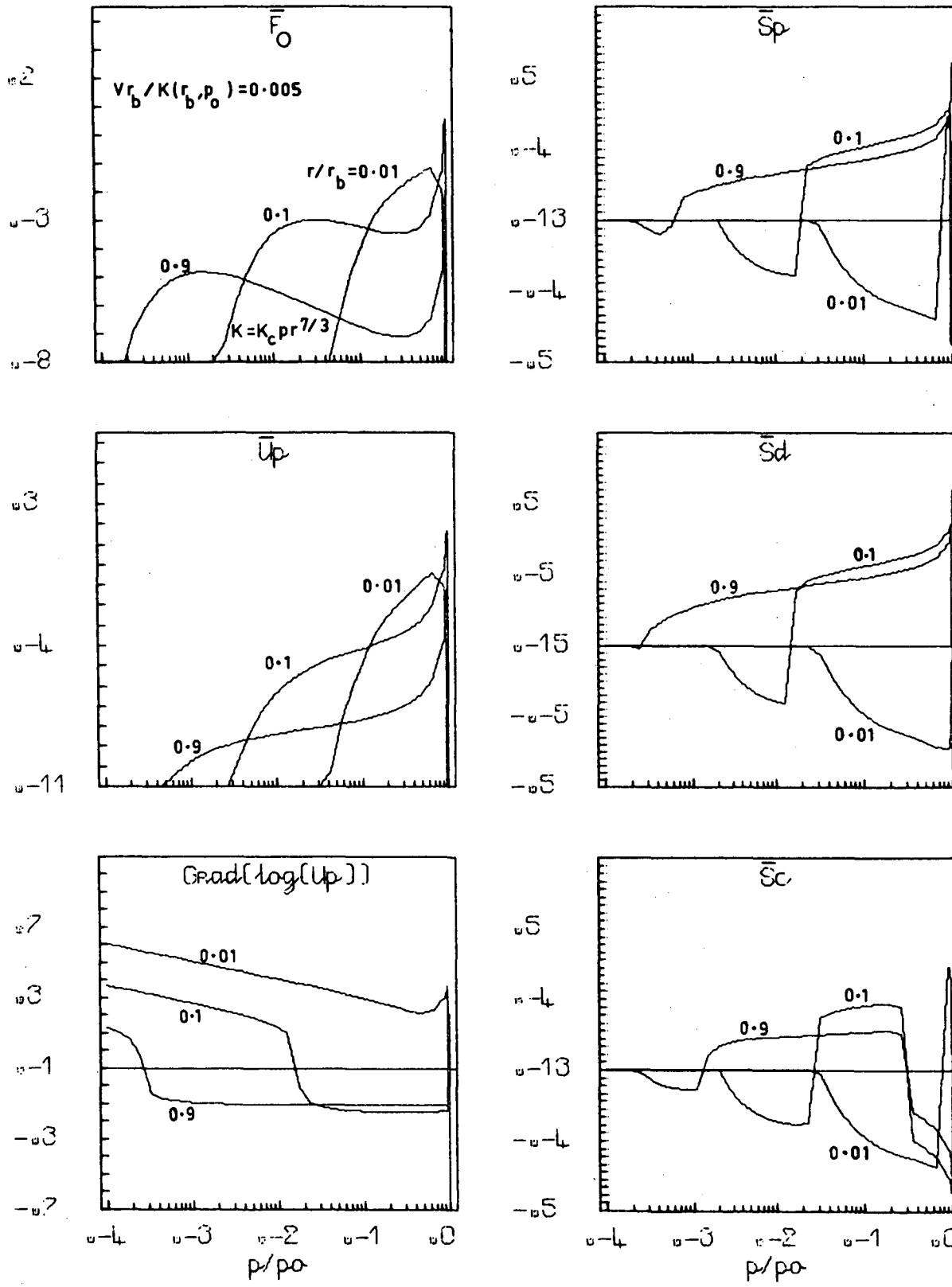
$\bar{F}_O$
$Vr_b/K(r_b,p_o)=0{\cdot}005$
$r/r_b=0{\cdot}01$
0·1
0·9
$K=K_c pr^{7/3}$
$\bar{S}p$
0·1
0·9
0·01
$\bar{U}p$
0·01
0·1
0·9
$\bar{S}d$
0·1
0·9
0·01
Grad[log(Up)]
0·01
0·1
0·9
$\bar{S}c$
0·1
0·9
0·01
p/po
p/po

Figure 10.1

Figure 10.2 - The momentum dependence of various physical quantities associated with a monoenergetic galactic spectrum of particles at heliocentric radius r_b, for the solution (10.1.2), in which $U_p \to N_g\, \delta(p-p_o)$ as $r \to r_b$, and the diffusion coefficient $K(r,p) = K_c\, p\, r^{7/3}$. The figure is drawn for $r/r_b = 0.1$, and for values 0.0005, 0.005 and 0.1 of the parameter $V\, r_b/K(r_b,p_o)$. Shown (in dimensionless form) are:

(a) the momentum average distribution function $F_o(r,p)$,
(b) the differential number density $U_p = 4\pi p^2 F_o$,
(c) the radial gradient $G_r = (1/U_p) \cdot (\partial U_p/\partial r)$.
(d) the radial differential current density S_p and its convective and diffusive components S_c and S_d, i.e.

$$S_c = -4\pi p^3 (V/3)\, \partial F_o/\partial p ,$$

$$S_d = -4\pi p^2 K(r,p)\, \partial F_o/\partial r ,$$

$$S_p = S_c + S_d .$$

Here

$$\overline{F}_o = p_o^3\, F_o / N_g ,$$

$$\overline{U}_p = p_o\, U_p / N_g ,$$

$$\mathrm{Grad}(\log (U_p)) = r_b\, G_r ,$$

$$\overline{S}_c = p_o\, S_c / (V\, N_g),$$

$$\overline{S}_d = p_o\, S_d / (V\, N_g),$$

$$\overline{S}_p = \overline{S}_c + \overline{S}_d = p_o\, S_p / (V\, N_g),$$

are dimensionless forms of F_o, U_p, G_r, S_c, S_d and S_p.

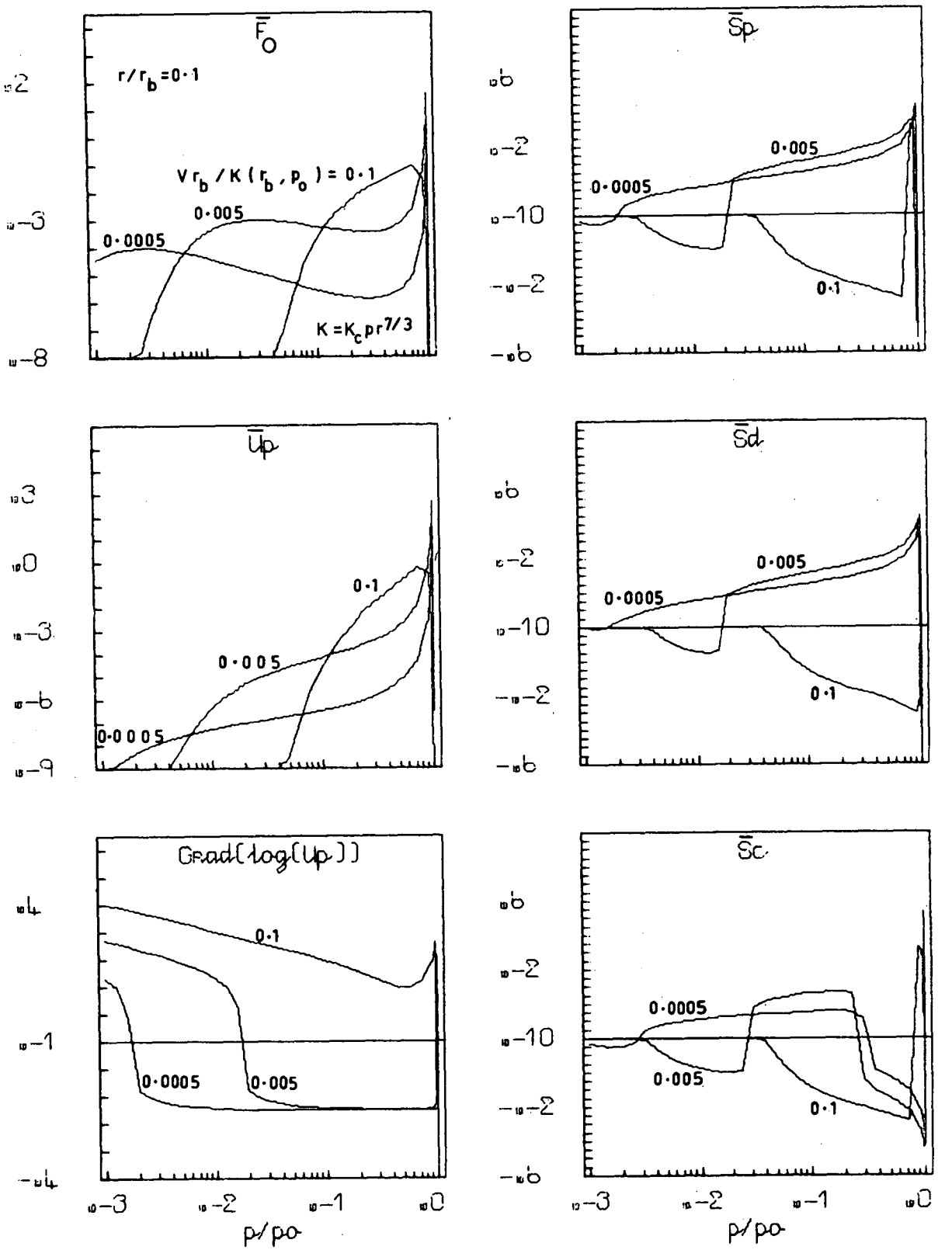
$\bar{F}_O$
$r/r_b = 0{\cdot}1$
$V r_b / K(r_b, p_o) = 0{\cdot}1$
0·005
0·0005
$K = K_c p r^{7/3}$
$\bar{S}p$
0·005
0·0005
0·1
$\bar{U}p$
0·1
0·005
0·0005
$\bar{S}d$
0·005
0·0005
0·1
Grad(log(Up))
0·1
0·0005
0·005
$\bar{S}c$
0·0005
0·005
0·1
p/po
p/po

Figure 10.2

Figure 10.3 - The momentum dependence of various physical quantities associated with a monoenergetic galactic spectrum of particles at heliocentric radius r_b, for the solution (10.1.2), in which $U_p \to N_g\ \delta(p-p_o)$ as $r \to r_b$, and the diffusion coefficient $K(r,p) = K_c\ p\ r^{7/3}$. The figure is drawn for $V\ r/K(r,p_o) = 0.11753$. It shows the dependence of the solution on the position of the boundary r_b, through the parameter r_b/r which has values of 1.01, 1.1, 2.0 and infinity. Shown (in dimensionless form) are:

(a) the momentum average distribution function $F_o(r,p)$,

(b) the differential number density $U_p = 4\pi p^2 F_o$,

(c) the radial gradient $G_r = (1/U_p)\ .\ (\partial U_p/\partial r)$

(d) the radial differential current density S_p and its convective and diffusive components S_c and S_d, i.e.,

$$S_c = -4\pi p^3 (V/3)\ \partial F_o/\partial p\ ,$$

$$S_d = -4\pi p^2 K(r,p)\ \partial F_o/\partial r\ ,$$

$$S_p = S_c + S_d\ .$$

Here

$$\overline{F}_o = p_o^3 F_o / N_g,$$

$$\overline{U}_p = p_o U_p / N_g,$$

$$\text{Grad}\ (\log(U_p)) = r_s G_r,$$

$$\overline{S}_c = p_o S_c / (V N_g),$$

$$\overline{S}_d = \overline{S}_c + \overline{S}_d = p_o S_p / (V N_g)\ ,$$

are dimensionless forms of F_o, U_p, G_r, S_c, S_d and S_p and $r_s = (K_c\ p_o/V)^{-3/4}$ is a characteristic length.

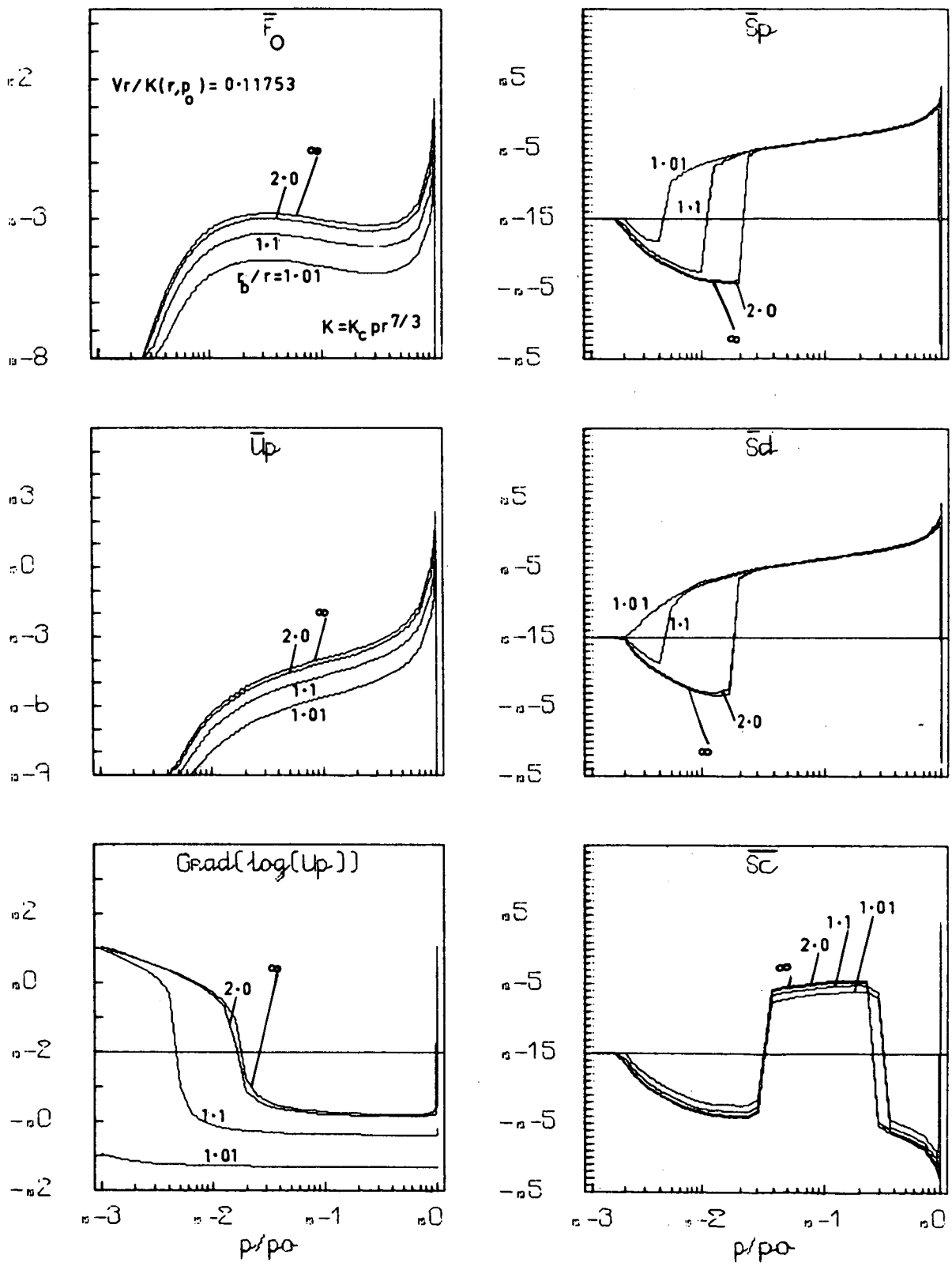
$\bar{r}_o$
Vr/K(r,p$_o$) = 0·11753
2·0
∞
1·1
r_b/r=1·01
K=K$_c$ pr$^{7/3}$
$\bar{S}_p$
1·01
1·1
2·0
∞
$\bar{U}_p$
2·0
∞
1·1
1·01
$\bar{S}_d$
1·01
1·1
2·0
∞
Grad[log[Up]]
2·0
∞
1·1
1·01
p/po
$\bar{S}_c$
1·01
1·1
2·0
∞
p/po

Figure 10.3

APPENDIX A

In this appendix we derive two sets of partial differential equations associated with the spherical symmetric similarity solutions of Chapter (5). These solutions, expressed in terms of F_o are of the form

$$F_o = a(z,t)\, g(z,\tau), \tag{A.1}$$

where the similarity variable z is a function of heliocentric radius r only, τ and t are functions of momentum p.

We obtain a partial differential equation for $F_o(z,t)$ in terms of the variables z and t. This equation is obtained by transforming the variables from $(x,t) \rightarrow (z,t)$ in the spherical symmetric, separable form of the transport equations (2.2.7) and (2.2.8).

The function a(z,t) and the variable τ are then chosen so that $g(z,\tau)$ satisfies an equation of the form

$$\frac{1}{q(z)} \frac{\partial}{\partial z}\left(p(z) \frac{\partial g}{\partial z} \right) = \frac{\partial g}{\partial \tau}, \tag{A.2}$$

with appropriate p(z) and q(z).

There are four cases to consider corresponding to the diffusion coefficients:

(i) $K(r,p) = K_o\, r^b\, p^{3(b-1)/4}, \quad b > 1,$

(ii) $K(r,p) = K_o\, r^b, \quad b < 1,$

(iii) $K(r,p) = K_o\, r^b, \quad b > 1,$

(iv) $K(r,p) = K_o\, r,$

and we now investigate these cases in detail.

Case (i) $K(r,p) = K_o\, r^b\, p^{3(b-1)/4}$

In this case the similarity variable z, and t are given by Equations (5.2.3) and (5.2.2), i.e.,

$$\begin{aligned} t &= 2K_o\, p^{3(1-b)/4} / (V(b-1)), \\ z &= x/t = V\, r^{(1-b)/2} / K_o, \\ x &= 2(rp^{3/2})^{(1-b)/2} / (b-1), \end{aligned} \tag{A.3}$$

and from Equation (2.2.7)

$$\frac{\partial^2 F_o}{\partial x^2} + \frac{2n+1}{x} \frac{\partial F_o}{\partial x} = \frac{\partial F_o}{\partial t}, \qquad (A.4)$$

is the transport equation for F_o.

Transforming the variables in (A.4) from $(x,t) \rightarrow (z,t)$ we have

$$\frac{\partial}{\partial x} = \frac{1}{t} \frac{\partial}{\partial z},$$

$$\frac{\partial^2}{\partial x^2} = \frac{1}{t^2} \frac{\partial^2}{\partial z^2}, \qquad (A.5)$$

$$\frac{\partial}{\partial t} = \frac{\partial}{\partial t} - \frac{z}{t} \frac{\partial}{\partial z}$$

for the transformations of the partial derivative operators. Using these transformations Equation (A.4) becomes

$$\frac{\partial^2 F_o}{\partial z^2} + \left(\frac{2n+1}{z} + zt \right) \frac{\partial F_o}{\partial z} = t^2 \frac{\partial F_o}{\partial t}, \qquad (A.6)$$

which is the transport equation in terms of z and t.

In order to transform the partial differential equation (A.6) to Sturm Liouville form, the similarity solution (5.2.5):

$$F_o = [\exp(-z^2 t/4)\ t^{-n-1}]\ z^{-n} \exp(-\chi/t)\ (A.I_m(\sqrt{\chi}\ z) + B.K_m(\sqrt{\chi}\ z)),$$

suggests that we choose

$$a(z,t) = \exp(-z^2 t/4)\ t^{-n-1}. \qquad (A.7)$$

as the expression for a(z,t) in Equation (A.1). Putting

$$\tau = -1/t,$$

$$F_o = a(z,t)\ g(z,\tau), \qquad (A.8)$$

Equation (A.6) for F_o reduces to

$$\frac{1}{z^{2n+1}} \frac{\partial}{\partial z} \left(z^{2n+1} \frac{\partial g}{\partial z} \right) = \frac{\partial g}{\partial \tau} \qquad (A.9)$$

Equation (A.9) for $g(z,\tau)$ has separated solutions which satisfy a

Sturm-Liouville equation and it is the equation for $g(z,\tau)$ that we set out to obtain.

Case (ii) $K(r,p) = K_o\, r^b, \quad b < 1$

In this case the similarity variable z, and t are given by Equations (5.2.10) and (5.2.11):

$$z = V\, r^{1-b} / (K_o(1-b)) = -x^2/(4t), \qquad (A.10)$$

$$t = K_o\, p^{3(1-b)/2} / (V\,(b-1)),$$

and the appropriate transport equation for F_o, in terms of the variables x and t is given in Equation (A.4).

Transforming the variables from (x,t) to (z,t) we have

$$\frac{\partial}{\partial x} = -\frac{x}{2t}\,\frac{\partial}{\partial t}\,,$$

$$\frac{\partial^2}{\partial x^2} = \frac{-1}{2t}\,\frac{\partial}{\partial z} - \frac{z}{t}\,\frac{\partial^2}{\partial z^2}\,, \qquad (A.11)$$

$$\frac{\partial}{\partial t} = \frac{\partial}{\partial t} - \frac{z}{t}\,\frac{\partial}{\partial z}\,,$$

for the transformation of partial derivatives. Using these transformations Equation (A.4) becomes

$$z\,\frac{\partial^2 F_o}{\partial z^2} + (n+1-z)\,\frac{\partial F_o}{\partial z} = -t\,\frac{\partial F_o}{\partial t}\,, \qquad (A.12)$$

which is the equation for F_o in terms of z and t.

Choosing

$$\tau = -\ell n(\,|t|\,), \qquad (A.13)$$

$$F_o(z,t) = g(z,\tau),$$

we find

$$\frac{1}{z^n e^{-z}}\,\frac{\partial}{\partial z}\left(\, z^{n+1} e^{-z}\,\frac{\partial g}{\partial z}\,\right) = \frac{\partial g}{\partial \tau} \qquad (A.14)$$

which is the required equation for $g(z,\tau)$.

Case (iii) $K(r,p) = K_o r^b, \quad b > 1$

The appropriate similarity variable z, and t are given by Equations (5.2.10) and (5.2.11), i.e.,

$$z = V r^{1-b} / (K_o(b-1)) = x^2 / (4t),$$
$$t = K_o p^{3(1-b)/2} / (V (b-1)), \tag{A.15}$$

and the transport equation for F_o, in terms of the variables x and t is given in Equation (A.4).

Transforming the variables from (x,t) to (z,t) we have

$$\frac{\partial}{\partial x} = \frac{x}{2t} \frac{\partial}{\partial z},$$
$$\frac{\partial^2}{\partial x^2} = \frac{1}{2t} \frac{\partial}{\partial z} + \frac{z}{t} \frac{\partial^2}{\partial z^2}, \tag{A.16}$$
$$\frac{\partial}{\partial t} = \frac{\partial}{\partial t} - \frac{z}{t} \frac{\partial}{\partial z},$$

for the transformation of partial derivatives and from Equations (A.4) and (A.16)

$$z \frac{\partial^2 F_o}{\partial z^2} + (n+1+z) \frac{\partial F_o}{\partial z} = t \frac{\partial F_o}{\partial t}, \tag{A.17}$$

is the equation for F_o in terms of z and t.

Choosing

$$\tau = \ell n(t) = -3(b-1) \ell n(p)/2, \tag{A.18}$$
$$F_o = g(z, \tau),$$

we find

$$\frac{1}{z^n e^z} \frac{\partial}{\partial z} \left(z^{n+1} e^z \frac{\partial g}{\partial z} \right) = \frac{\partial g}{\partial \tau}, \tag{A.19}$$

which is the required equation for $g(z, \tau)$.

Case (iv) $K(r,p) = K_o r$

The similarity variable z and the variable t for this case are given in Equations (5.2.15) and (5.2.18), i.e.,

$$z = \ell n(r) = -x + V\,t/K_o - \ell n(2)/2,$$
$$t = -3K_o\,\ell n(p)\,/\,(2V), \tag{A.20}$$

and from Equation (2.2.8)

$$\frac{\partial^2 F_o}{\partial x^2} - 2\frac{\partial F_o}{\partial x} = \frac{\partial F_o}{\partial t}\ , \tag{A.21}$$

is the transport equation for F_o.

Transforming the variables from $(x,t) \rightarrow (z,t)$ we have

$$\frac{\partial}{\partial x} = -\frac{\partial}{\partial z}\ ,$$
$$\frac{\partial^2}{\partial x^2} = \frac{\partial^2}{\partial z^2}\ , \tag{A.22}$$
$$\frac{\partial}{\partial t} = \frac{\partial}{\partial t} + \frac{V}{K_o}\frac{\partial}{\partial z}\ ,$$

as the transformations for the partial derivative operators. Using these transformations Equation (A.21) becomes

$$\frac{\partial^2 F_o}{\partial z^2} + 2c\frac{\partial F_o}{\partial z} = \frac{\partial F_o}{\partial t}\ , \tag{A.23}$$

where

$$c = 1 - V/(2K_o). \tag{A.24}$$

In this case we choose

$$F_o = g(z,\ t),$$

and

$$e^{-2cz}\frac{\partial}{\partial z}\left(\ e^{2cz}\ \frac{\partial g}{\partial z}\ \right) = \frac{\partial g}{\partial t}$$

is the standard form of the equation for g(z, t).

APPENDIX B

In this appendix we give an example of the derivation of a Green's function of Chapter (5) when the eigenspectrum is continuous. We consider the case where the diffusion coefficient

$$K(r,p) = K_o\, r^b\, p^{3(b-1)/4}, \quad b > 1, \tag{B.1}$$

and we have a monoenergetic source of momentum p_o located at radius r_o, between an outer free escape boundary at radius r_b and an inner boundary at $r = 0$.

We note that for diffusion coefficients of the form (B.1) the similarity solutions of the steady state spherically symmetric transport equation are of the form

$$F_o = a(z,t)\, g(z,\tau) \tag{B.2}$$

where

$$\begin{aligned} a(z,t) &= t^{m-1}\, e^{-z^2 t/4}, \\ z &= V\, r^{(1-b)/2} / K_o = x/t, \\ n &= (b+1) / (1-b), \quad m = |n|, \\ t &= 2\, K_o\, p^{3(1-b)/4} / (V\,(b-1)), \\ T &= t - t_o, \\ x &= 2\, (r\, p^{3/2})^{(1-b)/2} / (1-b), \\ \tau &= -1/t, \end{aligned} \tag{B.3}$$

and $g(z,\tau)$ satisfies the partial differential equation

$$\frac{\partial^2 g}{\partial z^2} + \frac{2n+1}{z}\,\frac{\partial g}{\partial z} = \frac{\partial g}{\partial \tau}, \tag{B.4}$$

(See Appendix (A)).

We initially find the Green's function for $g(z,\tau)$. This solution of Equation (B.4) is denoted by G_g; it satisfies the conditions:

$$\begin{aligned} &\text{(i)} \quad G_g \to \delta(z-z_o) \quad \text{as } \tau \to \tau_o, \quad \tau > \tau_o, \\ &\text{(ii)} \quad G_g(z_1,\tau) = G_g(\infty,\tau) = 0, \end{aligned} \tag{B.5}$$

where

$$z_1 = z(r_b), \quad z_o = z(r_o), \quad \tau_o = \tau(p_o),$$

and $0 < r_o < r_b < \infty$.

We shall show that the Green's function G_g satisfying Equations (B.4) and (B.5) is given by Equation (5.3.36), i.e.

$$G_g = z^m z_o^{1-m} \int_0^\infty s. [J_m(sz) Y_m(sz_1) - J_m(sz_1) Y_m(sz)] .$$

$$\frac{[J_m(sz_o)Y_m(sz_1) - J_m(sz_1)Y_m(sz_o)]}{J_m^2(sz_1) + Y_m^2(sz_1)} \exp[-s^2(\tau-\tau_o)] \, ds. \tag{B.6}$$

The Green's function for the distribution function F_o, denoted by G_F can then be obtained from Equation (B.2), i.e.,

$$G_F = a(z,t) G_g / a(z_o, t_o) ,$$

i.e.,

$$G_F = (t/t_o)^{m-1} \exp(-z^2 t/4 + z_o^2 t_o/4) G_g. \tag{B.7}$$

Derivation of G_g

The solution $g(z,\tau)$ of Equation (B.4) that we seek may be obtained by a Laplace transform technique. Putting

$$u(z,\lambda) = \int_0^\infty e^{-\lambda(\tau-\tau_o)} g(z,\tau) \, d\tau ,$$

and taking the Laplace transform of the partial differential equation (B.4) and the boundary conditions (B.5) we find that $u(z,\lambda)$ must satisfy the differential equation

$$\frac{d^2u}{dz^2} + \frac{1-2m}{z} \frac{du}{dz} - \lambda u = - \delta(z-z_o), \tag{B.8}$$

and the boundary conditions

$$u(z_1, \lambda) = 0, \tag{B.9a}$$

$$u(\infty, \lambda) \quad \text{is finite.} \tag{B.9b}$$

The general solution of the inhomogeneous equation (B.8) is

$$u = u_1\left(c_1 - \int^z [-\delta(y-z_o)] u_2(y)/W(u_1(y), u_2(y)) \, dy\right)$$

$$+ u_2\left(c_2 + \int^z [-\delta(y-z_o)] u_1(y)/W(u_1(y), u_2(y)) \, dy\right), \tag{B.10}$$

where c_1 and c_2 are arbitrary constants

and u_1 and u_2 are two independent solutions of the homogeneous equation (B.8) and $W(u_1, u_2)$ is their wronskian. (see Morse and Feshback (1953) Section (5.2), p.530, Vol.1).

Two independent solutions of the homogeneous equation (B.8) are

$$u_1 = z^m I_m(\sqrt{\lambda}\, z), \tag{B.11}$$

$$u_2 = z^m K_m(\sqrt{\lambda}\, z), \tag{B.12}$$

where $I_m(z)$ and $K_m(z)$ are modified Bessel functions of the first and second kind of argument z. The wronskian of u_1 and u_2 is

$$W(u_1(z), u_2(z)) = z^{2m-1}, \tag{B.13}$$

and

$$u_1 \to z^m e^{\sqrt{\lambda}z} / \sqrt{2\pi\sqrt{\lambda}\, z} \to \infty \quad \text{as } z \to \infty,$$
$$\text{for } |\arg(\sqrt{\lambda}\, z)| < \pi/2, \tag{B.14}$$
$$u_2 \to \sqrt{\pi}\, z^m e^{-\sqrt{\lambda}z} \sqrt{\sqrt{2/\lambda z}} \to 0, \quad \text{as } z \to \infty$$
$$\text{for } |\arg(\sqrt{\lambda}\, z)| < 3\pi/2.$$

(Abramowitz and Stegun 1965, Section (9.7))

specifies the asymptotic forms of u_1 and u_2 for large z.

The constants c_1 and c_2 in the solution (B.10) are determined by the boundary conditions (B.9). Using the asymptotic results (B.14) then the boundary condition (B.9b), which applies as $z \to \infty$, is satisfied if

$$c_1 = -\int^{\infty} (\delta(y-z_o)\, u_2(y,\lambda) / W(u_1, u_2))\, dy. \tag{B.15}$$

The homogeneous boundary condition at $z = z_1$ is satisfied if we choose

$$c_2 = \int^{z_1} (\delta(y-z_o)\, u_1(y,\lambda)/ W(u_1,u_2))\, dy + \left[u_1(z_1,\lambda)/u_2(z_1,\lambda)\right] \int_{z_1}^{\infty} (\delta(y-z_o)\, u_2(y)/W(u_1,u_2))dy. \tag{B.16}$$

Substituting the expressions (B.15), and (B.16) for c_1 and c_2

into the solution (B.10) we have

$$u(z,\lambda) = - u_1(z,\lambda) \int_z^\infty (\delta(y-z_o)\, u_2(y,\lambda) \,/\, W(u_1,u_2))\, dy$$
$$+ u_2(z,\lambda) \left[\int_z^{z_1} (\delta(y-z_o)\, u_1(y,\lambda)/W(u_1,u_2))\, dy \right.$$
$$\left. + (u_1(z_1,\lambda)/u_2(z_1,\lambda)) \int_{z_1}^\infty (\delta(y-z_o)\, u_2(y,\lambda)\,/W(u_1,u_2))\, dy \right]. \tag{B.17}$$

Substituting the expressions (B.11), (B.12) and (B.13) for u_1, u_2, $W(u_1,u_2)$ in the solution (B.17) we obtain

$$u(z,\lambda) = z^m I_m(\sqrt{\lambda}z) \int_z^\infty \delta(y-z_o)\, y^{1-m} K_m(\sqrt{\lambda}y)\, dy$$
$$+ z^m K_m(\sqrt{\lambda}z) \left[\int_{z_1}^z \delta(y-z_o) y^{1-m} I_m(\sqrt{\lambda}y)\, dy \right.$$
$$\left. - (I_m(\sqrt{\lambda}z_1)/K_m(\sqrt{\lambda}z_1)) \int_{z_1}^\infty \delta(y-z_o)\, y^{1-m} K_m(\sqrt{\lambda}y)\, dy \right]. \tag{B.18}$$

as the solution for $u(z,\lambda)$.

Carrying out the integrations in (B.18), the solution splits into two parts, and we have:

if $z_1 < z < z_o < \infty$

$$u(z,\lambda) = z^m z_o^{1-m} \quad w(z,z_o;\, z_1,\lambda), \tag{B.19}$$

and if $z_1 < z_o < z < \infty$,

$$u(z,\lambda) = z^m z_o^{1-m} \quad w(z_o,z;\, z_1,\lambda), \tag{B.20}$$

where

$$w(z,z_o;z_1,\lambda) = \frac{K_m(\sqrt{\lambda}\, z_o)}{K_m(\sqrt{\lambda}\, z_1)} \quad [I_m(\sqrt{\lambda}z)\, K_m(\sqrt{\lambda}z_1) - I_m(\sqrt{\lambda}z_1) K_m(\sqrt{\lambda}z)] \tag{B.21}$$

The required solution for $g(z,\tau)$ is now obtained by using the Bromwich contour integral formula for the inverse Laplace transform (see Spiegel (1970)).

i.e.,
$$g(z,\tau) = \frac{1}{2\pi i} \int_{c-i\infty}^{c+i\infty} u(z,\lambda)\, e^{\lambda(\tau-\tau_o)}\, d\lambda, \tag{B.22}$$

where c is a real non negative constant, chosen so that the inverse Laplace transform (B.22) is well defined.

Since the function $w(z,z_o;z_1,\lambda)$ occurs in (B.19), and the function $w(z_o,z;\ z_1,\lambda)$ occurs in (B.20) we need only consider the region $z_1 < z < z_o < \infty$ in the inversion process; the other part of the solution for $g(z,\tau)$ in the region $z_1 < z_o < z < \infty$ is obtained by interchanging z and z_o in the inverse Laplace transform of $w(z,z_o;z_1,\lambda)$.

We now consider the inverse Laplace transform of $u(z,\lambda)$ for the region $z_1 < z < z_o < \infty$, so that

$$u(z,\lambda) = z^m z_o^{1-m} \frac{K_m(\sqrt{\lambda}\ z_o)}{K_m(\sqrt{\lambda}\ z_1)} [I_m(\sqrt{\lambda}z)K_m(\sqrt{\lambda}z_1)-I_m(\sqrt{\lambda}z_1)K_m(\sqrt{\lambda}z)\ ]. \tag{B.23}$$

The function $u(z,\lambda)$ has a branch point at $\lambda = 0$. To compute $g(z,\tau)$ from the Bromwich integral (B.22), we make a branch cut along the negative $Re(\lambda)$ axis, and construct: a large circular arc GAHBC of radius R centred on $\lambda = 0$ with the points C and G a small distance ϵ above and below the negative $Re(\lambda)$ axis; a small circular arc FED of radius r, centred on $\lambda = 0$, with the points D and F a distance ϵ above and below the negative $Re(\lambda)$ axis respectively. The large and small arcs are joined above and below the branch cut by the straight line segments C D and G F. The straight line segment A B is parallel to the $Im(\lambda)$ axis and distance c from it, and as the radius R, of the large arc tends to infinity, A B becomes the straight line segment $(c - i\infty,\ c + i\infty)$ in the complex λ plane(see Figure (B.1)).

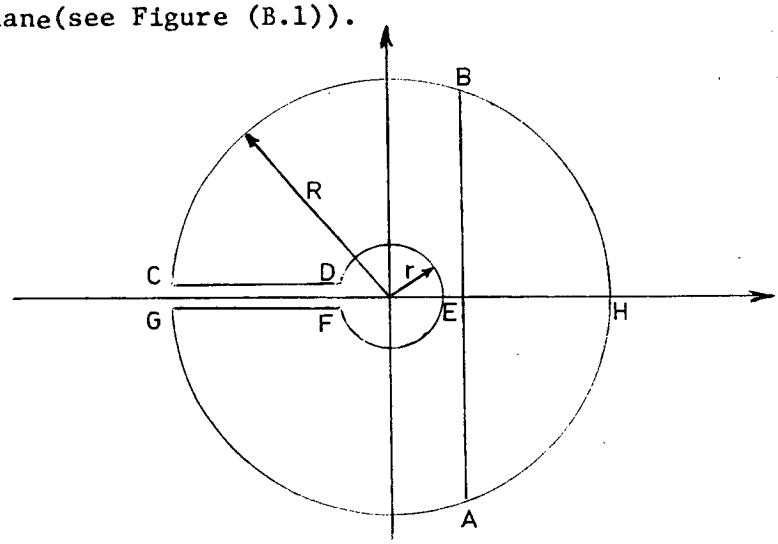

Figure B.1 Showing the Bromwich contours for the inversion of the Laplace transform. For $\tau > \tau_o$ the contour employed is A B C D E F G A, whereas for $\tau < \tau_o$ we use the contour A B H A.

For $\tau > \tau_o$ we first of all compute

$$g^*(z,\tau) = \int_A^B u(z,\lambda)\, e^{\lambda(\tau-\tau_o)}\, d\lambda,$$

by using Cauchy's theorem on the closed contour A B C D E F G A, whereas for $\tau < \tau_o$ we use Cauchy's theorem on the closed contour A B H A. The required transform (B.22) for $g(z,\tau)$ is then obtained by letting the radius of the large arc $R \to \infty$ and the radius of the small arc $r \to 0$.

Since $u(z,\lambda)$ has no poles within either contour, an application of Cauchy's theorem gives:

if $\tau > \tau_o$

$$g(z,\tau) = \frac{-1}{2\pi i} \lim_{\substack{r \to 0 \\ R \to \infty}} \int_{BCDEFGA} u(z,\lambda)\, e^{\lambda(\tau-\tau_o)}\, d\lambda, \qquad (B.24)$$

and if $\tau < \tau_o$

$$g(z,\tau) = -\frac{1}{2\pi i} \lim_{R \to \infty} \int_{BHA} u_1(z,\lambda)\, e^{\lambda(\tau-\tau_o)}\, d\lambda. \qquad (B.25)$$

Using the asymptotic results

$$K_m(x) \sim e^{-x}\sqrt{\frac{\pi}{2x}} \quad \text{as } x \to \infty, \quad |\arg(x)| < 3\pi/2 \qquad (B.26)$$

$$I_m(x) \sim \frac{e^x}{\sqrt{2\pi x}} \quad \text{as } x \to \infty, \quad |\arg(x)| < \pi/2,$$

(Abramowitz and Stegun (1965), Section (9.7))

and putting $\lambda = Re^{i\theta}$, with $|\theta| < \pi$, in the expression (B.23) for $u(z,\lambda)$ we have

$$|u(z,\lambda)| \sim \frac{z^m\, z_o^{1-m}}{2\sqrt{R\, z\, z_o}} \exp\left(-R\cos(\theta/2)\,|2z_1 - z_o - z|\right), \text{ as } R \to \infty$$

on the large circular arcs for sufficiently large R. From this last result it follows that the contribution to $g(z,\tau)$ from the integrals along the large circular arcs in (B.24) and (B.25) tend to zero as $R \to \infty$.

Using the expressions for $K_m(x)$ and $I_m(x)$ for small arguments

$$K_m(x) \sim \Gamma(m)\,(x/2)^{-m}/2, \text{ as } x \to 0, \quad (Re(m) > 0)$$

$$I_m(x) \sim (x/2)^m/\Gamma(m+1), \quad \text{as } x \to 0, \quad (m \neq -1, -2, \ldots)$$

and putting $\lambda = re^{i\theta}$ with $|\theta| < \pi$, in the expression (B.23) for $u(z,\lambda)$

we have

$$u(z,\lambda)\, d\lambda \sim re^{i\theta} d\theta \cdot z^m z_o^{1-m} (z_1/z_o)^m \Gamma(m) / (2\Gamma(m+1)) \cdot$$

$$[(z/z_1)^m - (z_1/z)^m]$$

on the small circular arc D E F. Thus the contribution to the contour integral (B.24) for $g(z,\tau)$ from the small circular arc D E F tends to zero as $r \to 0$.

Since the contributions to (B.24) and (B.25) from the circular arcs are zero in the limits as $r \to 0$ and $R \to \infty$ we have

if $\tau > \tau_o$

$$g(z,\tau) = \lim_{\substack{r \to 0 \\ R \to \infty}} \frac{-1}{2\pi i} (\int_{CD} + \int_{FG}) u(z,\lambda)\, e^{\lambda(\tau-\tau_o)}\, d\lambda, \qquad \text{(B.26)}$$

and if $\tau < \tau_o$

$$g(z,\tau) = 0. \qquad \text{(B.27)}$$

Using the transformations between modified Bessel functions and Bessel functions:

$$I_m(z) = \exp(-m\pi i/2)\ J_m(e^{i\pi/2} z), \quad -\pi < \arg(z) \le \pi/2,$$

$$K_m(z) = \frac{\pi i}{2} \exp(\frac{m\pi i}{2})\ H_m^{(1)}(e^{i\pi/2} z), \quad -\pi < \arg(z) \le \pi/2,$$

$$H_m^{(1)}(z) = J_m(z) + i\, Y_m(z) \qquad \text{(B.28)}$$

$$Y_m(z) = [J_m(z) \cos(m\pi) - J_{-m}(z)] / \sin(m\pi)$$

(Abramowitz and Stegun (1965), Section (9.6))

putting $\lambda = s^2 e^{i\pi}$, in the expression (B.23) for $u(z,\lambda)$ we have

$$\lim_{\substack{r \to 0 \\ R \to \infty}} -\frac{1}{2\pi i} \int_{CD} u(z,\lambda)\, e^{\lambda(\tau-\tau_o)}\, d\lambda$$

$$= \frac{z^m z_o^{1-m}}{2} \int_0^\infty s\, e^{-s^2(\tau-\tau_o)} [J_m(sz)\, Y_m(sz_1) - J_m(sz_1) Y_m(sz)]$$

$$[J_m(sz_o) Y_m(sz_1) - Y_m(sz_o) J_m(sz_o) - i\,(J_m(sz_o) J_m(sz_1)$$

$$+ Y_m(sz_o)\, Y_m(sz_1))] / [J_m^2(sz_1) + Y_m^2(sz_1)]\, ds. \qquad \text{(B.29)}$$

Using the relations (B.28) between modified Bessel functions and Bessel functions, putting $\lambda = s^2 e^{-i\pi}$, in the expression (B.23) for $u(z,\lambda)$ we have:

$$\lim_{\substack{r \to 0 \\ R \to \infty}} \frac{-1}{2\pi i} \int_{FG} u(z,\lambda)\, e^{\lambda(\tau-\tau_o)}\, d\lambda$$

$$= \frac{z^m z_o^{1-m}}{2} \int_0^\infty s\, e^{-s^2(\tau-\tau_o)} [J_m(sz)\, Y_m(sz_1) - Y_m(sz)\, J_m(sz_1)]$$

$$[J_m(sz_o)\, Y_m(sz_1) - J_m(sz_1)\, Y_m(sz_o) + i\,(J_m(sz_o)\, J_m(sz_1)$$

$$+ Y_m(sz_o)\, Y_m(sz_1))] \,/\, [J_m^2(sz_1) + Y_m^2(sz_1)]\, ds. \quad (B.30)$$

Substituting the results (B.29) and (B.30) into the expression (B.26) for $g(z,\tau)$ we obtain.

$$g(z,\tau) = z^m z_o^{1-m} \int_0^\infty s\, e^{-s^2(\tau-\tau_o)} [J_m(sz)\, Y_m(sz_1) - Y_m(sz) J_m(sz_1)] \cdot$$

$$[\, J_m(sz_o) Y_m(sz_1) - J_m(sz_1) Y_m(sz_o)] / [J_m^2(sz_1) + Y_m^2(sz_1)]\, ds. \quad (B.31)$$

The solution (B.31) is the Green's function that we set out to obtain; it has already been given in Equations (5.3.36) and (B.6).

We note that the solution (B.31) can be split into two parts: the first part is due to the source at (z_o, τ_o) and the second part is due to the boundary at $z = z_1$. If we let $z_1 \to 0$ ($r_b \to \infty$) in the solution (B.31), there will be no effect from the boundary. In this way we may identify the boundary and source terms in the solution (B.31). The source term is

$$S_g = z^m z_0^{1-m} \int_0^\infty s\, e^{-s^2(\tau-\tau_o)}\, J_m(sz)\, J_m(sz_o)\, ds \quad (B.32)$$

and the boundary term is

$$B_g = -z^m z_o^{1-m} \int_0^\infty s\, e^{-s^2(\tau-\tau_o)} \cdot J_m(sz_1) [J_m(sz).(J_m(sz_o) J_m(sz_1)$$

$$+ Y_m(sz_1)\, Y_m(sz_o)) + Y_m(sz)(J_m(sz_o) Y_m(sz_1) - J_m(sz_1) Y_m(sz_o))]$$

$$/ [J_m^2(sz_1) + Y_m^2(sz_1)]\, ds, \quad (B.33)$$

and

$$G_g = S_g + B_g \,. \tag{B.34}$$

Using the result

$$\int_0^\infty e^{-x^2\alpha} J_m(2\delta x)\, J_m(2\gamma x)\, dx$$

$$= \frac{1}{2\alpha}\; e^{-(\gamma^2+\delta^2)/\alpha}\; I_m\left(\frac{2\delta\gamma}{\alpha}\right), \qquad \mathrm{Re}(\beta) > -1 \tag{B.35}$$

(Gradshteyn and Ryzhik (1965), Section (6.61), p.710)

the source term S_g of Equation (B.32) reduces to

$$S_g = \frac{z^m\, z_o^{1-m}}{2(\tau-\tau_o)}\; \exp\left(\frac{-(z^2+z_o^2)}{4(\tau-\tau_o)}\right) I_m\left(\frac{z\, z_o}{2(\tau-\tau_o)}\right) . \tag{B.36}$$

The Green's function for the distribution function F_o corresponding to the result (B.36) is

$$G_F = (t/t_o)^{m-1} \exp\left((z_o^2\, t_o - z^2 t)/4\right) \cdot$$

$$\left[\; \frac{z^m\, z_o^{1-m}}{2(\tau-\tau_o)}\; \exp\left(-\frac{z^2+z_o^2}{4(\tau-\tau_o)}\right) I_m\left(\frac{z\, z_o}{2(\tau-\tau_o)}\right) \right] . \tag{B.37}$$

From the transformations (B.3) we have

$$x = 2(r\, p^{3/2})^{(1-b)/2} / (b-1) = zt$$

$$\tau = -1 / t,$$

$$T = t - t_o,$$

and upon expressing the result (B.37) in terms of x and t we have

$$G_F = t_o\; \frac{x^m\, x_o^{1-m}}{2T}\; \exp\left(-\frac{x^2+x_o^2}{4T}\right)\; I_m\left(\frac{x\, x_o}{2T}\right) . \tag{B.38}$$

This latter result is just t_o times the Green's function (5.3.12) with a free escape boundary at $r = \infty$.

APPENDIX C

In this appendix we derive the solutions of the steady-state spherically symmetric equation of transport given in Equations (6.3.25), which were initially obtained by Fisk and Axford (1969). In these solutions the momentum-average distribution function F_o satisfies the boundary conditions

$$\begin{aligned} &\text{(i)} \quad F_o \to N_g\, p^{-\mu-2} \quad \text{as} \quad r \to \infty, \quad \mu > 0, \\ &\text{(ii)} \quad F_o \text{ is finite as} \quad r \to 0, \end{aligned} \tag{C.1}$$

and the diffusion coefficient $K(r,p) = K_o\, p^a\, r^b$, where a, b, and K_o are constants, with $a > 0$, $b > 1$ and $K_o > 0$.

These solutions are obtained from the general galactic spectrum solution (6.3.17), i.e.,

$$F_o(r,p) = \frac{x^{2m}}{2^{2m}\Gamma(m)} \int_{t_s=t(p=\infty)}^{t_s=t(p)} \frac{Z(t_s)}{(t-t_s)^{m+1}} \exp\left(\frac{-x^2}{4(t-t_s)}\right) dt_s. \tag{C.2}$$

Here $z(t_s)$ specifies the galactic spectrum, i.e.

$$Z(t_s) = F_o(\infty, p_s) = N_g\, p_s^{-\mu-2},$$

and

$$\begin{aligned} t &= \begin{cases} -\varepsilon\, p^{\delta}/\delta & \text{if} \quad \delta = a + 3(1-b)/2 \neq 0, \\ -\varepsilon\, \ell n(p) & \text{if} \quad \delta = 0, \end{cases} \\ \varepsilon &= 3K_o / 2V, \\ t_s &= t(p_s), \\ x &= 2(rp^{3/2})^{(1-b)/2}/(1-b), \\ m &= (b+1)/(b-1). \end{aligned} \tag{C.3}$$

The solution of the boundary value problem (C.1) splits into three cases according as $\delta \gtrless 0$.

Case (i) $\delta > 0$ or $1 < b < 1 + 2a/3$

In order to obtain the Fisk and Axford result given in Equation (6.3.25a) we introduce the variables

$$y = (\mu+2) / \delta,$$
$$s = x^2 / [4(t-t_s)], \qquad (C.4)$$

and hence transform the integral (C.2) over t_s to an integral over s. To execute this transformation we note that

$$p_s = p\,(1 + \delta x^2 / (4\,\epsilon\, p^\delta\, s))^{1/\delta},$$
$$Z(t_s) = N_g\, p^{-\mu-2}\, s^y\, (s + \delta\, x^2 / (4\,\epsilon\, p^\delta))^{-y}, \qquad (C.5)$$
$$dt_s = x^2\, ds / (4s^2),$$

and the limits of integration over s are determined from the results:

$$s \to 0 \text{ as } t_s \to t(p=\infty) = -\infty,$$
and
$$s \to \infty \text{ as } t_s \to t. \qquad (C.6)$$

Using the transformations (C.4), (C.5) and (C.6) the solution (C.2) for F_o becomes

$$F_o(r,p) = \frac{N_g\, p^{-\mu-2}}{\Gamma(m)} \int_0^\infty (s+ \delta x^2/(4\,\epsilon p^\delta))^{-y}\, s^{y+m-1}\, e^{-s}\, ds. \qquad (C.7)$$

To proceed further we note that the second solution of Kummer's confluent hypergeometric equation, U(a,b,x) is given by the formula

$$U(a,b,x) = \frac{x^{1-b}}{\Gamma(a)} \int_0^\infty e^{-s}\, s^{a-1}\, (s+x)^{b-a-1}\, ds, \qquad (C.8)$$

(Slater (1960), Section (3.1.2))

where Re(a), Re(x) > 0, and that

$$U(a,b,x) = x^{1-b}\, U(1+a-b,\ 2-b,\ x), \qquad (C.9)$$

which is Kummer's transformation (Slater 1960, Section (1.4), p.38). Using the results (C.8) and (C.9) in the expression (C.6) for F_o we obtain

$$F_o = N_g\, p^{-\mu-2}\, \frac{\Gamma(\nu(\mu+2)/3+m)}{\Gamma(m)}\, U(\nu(\mu+2)/3, 2/(1-b),\ 2Vr^{1-b}p^{-a}/(\nu(1-b)^2K_o)), \qquad (C.10)$$

where

$$\nu = 3/\delta = 3/(a+3(1-b)/2),$$

is positive, i.e., $1 < b < 1 + 2a/3$.

This is the result of Fisk and Axford, and it is also given in Equation (6.3.25a).

Case (ii) $\delta = 0$ or $b = 1 + 2a/3$

To obtain the Fisk and Axford result, we introduce the variable

$$s = t - t_s = \varepsilon \ln(p_s/p). \tag{C.11}$$

Thus we have

$$\begin{aligned} p_s &= p \exp(s/\varepsilon) \\ Z(t_s) &= N_g p_s^{-\mu-2} = N_g p^{-\mu-2} \exp(-(\mu+2)s/\varepsilon) \\ dt_s &= -ds, \end{aligned} \tag{C.12}$$

and the limits of integration over s are determined by the results:

$$\begin{aligned} s &\to 0 \quad \text{as} \quad t_s \to t, \\ s &\to \infty \quad \text{as} \quad t_s \to t(\infty) = -\infty . \end{aligned} \tag{C.13}$$

Transforming the integration variable in the general solution (C.2) from t_s to s, and using the results (C.12) and (C.13) we obtain

$$F_o = N_g p^{-\mu-2} (x^2/4)^m \int_0^\infty \exp(-(\mu+2)s/\varepsilon - x^2/4s)\, s^{-m-1}\, ds/\Gamma(m). \tag{C.14}$$

as the solution for F_o. The result of Fisk and Axford (1969) is now obtained by using the Laplace transform

$$\int_0^\infty e^{-\lambda t} t^{-\nu-1} \exp(-\alpha/4t)dt = 2(\alpha/4\lambda)^{\nu/2} K_\nu(\sqrt{\alpha\lambda}), \tag{C.15}$$

where $\mathrm{Re}(\alpha)$, $\mathrm{Re}(\nu)$ and $\mathrm{Re}(\lambda)$ are positive and $K_\nu(x)$ is a modified Bessel function of the second kind of order ν and argument x (Erdelyi *et.al.* (1954), Vol.1, Section (4.5), p.146), with

$$\alpha = x^2,$$

$$\lambda = (\mu+2)/\epsilon,$$

$$\nu = m = (b+1)/(b-1)$$

in the integral (C.14). Hence

$$F_o = 2N_g\, p^{-\mu-2}\, (2(\mu+2)\, V r^{1-b}\, p^{-a}/(3(1-b)^2 K_o))^{m/2}/\, \Gamma(m)$$

$$K_m \left[2 \sqrt{(2(\mu+2)\, V\, r^{1-b}\, p^{-a}/\, (3(1-b)^2\, K_o))} \right], \qquad (C.17)$$

This is the solution for F_o cited in Equation (6.3.25b), and is the result we set out to obtain.

Case (iii) $\delta < 0$ or $b > 1 + 2a/3$

To obtain the Fisk and Axford result (6.3.25c) we introduce the variables

$$s = t\, /\, (t-t_s),$$

$$y = (\mu+2)\, /\, |\, \delta\, |, \qquad (C.18)$$

where

$$\delta = a + 3(1-b)/2.$$

Thus we have

$$p_s = p[(s-1)/s\,]^{1/\delta},$$

$$Z(t_s) = N_g\, p_s^{-\mu-2} = N_g\, p^{-\mu-2}\, [(s-1)/s]^y\,,$$

$$dt_s = t\, ds/\, s^2\,, \qquad (C.19)$$

$$s \to 1, \quad \text{as} \quad t_s \to t(\infty) = 0,$$

$$s \to \infty, \quad \text{as} \quad t_s \to t.$$

Transforming the integration variable in the general solution (C.2) from t_s to s and using the transformations (C.19) we have

$$F_o = N_g\, p^{-\mu-2} \left[|\delta| x^2/4\epsilon p^{\delta} \right]^m \int_1^{\infty} (s-1)^y\, s^{m-1-y}\, \exp(-|\delta| x^2 s/(4\epsilon p^{\delta}))\, ds, \qquad (C.20)$$

as the solution for F_o.

Using the formula

$$U(a,b,x) = \frac{e^x}{\Gamma(a)} \int_1^\infty e^{-x\omega}(\omega-1)^{a-1}\,\omega^{b-\alpha-1}\,d\omega, \qquad (C.21)$$

for U(a,b,x), which is one of the standard solutions of Kummer's confluent hypergeometric equation (Abramowitz and Stegun (1965), Section (13.1)) and using Kummer's transformation (C.9), the solution (C.20) for F_o becomes

$$F_o = N_g p^{-\mu-2} \frac{\Gamma(1-\nu(2+\mu)/3)}{\Gamma(m)} \exp\left[\, 2\,V\, r^{1-b} p^{-a}/(\nu(1-b)^2 K_o)\,\right]$$

$$U(2/(1-b)-\nu(\mu+2)/3,\ 2/(1-b),\ -2\,V r^{1-b} p^{-a}/(\nu(1-b)^2 K_o)). \qquad (C.22)$$

This is the solution (6.3.25c) which we set out to obtain.

APPENDIX D

In this appendix we obtain a solution of the spherically symmetric cosmic-ray equation of transport known as the convective solution. In this solution the effective radial diffusion coefficient is zero, and the solar wind velocity $\underline{V}$ is taken to be radial, so that the equation of transport (1.3.6), expressed in terms of the mean distribution function with respect to momentum $F_o(r,p)$ is

$$\frac{\partial F_o}{\partial t} + V \frac{\partial F_o}{\partial r} - \frac{p}{3r^2} \frac{d}{dr} (r^2 V) \frac{\partial F_o}{\partial p} = 0. \qquad (D.1)$$

The general solution of the first order, linear partial differential equation (D.1) may be expressed in terms of the solutions of the characteristic equations

$$\frac{dt}{1} = \frac{dr}{V} = \frac{dp}{\frac{-p}{3r^2} \frac{d}{dr} (r^2 V)} = \frac{dF_o}{0}, \qquad (D.2)$$

(Sneddon, Elements of Partial Differential Equations 1957). Here the symbol $dF_o/0$ is taken to mean that F_o is constant along the characteristic curves. The solutions of the characteristic equations (D.2) are

$$\begin{aligned} t - \int^r \frac{dx}{V(x)} &= c_1, \\ r\, p^{3/2}\, V^{1/2} &= c_2, \\ F_o &= c_3, \end{aligned} \qquad (D.3)$$

where c_1, c_2 and c_3 are arbitrary constants.

The general solution of the 'convective' equation of transport (D.1) is

$$F_o = H(c_1, c_2).$$

i.e.,

$$F_o(r,p) = H\left(t - \int^r \frac{dx}{V(x)},\ r\, p^{3/2}\, V^{1/2}\right) \qquad (D.4)$$

where H is an arbitrary function in two variables. In particular problems the function H is determined by the initial conditions and

the boundary conditions on the solution.

The steady state solution of the convective equation of transport (D.1), obtained when $\partial F_o/\partial t = 0$, is also determined by the characteristic curves (D.3). It is

$$F_o = G(c_2),$$

i.e.,

$$F_o(r,p) = G(r\, p^{3/2}\, V(r)^{1/2}), \tag{D.5}$$

where G is an arbitrary function in one independent variable.

We now show that the flow line equations (7.6.8) and (7.6.9) i.e.,

$$\frac{dr}{dt} = -\left(\frac{Vp}{3F_o}\,\frac{\partial F_o}{\partial p} + \frac{K(r,p)}{F_o}\,\frac{\partial F_o}{\partial p}\right), \tag{D.6}$$

$$\frac{dp}{dt} = \frac{pV}{3F_o}\,\frac{\partial F_o}{\partial r}, \tag{D.7}$$

for the general, steady state convective solution (D.5) have the general solution

$$r\, p^{3/2}\, V(r)^{1/2} = c, \tag{D.8}$$

where c is an arbitrary constant.

Substituting the expression (D.5) for $F_o(r,p)$ in the flow line equations (D.6) and (D.7), and putting $K(r,p) = 0$ we find

$$\frac{dr}{dt} = -\frac{Vp}{3\,G(z)}\,G'(z)\,\frac{\partial z}{\partial p}, \tag{D.9}$$

$$\frac{dp}{dt} = \frac{Vp}{3\,G(z)}\,G'(z)\,\frac{\partial z}{\partial r}, \tag{D.10}$$

where

$$z = r\, p^{3/2}\, V(r)^{1/2}. \tag{D.11}$$

Dividing Equation (D.9) by Equation (D.10) we have

$$\frac{dr}{dp} = -\frac{\partial z}{\partial p} \Big/ \frac{\partial z}{\partial r},$$

i.e.,

$$\frac{\partial z}{\partial r}\,dr + \frac{\partial z}{\partial p}\,dp = 0. \tag{D.12}$$

The general solution of the flow line equation (D.12) is

$$z = c,$$

i.e.,

$$r\, p^{3/2}\, v^{1/2} = c, \qquad \text{(D.13)}$$

where c is an arbitrary constant. This last result gives the flow lines (D.8) for the steady state, convective solution of the transport equation, which we set out to obtain.

APPENDIX E

In this appendix we prove that the coefficients a_k of the Hermite polynomial expansion (10.2.11a)

$$h_n(x) = \sum_{k=0}^{n} a_k \, p_k(x) = \sum_{i=0}^{n} \frac{h(t_i) \, p_{n+1}(x)}{(x-t_i) p'_{n+1}(t_i)} , \qquad (E.1)$$

are given by

$$a_k = \frac{1}{(n+1)} \sum_{i=0}^{n} h(t_i) \, p_k(t_i) \, / \, p_n^2(t_i), \quad k = 0(1)n, \qquad (E.2)$$

where $p_k(x)$ is a normalised Hermite polynomial, i.e.,

$$p_k(x) = \frac{(-1)^k e^{x^2}}{\sqrt{2^k \, k! \sqrt{\pi}}} \frac{d^k}{dx^k} (e^{-x^2}) = \frac{H_k(x)}{\sqrt{2^k \, k! \, \sqrt{\pi}}} \qquad (E.3)$$

and the t_i are roots of $p_{n+1}(x)$, i.e.,

$$p_{n+1}(t_i) = 0, \qquad i = 0(1)n. \qquad (E.4)$$

The polynomials $\{p_k(x)\}$ are orthonormal with respect to the weight function e^{-x^2} i.e.,

$$\int_{-\infty}^{\infty} e^{-x^2} \, p_m(x) \, p_j(x) dx = \delta_{mj}. \qquad (E.5)$$

Premultiplying Equation (E.1) by $e^{-x^2} \, p_m(x)$, integrating the resultant equation from $x = -\infty$ to $x = \infty$, and using the orthonormality condition (E.5) we have

$$a_m = \int_{-\infty}^{\infty} e^{-x^2} \, p_m(x) \left[\sum_{i=0}^{n} \frac{h(t_i) \, p_{n+1}(x)}{(x-t_i) \, p'_{n+1}(t_i)} \right] dx. \qquad (E.6)$$

We now express the function $p_{n+1}(x)/(x-t_i)$ in Equation (E.6) as a linear sum of the $p_k(x)$, $k = 0(1)n$, by using the Christoffel Darboux identity for orthonormal polynomials. In this case the Christoffel Darboux identity is

$$\sqrt{2/(n+1)} \sum_{k=0}^{n+1} p_k(x) \, p_k(y) = \frac{(p_{n+2}(x) \, p_{n+1}(y) - p_{n+1}(x) \, p_{n+2}(y))}{(x - y)} , \qquad (E.7)$$

(Szëgo (1967) Section (3.2), p.42, or Abramowitz and Stegun (1965), Section (22.12), p.785). Putting $y = t_i$ in the Christoffel Darboux identity (E.7) and using $p_{n+1}(t_i) = 0$ we obtain,

$$\frac{p_{n+1}(x)}{(x-t_i)} = -\sqrt{\frac{2}{n+2}} \sum_{k=0}^{n} p_k(x)\, p_k(t_i) \,/\, p_{n+2}(t_i), \quad \text{(E.8)}$$

which is the expression we seek.

Substituting the expression (E.8) in the expression (E.6) for a_m, and using the orthonormality conditions (E.5) we find

$$a_m = -\sqrt{2/(n+2)} \sum_{i=0}^{n} h(t_i)\, p_m(t_i) \,/[p'_{n+1}(t_i)\, p_{n+2}(t_i)] \,. \quad \text{(E.9)}$$

From the properties of the Hermite polynomials $H_k(x)$ we have

$$p_{k+1}(x) = \sqrt{2/(k+1)}\; x\, p_k(x) - \sqrt{k/(k+1)}\; p_{k-1}(x), \quad k \geq 1, \quad \text{(E.10)}$$

$$p'_{k+1}(x) = \sqrt{2(k+1)}\; p_k(x),$$

and hence

$$p'_{n+1}(t_i) = \sqrt{2(n+1)}\; p_n(t_i), \quad \text{(E.11)}$$

$$p_{n+2}(t_i) = -\sqrt{(n+1)/(n+2)}\; p_n(t_i),$$

(Abramowitz and Stegun (1965), Chapter 22). Substituting the results (E.11) in Equation (E.9) we obtain

$$a_m = \frac{1}{(n+1)} \sum_{i=0}^{n} h(t_i)\, p_m(t_i) \,/\, p_n^2(t_i). \quad \text{(E.12)}$$

This is the expansion for a_m given in Equation (E.2), and it is the result we set out to obtain.

APPENDIX F

In this appendix we show that if

$$h_n(x) = \sum_{k=0}^{n} a_k \, p_k(x) = \sum_{i=0}^{n} \frac{h(t_i) \; p_{n+1}(x)}{(x-t_i) \; p'_{n+1}(t_i)} \quad , \qquad (F.1)$$

is the Hermite polynomial approximation of order n to the function h(x), where $p_k(x)$ is a normalised Hermite polynomial (cf. Equation (10.2.10)), then the error in approximating the integral

$$i = \int_{-\infty}^{\infty} e^{-x^2} \sin(\alpha x) \; h(x) \; dx, \qquad (F.2)$$

by

$$i^{(n)} = \int_{-\infty}^{\infty} e^{-x^2} \sin(\alpha x) \; h_n(x) \; dx, \qquad (F.3)$$

is given by

$$R_i^{(n)} = i - i^{(n)} = \frac{1}{2\pi i} \int_C \frac{h(z) \; q(z,\alpha)}{p_{n+1}(z)} \; dz, \qquad (F.4)$$

where

$$q(z,\alpha) = \int_{-\infty}^{\infty} e^{-t^2} \sin(\alpha t) \; p_{n+1}(t) \; / \; (z-t) \; dt. \qquad (F.5)$$

Here h(z) is assumed analytic along the Re(z) axis and

$C = C^+(0,0) \cup C^-(0,0)$ is a contour in the complex z plane defined by Donaldson and Elliott (1972) (see below).

We then use the error formula (F.4) to derive the result (10.2.29a), i.e. if

$$\begin{aligned} h(x) &= m(x) \; / \; s_o(x), \\ s_o(x) &= \nu^2 \; (x-z_1)(x-\bar{z}_1)(x+z_1)(x+\bar{z}_1), \\ z_1 &= \sqrt{3/\nu} \; e^{i\pi/3} \; , \end{aligned} \qquad (F.6)$$

and m(x) is an odd polynomial of degree less than n, then

$$R_i^{(n)} = -2 \; \mathrm{Im}(m(z_1) \; q(z_1,\alpha) \; / \; (3\sqrt{3} \; \nu \; z_1 \; p_{n+1}(z_1))). \qquad (F.7)$$

is the error (F.4) for the function h(x) of Equation (F.6).

We now proceed to obtain the general result (F.4). For convenience let $g(\alpha,z)$ denote the integrand of the contour integral in

Equation (F.4). In the present application of the more general result of Donaldson and Elliott (1972) we may choose $C^+(0,0)$ to be the upper edge of $(-\infty, \infty)$, i.e., the line $\mathrm{Im}(z) = \varepsilon > 0$, with ε sufficiently small so that $h(z)$ has no singularities in the region $|\mathrm{Im}(z)| < \varepsilon$, together with semi-circular indentations of radius δ around each of the singularities of $g(\alpha,z)$ on $(-\infty, \infty)$. The function $g(\alpha, z)$ has simple poles at the roots of $p_{n+1}(z)$, i.e., at $z = t_k$, $k = 0(1)n$. The semicircle around t_k is denoted by γ_k^+ for $k = 0(1)n$. $C^-(0,0)$ is chosen similarly in the $\mathrm{Im}(z) < 0$ plane but with corresponding semicircular indentations γ_k^- (see Figure (F.1)).

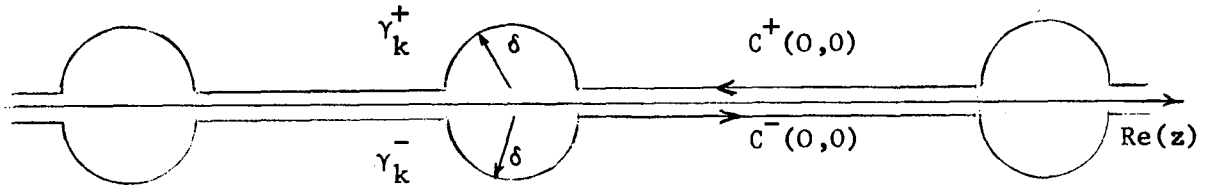

Figure F.1. Illustrating the contour $C = C^+(0,0) \cup C^-(0,0)$.

Having defined the contour C we may write the contour integral (F.4) as

$$R_i^{(n)} = \frac{1}{2\pi i}\left[\sum_{k=1}^{n}\left(\int_{t_{k-1}+\delta}^{t_k-\delta}\right) + \int_{-\infty}^{t_0-\delta} + \int_{t_{n+\delta}}^{\infty}\right] g^*(\alpha,x)\,dx$$

$$+ \frac{1}{2\pi i}\sum_{k=0}^{n}\left(\int_{\gamma_k^-} + \int_{\gamma_k^+}\right) g(\alpha,z)\,dz, \qquad (F.8)$$

where

$$g^*(\alpha,x) = g(\alpha,x-i\varepsilon) - g(\alpha, x+i\varepsilon). \qquad (F.9)$$

Since $g(\alpha,z)$ is the integrand of the contour integral (F.4), and since $h(z)$ and $p_{n+1}(z)$ are continuous across the Re(z) axis we have

$$g^*(\alpha,x) = h(x)\,(q(x-i\varepsilon,\alpha) - q(x+i\varepsilon,\alpha)) \,/\, p_{n+1}(x). \qquad (F.10)$$

For x real we define $q(x,\alpha)$ to be the Cauchy principal value integral

$$q(x,\alpha) = \int_{-\infty}^{\infty} e^{-t^2} \sin(\alpha t)\, p_{n+1}(t) \,/\, (x-t)\,dt, \qquad (F.11)$$

Accounting for the pole at $z = x$ it is easily shown that

$$q(x-i\varepsilon,\alpha) = q(x,\alpha) + \pi i\, e^{-x^2} \sin(\alpha x)\, p_{n+1}(x)$$
$$q(x+i\varepsilon,\alpha) = q(x,\alpha) - \pi i\, e^{-x^2} \sin(\alpha x)\, p_{n+1}(x). \tag{F.12}$$

Substituting the results (F.12) in Equation (F.10) we have

$$g^*(\alpha,x) = 2\pi i\, e^{-x^2} \sin(\alpha x)\, h(x). \tag{F.13}$$

Also from a well known result we have

$$\frac{1}{2\pi i} \int_{\gamma_k^-} g(\alpha,z)\, dz = h(t_k)\, q(t_k - i\varepsilon,\alpha) / (2\, p'_{n+1}(t_k)),$$
$$\frac{1}{2\pi i} \int_{\gamma_k^+} g(\alpha,z)\, dz = h(t_k)\, q(t_k + i\varepsilon,\alpha) / (2\, p'_{n+1}(t_k)), \tag{F.14}$$

and hence using the results (F.12) we have

$$\frac{1}{2\pi i} \left(\int_{\gamma_k^-} + \int_{\gamma_k^+} \right) g(\alpha,z)\, dz = h(t_k)\, q(t_k,\alpha) / p'_{n+1}(t_k). \tag{F.15}$$

Substituting the results (F.15), (F.13) in the result (F.8) and letting both ε and $\delta \to 0$ we have

$$R_i^{(n)} = \int_{-\infty}^{\infty} e^{-x^2} \sin(\alpha x)\, h(x)\, dx + \sum_{k=0}^{n} h(t_k)\, q(t_k,\alpha) / p'_{n+1}(t_k). \tag{F.16}$$

Using the definition (F.11) for $q(x,\alpha)$ in this latter expression for $R_i^{(n)}$ we obtain

$$R_i^{(n)} = \int_{-\infty}^{\infty} e^{-x^2} \sin(\alpha x)\, [h(x) - h_n(x)]\, dx = i - i^{(n)}, \tag{F.17}$$

which is the result (F.4) which we set out to prove.

We now use the contour integral expression for the remainder $R_i^{(n)}$, given in Equation (F.4) to show that for

$$h(x) = m(x) / (\nu^2 (x-z_1)(x+z_1)(x-\bar{z}_1)(x+\bar{z}_1)),$$
$$z_1 = \sqrt{3}/\nu\, e^{i\pi/3}, \tag{F.18}$$

and $m(x)$ is an odd polynomial of degree less than n, that

$$R_i^{(n)} = -2\,\mathrm{Im}\left[m(z_1)\, q(z_1,\alpha) \,/\, (3\sqrt{3}\,\nu\, z_1\, p_{n+1}(z_1)) \right] . \qquad (F.19)$$

To obtain the result (F.19) we introduce contours C_1 and C_2 in the complex z plane. The contour C_1 is a large semi-circular arc of radius R in the $\mathrm{Im}(z) > 0$ half plane with suitable indentations to circle the poles of h(z) at $z = z_1$ and $z = -\bar{z}_1$. The contour C_2 is a similar semi-circular arc of radius R in the $\mathrm{Im}(z) < 0$ half plane with indentations to circle the poles of h(z) at $z = \bar{z}_1$ and $z = -z_1$ (see Figure (F.2)).

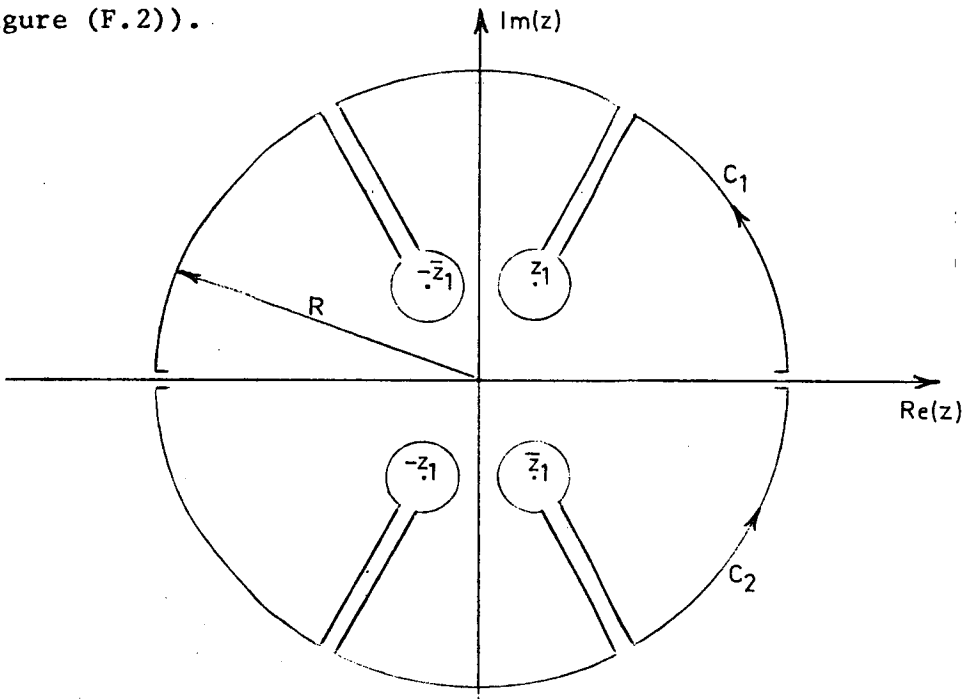

Figure F.2 Showing the contours C_1 and C_2 in the complex z plane.

Consider the contour integral

$$I = \frac{1}{2\pi i} \int_{C_1 \cup C_2} h(z)\, q(z,\alpha) \,/\, p_{n+1}(z)\; dz. \qquad (F.20)$$

As the radius R of the large circular arcs of C_1 and C_2 tends to infinity, an application of Cauchy's theorem, and using the result (F.4) gives

$$R_i^{(n)} = \lim_{R \to \infty} \frac{1}{2\pi i} \int_{C_1 \cup C_2} h(z)\, q(z,\alpha) \,/\, p_{n+1}(z)\; dz. \qquad (F.21)$$

If $h(z) \sim O(|z|^k)$ as $|z| \to \infty$ and we choose $n > k$ the contribution to the integral (F.20) from the large circular arcs of C_1 and C_2 tends to zero as $R \to \infty$.

As the radius r of the circular indentations around the poles of h(z) tends to zero and as $R \to \infty$, the principal contribution to the integral (F.20) comes from the indentations around the poles of h(z), and we find that $R_i^{(n)}$ is minus the sum of the residues of h(z) $q(z,\alpha) / p_{n+1}(z)$ at the poles of h(z), i.e.,

$$R_i^{(n)} = -\frac{1}{\nu^2}\Big[m(z_1)\, q(z_1,\alpha) / (2(z_1+\bar{z}_1)\, z_1(z_1-\bar{z}_1)\, p_{n+1}(z_1))$$
$$+ m(\bar{z}_1)\, q(\bar{z}_1,\alpha) / (2\bar{z}_1(\bar{z}_1-z_1)(z_1+\bar{z}_1)\, p_{n+1}(\bar{z}_1))$$
$$+ m(-z_1) q(-z_1,\alpha) / (2z_1(\bar{z}_1-z_1)(z_1+\bar{z}_1)\, p_{n+1}(z_1))$$
$$+ m(-\bar{z}_1)\, q(-\bar{z}_1,\alpha) / (2\bar{z}_1(z_1+\bar{z}_1)(z_1-\bar{z}_1)\, p_{n+1}(-\bar{z}_1))\Big]. \tag{F.22}$$

Using the results

$$\begin{aligned} p_{n+1}(-z) &= (-1)^{n+1}\, p_{n+1}(z), \\ q(-z,\alpha) &= (-1)^{n+1}\, q(z,\alpha) \\ m(-z) &= -m(z). \\ z_1 &= \sqrt{3/\nu}\, e^{i\pi/3}, \end{aligned} \tag{F.23}$$

the result (F.22) for $R_i^{(n)}$ reduces to

$$R_i^{(n)} = -\frac{2}{3\sqrt{3}\nu}\ \mathrm{Im}\left(\frac{m(z_1)\, q(z_1,\alpha)}{z_1\, p_{n+1}(z_1)}\right) \tag{F.24}$$

which is the expression for $R_i^{(n)}$ given in Equations (10.2.29a) and (F.7).

APPENDIX G

In this appendix we derive the momentum rate $\langle \dot{p}' \rangle$ which is the average time rate of change of momentum of cosmic-ray particles when the particle momentum p' is specified relative to the wind frame, and its position, $\underline{x}$, is specified in the fixed frame.

In our analysis we use the relativistic transformations of velocity $\underline{v}$ and momentum $\underline{p}$ accurate to $O\left(\frac{V}{c}\right)^2$ between fixed and solar wind frames of reference. These transformations are

$$\underline{v}' = \underline{v} - \underline{V} + \frac{\underline{V} \cdot \underline{v}}{c^2} \underline{v} + O\left(\frac{V^2}{c^2} v\right) , \qquad (G.1)$$

$$\underline{p}' = \underline{p} - m \underline{V}(\underline{x}) + O\left(\frac{V^2}{c^2} p\right) , \qquad (G.2)$$

where m is the relativistic particle mass in the fixed frame and $\underline{V}$ is the solar wind velocity.

The momentum $\underline{p}'$ in Equation (G.2) varies with position due to the spatial dependence of the solar and wind velocity $\underline{V}(\underline{x})$, as well as due to the Lorentz force. Thus focussing our attention on an individual particle we have

$$\frac{dp_i'}{dt} = \frac{\partial p_i'}{\partial x_j} \frac{dx_j}{dt} + \frac{\partial p_i'}{\partial p_j} \frac{dp_j}{dt} \qquad (G.3)$$

as the time rate of change of the i^{th} component p_i' of $\underline{p}'$. Here we use the summation convention and the notation of tensor calculus;

$$\frac{dp_j}{dt} = \frac{q}{c} \epsilon_{j\ell m} (v_\ell - V_\ell) B_m , \qquad (G.4)$$

is the Lorentz force on the particle and $\frac{dx_j}{dt} = v_j$ is the particle velocity.

Using the transformations (G.1) and (G.2) we have

$$\frac{dp_j}{dt} = \frac{q}{c} \epsilon_{j\ell m} v_\ell' B_m \left(1 - \frac{V_s v_s'}{c^2}\right) , \qquad (G.5)$$

$$\frac{\partial p_i'}{\partial p_j} = \delta_{ij} - \frac{v_j' V_i}{c^2} + O\left(\frac{V^2}{v^2}\right), \qquad (G.6)$$

$$\frac{\partial p_i'}{\partial x_j} = - m \frac{\partial V_i}{\partial x_j} . \qquad (G.7)$$

Substituting the results (G.5), (G.6) and(G.7) in the expression (G.3) for $\frac{dp_i'}{dt}$ we obtain

$$\frac{dp_i'}{dt} = - p_j \frac{\partial V_i}{\partial x_j} + \left(\delta_{ij} - \frac{v_j' V_i}{c^2}\right) \frac{q}{c} \varepsilon_{j\ell m} v_\ell' B_m \left(1 - \frac{V_s v_s'}{c^2}\right),$$

i.e.,

$$\frac{dp_i'}{dt} = - p_j \frac{\partial V_i}{\partial x_j} + \frac{q}{c} \varepsilon_{ijk} v_j' B_k \left(1 - \frac{V_s v_s'}{c^2}\right) . \qquad (G.8)$$

However we are not interested in $\frac{dp_i'}{dt}$ but $\frac{dp'}{dt}$. This latter quantity is given by

$$\frac{dp'}{dt} = \frac{p_i'}{p'} \frac{dp_i'}{dt} . \qquad (G.9)$$

Substituting for $\frac{dp_i'}{dt}$ from Equation (G.8) in the result (G.9), and using the momentum transformations (G.2) we obtain

$$\frac{dp'}{dt} = \frac{- p_i'}{p'} (p_j' + m V_j) \frac{\partial V_i}{\partial x_j} . \qquad (G.10)$$

The result (G.10) gives the rate of change of momentum p' of an individual particle with time. Note that it depends on the direction of the particle momentum p_i' and is independent of the magnetic field $\underline{B}$.

In order to find the average value of $\frac{dp'}{dt}$ for a group of particles, all with momentum of magnitude p', but with different directions we proceed as follows: We introduce the distribution function $F^*(\underline{r}, \underline{p}', t)$ in position-momentum space in which the position $\underline{r}$ is specified in the fixed frame of reference and the momentum $\underline{p}'$is specified in the solar wind frame. Since the cosmic-ray distribution must be near isotropic for the transport equations to be valid we may write -

$$F^*(\underline{r},\underline{p}',t) \simeq F_0^*(\underline{r},p',t) + F_{1i}^*(\underline{r},p',t)(p_i'/p'), \qquad (G.11)$$

where F_0^* is the isotropic part of the distribution function and $F_{1j}^* \sim O(\frac{V}{v}, F_0^*)$ is usually associated with cosmic-ray anisotropies or streaming.

For such a distribution of particles, the average value of $\frac{dp'}{dt}$ is given by

$$\langle \dot{p}' \rangle = \frac{\int \frac{dp'}{dt} F^*(\underline{r},\underline{p}',t)\, d\Omega'}{\int F^*(\underline{r},\underline{p}',t)\, d\Omega'} , \qquad (G.12).$$

where the solid angle integrations with respect to $d\Omega'$ are over all directions of $\underline{p}'$.

Substituting the expressions (G.10) and (G.11) for $\frac{dp'}{dt}$ and F^* in the definition (G.12) for $\langle \dot{p}' \rangle$ and using the results

$$\begin{aligned} &\int d\Omega' = 4\pi, \\ &\int \tilde{v}_i\, d\Omega' = 0, \\ &\int \tilde{v}_i \tilde{v}_j\, d\Omega' = \frac{4\pi\delta_{ij}}{3}, \end{aligned} \qquad (G.13)$$

where $\tilde{v}_i = p_i'/p'$ we obtain,

$$\langle \dot{p}' \rangle = \frac{-p'}{3} \underline{\nabla} \cdot \underline{V} \left(1 + O\left(\frac{V^2}{v^2}\right)\right). \qquad (G.14)$$

This is the rate $\langle \dot{p}' \rangle$ quoted in the text in Equation (1.3.7).

REFERENCES

Abramowitz, M. and Stegun, I.A. : 1965, Handbook of Mathematical Functions, Dover, New York.

Axford, W.I. : 1965a, The modulation of galactic cosmic-rays in the interplanetary medium, *Planet.Space Sci.*, 13, 115.

Axford, W.I. : 1965b, Anisoptropic diffusion of solar cosmic-rays, *Planet.Space Sci.*, 13, 1301.

Axford, W.I. : 1970a, Energetic solar particles in the interplanetary medium, Review Paper, *Symposium on Solar Terrestrial Physics, Leningrad*, May 1970.

Axford, W.I. : 1970b. A review of theoretical work on the effects of solar wind transport on energetic solar particles, *paper presented at Seminar on Cosmic-Ray Generation on the Sun*, U.S.S.R. Academy of Science, Leningrad, December 1970.

Badhwar, G.D., Deney, C.L., Dennis, B.R. and Kaplon, M.F. : 1967, Measurements of the low-energy cosmic radiation during the summer of 1966, *Phys.Rev.*, 163, 1327.

Belov, A.V. and Dorman, L.I. : 1969, Modulation of the intensity of galactic cosmic-rays by the solar wind in the presence of azimuthal asymmetry, *Geomagn. and Aeron.*, Vol.9, No.6, 783.

Belov, A.V. and Dorman, L.I. : 1971, Spherical cone in the solar wind that modulates cosmic-rays, *Geomagn. and Aeron*, Vol.11, No.2, 273.

Beuerman, K.P., Rice, C.J., Stone, E.C. and Vogt, R.E. : 1969, Cosmic-ray negatron and position spectra between 12 and 220 MeV, *Phys. Rev.Letters*, 22, 412.

Biermann, L. : 1951, Kometenschweife und solare Korpuskularstrahlung, *Z.Astrophys.*, 29, 274.

Birmingham, T.J. and Jones, F.C. : 1975, Cosmic-ray-diffusion report of the workshop on cosmic-ray diffusion theory, NASA *Technical Note* JN D-7873.

Bluman, G.W. : 1967, Construction of Solutions to Partial Differential Equations by the use of Transformation Groups, Ph.D. Thesis, California Institute of Technology, 1967.

Bluman, G.W. : 1969, The general similarity solution of the heat equation, *J. Math. and Mechanics*, Vol.18, No.11, 1025.

Bluman, G.W. : 1974, Application of the general similarity solution of the heat equation to boundary-value problems, *Quart. J. of Appl. Math.*, Vol.31, No.4, 403.

Burger, J.J. : 1971, A phenomenological approach to the solar modulation of cosmic-rays, *Astrophys. J.*, 166, 651.

Burger, J.J. and Swanenburg, B.N. : 1971, Long-term solar modulation of cosmic-ray electrons with energies above 0.5 GeV, *Proc. 12th Int. Conf. on Cosmic-Rays, Hobart,* Conference Papers, 5, 1858.

Burger, J.J. and Swanenburg, B.N. : 1973, Energy dependent time lag in the long term modulation of cosmic-rays, *J. Geophys.Res.*, 78, 292.

Caldwell, J., Evenson, P., Jordan, S. and Meyer, P. : 1975, The Cosmic-ray electron spectrum in 1973 and 1974, *Proc. 14th Int. Conf. on Cosmic-Rays, Munich,* 3, 1000.

Cecchini, S. and Quenby, J.J. : 1975, Three-dimensional models of galactic cosmic-ray modulation, *Proc. 14th Int. Conf. on Cosmic-Rays, Munich,* 3, 911.

Clenshaw, C.W. : 1955, A note on the summation of Chebyshev series, *Math. Comp.*, 9, 118.

Cocconi, G. : 1951, On the origin of cosmic radiation, *Phys. Rev.*, 83, 1193.

Compton, A.H. and Getting, I.A. : 1935, An apparent effect of galactic rotation on the intensity of cosmic-rays, *Phys. Rev.*, 47, 817.

Dolginov, A.Z. and Toptygin, I.N. : 1967, Diffusion of cosmic particles in the interplanetary medium, *Geomag. and Aeron.*, 7, 785.

Dolginov, A.Z. and Toptygin, I.N. : 1968, Cosmic-rays in the interplanetary magnetic fields, *Icarus*, 8, 54.

Donaldson, J.D. and Elliot, D. : 1972, A unified approach to quadrature rules with asymptotic estimates of their remainders, *Siam. J. Numer. Anal.*, 9, 573

Dorman, L.I. : 1965, Galactic and solar cosmic rays in interplanetary space, *Proc. 9th Int. Conf. on Cosmic Rays, London,* 1, 292.

Dorman, L.I. and Kats, M.E. : 1971, Study of cosmic-rays propagation in the interplanetary medium on the basis of the kinetic equation, *Proc.12th Int. Conf. on Cosmic-Rays, Hobart,* Conf. Papers, 7, 2682.

Dorman, L.I. and Kobylinsky, Z. : 1973, Modulation of the spectrum, the radial and transverse gradients of galactic cosmic rays in a combined model of anisotropic diffusion including convection, and adiabatic cooling of particles in inter-

planetary space, *Proc. 13th Int. Conf. on Cosmic-Rays, Denver*, 2, 771.

Dorman, L.I., Kobylinsky, Z. and Khadakhanova, T.S. : 1973, Modulation of galactic cosmic-rays by solar wind which is unsymmetric in solar latitude, *Geomag. and Aeron.*, Vol. 12, No.1, 16.

Dorman, L.I. and Milovinova, N.P. : 1973, Galactic cosmic-ray density distribution in interplanetary space expected on the basis of anisotropic diffusion theory including the actual distribution of solar activity over the solar disc, *Proc. 13th Int. Conf. on Cosmic-Rays, Denver*, 2, 713.

Dorman, L.I. and Milovinova, N.P. : 1975, Expected spatial distribution of cosmic-rays in interplanetary space including the real helioatitude distribution of solar activity, *Proc. 14th Int. Conf. on Cosmic-Rays, Munich*, 3, 917.

Earl, J.A. : 1973, Diffusion of charged particles in a random magnetic field, *Astrophys. J.*, 180, 227.

Earl, J.A. : 1974a, Coherent propagation of charged particle bunches in random magnetic fields, *Astrophys. J.*, 188, 379.

Earl, J.A. : 1974b, The diffusive idealisation of charged particle transport in random magnetic fields, *Astrophys. J.*, 193, 231.

Eisenhart, L.P. : 1933, Continuous groups of transformations, Dover, New York, (1933).

Elliot, D. : Uniform asymptotic expansions of classical orthogonal polynomials and some associated functions, Tech. Report 21, University of Tasmania, Hobart, Australia (undated).

Englade, R.C. : 1971a, A computational model for solar flare particle propagation, *J. Geophys.Res.*, 76, 768.

Englade, R.C. : 1971b, Effect of solar boundary condition on flare particle propagation, *J. Geophys.Res.*, 76, 6190.

Erdelyi, A., Magnus, W., Oberhettinger, F., and Tricomi, G. : 1954, Tables of Integral Transforms, Vol. 1, McGraw Hill.

Erdelyi, A. : 1956, Asymptotic Expansions, Dover.

Fan, C.Y., Gloeckler, G. and Simpson, J.A. : 1965, Solar modulation of the galactic helium spectrum above 30 MeV per nucleon, *Proc. 9th Int. Conf. on Cosmic-Rays, London :* Institute of Physics and the Physical Society, I, 380.

Fanselow, J.L., Hartmann, R.C., Hildebrand, R.H. and Meyer, P. : 1969, Charge composition and energy spectrum of primary cosmic-ray

electrons, *Astrophys. J.*, 158, 771.

Fermi, E. : 1949, On the origin of cosmic radiation, *Phys.Rev.*, 75, 1169.

Fisk, L.A. and Axford, W.I. : 1968, Effect of energy changes on solar cosmic-rays, *J. Geophys. Res.*, 73, 4396.

Fisk, L.A. : 1969, Behaviour of Cosmic-Rays in the Interplanetary medium, Ph.D. thesis, University of California at San Diego.

Fisk, L.A. and Axford, W.I. : 1969, Solar modulation of galatic cosmic-rays, 1, *J. Geophys. Res.*, 74, 4973.

Fisk, L.A., Gleeson, L.J. and Axford, W.I. : 1969, Approximations in the theory of solar cycle modulation, *Proc. 11th Int. Conf. on Cosmic-Rays, Budapest*, 2, 105.

Fisk, L.A., Forman, M.A. and Goldstein, M.L. : 1973, Modulation of low energy galactic cosmic-rays, *Proc. 13th Int. Conf. on Cosmic-Rays, Denver*, 2, 771.

Fisk, L.A., Goldstein, M.L., Klimas, A.J. and Sandri, G. : 1974, The Fokker-Planck coefficient for pitch angle scattering of cosmic-rays, *Astrophys. J.*, 190, 417.

Fisk, L.A. : 1975, Possible evidence for latitude-dependent cosmic-ray modulation, *Proc. 14th Int. Conf. on Cosmic-Rays, Munich*, 3, 905.

Forbush, S.E. : 1937, On the effects of cosmic-ray intensity observed during the recent magnetic storm, *Phys. Rev.*, 51, 1108.

Forbush, S.E. : 1954, World-wide cosmic-ray variations, 1937-1952, *J. Geophys. Res.*, 59, 525.

Forman, M.A. : 1970, The Compton-Getting effect for cosmic-ray particles and photons and the Lorentz-invariance of distribution functions, *Planet.Space Sci.*, 18, 25.

Forman, M.A. : 1971a, Convection dominated transport of solar cosmic-rays, *J. Geophys. Res.*, 76, 759.

Forman, M.A. : 1971b, Convection dominated transport of solar cosmic-rays, *Proc. 12th Int. Conf. on Cosmic-Rays, Hobart*, 2, 501.

Forman, M.A., Jokipii, J.R. and Owens, A.J. : 1974, Cosmic-ray streaming perpendicular to the mean magnetic field, *Astrophys. J.*, 192, 535.

Forman, M.A. and Gleeson, L.J. : 1975, Cosmic-ray streaming and anisotropies, *Astrophys. and Space Sci.*, 32, 77.

Freir, P.S. and Waddington, C.J. : 1965, Modulation of cosmic-rays by an electric field, *Proc. 9th Int. Conf. on Cosmic-Rays, London*, 1, 176.

Freir, P.S., Long, C.E., Cleghorn, T.F. and Waddington, C.J. : 1971, The charge and energy spectra of heavy cosmic-ray nuclei, *Proc. 12th Int. Conf. on Cosmic-Rays, Hobart*, Conf. Papers, 1, 252.

Fulks, G., Meyer, P. and L'Heureux, J. : 1973, The Cosmic-ray electron spectrum and its modulation from 1968 through 1972, *Proc. 13th Int. Conf. on Cosmic-Rays, Denver*, 2, 753.

Gleeson, L.J. and Axford, W.I. : 1967, Cosmic-rays in the interplanetary medium, *Astrophys. J. Lett.*, 149, L115.

Gleeson, L.J. and Axford, W.I. : 1968a, The Compton-Getting effect, *Astrophys. Space Sci.*, 2, 431.

Gleeson, L.J. and Axford, W.I. : 1968b, The solar radial gradient of galactic cosmic-rays, *Canad.J. of Physics*, 46, S937.

Gleeson, L.J. and Axford, W.I. : 1968c, Solar modulation of galactic cosmic-rays, *Astrophys. J.*, 154, 1011.

Gleeson, L.J. : 1969, The equations describing the cosmic-ray gas in the interplanetary region, *Planet.Space Sci.*, 17, 31.

Gleeson, L.J. : 1970, Convective transport of low energy cosmic-rays in the interplanetary region, *Astrophys. and Space Sci.*, 10, 471.

Gleeson, L.J. : 1971, Steady-state solar modulation of cosmic-rays, Rapporteur Paper, *Proc. 12th Int. Conf. on Cosmic-Rays, Hobart*, August 1971.

Gleeson, L.J. and Ng, C.K., : 1971, Energy changes of cosmic-rays in interplanetary space, *J. Geophys.Res.*, 76, 8434.

Gleeson, L.J. and Urch, I.H. : 1971, Energy losses and modulation of galactic cosmic-rays, *Astrophys. Space Sci.*, 11, 288.

Gleeson, L.J. : 1972, Cosmic-ray propagation and modulation in the interplanetary medium, *Proc. Solar Terrestrial Relations Conf. Calgary*, August 28 - September 1, 1972, 79.

Gleeson, L.J. and Urch, I.H. : 1973, A study of the force-field equation for the propagation of galactic cosmic-rays, *Astrophys. and Space Sci.*, 25, 387.

Gleeson, L.J. and Webb, G.M. : 1974, Cosmic-ray energy changes, *Proc. Astron.Soc.Aust.*, Vol.2, No.5, 297.

Gleeson, L.J. and Webb, G.M. : 1975, Modulation and spectral redistribution of galactic cosmic-rays, *Proc. 14th Int. Conf. on Cosmic-rays, Munich*, 3, 893.

Gloeckler, G. and Jokipii, J.R. : 1966, Low-energy cosmic-ray modulation related to the observed interplanetary magnetic field irregularities, *Phys. Rev. Letters*, 17, 203.

Gloeckler, G. and Jokipii, J.R. : 1967, Solar modulation and energy density of galactic cosmic-rays, *Astrophys. J.*, 148, L41.

Goldstein, M.L., Fisk, L.A. and Ramaty, R. : 1970a, Interstellar cosmic-ray spectra from non-thermal radio background from 0.4 to 400 MHz, *Phys. Rev. Letters*, 24, 1193.

Goldstein, M.L., Ramaty, R. and Fisk, L.A. : 1970b, Energy losses of cosmic-rays in the interplanetary medium, *Phys. Rev. Letters*, 25, 832.

Gradshteyn, I.S. and Ryzhik, I.M. : 1965, Tables of Integrals, Series and Products, New York Academic Press.

Hall, D.E. and Sturrock, P.A. : 1967, Diffusion, scattering and acceleration of particles by stochastic magnetic fields, *Phys. Fluids*, 10, 2620.

Hammarling, S.J. : 1970, Latent Roots and Latent Vectors, Adam Hilger (1970).

Hasselman, K. and Wibberenz, G. : 1968, Scattering of charged particles by random electromagnetic fields, *Zs.f.Geophys.*, 34, 353.

Hasselman, K. and Wibberenz, G. : 1970, A note on the parallel diffusion coefficient, *Astrophys. J.*, 162, 1049.

Hatton, C.J. : 1971, The neutron monitor, Progress in Elementary Particle and Cosmic-Ray Physics, 10, 1.

Hess, V.F. : 1911, *Physikal.Zeits.*, 12, 998.

Hess, V.F. : 1912, *Physikal.Zeits.*, 13, 1084.

Hess, V.F. and Graziadei, T.H. : 1936, The diurnal variation of cosmic-radiation, *J. Geophys. Res.* (Terr. Mag.), 41, 9.

Hess, V.F. and Steinmaurer, R. : 1933, *Proceedings of the Berlin Academy of Sciences*, 15, 521.

Hsieh, K.C. : 1970, Study of solar modulation of low energy cosmic-rays, *Astrophys. J.*, 159, 61.

Jokipii, J.R. : 1966, Cosmic-ray propagation, 1. Charged particles in a random magnetic field, *Astrophys. J.*, 146, 480.

Jokipii, J.R. : 1967, Cosmic-ray propagation, 2. Diffusion in the interplanetary magnetic field, *Astrophys. J.*, 149, 405.

Jokipii, J.R. and Parker, E.N. : 1967, Energy changes of cosmic rays in the solar system, *Planet. Space Sci.*, 15, 1375.

Jokipii, J.R. : 1968a, Addendum and erratum to cosmic-ray propagation, 1, *Astrophys. J.*, 152, 671.

Jokipii, J.R. : 1968b, Backscatter and diffusion of cosmic-rays in a random magnetic field, *Astrophys. J.*, 152, 997.

Jokipii, J.R. and Parker, E.N. : 1969, Stochastic aspects of magnetic lines of force with application to cosmic-ray propagation, *Astrophys. J.*, 155, 777.

Jokipii, J.R. and Parker, E.N. : 1970, On the convection, diffusion and adiabatic deceleration of cosmic-rays in the solar wind, *Astrophys. J.*, 160, 735.

Jokipii, J.R. : 1971, Propagation of cosmic-rays in the solar wind, *Revs. Geophys. Space Sci.* 9, 27.

Jokipii, J.R. : 1972, Fokker-Planck equations for charged-particle transport in random fields, *Astrophys. J.*, 172, 319.

Jokipii, J.R. : 1973a, Radial variation of magnetic fluctuations and the cosmic-ray diffusion tensor in the solar wind, *Astrophys. J.*, 182, 585.

Jokipii, J.R. : 1973b, Turbulence and scintillations in the interplanetary plasma, *Ann. Rev. Astron. Astrophys.*, 11, 1.

Jokipii, J.R. and Lerche, I. : 1973, On the transport of charged particles in turbulent fields : comparison of an exact solution of the quasi-linear approximation, *Plasma Phys.*, 15, 619.

Jokipii, J.R. : 1974, Pitch angle scattering of charged particles in a random magnetic field, *Astrophys. J.*, 194, 465.

Jones, F.C., Birmingham, T.J. and Kaiser, T.B. : 1973a, Investigation of resonance integrals occurring in cosmic-ray diffusion theory, *Astrophys. J.*, 180, L139.

Jones, F.C., Kaiser, T.B. and Birmingham, T.J. : 1973b, New approach to cosmic-ray diffusion theory, *Phys. Rev. Letters*, 31, 485.

Jones, F.C. and Birmingham, T.J. : 1975, When is quasi-linear theory exact, *Plasma Phys.*, 17, 15.

Kaiser, T.B. : 1973, The behaviour of charged particle distributions in time-independent stochastic magnetic fields, Ph.D. thesis, Techn. Report No. 74-033, University of Maryland.

Kaiser, T.B., Jones, F.C. and Birmingham, T.J. : 1973, Cosmic-rays in a random magnetic field: breakdown of the quasi-linear derivation of the kinetic equation, *Astrophys.J.*, 180, 239.

Klimas, A.J. and Sandri, G. : 1971, Foundation of the theory of cosmic-ray transport in random magnetic fields, *Astrophys. J.*, 169, 41.

Klimas, A.J. and Sandri, G. : 1972, A critical review of recent work in cosmic-ray transport theory, *Proc. Solar Terrestrial Relations Conf., Calgary*, Canada, 493.

Klimas, A.J. and Sandri, G. : 1973, A rigorous cosmic-ray transport equation with no restrictions on particle energy, *Astrophys. J.*, 180, 937.

Krimsky, G.F. : 1964, *Geomag. and Aeron.*, 4, 763.

Kulsrud, R. and Pearce, W.P. : 1969, The effect of wave-particle interactions in the propagation of cosmic-rays, *Astrophys. J.*, 156, 445.

Lee, M.E. and Lerche, I. : 1974, Waves and irregularities in the solar wind, *Rev. Geophys. and Space Sci.*, 12, 671.

Lerche, I. : 1967, Unstable magneto-sonic modes in a relativistic plasma, *Astrophys. J.*, 147, 689.

Lerche, I. : 1974, On Kraichnan's direct interaction approximation applied to charged particle transport in turbulent magnetic fields, *Astrophys. J.*, 193, 711.

Lerche, I. : 1974, A variational approach to charged particle transport, *Astrophys. J.*, 193, 711.

Lentz, G.A., McKibben, R.B., O'Gallagher, J.J., Perkins, M., Simpson, J.A. and Tuzzolino, A.J. : 1973, Heliospheric intensity gradients of galactic cosmic-ray nuclei and electrons from Pioneer 10, *Proc. 13th Int. Conf. on Cosmic-Rays, Denver*, 2, 743.

Lezniak, J.A. and Webber, W.R. : 1971, Solar modulation of cosmic-ray protons, helium nuclei and electrons, (a comparison of experiment with theory), *J.Geophys.Res.*, 76, 1605.

Lie, S. : 1881, Über die Integration durche bestimmte Integrale von einer Klasse linearer partieller Differentialgleichungen, Arch. Math., VI, 328 (1881).

Lietti, B. and Quenby, J.J. : 1968, The daily variation second harmonic and cosmic-ray intensity gradient perpendicular to the ecliptic, *Canad. J. Phys.*, 46, S942.

Lockwood, J.A. and Webber, W.R. : 1967, The eleven-year solar modulation of cosmic-rays as deduced from neutron monitor variation and

direct measurements at low energies, *J.Geophys.Res.*, 72,5977.

Lupton, J.E. and Stone, E.C. : 1971, Transport of solar flare protons - Comparisons of a new analytic model with spacecraft measurements, *Proc. 12th Int. Conf. on Cosmic-Rays, Hobart*, Conf. Papers, 2, 492.

Lupton, J.E. and Stone, E.C. : 1973, Solar flare particle propagation: Comparison of a new analytic solution with spacecraft measurements, *J.Geophys. Res.*, 78, 1007.

McCracken, K.G. and Rao, U.R. : 1970, Solar cosmic-ray phenomena, *Space.Sci.Rev.*, 11, 155.

Melrose, D.B. and Wentzel, D.G. : 1970, Interaction between cosmic-ray electrons and cosmic-ray protons, *Astrophys.J.*, 161, 457.

Meyer, P., Parker, E.N. and Simpson, J.A. : 1956, Solar cosmic-rays of February 1956 and their propagation through interplanetary space, *Phys. Rev.*, 104, 768.

Meyer, P., Schmidt, P.J. and L'Heureux, L.J. : 1971, Measurements of the primary cosmic-ray electron spectrum between 20 MeV and 20 GeV and its changes with time, *Proc. 12th Int. Conf. on Cosmic-Rays, Hobart*, Conf. Papers, 2, 548.

Moraal, H. : 1973, The force-field approach to neutron monitor observations of the eleven-year cosmic-ray modulation cycle, Ph.D. thesis, Potchefstroom University, South Africa.

Moraal, H. : 1975, Modulation Observations, *Proc. 14th Int. Conf. on Cosmic-Rays, Munich*, (Rapporteur paper - in press).

Moraal, H. and Gleeson, L.J. : 1975, Three-dimensional models of the galactic cosmic-ray modulation, *Proc. 14th Int. Conf. on Cosmic-Rays, Munich*, 3, 910.

Morse, P.M. and Feshback, H. : 1953, Methods of Theoretical Physics, Vol. 1, McGraw-Hill, International student edition.

Müller, E.A. and Matschat, K. : 1962, Über das Auffinden von Ähnlichkeitslösungen partieller Differentialgleichungssysteme unter Benutzung von Transformationsgruppen, mit Anwendung auf Probleme der Strömungphysik, *Miszellaneen der Angewandten Mechanik*, Berlin, 1962, p. 190.

Ng, C.K. and Gleeson, L.J. : 1971a, The propagation of solar cosmic-ray bursts, *Solar Phys.*, 20, 166.

Ng, C.K. and Gleeson, L.J. : 1971b, On the propagation of solar cosmic-rays, *Proc. 12th Int. Conf. on Cosmic-Rays, Hobart*, Conf. Papers, 2, 498.

Ng, C.K. : 1972, Propagation of Solar-Flare Cosmic-Rays, Ph.D. thesis, Monash University, Australia.

Ng, C.K. and Gleeson, L.J. : 1975, A model for the propagation of solar-flare cosmic-rays, *Proc. 14th Int. Conf. on Cosmic-Rays, Munich*, 4, 1744.

Noerdlinger, P.D. : 1968, An improved model for cosmic-ray propagation, *Phys.Rev.Letters*, 20, 1513.

O'Gallagher, J.J. and Simpson, J.A. : 1967, The heliocentric intensity gradients of cosmic-ray protons and helium during minimum solar modulation,*Astrophys. J.*, 147, 819.

O'Gallagher, J.J. : 1973, Cosmic-ray hysteresis as evidence for time-dependent diffusive processes in the long term modulation, *Proc. 13th Int. Conf. on Cosmic-Rays, Denver*, Conf. Papers, 2, 1135.

Ormes, J.F. and Webber, W.R. : 1968, Proton and helium nuclei cosmic-ray spectra and modulation between 100 and 2000 MeV/nucleon, *J. Geophys.Res.*, 73, 4231.

Ovsjannikov, L.V. : 1962, Gruppovye Svoystva Differentsialny Uravnenii, Novosibirsk, (1962), (Group Properties of Differential Equations, translated by G.W. Bluman, 1967).

Owens, A.J. and Jokipii, J.R. : 1971, Cosmic-ray modulation by an angle-dependent solar wind, *Astrophys.J.*, 167, 169.

Owens, A.J. : 1974a, Cosmic-ray scintillations, 2, general theory of interplanetary scintillations, *J.Geophys.Res.*, 79, 895.

Owens, A.J. : 1974b, The effects of non linear terms in cosmic-ray diffusion theory, *Astrophys. J.*, 191, 235.

Paget, D.F. and Elliot, D. : 1972, An algorithm for the numerical evaluation of certain Cauchy principal value integrals, *Numer.Math.*, 19, 373.

Parker, E.N. : 1958a, Dynamics of the interplanetary gas and magnetic field. *Astrophys, J.* 128, 664.

Parker, E.N. : 1958b, Cosmic-ray modulation by the solar wind, *Phys.Rev.*, 110, 1445.

Parker, E.N. : 1963, Interplanetary Dynamical Processes, Interscience, New York.

Parker, E.N. : 1964, Theory of streaming of cosmic-rays and the diurnal variation, *Planet. Space Sci.*, 12, 735.

Parker, E.N. : 1965, The passage of energetic charged particles through interplanetary space, *Planet. Space Sci.*, 13. 9.

Parker, E.N. : 1966, The effect of adiabatic deceleration on the

cosmic-ray spectrum in the solar system, *Planet.Space Sci.*, 14, 371.

Quenby, J.J. : 1965, Cosmic-rays and the interplanetary magnetic field, *Proc. 9th Int.Conf. on Cosmic Rays, London*, 1, 3.

Quenby, J.J. : 1967, Time variations of the cosmic-ray intensity, *Handbuch der Physik XLVI/2, Cosmic Rays*, Springer Verlag, Berlin, 46, No.2, 310.

Quenby, J.J. : 1973, Particle propagation in interplanetary space (theory), RapporteurPaper, *Proc. 13th Int. Conf. on Cosmic Rays, Denver*, Conf. Papers, 5, 3731.

Ramaty, R. and Lingfelter, R.E. : 1969, Cosmic-ray deuterium and helium-3 of secondary origin and the residual modulation of cosmic-rays, *Astrophys. J.*, 155, 587.

Roelof, E.C. : 1966, Ph.D. thesis, University of California, Berkely.

Roelof, E.C. : 1968, Transport of cosmic-rays in the interplanetary medium, *Canad. J. Phys.*, 46, S990.

Silberberg, R. : 1966, Cosmic-ray modulations in the solar system and in interstellar space, *Phys.Rev.*, 148, 1247.

Simpson, J.A. and Fagot, W.C. : 1953, Cosmic radiation intensity time variations, *Phys.Rev.*, 90, 934.

Singer, S.F., Laster, H. and Lenchek, A.M. : 1962, Forbush decreases produced by diffusive deceleration mechanism in interplanetary space, *J.Phys. Soc.Japan*, 17, (Suppl.A-11), 583.

Slater, L.J. : 1960, Confluent Hypergeometric Functions, Cambridge University Press, London (1960).

Sneddon, I.N. : 1957, Elements of Partial Differential Equations, McGraw-Hill, International Student Edition (1957).

Sneddon, I.N. : 1961, Special Functions of Mathematical Physics and Chemistry, New York, Interscience.

Spiegel, M.R. : 1970, Laplace Transforms, McGraw-Hill, (Schaum outline series).

Subramanian, G. and Sarabhai, V. : 1969, Consequences of the distribution of galactic cosmic-ray density in the solar system, *Astrophys. J.*, 149, 417.

Szegö, G : 1967, Orthogonal Polynomials, A.M.S. Colloquim Publications, vol.23, (1939), 3rd edition (1967).

Terletskii, Ia.P. and Logunov, A.A. : 1951, Energeticheskii spectr. pervichnoi komponenti kosmicheskikh luchei, *J.Exptl.Theoret.Phys.*, (U.S.S.R), 21, 567.

Toptygin, I.N. : 1973, Direct and inverse problem of cosmic-ray propagation in interplanetary space, *Geomag. and Aeron.*, 13, 181.

Titchmarsh, E.C. : 1962, Eigenfunction Expansions associated with second order differential equations, Oxford University Press (1962).

Urch, I.H. : 1971, Theoretical studies of the interplanetary medium, Ph.D. thesis, University of Adelaide, Australia.

Urch, I.H. and Gleeson, L.J. : 1971, Energy changes of solar cosmic-ray particles, *Proc. 12th Int. Conf. on Cosmic-Rays, Hobart*, Conf. Papers, 2, 504.

Urch, I.H. and Gleeson, L.J. : 1972a, Radial gradients and anisotropies due to galactic cosmic-rays, *Astrophys and Space Sci.* 16, 55.

Urch, I.H. and Gleeson, L.J. : 1972b, Galactic cosmic-ray modulation from 1965-1970, *Astrophys. and Space Sci.*, 17, 426.

Urch, I.H. and Gleeson, L.J. : 1973, Energy losses of cosmic-rays in the interplanetary medium, *Astrophys and Space Sci.*, 20, 177.

Urch, I.H. : 1974, Cosmic-ray particle diffusion and the Fokker-Planck equation, *Proc. Astron. Soc. of Aust.*, Vol.2, No.5, 306.

Van Allen, J.A. : 1973, Heliocentric dependence of galactic cosmic ray intensity to and beyond 3.3 AU, *Proc. 13th Int. Conf. on Cosmic-Rays, Denver*, 2, 750.

Volk, H.J. : 1973, Non-linear perturbation theory for cosmic-ray propagation, *Astrophys. and Space Sci.*, 25, 471.

Volk, H.J., Morfill, G., Alpers, W. and Lee, M.A. : 1974, Spatial dependence of the pitch angle and associated spatial diffusion coefficients for cosmic-rays in interplanteary space, *Astrophys. Space and Sci.*, 26, 403.

Wang, R.J. : 1970, Dynamics of the eleven-year modulation of galactic cosmic-rays, *Astrophys. J.*, 160, 261.

Webb, G.M. and Gleeson, L.J. : 1973, Monoenergetic source solutions of the steady-state cosmic-ray equation of transport, *Proc. 13th Int. Conf. on Cosmic-Rays, Denver*, (University of Denver, 1973), Conf.Papers, 5, 3253.

Webb, G.M. and Gleeson, L.J.: 1974, Solutions of the cosmic-ray equation of transport, *Proc. Astron. Soc. of Australia*, Vol.2, No.5, 299.

Webb, S. and Quenby, J.J. : 1973a, Numerical studies of the transport of solar protons in interplanetary space, *Planet.Space Sci.*, 21, 23.

Webb, S. and Quenby, J.J. : 1973b, Numerical studies of the interaction of energetic charged particles with interplanetary field discontinuities, *Proc. 13th Int. Conf. of Cosmic-Rays, Denver*, Conf. Papers, 2, 1343.

Webber, W.R. : 1969, Survey-paper given at the *Seminar on the Study of Interplanetary Space Physics by means of Cosmic Rays*, Leningrad, U.S.S.R., June 4-7, 1969.

Webber, W.R. and Chotowski, C. : 1967, A determination of the energy spectrum of extraterrestrial electrons in the energy range 70-2000 MeV, *J.Geophys.Res.*, 72, 2783.

Webber, W.R. and Lezniak, J.A. : 1973, Interplanetary radial gradients of galactic cosmic ray protons and helium nuclei: Pioneer 8 and 9 measurements from 0.75 to 1.1 A.U., *J. Geophys. Res.*, 78, 1979.

Webber, W.R. and Lezniak, J.A. : 1974, The comparative spectra of cosmic-ray protons and helium nuclei, *Astrophys. and Space Sci.*, 30, 361.

Wibberenz, G. : 1971, Solar particle propagation, Rapporteur Paper, *Proc.12th Int. Conf. on Cosmic-Rays, Hobart.*

Zakharchenko, V.F. : 1971, The Fokker-Planck equation with convection and non symmetrical scattering of cosmic-ray particles, *Proc. 12th Int. Conf. on Cosmic-Rays, Hobart*, Conference Papers, 2, 800.

Zakharchenko, V.F. : 1973, Contribution to the theory of cosmic-ray propagation with anisotropic particle scattering, *Geomag. and Aeron.*, Vol.13, No.1, 11.